HI Selected Galaxies in the Sloan Digital Sky Survey

Andrew Alan West

A dissertation submitted in partial fulfillment
of the requirements for the degree of

Doctor of Philosophy

University of Washington

2005

Program Authorized to Offer Degree: Department of Astronomy

University of Washington

Graduate School

This is to certify that I have examined this copy of a doctoral dissertation by

Andrew Alan West

and have found that it is complete and satisfactory in all respects,
and that any and all revisions required by the final
examining committee have been made.

Chair of Supervisory Committee:

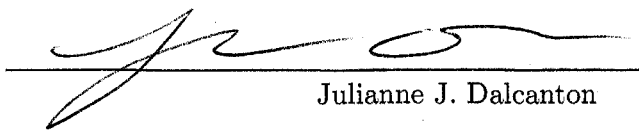

Julianne J. Dalcanton

Reading Committee:

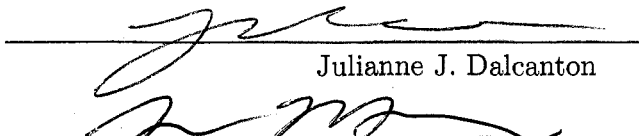

Julianne J. Dalcanton

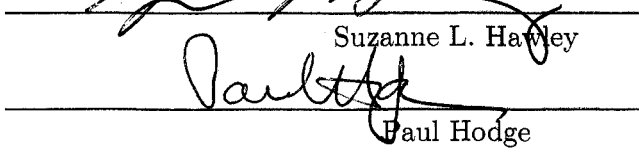

Suzanne L. Hawley

Paul Hodge

Date: 7/5/05

In presenting this dissertation in partial fulfillment of the requirements for the doctoral degree at the University of Washington, I agree that the Library shall make its copies freely available for inspection. I further agree that extensive copying of this dissertation is allowable only for scholarly purposes, consistent with "fair use" as prescribed in the U.S. Copyright Law. Requests for copying or reproduction of this dissertation may be referred to Proquest Information and Learning, 300 North Zeeb Road, Ann Arbor, MI 48106-1346, to whom the author has granted "the right to reproduce and sell (a) copies of the manuscript in microform and/or (b) printed copies of the manuscript made from microform."

Signature _____

Date 7/5/05

University of Washington

Abstract

HI Selected Galaxies in the Sloan Digital Sky Survey

Andrew Alan West

Chair of the Supervisory Committee:
Professor Julianne J. Dalcanton
Department Astronomy

We present the results from a study of HI selected galaxies that fall within both the HI Parkes All Sky Survey (HIPASS) and the Sloan Digital Sky Survey (SDSS). By comparing the optical properties derived from the SDSS five-band photometry with the HI properties from HIPASS, we are able to probe the relationship between the stellar population and the neutral gas over a range of Hubble types. Our HIPASS/SDSS catalog provides a uniform data set that is used to investigate the physical factors that contribute to star formation on global scales in galaxies. The HI selection has allowed us to identify a significant group of low surface brightness galaxies not included in most SDSS studies. We also find that the colors of the HI selected galaxies are offset from those of a volume-limited sample of SDSS galaxies. This can be explained by a recent burst of star formation in the HI selected galaxies and may point to a recent acquisition of cold gas. We synthesize model galaxy colors using the Bruzual & Charlot (2003) population synthesis grids and use these colors to derive rough star formation histories and metallicities for the HIPASS/SDSS sample galaxies. Many of the HIPASS/SDSS galaxies have colors that do not fall on the Bruzual & Charlot model grids. However, most of the discrepant sources can be explained as galaxies whose colors are dominated by emission lines rather than the underlying stellar populations. We also utilize the dynamical information derived from the HI line widths and investigate the Tully-Fisher relation in HI selected galaxies. The combination of HI and optical data allow us to examine the "baryonic" Tully-Fisher (BTF) relation. We find that the scatter

in the (BTF) correlates with the baryonic mass fraction and is predicted by fundamental disk galaxy formation scenarios. In addition, the construction of this catalog has let to a set of tools to aid in the analysis of large nearby galaxies in the SDSS.

TABLE OF CONTENTS

LIST OF FIGURES

LIST OF TABLES

ACKNOWLEDGMENTS

As I prepare to finish this final stage of my formal academic training, I can't help but be thankful for all of the help and support I have received over the years. This thesis is the product of years of effort and although it seems cliché to say, I was only able to accomplish this task with the help of countless people and many institutions. I can't include everyone in these acknowledgments, but I can highlight those individuals who have had the greatest influence on me and my academic growth:

- *Catherine:* I am sure that everyone thinks that their partner is the smartest, the prettiest, the most supportive or the best friend- but it's really true for me. Catherine Foster has been supportive of my academic and personal goals for the entirety of our 8+ year relationship. She has endured my countless 16 hour days at work, tireless travel schedule and put up with sleepless nights when I was stressed. She has done this while working on her own studies. She now sets forth for her own Ph.D., looking at the isotope ratios in fish bones to determine ancient ocean temperatures - what a nerd (I love it!). Thanks Catherine for your love and t-time. I am so excited that we will be supporting each other forever.

- *My family:* I was taught from an early age that education was of utmost importance. Both of my parents are educators and I was fortunate to grow up in an environment that supported my "nerdy" tendencies. I thank Mom, Dad, Leslie, Ethan, Grammy and Poppa for all of their love and support over that last 23 years of my education. I am also thankful to be marrying into an equally supportive family that has given me a tremendous amount of encouragement over the past 8 years. Thanks to Richard, Margaret and Susan for including me in your family and sharing your love with me.

- *Teachers:* I am most thankful for the myriad of teachers and mentors who have touched my life over the past 23 years. Linda Valenziano, Bonnie Springer, Bruce Bowen, Sid Bishop, Gary Cavender, Christian LaPotre, Richard Whipkey, Ingrid Erich, Rita Meyers, Pat Alto, Roland Neilson, John Mattern, Steve Boughn, Ken Kellermann, Bruce Partridge, Debbie Haarsma, Anne McGuire, Michael Johns, Walter Smith, Željko Ivezić and Tony Irving have all played a vital role in my arrival at the Ph.D. I would like to give special thanks to my advisor Julianne Dalcanton for her support over the past couple of years and her constant belief in my abilities. I also have to thank my second advisor and mentor Suzanne Hawley for showing me the beauty of cool stars, teaching me to be a true winner and always keeping me on track.

- *Friends:* I have always had the fortune of a strong friend base. It all started with Sean Newton and has worked it's way to Sean Raymond. I would like to give thanks to Sean N., Sharia, Damon, Christine, Blake, Cookie, Muffin, Anil, Kevin, Verno, and Bochanski for letting me be a part of your life. It is also important to acknowledge the support of Dr. Maritza Tavarez (aka. Wonder Woman), who helped me work out problems with my science and allowed me to vent my frustration on many occasions. I have to give special thanks to Chris Laws and Sean Raymond for making graduate school a ridiculously fun experience. The "baseball 3" will live again my friends and we will teach our children that sliding head first into third base in the 11th inning is worth 12 points! See you both at Coastanoa!

- *Dr. Sean Raymond:* I got lucky! When I heard that there was only one other person in my graduate school class, I was frightened. Given the social skills of many astronomers, it wasn't clear that the "other" would be someone with whom I would relate. But as luck would have it, I got Sean Raymond. He is my best buddy, the "Reverend" who will marry me and the part of graduate school that I will most miss. Thank you Dr. Raymond for your love, your support, for introducing me to Irish music, forcing me

to ski Peak 8, teaching me about "die and pong" and instructing me on the art of bathtub photography. Your friendship is at the top of my grad school highlight show.

- *Sports:* I am a very competitive person. The athletic field has been an excellent outlet for me. I thank Jerry, Cliff, Tom, Rich, the Goats, the Infrared Sox, the Adiabats and the Foragers. In particular I would like to thank Warped Disks for the awesome "Westies", the great flow and awesome memories. My new ACL and I will be back for Potlatch 2006!

- *Collaborators:* I have been fortunate to be involved in many projects while a graduate student. I thank my many collaborators for their contribution to my learning. In particular I would like to thank Diego Garcia-Appadoo, Mike Disney, Julianne Dalcanton, Connie Rockosi, and Željko Ivezić for their considerable help on this thesis project.

- *Students:* I have learned a tremendous amount from those whom I was allowed to teach. I thank all of my Upward Bound, McNair, 101, 150, 221, and 481 students for your thoughtful questions and comments and for helping me to become a better teacher. In particular I would like to thank the undergraduates with whom I have closely worked. Thanks to Misty Bentz, Willow Brim, Robert Farris, and Laura Kushner for helping me with research and assisting in my growth as a mentor and advisor.

- *Financial Support:* I could not get through grad school without the financial support of the following organizations and individuals: Julianne Dalcanton, Suzanne Hawley, Tom Quinn, McNair, Upward Bound, AAS, NSF, the Jacobsen Fund, Sigma Xi, ADVANCE, the Royalty Research Grant, the Astronaut Scholarship Foundation, ARCS, MESA, University Tutoring, SDSS and Mike Disney.

DEDICATION

This thesis is dedicated to my grandmother, Barbara Bassett, who has always supported my passion for astronomy and the night sky. Some of my earliest memories are of my "Grammy" telling me to look up at the moon every night so that she and I might gaze upon the same object even though we were separated by hundreds of miles. She bought me my first telescope, which opened my eyes to the moons of Jupiter, the Orion Nebula and countless other astronomical wonders. Throughout my long academic career, she has followed the popular coverage of astronomy and saved almost every astronomically related newspaper article published in her local newspaper. I feel blessed to have had her support at every stage of my academic growth. Thank you Grammy for always believing in me, I made it at long last - I'm a doctor now!

Chapter 1

INTRODUCTION

1.1 Gas and Galaxy Evolution

Galaxies steadily evolve by accreting gas and converting that gas into stars. Throughout this process, galaxies gradually transform from systems whose baryonic content is dominated by gas, into systems that are dominated by stars. In the local universe we see examples of galaxies spanning this spectrum of star formation history. At the beginning of the spectrum are gas rich, low surface brightness (LSB) galaxies that have either just begun the process of star formation or have been processing their gas with extremely small efficiency. At the other end are the gas poor galaxies that are generally devoid of gas and that typically have formed the bulk of their stars in the distant past.

These "gas rich" and "gas poor" galaxies represent the starting and ending points of the evolution of galaxies. Examples of the former reveal glimpses of the stages through which most disk galaxies must have passed early in their evolution. Examples of the latter are candidates for some of the oldest galactic systems ever assembled. Nearby examples of both types of galaxies represent important laboratories for studying critical epochs in the history of galaxy formation.

Between these two extremes lie "normal" galaxies that have formed substantial stellar populations but have retained some amount of their primordial gas, and thus lie on a continuum between the gas rich and the gas poor systems. Presumably, the degree to which these galaxies have traveled down their evolutionary paths from gas rich to gas poor is tightly coupled to global properties of the galaxies, such as mass, environment, internal motions, and metal content. A galaxy's evolution is also complicated by the fact that it can lose gas to tidal stripping and supernova blowout and acquire gas through infall; the

evolutionary path is not always smooth or identical. One of the underlying goals of this thesis is to characterize some of the critical properties that control galaxy evolution for a large spectrum of galaxy evolutionary stages, from the unevolved gas rich systems, through the normal galaxy population, to the very gas poor.

Creating a sample that bridges these two regimes requires the union of two radically different methods of identifying galaxies. Stars dominate the light output of most galaxies in the visible regime, and thus galaxies detected by traditional "optical" imaging have a well developed population of stars. In contrast, the natural way to identify gas rich, less evolved galaxies is by their 21 cm radio emission. This emission line is caused by the hyperfine ground-state transition of neutral Hydrogen (HI), the most abundant form of gas in most galaxies. Selecting on HI reveals galaxies entirely based on their gas content, independent of their starlight, and thus easily finds systems with intact gas reservoirs. Characterizing both the stellar and gas properties of galaxies selected in the radio and in the optical will therefore yield information about the entire continuum of galaxy star formation histories.

Aside from its importance for global star formation, a sample of gaseous and stellar information for galaxies in the nearby universe also allows for a more complete census of the local baryons. Too often, galaxy studies neglect the fact that HI dominates the baryonic content of many galaxies. The baryonic makeup of the nearby universe puts important observational constraints on simulations of galaxy formation and evolution as well as revealing reservoirs of mass that were previously undetected because of their optical LSB nature (Disney 1976). The HI data also provide kinematic information related to the dark matter content of the galaxies. Therefore, with both optical and HI information, we can probe how the baryonic content relates to total mass of the galaxy.

The aim of this thesis is to present the first step toward an inventory of the HI and optical properties of galaxies in the local universe. This thesis focuses on an HI selected sample and therefore identifies many systems that have retained much of their primordial HI. It lacks the systems that have used their entire gas supply and are dominated by stars. A project is underway to fill in the gas poor systems and complete the nearby baryonic census, but it will not be included in this work.

This thesis combines data from two high quality surveys, the HI Parkes All Sky Survey[1] (HIPASS; Barnes et al. 2001; Meyer et al. 2004; Zwaan et al. 2004) and the Sloan Digital Sky Survey[2] (SDSS; York et al. 2000; Gunn et al. 1998; Fukugita et al. 1996; Hogg et al. 2001; Smith et al. 2002; Pier et al. 2003). The HI data (HIPASS) are acquired using the multibeam receiver on the 64m Parkes telescope in Parkes, Australia. The SDSS is a deep, 5-band optical survey of the northern sky using the 2.5m telescope at the Apache Point Observatory in New Mexico. The combination of these two surveys has created a rich compendium of stellar and HI parameters for galaxies at various evolutionary states that are used to explore how global star formation proceeds in galaxies as a function of their physical parameters.

1.2 Previous HI Observations

HI has historically been used as a means to measure the kinematics of disk galaxies. The 21cm hyper-fine transition for HI was predicted by van de Hulst (1945) and the first HI observations were carried out to study the motions and structure of the Milky Way (Ewen & Purcell 1951; Muller & Oort 1951). HI synthesis measurements have since been used to map the kinematics and structure of HI in many extragalactic systems and were important to the eventual recognition of dark matter in galaxies (Bosma 1978; van Albada 1985). Because of the large amount of observing time needed to complete HI observations, the first blind[3] HI survey was not published until 1977 (Shostak 1977). The Shostak survey observed for

---

[1]The Parkes telescope is part of the Australia Telescope which is funded by the Commonwealth of Australia for operation as a National Facility managed by CSIRO.

[2]Funding for the Sloan Digital Sky Survey (SDSS) has been provided by the Alfred P. Sloan Foundation, the Participating Institutions, the National Aeronautics and Space Administration, the National Science Foundation, the U.S. Department of Energy, the Japanese Monbukagakusho, and the Max Planck Society. The SDSS Web site is http://www.sdss.org/.

The SDSS is managed by the Astrophysical Research Consortium (ARC) for the Participating Institutions. The Participating Institutions are The University of Chicago, Fermilab, the Institute for Advanced Study, the Japan Participation Group, The Johns Hopkins University, the Korean Scientist Group, Los Alamos National Laboratory, the Max-Planck-Institute for Astronomy (MPIA), the Max-Planck-Institute for Astrophysics (MPA), New Mexico State University, University of Pittsburgh, University of Portsmouth, Princeton University, the United States Naval Observatory, and the University of Washington.

[3]The term "blind" is used to indicate that a survey uses no prior knowledge of astronomical sources and is therefore blind to previous detections

several days on the NRAO 300 ft telescope and yielded only one detection. Many subsequent HI surveys were pointed toward optical over-densities in order to increase the number of detections. This method was a successful tactic that yielded many HI detections as well as several new LSB systems (Lo & Sargent 1979; Haynes & Roberts 1979; Fisher & Tully 1981; McMahon 1993; Dickey 1997; Barnes 1997). Other HI surveys were directed at under-dense regions and although they were able to detect extragalactic HI, they yielded no new population of LSB galaxies (Krumm & Brosch 1984; Szomoru et al. 1996).

Until recently, most of the HI surveys were targeted at specific locations and little was known about the distribution of HI in the Universe independent of optical properties. Henning (1992; 1995) used the NRAO 300 ft telescope (with a better receiver than that of Shostak 1977) to conduct an HI blind survey and recovered 39 sources, half of which were not previously known. Large blind surveys followed using the Arecibo 300m telescope, yielding hundreds of sources and allowing for the first statistically sound studies of the HI mass function (Zwaan et al. 1997; Spitzak & Schneider 1998; Rosenberg & Schneider 2000; Rosenberg & Schneider 2002). These blind surveys also identified many LSB galaxies that were previously unidentified and paved the way for more complete studies of the baryonic content of nearby galaxies (Rosenberg, Schneider & Posson-Brown 2005).

The HIPASS blind HI survey, as of its first data release, has identified over 4000 HI sources (Meyer et al. 2004). Although it has a larger beam (15.5′ versus 3.3′) and a larger system noise than the Arecibo surveys, it covers a much larger sky area and has a velocity coverage that is twice that of the Arecibo surveys. The uniformity, velocity depth and scale of HIPASS make it an ideal survey with which to probe the gas content of the nearby Universe.

1.3 The Need for a Uniform Sample

Many previous studies have investigated the relationships between gas and stars in galaxies (e.g., Roberts 1963; Fisher & Tully 1981; Scodeggio & Gavazzi 1993; Kennicutt, Tablyn & Condon 1994; McGaugh & de Blok 1997; Haynes et al. 1999; Burkholder, Impey & Sprayberry 2001; Swaters et al. 2002; Iglesias-Paramo et al. 2003; Karachentsev et al.

2004; Helmboldt et al. 2004; Rosenberg, et al. 2005). However, most of the studies have utilized data that are not taken in a uniform manner. Typically these samples are limited in size and the inhomogeneities create additional scatter in the derived relationships. Because many of the gas/star relationships have significant scatter themselves, it is difficult to probe the intrinsic scatter without the use of a uniform sample. The advent of large astronomical surveys allows for large quantities of data to be taken with a high level of uniformity. Unions of these large surveys yield multi-wavelength, uniform data sets with small systemic errors and large sample sizes (Salim et al. 2005; Agüeros et al. 2005; Covey et al. 2005).

The most relevant of these marriages to this thesis work is the combination of the Arecibo Duel Beam and Slice Surveys with the Two Micron All Sky Survey (2MASS; Jarrett et al. 2000; Rosenberg et al. 2005). They investigate how the infrared stellar light compares to the HI gas emission. Although Rosenberg et al. (2005) are able to probe the baryonic content of a large sample of galaxies, they are limited by the shallow depth of 2MASS, which does not have data for many of the LSB galaxies in the sample. Therefore their study excludes the galaxies at the extreme gas rich end of the evolutionary spectrum.

The union of SDSS and HIPASS for this thesis provides the desired uniformity in both the optical and the radio (HI) data, along with remarkable depth in the optical SDSS data. Although there is only a small area of SDSS/HIPASS overlap, enough data exist for the construction of a a uniform HI selected catalog that can be used to probe how the baryonic content of galaxies changes as a function of other physical parameters.

1.4 Brief Thesis Outline

Chapter 2 describes the SDSS and HIPASS samples and discusses the methods by which the HI selected sample is created. In this chapter distances and masses are derived from the HI data.

Because the SDSS is not optimized for studying large galaxies, there are several problems associated with a catalog level treatment of nearby galaxy science. Chapter 3 outlines the techniques for the accurate extraction of photometric parameters of large galaxies in SDSS. Photometric properties and uncertainties of the HI selected galaxies are measured and

various physical parameters from these data are derived.

Chapter 4 examines the relationships between gas, stars and dark matter by investigating trends in the gas fraction of systems and examining the distribution of HI in the HIPASS/SDSS galaxies.

Chapter 5 specifically examines how the observed optical colors of galaxies relate to the gas content. Population synthesis models are compared to the HIPASS/SDSS sample colors in order to estimate star formation histories and metallicities. We show that HI selected galaxies have different colors than their gas poor counterparts and explain this difference as a product of recent star formation. We also suggest that a transition from stable to unstable disks is responsible for a change in the color dispersion of galaxies. And lastly, we investigate how emission lines can dominate the colors of galaxies and explain many of the discrepancies between the predicted model and observed sample colors.

Chapter 6 utilizes the width of the HI emission line to investigate the dynamics of the HIPASS/SDSS galaxies. The slope and scatter for various manifestations of the Tully-Fisher relation is derived and we show that the scatter in the Baryonic Tully-Fisher relation may be explained by differences in the physical structure of galaxies.

Two appendices are included in this thesis. The first gives a detailed discussion of the problems that the SDSS has in calculating accurate photometry for large galaxies. By simulating a set of fake galaxies, we derive quantitative solutions for remedying the problems and apply these solutions to real data. The second appendix is a collection of the images and spectra for the HIPASS/SDSS galaxies.

Chapter 2

HI SELECTED GALAXIES - SAMPLE SELECTION

2.1 Introduction

Building a uniform sample of HI selected galaxies requires a number of steps. Although both the SDSS and HIPASS surveys produce uniform, high quality data sets, there are some "impedance matching" problems that must be sorted out before useful science can come from their union. The fact that the Parkes HI beam size is many arcminutes makes the catalog matching to SDSS (with resolution of 1-2 arcseconds) quite time consuming. In this chapter we will discuss the process by which we construct the HIPASS/SDSS catalog. We will also discuss the methods for deriving physical quantities from the HI data and will present some of the limits and ranges of the HI selected sample. By comparing these data with a volume-limited SDSS sample, we will briefly show some of the ways in which this sample differs from an optically selected sample and discuss an ongoing project to build a more complete volume-limited sample of galaxies in the nearby Universe.

2.2 Survey Descriptions and Sample Selection

2.2.1 HIPASS Survey

The HI data come from a subset of the HI Parkes All Sky Survey (HIPASS; Barnes et al. 2001; Meyer et al. 2004; Zwaan et al. 2004). HIPASS is a blind HI survey of the southern sky that covers a velocity range from -1280 to 12700 km/s with an RMS noise of 13 mJy, using the multibeam receiver on the 64m radio telescope in Parkes, Australia. The main survey covers the entire southern sky below $\delta < +2$. A northern extension between $+2 < \delta < +10$ was also observed with the same survey characteristics and is important for this thesis study because of its substantial overlap with the SDSS data. The velocity resolution of the HIPASS HI spectra is 18.0 km/s and assuming a 200 km/s HI galaxy profile, the 3σ HI

mass limit of the survey is $10^6 \times D^2_{Mpc} M_\odot$. All HIPASS data is stored in three dimensional data cubes (ra-dec-velocity). For detailed descriptions of the data acquisition, calibration and reliability see Barnes et al. (2001), Meyer et al. (2004), and Zwaan et al. (2004).

The HIPASS data cubes were searched by my collaborator from Cardiff University, Diego Garcia-Appadoo, using an automated search code written in MIRIAD. He extracted 1164 sources from a 5738 square degree region of the sky ($-6 < \delta < +10$) where the SDSS overlaps were likely to occur. For each source detection, the HI spectrum was extracted by fitting a baseline relation to the background flux (Barnes et al. 2001). From each spectrum, the source position, recessional velocity, 20% peak velocity width, peak and integrated fluxes were all measured. The extracted HI velocity and flux measures for the SDSS-HIPASS sample can be found in Table 2.1. The parameter uncertainties are investigated by Zwaan et al. (2004) and can be found in Table 2.2. For further details on the source extraction and parameter measurement for the HIPASS-SDSS data, see the description in Garcia-Appadoo (2005).

Table 2.1. HI Extracted Parameters

HIPASS Name	Heliocentric Velocity (km/s)	W_{20} (km/s)	S_{peak} (Jy)	S_{int} (Jy km/s)	Distance (Mpc)	HI Mass 10^9 $M_\odot$
HIPEQ0014-00	3914.3	290.0	0.0745	17.182	56.5	12.901
HIPEQ0027-01a	3848.2	223.3	0.0393	6.603	55.4	4.771
HIPEQ0033-01	1972.4	146.0	0.1308	17.244	27.9	3.162
HIPEQ0043-00	4124.0	287.4	0.0640	13.808	59.5	11.501
HIPEQ0051-00	1616.4	172.7	0.1166	14.840	22.7	1.801
HIPEQ0058+00	5338.0	155.6	0.0478	4.968	77.5	7.028
HIPEQ0107+01	626.2	59.5	0.0632	3.805	8.5	0.064
HIPEQ0119+00	4307.0	78.0	0.0500	3.900	62.1	3.539
HIPEQ0120-00	1712.0	129.2	0.0392	3.883	24.0	0.526
HIPEQ0122+00	2324.7	265.8	0.1592	33.231	33.0	8.502
HIPEQ0123-00	7282.8	60.0	0.0493	2.952	106.6	7.904
HIPEQ0126+00a	5336.0	84.0	0.0550	4.600	77.3	6.481
HIPEQ0126-00b	1898.3	98.6	0.0393	3.287	26.6	0.549
HIPEQ0154-00	5661.6	93.1	0.0423	3.764	82.0	5.968
HIPEQ0222-00	1534.8	143.6	0.0590	7.271	21.1	0.766
HIPEQ0228-01	1604.8	155.5	0.1306	15.998	22.1	1.841
HIPEQ0230+00	1523.0	27.5	0.0470	1.374	21.1	0.000
HIPEQ0230-01	1501.1	331.4	0.0422	7.838	20.6	0.783
HIPEQ0231+00	6245.0	157.0	0.0470	7.400	90.7	14.342
HIPEQ0236+00	6452.4	298.9	0.0412	7.231	93.8	15.001
HIPEQ0238+00	1457.0	109.0	0.0850	9.300	20.1	0.881
HIPEQ0240+01	1176.4	54.3	0.0953	5.739	16.0	0.348
HIPEQ0241+00	991.6	388.0	0.4095	119.340	13.3	4.990
HIPEQ0244+00	2771.3	70.2	0.0337	2.990	39.2	1.080
HIPEQ0246-00a	2744.1	308.9	0.1548	27.592	38.7	9.726
HIPEQ0246-00b	1508.6	216.8	0.1649	32.092	20.7	3.240
HIPEQ0249-00	6493.2	118.3	0.0252	2.634	94.3	5.521
HIPEQ0249-00a	2632.0	132.0	0.0880	11.600	37.0	3.747
HIPEQ0249-00b	6953.4	258.6	0.0396	7.840	101.3	18.936
HIPEQ0251-01	1498.1	104.5	0.2780	27.989	20.5	2.767
HIPEQ0300+00	2831.9	211.9	0.0517	9.885	39.9	3.716
HIPEQ0301-00	2624.8	110.5	0.0725	6.504	36.9	2.082
HIPEQ0306-00	3185.8	196.7	0.0802	13.101	45.1	6.265
HIPEQ0316-00	6826.0	74.9	0.0400	1.699	99.3	3.945
HIPEQ0320-06	2313.6	227.3	0.0915	18.638	31.9	4.463
HIPEQ0351-00	9031.1	117.1	0.0355	3.742	132.9	15.565
HIPEQ0809+00	1798.5	151.2	0.0451	5.291	25.1	0.787
HIPEQ0821+03b	4056.6	255.0	0.0446	6.824	58.4	5.488
HIPEQ0821-00	1802.3	72.1	0.1557	13.743	25.1	2.048
HIPEQ0822-00	4459.7	131.9	0.0514	5.780	64.1	5.591
HIPEQ0825-00	4914.0	466.5	0.0550	12.116	70.9	14.336
HIPEQ0855+02	3779.1	127.1	0.0572	5.602	54.4	3.908
HIPEQ0856+00	2493.4	146.1	0.0692	9.196	35.4	2.715
HIPEQ0923-00	3471.1	234.2	0.0513	9.441	49.8	5.508
HIPEQ0930+04	5244.2	68.6	0.0865	5.988	76.4	8.242
HIPEQ0936+01	4874.8	271.0	0.0524	11.318	70.7	13.342
HIPEQ0942+00	1880.4	129.4	0.4903	59.186	26.7	9.930
HIPEQ0944-00b	1219.8	124.6	0.0552	6.498	17.1	0.446
HIPEQ0945+01	1853.0	265.2	0.0787	16.602	26.4	2.727
HIPEQ0946+02	1927.2	177.2	0.0699	13.405	27.6	2.402
HIPEQ0947+00a	1763.5	211.9	0.1130	19.309	25.0	2.849
HIPEQ0947+00b	1850.1	113.5	0.0769	8.050	26.3	1.313
HIPEQ0953+01	1284.0	329.5	0.2129	55.139	18.2	4.302
HIPEQ0954+01a	1796.8	125.7	0.0578	6.621	25.7	1.026
HIPEQ0954+02a	7192.1	61.1	0.0535	3.643	105.7	9.597
HIPEQ0955+04a	1813.4	221.5	0.0567	11.498	26.1	1.840
HIPEQ0958+01	1804.7	112.9	0.0566	5.821	25.8	0.910
HIPEQ1000+03	2053.1	361.5	0.0759	23.072	29.5	4.732
HIPEQ1010+05	4066.8	125.7	0.0419	5.672	59.2	4.685

Table 2.1—Continued

HIPASS Name	Heliocentric Velocity (km/s)	W_{20} (km/s)	S_{peak} (Jy)	S_{int} (Jy km/s)	Distance (Mpc)	HI Mass 10^9 $M_\odot$
HIPEQ1014+03	1216.8	434.2	0.3258	115.350	17.5	8.290
HIPEQ1015+02	1272.7	144.3	0.0975	12.705	18.2	0.994
HIPEQ1026+03	2141.5	241.1	0.1218	22.280	31.0	5.030
HIPEQ1028+03	1147.3	110.5	0.0451	4.529	16.5	0.292
HIPEQ1031+04	1172.6	180.3	0.2041	33.012	17.0	2.244
HIPEQ1039+01	706.7	47.6	0.0715	4.099	10.1	0.099
HIPEQ1041+00	5541.2	103.7	0.0459	4.556	81.0	7.040
HIPEQ1046+01	982.7	233.2	0.2557	46.779	14.1	2.200
HIPEQ1050+01	1589.0	120.2	0.0300	3.937	22.9	0.485
HIPEQ1051+04a	1038.6	153.6	0.1007	11.635	15.2	0.630
HIPEQ1052+00	1808.6	88.0	0.0688	5.674	26.0	0.902
HIPEQ1053+02	1045.0	87.5	0.1053	9.003	15.1	0.485
HIPEQ1055+02	1040.0	84.2	0.0370	3.444	15.0	0.184
HIPEQ1101+03	1122.1	302.6	0.1491	35.887	16.3	2.259
HIPEQ1109-00	3810.1	336.5	0.0818	19.888	55.3	14.345
HIPEQ1110+01	991.3	70.8	0.0752	5.341	14.3	0.258
HIPEQ1113+05	2524.9	82.9	0.0529	4.020	36.9	1.288
HIPEQ1117+04a	1572.9	350.7	0.0610	14.545	23.0	1.814
HIPEQ1119+02	1576.0	214.0	0.2700	57.800	22.9	7.155
HIPEQ1124+03	1368.3	107.1	0.2263	23.513	20.0	2.215
HIPEQ1127-01	962.3	82.6	0.0958	8.944	13.8	0.404
HIPEQ1131-02	4676.6	106.6	0.1527	18.474	68.1	20.194
HIPEQ1133-03	1603.8	139.1	0.1276	15.508	23.0	1.926
HIPEQ1136+00	1099.3	90.2	0.0782	6.841	16.0	0.412
HIPEQ1138+03	5492.2	102.3	0.0541	5.432	80.8	8.347
HIPEQ1143-01	1695.0	58.0	0.0670	3.900	24.5	0.551
HIPEQ1145+02	1007.5	29.6	0.1308	5.914	14.8	0.305
HIPEQ1148-02	1724.5	223.4	0.1675	28.490	24.9	4.157
HIPEQ1151-02	3832.4	224.1	0.0363	6.686	55.7	4.886
HIPEQ1152+01	6022.2	136.1	0.0373	5.370	88.6	9.942
HIPEQ1152-02	1053.9	59.9	0.1138	7.445	15.2	0.404
HIPEQ1152-03b	1634.8	60.8	0.0910	5.934	23.5	0.771
HIPEQ1155+01	1878.8	175.9	0.0950	14.116	27.4	2.496
HIPEQ1200-00	1928.5	54.2	0.1237	7.063	28.1	1.309
HIPEQ1200-01	1459.3	319.3	0.2420	65.298	21.2	6.895
HIPEQ1202+01	1966.4	303.2	0.0997	18.746	28.8	3.653
HIPEQ1204-01	1468.4	96.3	0.1026	8.832	21.3	0.943
HIPEQ1204-02	5887.0	42.6	0.0940	3.250	86.3	5.708
HIPEQ1210+02	1331.2	82.8	0.1253	10.739	19.6	0.972
HIPEQ1215+04a	2171.0	85.1	0.0405	3.764	32.0	0.908
HIPEQ1216-03	5054.8	127.1	0.0467	5.736	73.9	7.376
HIPEQ1218+00	932.9	59.8	0.3350	21.186	13.8	0.946
HIPEQ1218-01	5587.1	297.6	0.0584	9.292	82.0	14.732
HIPEQ1219+03	1516.2	55.8	0.0420	2.134	22.4	0.253
HIPEQ1220+00	889.7	70.6	0.0657	4.568	13.2	0.186
HIPEQ1220+01	1587.6	184.1	0.0434	6.264	23.3	0.802
HIPEQ1221+03	2552.7	343.5	0.0957	15.570	37.5	5.163
HIPEQ1223+00	2040.3	84.5	0.0961	7.999	29.8	1.677
HIPEQ1223-03b	1989.3	371.8	0.0511	11.122	28.8	2.173
HIPEQ1224+00	2051.0	125.0	0.0480	6.000	30.0	1.268
HIPEQ1224+03b	923.5	50.9	0.1973	10.728	13.9	0.486
HIPEQ1225+00	2130.2	98.6	0.0440	4.396	31.1	1.005
HIPEQ1226+02	1678.7	186.6	0.0868	14.265	24.7	2.057
HIPEQ1227+01	1286.5	63.2	0.4925	33.319	19.0	2.834
HIPEQ1228+02	1559.4	168.3	0.0870	13.524	23.0	1.691
HIPEQ1228+03	894.1	125.7	0.0596	7.056	13.5	0.302
HIPEQ1229+00	2222.8	109.5	0.0463	4.377	32.5	1.092
HIPEQ1230+02	1627.9	39.5	0.0973	3.699	24.0	0.503
HIPEQ1230+03	5137.1	121.0	0.0424	4.233	75.7	5.717

Table 2.1—Continued

HIPASS Name	Heliocentric Velocity (km/s)	W_{20} (km/s)	S_{peak} (Jy)	S_{int} (Jy km/s)	Distance (Mpc)	HI Mass 10^9 $M_\odot$
HIPEQ1232+00a	1519.6	156.9	0.3015	41.465	22.3	4.861
HIPEQ1232+00b	1126.9	304.3	0.5045	118.380	16.6	7.698
HIPEQ1233-02	2461.6	68.3	0.0923	6.743	35.8	2.034
HIPEQ1236+03	1432.4	118.9	0.0588	6.539	21.3	0.696
HIPEQ1239-00	1070.3	198.7	1.0554	159.450	15.8	9.356
HIPEQ1241+01	1695.0	143.2	0.0800	9.251	25.0	1.358
HIPEQ1241-02	1431.0	99.1	0.0570	4.860	20.8	0.496
HIPEQ1242+03b	742.4	138.5	0.0488	6.794	11.4	0.208
HIPEQ1242-00	1708.0	216.2	0.2110	39.319	25.0	5.812
HIPEQ1242-01a	1101.0	144.2	0.1690	21.042	16.2	1.298
HIPEQ1242-01b	3172.0	293.3	0.1190	23.269	46.3	11.765
HIPEQ1243-00	2605.0	193.2	0.1670	21.267	38.1	7.264
HIPEQ1244+00	1167.0	103.1	0.1090	7.329	17.3	0.515
HIPEQ1244-02	1576.0	108.1	0.1140	9.892	23.0	1.231
HIPEQ1245-00	1510.0	348.4	0.3310	75.701	22.2	8.762
HIPEQ1249+03	722.5	156.2	0.4249	54.568	11.1	1.584
HIPEQ1249+04	2642.4	74.2	0.0969	7.276	39.0	2.611
HIPEQ1250+05	648.7	168.4	0.3413	48.728	10.2	1.190
HIPEQ1253+01	1138.1	278.1	0.0710	13.736	17.0	0.930
HIPEQ1253+02	998.7	426.1	0.0565	12.022	15.0	0.638
HIPEQ1253+04	718.4	74.5	0.2272	18.309	11.1	0.535
HIPEQ1255+00	1311.4	186.9	0.1526	23.531	19.4	2.082
HIPEQ1255+02	2759.5	362.6	0.0560	13.920	40.6	5.416
HIPEQ1255-00	1115.0	92.1	0.0430	3.440	16.5	0.221
HIPEQ1256+03	654.4	188.8	0.1117	15.185	10.2	0.371
HIPEQ1257+02	923.3	102.1	0.0491	4.854	14.0	0.223
HIPEQ1257-01	2821.3	293.0	0.0826	19.820	41.2	7.932
HIPEQ1258+02	2731.4	131.6	0.0687	8.896	40.2	3.393
HIPEQ1300+02a	875.8	51.3	0.0561	2.729	13.3	0.113
HIPEQ1300+02b	960.0	98.7	0.1964	25.628	14.5	1.271
HIPEQ1303+03	2844.1	112.0	0.0776	7.438	42.0	3.090
HIPEQ1304-02	1265.7	77.5	0.0777	6.237	18.5	0.505
HIPEQ1304-03	1357.7	113.9	0.3828	41.302	19.8	3.824
HIPEQ1307-00	5324.1	190.2	0.0705	13.341	78.3	19.291
HIPEQ1308-02	5260.2	175.3	0.0499	7.641	77.3	10.758
HIPEQ1311+03a	3008.4	160.3	0.0549	7.527	44.4	3.495
HIPEQ1312+03	8068.5	115.9	0.0399	4.627	120.2	15.748
HIPEQ1312+05	908.0	79.2	0.0498	3.569	14.0	0.165
HIPEQ1313+06	6906.1	191.1	0.0426	7.990	102.7	19.857
HIPEQ1317-00	1223.2	105.3	0.0470	4.945	18.1	0.383
HIPEQ1318-01	5637.7	101.9	0.0595	5.302	83.1	8.618
HIPEQ1320+05	958.8	85.2	0.0589	4.827	14.8	0.248
HIPEQ1327+02	1020.0	53.6	0.0572	3.047	15.5	0.172
HIPEQ1329-00	3213.2	159.5	0.0479	6.882	47.2	3.612
HIPEQ1332+01	3234.9	107.4	0.0476	4.047	47.7	2.169
HIPEQ1335+01	5160.1	238.6	0.0535	7.518	76.2	10.281
HIPEQ1341+05	6843.2	228.9	0.0445	8.640	101.8	21.096
HIPEQ1348+03	1157.3	196.4	0.0929	13.357	17.7	0.981
HIPEQ1352+02a	4575.3	280.5	0.0692	12.897	67.7	13.907
HIPEQ1352-01	1388.1	203.5	0.2098	29.880	20.6	2.999
HIPEQ1400+02	3561.4	239.3	0.0466	8.429	52.6	5.499
HIPEQ1411-01	1539.0	240.8	0.3718	64.392	22.9	7.948
HIPEQ1415+04	5672.7	59.7	0.0532	3.243	84.2	5.422
HIPEQ1416+03	1466.0	100.2	0.0762	7.151	22.2	0.831
HIPEQ1422-00	1625.8	196.5	0.1652	28.627	24.2	3.963
HIPEQ1429-00	1532.2	196.7	0.2942	49.763	22.9	6.167
HIPEQ1432+00	1655.0	194.3	0.0370	4.617	24.7	0.666
HIPEQ1433+01	1816.4	65.8	0.0553	3.379	27.2	0.588
HIPEQ1433+02	1483.2	86.6	0.0550	5.177	22.4	0.615

Table 2.1—Continued

HIPASS Name	Heliocentric Velocity (km/s)	W_{20} (km/s)	S_{peak} (Jy)	S_{int} (Jy km/s)	Distance (Mpc)	HI Mass 10^9 $M_\odot$
HIPEQ1437+02	1753.0	291.3	0.1100	25.350	26.3	0.000
HIPEQ1437-00	1872.8	150.6	0.0476	5.786	27.9	1.059
HIPEQ1439+02	1567.7	95.0	0.0727	6.065	23.7	0.802
HIPEQ1439-00	1752.7	182.5	0.1921	29.396	26.1	4.722
HIPEQ1440+02	1629.0	121.4	0.0303	3.346	24.5	0.474
HIPEQ1444+01a	1566.1	323.8	0.1458	35.248	23.6	4.622
HIPEQ1500+01	1337.9	322.7	0.0480	13.516	20.3	1.319
HIPEQ1504+02	9254.7	170.5	0.0386	5.077	138.8	23.041
HIPEQ1504-00	1792.7	196.9	0.0544	9.469	26.8	1.596
HIPEQ1507+01	2530.2	204.8	0.1035	18.116	37.7	6.056
HIPEQ1542+00	1910.1	249.6	0.1144	20.080	28.7	3.884
HIPEQ1544+02	3824.5	104.1	0.0819	8.610	56.8	6.551
HIPEQ1545+00	3783.8	115.0	0.0618	7.149	56.1	5.301
HIPEQ1601+01a	1915.7	234.1	0.0572	9.411	28.8	1.844
HIPEQ1609-00	1490.7	97.6	0.0751	6.981	22.6	0.836
HIPEQ1613-00	2086.2	151.4	0.0551	7.562	31.1	1.728
HIPEQ1614+00	1971.6	113.5	0.0800	8.252	29.6	1.704
HIPEQ1614-00	2018.3	361.5	0.1715	38.188	30.2	8.208
HIPEQ2036-04	6097.2	371.2	0.0583	14.154	89.8	26.879
HIPEQ2314+00	4333.0	70.8	0.0610	2.979	63.0	2.788
HIPEQ2324-00	2679.1	113.6	0.0995	11.226	38.6	3.943
HIPEQ2335+01	2576.3	82.8	0.1303	9.529	37.1	3.098
HIPEQ2336+00	2566.0	307.0	0.1070	32.800	36.9	10.536
HIPEQ2337+00	2658.0	111.2	0.1180	9.496	38.3	3.277
HIPEQ2340+01	1856.5	187.2	0.0589	9.616	26.6	1.609

Table 2.2. HI Parameter Uncertainties

parameter	uncertainty
$\sigma(S_{peak})$	11.0 mJy
$\sigma(S_{int})$	0.5 $S_{int}^{0.5}$ Jy km/s
$\sigma(W_{20})$	7.5 km/s
$\sigma(V_{hel})$	$1.0\times10^4 S_p^{-2}$+5 km/s

2.2.2 SDSS Survey

The optical data for this study come from the Sloan Digital Sky Survey (SDSS; York et al. 2000; Gunn et al. 1998; Fukugita et al. 1996; Hogg et al. 2001; Smith et al. 2002; Pier et al. 2003) Data Release 2 (DR2; Abazajian et al. 2004) sky area. The actual photometry used in this thesis were obtained from the Data Release 3 (DR3; Abazajian et al. 2005a) photometric pipelines, but new searches for HIPASS matches on the additional DR3 area were not performed. The DR2 area is 3324 deg.^{2}, about half of which overlaps with the searched HIPASS region discussed above (see Figure 2.1). The SDSS data is taken in five photometric bands (*ugriz*) and has point source magnitude limits of 22.0, 22.2, 22.2 ,21.3, & 20.5 respectively at the 95% completeness level. The pixel scale of SDSS is 0.396″/pixel and the average seeing is 1.4″. The time delay and integrate (TDI) method for SDSS observations allows for extremely accurate flat fielding, and photometric calibration at the 2-3% level. Automatic pipelines reduce the raw data and store the derived quantities in catalog tables. Although all of the photometric parameters for SDSS objects are stored in an online database, for galaxies with large angular extents, the SDSS catalog data are unreliable (see Apendix A). Therefore, aside from the initial catalog matching described below, no SDSS catalog data were used for this study. All photometric quanities were obtained using a new set of techniques optimized for reducing large galaxy photometry (see Chapter 3).

SDSS data is taken in 2.5 degree wide `runs` along great circles. Each `run` is broken up into 6 `camcols` (one for each SDSS camera column), and many $13' \times 9'$ frames or `fields`. These `fields` are passed through a version of the photometric pipeline and individual objects are assigned an `object_id`. The version of the pipeline is indicated by its `rerun` value. Thus,

every object in the SDSS catalog has a unique set combination of `run`, `rerun`, `camcol`, `field` and `object_id`. Because the photometry in this thesis does not come from the SDSS catalog, the description of the photometric methods contains several SDSS data products that may be unfamiliar to the catalog-level user. We define the most frequently used data products below:

- `fpC` file – Corrected frame or `field` that is a segment of an SDSS `run`. These files have had all photometric and astrometric processing performed on them with the exception of sky subtraction. The five filters are slightly offset from each other requiring small shifts for image combining and comparison.

- `fpAtlas` image – Atlas image for an object that is identified by the SDSS photometric software. These images have been fully processed including sky subtraction and are useful for visually inspecting the quality of deblending (see Chapter 3 and Appendix A).

- `tsObj` file – Binary fits table of photometric values derived from objects in a particular `field`.

- `fpBIN` file – 4×4 binned image of an SDSS `field` after sky subtraction. These files also contain the 128×128 binned sky values and are needed for reconstructing the SDSS calculated sky.

- `fpFieldStat` file – Contains a statistical summary for one `field`.

- `tsField` file – Binary fits table of observational information for one `field` including photometric offsets, gains, atmospheric extinction measures and airmass.

2.2.3 Comparison Sample

To compare the HI selected HIPASS/SDSS galaxies to an optically selected sample, we use the Data Release 4 (DR4; Abazajian et al. 2005b) "main" galaxy sample that is defined

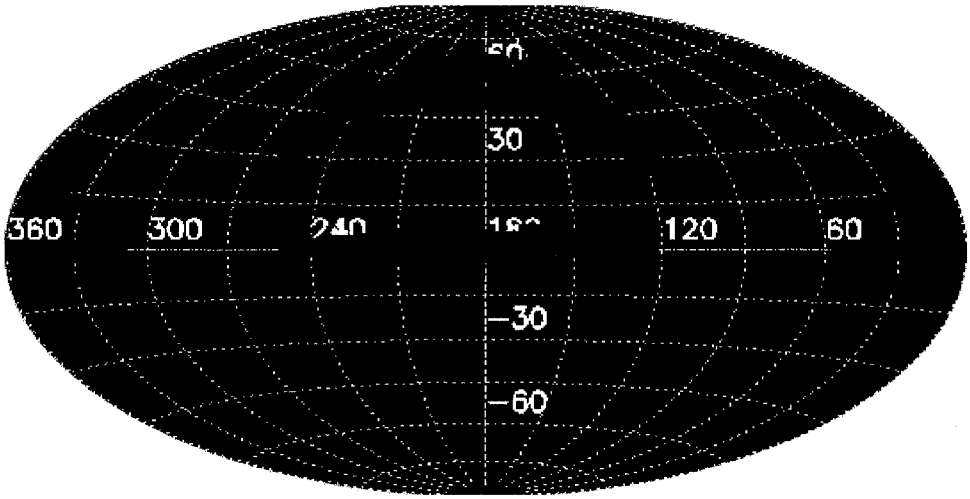

Figure 2.1 SDSS Data Release 2 (DR2) sky area (red). Most of the overlap with HIPASS comes from the strips on and below the celestial equator.

as having $r_{Petrosian} < 17.77$ (Strauss et al. 2002). We apply a secondary cut of $0.01 < z < 0.04$ to ensure that a small volume is being sampled. Most SDSS galaxy studies use a redshift cut of 0.02 (e.g., Blanton et al. 2003a) at the low end so as not to include bad deblends or other large galaxy effects (see Appendix A) but we use a slightly smaller lower bound because the majority of the HIPASS/SDSS sample is very nearby. This sample is used throughout this thesis as a comparison sample for many galaxy properties. We apply all of the same photometric corrections discussed in Chapter 3 to these data and have tested that their properties do not drastically change as a function of different volume cuts. Because there were no major photometry changes between DR4 and DR3, there is no concern in comparing a DR4 data set (main comparison sample) with one drawn from DR3 (HIPASS/SDSS sample). Because of the surface brightness limit for SDSS spectroscopic observations (Strauss et al. 2002), this comparison sample does not contain any galaxies with $\mu_r > 23.0$ where μ_r is the Petrosian surface brightness (within the 50% radius).

2.3 *Matching/ Confirmation*

2.3.1 SDSS Photometry

The catalog matching began by searching the DR2 `tsObj` files for all SDSS sources within $10'$ of the HIPASS source positions. A web-page showing the field for each matching SDSS object was created and all candidate objects were sorted by inverse object size (large to small) to ease visual inspection. Over 1.16 million SDSS objects were found inside the HIPASS source beam areas. At every HIPASS source position, the candidate SDSS objects were visually inspected and potential counterpart galaxies were identified.

In order to be included in the HIPASS-SDSS sample, each candidate galaxy had to meet 4 criteria:

- The HIPASS recessional velocity must agree to within twice the W_{20} value of the optically derived redshift.
- There must be no more than 1 detectable galaxy within the HIPASS beam at the same redshift.
- The candidate galaxy must not extend across two or more SDSS fields.
- All galaxies must be at least $1'$ away from any saturated foreground stars.

To test the first criterion, we obtained a redshift for each candidate galaxy. SDSS spectra were available for ~80% of the candidate galaxies and redshifts were easliy calculated from them. For the remaining candidates, we searched the NED[1] database and acquired redshifts for all but $\sim$ 20 galaxies. The remaining sources were spectroscopically observed using the Apache Point Observatory's (APO) ARC 3.5m telescope from February 2002 to July 2003. All of the sources were observed with long integrations on the Dual Imaging Spectrograph (DIS) with a $1.5''$ slit and with the high resolution gratings. Most of the galaxies in the

[1]This research has made use of the NASA/IPAC Extragalactic Database (NED) which is operated by the Jet Propulsion Laboratory, California Institute of Technology, under contract with the National Aeronautics and Space Administration

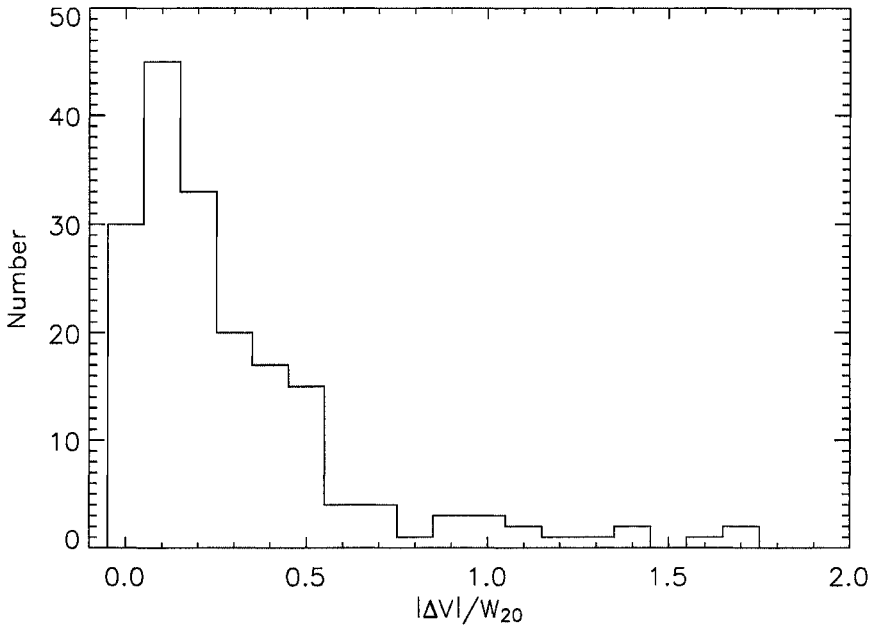

Figure 2.2 Distribution of the ratio of the absolute value of the recessional velocity difference (SDSS-HIPASS) to the W_{20} HI line width for the HIPASS/SDSS galaxies that had SDSS spectra. Most of the galaxies have HI and optical recessional velocities that match to within half of the HI line width.

HIPASS/SDSS sample are currently forming stars and have emission lines that can be unambiguously identified and easily measured for accurate redshift determination (see Figure 2.4). Figure 2.2 shows the distribution of the ratio of the absolute value of the recessional velocity difference (SDSS-HIPASS) to the W_{20} HI line width. Most of the galaxies have HI and optical resessional velocities that match to within half of the HI line width.

After obtaining redshifts for all of the candidate sources, we were able to identify 310 HIPASS sources that had SDSS galaxies within the HIPASS beam and at the same redshift. It is important to note that *every* HIPASS source in the SDSS footprint was found to have an optical counterpart.

87 of the sources did not meet the second criterion because of multiple SDSS galaxies within a single HIPASS beam. Some of these sources had as many as 5 galaxies at the same redshift. This criterion was applied because of the importance in knowing the quantity

of HI in each individual galaxy. With multiple galaxies in the HIPASS beam, only the total HI of the group is measured, and without higher resolution observations, this problem cannot be resolved. The high percentage of HIPASS sources containing galaxy groups brings into question the ability to correctly measure the HI mass function with the HIPASS data (Zwaan et al. 2005). This may introduce a bias against galaxies in higher density regions. HI data acquired with a larger telescope aperture (and therefore a smaller beam) is required to test how much bias is introduced. We leave the bias analysis for future study.

Twenty of the galaxies were positioned in such a way and/or had angular extents so large that they fell over multiple SDSS fields (criterion #3). At the time of sample selection, no techniques were available to accurately obtain the photometry for galaxies with flux spread over multiple fields. This also introduces a bias against the largest nearby galaxies. The sky subtraction method that will be discussed in Chapter 3, currently makes it possible to obtain good photometry for angularly large galaxies in SDSS. Although these systems are not included in this thesis study, many of them will appear in the SDSS Nearby Galaxy Atlas (West et al. 2005).

Three additional galaxies were removed because of their close proximity to saturated foreground stars (criterion #4). The stars were close enough to the galaxies that scattered light would greatly effect galaxy photometry. The random superposition of stars in front of galaxies should not introduce any additional bias due to criterion #4.

The SDSS-HIPASS sample that will be studied in the thesis consists of the 200 galaxies that passed all four criteria. Their survey names, central SDSS positions, other catalog names, and morphological types from NED can be found in Table 2.3. The position centers are those used for photometry (see Chapter 3). Optical images and the HI spectrum for each source can be found in Appendix B. For the remainder of this thesis we will refer to objects both in the text and in tables by their HIPASS Equatorial catalog name.

Figure 2.3 shows the distribution of the HIPASS-SDSS central position differences. Most of the SDSS sources fall within $2'$ of the HIPASS position. This is consistent with the positional uncertainty of $1.3'$ quoted in both Meyer et al. (2003) and Zwaan et al. (2004). Figure 2.3 demonstrates the challenge of matching two surveys with drastically different angular resolutions. The observation that there are significant offsets in the central positions

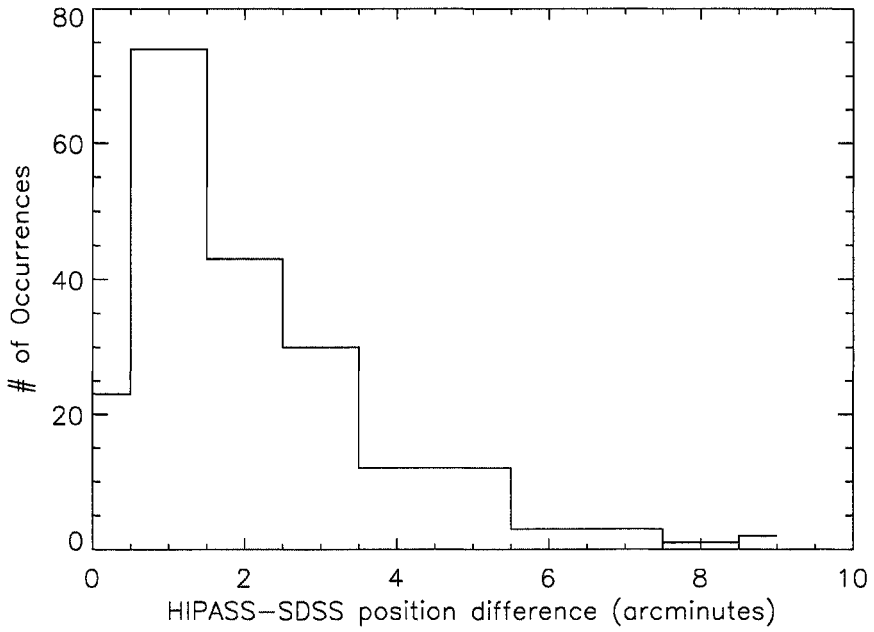

Figure 2.3 The distribution of the HIPASS-SDSS central position differences. Most of the SDSS sources fall within 2′ of the HIPASS position. This is consistent with the positional uncertainty of 1.3′ quoted in both Meyer et al. (2003) and Zwaan et al. (2004).

of some sources may suggest that the peak HI and peak optical positions differ by as much as a few arcminutes. HI synthesis data are required to confirm this.

Table 2.3. Galaxy Names

SDSS Name	RA h	RA m	RA s	DEC °	DEC ′	DEC ″	Other Name	HIPASS Name	Morphological Type
SDSS J001431.87−004415.0	00	14	31.87	−00	44	15.0	UGC00139	HIPEQ0014−00	SAB(s)c
SDSS J002749.46−011160.0	00	27	49.46	−01	11	60.0	UGC00272	HIPEQ0027−01a	SAB(s)d
SDSS J003321.96−010718.8	00	33	21.96	−01	07	18.8	UGC00328	HIPEQ0033−01	SB(rs)dm
SDSS J004327.77−000730.4	00	43	27.77	−00	07	30.4	NGC0237	HIPEQ0043−00	SAB(rs)cd
SDSS J005159.59−002911.8	00	51	59.59	−00	29	11.8	ARK018	HIPEQ0051−00	Sb
SDSS J005848.82+003512.1	00	58	48.82	+00	35	12.1	IC1607/UGC00611	HIPEQ0058+00	Sb
SDSS J010746.30+010349.0	01	07	46.30	+01	03	49.0	UGC00695	HIPEQ0107+01	Sc
SDSS J011958.78+004318.5	01	19	58.78	+00	43	18.5	LSBC_F827−05	HIPEQ0119+00	Sd
SDSS J012006.58−001219.1	01	20	06.58	−00	12	19.1	UGC00866	HIPEQ0120−00	Sdm
SDSS J012209.10+005644.9	01	22	09.10	+00	56	44.9	NGC0493	HIPEQ0122+00	SAB(s)cd
SDSS J012313.63−002307.4	01	23	13.63	−00	23	07.4	UGC00929	HIPEQ0123−00	Scd
SDSS J012629.18+003257.5	01	26	29.18	+00	32	57.5	UGC01018	HIPEQ0126+00a	Im
SDSS J012646.39−003845.6	01	26	46.39	−00	38	45.6	UM323	HIPEQ0126−00b	BCD
SDSS J015440.92−000837.3	01	54	40.92	−00	08	37.3	UGC01382	HIPEQ0154−00	E
SDSS J022229.88−003704.1	02	22	29.88	−00	37	04.1	UGC01839	HIPEQ0222−00	Sdm
SDSS J022827.74−010908.6	02	28	27.74	−01	09	08.6	NGC0941	HIPEQ0228−01	SAB(rs)c
SDSS J023017.09+005619.3	02	30	17.09	+00	56	19.3	UGC01981	HIPEQ0230+00	IB(s)m
SDSS J023033.12−010632.4	02	30	33.12	−01	06	32.4	NGC0955	HIPEQ0230−01	Sab
SDSS J023143.25+001738.4	02	31	43.25	+00	17	38.4	UGC01998	HIPEQ0231+00	Scd
SDSS J023623.52+004229.2	02	36	23.52	+00	42	29.2	UGC02091	HIPEQ0236+00	Sc
SDSS J023848.50+003114.2	02	38	48.50	+00	31	14.2	APMUKS_B023614.54+001818.0	HIPEQ0238+00	LSB
SDSS J024022.80+011349.1	02	40	22.80	+01	13	49.1	UGC02162	HIPEQ0240+01	IB(s)m
SDSS J024144.78+002642.4	02	41	44.78	+00	26	42.4	NGC1055	HIPEQ0241+00	SBb
SDSS J024420.93+004034.3	02	44	20.93	+00	40	34.3	UGC02216	HIPEQ0244+00	Im
SDSS J024633.55−001450.6	02	46	33.55	−00	14	50.6	NGC1090	HIPEQ0246−00a	SB(rs)bc
SDSS J024625.32−002956.4	02	46	25.32	−00	29	56.4	NGC1087	HIPEQ0246−00b	SAB(rs)c
SDSS J024940.92−003125.0	02	49	40.92	−00	31	25.0	CGCG389−028	HIPEQ0249−00	SB(rs)b
SDSS J024852.54−002101.4	02	48	52.54	−00	21	01.4	UGCA042	HIPEQ0249−00a	dI
SDSS J024927.74−005225.3	02	49	27.74	−00	52	25.3	UGC02311	HIPEQ0249−00b	SB(r)b
SDSS J025151.62−011026.8	02	51	51.62	−01	10	26.8	UGC02345	HIPEQ0251−01	SB(rs)m
SDSS J030040.08+000113.1	03	00	40.08	+00	01	13.1	UGC02479	HIPEQ0300+00	Sdm
SDSS J030103.14−004435.9	03	01	03.14	−00	44	35.9	UGC02482	HIPEQ0301−00	Sdm
SDSS J030652.42−004741.3	03	06	52.42	−00	47	41.3	NGC1211	HIPEQ0306−00	SB(r)0/a
SDSS J031631.90−002803.7	03	16	31.90	−00	28	03.7	UGC02628	HIPEQ0316−00	SB(s)bc
SDSS J032009.53−061542.5	03	20	09.53	−06	15	42.5	NGC1299	HIPEQ0320−06	SB(rs)b
SDSS J035140.44−003038.2	03	51	40.44	−00	30	38.2	ARK103	HIPEQ0351−00	Spiral
SDSS J080924.12+003634.6	08	09	24.12	+00	36	34.6	UGC04254	HIPEQ0809+00	SB(rs)m
SDSS J082210.58+031604.4	08	22	10.58	+03	16	04.4	IC0503	HIPEQ0821+03b	SBa
SDSS J082126.21−002510.2	08	21	26.21	−00	25	10.2	UGC04358	HIPEQ0821−00	IrS
SDSS J082228.66−010244.2	08	22	28.66	−01	02	44.2	UGC04370	HIPEQ0822−00	SB(rs)d
SDSS J082501.90−003530.1	08	25	01.90	−00	35	30.1	NGC2590	HIPEQ0825−00	SA(s)bc

Table 2.3—Continued

SDSS Name	RA h	RA m	RA s	DEC °	DEC ′	DEC ″	Other Name	HIPASS Name	Morphological Type
SDSS J085552.25+023125.0	08	55	52.25	+02	31	25.0	UGC04673	HIPEQ0855+02	SB(s)d
SDSS J085640.66+002231.4	08	56	40.66	+00	22	31.4	UGC04684	HIPEQ0856+00	SA(rs)dm
SDSS J092315.60−004341.2	09	23	15.60	−00	43	41.2	UGC04996	HIPEQ0923−00	SAB(s)bc
SDSS J093015.17+040838.4	09	30	15.17	+04	08	38.4	NGC2900	HIPEQ0930+04	SBcd
SDSS J093626.76+011129.8	09	36	26.76	+01	11	29.8	SDSSJ093626.69+01112	HIPEQ0936+01	...
SDSS J094203.46+002012.5	09	42	03.46	+00	20	12.5	NGC2967	HIPEQ0942+00	SA(s)c
SDSS J094446.32−004118.2	09	44	46.32	−00	41	18.2	SDSSJ094446.23−00411	HIPEQ0944−00b	...
SDSS J094603.48+014004.4	09	46	03.48	+01	40	04.4	UGC05228	HIPEQ0945+01	SB(s)c
SDSS J094551.91+025839.4	09	45	51.91	+02	58	39.4	UGC05224	HIPEQ0946+02	...
SDSS J094653.81+003028.4	09	46	53.81	+00	30	28.4	UGC05238	HIPEQ0947+00a	SB(s)dm
SDSS J094705.30+005752.9	09	47	05.30	+00	57	52.9	UGC05242	HIPEQ0947+00b	SB(s)m
SDSS J095340.78+013443.7	09	53	40.78	+01	34	43.7	NGC3044	HIPEQ0953+01	B(s)c
SDSS J095359.23+020019.8	09	53	59.23	+02	00	19.8	[ISI96]0951+0214	HIPEQ0954+01a	dI
SDSS J095410.58+021714.3	09	54	10.58	+02	17	14.3	CGCG035−083	HIPEQ0954+02a	...
SDSS J095517.76+041613.1	09	55	17.76	+04	16	13.1	NGC3055	HIPEQ0955+04a	SAB(s)c
SDSS J095829.09+014137.3	09	58	29.09	+01	41	37.3	LSBC_L1−099	HIPEQ0958+01	dI
SDSS J100026.98+032228.6	10	00	26.98	+03	22	28.6	UGC05376	HIPEQ1000+03	Sdm
SDSS J101037.22+050900.7	10	10	37.22	+05	09	00.7	CGCG036−048	HIPEQ1010+05	...
SDSS J101414.21+032802.6	10	14	14.21	+03	28	02.6	NGC3169	HIPEQ1014+03	SA(s)a
SDSS J101555.25+024112.5	10	15	55.25	+02	41	12.5	UGC05539	HIPEQ1015+02	IBm
SDSS J102641.71+035141.8	10	26	41.71	+03	51	41.8	NGC3246	HIPEQ1026+03	SABdm
SDSS J102837.97+033336.4	10	28	37.97	+03	33	36.4	UGC05677	HIPEQ1028+03	Sdm
SDSS J103113.51+042810.9	10	31	13.51	+04	28	10.9	UGC05708	HIPEQ1031+04	SBd
SDSS J103925.13+014306.6	10	39	25.13	+01	43	06.6	UGC05797	HIPEQ1039+01	dIn
SDSS J104153.42+004735.5	10	41	53.42	+00	47	35.5	UGC05823	HIPEQ1041+00	Im
SDSS J104612.53+014850.8	10	46	12.53	+01	48	50.8	NGC3365	HIPEQ1046+01	Scd
SDSS J105008.95+011555.4	10	50	08.95	+01	15	55.4	LSBC_L1−134	HIPEQ1050+01	dI
SDSS J105134.94+043459.5	10	51	34.94	+04	34	59.5	UGC05974	HIPEQ1051+04a	Scd
SDSS J105248.70+000202.4	10	52	48.70	+00	02	02.4	CGCG010−041	HIPEQ1052+00	...
SDSS J105318.74+023734.7	10	53	18.74	+02	37	34.7	LSBC_L1−137	HIPEQ1053+02	dIn
SDSS J105538.95+022340.6	10	55	38.95	+02	23	40.6	CGCG038−051	HIPEQ1055+02	...
SDSS J110116.15+033741.5	11	01	16.15	+03	37	41.5	NGC3495	HIPEQ1101+03	Sd
SDSS J110925.18−000548.8	11	09	25.18	−00	05	48.8	IC0673	HIPEQ1109−00	(R')SAB(rs)c
SDSS J111054.58+010532.3	11	10	54.58	+01	05	32.3	CGCG011−018	HIPEQ1110+01	dIn
SDSS J111312.17+051201.4	11	13	12.17	+05	12	01.4	CGCG039−073	HIPEQ1113+05	...
SDSS J111730.14+043318.7	11	17	30.14	+04	33	18.7	NGC3604	HIPEQ1117+04a	SA(s)a pec
SDSS J112015.41+023138.3	11	20	15.41	+02	31	38.3	UGC06345	HIPEQ1119+02	IB(s)m
SDSS J112424.70+031934.0	11	24	24.70	+03	19	34.0	NGC3664	HIPEQ1124+03	SB(s)m
SDSS J112712.14−005941.3	11	27	12.14	−00	59	41.3	UGC06457	HIPEQ1127−01	dIn
SDSS J113131.99−021833.1	11	31	31.99	−02	18	33.1	UGC06510	HIPEQ1131−02	SAB(rs)cd
SDSS J113345.17−032616.8	11	33	45.17	−03	26	16.8	CGCG012−022	HIPEQ1133−03	SAB(s)dm

Table 2.3—Continued

SDSS Name	RA h	RA m	RA s	DEC °	DEC ′	DEC ″	Other Name	HIPASS Name	Morphological Type
SDSS J113636.62+004900.1	11	36	36.62	+00	49	00.1	UGC06578	HIPEQ1136+00	...
SDSS J113854.82+033449.4	11	38	54.82	+03	34	49.4	MRK1302	HIPEQ1138+03	(R')SB(r)b
SDSS J114345.46−011634.3	11	43	45.46	−01	16	34.3	New	HIPEQ1143−01	...
SDSS J114454.07+020949.3	11	44	54.07	+02	09	49.3	[RC3]1142.4+0226	HIPEQ1145+02	Im
SDSS J114850.33−020155.9	11	48	50.33	−02	01	55.9	UGC06780	HIPEQ1148−02	SAB(s)d
SDSS J115156.30−023833.0	11	51	56.30	−02	38	33.0	UGC06838	HIPEQ1151−02	SAab
SDSS J115243.42+014428.0	11	52	43.42	+01	44	28.0	UGC06854	HIPEQ1152+01	SB(rs)bc
SDSS J115237.22−022810.2	11	52	37.22	−02	28	10.2	UGC06850	HIPEQ1152−02	BCD
SDSS J115231.30−034028.2	11	52	31.30	−03	40	28.2	UGCA249	HIPEQ1152−03b	IB(s)m
SDSS J115536.94+011412.5	11	55	36.94	+01	14	12.5	UGC06903	HIPEQ1155+01	SB(s)cd
SDSS J120047.64−000122.8	12	00	47.64	−00	01	22.8	NGC4030b	HIPEQ1200−00	SAB(s)m
SDSS J120023.33−010559.3	12	00	23.33	−01	05	59.3	NGC4030	HIPEQ1200−01	SA(s)bc
SDSS J120242.34+015837.2	12	02	42.34	+01	58	37.2	NGC4045	HIPEQ1202+01	SAB(r)a
SDSS J120420.35−013149.8	12	04	20.35	−01	31	49.8	UGC07053	HIPEQ1204−01	IAB(s)m
SDSS J120447.16−024314.2	12	04	47.16	−02	43	14.2	UGC07065	HIPEQ1204−02	(R')SB(r)0/a
SDSS J121103.74+020022.7	12	11	03.74	+02	00	22.7	UGC07178	HIPEQ1210+02	IAB(rs)m
SDSS J121600.55+043902.2	12	16	00.55	+04	39	02.2	VCC0172	HIPEQ1215+04a	IAm
SDSS J121608.40−033413.1	12	16	08.40	−03	34	13.1	CGCG013−114	HIPEQ1216−03	SAB(s)cd
SDSS J121756.38+002600.6	12	17	56.38	+00	26	00.6	UGC07332	HIPEQ1218+00	IB(s)m
SDSS J121808.69−010352.2	12	18	08.69	−01	03	52.2	NGC4202	HIPEQ1218−01	SAB(rs)bc
SDSS J121909.84+035122.7	12	19	09.84	+03	51	22.7	UGC07354	HIPEQ1219+03	E
SDSS J122021.24+002204.1	12	20	21.24	+00	22	04.1	CGCG014−010	HIPEQ1220+00	Sm?
SDSS J122027.50+012811.3	12	20	27.50	+01	28	11.3	UGC07394	HIPEQ1220+01	SAd
SDSS J122102.33+034317.0	12	21	02.33	+03	43	17.0	NGC4289	HIPEQ1221+03	SA(s)cd
SDSS J122412.53+003358.3	12	24	12.53	+00	33	58.3	DDO121	HIPEQ1223+00	IB(s)m
SDSS J122353.76−032635.2	12	23	53.76	−03	26	35.2	NGC4348	HIPEQ1223−03b	SAbc
SDSS J122430.53+000418.5	12	24	30.53	+00	04	18.5	KDG118	HIPEQ1224+00	Irr
SDSS J122439.91+031810.1	12	24	39.91	+03	18	10.1	VCC0739	HIPEQ1224+03b	S
SDSS J122542.79+003420.3	12	25	42.79	+00	34	20.3	NGC4385	HIPEQ1225+00	SB(rs)0
SDSS J122658.44+022936.6	12	26	58.44	+02	29	36.6	NGC4409	HIPEQ1226+02	SB(r)bc
SDSS J122745.86+013601.8	12	27	45.86	+01	36	01.8	HI1225+01	HIPEQ1227+01	dIn
SDSS J122901.87+024324.6	12	29	01.87	+02	43	24.6	UGC07612	HIPEQ1228+02	Sm
SDSS J122858.90+033413.4	12	28	58.90	+03	34	13.4	NGC4457	HIPEQ1228+03	(R)SAB(s)0/a
SDSS J122932.66+005021.5	12	29	32.66	+00	50	21.5	UGC07625	HIPEQ1229+00	Sm
SDSS J123013.78+023728.6	12	30	13.78	+02	37	28.6	UGC07642	HIPEQ1230+02	Sdm
SDSS J123012.00+033440.8	12	30	12.00	+03	34	40.8	VCC1262	HIPEQ1230+03	BCD
SDSS J123228.08+002319.3	12	32	28.08	+00	23	19.3	NGC4517A	HIPEQ1232+00a	SB(rs)dm
SDSS J123244.76+000655.1	12	32	44.76	+00	06	55.1	NGC4517	HIPEQ1232+00b	SA(s)cd
SDSS J123346.42−023916.9	12	33	46.42	−02	39	16.9	UGC07710	HIPEQ1233−02	IAB(s)m
SDSS J123641.74+030626.3	12	36	41.74	+03	06	26.3	UGC07780	HIPEQ1236+03	Sdm
SDSS J123918.14−003153.0	12	39	18.14	−00	31	53.0	NGC4592	HIPEQ1239−00	SA(s)dm

Table 2.3—Continued

SDSS Name	RA h	RA m	RA s	DEC °	DEC ′	DEC ″	Other Name	HIPASS Name	Morphological Type
SDSS J124111.45+012435.3	12	41	11.45	+01	24	35.3	UGC07841	HIPEQ1241+01	SA(r)b
SDSS J124122.80−030332.0	12	41	22.80	−03	03	32.0	CGCG014−104	HIPEQ1241−02	SA0
SDSS J124231.01+035727.0	12	42	31.01	+03	57	27.0	NGC4630	HIPEQ1242+03b	IB(s)m
SDSS J124231.87−000454.8	12	42	31.87	−00	04	54.8	NGC4632	HIPEQ1242−00	SAc
SDSS J124232.42−012102.9	12	42	32.42	−01	21	02.9	NGC4629	HIPEQ1242−01a	SAB(s)m
SDSS J124257.31−011346.9	12	42	57.31	−01	13	46.9	UGC07883	HIPEQ1242−01b	SA(s)cd
SDSS J124350.98−003345.4	12	43	50.98	−00	33	45.4	NGC4653	HIPEQ1243−00	SAB(rs)cd
SDSS J124428.39+002757.2	12	44	28.39	+00	27	57.2	UGC07911	HIPEQ1244+00	(R')SB(s)m
SDSS J124433.29−021909.8	12	44	33.29	−02	19	09.8	UGC07913	HIPEQ1244−02	SAB(s)m
SDSS J124508.16−002742.8	12	45	08.16	−00	27	42.8	NGC4666	HIPEQ1245−00	SABc
SDSS J124911.52+032322.6	12	49	11.52	+03	23	22.6	NGC4701	HIPEQ1249+03	SA(s)cd
SDSS J124914.88+043926.3	12	49	14.88	+04	39	26.3	UGC07976	HIPEQ1249+04	Sdm
SDSS J124957.72+051840.7	12	49	57.72	+05	18	40.7	NGC4713	HIPEQ1250+05	SAB(rs)d
SDSS J125321.41+011606.2	12	53	21.41	+01	16	06.2	NGC4771	HIPEQ1253+01	SAd
SDSS J125329.04+021006.6	12	53	29.04	+02	10	06.6	NGC4772	HIPEQ1253+02	SA(s)a
SDSS J125314.47+042749.7	12	53	14.47	+04	27	49.7	NGC4765	HIPEQ1253+04	S0/a
SDSS J125512.67+000659.8	12	55	12.67	+00	06	59.8	UGC08041	HIPEQ1255+00	SB(s)d
SDSS J125515.50+025347.0	12	55	15.50	+02	53	47.0	NGC4799	HIPEQ1255+02	S
SDSS J125539.36−001547.9	12	55	39.36	−00	15	47.9	UGC08048	HIPEQ1255−00	Sm
SDSS J125604.42+034846.4	12	56	04.42	+03	48	46.4	UGC08055	HIPEQ1256+03	ImV
SDSS J125744.35+024128.3	12	57	44.35	+02	41	28.3	UGC08074	HIPEQ1257+02	Sm
SDSS J125712.14−014224.5	12	57	12.14	−01	42	24.5	UGC08067	HIPEQ1257−01	Sb
SDSS J125822.30+024733.4	12	58	22.30	+02	47	33.4	UGC08084	HIPEQ1258+02	SB(s)dm
SDSS J125958.03+020259.3	12	59	58.03	+02	02	59.3	UGC08105	HIPEQ1300+02a	dIn
SDSS J130036.55+023002.2	13	00	36.55	+02	30	02.2	NGC4900	HIPEQ1300+02b	SB(rs)c
SDSS J130305.74+035929.0	13	03	05.74	+03	59	29.0	UGC08153	HIPEQ1303+03	Sd
SDSS J130431.87−025917.5	13	04	31.87	−02	59	17.5	LCRS_B130157.2−024313	HIPEQ1304−02	...
SDSS J130431.82−033425.3	13	04	31.82	−03	34	25.3	UGCA322	HIPEQ1304−03	SAB(s)dm
SDSS J130738.66−005632.6	13	07	38.66	−00	56	32.6	IC0849	HIPEQ1307−00	SAB(rs)cd
SDSS J130843.06−020806.0	13	08	43.06	−02	08	06.0	UGC08223	HIPEQ1308−02	SBcd
SDSS J131123.21+032441.8	13	11	23.21	+03	24	41.8	UGC08263	HIPEQ1311+03a	SBc
SDSS J131207.15+031156.4	13	12	07.15	+03	11	56.4	NGC5013	HIPEQ1312+03	...
SDSS J131205.95+052836.5	13	12	05.95	+05	28	36.5	UGC08276	HIPEQ1312+05	Im
SDSS J131320.83+060341.4	13	13	20.83	+06	03	41.4	NGC5027	HIPEQ1313+06	SB(r)b
SDSS J131742.65−010005.4	13	17	42.65	−01	00	05.4	UM559	HIPEQ1317−00	...
SDSS J131810.03−011438.0	13	18	10.03	−01	14	38.0	UGC08360	HIPEQ1318−01	SAB(r)cd
SDSS J132032.18+052422.7	13	20	32.18	+05	24	22.7	UGC08382	HIPEQ1320+05	IBm
SDSS J132811.81+021643.7	13	28	11.81	+02	16	43.7	LEDA135827	HIPEQ1327+02	dIn
SDSS J132925.42−002355.0	13	29	25.42	−00	23	55.0	UGC08473	HIPEQ1329−00	Im
SDSS J133230.72+015051.0	13	32	30.72	+01	50	51.0	UGC08521	HIPEQ1332+01	(R)SB(r)ab
SDSS J133524.50+012437.4	13	35	24.50	+01	24	37.4	NGC5227	HIPEQ1335+01	(R')SB(r)b

Table 2.3—Continued

SDSS Name	RA h	RA m	RA s	DEC °	DEC ′	DEC ″	Other Name	HIPASS Name	Morphological Type
SDSS J134105.11+050619.8	13	41	05.11	+05	06	19.8	UGC08657	HIPEQ1341+05	Sbc
SDSS J134816.08+035702.5	13	48	16.08	+03	57	02.5	NGC5300	HIPEQ1348+03	SAB(r)c
SDSS J135256.54+024902.3	13	52	56.54	+02	49	02.3	NGC5335	HIPEQ1352+02a	SB(r)b
SDSS J135254.50−010653.3	13	52	54.50	−01	06	53.3	NGC5334	HIPEQ1352−01	SB(rs)c
SDSS J140045.77+020117.0	14	00	45.77	+02	01	17.0	UGC08924	HIPEQ1400+02	Sc
SDSS J141137.73−010929.9	14	11	37.73	−01	09	29.9	NGC5496	HIPEQ1411−01	SBcd
SDSS J141526.33+042429.9	14	15	26.33	+04	24	29.9	NGC5521	HIPEQ1415+04	S
SDSS J141657.05+035003.1	14	16	57.05	+03	50	03.1	KKR05	HIPEQ1416+03	Im
SDSS J142223.59−002318.2	14	22	23.59	−00	23	18.2	NGC5584	HIPEQ1422−00	SAB(rs)cd
SDSS J142934.68−000106.2	14	29	34.68	−00	01	06.2	UGC09299	HIPEQ1429−00	SAB(s)d
SDSS J143228.32+001739.5	14	32	28.32	+00	17	39.5	UGC09348	HIPEQ1432+00	S0
SDSS J143353.30+012905.6	14	33	53.30	+01	29	05.6	[ISI96]1431+0142	HIPEQ1433+01	dI
SDSS J143245.22+025452.6	14	32	45.22	+02	54	52.6	CGCG047−085	HIPEQ1433+02	SB
SDSS J143741.16+021728.0	14	37	41.16	+02	17	28.0	NGC5690	HIPEQ1437+02	Sc
SDSS J143753.52−002355.7	14	37	53.52	−00	23	55.7	NGC5691	HIPEQ1437−00	SAB(s)a
SDSS J143904.27+025657.5	14	39	04.27	+02	56	57.5	UGC09432	HIPEQ1439+02	Im
SDSS J143949.46−004309.5	14	39	49.46	−00	43	09.5	NGC5705	HIPEQ1439−00	SB(rs)d
SDSS J144058.25+021112.1	14	40	58.25	+02	11	12.1	NGC5725	HIPEQ1440+02	SB(s)d
SDSS J144056.14−001905.9	14	40	56.14	−00	19	05.9	NGC5719	HIPEQ1440−00	SAB(s)ab
SDSS J144424.50+014048.0	14	44	24.50	+01	40	48.0	NGC5740	HIPEQ1444+01a	SAB(rs)b
SDSS J150000.26+015329.0	15	00	00.26	+01	53	29.0	NGC5806	HIPEQ1500+01	SAB(s)b
SDSS J150429.71+021959.5	15	04	29.71	+02	19	59.5	CGCG048−099	HIPEQ1504+02	...
SDSS J150430.10−005105.4	15	04	30.10	−00	51	05.4	UGC09682	HIPEQ1504−00	SB(s)m
SDSS J150707.68+013240.2	15	07	07.68	+01	32	40.2	NGC5850	HIPEQ1507+01	SB(r)b
SDSS J154159.81+004246.1	15	41	59.81	+00	42	46.1	UGC09977	HIPEQ1542+00	Sc
SDSS J154500.26+022803.7	15	45	00.26	+02	28	03.7	CGCG050−091	HIPEQ1544+02	...
SDSS J154514.35+004619.6	15	45	14.35	+00	46	19.6	UGC10005	HIPEQ1545+00	SA(s)d
SDSS J160134.06+014228.1	16	01	34.06	+01	42	28.1	IC1158	HIPEQ1601+01a	SAB(r)c
SDSS J160943.90−000651.8	16	09	43.90	−00	06	51.8	UGC10229	HIPEQ1609−00	Im
SDSS J161329.16−005301.3	16	13	29.16	−00	53	01.3	VV370	HIPEQ1613−00	Sm
SDSS J161433.00+004920.3	16	14	33.00	+00	49	20.3	UGC10290	HIPEQ1614+00	SB(s)m
SDSS J161424.84−001229.9	16	14	24.84	−00	12	29.9	UGC10288	HIPEQ1614−00	Sc
SDSS J203623.33−043709.5	20	36	23.33	−04	37	09.5	NGC6941	HIPEQ2036−04	SAB(rs)b
SDSS J231432.98+001407.4	23	14	32.98	+00	14	07.4	UGC12446	HIPEQ2314+00	Sa
SDSS J232423.47−000625.6	23	24	23.47	−00	06	25.6	UGC12578	HIPEQ2324−00	SB(s)m
SDSS J233539.86+011150.6	23	35	39.86	+01	11	50.6	UGC12690	HIPEQ2335+01	SB(s)m
SDSS J233631.49+001749.9	23	36	31.49	+00	17	49.9	NGC7716	HIPEQ2336+00	SAB(r)b
SDSS J233723.83+002331.2	23	37	23.83	+00	23	31.2	UGC12709	HIPEQ2337+00	SAB(s)m
SDSS J234020.78+011443.8	23	40	20.78	+01	14	43.8	UGC127	HIPEQ2340+01	S0/a

2.3.2 Spectra

159 of the galaxies have SDSS fiber spectra. The spectra were identified by visually inspecting each galaxy in the DR3 Finding Chart Tool[2] with the S option selected to plot all spectra positions. At each spectrum position the coordinates were recorded and piped into the DR3 Spectro CrossID server[3] to recover the plate, mjd and fiber. Because of the deblending problems (see Appendix A), some of the galaxies have multiple spectra (as many as 5). Although these spectra are useful for obtaining redshifts, and isolated metallicity information, their small apertures (3″) and irregular placement make them highly susceptible to aperture effects. Because the spectral targeting engine places the fibers on both central bulges and HII regions, the spectra do not provide a uniform method of examining the global spectroscopic properties of these galaxies. We will therefore not include any analysis of the spectral data in this thesis but include the positions and catalog information for the matching spectra in Table 2.4 for completeness.

[2]http://cas.sdss.org/astro/en/tools/chart/chart.asp

[3]http://cas.sdss.org/astro/en/tools/crossid/speclist.asp

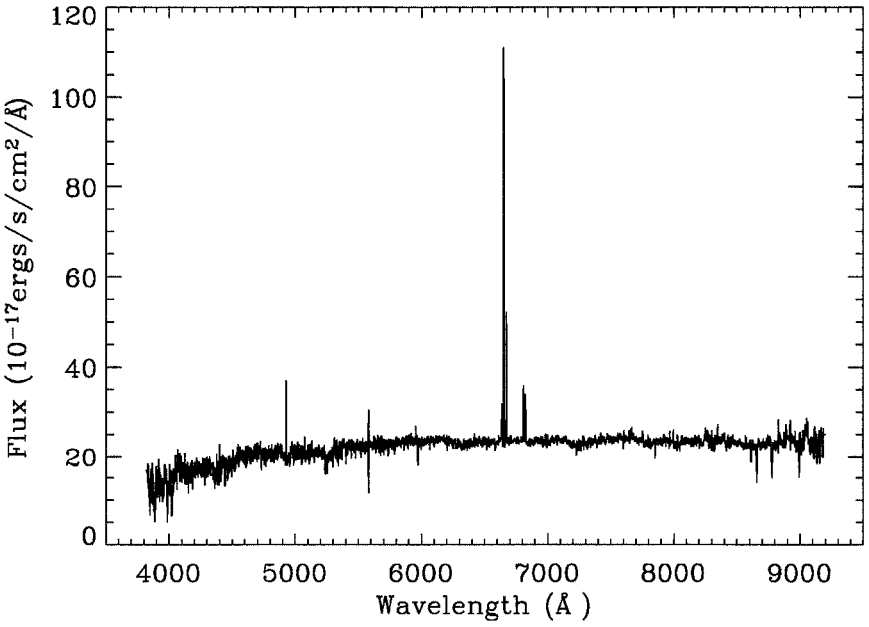

Figure 2.4 SDSS fiber spectrum of HIPASS/SDSS galaxy HIPEQ0014-00. Strong emission lines created by star forming regions in the galaxy allow for an accurate and unambiguous redshift determination.

Table 2.4. SDSS Spectra

HIPASS Name	RA	DEC	Plate	MJD	Fiber
HIPEQ0014-00	3.632750	-0.737557	389	51795	208
HIPEQ0027-01a	6.957241	-1.199990	391	51782	130
HIPEQ0033-01	8.342062	-1.121294	392	51793	284
HIPEQ0043-00	10.865800	-0.128086	393	51794	191
HIPEQ0051-00	12.998420	-0.486708	394	51913	182
HIPEQ0058+00	14.703581	0.587256	395	51783	441
HIPEQ0119+00	19.994598	0.722308	398	51789	532
HIPEQ0120-00	20.028474	-0.205370	398	51789	111
HIPEQ0122+00	20.526497	0.937963	399	51817	323
...	20.542581	0.949376	399	51817	339
...	20.557737	0.958730	399	51817	324
HIPEQ0123-00	20.807111	-0.385269	399	51817	185
HIPEQ0126+00a	21.622421	0.548957	399	51817	547
HIPEQ0126-00b	21.694154	-0.646127	399	51817	140
HIPEQ0154-00	28.650150	-0.156335	403	51871	271
...	28.671011	-0.143342	403	51871	266
HIPEQ0222-00	35.625385	-0.617390	406	51869	254
HIPEQ0228-01	37.102403	-1.149843	407	51820	259
HIPEQ0230-01	37.637702	-1.111188	407	51820	135
HIPEQ0231+00	37.930696	0.293456	407	51820	496
HIPEQ0236+00	39.098442	0.708578	408	51821	361
HIPEQ0241+00	40.436214	0.442986	408	51821	546
HIPEQ0244+00	41.087900	0.675389	408	51821	627
HIPEQ0246-00a	41.626471	-0.242086	409	51871	225
...	41.645166	-0.250249	409	51871	227
HIPEQ0246-00b	41.604852	-0.498649	409	51871	237
HIPEQ0249-00a	42.219316	-0.351111	409	51871	143
HIPEQ0249-00b	42.366452	-0.872991	409	51871	41
...	42.398957	-0.888892	409	51871	48
HIPEQ0249-00	42.420380	-0.523335	409	51871	114
HIPEQ0300+00	45.167485	0.020371	411	51817	270
HIPEQ0301-00	45.263684	-0.743466	411	51817	257
HIPEQ0306-00	46.718416	-0.794484	411	51817	20
HIPEQ0316-00	49.132665	-0.468139	413	51929	222
HIPEQ0320-06	50.037589	-6.263665	460	51924	378
HIPEQ0855+02	133.967889	2.524287	565	52225	132
HIPEQ0856+00	134.169461	0.375001	468	51912	61
HIPEQ0923-00	140.819362	-0.730928	474	52000	254
HIPEQ0930+04	142.563279	4.144214	569	52264	352
HIPEQ0936+01	144.111204	1.191351	477	52026	242
HIPEQ0942+00	145.512414	0.339172	266	51630	387
...	145.519514	0.336411	476	52314	622
HIPEQ0944-00b	146.192611	-0.688427	266	51630	99
HIPEQ0946+02	146.469881	2.978372	570	52266	55
HIPEQ0945+01	146.510614	1.672064	480	51989	471
HIPEQ0947+00a	146.723488	0.507350	267	51608	360
...	146.725313	0.508233	266	51630	556
HIPEQ0947+00b	146.772901	0.964255	266	51630	574
HIPEQ0953+01	148.394808	1.590095	481	51908	180
HIPEQ0954+02a	148.544531	2.287192	500	51994	399
HIPEQ0955+04a	148.818214	4.267733	572	52289	348
...	148.825262	4.270016	571	52286	597
HIPEQ1000+03	150.112801	3.374386	572	52289	96
HIPEQ1010+05	152.654965	5.150673	573	52325	610
HIPEQ1014+03	153.558712	3.465168	574	52355	214
HIPEQ1015+02	153.979157	2.685483	502	51957	616
...	153.979157	2.685483	574	52355	84
HIPEQ1026+03	156.674201	3.861923	575	52319	109
HIPEQ1039+01	159.854832	1.718383	506	52022	262
HIPEQ1041+00	160.472555	0.793204	274	51913	509

Table 2.4—Continued

HIPASS Name	RA	DEC	Plate	MJD	Fiber
HIPEQ1046+01	161.552443	1.813285	507	52353	314
HIPEQ1050+01	162.537024	1.264961	507	52353	245
HIPEQ1051+04a	162.894817	4.583507	579	52338	182
HIPEQ1052+00	163.202647	0.034450	276	51909	197
HIPEQ1053+02	163.327675	2.626031	507	52353	550
HIPEQ1055+02	163.913206	2.395755	508	52366	357
HIPEQ1109-00	167.355478	-0.097712	278	51900	197
HIPEQ1110+01	167.726184	1.091985	278	51900	534
HIPEQ1113+05	168.302112	5.196332	835	52326	421
HIPEQ1119+02	170.061247	2.522488	510	52381	637
HIPEQ1127-01	171.801047	-0.994666	281	51614	201
HIPEQ1131-02	172.883651	-2.309190	326	52375	585
HIPEQ1133-03	173.438607	-3.437008	327	52294	205
HIPEQ1136+00	174.153584	0.816870	282	51658	532
HIPEQ1138+03	174.728893	3.580877	513	51989	603
...	...	174.730792	3.600690	513	51989	601
HIPEQ1148-02	177.210023	-2.032235	330	52370	344
HIPEQ1151-02	177.984014	-2.642419	330	52370	200
HIPEQ1152-03b	178.133501	-3.671482	330	52370	205
HIPEQ1152-02	178.154970	-2.469419	329	52056	633
...	...	178.156981	-2.468419	330	52370	471
HIPEQ1152+01	178.181001	1.740770	515	52051	215
HIPEQ1155+01	178.903945	1.237171	285	51930	334
HIPEQ1200-01	180.083719	-1.106492	285	51930	49
...	...	180.096241	-1.097719	331	52368	405
...	...	180.109478	-1.102220	285	51930	42
HIPEQ1200-00	180.194068	-0.021377	285	51930	541
HIPEQ1202+01	180.675992	1.976807	516	52017	119
HIPEQ1204-01	181.084447	-1.530284	331	52368	613
HIPEQ1204-02	181.196685	-2.720079	331	52368	35
HIPEQ1210+02	182.765506	2.006052	518	52282	313
HIPEQ1215+04a	184.001528	4.650964	843	52378	101
HIPEQ1216-03	184.035531	-3.570137	333	52313	250
HIPEQ1218-01	184.535644	-1.064118	288	52000	257
HIPEQ1219+03	184.791156	3.856523	844	52378	41
HIPEQ1220+01	185.115258	1.469741	519	52283	282
HIPEQ1223-03b	185.974942	-3.442919	334	51993	291
HIPEQ1224+03b	186.166777	3.302825	519	52283	532
HIPEQ1226+02	186.743428	2.489796	519	52283	640
...	...	186.743741	2.494349	520	52288	309
HIPEQ1228+02	187.258916	2.723194	520	52288	395
HIPEQ1229+00	187.386229	0.839536	289	51990	570
HIPEQ1230+03	187.550447	3.577744	520	52288	380
HIPEQ1230+02	187.556304	2.624993	520	52288	431
HIPEQ1232+00a	188.115492	0.385521	290	51941	350
...	...	188.116444	0.390624	289	51990	627
HIPEQ1233-02	188.440683	-2.652105	334	51993	33
HIPEQ1236+03	189.175336	3.108392	520	52288	625
HIPEQ1239-00	189.828066	-0.531949	290	51941	61
HIPEQ1241+01	190.298339	1.410283	521	52326	90
HIPEQ1241-02	190.345367	-3.057827	335	52000	18
HIPEQ1242+03b	190.629446	3.959162	846	52407	2
HIPEQ1242-01a	190.636140	-1.350666	336	51999	330
HIPEQ1242-01b	190.738583	-1.229430	291	51928	128
HIPEQ1243-00	190.962113	-0.561232	291	51928	190
HIPEQ1244+00	191.119882	0.468068	291	51928	513
HIPEQ1244-02	191.138219	-2.319038	336	51999	187
HIPEQ1249+03	192.297324	3.387699	522	52024	569
HIPEQ1249+04	192.315396	4.655775	847	52426	152
HIPEQ1250+05	192.491139	5.311405	847	52426	556

Table 2.4—Continued

HIPASS Name	RA	DEC	Plate	MJD	Fiber
HIPEQ1253+04	193.310061	4.463112	847	52426	40
HIPEQ1253+01	193.338405	1.269101	523	52026	250
HIPEQ1253+02	193.367972	2.173186	523	52026	272
... ...	193.368844	2.166994	522	52024	34
HIPEQ1255+00	193.802728	0.116650	292	51609	630
HIPEQ1255+02	193.814721	2.896639	523	52026	476
HIPEQ1255-00	193.912055	-0.264898	293	51994	221
HIPEQ1257-01	194.304017	-1.711065	338	51694	374
HIPEQ1257+02	194.435776	2.691733	523	52026	543
HIPEQ1300+02a	194.992002	2.049279	523	52026	76
HIPEQ1300+02b	195.163539	2.500726	524	52027	266
... ...	195.165273	2.508513	523	52026	34
HIPEQ1303+03	195.774655	3.991876	849	52439	136
HIPEQ1304-02	196.132638	-2.988038	339	51692	166
HIPEQ1304-03	196.109674	-3.584624	339	51692	97
... ...	196.129976	-3.572413	339	51692	84
... ...	196.133541	-3.588389	339	51692	89
... ...	196.134467	-3.556145	339	51692	83
... ...	196.158112	-3.566064	339	51692	53
HIPEQ1307-00	196.911222	-0.942461	294	51986	87
HIPEQ1308-02	197.179850	-2.130632	339	51692	583
... ...	197.184154	-2.132882	340	51990	351
HIPEQ1311+03a	197.846921	3.411447	850	52338	84
HIPEQ1312+03	198.015559	3.171944	525	52295	454
... ...	198.059324	3.234651	525	52295	453
HIPEQ1312+05	198.027311	5.475700	850	52338	503
HIPEQ1313+06	198.337442	6.061269	850	52338	571
HIPEQ1317-00	199.429970	-1.001060	296	51984	285
HIPEQ1318-01	199.541978	-1.243678	296	51984	243
... ...	199.541986	-1.243671	341	51690	326
HIPEQ1320+05	200.133546	5.408202	851	52376	541
HIPEQ1327+02	202.050814	2.278485	527	52342	481
HIPEQ1329-00	202.355123	-0.399040	297	51959	70
HIPEQ1332+01	203.128186	1.847701	527	52342	24
HIPEQ1335+01	203.852316	1.410596	528	52022	137
HIPEQ1341+05	205.271696	5.105801	853	52374	628
HIPEQ1348+03	207.066824	3.950865	854	52373	29
HIPEQ1352-01	208.226914	-1.114633	300	51943	2
HIPEQ1352+02a	208.235657	2.814274	530	52026	585
HIPEQ1400+02	210.190708	2.022034	531	52028	112
HIPEQ1411-01	212.907426	-1.156185	916	52378	442
... ...	212.907750	-1.159105	303	51615	297
HIPEQ1415+04	213.848835	4.408523	583	52055	178
HIPEQ1416+03	214.238635	3.836137	584	52049	315
HIPEQ1422-00	215.599029	-0.387669	304	51957	113
HIPEQ1429-00	217.394166	-0.018234	305	51613	54
HIPEQ1432+00	218.121186	0.292890	306	51637	507
HIPEQ1433+02	218.187374	2.913265	585	52027	49
... ...	218.188098	2.915015	535	51999	563
HIPEQ1437-00	219.468914	-0.398685	307	51663	185
HIPEQ1439+02	219.766477	2.947061	536	52024	536
HIPEQ1439-00	219.958461	-0.706355	307	51663	99
HIPEQ1440-00	220.234835	-0.318219	307	51663	68
HIPEQ1440+02	220.242984	2.186262	536	52024	552
... ...	220.243978	2.183975	537	52027	358
HIPEQ1444+01a	221.101864	1.679772	536	52024	40
HIPEQ1444+01a	221.101864	1.679772	537	52027	240
HIPEQ1500+01	225.000579	1.890904	539	52017	398
... ...	225.001661	1.891329	538	52029	639
HIPEQ1504+02	226.123884	2.333028	539	52017	548

Table 2.4—Continued

HIPASS Name	RA	DEC	Plate	MJD	Fiber
HIPEQ1507+01	226.780099	1.543908	540	51996	280
... ...	226.782027	1.544240	539	52017	40
HIPEQ1542+00	235.497978	0.712604	315	51663	541
HIPEQ1544+02	236.251464	2.467996	594	52045	240
HIPEQ1545+00	236.309919	0.772177	342	51691	430
HIPEQ1609-00	242.433160	-0.115139	345	51690	161
HIPEQ1613-00	243.370727	-0.883496	345	51690	16
HIPEQ1614+00	243.637159	0.821472	346	51693	375
HIPEQ2036-04	309.097805	-4.618743	634	52164	328
HIPEQ2314+00	348.638024	0.235979	382	51816	437
... ...	348.640049	0.234591	381	51811	624
HIPEQ2335+01	353.917023	1.198135	384	51821	564
HIPEQ2337+00	354.350001	0.391670	385	51877	382
HIPEQ2340+01	355.086363	1.245770	385	51877	413

2.4 Deriving HI Properties

Single dish HI observations contain a wealth of information. In this section we will use the HI data to derive distances and HI masses for the HI selected sample. Most extragalactic HI studies ignore the subtleties surrounding the radiative transfer of HI emission. Although we will only give a cursory overview of HI radiative transfer in this section, we will show that some of the assumptions made when deriving quantities such as the HI mass can be problematic.

2.4.1 Distance

One of the simplest ways to calculate a distance is by applying the Hubble Law (Hubble 1929) to the recessional velocity. Complexity arises from both cosmological factors that can change the value of the "Hubble Constant" and local mass structures such as the Virgo cluster that can distort the expansion flow. These must be corrected before an accurate distance can be estimated. For this study, we adopt a cosmology with H_0=70 km/s/Mpc, Ω_M=0.3 and Ω_Λ=0.7.

Because of the limits of the HIPASS survey, the HI selected sample only probes the very nearby Universe. Figure 2.5 shows the redshift distribution of the HI selected galaxies (red) with the redshift distribution of a volume-limited sample of SDSS galaxies (black) from the DR4 main galaxy sample. As compared to the galaxies included in most SDSS studies, the galaxies in the HI selected sample have very small distances. Although this means that the HI selected sample probes a smaller volume than other SDSS studies, the volume it samples is more complete (although it is still missing gas-free galaxies and others eliminated by the selection criteria).

Many of the measured recessional velocities are likely to be influenced by infall toward Virgo. We correct for Virgo infall using the `IDL` routine `v_converter`, which derives velocity corrections from the LEDA database (Theureau et al. 1998; Terry et al. 2002).

The velocities are then converted into redshifts and the luminosity distance is derived using:

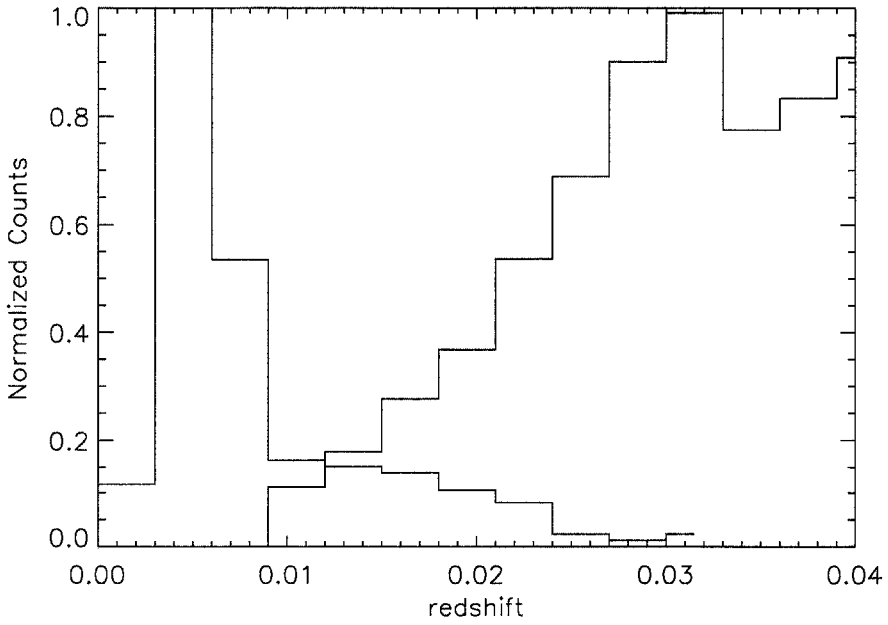

Figure 2.5 The redshift distribution of the HI selected galaxies (red) with the redshift distribution of a volume limited sample of SDSS galaxies (black) from the Data Release 4 (DR4) main galaxy sample. The HI selected sample probes galaxies that are much closer than most SDSS galaxy studies.

$$d_L = \frac{c}{H_0}(1+z)\int_0^z \frac{dz'}{\sqrt{(1+z')^3+\Omega_M+\Omega_\Lambda}}. \tag{2.1}$$

The derived distances can be found in Table 2.1.

2.4.2 HI Mass

For most blackbodies produced in nature (stars), the emission in the radio falls on the Rayleigh-Jeans tail. Because of this, radio astronomers have historically measured intensity in "brightness temperature" units that can be defined by the Rayleigh-Jeans approximation for the Planck Law:

$$T_B = \frac{c^2 I_\nu}{\nu^2 k} \tag{2.2}$$

where T_B is the brightness temperature, c is the speed of light, I_ν is the measured intensity, k is the Boltzmann constant and ν is the observed frequency.

In the absence of a strong background source, T_B can be expressed in relation to the kinetic temperature and the optical depth of the astronomical source by the equation:

$$T_B = \left(1 - e^{-\tau}\right) T_{kin} \tag{2.3}$$

where τ is the optical depth and T_{kin} is the kinetic temperature of the source. For large values of τ, $T_B = T_{kin}$ and for small values of τ, $T_B = \tau T_{kin}$.

The optical depth for HI is determined by the absorption cross section of the HI atoms at an observed frequency ν and is given by:

$$\tau = \frac{n}{1.823 \times 10^{18} T_{kin}} \tag{2.4}$$

where n is the column density of HI atoms in cm^{-2}.

In the optically thin case ($\tau \ll 1$), the column density can be written as:

$$n = 1.823 \times 10^{18} \int T_B d\nu \tag{2.5}$$

which only depends on the integrated flux in the beam. The integral is required because most radio receivers separate the flux over multiple channels within some bandwidth. In the case of the HIPASS receiver, the channel separation is 0.06 MHz and the bandwidth is 64 MHz.

From the column density inside the beam, the mass in HI is given by:

$$\mathrm{M_{HI}} = 2.356 \times 10^5 D^2 \int Sdv \tag{2.6}$$

where D is the distance in Mpc and $\int Sdv$ is the integrated flux in Jy·km/s. We use this relation to derive HI masses for the HI selected sample. These values can be found in Table 2.1 and Figure 2.6 shows the distribution of derived HI masses.

What is often neglected is that this expression for the HI mass is *only* valid in the optically thin limit. In reality, optically thick regions of HI are common (Braun 1997). Although these regions may not act to saturate the entire column of HI, their contribution to the total HI mass will be underestimated. Therefore, the HI mass derived in Equation 2.6 should be considered a lower limit. This is especially true for HI gas in the coldest phase. Equation 2.4 shows that the colder gas will become optically thick at a lower column density than warmer HI. Therefore, the cold HI phase in many galaxies likely contains many optically thick regions.

Because there is no spatial information associated with the HIPASS data, the τ_{HI} values for the galaxies in this sample cannot be directly probed. Therefore, for the remainder of this thesis the derived HI masses based on the optically thin assumption are used and the reader is reminded that these should be considered lower limits.

2.4.3 W_{20}

The width of the HI emission line is primarily due to the rotation velocity of the galaxy. This measure is important for studying the internal dynamics and mass of a galaxy. The 20% line width ($\mathrm{W_{20}}$) values are included in Table 2.1 but the true velocities need to be corrected for inclination effects. Because the optically derived inclinations of the sample galaxies are not presented until Chapter 3, the details of the inclination corrections and the

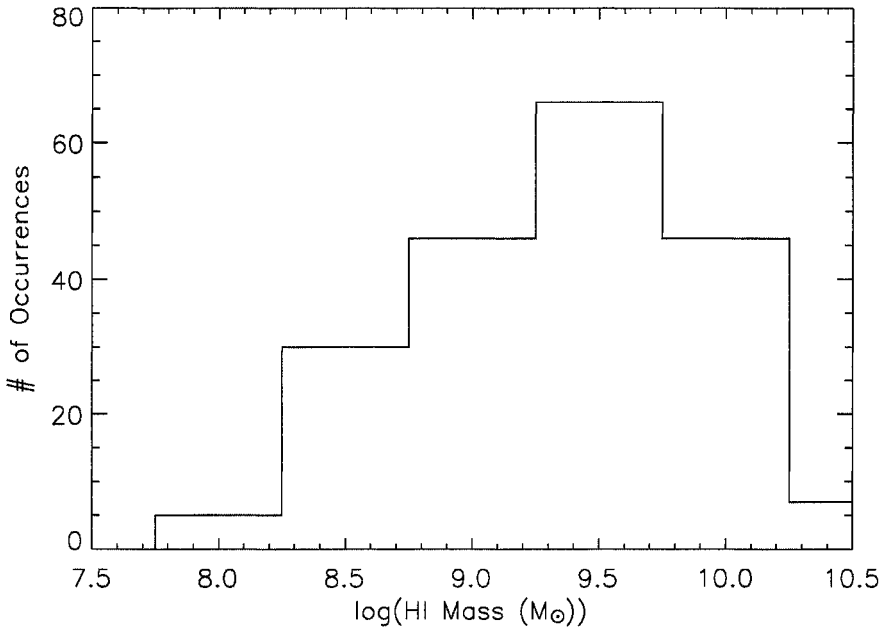

Figure 2.6 The HI mass distribution for the HI selected sample of SDSS galaxies.

corrected velocities are left to a later discussion.

2.5 Reverse List

Ideally there would be an equivalent optically selected catalog or volume limited sample to which the results from this HI selected sample could be compare. As seen in Figure 2.5, the HI selected sample is made up nearby galaxies, whereas the SDSS main sample has few galaxies closer than 100 Mpc. This is not because SDSS does not have data for nearby sources (it obviously does). It is instead, that the SDSS photometric pipeline is not optimized for nearby galaxy photometry, creating a variety of problems that make the data unreliable at the catalog level (see Appendix A).

A project is currently underway to create a nearby, volume limited sample, with some level of HI information. Using the DR3 spectroscopic data, we have selected all SDSS sources with recessional velocities < 3000 km/s that overlap with the HIPASS area. Diego Garcia-Appadoo is searching the HIPASS data cubes at every three-dimensional position

and recording the HI emission properties (or upper limits). We have dubbed this catalog the "reverse list" and when complete it will allow us to examine how properties of HI selected galaxies compare with a more uniformly drawn sample from a similar volume. Of course because of observational limits from spectroscopy, the galaxies that were not targeted for spectra (Strauss et al. 2002) will not be included in the reverse list. Until the reverse list is completed, we will use the volume limited DR4 main galaxy sample for comparisons between the HI selected sample and a more traditionally drawn catalog.

Chapter 3

HI SELECTED GALAXIES - PHOTOMETRY

3.1 Introduction

Large galaxy photometry in SDSS in non-trivial. In almost every SDSS galaxy study to date, large, nearby galaxies have been purposefully avoided because of the challenge in correctly extracting their photometric quantities (see Appendix A). The problems with deblending and sky subtraction certainly preclude an automated catalog-level analysis of large galaxies, and the inclination problems in the Petrosian quantities derived by SDSS adversely affect the photometry of even galaxies with small angular sizes. In this chapter we will discuss the process by which we address the problems with SDSS photometry and outline the method used to remedy the situation. We then apply these techniques to derive photometry for the HIPASS/SDSS sample (see Chapter 2). For completeness, we will also give a variety of other quantities that may be useful for comparison with other datasets and surveys.

3.2 Creating New Atlas Images

3.2.1 Reconstruction of Atlas Images

Although the SDSS photometric software has problems with large galaxies, it still does some things very well, in particular the removal of foreground stars from galaxy images. To preserve the good qualities of `PHOTO's` overenthusiastic deblender, we have reconstructed optical images of the galaxies with foreground stars removed as follows. First, for each deblended galaxy, we downloaded all of the `atlas images` within a $5'$ radius of the galaxy center. We visually inspected each `atlas image` and identified the `children` that belonged to each galaxy. For the most part, the appropriate `children` were easy to identify because of their uniform colors and extended morphology. In a few cases however, confusion between an HI region and a foreground star made the choice difficult. In these cases, we examined

the colors of the star-like objects and included them as children if they fell off the stellar locus as described by Covey et al. (2005). The `object_id` for each likely part of each galaxy was saved. The images from the deblended galaxy were mosaicked together to create a galaxy image uncontaminated by stars. Because we used `atlas images` that were produced after SDSS sky subtraction, the new galaxy images were still plagued with the sky subtraction problems (see Appendix A). However, these reconstructed images were useful in determining the quality and completeness of our `child` identification. Each reconstructed image was visually inspected to ensure that it did not have significant missing `children` and that bright stars and their artifacts were not included in the reconstructed images.

To properly reconstruct the images of the galaxies with their original sky, we wrote a script that uses the `tsobj`, `fpAtlas`, `fpBIN` and `fpFieldStat` SDSS files and rebuilds corrected frames (`fpC` files) with a specified list of atlas images. The resulting images contain only the galaxy superimposed on a restored image of the sky. We ran this script and obtained single galaxy `fpC` files as well as reconstructed sky images for every field. The latter were useful in correcting for the error in the SDSS sky subtraction discussed in Appendix A (also see §3.3 below).

Finally, we used the IDL procedure `HASTROM` to align all five SDSS bands to the same pixel coordinates and then used the function `HEXTRACT` to make cutouts of each galaxy while still preserving the astrometric (and other header) information.

3.2.2 Masking Out Stars

Twelve of the galaxies in the sample were so badly deblended by `photo` that we decided to use the `atlas image` of the `parent` for determining the photometric properties. We used the same software described above to create an `fpC` file of the galaxy and the reconstructed sky. The only difference was that we gave the program the `object_id` of the `parent` object rather than a list of the appropriate `children`. We aligned and extracted the atlas images in the same manner as described above. The major difficulty in using the `parent` images is that foreground stars are not removed. Therefore, before moving on to sky subtraction, we had to remove the stars from the atlas images. We adapted a set of IDL routines written

by Julianne Dalcanton to mask out the bright stars and fill in the masked out regions by interpolating from surrounding pixels. This method is time consuming but essential when deblending effects are severe.

3.3 Sky Subtraction

3.3.1 Sky Subtraction of SDSS Fields

As outlined in Appendix A, sky subtraction errors can be on the order of 1 magnitude in the SDSS catalog data. It is essential to address the sky subtraction problems when a galaxy exceeds $\sim$5 arcmin.^{2}. The sky subtraction method that we used is a variation on the method used by Maritza Tavarez for her thesis (Tavarez 2005). The procedure for sky subtraction is as follows:

A subregion of the original corrected frames (`fpC` files) is used to calculate the sky background for each galaxy. These frames are produced from the standard SDSS pipeline and are thus different from the reconstructed `fpC` files in that they include ALL of the sources in the fields and not just the galaxy in question (see previous section). We again use IDL's `HASTROM` to align each filter to the r-band pixel coordinate system. We then use IDL's `HEXTRACT` to cut out a section of the `fpC` file that includes the galaxy. We use subregions rather than the entire field to decrease processing time. We will show in the following section that the choice to do sky subtraction on a subregion of a field, rather than the entire field itself does not make a significant difference in the determination of the sky.

We next run `SExtractor` on the r-band subregion requiring 5 adjacent pixels to be above a threshold level of 1.5σ. Sources are extracted and a mask is built based on the SExtractor output. Foreground and background object are masked with apertures that are 5 times the object area (as calculated by `SExtractor`. The mask is then multiplied by all 5 `fpC` files (u, g, r, i, z) to create a "sky only" image. Due to the slight pixel offsets between SDSS images in different filters, every non-r-band image has some area that does not overlap the r-band. These pixels are also masked and not included in the sky calculation. Each mask is then reviewed by eye in a high contrast image to ensure that no resolved object flux is being included in the sky value. For the HI selected sample, ten of the sources have

surface brightnesses so low that the SExtractor threshold does not adequately mask the galaxies. For these objects, we grew the insufficient SExtractor masks by a factor of $\sim$20 times until the high contrast images no longer included galaxy flux. The sky pixels are then fit with a tilted plane model. The sky model, the sky pixels, and the sky subtracted galaxy image are all saved for each filter. The resulting model sky image is subtracted from the reconstructed galaxy image, yielding a correctly sky subtracted, non-deblended, reconstructed atlas images with no foreground or background objects.

3.3.2 Verifying Sky Subtraction Accuracy

In this section we explore various methods of calculating the sky background and show that almost all of the methods return similar results. We use the differences among sky subtraction techniques to characterize the uncertainty in determining the sky background.

There are many available options for fitting a sky background to an SDSS field. Should an entire field be used, or a cutout of a field? Should the sky be fit with a plane surface, or with a multiple order surface? And how does the areas of the galaxy mask affect the fit, especially for multiple order fits? To answer these questions, we have selected a sparsely populated field from the SDSS as a test field and created twelve different variations on which to test various sky subtraction methods. The twelve different methods are the combination of three different sky field cutouts and four different surface fits, ranging from first to fourth order respectively. The different sky fields are:

- An SDSS field with all of the objects masked out. We will call the combination of this method with the four surface fits, models 1-4 (where the surface fits are in increasing order).

- An SDSS field with all of the objects masked out and the mask of HIPEQ0014-00 (a medium/large sized galaxy in the sample with an area of 1.4 arcmin.^{2}) superimposed on the field. This leaves a large "hole" in the image at the galaxy location. We will call the combination of this method with the four surface fits, models 5-8 (where the surface fits are in increasing order).

- A $4' \times 5'$ subregion of an SDSS field with all of the objects masked out and the mask of HIPEQ0014-00 superimposed on the cutout. We will call the combination of this method with the four surface fits, models 9-12 (where the surface fits are in increasing order).

Each of the twelve methods was run on all 5 bands of the sparsely populated SDSS test image.

To quantify the differences among the various methods, we calculate the average residual counts per pixel in the area under the HIPEQ0014-00 mask. We assume that a perfect sky subtraction yields a mean sky level of zero. Thus, any non-zero mean sky level is a measure of the sky subtraction uncertainty, and is reported as the residual. This analysis adequately reproduces the manner in which actual sky subtraction of a galaxy field is calculated and reports the relevant residuals that affect galaxy photometry. For an $r \sim 13$ galaxy with an aperture area of $4\square'$, a residual of 1 count/pixel results in a 0.2 change in the magnitude. A residual of 0.1 counts/pixel would result in a 0.01 change in magnitude for the same galaxy. Figure 3.1 plots the residuals in all five SDSS bands for each of the twelve methods. The maximum residual is 0.1 counts/pixel and the rms is 0.04 counts/pixel. Figure 3.2 shows the residuals as a function of color (top), fit order (middle) and area schema (bottom). The residuals show no clear trend with either the fit order or the area schema. However, the i-band data have systematically larger residuals while the z-band's are systematically smaller. This may be due to objects that are uniquely in the i and z bands and therefore not properly removed with the r-band masks.

All of the methods have residuals are that well below other per pixel uncertainties (e.g. the `Dark Variance` varies between 0.9 and 3.9 counts/pixel) that will be described below. Therefore, we conclude that choosing any of these methods will not have an effect of more than $\sim 0.01^m$ on the resulting photometry.

For the photometry presented in this chapter, we've adopted a tilted plane fit to a subregion of the SDSS field for the sky subtraction (method 9). This approach is computationally the fastest method and, although the z-band residual is slightly worse than other methods, the deviation is still not significant. For completeness we use the largest absolute residual

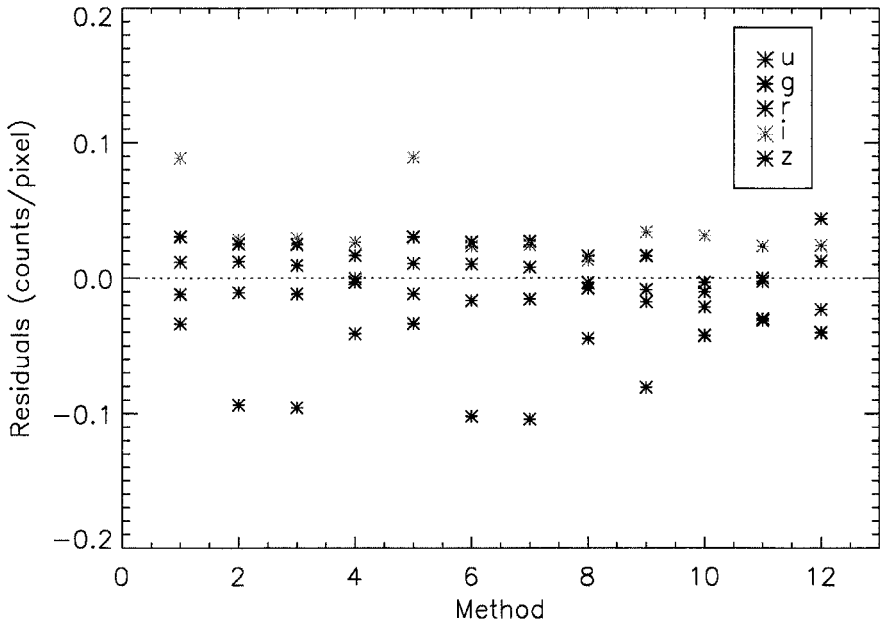

Figure 3.1 Residuals from the 12 different methods of sky subtraction of the same SDSS field. The colors represent the five SDSS bands. Most methods have comparable residuals and all are below other "per pixel" uncertainties. "Method 9" is used in this study.

in each band (regardless of method) as a measure of the uncertainty in the sky value. This is added to the uncertainty analysis described below. Figure 3.3 shows the residuals from Figure 3.1 with the SDSS residual (defined as the mean difference between the SDSS sky and the method presented in this thesis) for HIPASS/SDSS galaxy HIPEQ0014-00. This figure demonstrates the improvement we have made over the SDSS pipeline sky subtraction for a galaxy that is less than 2 arcminutes in extent. This improved sky subtraction changes the r-band magnitude of HIPEQ0014-00 by 0.19 magnitudes.

3.4 Model Fitting

To quantify the galaxies' sizes, surface brightnesses, and orientations, their reconstructed sky subtracted images are run through two different model fitting routines. Both fitting routines use the Levenberg-Marquardt (LM) minimization technique to calculate a two-dimensional surface fit to a galaxy image. The first routine fits a single Sérsic (1968) profile

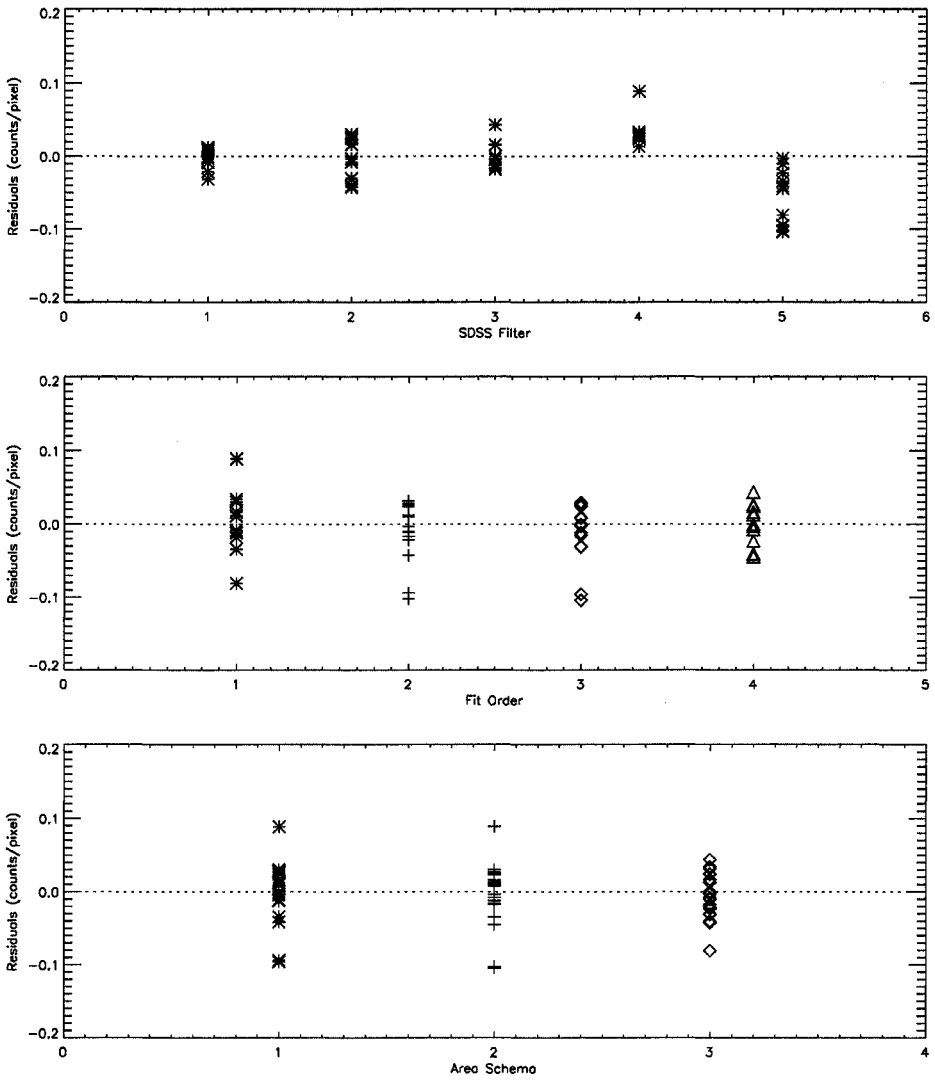

Figure 3.2 Sky subtraction residuals as a function of color (top), fit order (middle), and area schema (bottom). The colors represent the 5 SDSS bands and have the same values as Figure 3.1. The residuals have no trend with either the fit order or the area schema. However, the i and z bands have systematic deviations from 0 that are likely due to sources not being properly removed using the r-band mask.

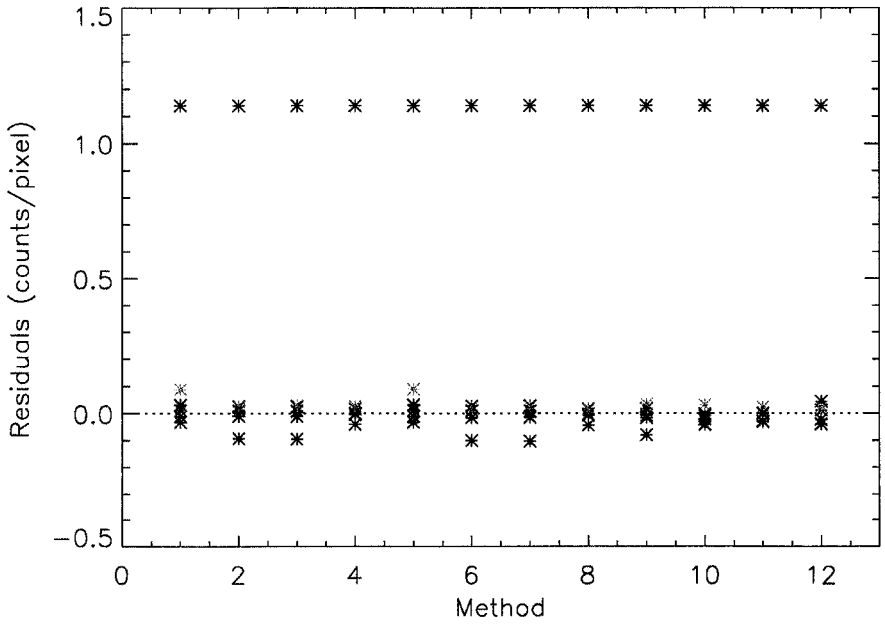

Figure 3.3 Residuals from the 12 different methods of sky subtraction of the same SDSS field. The colors represent the five SDSS bands and follow the same schema as Figure 3.1. The difference between the SDSS sky and the method presented in this thesis is overplotted for reference. Note that the sky subtraction residuals from my method are an order of magnitude smaller than the SDSS errors.

and the second fits a two component, double exponential disk. Below we discuss the specifics of both fitting methods and present the model fit parameters. All fits were performed on the r-band images. Although changes in the fit parameters between band passes might be of some scientific interest, there is considerable computational time required to run the models and many of these color difference will be identified using other photometric quantities.

3.4.1 Sérsic Fits

We used the LM IDL routine `MPFIT2DFUN` with the following Sérsic functional form:

$$I(r) = I_0 e^{-(r/h)^{\frac{1}{n}}} \tag{3.1}$$

where I is the surface brightness, h is a scale length and n is the Sérsic parameter. The variable r is defined to be:

$$r = \sqrt{[(x - x_0)\cos(\theta) + (y - y_0)\sin(\theta)]^2 + \frac{[(x - x_0)\sin(\theta) - (y - y_0)\cos(\theta)]^2}{1 - e^2}} \tag{3.2}$$

where $x0$ and $y0$ are the image centers, θ is the position angle, and e is the eccentricity. Because of the small number of parameters (7), the minimization was robust over a range of starting values and consistently converged to the same best-fit values. The starting centers were estimated by inspecting each r-band image. The central intensity was started at the maximum pixel value, the position angle was started at $\pi/4$, the Sérsic index was started at 1, the eccentricity was started at 0.8, and the starting h value was scaled from the image size to be 0.05 times the maximum r value (assuming a circle). All parameters were allowed to vary within reasonable limits. The input image pixels were weighted with a uniform value provided they met three criteria: 1) They must be inside the mask created for sky subtraction (see above); 2) they must have a value greater than the sky noise calculated in the previous section; and 3) they cannot be within a 10 pixel radius of the center. This last criterion was essential for the sources with large Sérsic indices because these models do not include the effects of seeing. Galaxies with steep profiles near the center will not be well fit because the seeing will smooth out the steep profile. Future versions will include

a convolution of the model with the observed psf. The last criterion made no significant difference for the "pure disk" galaxies.

The principal motivation for doing these fits was to obtain sensible aperture shapes and Sérsic index values. Table 3.1 gives the best fit Sérsic model parameters for all of the galaxies in the sample. The "Aperture Type" signifies the quality of the Sérsic fit. If the fit was able to accurately reproduce the galaxy image, then an elliptical aperture was used for photometry and the fit parameters were considered "good". Some of the galaxies are not well fit by the Sérsic model, resulting in large $\tilde{\chi}^2$ values. The elliptical shape of some of these large $\tilde{\chi}^2$ systems was well fit and these were included in the ellipse aperture photometry. 47 of the galaxies were not at all well fit by this simple profile because of their irregular morphologies or low surface brightness (LSB). For the irregular and LSB galaxies the parameters are not reliable and a default circular aperture is used for photometry. Although the lack of seeing in the models may introduce uncertainty into the exact Sérsic profile derived (see above), it has little effect on the aperture shape. Appendix B shows the fits for all of the galaxies in the sample.

Table 3.1. Aperture Choice and Sércic Parameters

HIPASS Name	Aperture Type	Angle (°)	Eccentricity	I_0 (mag/□″)[a]	h (″)	Sércic $\frac{1}{n}$	$\tilde{\chi}^2$
HIPEQ0014-00	ellipse	78.7	0.892	18.34	1.244	0.420	6.2
HIPEQ0027-01a	ellipse	124.6	0.920	18.84	0.339	0.289	3.0
HIPEQ0033-01	circle	...	...	...	...	...	...
HIPEQ0043-00	ellipse	7.4	0.736	17.71	1.754	0.524	37.0
HIPEQ0051-00	ellipse	0.0	0.855	17.93	1.765	0.709	15.9
HIPEQ0058+00	ellipse	88.6	0.224	17.00	0.152	0.329	12.0
HIPEQ0107+01	circle	...	...	...	...	...	...
HIPEQ0119+00	circle	...	...	...	...	...	...
HIPEQ0120-00	ellipse	54.1	0.936	20.71	7.609	0.540	5.0
HIPEQ0122+00	ellipse	58.0	0.972	19.84	18.639	0.635	10.9
HIPEQ0123-00	ellipse	4.7	0.348	17.43	0.129	0.312	10.1
HIPEQ0126+00a	circle	...	...	...	...	...	...
HIPEQ0126-00b	circle	...	...	...	...	...	...
HIPEQ0154-00	ellipse	54.1	0.518	15.52	0.216	0.449	47.5
HIPEQ0222-00	ellipse	45.0	0.989	20.61	9.040	0.463	3.7
HIPEQ0228-01	circle	...	...	...	...	...	...
HIPEQ0230+00	circle	...	...	...	...	...	...
HIPEQ0230-01	ellipse	18.5	0.910	15.23	0.568	0.428	336.5
HIPEQ0231+00	ellipse	132.2	0.799	19.35	0.398	0.308	4.3
HIPEQ0236+00	ellipse	169.5	0.953	19.62	6.966	0.749	6.7
HIPEQ0238+00	circle	...	...	...	...	...	...
HIPEQ0240+01	circle	...	...	...	...	...	...
HIPEQ0241+00	ellipse	101.8	0.941	18.11	6.100	0.445	130.2
HIPEQ0244+00	ellipse	14.1	0.941	19.87	0.571	0.264	4.3
HIPEQ0246-00a	ellipse	106.6	0.863	17.13	0.343	0.305	22.5
HIPEQ0246-00b	ellipse	180.0	0.505	18.02	3.008	0.433	181.0
HIPEQ0249-00	ellipse	90.7	0.612	16.77	0.209	0.407	45.1
HIPEQ0249-00a	circle	...	...	...	...	...	...
HIPEQ0249-00b	ellipse	46.3	0.691	16.09	0.198	0.374	42.4
HIPEQ0251-01	ellipse	57.0	0.935	21.40	8.208	0.243	2.3
HIPEQ0300+00	ellipse	24.6	0.953	19.85	1.848	0.359	1.9
HIPEQ0301-00	ellipse	140.4	0.829	19.44	0.296	0.255	1.9
HIPEQ0306-00	ellipse	152.6	0.520	15.20	0.280	0.416	38.9
HIPEQ0316-00	ellipse	125.9	0.949	18.21	1.165	0.414	6.1
HIPEQ0320-06	ellipse	48.9	0.858	17.70	3.267	0.625	76.0
HIPEQ0351-00	ellipse	51.7	0.772	15.98	0.190	0.426	25.3
HIPEQ0809+00	ellipse	93.3	0.792	18.98	1.352	0.390	12.8
HIPEQ0821+03b	ellipse	137.6	0.739	16.59	0.240	0.365	57.8
HIPEQ0821-00	circle	...	...	...	...	...	...
HIPEQ0822-00	ellipse	128.3	0.882	17.60	0.209	0.311	27.3
HIPEQ0825-00	ellipse	80.3	0.916	16.56	0.506	0.384	68.4
HIPEQ0855+02	ellipse	67.3	0.846	19.04	0.028	0.187	5.1
HIPEQ0856+00	ellipse	157.6	0.543	18.68	0.340	0.305	15.8
HIPEQ0923-00	ellipse	129.5	0.939	19.24	3.445	0.526	8.8
HIPEQ0930+04	ellipse	75.6	0.888	18.14	0.485	0.339	9.7
HIPEQ0942+00	ellipse	137.1	0.478	17.59	2.020	0.447	47.3
HIPEQ0944-00b	ellipse	154.9	0.816	20.04	0.983	0.354	2.9
HIPEQ0945+01	ellipse	122.8	0.962	19.11	11.342	0.657	10.8
HIPEQ0946+02	ellipse	74.7	0.952	19.86	0.713	0.272	2.6
HIPEQ0947+00a	ellipse	53.4	0.912	19.09	0.929	0.327	3.2
HIPEQ0947+00b	ellipse	13.4	0.854	19.99	0.181	0.203	1.3
HIPEQ0953+01	ellipse	115.0	0.994	19.25	38.675	0.931	144.0
HIPEQ0954+02a	ellipse	4.0	0.197	18.60	0.220	0.297	4.0
HIPEQ0955+04a	ellipse	68.8	0.886	15.75	0.116	0.294	132.0
HIPEQ0958+01	circle	...	...	...	...	...	...
HIPEQ1000+03	ellipse	153.2	0.957	17.66	2.936	0.585	21.8
HIPEQ1010+05	circle	...	...	...	...	...	...
HIPEQ1014+03	ellipse	31.2	0.831	16.89	8.370	0.960	5102.6
HIPEQ1015+02	ellipse	36.3	0.924	19.59	0.021	0.157	3.3
HIPEQ1026+03	ellipse	94.6	0.875	18.42	0.827	0.348	9.9

Table 3.1—Continued

HIPASS Name	Aperture Type	Angle (°)	Eccentricity	I_0 (mag/□″)[a]	h (″)	Sérsic $\frac{1}{n}$	$\tilde{\chi}^2$
HIPEQ1028+03	ellipse	6.0	0.984	21.34	16.645	0.580	2.1
HIPEQ1039+01	circle	...	...	...	...	...	...
HIPEQ1041+00	ellipse	113.6	0.564	18.90	0.275	0.297	5.9
HIPEQ1046+01	ellipse	160.5	0.984	19.12	5.677	0.426	8.7
HIPEQ1050+01	ellipse	127.5	0.911	21.67	6.056	0.396	1.1
HIPEQ1051+04a	ellipse	122.3	0.905	19.69	4.020	0.493	5.3
HIPEQ1052+00	ellipse	60.6	0.816	18.83	2.967	1.000	5.7
HIPEQ1053+02	circle	...	...	...	...	...	...
HIPEQ1055+02	circle	...	...	...	...	...	...
HIPEQ1101+03	ellipse	22.1	0.975	20.04	48.254	0.888	39.9
HIPEQ1109-00	ellipse	162.0	0.900	18.04	2.686	0.655	9.5
HIPEQ1110+01	circle	...	...	...	...	...	...
HIPEQ1113+05	ellipse	0.0	0.670	19.85	1.803	0.399	6.5
HIPEQ1117+04a	ellipse	23.3	0.633	14.78	0.232	0.420	354.9
HIPEQ1119+02	circle	...	...	...	...	...	...
HIPEQ1124+03	circle	...	...	...	...	...	...
HIPEQ1127-01	ellipse	169.6	0.586	19.13	0.203	0.262	6.7
HIPEQ1131-02	ellipse	0.0	0.269	17.14	0.083	0.275	35.4
HIPEQ1133-03	ellipse	42.5	0.827	20.62	4.577	0.435	4.2
HIPEQ1136+00	circle	...	...	...	...	...	...
HIPEQ1138+03	ellipse	36.0	0.461	16.45	0.309	0.484	40.2
HIPEQ1143-01	circle	...	...	...	...	...	...
HIPEQ1145+02	circle	...	...	...	...	...	...
HIPEQ1148-02	ellipse	11.5	0.804	18.68	0.253	0.286	10.6
HIPEQ1151-02	ellipse	108.9	0.860	19.43	5.031	0.994	10.8
HIPEQ1152+01	ellipse	24.7	0.732	17.14	0.121	0.316	87.6
HIPEQ1152-02	circle	...	...	...	...	...	...
HIPEQ1152-03b	circle	...	...	...	...	...	...
HIPEQ1155+01	ellipse	115.4	0.743	18.64	0.163	0.245	17.2
HIPEQ1200-00	ellipse	41.9	0.780	21.57	3.345	0.242	3.2
HIPEQ1200-01	ellipse	34.4	0.559	16.22	1.380	0.428	112.5
HIPEQ1202+01	ellipse	38.0	0.381	15.63	0.227	0.364	108.0
HIPEQ1204-01	circle	...	...	...	...	...	...
HIPEQ1204-02	ellipse	8.0	0.541	16.70	0.427	0.502	45.9
HIPEQ1210+02	circle	...	...	...	...	...	...
HIPEQ1215+04a	ellipse	140.1	0.901	19.73	4.876	0.671	7.0
HIPEQ1216-03	ellipse	104.5	0.106	18.26	0.285	0.343	5.0
HIPEQ1218+00	circle	...	...	...	...	...	...
HIPEQ1218-01	ellipse	133.8	0.789	18.18	1.585	0.527	19.9
HIPEQ1219+03	ellipse	17.6	0.492	17.45	0.192	0.334	24.6
HIPEQ1220+00	ellipse	42.2	0.960	21.51	13.317	0.525	1.5
HIPEQ1220+01	ellipse	146.4	0.990	20.13	11.508	0.622	5.7
HIPEQ1221+03	ellipse	1.8	0.963	17.41	0.860	0.403	27.7
HIPEQ1223+00	circle	...	...	...	...	...	...
HIPEQ1223-03b	ellipse	37.5	0.968	17.96	8.136	0.698	38.3
HIPEQ1224+00	circle	...	...	...	...	...	...
HIPEQ1224+03b	circle	...	...	...	...	...	...
HIPEQ1225+00	ellipse	101.8	0.723	15.00	0.266	0.467	345.0
HIPEQ1226+02	ellipse	11.6	0.901	19.36	23.301	1.571	282.1
HIPEQ1227+01	circle	...	...	...	...	...	...
HIPEQ1228+02	ellipse	129.3	0.930	20.21	0.163	0.181	3.5
HIPEQ1228+03	ellipse	72.1	0.604	13.95	0.344	0.443	914.9
HIPEQ1229+00	ellipse	73.4	0.981	21.14	4.234	0.365	1.2
HIPEQ1230+02	circle	...	...	...	...	...	...
HIPEQ1230+03	circle	...	...	...	...	...	...
HIPEQ1232+00a	ellipse	29.1	0.833	19.47	0.565	0.257	8.1
HIPEQ1232+00b	ellipse	82.2	0.992	19.90	83.491	0.763	61.8
HIPEQ1233-02	circle	...	...	...	...	...	...
HIPEQ1236+03	ellipse	44.2	0.955	21.34	6.717	0.375	1.2
HIPEQ1239-00	ellipse	92.4	0.956	19.78	32.004	0.991	53.0

Table 3.1—Continued

HIPASS Name	Aperture Type	Angle (°)	Eccentricity	I_0 (mag/$\Box''$)[a]	h ($''$)	Sércic $\frac{1}{n}$	$\tilde{\chi}^2$
HIPEQ1241+01	ellipse	142.0	0.794	19.34	5.770	1.066	13.5
HIPEQ1241-02	ellipse	146.3	0.923	19.54	6.258	0.727	6.5
HIPEQ1242+03b	ellipse	168.7	0.785	17.61	1.037	0.399	84.9
HIPEQ1242-00	ellipse	59.4	0.928	19.51	30.240	1.127	189.2
HIPEQ1242-01a	ellipse	75.2	0.666	19.84	4.752	0.547	8.5
HIPEQ1242-01b	ellipse	69.0	0.962	20.01	15.139	0.717	24.6
HIPEQ1243-00	ellipse	14.4	0.679	17.94	0.356	0.300	15.4
HIPEQ1244+00	ellipse	44.7	0.890	19.40	0.190	0.219	8.7
HIPEQ1244-02	circle	...	...	...	...	...	...
HIPEQ1245-00	ellipse	36.7	0.948	17.40	11.551	0.699	2404.7
HIPEQ1249+03	ellipse	35.8	0.659	18.04	3.581	0.601	90.8
HIPEQ1249+04	ellipse	171.7	0.811	19.17	0.022	0.186	3.4
HIPEQ1250+05	ellipse	84.3	0.677	18.59	4.896	0.511	104.6
HIPEQ1253+01	ellipse	133.6	0.966	19.23	23.602	0.896	22.0
HIPEQ1253+02	ellipse	150.5	0.455	15.01	0.172	0.349	102.0
HIPEQ1253+04	ellipse	86.1	0.842	17.46	3.416	0.764	47.4
HIPEQ1255+00	ellipse	126.5	0.407	19.24	1.319	0.327	41.2
HIPEQ1255+02	ellipse	88.1	0.933	16.38	1.375	0.547	92.8
HIPEQ1255-00	ellipse	60.1	0.977	20.47	0.189	0.183	1.9
HIPEQ1256+03	circle	...	...	...	...	...	...
HIPEQ1257+02	circle	...	...	...	...	...	...
HIPEQ1257-01	ellipse	137.3	0.970	19.15	10.145	0.783	15.3
HIPEQ1258+02	ellipse	73.3	0.900	19.11	0.380	0.278	6.4
HIPEQ1300+02a	circle	...	...	...	...	...	...
HIPEQ1300+02b	ellipse	136.7	0.726	16.24	0.090	0.258	191.0
HIPEQ1303+03	ellipse	167.6	0.282	19.32	0.169	0.252	4.7
HIPEQ1304-02	ellipse	117.0	0.798	20.25	1.896	0.442	8.1
HIPEQ1304-03	ellipse	52.9	0.652	21.29	13.144	0.362	24.9
HIPEQ1307-00	ellipse	73.1	0.651	18.91	3.156	0.580	23.0
HIPEQ1308-02	ellipse	61.8	0.535	18.17	0.384	0.346	17.0
HIPEQ1311+03a	ellipse	120.3	0.955	19.53	4.334	0.744	3.4
HIPEQ1312+03	ellipse	139.0	0.774	16.32	0.179	0.401	37.2
HIPEQ1312+05	circle	...	...	...	...	...	...
HIPEQ1313+06	ellipse	111.4	0.484	17.22	0.265	0.359	22.7
HIPEQ1317-00	ellipse	82.5	0.963	21.40	15.267	0.693	17.6
HIPEQ1318-01	ellipse	117.8	0.587	17.73	0.077	0.257	22.6
HIPEQ1320+05	ellipse	137.0	0.946	20.71	8.453	0.488	4.1
HIPEQ1327+02	circle	...	...	...	...	...	...
HIPEQ1329-00	ellipse	171.6	0.916	20.11	0.414	0.260	2.5
HIPEQ1332+01	ellipse	137.3	0.594	15.49	0.181	0.421	225.9
HIPEQ1335+01	ellipse	145.8	0.723	15.93	0.127	0.354	77.3
HIPEQ1341+05	ellipse	30.9	0.668	17.07	0.246	0.419	32.2
HIPEQ1348+03	ellipse	143.7	0.746	18.90	1.727	0.338	31.7
HIPEQ1352+02a	ellipse	147.2	0.719	16.04	0.252	0.392	49.1
HIPEQ1352-01	ellipse	21.1	0.695	19.85	7.819	0.448	31.4
HIPEQ1400+02	ellipse	119.3	0.976	19.69	8.388	0.689	6.2
HIPEQ1411-01	ellipse	172.0	0.983	19.40	8.585	0.454	18.2
HIPEQ1415+04	ellipse	91.3	0.285	17.87	0.211	0.360	8.9
HIPEQ1416+03	circle	...	...	...	...	...	...
HIPEQ1422-00	ellipse	153.7	0.760	19.33	4.339	0.400	49.5
HIPEQ1429-00	ellipse	91.5	0.842	19.19	1.362	0.390	17.0
HIPEQ1432+00	ellipse	117.6	0.978	19.33	10.285	0.769	8.4
HIPEQ1433+01	circle	...	...	...	...	...	...
HIPEQ1433+02	ellipse	178.4	0.782	18.61	0.799	0.412	10.8
HIPEQ1437+02	ellipse	140.5	0.971	19.08	20.528	0.769	176.8
HIPEQ1437-00	ellipse	97.2	0.873	17.29	1.547	0.452	176.9
HIPEQ1439-00	ellipse	61.2	0.911	18.72	0.669	0.300	12.4
HIPEQ1440+02	ellipse	16.8	0.745	19.49	5.711	0.726	20.3
HIPEQ1444+01a	ellipse	149.6	0.775	15.59	0.174	0.330	170.6
HIPEQ1500+01	ellipse	166.7	0.821	15.31	0.177	0.324	280.7

Table 3.1—Continued

HIPASS Name	Aperture Type	Angle (°)	Eccentricity	I_0 (mag/□″)[a]	h (″)	Sércic $\frac{1}{n}$	$\tilde{\chi}^2$
HIPEQ1504+02	ellipse	19.2	0.576	18.17	0.240	0.346	8.7
HIPEQ1504-00	ellipse	159.5	0.966	20.06	2.830	0.361	6.3
HIPEQ1507+01	ellipse	82.3	0.292	15.39	0.261	0.372	146.7
HIPEQ1542+00	ellipse	77.5	0.986	19.67	8.300	0.461	9.5
HIPEQ1544+02	ellipse	128.3	0.499	18.77	0.959	0.423	6.6
HIPEQ1545+00	ellipse	125.5	0.439	19.15	0.018	0.183	4.4
HIPEQ1601+01a	ellipse	134.0	0.834	18.77	0.633	0.281	17.5
HIPEQ1609-00	circle	...	...	...	...	...	...
HIPEQ1613-00	circle	...	...	...	...	...	...
HIPEQ1614+00	ellipse	169.0	0.527	19.26	0.025	0.174	7.8
HIPEQ1614-00	ellipse	90.7	0.992	18.97	5.846	0.429	26.7
HIPEQ2036-04	ellipse	107.5	0.770	16.15	0.169	0.350	78.6
HIPEQ2314+00	ellipse	69.0	0.400	19.35	5.529	0.910	35.1
HIPEQ2324-00	circle	...	...	...	...	...	...
HIPEQ2335+01	circle	...	...	...	...	...	...
HIPEQ2336+00	ellipse	30.0	0.684	15.48	0.042	0.269	18.9
HIPEQ2337+00	circle	...	...	...	...	...	...
HIPEQ2340+01	ellipse	78.8	0.875	18.85	1.933	0.509	11.3

[a]Model central surface brightness has been converted to mag/□″ and corrected for Milky Way extinction using the photometric calibrations discussed in §3.5

Note. — Sérsic fit parameters for galaxies with circular aperture photometry are not included

3.4.2 Bulge/Disk Fits

We also complete two-component, 2D fits using the same Levenberg-Marquardt minimization. We use the fact that Sérsic bulge fits for late-type galaxies favor n=1 (exponential disk; e.g. MacArthur, Courteau & Holtzman 2003) and fit the surface brightness profile as a double-exponential with the form:

$$I(r) = I_{0,a}e^{-(r_a/h_a)} + I_{0,b}e^{-(r_b/h_b)} \tag{3.3}$$

where $I_{0,a}$ and $I_{0,b}$ are the central surface brightnesses of the bulge and disk respectively, the h values are two scale lengths of the inner and outer regions and the r values are defined to be the same as Equation 4.2. All of the image pixels have uniform fitting weight provided they are inside the sky subtraction mask and have a value above the calculated sky noise. All position angles are started at $\pi/2$, all eccentricities are started at 0.7, all I_0 values are started at 0.5 times the maximum pixel value and the two scale lengths for each image are started at 1/10 and 1/50 of the major axis of the image respectively. All of these values are allowed to vary during the fit within reasonable limits. However, the addition of more parameters (14 in total) makes the two-component fit less stable against initial condition and parameter constraint variations. Therefore, three different versions of the double exponential fits were run on the r-band galaxy images. The difference between the three fitting methods comes in the determination and variation of the image centers. The first method uses the brightest pixel as the center for both components and allows the centers to vary by as much as 15 pixels in any direction. The second method uses the same user-defined centers used in the Sérsic fits and allows the centers to vary by as much as 25 pixels in any direction. The third method also used the user-defined centers but allows the centers to vary by as much as 5 pixels in any direction. The choice between the 3 methods was determined by the smallest $\tilde{\chi}^2$ value of the fit.

The resulting best two component fit can be seen in Appendix B. Again, the LSB and irregular galaxies were not well fit by these models. Table 3.2 shows the two component fit parameters for the all of the galaxies in the sample.

Table 3.2. Two Component Fit Parameters

	Disk				Bulge				
HIPASS Name	Angle (°)	Eccentricity	I_0 (mag/□″)[a]	h (″)	Angle (°)	Eccentricity	I_0 (mag/□″)[a]	h (″)	$\tilde{\chi}^2$
HIPEQ0014-00	79.9	0.924	22.60	114.76	78.4	0.890	19.45	6.60	4.3
HIPEQ0027-01a	124.2	0.917	22.17	50.26	125.4	0.927	20.34	4.73	3.1
HIPEQ0033-01	...	...	...	...	...	...	...	...	...
HIPEQ0043-00	0.2	0.801	19.20	9.74	56.7	0.822	18.40	1.75	28.3
HIPEQ0051-00	176.9	0.799	22.79	63.53	176.9	0.861	18.29	2.72	7.1
HIPEQ0058+00	126.5	0.259	19.61	7.13	71.1	0.498	18.15	0.72	11.7
HIPEQ0059+01	0.0	0.789	22.25	18.09	0.0	0.705	20.00	1.06	1.2
HIPEQ0107+01	...	...	...	...	...	...	...	...	...
HIPEQ0119+00	...	...	...	...	...	...	...	...	...
HIPEQ0120-00	59.0	0.956	23.20	130.28	52.8	0.933	21.22	10.60	4.1
HIPEQ0122+00	57.7	0.985	21.09	67.51	54.7	0.899	20.35	10.04	8.9
HIPEQ0123-00	23.2	0.328	20.60	10.88	158.3	0.356	18.62	1.06	10.5
HIPEQ0126+00a	...	...	...	...	...	...	...	...	...
HIPEQ0126-00b	...	...	...	...	...	...	...	...	...
HIPEQ0154-00	57.9	0.650	19.49	6.86	51.3	0.468	16.56	0.92	18.2
HIPEQ0222-00	46.8	0.964	23.22	178.20	44.9	0.991	21.33	18.91	3.2
HIPEQ0228-01	...	...	...	...	...	...	...	...	...
HIPEQ0230+00	...	...	...	...	...	...	...	...	...
HIPEQ0230-01	18.9	0.969	17.77	11.89	21.7	0.670	16.15	1.22	77.0
HIPEQ0231+00	150.6	0.848	22.75	60.29	122.9	0.818	20.68	4.13	3.5
HIPEQ0236+00	168.3	0.960	23.54	306.50	169.7	0.954	19.88	8.82	5.2
HIPEQ0238+00	...	...	...	...	...	...	...	...	...
HIPEQ0240+01	...	...	...	...	...	...	...	...	...
HIPEQ0241+00	104.6	0.849	20.85	75.99	101.6	0.973	19.03	21.66	86.0
HIPEQ0244+00	18.2	0.956	23.32	300.56	14.5	0.943	21.34	10.61	3.3
HIPEQ0246-00a	104.0	0.881	20.25	32.33	106.4	0.813	18.50	3.00	20.9
HIPEQ0246-00b	15.9	0.662	19.63	29.65	123.6	0.889	17.94	2.34	117.4
HIPEQ0247-00	94.0	0.725	18.78	6.94	97.3	0.533	16.85	0.85	22.6
HIPEQ0249-00	86.5	0.787	21.17	18.24	77.6	0.380	17.64	0.96	14.9
HIPEQ0249-00a	...	...	...	...	...	...	...	...	...
HIPEQ0249-00b	41.8	0.858	19.48	10.57	101.5	0.446	17.11	0.96	18.4
HIPEQ0251-01	30.8	0.650	23.00	275.84	59.1	0.973	22.70	21.87	2.2
HIPEQ0300+00	32.7	0.939	23.04	242.75	23.7	0.954	20.94	9.28	1.5
HIPEQ0301-00	0.0	0.308	22.74	103.25	0.0	0.389	20.85	3.91	1.8
HIPEQ0305-00	148.0	0.972	22.54	70.23	157.3	0.933	19.93	2.97	2.8
HIPEQ0306-00	147.6	0.744	18.37	7.71	180.0	0.254	16.41	1.21	34.1
HIPEQ0316-00	125.8	0.963	20.03	14.30	126.3	0.674	19.14	1.19	5.9
HIPEQ0317-00	61.7	0.749	19.28	9.23	85.3	0.438	16.70	0.74	31.7
HIPEQ0320-06	49.7	0.885	18.77	10.11	46.8	0.528	18.28	1.43	56.2
HIPEQ0351-00	52.0	0.934	19.07	5.82	125.1	0.289	16.87	0.53	8.9

Table 3.2—Continued

	Disk				Bulge				
HIPASS Name	Angle (°)	Eccentricity	I_0 (mag/□″)[a]	h (″)	Angle (°)	Eccentricity	I_0 (mag/□″)[a]	h (″)	$\tilde{\chi}^2$
HIPEQ0809+00	82.1	0.853	21.20	24.88	119.9	0.857	20.25	4.69	13.0
HIPEQ0821+03b	128.3	0.834	19.52	9.83	154.3	0.554	17.66	1.01	44.6
HIPEQ0821-00	...	...	...	...	...	...	...	...	...
HIPEQ0822-00	128.7	0.890	20.72	17.81	123.8	0.862	18.57	1.44	17.4
HIPEQ0825-00	77.6	0.950	19.71	18.66	83.8	0.872	17.88	2.66	59.0
HIPEQ0855+02	59.6	0.670	22.79	95.69	67.9	0.951	20.54	4.39	3.7
HIPEQ0856+00	180.0	0.100	23.04	199.37	153.4	0.647	20.10	5.66	8.6
HIPEQ0923-00	124.9	0.954	22.57	71.03	130.1	0.937	22.57	7.66	7.6
HIPEQ0930+04	92.3	0.701	22.00	38.26	73.2	0.935	19.59	5.96	8.4
HIPEQ0934+00	90.8	0.100	23.56	196.81	90.5	0.817	19.46	5.94	13.0
HIPEQ0936+01	40.9	0.952	20.89	5.41	34.5	0.900	20.61	2.18	1.0
HIPEQ0942+00	0.0	0.206	19.28	17.01	128.8	0.694	18.12	2.03	40.5
HIPEQ0944-00b	180.0	0.100	23.32	160.43	155.8	0.841	21.10	5.38	2.2
HIPEQ0945+01	130.9	0.968	22.85	376.99	122.4	0.963	19.49	16.97	8.4
HIPEQ0946+02	76.0	0.835	23.19	207.93	74.9	0.965	21.14	10.14	1.9
HIPEQ0947+00a	48.7	0.929	22.49	112.32	55.8	0.905	20.33	7.38	2.4
HIPEQ0947+00b	14.0	0.855	22.92	183.25	12.9	0.856	21.48	5.73	1.2
HIPEQ0953+01	115.0	0.994	19.43	44.17	105.3	0.970	19.43	4.62	80.3
HIPEQ0954+01a	0.0	0.100	23.22	53.00	121.0	0.987	21.27	0.43	0.2
HIPEQ0954+02a	38.2	0.369	22.90	89.29	0.0	0.253	20.28	4.78	3.7
HIPEQ0955+04a	65.2	0.890	19.36	19.25	70.3	0.841	16.83	1.21	72.2
HIPEQ0958+01	...	...	...	...	...	...	...	...	...
HIPEQ1000+03	154.3	0.958	21.55	41.53	152.5	0.960	18.28	6.32	19.8
HIPEQ1010+05	...	...	...	...	...	...	...	...	...
HIPEQ1014+03	53.4	0.821	19.15	27.99	53.0	0.750	16.06	3.59	365.3
HIPEQ1015+02	44.2	0.898	23.14	261.76	29.9	0.950	21.36	7.65	2.6
HIPEQ1026+03	97.3	0.875	21.82	49.86	92.8	0.873	19.85	6.85	10.0
HIPEQ1028+03	15.6	0.898	23.19	86.01	5.9	0.990	21.78	18.19	1.9
HIPEQ1031+04	0.0	0.968	22.87	232.71	0.0	0.974	21.04	15.61	14.0
HIPEQ1039+01	...	...	...	...	...	...	...	...	...
HIPEQ1041+00	0.0	0.492	21.71	20.47	98.9	0.913	21.71	3.51	5.5
HIPEQ1046+01	159.7	0.980	23.19	476.78	160.4	0.985	20.23	29.16	8.6
HIPEQ1050+01	99.8	0.878	23.37	125.93	130.6	0.932	22.55	8.22	1.1
HIPEQ1051+04a	142.7	0.978	23.13	309.04	119.5	0.906	20.33	9.39	3.6
HIPEQ1052+00	71.4	0.722	19.80	3.60	62.5	0.766	18.91	1.73	3.1
HIPEQ1053+02	...	...	...	...	...	...	...	...	...
HIPEQ1055+02	...	...	...	...	...	...	...	...	...
HIPEQ1101+03	22.1	0.975	20.27	59.77	32.7	0.727	19.66	2.44	34.2
HIPEQ1109-00	162.1	0.902	18.58	5.52	0.0	0.991	17.61	0.42	13.1
HIPEQ1110+01	...	...	...	...	...	...	...	...	...

Table 3.2—Continued

	Disk				Bulge				
HIPASS Name	Angle (°)	Eccentricity	I_0 (mag/□″)[a]	h (″)	Angle (°)	Eccentricity	I_0 (mag/□″)[a]	h (″)	$\tilde{\chi}^2$
HIPEQ1113+05	57.0	0.769	23.01	89.82	7.2	0.742	20.87	7.79	5.5
HIPEQ1117+04a	20.1	0.796	18.36	8.04	23.9	0.491	15.81	0.99	142.9
HIPEQ1119+02	...	...	...	...	...	...	...	...	...
HIPEQ1124+03	...	...	...	...	...	...	...	...	...
HIPEQ1127-01	180.0	0.100	23.41	271.66	167.6	0.628	20.81	6.94	4.4
HIPEQ1131-02	66.7	0.348	20.94	21.33	0.0	0.541	18.65	1.86	34.6
HIPEQ1133-03	73.5	0.920	23.34	257.40	37.7	0.839	21.38	10.84	3.8
HIPEQ1136+00	155.5	0.861	19.74	5.86	78.9	0.595	18.16	0.58	13.7
HIPEQ1138+03	36.5	0.915	20.97	19.52	0.4	0.191	17.32	1.05	9.0
HIPEQ1143-01	...	...	...	...	...	...	...	...	...
HIPEQ1145+02	...	...	...	...	...	...	...	...	...
HIPEQ1148-02	14.8	0.914	22.78	127.46	7.6	0.646	19.90	3.64	5.1
HIPEQ1151-02	118.6	0.826	23.54	198.40	108.4	0.856	19.39	4.47	6.8
HIPEQ1152+01	80.4	0.756	20.95	16.84	10.7	0.895	18.15	1.49	43.2
HIPEQ1152-02	...	...	...	...	...	...	...	...	...
HIPEQ1152-03b	...	...	...	...	...	...	...	...	...
HIPEQ1155+01	136.2	0.578	22.07	56.03	105.5	0.919	19.93	4.89	12.2
HIPEQ1200-00	40.1	0.801	23.24	177.48	46.7	0.780	21.64	3.41	2.8
HIPEQ1200-01	35.7	0.588	18.57	20.58	30.3	0.463	17.22	3.29	151.2
HIPEQ1202+01	17.6	0.421	19.23	13.04	63.6	0.480	16.69	1.44	47.3
HIPEQ1204-01	...	...	...	...	...	...	...	...	...
HIPEQ1204-02	15.9	0.854	21.81	38.71	173.7	0.390	17.54	1.40	15.3
HIPEQ1210+02	...	...	...	...	...	...	...	...	...
HIPEQ1215+04a	140.8	0.901	20.41	9.89	0.0	0.100	20.67	1.58	6.9
HIPEQ1216-03	80.2	0.296	22.11	28.65	0.0	0.169	19.65	2.79	4.8
HIPEQ1218+00	...	...	...	...	...	...	...	...	...
HIPEQ1218-01	135.7	0.877	22.73	85.16	134.1	0.783	18.99	4.68	16.8
HIPEQ1219+03	42.1	0.587	20.43	10.07	79.3	0.642	18.65	1.64	10.5
HIPEQ1220+00	40.7	0.905	23.52	248.69	42.5	0.962	21.98	13.85	1.3
HIPEQ1220+01	146.3	0.995	21.35	40.17	146.2	0.964	20.86	7.14	5.0
HIPEQ1221+03	0.9	0.974	22.34	133.67	1.8	0.961	18.68	6.22	19.9
HIPEQ1223+00	...	...	...	...	...	...	...	...	...
HIPEQ1223-03b	36.7	0.983	19.25	25.02	41.0	0.907	18.55	5.37	25.7
HIPEQ1224+00	...	...	...	...	...	...	...	...	...
HIPEQ1224+03b	180.0	0.464	22.88	89.33	131.8	0.654	20.12	5.40	9.0
HIPEQ1225+00	95.3	0.892	19.81	18.17	102.9	0.680	15.93	1.06	67.2
HIPEQ1226+02	10.9	0.940	19.27	15.55	14.8	0.914	19.80	15.07	276.5
HIPEQ1227+01	...	...	...	...	...	...	...	...	...
HIPEQ1228+02	133.2	0.849	23.02	162.21	127.8	0.970	22.24	14.44	3.4
HIPEQ1228+03	72.7	0.663	18.32	14.18	70.9	0.628	15.03	1.70	255.3

Table 3.2—Continued

	Disk				Bulge				
HIPASS Name	Angle (°)	Eccentricity	I_0 (mag/□″)[a]	h (″)	Angle (°)	Eccentricity	I_0 (mag/□″)[a]	h (″)	$\tilde{\chi}^2$
HIPEQ1229+00	71.6	0.928	23.37	124.74	73.3	0.985	22.07	10.77	1.1
HIPEQ1230+02	...	...	...	...	...	...	...	...	...
HIPEQ1230+03	...	...	...	...	...	...	...	...	...
HIPEQ1232+00a	31.1	0.818	22.63	127.29	27.3	0.857	21.20	12.49	7.7
HIPEQ1232+00b	81.2	0.987	21.42	180.11	82.6	0.995	20.28	83.19	50.9
HIPEQ1233-02	...	...	...	...	...	...	...	...	...
HIPEQ1236+03	49.9	0.991	23.15	201.17	36.7	0.923	22.24	9.17	1.2
HIPEQ1239-00	94.6	0.992	20.86	35.70	92.3	0.934	20.08	30.13	43.4
HIPEQ1241+01	128.6	0.897	23.43	212.65	142.2	0.795	19.24	4.84	10.1
HIPEQ1241-02	0.0	0.100	23.50	310.86	146.2	0.925	19.80	8.15	3.9
HIPEQ1242+03b	0.0	0.793	19.59	15.09	0.0	0.100	18.24	1.50	41.6
HIPEQ1242-00	60.1	0.942	19.98	35.95	78.3	0.776	19.30	7.45	91.3
HIPEQ1242-01a	134.2	0.654	23.35	266.11	73.9	0.685	20.41	9.53	6.7
HIPEQ1242-01b	69.3	0.964	20.46	25.69	61.7	0.768	19.90	1.11	22.1
HIPEQ1243-00	14.9	0.700	20.79	28.72	17.9	0.508	19.37	2.74	19.0
HIPEQ1244+00	31.4	0.668	23.04	181.21	47.0	0.942	21.11	12.24	6.6
HIPEQ1244-02	...	...	...	...	...	...	...	...	...
HIPEQ1245-00	40.1	0.972	18.57	34.43	46.2	0.896	16.59	3.53	335.1
HIPEQ1249+03	53.3	0.786	22.39	80.89	39.1	0.635	18.62	7.43	73.3
HIPEQ1249+04	0.0	0.634	22.88	69.15	0.0	0.872	21.44	5.08	3.2
HIPEQ1250+05	85.9	0.617	19.89	23.17	83.7	0.919	19.11	3.99	94.7
HIPEQ1253+01	133.7	0.972	19.53	31.05	180.0	0.100	20.33	4.39	19.4
HIPEQ1253+02	148.3	0.653	18.67	13.03	94.8	0.100	16.26	1.31	113.3
HIPEQ1253+04	65.8	0.782	19.25	8.22	93.1	0.899	17.90	3.90	35.3
HIPEQ1255+00	0.0	0.710	21.32	44.29	163.0	0.536	18.56	1.06	34.1
HIPEQ1255+02	88.0	0.952	18.02	7.63	90.4	0.848	17.11	1.26	49.0
HIPEQ1255-00	60.0	0.918	23.41	232.85	60.3	0.988	22.40	17.02	1.7
HIPEQ1256+03	...	...	...	...	...	...	...	...	...
HIPEQ1257+02	...	...	...	...	...	...	...	...	...
HIPEQ1257-01	137.3	0.974	19.58	16.07	0.0	0.100	19.81	1.34	13.4
HIPEQ1258+02	71.3	0.575	22.78	91.33	72.3	0.953	20.36	6.88	4.0
HIPEQ1300+02a	...	...	...	...	...	...	...	...	...
HIPEQ1300+02b	127.6	0.513	19.76	25.88	140.6	0.905	17.71	2.45	117.2
HIPEQ1303+03	15.1	0.664	22.76	73.73	116.9	0.577	20.78	3.97	3.8
HIPEQ1304-02	52.5	0.853	23.31	130.28	118.5	0.843	21.01	5.23	6.3
HIPEQ1304-03	24.6	0.785	22.67	147.94	88.6	0.909	22.01	14.39	23.9
HIPEQ1307-00	118.3	0.378	22.50	41.27	74.8	0.661	19.53	6.54	20.6
HIPEQ1308-02	111.4	0.537	21.11	16.90	46.8	0.823	19.49	3.00	15.5
HIPEQ1311+03a	109.3	0.987	23.20	187.70	120.9	0.955	19.74	5.17	1.8
HIPEQ1312+03	139.5	0.895	19.52	6.40	0.0	0.203	17.33	0.62	19.6

Table 3.2—Continued

	Disk				Bulge				
HIPASS Name	Angle (°)	Eccentricity	I_0 (mag/□″)[a]	h (″)	Angle (°)	Eccentricity	I_0 (mag/□″)[a]	h (″)	$\tilde{\chi}^2$
HIPEQ1312+05	...	...	...	...	...	...	...	...	...
HIPEQ1313+06	89.4	0.477	20.30	11.47	0.0	0.100	18.24	1.25	16.0
HIPEQ1317-00	74.3	0.999	22.14	32.62	92.0	0.939	22.03	22.35	16.5
HIPEQ1318-01	124.7	0.515	21.14	21.38	104.0	0.541	18.70	1.12	14.9
HIPEQ1320+05	16.8	0.515	23.06	94.69	136.7	0.959	21.30	13.83	3.5
HIPEQ1327+02	...	...	...	...	...	...	...	...	...
HIPEQ1329-00	180.0	0.811	23.30	134.92	168.0	0.943	21.45	6.49	2.0
HIPEQ1332+01	138.5	0.822	19.48	9.82	0.0	0.100	16.28	0.65	54.9
HIPEQ1335+01	141.8	0.874	19.88	12.62	175.4	0.488	16.93	0.80	31.6
HIPEQ1337+05	8.5	0.823	22.19	38.06	133.2	0.802	19.42	4.38	14.6
HIPEQ1341+05	2.0	0.656	21.23	12.88	40.9	0.704	18.03	1.18	18.4
HIPEQ1348+03	144.3	0.744	20.86	41.81	163.2	0.656	19.29	1.91	30.9
HIPEQ1352+02a	148.5	0.822	20.72	23.61	0.0	0.276	17.30	1.62	37.2
HIPEQ1352-01	15.8	0.702	21.18	49.95	48.4	0.913	20.49	6.57	30.4
HIPEQ1400+02	117.8	0.990	23.18	230.08	119.1	0.975	20.01	11.11	4.4
HIPEQ1411-01	172.2	0.985	22.51	191.73	171.7	0.984	20.35	27.39	18.1
HIPEQ1415+04	75.8	0.470	21.17	10.27	117.0	0.523	19.17	1.59	8.3
HIPEQ1416+03	...	...	...	...	...	...	...	...	...
HIPEQ1422-00	152.6	0.764	20.92	45.73	32.3	0.782	19.52	2.98	40.6
HIPEQ1427+01	170.4	0.852	20.73	20.45	167.5	0.720	18.17	1.81	18.8
HIPEQ1429-00	77.5	0.898	22.47	64.29	100.6	0.831	20.28	6.52	13.2
HIPEQ1432+00	110.7	0.975	23.39	312.05	117.5	0.979	19.56	12.90	6.1
HIPEQ1433+01	...	...	...	...	...	...	...	...	...
HIPEQ1433+02	0.0	0.709	22.59	50.18	179.2	0.792	19.69	4.12	7.8
HIPEQ1437+02	180.0	0.100	22.43	86.71	140.6	0.979	22.43	26.37	150.9
HIPEQ1437-00	104.6	0.755	19.30	13.62	94.6	0.971	18.01	3.69	111.8
HIPEQ1439+02	56.3	0.608	23.26	187.75	39.4	0.819	22.51	8.84	1.6
HIPEQ1439-00	63.1	0.809	22.22	78.02	60.4	0.952	20.19	10.63	9.3
HIPEQ1440+02	69.3	0.927	23.23	209.88	14.7	0.753	19.76	7.38	16.2
HIPEQ1440-00	98.5	0.946	19.63	26.04	97.7	0.923	16.98	4.26	154.0
HIPEQ1444+01a	150.6	0.847	19.28	18.48	156.6	0.691	16.53	1.22	58.7
HIPEQ1500+01	170.7	0.897	19.25	24.68	157.6	0.729	16.55	1.77	117.0
HIPEQ1504+02	13.1	0.720	21.84	22.13	36.7	0.416	19.43	1.88	7.7
HIPEQ1504-00	0.0	0.930	22.60	92.24	0.0	0.847	21.18	6.88	9.3
HIPEQ1507+01	115.4	0.815	19.85	29.63	180.0	0.292	16.69	2.27	86.6
HIPEQ1542+00	77.3	0.993	21.31	71.89	78.8	0.927	20.46	7.07	7.7
HIPEQ1544+02	83.4	0.771	22.80	86.22	133.0	0.542	19.84	4.77	4.9
HIPEQ1545+00	95.4	0.302	22.89	85.55	107.1	0.572	20.60	2.44	3.2
HIPEQ1601+01a	112.9	0.424	22.99	287.89	134.4	0.858	20.68	20.36	17.4
HIPEQ1609-00	...	...	...	...	...	...	...	...	...

Table 3.2—Continued

	Disk				Bulge				
HIPASS Name	Angle (°)	Eccentricity	I_0 (mag/□″)[a]	h (″)	Angle (°)	Eccentricity	I_0 (mag/□″)[a]	h (″)	$\tilde{\chi}^2$
HIPEQ1613-00	...	...	...	...	...	...	...	...	...
HIPEQ1614+00	0.0	0.100	22.80	113.09	0.0	0.760	21.38	6.79	7.2
HIPEQ1614-00	90.6	0.993	21.09	75.58	90.8	0.989	19.95	11.82	25.1
HIPEQ2036-04	113.7	0.740	20.51	19.81	108.2	0.723	17.24	1.37	35.4
HIPEQ2314+00	105.1	0.457	19.46	6.01	132.6	0.889	20.55	3.58	28.5
HIPEQ2324-00	...	...	...	...	...	...	...	...	...
HIPEQ2335+01	...	...	...	...	...	...	...	...	...
HIPEQ2336+00	30.9	0.656	19.57	14.24	54.5	0.670	16.10	1.40	41.4
HIPEQ2337+00	...	...	...	...	...	...	...	...	...
HIPEQ2340+01	69.5	0.923	22.72	73.78	79.8	0.873	19.61	5.27	7.9

[a]Model central surface brightness has been converted to mag/□″ and corrected for Milky Way extinction using the photometric calibrations discussed in §4.5

Note. — Model fit parameters for galaxies with circular aperture photometry are not included

3.5 Petrosian Photometry

In this section, we discuss the steps followed to derive Petrosian quantities for the HIPASS/SDSS sample. As discussed in Appendix A, Petrosian (1976) photometry recovers most of the galaxy flux for a variety of morphological types and is robust against most changes in the surface brightness profile. This photometric method has fewer biases than when measuring total galaxy flux with apertures based on isophotes or fractions of the central surface brightness. A modified Petrosian photometric systems has been adopted by SDSS.

Petrosian quantities were adopted for this thesis to be consistent with SDSS photometry and compare our results to the greater SDSS sample. As discussed in Appendix A, there are significant problems with the circular apertures that the SDSS photometric pipeline uses to extract Petrosian quantities. We have remedied this problem by allowing for elliptical apertures in our Petrosian photometric pipeline. For the galaxies with high quality Sérsic fits, we adapt the SDSS photometric methods to include elliptically shaped photometric apertures. We also measure every galaxy with a circular aperture for comparison with standard SDSS outputs. These circular measurements are adopted for galaxies whose Sérsic fits were of poor quality. They also provide empirical constraints on how the inclination of a galaxy affects the derived Petrosian quantities (see Appendix A).

The first step in deriving Petrosian quantities is to calculate the Petrosian radius. Following the SDSS prescription, we define the Petrosian ratio as:

$$R_P(r) \equiv \frac{\int_{0.8r}^{1.25r} dr' 2\pi r' I(r') / [\pi(1.25^2 - 0.8^2) r^2]}{\int_0^r dr' 2\pi r' I(r') / (\pi r^2)} \tag{3.4}$$

where $I(r)$ is the azimuthally averaged surface brightness profile. We perform the integration by taking 1 pixel steps and calculating the subsequent Petrosian ratio at every pixel from the galaxy center. In the SDSS pipeline, the Petrosian radius r_P is defined as the radius at which $R_P(r)$ is equal to 0.2 (see Blanton et al. 2001, Yasuda et al. 2001). The Petrosian flux f_P in any band is defined as the flux within 2.0 Petrosian radii:

$$f_P \equiv \int_0^{2r_P} 2\pi r' I(r') dr' \tag{3.5}$$

Our method differs from the SDSS method in that we use both elliptical apertures

defining the elliptical r as described in Equation 3.2, in addition to the standard SDSS circular apertures.

To correctly measure colors of the galaxies, it is important that magnitude determination for all five bands use the *same* aperture. Mimicking SDSS, we use the derived r-band aperture for all bands. Once the Petrosian flux is measured using the r-band aperture, other Petrosian quantities can be measured in each band independently.

In some cases the Petrosian radius is so large that the derived aperture (r_P) far exceeds the observed boundaries of the galaxy. In these cases, large amounts of sky pixels are included in the galaxy flux. Although, in the perfect case, the summation of all sky pixels is zero, we know from the section on sky subtraction that small residuals exist. Therefore, as Petrosian radius increases, so does the error from the sky subtraction residuals. Due to their uncertain, irregular surface brightness profiles, most of the cases where the Petrosian radius is exceedingly large are LSB galaxies. The resulting flux errors are particularly large for these LSB systems because the integrated sky subtraction residuals can be a large fraction of the total galaxy flux. A similar problem is present in the SDSS photometric pipeline (Lupton, private communication). SDSS corrects for this by using the statistically defined edges of atlas images as the maximum possible photometric boundaries. We impose a similar maximum size for the Petrosian radius using the masks created in sky subtraction for each r-band image as the photometric boundaries. For most of the galaxies, the integration of Petrosian magnitudes rarely reaches the mask boundaries, indicating that the galaxy flux is correctly masked out in the sky determination. The only galaxies that reach the mask boundary are the very LSB galaxies (29% of the HIPASS/SDSS sample), whose Petrosian radius is not well defined (Lupton, private communication).

Once a Petrosian flux is calculated, we convert all fluxes to asinh magnitudes (or "Luptitudes" as they are affectionately known; Lupton, Gunn & Szalay 1999) using the relation:

$$mag = -\frac{2.5}{\ln(10)}\left[\text{asinh}\left(\left(\frac{f}{f_0}\right)/2b\right) + \ln(b)\right] \tag{3.6}$$

where b is the softening parameter (a constant for each filter) and $\frac{f}{f_0}$ is given by:

$$\frac{f}{f_0} = \frac{counts}{exptime} 10^{0.4(aa+kk\times airmass)}. \tag{3.7}$$

Here the aa is the m_{zp}, measured for each field, the kk is the extinction coefficient in magnitudes, and the exposure time is the standard SDSS value of 53.907456 seconds. The values for the *airmass*, aa, and kk were all pulled from the corresponding `tsField` files. Asinh magnitudes were computed for both the elliptical and circular apertures. The resulting magnitudes, calculated using each method (elliptical and circular apertures) can be found in Tables 3.3 and 3.4 respectively.

For most of the galaxies in the HIPASS/SDSS sample, the main contribution to the photometric uncertainty is dominated by the Poisson noise of the subtracted sky. The Poisson variable for CCD photometry is photo_electrons. We convert from counts to photo_electrons using the following relation:

$$photo\_electrons = counts \times gain \tag{3.8}$$

where the *gain* is a variable quantity that is also stored for each filter in each `field` in the `tsField` files.

The photometric error is then derived to be:

$$error(counts) = \sqrt{\frac{counts + sky}{gain} + N_{pix}(dark\_variance + skyErr)} \tag{3.9}$$

where *counts* is the galaxy flux in counts, *sky* is the integrated sky flux in the object aperture, N_{pix} is the number of pixels in the object aperture, *dark_variance* is a combination of the dark current and the read noise per pixel that is found in the `tsField` files and significantly varies from field to field and filter to filter. The *skyErr* term is the maximum residual from sky subtraction in each of the five band passes. The uncertainties from Equation 3.9 (in counts) are then converted to magnitudes using Equation 3.6.

The asinh function (or log for that matter) is not symmetric and therefore photometric errors are also not perfectly symmetric. We therefore calculate both the positive and negative errors for all photometric quantities derived in this thesis. The magnitude uncertainties are included in Tables 3.3 and 3.4. These errors do not include the uncertainty in the overall

photometric calibration, which are 2%, 3%, 2%, 2% and 3% for r, $u-g$, $g-r$, $r-i$ and $i-z$ respectively (Abazajian et al. 2005).

Table 3.3. Elliptical Petrosian Photometry of HI Selected Sources

HIPASS Name	u^a	g^a	r^a	i^a	z^a	Edge Correction[b]
HIPEQ0014-00	$14.68\pm^{0.019}_{0.020}$	$13.77\pm^{0.003}_{0.003}$	$13.39\pm^{0.003}_{0.003}$	$13.17\pm^{0.003}_{0.003}$	$13.01\pm^{0.011}_{0.011}$	...
HIPEQ0027-01a	$15.52\pm^{0.027}_{0.028}$	$14.66\pm^{0.006}_{0.006}$	$14.27\pm^{0.005}_{0.005}$	$14.09\pm^{0.007}_{0.007}$	$14.04\pm^{0.024}_{0.025}$	...
HIPEQ0033-01	$15.94\pm^{0.048}_{0.050}$	$15.06\pm^{0.011}_{0.011}$	$14.74\pm^{0.009}_{0.009}$	$14.54\pm^{0.013}_{0.013}$	$14.46\pm^{0.042}_{0.044}$	...
HIPEQ0043-00	$14.41\pm^{0.007}_{0.007}$	$13.31\pm^{0.001}_{0.001}$	$12.78\pm^{0.001}_{0.001}$	$12.50\pm^{0.001}_{0.001}$	$12.27\pm^{0.004}_{0.004}$	...
HIPEQ0051-00	$15.87\pm^{0.016}_{0.017}$	$14.91\pm^{0.002}_{0.002}$	$14.46\pm^{0.002}_{0.002}$	$14.23\pm^{0.003}_{0.003}$	$14.10\pm^{0.009}_{0.010}$	...
HIPEQ0058+00	$14.97\pm^{0.012}_{0.012}$	$13.94\pm^{0.002}_{0.002}$	$13.46\pm^{0.002}_{0.002}$	$13.20\pm^{0.002}_{0.002}$	$13.06\pm^{0.007}_{0.007}$	...
HIPEQ0107+01	$15.80\pm^{0.031}_{0.032}$	$14.96\pm^{0.005}_{0.005}$	$14.68\pm^{0.006}_{0.006}$	$14.54\pm^{0.009}_{0.009}$	$14.51\pm^{0.031}_{0.031}$	...
HIPEQ0119+00	$17.87\pm^{0.105}_{0.116}$	$17.05\pm^{0.020}_{0.020}$	$16.74\pm^{0.022}_{0.023}$	$16.60\pm^{0.034}_{0.035}$	$16.46\pm^{0.097}_{0.107}$	...
HIPEQ0120-00	$16.06\pm^{0.041}_{0.042}$	$15.19\pm^{0.007}_{0.007}$	$14.80\pm^{0.007}_{0.007}$	$14.60\pm^{0.009}_{0.009}$	$14.48\pm^{0.035}_{0.036}$	0.11
HIPEQ0122+00	$13.51\pm^{0.013}_{0.013}$	$12.68\pm^{0.002}_{0.002}$	$12.31\pm^{0.002}_{0.002}$	$12.02\pm^{0.003}_{0.003}$	$11.82\pm^{0.008}_{0.008}$	...
HIPEQ0123-00	$15.00\pm^{0.017}_{0.017}$	$14.14\pm^{0.003}_{0.003}$	$13.73\pm^{0.003}_{0.003}$	$13.49\pm^{0.004}_{0.004}$	$13.28\pm^{0.012}_{0.012}$	...
HIPEQ0126+00a	$18.57\pm^{0.255}_{0.334}$	$16.84\pm^{0.022}_{0.023}$	$16.50\pm^{0.023}_{0.024}$	$16.33\pm^{0.036}_{0.037}$	$16.31\pm^{0.111}_{0.124}$	...
HIPEQ0126-00b	$16.36\pm^{0.023}_{0.024}$	$15.72\pm^{0.004}_{0.004}$	$15.54\pm^{0.005}_{0.005}$	$15.54\pm^{0.008}_{0.008}$	$15.56\pm^{0.029}_{0.030}$	...
HIPEQ0154-00	$15.76\pm^{0.021}_{0.021}$	$14.07\pm^{0.002}_{0.002}$	$13.29\pm^{0.001}_{0.001}$	$12.88\pm^{0.001}_{0.001}$	$12.65\pm^{0.004}_{0.004}$	...
HIPEQ0222-00	$16.11\pm^{0.076}_{0.082}$	$15.04\pm^{0.009}_{0.010}$	$14.63\pm^{0.010}_{0.010}$	$14.46\pm^{0.011}_{0.011}$	$14.48\pm^{0.042}_{0.043}$	0.17
HIPEQ0228-01	$13.52\pm^{0.008}_{0.008}$	$12.66\pm^{0.002}_{0.002}$	$12.28\pm^{0.001}_{0.001}$	$12.07\pm^{0.002}_{0.002}$	$11.97\pm^{0.006}_{0.006}$	...
HIPEQ0230+00	$17.54\pm^{0.131}_{0.149}$	$15.64\pm^{0.014}_{0.014}$	$14.93\pm^{0.009}_{0.009}$	$14.51\pm^{0.011}_{0.011}$	$14.83\pm^{0.044}_{0.046}$	...
HIPEQ0230-01	$14.02\pm^{0.006}_{0.006}$	$12.44\pm^{0.001}_{0.001}$	$11.68\pm^{0.000}_{0.000}$	$11.26\pm^{0.000}_{0.000}$	$11.03\pm^{0.001}_{0.001}$	...
HIPEQ0231+00	$16.38\pm^{0.055}_{0.058}$	$15.22\pm^{0.006}_{0.006}$	$14.86\pm^{0.007}_{0.007}$	$14.68\pm^{0.009}_{0.009}$	$14.49\pm^{0.033}_{0.034}$	...
HIPEQ0236+00	$16.14\pm^{0.033}_{0.034}$	$14.95\pm^{0.004}_{0.004}$	$14.34\pm^{0.004}_{0.004}$	$13.98\pm^{0.004}_{0.004}$	$13.79\pm^{0.011}_{0.011}$	...
HIPEQ0238+00	$17.37\pm^{0.129}_{0.147}$	$16.47\pm^{0.023}_{0.023}$	$16.31\pm^{0.026}_{0.027}$	$16.16\pm^{0.040}_{0.041}$	$16.04\pm^{0.110}_{0.122}$	...
HIPEQ0240+01	$16.96\pm^{0.139}_{0.159}$	$16.15\pm^{0.023}_{0.023}$	$16.04\pm^{0.031}_{0.032}$	$15.88\pm^{0.041}_{0.042}$	$15.41\pm^{0.091}_{0.099}$	...
HIPEQ0241+00	$12.38\pm^{0.005}_{0.005}$	$11.00\pm^{0.001}_{0.001}$	$10.22\pm^{0.000}_{0.000}$	$9.81\pm^{0.000}_{0.000}$	$9.55\pm^{0.001}_{0.001}$	0.05
HIPEQ0244+00	$15.91\pm^{0.043}_{0.044}$	$15.12\pm^{0.008}_{0.008}$	$14.73\pm^{0.008}_{0.008}$	$14.50\pm^{0.011}_{0.011}$	$14.36\pm^{0.030}_{0.031}$	0.38
HIPEQ0246-00a	$13.36\pm^{0.008}_{0.009}$	$12.25\pm^{0.001}_{0.001}$	$11.67\pm^{0.001}_{0.001}$	$11.39\pm^{0.001}_{0.001}$	$11.12\pm^{0.003}_{0.003}$	...
HIPEQ0246-00b	$12.11\pm^{0.004}_{0.004}$	$11.12\pm^{0.000}_{0.000}$	$10.70\pm^{0.001}_{0.001}$	$10.48\pm^{0.001}_{0.001}$	$10.33\pm^{0.002}_{0.002}$	...
HIPEQ0249-00	$15.61\pm^{0.030}_{0.031}$	$14.48\pm^{0.003}_{0.003}$	$13.97\pm^{0.003}_{0.003}$	$13.68\pm^{0.003}_{0.003}$	$13.50\pm^{0.010}_{0.010}$	...
HIPEQ0249-00a	$16.51\pm^{0.068}_{0.073}$	$15.91\pm^{0.014}_{0.014}$	$15.73\pm^{0.017}_{0.017}$	$15.73\pm^{0.026}_{0.027}$	$15.44\pm^{0.076}_{0.081}$	...
HIPEQ0249-00b	$14.55\pm^{0.013}_{0.013}$	$13.46\pm^{0.002}_{0.002}$	$12.90\pm^{0.002}_{0.002}$	$12.57\pm^{0.002}_{0.002}$	$12.36\pm^{0.005}_{0.005}$	...
HIPEQ0251-01	$15.09\pm^{0.037}_{0.038}$	$14.34\pm^{0.009}_{0.009}$	$14.05\pm^{0.007}_{0.007}$	$13.91\pm^{0.010}_{0.010}$	$13.69\pm^{0.028}_{0.029}$	...
HIPEQ0300+00	$16.24\pm^{0.074}_{0.079}$	$15.18\pm^{0.008}_{0.008}$	$14.83\pm^{0.008}_{0.008}$	$14.64\pm^{0.010}_{0.010}$	$14.56\pm^{0.042}_{0.044}$	...
HIPEQ0301-00	$15.37\pm^{0.043}_{0.045}$	$14.84\pm^{0.007}_{0.008}$	$14.63\pm^{0.008}_{0.008}$	$14.49\pm^{0.010}_{0.010}$	$14.43\pm^{0.033}_{0.034}$	...
HIPEQ0306-00	$14.39\pm^{0.012}_{0.012}$	$12.72\pm^{0.001}_{0.001}$	$11.99\pm^{0.001}_{0.001}$	$11.59\pm^{0.001}_{0.001}$	$11.36\pm^{0.002}_{0.002}$	...
HIPEQ0316-00	$15.90\pm^{0.052}_{0.055}$	$14.46\pm^{0.004}_{0.004}$	$13.85\pm^{0.004}_{0.004}$	$13.50\pm^{0.004}_{0.004}$	$13.22\pm^{0.010}_{0.010}$	...
HIPEQ0320-06	$14.13\pm^{0.006}_{0.006}$	$13.05\pm^{0.001}_{0.001}$	$12.59\pm^{0.001}_{0.001}$	$12.33\pm^{0.001}_{0.001}$	$12.16\pm^{0.003}_{0.003}$	...
HIPEQ0351-00	$15.93\pm^{0.033}_{0.034}$	$14.80\pm^{0.003}_{0.003}$	$14.29\pm^{0.003}_{0.003}$	$14.02\pm^{0.003}_{0.003}$	$13.83\pm^{0.008}_{0.008}$	...
HIPEQ0809+00	$14.68\pm^{0.011}_{0.011}$	$13.85\pm^{0.002}_{0.002}$	$13.49\pm^{0.002}_{0.002}$	$13.33\pm^{0.003}_{0.003}$	$13.19\pm^{0.010}_{0.010}$	...
HIPEQ0821+03b	$15.08\pm^{0.010}_{0.011}$	$13.84\pm^{0.001}_{0.001}$	$13.26\pm^{0.001}_{0.001}$	$12.94\pm^{0.001}_{0.001}$	$12.72\pm^{0.004}_{0.004}$	...
HIPEQ0821-00	$15.98\pm^{0.025}_{0.026}$	$15.26\pm^{0.006}_{0.006}$	$15.11\pm^{0.007}_{0.007}$	$15.14\pm^{0.011}_{0.011}$	$14.99\pm^{0.035}_{0.036}$	...
HIPEQ0822-00	$14.99\pm^{0.014}_{0.014}$	$14.13\pm^{0.003}_{0.003}$	$13.70\pm^{0.003}_{0.003}$	$13.46\pm^{0.003}_{0.003}$	$13.25\pm^{0.010}_{0.010}$	0.03
HIPEQ0825-00	$14.49\pm^{0.012}_{0.012}$	$13.34\pm^{0.002}_{0.002}$	$12.58\pm^{0.001}_{0.001}$	$12.13\pm^{0.001}_{0.001}$	$11.77\pm^{0.003}_{0.003}$	0.01
HIPEQ0855+02	$15.46\pm^{0.051}_{0.054}$	$14.54\pm^{0.008}_{0.008}$	$14.21\pm^{0.009}_{0.009}$	$14.02\pm^{0.012}_{0.012}$	$13.91\pm^{0.041}_{0.042}$	...
HIPEQ0856+00	$14.61\pm^{0.020}_{0.021}$	$13.91\pm^{0.005}_{0.005}$	$13.67\pm^{0.006}_{0.006}$	$13.33\pm^{0.006}_{0.007}$	$13.24\pm^{0.022}_{0.022}$	...
HIPEQ0923-00	$15.19\pm^{0.017}_{0.017}$	$14.36\pm^{0.003}_{0.003}$	$14.05\pm^{0.003}_{0.003}$	$13.87\pm^{0.004}_{0.004}$	$13.75\pm^{0.013}_{0.013}$	...
HIPEQ0930+04	$14.31\pm^{0.011}_{0.011}$	$13.93\pm^{0.003}_{0.003}$	$13.43\pm^{0.002}_{0.002}$	$13.24\pm^{0.003}_{0.003}$	$12.71\pm^{0.008}_{0.008}$	...

Table 3.3—Continued

HIPASS Name	u[a]	g[a]	r[a]	i[a]	z[a]	Edge Correction[b]
HIPEQ0936+01	$17.61\pm^{0.049}_{0.051}$	$16.81\pm^{0.010}_{0.010}$	$16.62\pm^{0.011}_{0.011}$	$16.60\pm^{0.017}_{0.018}$	$16.41\pm^{0.052}_{0.054}$	...
HIPEQ0942+00	$12.62\pm^{0.004}_{0.004}$	$11.61\pm^{0.001}_{0.001}$	$11.14\pm^{0.001}_{0.001}$	$10.88\pm^{0.001}_{0.001}$	$10.66\pm^{0.002}_{0.002}$	...
HIPEQ0944-00b	$16.68\pm^{0.043}_{0.045}$	$15.73\pm^{0.007}_{0.007}$	$15.45\pm^{0.009}_{0.009}$	$15.54\pm^{0.014}_{0.014}$	$15.25\pm^{0.039}_{0.040}$	...
HIPEQ0945+01	$13.88\pm^{0.021}_{0.022}$	$12.90\pm^{0.003}_{0.003}$	$12.43\pm^{0.002}_{0.002}$	$12.20\pm^{0.003}_{0.003}$	$11.95\pm^{0.009}_{0.009}$	...
HIPEQ0946+02	$15.57\pm^{0.036}_{0.037}$	$14.74\pm^{0.009}_{0.009}$	$14.34\pm^{0.007}_{0.007}$	$14.18\pm^{0.009}_{0.009}$	$14.00\pm^{0.024}_{0.025}$	...
HIPEQ0947+00a	$14.96\pm^{0.034}_{0.035}$	$14.03\pm^{0.005}_{0.005}$	$13.61\pm^{0.005}_{0.005}$	$13.37\pm^{0.006}_{0.006}$	$13.21\pm^{0.016}_{0.017}$	...
HIPEQ0947+00b	$15.72\pm^{0.062}_{0.066}$	$15.06\pm^{0.011}_{0.011}$	$14.78\pm^{0.012}_{0.013}$	$14.77\pm^{0.018}_{0.019}$	$14.76\pm^{0.061}_{0.065}$	...
HIPEQ0953+01	$12.92\pm^{0.005}_{0.005}$	$11.99\pm^{0.001}_{0.001}$	$11.59\pm^{0.001}_{0.001}$	$11.38\pm^{0.001}_{0.001}$	$10.97\pm^{0.004}_{0.004}$	...
HIPEQ0954+01a	$18.80\pm^{0.236}_{0.302}$	$18.38\pm^{0.067}_{0.071}$	$18.13\pm^{0.088}_{0.096}$	$18.16\pm^{0.146}_{0.169}$	$17.86\pm^{0.442}_{0.757}$	...
HIPEQ0954+02a	$15.51\pm^{0.018}_{0.018}$	$14.29\pm^{0.003}_{0.003}$	$14.00\pm^{0.003}_{0.003}$	$13.69\pm^{0.005}_{0.005}$	$14.11\pm^{0.018}_{0.018}$	...
HIPEQ0955+04a	$13.18\pm^{0.005}_{0.005}$	$12.27\pm^{0.001}_{0.001}$	$11.82\pm^{0.001}_{0.001}$	$11.62\pm^{0.001}_{0.001}$	$11.42\pm^{0.003}_{0.003}$	...
HIPEQ0958+01	$17.89\pm^{0.201}_{0.246}$	$17.02\pm^{0.036}_{0.038}$	$16.95\pm^{0.054}_{0.057}$	$17.26\pm^{0.113}_{0.127}$	$17.24\pm^{0.412}_{0.672}$	...
HIPEQ1000+03	$14.77\pm^{0.011}_{0.011}$	$13.56\pm^{0.001}_{0.001}$	$12.92\pm^{0.001}_{0.001}$	$12.51\pm^{0.001}_{0.001}$	$12.23\pm^{0.003}_{0.003}$	...
HIPEQ1010+05	$16.45\pm^{0.025}_{0.026}$	$15.12\pm^{0.004}_{0.004}$	$14.67\pm^{0.004}_{0.004}$	$14.45\pm^{0.004}_{0.004}$	$14.43\pm^{0.014}_{0.014}$	...
HIPEQ1014+03	$12.17\pm^{0.004}_{0.004}$	$10.65\pm^{0.000}_{0.000}$	$9.94\pm^{0.000}_{0.000}$	$9.52\pm^{0.000}_{0.000}$	$9.29\pm^{0.001}_{0.001}$	...
HIPEQ1015+02	$15.38\pm^{0.046}_{0.048}$	$14.73\pm^{0.010}_{0.010}$	$14.50\pm^{0.012}_{0.012}$	$14.29\pm^{0.017}_{0.017}$	$14.29\pm^{0.060}_{0.064}$	...
HIPEQ1026+03	$14.27\pm^{0.012}_{0.013}$	$13.20\pm^{0.002}_{0.002}$	$12.88\pm^{0.002}_{0.002}$	$12.72\pm^{0.002}_{0.002}$	$12.31\pm^{0.007}_{0.007}$	...
HIPEQ1028+03	$16.26\pm^{0.042}_{0.044}$	$15.29\pm^{0.009}_{0.009}$	$15.19\pm^{0.010}_{0.010}$	$15.01\pm^{0.012}_{0.012}$	$14.80\pm^{0.032}_{0.033}$	...
HIPEQ1031+04	$14.68\pm^{0.018}_{0.018}$	$13.65\pm^{0.003}_{0.003}$	$13.47\pm^{0.004}_{0.004}$	$13.12\pm^{0.004}_{0.004}$	$13.71\pm^{0.019}_{0.019}$	0.89
HIPEQ1039+01	$15.48\pm^{0.022}_{0.023}$	$14.52\pm^{0.003}_{0.003}$	$14.15\pm^{0.004}_{0.004}$	$13.91\pm^{0.004}_{0.004}$	$13.80\pm^{0.016}_{0.017}$	0.01
HIPEQ1041+00	$15.31\pm^{0.016}_{0.016}$	$14.55\pm^{0.003}_{0.003}$	$14.18\pm^{0.004}_{0.004}$	$13.93\pm^{0.005}_{0.005}$	$13.81\pm^{0.015}_{0.015}$	...
HIPEQ1046+01	$13.84\pm^{0.015}_{0.015}$	$12.85\pm^{0.002}_{0.002}$	$12.36\pm^{0.002}_{0.002}$	$12.16\pm^{0.003}_{0.003}$	$11.68\pm^{0.010}_{0.010}$	...
HIPEQ1050+01	$18.23\pm^{0.134}_{0.153}$	$17.13\pm^{0.027}_{0.027}$	$16.67\pm^{0.023}_{0.023}$	$16.57\pm^{0.034}_{0.035}$	$16.86\pm^{0.150}_{0.175}$	...
HIPEQ1051+04a	$14.76\pm^{0.018}_{0.018}$	$14.08\pm^{0.003}_{0.003}$	$13.70\pm^{0.004}_{0.004}$	$13.59\pm^{0.005}_{0.005}$	$13.47\pm^{0.019}_{0.019}$	...
HIPEQ1052+00	$16.06\pm^{0.012}_{0.012}$	$15.27\pm^{0.002}_{0.002}$	$14.99\pm^{0.003}_{0.003}$	$14.85\pm^{0.004}_{0.004}$	$14.71\pm^{0.014}_{0.014}$	...
HIPEQ1053+02	$15.82\pm^{0.023}_{0.024}$	$15.51\pm^{0.006}_{0.006}$	$15.35\pm^{0.008}_{0.008}$	$15.23\pm^{0.012}_{0.013}$	$15.24\pm^{0.044}_{0.046}$	...
HIPEQ1055+02	$16.60\pm^{0.035}_{0.036}$	$15.95\pm^{0.007}_{0.007}$	$15.81\pm^{0.009}_{0.009}$	$15.82\pm^{0.015}_{0.015}$	$15.76\pm^{0.065}_{0.069}$	...
HIPEQ1101+03	$12.73\pm^{0.007}_{0.007}$	$11.74\pm^{0.001}_{0.001}$	$11.35\pm^{0.001}_{0.001}$	$11.03\pm^{0.001}_{0.001}$	$10.78\pm^{0.002}_{0.002}$	...
HIPEQ1109-00	$15.32\pm^{0.011}_{0.012}$	$14.12\pm^{0.002}_{0.002}$	$13.52\pm^{0.002}_{0.002}$	$13.20\pm^{0.002}_{0.002}$	$12.99\pm^{0.006}_{0.006}$	...
HIPEQ1110+01	$16.45\pm^{0.036}_{0.038}$	$15.62\pm^{0.007}_{0.007}$	$15.35\pm^{0.008}_{0.008}$	$15.30\pm^{0.013}_{0.013}$	$15.27\pm^{0.046}_{0.048}$	...
HIPEQ1113+05	$15.49\pm^{0.021}_{0.021}$	$14.46\pm^{0.004}_{0.004}$	$14.28\pm^{0.004}_{0.004}$	$14.08\pm^{0.005}_{0.005}$	$14.48\pm^{0.018}_{0.018}$	...
HIPEQ1117+04a	$13.68\pm^{0.005}_{0.005}$	$12.51\pm^{0.001}_{0.001}$	$11.95\pm^{0.001}_{0.001}$	$11.67\pm^{0.001}_{0.001}$	$11.47\pm^{0.002}_{0.002}$	0.17
HIPEQ1119+02	$14.07\pm^{0.017}_{0.018}$	$13.52\pm^{0.004}_{0.004}$	$13.32\pm^{0.005}_{0.005}$	$13.12\pm^{0.006}_{0.006}$	$13.16\pm^{0.030}_{0.030}$	...
HIPEQ1124+03	$13.52\pm^{0.010}_{0.010}$	$12.91\pm^{0.002}_{0.002}$	$12.69\pm^{0.002}_{0.002}$	$12.55\pm^{0.004}_{0.004}$	$12.38\pm^{0.011}_{0.011}$	...
HIPEQ1127-01	$15.21\pm^{0.018}_{0.018}$	$14.37\pm^{0.004}_{0.004}$	$14.01\pm^{0.004}_{0.004}$	$13.80\pm^{0.006}_{0.006}$	$13.47\pm^{0.015}_{0.015}$	...
HIPEQ1131-02	$13.94\pm^{0.010}_{0.011}$	$13.05\pm^{0.002}_{0.002}$	$12.61\pm^{0.002}_{0.002}$	$12.34\pm^{0.002}_{0.002}$	$12.19\pm^{0.009}_{0.009}$	...
HIPEQ1133-03	$15.37\pm^{0.021}_{0.021}$	$14.58\pm^{0.005}_{0.005}$	$14.30\pm^{0.005}_{0.005}$	$14.11\pm^{0.007}_{0.007}$	$13.97\pm^{0.022}_{0.022}$	...
HIPEQ1136+00	$15.46\pm^{0.008}_{0.008}$	$14.71\pm^{0.002}_{0.002}$	$14.60\pm^{0.003}_{0.003}$	$14.57\pm^{0.004}_{0.004}$	$14.58\pm^{0.014}_{0.014}$	...
HIPEQ1138+03	$15.58\pm^{0.023}_{0.023}$	$14.35\pm^{0.003}_{0.003}$	$13.77\pm^{0.002}_{0.002}$	$13.46\pm^{0.003}_{0.003}$	$13.27\pm^{0.009}_{0.009}$	...
HIPEQ1143-01	$18.19\pm^{0.143}_{0.164}$	$17.51\pm^{0.030}_{0.031}$	$17.25\pm^{0.039}_{0.041}$	$17.16\pm^{0.060}_{0.063}$	$17.19\pm^{0.210}_{0.260}$	...
HIPEQ1145+02	$17.50\pm^{0.177}_{0.212}$	$17.00\pm^{0.045}_{0.047}$	$16.74\pm^{0.054}_{0.057}$	$16.87\pm^{0.100}_{0.111}$	$18.89\pm^{1.384}_{8.302}$	...
HIPEQ1148-02	$14.67\pm^{0.021}_{0.021}$	$13.83\pm^{0.004}_{0.004}$	$13.51\pm^{0.005}_{0.005}$	$13.24\pm^{0.006}_{0.006}$	$13.23\pm^{0.020}_{0.021}$	0.05
HIPEQ1151-02	$16.12\pm^{0.015}_{0.016}$	$15.07\pm^{0.003}_{0.003}$	$14.66\pm^{0.003}_{0.003}$	$14.47\pm^{0.004}_{0.004}$	$14.33\pm^{0.014}_{0.014}$	...
HIPEQ1152+01	$14.97\pm^{0.014}_{0.014}$	$14.14\pm^{0.002}_{0.002}$	$13.79\pm^{0.003}_{0.003}$	$13.58\pm^{0.003}_{0.003}$	$13.46\pm^{0.012}_{0.012}$	...
HIPEQ1152-02	$14.83\pm^{0.006}_{0.006}$	$14.29\pm^{0.001}_{0.001}$	$14.25\pm^{0.002}_{0.002}$	$14.42\pm^{0.004}_{0.004}$	$14.45\pm^{0.017}_{0.017}$	...

Table 3.3—Continued

HIPASS Name	u^a	g^a	r^a	i^a	z^a	Edge Correction[b]
HIPEQ1152-03b	$15.22\pm^{0.024}_{0.024}$	$14.35\pm^{0.005}_{0.005}$	$14.09\pm^{0.005}_{0.005}$	$13.93\pm^{0.008}_{0.008}$	$13.84\pm^{0.025}_{0.025}$	···
HIPEQ1155+01	$14.16\pm^{0.013}_{0.013}$	$13.08\pm^{0.002}_{0.002}$	$12.61\pm^{0.002}_{0.002}$	$12.38\pm^{0.003}_{0.003}$	$12.14\pm^{0.007}_{0.007}$	···
HIPEQ1200-00	$15.92\pm^{0.049}_{0.051}$	$15.03\pm^{0.010}_{0.010}$	$14.64\pm^{0.011}_{0.011}$	$14.40\pm^{0.013}_{0.014}$	$14.43\pm^{0.052}_{0.054}$	···
HIPEQ1200-01	$11.76\pm^{0.002}_{0.002}$	$10.62\pm^{0.000}_{0.000}$	$10.03\pm^{0.000}_{0.000}$	$9.69\pm^{0.000}_{0.000}$	$9.46\pm^{0.001}_{0.001}$	···
HIPEQ1202+01	$13.60\pm^{0.010}_{0.010}$	$12.19\pm^{0.001}_{0.001}$	$11.48\pm^{0.001}_{0.001}$	$11.08\pm^{0.001}_{0.001}$	$10.79\pm^{0.002}_{0.002}$	···
HIPEQ1204-01	$15.93\pm^{0.057}_{0.060}$	$15.37\pm^{0.013}_{0.013}$	$15.05\pm^{0.015}_{0.015}$	$14.97\pm^{0.023}_{0.024}$	$14.72\pm^{0.066}_{0.071}$	···
HIPEQ1204-02	$15.66\pm^{0.019}_{0.019}$	$14.28\pm^{0.002}_{0.002}$	$13.66\pm^{0.002}_{0.002}$	$13.32\pm^{0.002}_{0.002}$	$13.08\pm^{0.007}_{0.007}$	···
HIPEQ1210+02	$16.09\pm^{0.087}_{0.095}$	$15.27\pm^{0.014}_{0.014}$	$14.91\pm^{0.016}_{0.016}$	$14.77\pm^{0.022}_{0.023}$	$14.54\pm^{0.070}_{0.075}$	···
HIPEQ1215+04a	$15.69\pm^{0.018}_{0.018}$	$14.74\pm^{0.003}_{0.003}$	$14.46\pm^{0.004}_{0.004}$	$14.32\pm^{0.005}_{0.005}$	$14.25\pm^{0.020}_{0.021}$	···
HIPEQ1216-03	$15.25\pm^{0.017}_{0.018}$	$14.38\pm^{0.004}_{0.004}$	$13.97\pm^{0.003}_{0.003}$	$13.75\pm^{0.005}_{0.005}$	$13.49\pm^{0.013}_{0.013}$	···
HIPEQ1218+00	$16.01\pm^{0.050}_{0.052}$	$15.13\pm^{0.010}_{0.010}$	$14.69\pm^{0.010}_{0.010}$	$14.59\pm^{0.016}_{0.016}$	$14.54\pm^{0.048}_{0.051}$	···
HIPEQ1218-01	$15.47\pm^{0.014}_{0.014}$	$14.22\pm^{0.002}_{0.002}$	$13.64\pm^{0.002}_{0.002}$	$13.33\pm^{0.002}_{0.002}$	$13.14\pm^{0.006}_{0.006}$	···
HIPEQ1219+03	$14.84\pm^{0.010}_{0.010}$	$14.00\pm^{0.002}_{0.002}$	$13.65\pm^{0.002}_{0.002}$	$13.53\pm^{0.003}_{0.003}$	$13.37\pm^{0.010}_{0.010}$	···
HIPEQ1220+00	$16.53\pm^{0.040}_{0.041}$	$15.64\pm^{0.007}_{0.007}$	$15.49\pm^{0.010}_{0.010}$	$15.40\pm^{0.014}_{0.014}$	$15.39\pm^{0.063}_{0.067}$	···
HIPEQ1220+01	$15.77\pm^{0.044}_{0.046}$	$14.74\pm^{0.008}_{0.008}$	$14.33\pm^{0.007}_{0.007}$	$14.11\pm^{0.010}_{0.011}$	$13.96\pm^{0.034}_{0.036}$	···
HIPEQ1221+03	$15.17\pm^{0.019}_{0.020}$	$14.07\pm^{0.003}_{0.003}$	$13.30\pm^{0.002}_{0.002}$	$12.85\pm^{0.002}_{0.002}$	$12.46\pm^{0.006}_{0.006}$	···
HIPEQ1223+00	$16.16\pm^{0.052}_{0.054}$	$15.49\pm^{0.013}_{0.013}$	$15.21\pm^{0.015}_{0.015}$	$15.11\pm^{0.023}_{0.023}$	$14.93\pm^{0.062}_{0.065}$	···
HIPEQ1223-03b	$13.99\pm^{0.008}_{0.008}$	$12.66\pm^{0.001}_{0.001}$	$11.96\pm^{0.001}_{0.001}$	$11.54\pm^{0.001}_{0.001}$	$11.25\pm^{0.003}_{0.003}$	···
HIPEQ1224+00	$17.94\pm^{0.114}_{0.127}$	$17.11\pm^{0.023}_{0.023}$	$16.77\pm^{0.026}_{0.026}$	$16.67\pm^{0.037}_{0.038}$	$16.62\pm^{0.153}_{0.178}$	···
HIPEQ1224+03b	$14.75\pm^{0.021}_{0.022}$	$13.87\pm^{0.004}_{0.004}$	$13.55\pm^{0.004}_{0.004}$	$13.36\pm^{0.007}_{0.007}$	$13.28\pm^{0.022}_{0.023}$	···
HIPEQ1225+00	$13.77\pm^{0.005}_{0.005}$	$12.75\pm^{0.001}_{0.001}$	$12.20\pm^{0.001}_{0.001}$	$11.92\pm^{0.001}_{0.001}$	$11.69\pm^{0.003}_{0.003}$	···
HIPEQ1226+02	$13.43\pm^{0.004}_{0.004}$	$12.45\pm^{0.001}_{0.001}$	$12.01\pm^{0.001}_{0.001}$	$11.79\pm^{0.001}_{0.001}$	$11.59\pm^{0.003}_{0.003}$	0.09
HIPEQ1227+01	$16.79\pm^{0.087}_{0.094}$	$16.36\pm^{0.028}_{0.029}$	$16.24\pm^{0.033}_{0.034}$	$16.25\pm^{0.057}_{0.060}$	$16.03\pm^{0.168}_{0.198}$	···
HIPEQ1228+02	$15.27\pm^{0.034}_{0.036}$	$14.44\pm^{0.006}_{0.006}$	$14.13\pm^{0.007}_{0.007}$	$13.95\pm^{0.010}_{0.010}$	$13.83\pm^{0.041}_{0.043}$	···
HIPEQ1228+03	$12.74\pm^{0.003}_{0.003}$	$11.17\pm^{0.000}_{0.000}$	$10.48\pm^{0.000}_{0.000}$	$10.11\pm^{0.000}_{0.000}$	$9.87\pm^{0.001}_{0.001}$	···
HIPEQ1229+00	$17.57\pm^{0.102}_{0.112}$	$16.61\pm^{0.017}_{0.017}$	$16.19\pm^{0.018}_{0.018}$	$16.15\pm^{0.027}_{0.028}$	$16.22\pm^{0.099}_{0.109}$	···
HIPEQ1230+02	$16.19\pm^{0.046}_{0.048}$	$15.32\pm^{0.008}_{0.008}$	$15.13\pm^{0.010}_{0.010}$	$15.03\pm^{0.015}_{0.015}$	$15.02\pm^{0.070}_{0.074}$	···
HIPEQ1230+03	$16.33\pm^{0.023}_{0.023}$	$15.56\pm^{0.004}_{0.004}$	$15.38\pm^{0.005}_{0.005}$	$15.27\pm^{0.008}_{0.008}$	$15.24\pm^{0.029}_{0.030}$	···
HIPEQ1232+00a	$13.78\pm^{0.012}_{0.012}$	$12.80\pm^{0.002}_{0.002}$	$12.41\pm^{0.002}_{0.002}$	$12.20\pm^{0.003}_{0.003}$	$12.17\pm^{0.013}_{0.013}$	0.01
HIPEQ1232+00b	$12.01\pm^{0.004}_{0.004}$	$10.91\pm^{0.001}_{0.001}$	$10.24\pm^{0.000}_{0.000}$	$9.84\pm^{0.001}_{0.001}$	$9.49\pm^{0.002}_{0.002}$	···
HIPEQ1233-02	$15.49\pm^{0.042}_{0.044}$	$14.81\pm^{0.010}_{0.010}$	$14.41\pm^{0.012}_{0.012}$	$14.26\pm^{0.016}_{0.017}$	$14.28\pm^{0.066}_{0.071}$	···
HIPEQ1236+03	$16.53\pm^{0.063}_{0.066}$	$15.79\pm^{0.013}_{0.013}$	$15.50\pm^{0.015}_{0.015}$	$15.34\pm^{0.024}_{0.024}$	$15.27\pm^{0.076}_{0.082}$	···
HIPEQ1239-00	$12.84\pm^{0.004}_{0.004}$	$11.99\pm^{0.001}_{0.001}$	$11.64\pm^{0.001}_{0.001}$	$11.47\pm^{0.001}_{0.001}$	$11.35\pm^{0.003}_{0.003}$	0.06
HIPEQ1241+01	$15.67\pm^{0.014}_{0.014}$	$14.65\pm^{0.003}_{0.003}$	$14.20\pm^{0.002}_{0.002}$	$13.94\pm^{0.003}_{0.003}$	$13.76\pm^{0.010}_{0.010}$	···
HIPEQ1241-02	$15.45\pm^{0.019}_{0.019}$	$14.46\pm^{0.003}_{0.003}$	$14.00\pm^{0.003}_{0.003}$	$13.71\pm^{0.004}_{0.004}$	$13.51\pm^{0.012}_{0.013}$	···
HIPEQ1242+03b	$13.64\pm^{0.006}_{0.006}$	$12.64\pm^{0.001}_{0.001}$	$12.09\pm^{0.001}_{0.001}$	$11.80\pm^{0.001}_{0.001}$	$11.63\pm^{0.003}_{0.003}$	···
HIPEQ1242-00	$12.91\pm^{0.004}_{0.004}$	$11.91\pm^{0.001}_{0.001}$	$11.45\pm^{0.001}_{0.001}$	$11.22\pm^{0.001}_{0.001}$	$10.97\pm^{0.002}_{0.002}$	···
HIPEQ1242-01a	$14.54\pm^{0.012}_{0.012}$	$13.76\pm^{0.002}_{0.002}$	$13.45\pm^{0.003}_{0.003}$	$13.24\pm^{0.004}_{0.004}$	$13.05\pm^{0.012}_{0.012}$	···
HIPEQ1242-01b	$14.88\pm^{0.019}_{0.019}$	$13.70\pm^{0.002}_{0.002}$	$13.19\pm^{0.002}_{0.003}$	$12.92\pm^{0.003}_{0.003}$	$12.78\pm^{0.010}_{0.011}$	0.39
HIPEQ1243-00	$13.39\pm^{0.007}_{0.007}$	$12.46\pm^{0.001}_{0.001}$	$12.04\pm^{0.001}_{0.001}$	$11.76\pm^{0.002}_{0.002}$	$11.56\pm^{0.004}_{0.004}$	···
HIPEQ1244+00	$14.32\pm^{0.014}_{0.014}$	$13.41\pm^{0.003}_{0.003}$	$13.14\pm^{0.003}_{0.003}$	$13.39\pm^{0.007}_{0.007}$	$12.89\pm^{0.014}_{0.015}$	···
HIPEQ1244-02	$15.59\pm^{0.040}_{0.041}$	$14.88\pm^{0.008}_{0.008}$	$14.63\pm^{0.010}_{0.010}$	$14.54\pm^{0.016}_{0.016}$	$14.38\pm^{0.061}_{0.065}$	···
HIPEQ1245-00	$12.24\pm^{0.003}_{0.003}$	$10.98\pm^{0.000}_{0.000}$	$10.25\pm^{0.000}_{0.000}$	$9.83\pm^{0.000}_{0.000}$	$9.53\pm^{0.001}_{0.001}$	···
HIPEQ1249+03	$13.40\pm^{0.004}_{0.005}$	$12.49\pm^{0.001}_{0.001}$	$12.11\pm^{0.001}_{0.001}$	$11.91\pm^{0.001}_{0.001}$	$11.78\pm^{0.003}_{0.003}$	···
HIPEQ1249+04	$16.01\pm^{0.036}_{0.037}$	$15.08\pm^{0.007}_{0.007}$	$14.85\pm^{0.009}_{0.009}$	$14.72\pm^{0.013}_{0.013}$	$15.35\pm^{0.061}_{0.064}$	···

Table 3.3—Continued

HIPASS Name	u^a	g^a	r^a	i^a	z^a	Edge Correction[b]
HIPEQ1250+05	$12.55\pm^{0.003}_{0.003}$	$11.84\pm^{0.001}_{0.001}$	$11.53\pm^{0.001}_{0.001}$	$11.41\pm^{0.001}_{0.001}$	$11.21\pm^{0.003}_{0.003}$	···
HIPEQ1253+01	$13.55\pm^{0.009}_{0.009}$	$12.32\pm^{0.001}_{0.001}$	$11.67\pm^{0.001}_{0.001}$	$11.29\pm^{0.001}_{0.001}$	$11.01\pm^{0.003}_{0.004}$	···
HIPEQ1253+02	$13.11\pm^{0.008}_{0.008}$	$11.58\pm^{0.001}_{0.001}$	$10.87\pm^{0.001}_{0.001}$	$10.47\pm^{0.001}_{0.001}$	$10.21\pm^{0.002}_{0.002}$	···
HIPEQ1253+04	$13.88\pm^{0.004}_{0.004}$	$13.05\pm^{0.001}_{0.001}$	$12.75\pm^{0.001}_{0.001}$	$12.63\pm^{0.001}_{0.001}$	$12.56\pm^{0.003}_{0.003}$	···
HIPEQ1255+00	$13.38\pm^{0.007}_{0.007}$	$12.45\pm^{0.001}_{0.001}$	$12.00\pm^{0.001}_{0.001}$	$11.78\pm^{0.002}_{0.002}$	$11.68\pm^{0.006}_{0.006}$	···
HIPEQ1255+02	$14.78\pm^{0.009}_{0.009}$	$13.39\pm^{0.001}_{0.001}$	$12.72\pm^{0.001}_{0.001}$	$12.34\pm^{0.001}_{0.001}$	$12.09\pm^{0.003}_{0.003}$	···
HIPEQ1255-00	$16.46\pm^{0.060}_{0.063}$	$15.62\pm^{0.012}_{0.012}$	$15.23\pm^{0.013}_{0.013}$	$15.06\pm^{0.017}_{0.018}$	$14.90\pm^{0.057}_{0.061}$	···
HIPEQ1256+03	$16.76\pm^{0.099}_{0.109}$	$15.85\pm^{0.016}_{0.017}$	$15.77\pm^{0.021}_{0.022}$	$15.77\pm^{0.031}_{0.032}$	$16.07\pm^{0.147}_{0.169}$	···
HIPEQ1257+02	$15.71\pm^{0.038}_{0.039}$	$15.11\pm^{0.008}_{0.008}$	$14.82\pm^{0.009}_{0.010}$	$14.71\pm^{0.015}_{0.015}$	$14.56\pm^{0.060}_{0.063}$	···
HIPEQ1257-01	$14.73\pm^{0.010}_{0.010}$	$13.73\pm^{0.002}_{0.002}$	$13.22\pm^{0.002}_{0.002}$	$12.94\pm^{0.003}_{0.003}$	$12.76\pm^{0.008}_{0.008}$	···
HIPEQ1258+02	$15.11\pm^{0.033}_{0.034}$	$14.14\pm^{0.005}_{0.005}$	$13.81\pm^{0.006}_{0.006}$	$13.59\pm^{0.008}_{0.008}$	$13.45\pm^{0.032}_{0.033}$	···
HIPEQ1300+02a	$15.65\pm^{0.031}_{0.032}$	$14.53\pm^{0.004}_{0.004}$	$14.12\pm^{0.005}_{0.005}$	$13.93\pm^{0.006}_{0.006}$	$13.80\pm^{0.023}_{0.024}$	0.28
HIPEQ1300+02b	$12.36\pm^{0.003}_{0.003}$	$11.49\pm^{0.001}_{0.001}$	$11.08\pm^{0.001}_{0.001}$	$10.80\pm^{0.001}_{0.001}$	$10.55\pm^{0.003}_{0.003}$	···
HIPEQ1303+03	$15.17\pm^{0.025}_{0.026}$	$14.30\pm^{0.006}_{0.006}$	$14.03\pm^{0.005}_{0.005}$	$13.86\pm^{0.007}_{0.007}$	$13.82\pm^{0.022}_{0.022}$	···
HIPEQ1304-02	$16.88\pm^{0.044}_{0.046}$	$16.01\pm^{0.008}_{0.008}$	$15.55\pm^{0.009}_{0.009}$	$15.41\pm^{0.012}_{0.012}$	$15.50\pm^{0.050}_{0.052}$	1.37
HIPEQ1304-03	$13.61\pm^{0.011}_{0.011}$	$12.76\pm^{0.002}_{0.002}$	$12.52\pm^{0.003}_{0.003}$	$12.41\pm^{0.004}_{0.004}$	$12.44\pm^{0.014}_{0.014}$	0.01
HIPEQ1307-00	$14.53\pm^{0.007}_{0.007}$	$13.64\pm^{0.002}_{0.002}$	$13.29\pm^{0.002}_{0.002}$	$13.12\pm^{0.002}_{0.002}$	$12.99\pm^{0.006}_{0.006}$	···
HIPEQ1308-02	$15.00\pm^{0.013}_{0.013}$	$14.00\pm^{0.002}_{0.002}$	$13.57\pm^{0.002}_{0.002}$	$13.37\pm^{0.003}_{0.003}$	$13.11\pm^{0.012}_{0.012}$	0.03
HIPEQ1311+03a	$16.50\pm^{0.031}_{0.032}$	$15.56\pm^{0.005}_{0.005}$	$15.24\pm^{0.005}_{0.005}$	$15.09\pm^{0.008}_{0.008}$	$14.95\pm^{0.026}_{0.027}$	···
HIPEQ1312+03	$16.16\pm^{0.024}_{0.025}$	$14.73\pm^{0.003}_{0.003}$	$14.17\pm^{0.002}_{0.002}$	$13.87\pm^{0.003}_{0.003}$	$13.69\pm^{0.010}_{0.010}$	···
HIPEQ1312+05	$17.46\pm^{0.103}_{0.114}$	$16.43\pm^{0.018}_{0.018}$	$16.21\pm^{0.022}_{0.022}$	$16.07\pm^{0.033}_{0.034}$	$16.47\pm^{0.150}_{0.174}$	···
HIPEQ1313+06	$15.12\pm^{0.016}_{0.016}$	$13.86\pm^{0.002}_{0.002}$	$13.31\pm^{0.002}_{0.002}$	$13.02\pm^{0.002}_{0.002}$	$12.81\pm^{0.005}_{0.005}$	···
HIPEQ1317-00	$16.32\pm^{0.029}_{0.030}$	$15.65\pm^{0.008}_{0.008}$	$15.55\pm^{0.010}_{0.010}$	$15.61\pm^{0.017}_{0.017}$	$15.54\pm^{0.053}_{0.056}$	···
HIPEQ1318-01	$14.74\pm^{0.013}_{0.013}$	$13.81\pm^{0.002}_{0.002}$	$13.30\pm^{0.002}_{0.002}$	$13.00\pm^{0.003}_{0.003}$	$12.72\pm^{0.008}_{0.008}$	···
HIPEQ1320+05	$15.51\pm^{0.031}_{0.032}$	$14.87\pm^{0.006}_{0.006}$	$14.43\pm^{0.006}_{0.006}$	$14.30\pm^{0.008}_{0.008}$	$13.61\pm^{0.025}_{0.025}$	···
HIPEQ1327+02	$17.12\pm^{0.078}_{0.084}$	$16.30\pm^{0.014}_{0.014}$	$16.12\pm^{0.018}_{0.019}$	$16.12\pm^{0.030}_{0.031}$	$16.06\pm^{0.116}_{0.130}$	···
HIPEQ1329-00	$16.66\pm^{0.048}_{0.050}$	$15.84\pm^{0.010}_{0.010}$	$15.46\pm^{0.011}_{0.011}$	$15.32\pm^{0.015}_{0.015}$	$15.12\pm^{0.048}_{0.050}$	···
HIPEQ1332+01	$14.87\pm^{0.014}_{0.014}$	$13.62\pm^{0.002}_{0.002}$	$13.02\pm^{0.001}_{0.001}$	$12.68\pm^{0.002}_{0.002}$	$12.46\pm^{0.005}_{0.005}$	···
HIPEQ1335+01	$14.67\pm^{0.015}_{0.015}$	$13.48\pm^{0.002}_{0.002}$	$12.95\pm^{0.002}_{0.002}$	$12.65\pm^{0.002}_{0.002}$	$12.47\pm^{0.008}_{0.008}$	···
HIPEQ1341+05	$15.67\pm^{0.023}_{0.024}$	$14.65\pm^{0.003}_{0.003}$	$14.29\pm^{0.004}_{0.004}$	$14.08\pm^{0.004}_{0.004}$	$13.98\pm^{0.018}_{0.018}$	1.03
HIPEQ1348+03	$13.05\pm^{0.006}_{0.006}$	$11.99\pm^{0.001}_{0.001}$	$11.54\pm^{0.001}_{0.001}$	$11.28\pm^{0.001}_{0.001}$	$10.89\pm^{0.004}_{0.004}$	···
HIPEQ1352+02a	$14.34\pm^{0.017}_{0.017}$	$13.07\pm^{0.002}_{0.002}$	$12.41\pm^{0.002}_{0.002}$	$12.06\pm^{0.002}_{0.002}$	$11.82\pm^{0.006}_{0.006}$	···
HIPEQ1352-01	$13.00\pm^{0.006}_{0.006}$	$11.98\pm^{0.001}_{0.001}$	$11.54\pm^{0.001}_{0.001}$	$11.25\pm^{0.001}_{0.001}$	$11.15\pm^{0.004}_{0.004}$	···
HIPEQ1400+02	$15.58\pm^{0.032}_{0.033}$	$14.58\pm^{0.005}_{0.005}$	$14.16\pm^{0.005}_{0.005}$	$13.94\pm^{0.006}_{0.006}$	$13.71\pm^{0.020}_{0.021}$	···
HIPEQ1411-01	$13.55\pm^{0.010}_{0.010}$	$12.61\pm^{0.002}_{0.002}$	$12.28\pm^{0.002}_{0.002}$	$12.18\pm^{0.003}_{0.003}$	$11.99\pm^{0.008}_{0.008}$	···
HIPEQ1415+04	$15.49\pm^{0.016}_{0.016}$	$15.01\pm^{0.003}_{0.003}$	$14.68\pm^{0.004}_{0.004}$	$14.44\pm^{0.005}_{0.005}$	$14.03\pm^{0.013}_{0.013}$	···
HIPEQ1416+03	$16.81\pm^{0.084}_{0.091}$	$16.06\pm^{0.015}_{0.015}$	$15.69\pm^{0.017}_{0.017}$	$15.69\pm^{0.024}_{0.025}$	$15.45\pm^{0.094}_{0.103}$	···
HIPEQ1422-00	$12.83\pm^{0.005}_{0.005}$	$11.89\pm^{0.001}_{0.001}$	$11.50\pm^{0.001}_{0.001}$	$11.33\pm^{0.001}_{0.001}$	$11.14\pm^{0.004}_{0.004}$	···
HIPEQ1429-00	$14.81\pm^{0.012}_{0.012}$	$14.01\pm^{0.002}_{0.002}$	$13.75\pm^{0.003}_{0.003}$	$13.60\pm^{0.004}_{0.004}$	$13.49\pm^{0.015}_{0.015}$	0.02
HIPEQ1432+00	$15.12\pm^{0.017}_{0.017}$	$14.02\pm^{0.002}_{0.002}$	$13.51\pm^{0.002}_{0.002}$	$13.22\pm^{0.003}_{0.003}$	$13.01\pm^{0.011}_{0.011}$	···
HIPEQ1433+01	$17.74\pm^{0.247}_{0.320}$	$16.81\pm^{0.037}_{0.038}$	$16.70\pm^{0.053}_{0.055}$	$16.44\pm^{0.067}_{0.071}$	$16.80\pm^{0.322}_{0.459}$	···
HIPEQ1433+02	$15.30\pm^{0.017}_{0.017}$	$14.50\pm^{0.003}_{0.003}$	$14.26\pm^{0.004}_{0.004}$	$14.22\pm^{0.007}_{0.007}$	$14.12\pm^{0.021}_{0.022}$	···
HIPEQ1437+02	$12.88\pm^{0.005}_{0.005}$	$12.16\pm^{0.001}_{0.001}$	$11.41\pm^{0.001}_{0.001}$	$11.13\pm^{0.001}_{0.001}$	$10.74\pm^{0.003}_{0.003}$	0.03
HIPEQ1437-00	$13.54\pm^{0.004}_{0.004}$	$12.45\pm^{0.001}_{0.001}$	$12.01\pm^{0.001}_{0.001}$	$11.77\pm^{0.001}_{0.001}$	$11.66\pm^{0.003}_{0.003}$	···
HIPEQ1439+02	$16.50\pm^{0.077}_{0.082}$	$15.40\pm^{0.015}_{0.015}$	$14.98\pm^{0.014}_{0.014}$	$14.72\pm^{0.017}_{0.017}$	$14.69\pm^{0.059}_{0.062}$	···

Table 3.3—Continued

HIPASS Name	u^a	g^a	r^a	i^a	z^a	Edge Correction[b]
HIPEQ1439-00	$13.81\pm^{0.011}_{0.012}$	$12.94\pm^{0.002}_{0.002}$	$12.55\pm^{0.002}_{0.002}$	$12.27\pm^{0.002}_{0.002}$	$12.22\pm^{0.008}_{0.008}$	...
HIPEQ1440+02	$15.00\pm^{0.014}_{0.014}$	$13.96\pm^{0.002}_{0.002}$	$13.69\pm^{0.002}_{0.002}$	$13.44\pm^{0.003}_{0.003}$	$13.86\pm^{0.012}_{0.012}$	...
HIPEQ1444+01a	$13.44\pm^{0.007}_{0.007}$	$12.16\pm^{0.001}_{0.001}$	$11.58\pm^{0.001}_{0.001}$	$11.24\pm^{0.001}_{0.001}$	$10.97\pm^{0.003}_{0.003}$	...
HIPEQ1500+01	$13.11\pm^{0.007}_{0.007}$	$11.76\pm^{0.001}_{0.001}$	$11.08\pm^{0.001}_{0.001}$	$10.71\pm^{0.001}_{0.001}$	$10.44\pm^{0.002}_{0.002}$	0.01
HIPEQ1504+02	$15.98\pm^{0.032}_{0.033}$	$14.95\pm^{0.005}_{0.005}$	$14.62\pm^{0.005}_{0.005}$	$14.47\pm^{0.007}_{0.007}$	$14.50\pm^{0.025}_{0.026}$	...
HIPEQ1504-00	$15.65\pm^{0.034}_{0.035}$	$14.62\pm^{0.007}_{0.007}$	$14.23\pm^{0.006}_{0.006}$	$14.04\pm^{0.008}_{0.008}$	$14.02\pm^{0.028}_{0.029}$	...
HIPEQ1507+01	$12.90\pm^{0.010}_{0.011}$	$11.41\pm^{0.001}_{0.001}$	$10.76\pm^{0.001}_{0.001}$	$10.38\pm^{0.001}_{0.001}$	$10.08\pm^{0.003}_{0.003}$	...
HIPEQ1542+00	$14.78\pm^{0.032}_{0.033}$	$13.61\pm^{0.004}_{0.004}$	$13.06\pm^{0.004}_{0.004}$	$12.76\pm^{0.005}_{0.005}$	$12.54\pm^{0.012}_{0.012}$	0.10
HIPEQ1544+02	$15.77\pm^{0.035}_{0.036}$	$14.57\pm^{0.004}_{0.004}$	$14.06\pm^{0.004}_{0.004}$	$14.01\pm^{0.005}_{0.005}$	$13.44\pm^{0.013}_{0.013}$	...
HIPEQ1545+00	$15.60\pm^{0.045}_{0.047}$	$14.93\pm^{0.010}_{0.010}$	$14.52\pm^{0.011}_{0.011}$	$14.33\pm^{0.016}_{0.017}$	$13.86\pm^{0.036}_{0.037}$	...
HIPEQ1601+01a	$13.52\pm^{0.017}_{0.017}$	$12.60\pm^{0.002}_{0.002}$	$12.26\pm^{0.002}_{0.002}$	$11.84\pm^{0.002}_{0.002}$	$11.77\pm^{0.007}_{0.007}$	...
HIPEQ1609-00	$16.59\pm^{0.080}_{0.087}$	$15.75\pm^{0.015}_{0.015}$	$15.73\pm^{0.022}_{0.022}$	$15.74\pm^{0.035}_{0.036}$	$15.76\pm^{0.133}_{0.151}$	...
HIPEQ1613-00	$15.26\pm^{0.023}_{0.024}$	$14.35\pm^{0.003}_{0.003}$	$14.25\pm^{0.004}_{0.004}$	$14.14\pm^{0.006}_{0.006}$	$13.78\pm^{0.018}_{0.018}$	...
HIPEQ1614+00	$14.58\pm^{0.021}_{0.022}$	$13.82\pm^{0.004}_{0.004}$	$13.56\pm^{0.005}_{0.005}$	$13.49\pm^{0.009}_{0.009}$	$13.36\pm^{0.025}_{0.026}$	...
HIPEQ1614-00	$14.83\pm^{0.031}_{0.032}$	$13.34\pm^{0.003}_{0.003}$	$12.64\pm^{0.002}_{0.002}$	$12.24\pm^{0.002}_{0.002}$	$11.95\pm^{0.006}_{0.006}$	0.08
HIPEQ2036-04	$14.88\pm^{0.017}_{0.018}$	$13.34\pm^{0.002}_{0.002}$	$12.54\pm^{0.002}_{0.002}$	$12.11\pm^{0.002}_{0.002}$	$11.97\pm^{0.005}_{0.005}$	...
HIPEQ2314+00	$15.14\pm^{0.013}_{0.013}$	$14.15\pm^{0.002}_{0.002}$	$13.77\pm^{0.002}_{0.002}$	$13.56\pm^{0.002}_{0.002}$	$13.40\pm^{0.009}_{0.009}$	...
HIPEQ2324-00	$14.79\pm^{0.021}_{0.022}$	$14.21\pm^{0.004}_{0.004}$	$14.05\pm^{0.006}_{0.006}$	$13.99\pm^{0.009}_{0.009}$	$13.81\pm^{0.031}_{0.032}$	...
HIPEQ2335+01	$16.40\pm^{0.103}_{0.113}$	$15.74\pm^{0.018}_{0.019}$	$15.25\pm^{0.018}_{0.019}$	$15.09\pm^{0.027}_{0.027}$	$14.81\pm^{0.074}_{0.080}$	...
HIPEQ2336+00	$13.67\pm^{0.007}_{0.007}$	$12.45\pm^{0.001}_{0.001}$	$11.88\pm^{0.001}_{0.001}$	$11.53\pm^{0.001}_{0.001}$	$11.24\pm^{0.003}_{0.003}$	...
HIPEQ2337+00	$15.04\pm^{0.043}_{0.044}$	$14.18\pm^{0.006}_{0.006}$	$13.81\pm^{0.007}_{0.007}$	$13.62\pm^{0.009}_{0.009}$	$13.59\pm^{0.042}_{0.044}$	...
HIPEQ2340+01	$15.75\pm^{0.027}_{0.027}$	$14.67\pm^{0.003}_{0.003}$	$14.16\pm^{0.003}_{0.003}$	$13.90\pm^{0.004}_{0.004}$	$13.78\pm^{0.014}_{0.014}$	...

[a]Uncertainties are based on the photometric errors described in §3.5 and *do not* account for calibration errors or other uncertainties.

[b]Edge corrections are determined using the r-band images of galaxies that are close to the edges of SDSS `fields`

Table 3.4. Circular Petrosian Photometry of HI Selected Sources

HIPASS Name	u^a	g^a	r^a	i^a	z^a	Edge Correction[b]
HIPEQ0014-00	$14.65\pm^{0.019}_{0.019}$	$13.75\pm^{0.003}_{0.003}$	$13.37\pm^{0.003}_{0.003}$	$13.15\pm^{0.003}_{0.003}$	$12.99\pm^{0.011}_{0.011}$	...
HIPEQ0027-01a	$15.53\pm^{0.023}_{0.023}$	$14.66\pm^{0.005}_{0.005}$	$14.28\pm^{0.004}_{0.004}$	$14.10\pm^{0.006}_{0.006}$	$14.06\pm^{0.020}_{0.021}$	...
HIPEQ0033-01	$15.94\pm^{0.048}_{0.050}$	$15.06\pm^{0.011}_{0.011}$	$14.74\pm^{0.009}_{0.009}$	$14.54\pm^{0.013}_{0.013}$	$14.46\pm^{0.042}_{0.044}$	...
HIPEQ0043-00	$14.41\pm^{0.007}_{0.007}$	$13.31\pm^{0.001}_{0.001}$	$12.78\pm^{0.001}_{0.001}$	$12.50\pm^{0.001}_{0.001}$	$12.27\pm^{0.004}_{0.004}$	...
HIPEQ0051-00	$15.88\pm^{0.015}_{0.015}$	$14.93\pm^{0.002}_{0.002}$	$14.48\pm^{0.002}_{0.002}$	$14.24\pm^{0.002}_{0.002}$	$14.11\pm^{0.009}_{0.009}$	...
HIPEQ0058+00	$14.97\pm^{0.012}_{0.012}$	$13.94\pm^{0.002}_{0.002}$	$13.46\pm^{0.002}_{0.002}$	$13.20\pm^{0.002}_{0.002}$	$13.06\pm^{0.007}_{0.007}$	...
HIPEQ0107+01	$15.80\pm^{0.031}_{0.032}$	$14.96\pm^{0.005}_{0.005}$	$14.68\pm^{0.006}_{0.006}$	$14.54\pm^{0.009}_{0.009}$	$14.51\pm^{0.031}_{0.032}$	...
HIPEQ0119+00	$17.85\pm^{0.097}_{0.107}$	$17.04\pm^{0.019}_{0.019}$	$16.74\pm^{0.021}_{0.021}$	$16.57\pm^{0.031}_{0.032}$	$16.45\pm^{0.092}_{0.100}$	...
HIPEQ0120-00	$16.09\pm^{0.033}_{0.034}$	$15.20\pm^{0.005}_{0.005}$	$14.81\pm^{0.006}_{0.006}$	$14.60\pm^{0.007}_{0.007}$	$14.47\pm^{0.027}_{0.028}$	0.01
HIPEQ0122+00	$13.51\pm^{0.008}_{0.008}$	$12.68\pm^{0.001}_{0.001}$	$12.31\pm^{0.001}_{0.001}$	$12.02\pm^{0.002}_{0.002}$	$11.82\pm^{0.005}_{0.005}$	...
HIPEQ0123-00	$15.00\pm^{0.017}_{0.017}$	$14.14\pm^{0.003}_{0.003}$	$13.73\pm^{0.003}_{0.003}$	$13.49\pm^{0.004}_{0.004}$	$13.28\pm^{0.012}_{0.012}$	...
HIPEQ0126+00a	$18.57\pm^{0.254}_{0.333}$	$16.84\pm^{0.022}_{0.023}$	$16.50\pm^{0.023}_{0.024}$	$16.33\pm^{0.036}_{0.037}$	$16.31\pm^{0.111}_{0.124}$	...
HIPEQ0126-00b	$16.33\pm^{0.023}_{0.023}$	$15.72\pm^{0.004}_{0.004}$	$15.53\pm^{0.005}_{0.005}$	$15.54\pm^{0.007}_{0.008}$	$15.56\pm^{0.029}_{0.030}$	...
HIPEQ0154-00	$15.76\pm^{0.021}_{0.021}$	$14.06\pm^{0.002}_{0.002}$	$13.28\pm^{0.001}_{0.001}$	$12.88\pm^{0.001}_{0.001}$	$12.65\pm^{0.004}_{0.004}$	...
HIPEQ0222-00	$16.14\pm^{0.045}_{0.047}$	$15.04\pm^{0.005}_{0.005}$	$14.63\pm^{0.006}_{0.006}$	$14.48\pm^{0.006}_{0.006}$	$14.47\pm^{0.024}_{0.024}$	0.10
HIPEQ0228-01	$13.52\pm^{0.008}_{0.008}$	$12.66\pm^{0.002}_{0.002}$	$12.28\pm^{0.001}_{0.001}$	$12.07\pm^{0.002}_{0.002}$	$11.97\pm^{0.006}_{0.006}$	...
HIPEQ0230+00	$17.54\pm^{0.133}_{0.151}$	$15.64\pm^{0.014}_{0.015}$	$14.94\pm^{0.009}_{0.009}$	$14.51\pm^{0.011}_{0.011}$	$14.84\pm^{0.045}_{0.047}$	...
HIPEQ0230-01	$14.07\pm^{0.006}_{0.006}$	$12.44\pm^{0.001}_{0.001}$	$11.68\pm^{0.000}_{0.000}$	$11.26\pm^{0.000}_{0.000}$	$11.04\pm^{0.001}_{0.001}$	...
HIPEQ0231+00	$16.35\pm^{0.048}_{0.050}$	$15.22\pm^{0.006}_{0.006}$	$14.86\pm^{0.006}_{0.006}$	$14.67\pm^{0.008}_{0.008}$	$14.48\pm^{0.029}_{0.030}$	...
HIPEQ0236+00	$16.21\pm^{0.027}_{0.028}$	$14.96\pm^{0.003}_{0.003}$	$14.34\pm^{0.003}_{0.003}$	$13.99\pm^{0.003}_{0.003}$	$13.80\pm^{0.009}_{0.009}$	...
HIPEQ0238+00	$17.37\pm^{0.119}_{0.134}$	$16.47\pm^{0.021}_{0.021}$	$16.31\pm^{0.024}_{0.025}$	$16.16\pm^{0.037}_{0.038}$	$16.04\pm^{0.101}_{0.112}$	...
HIPEQ0240+01	$17.01\pm^{0.134}_{0.152}$	$16.20\pm^{0.022}_{0.022}$	$16.07\pm^{0.030}_{0.031}$	$15.92\pm^{0.039}_{0.041}$	$15.44\pm^{0.087}_{0.094}$	...
HIPEQ0241+00	$12.38\pm^{0.005}_{0.005}$	$11.00\pm^{0.001}_{0.001}$	$10.22\pm^{0.000}_{0.000}$	$9.81\pm^{0.000}_{0.000}$	$9.55\pm^{0.001}_{0.001}$	0.05
HIPEQ0244+00	$15.98\pm^{0.036}_{0.037}$	$15.17\pm^{0.006}_{0.006}$	$14.77\pm^{0.007}_{0.007}$	$14.56\pm^{0.009}_{0.009}$	$14.44\pm^{0.025}_{0.026}$	...
HIPEQ0246-00a	$13.35\pm^{0.007}_{0.007}$	$12.24\pm^{0.001}_{0.001}$	$11.67\pm^{0.001}_{0.001}$	$11.38\pm^{0.001}_{0.001}$	$11.12\pm^{0.003}_{0.003}$	...
HIPEQ0246-00b	$12.10\pm^{0.004}_{0.004}$	$11.12\pm^{0.000}_{0.000}$	$10.70\pm^{0.001}_{0.001}$	$10.48\pm^{0.001}_{0.001}$	$10.33\pm^{0.002}_{0.002}$	...
HIPEQ0249-00	$15.62\pm^{0.029}_{0.030}$	$14.49\pm^{0.003}_{0.003}$	$13.97\pm^{0.003}_{0.003}$	$13.68\pm^{0.003}_{0.003}$	$13.51\pm^{0.009}_{0.010}$	...
HIPEQ0249-00a	$16.49\pm^{0.066}_{0.071}$	$15.91\pm^{0.014}_{0.014}$	$15.73\pm^{0.017}_{0.017}$	$15.73\pm^{0.026}_{0.026}$	$15.44\pm^{0.075}_{0.081}$	...
HIPEQ0249-00b	$14.62\pm^{0.012}_{0.012}$	$13.49\pm^{0.002}_{0.002}$	$12.92\pm^{0.001}_{0.001}$	$12.59\pm^{0.002}_{0.002}$	$12.39\pm^{0.004}_{0.004}$	...
HIPEQ0251-01	$15.08\pm^{0.035}_{0.036}$	$14.34\pm^{0.008}_{0.008}$	$14.06\pm^{0.007}_{0.007}$	$13.92\pm^{0.010}_{0.010}$	$13.71\pm^{0.027}_{0.027}$	...
HIPEQ0300+00	$16.22\pm^{0.058}_{0.061}$	$15.17\pm^{0.006}_{0.006}$	$14.83\pm^{0.006}_{0.006}$	$14.64\pm^{0.008}_{0.008}$	$14.54\pm^{0.033}_{0.034}$	...
HIPEQ0301-00	$15.36\pm^{0.038}_{0.040}$	$14.82\pm^{0.007}_{0.007}$	$14.62\pm^{0.007}_{0.007}$	$14.49\pm^{0.009}_{0.009}$	$14.42\pm^{0.029}_{0.030}$	...
HIPEQ0306-00	$14.40\pm^{0.012}_{0.012}$	$12.73\pm^{0.001}_{0.001}$	$12.00\pm^{0.001}_{0.001}$	$11.60\pm^{0.001}_{0.001}$	$11.37\pm^{0.002}_{0.002}$	...
HIPEQ0316-00	$15.95\pm^{0.041}_{0.042}$	$14.46\pm^{0.003}_{0.003}$	$13.85\pm^{0.003}_{0.003}$	$13.51\pm^{0.003}_{0.003}$	$13.22\pm^{0.007}_{0.008}$	...
HIPEQ0320-06	$14.14\pm^{0.006}_{0.006}$	$13.06\pm^{0.001}_{0.001}$	$12.60\pm^{0.001}_{0.001}$	$12.34\pm^{0.001}_{0.001}$	$12.17\pm^{0.003}_{0.003}$	...
HIPEQ0351-00	$15.92\pm^{0.030}_{0.031}$	$14.79\pm^{0.003}_{0.003}$	$14.29\pm^{0.003}_{0.003}$	$14.02\pm^{0.003}_{0.003}$	$13.84\pm^{0.007}_{0.008}$	...
HIPEQ0809+00	$14.69\pm^{0.010}_{0.010}$	$13.85\pm^{0.002}_{0.002}$	$13.49\pm^{0.002}_{0.002}$	$13.33\pm^{0.003}_{0.003}$	$13.20\pm^{0.009}_{0.009}$	...
HIPEQ0821+03b	$15.09\pm^{0.010}_{0.010}$	$13.84\pm^{0.001}_{0.001}$	$13.27\pm^{0.001}_{0.001}$	$12.94\pm^{0.001}_{0.001}$	$12.73\pm^{0.004}_{0.004}$	...
HIPEQ0821-00	$15.95\pm^{0.031}_{0.032}$	$15.22\pm^{0.007}_{0.007}$	$15.08\pm^{0.008}_{0.008}$	$15.14\pm^{0.014}_{0.014}$	$14.96\pm^{0.043}_{0.044}$	...
HIPEQ0822-00	$15.04\pm^{0.013}_{0.013}$	$14.15\pm^{0.003}_{0.003}$	$13.72\pm^{0.002}_{0.002}$	$13.47\pm^{0.003}_{0.003}$	$13.29\pm^{0.009}_{0.009}$	0.03
HIPEQ0825-00	$14.60\pm^{0.011}_{0.011}$	$13.35\pm^{0.001}_{0.001}$	$12.58\pm^{0.001}_{0.001}$	$12.14\pm^{0.001}_{0.001}$	$11.81\pm^{0.003}_{0.003}$	...
HIPEQ0855+02	$15.46\pm^{0.049}_{0.051}$	$14.54\pm^{0.007}_{0.007}$	$14.21\pm^{0.009}_{0.009}$	$14.02\pm^{0.011}_{0.012}$	$13.91\pm^{0.039}_{0.040}$	...
HIPEQ0856+00	$14.68\pm^{0.015}_{0.015}$	$13.91\pm^{0.003}_{0.003}$	$13.63\pm^{0.004}_{0.004}$	$13.34\pm^{0.004}_{0.004}$	$13.24\pm^{0.015}_{0.015}$	...
HIPEQ0923-00	$15.23\pm^{0.014}_{0.015}$	$14.36\pm^{0.002}_{0.002}$	$14.06\pm^{0.003}_{0.003}$	$13.88\pm^{0.003}_{0.003}$	$13.79\pm^{0.011}_{0.011}$	...
HIPEQ0930+04	$14.34\pm^{0.012}_{0.012}$	$13.95\pm^{0.003}_{0.003}$	$13.45\pm^{0.002}_{0.003}$	$13.26\pm^{0.003}_{0.003}$	$12.73\pm^{0.008}_{0.008}$	...

Table 3.4—Continued

HIPASS Name	u^a	g^a	r^a	i^a	z^a	Edge Correction[b]
HIPEQ0936+01	$17.58\pm^{0.039}_{0.040}$	$16.81\pm^{0.008}_{0.008}$	$16.64\pm^{0.009}_{0.009}$	$16.61\pm^{0.014}_{0.014}$	$16.51\pm^{0.045}_{0.047}$	...
HIPEQ0942+00	$12.62\pm^{0.004}_{0.004}$	$11.61\pm^{0.001}_{0.001}$	$11.14\pm^{0.001}_{0.001}$	$10.88\pm^{0.001}_{0.001}$	$10.66\pm^{0.002}_{0.002}$	...
HIPEQ0944-00b	$16.67\pm^{0.044}_{0.046}$	$15.72\pm^{0.007}_{0.007}$	$15.45\pm^{0.009}_{0.009}$	$15.53\pm^{0.015}_{0.015}$	$15.24\pm^{0.040}_{0.041}$	...
HIPEQ0945+01	$13.97\pm^{0.016}_{0.016}$	$12.91\pm^{0.002}_{0.002}$	$12.45\pm^{0.002}_{0.002}$	$12.23\pm^{0.002}_{0.002}$	$12.02\pm^{0.007}_{0.007}$	...
HIPEQ0946+02	$15.55\pm^{0.031}_{0.032}$	$14.74\pm^{0.008}_{0.008}$	$14.35\pm^{0.006}_{0.006}$	$14.17\pm^{0.008}_{0.008}$	$13.98\pm^{0.021}_{0.021}$	...
HIPEQ0947+00a	$14.96\pm^{0.026}_{0.027}$	$14.03\pm^{0.004}_{0.004}$	$13.61\pm^{0.004}_{0.004}$	$13.37\pm^{0.005}_{0.005}$	$13.21\pm^{0.013}_{0.013}$	...
HIPEQ0947+00b	$15.72\pm^{0.054}_{0.057}$	$15.06\pm^{0.010}_{0.010}$	$14.78\pm^{0.011}_{0.011}$	$14.77\pm^{0.016}_{0.016}$	$14.76\pm^{0.053}_{0.056}$	...
HIPEQ0953+01	$13.09\pm^{0.003}_{0.003}$	$12.09\pm^{0.001}_{0.001}$	$11.67\pm^{0.001}_{0.001}$	$11.49\pm^{0.001}_{0.001}$	$11.09\pm^{0.002}_{0.002}$	0.05
HIPEQ0954+01a	$18.80\pm^{0.230}_{0.293}$	$18.38\pm^{0.065}_{0.069}$	$18.13\pm^{0.085}_{0.093}$	$18.16\pm^{0.142}_{0.163}$	$17.86\pm^{0.431}_{0.726}$	...
HIPEQ0954+02a	$15.51\pm^{0.018}_{0.018}$	$14.30\pm^{0.003}_{0.003}$	$14.01\pm^{0.003}_{0.003}$	$13.69\pm^{0.005}_{0.005}$	$14.11\pm^{0.018}_{0.018}$	...
HIPEQ0955+04a	$13.21\pm^{0.005}_{0.005}$	$12.26\pm^{0.001}_{0.001}$	$11.82\pm^{0.001}_{0.001}$	$11.62\pm^{0.001}_{0.001}$	$11.44\pm^{0.003}_{0.003}$	...
HIPEQ0958+01	$17.89\pm^{0.156}_{0.182}$	$17.02\pm^{0.028}_{0.028}$	$16.95\pm^{0.041}_{0.043}$	$17.26\pm^{0.087}_{0.095}$	$17.24\pm^{0.326}_{0.467}$	...
HIPEQ1000+03	$14.83\pm^{0.010}_{0.010}$	$13.60\pm^{0.001}_{0.001}$	$12.95\pm^{0.001}_{0.001}$	$12.55\pm^{0.001}_{0.001}$	$12.29\pm^{0.003}_{0.003}$	...
HIPEQ1010+05	$16.44\pm^{0.023}_{0.024}$	$15.13\pm^{0.004}_{0.004}$	$14.68\pm^{0.003}_{0.003}$	$14.46\pm^{0.004}_{0.004}$	$14.45\pm^{0.013}_{0.013}$	...
HIPEQ1014+03	$12.20\pm^{0.004}_{0.004}$	$10.68\pm^{0.000}_{0.000}$	$9.97\pm^{0.000}_{0.000}$	$9.54\pm^{0.000}_{0.000}$	$9.31\pm^{0.001}_{0.001}$	...
HIPEQ1015+02	$15.42\pm^{0.042}_{0.043}$	$14.74\pm^{0.009}_{0.009}$	$14.52\pm^{0.011}_{0.011}$	$14.32\pm^{0.016}_{0.016}$	$14.38\pm^{0.058}_{0.061}$	...
HIPEQ1026+03	$14.27\pm^{0.011}_{0.011}$	$13.21\pm^{0.002}_{0.002}$	$12.88\pm^{0.002}_{0.002}$	$12.72\pm^{0.002}_{0.002}$	$12.32\pm^{0.006}_{0.006}$	...
HIPEQ1028+03	$16.26\pm^{0.030}_{0.031}$	$15.29\pm^{0.007}_{0.007}$	$15.19\pm^{0.007}_{0.007}$	$15.01\pm^{0.009}_{0.009}$	$14.80\pm^{0.023}_{0.023}$	...
HIPEQ1031+04	$14.74\pm^{0.013}_{0.013}$	$13.67\pm^{0.002}_{0.002}$	$13.49\pm^{0.003}_{0.003}$	$13.16\pm^{0.003}_{0.003}$	$13.76\pm^{0.013}_{0.013}$	0.22
HIPEQ1039+01	$15.48\pm^{0.023}_{0.023}$	$14.52\pm^{0.003}_{0.003}$	$14.15\pm^{0.004}_{0.004}$	$13.91\pm^{0.005}_{0.005}$	$13.79\pm^{0.016}_{0.017}$	0.10
HIPEQ1041+00	$15.32\pm^{0.016}_{0.016}$	$14.56\pm^{0.003}_{0.003}$	$14.18\pm^{0.004}_{0.004}$	$13.94\pm^{0.005}_{0.005}$	$13.82\pm^{0.015}_{0.015}$	...
HIPEQ1046+01	$13.90\pm^{0.010}_{0.010}$	$12.87\pm^{0.001}_{0.001}$	$12.38\pm^{0.001}_{0.001}$	$12.18\pm^{0.002}_{0.002}$	$11.73\pm^{0.006}_{0.006}$	...
HIPEQ1050+01	$18.20\pm^{0.114}_{0.128}$	$17.13\pm^{0.023}_{0.024}$	$16.67\pm^{0.020}_{0.021}$	$16.56\pm^{0.030}_{0.031}$	$16.90\pm^{0.136}_{0.155}$	...
HIPEQ1051+04a	$14.76\pm^{0.015}_{0.015}$	$14.07\pm^{0.003}_{0.003}$	$13.69\pm^{0.003}_{0.003}$	$13.59\pm^{0.004}_{0.004}$	$13.46\pm^{0.016}_{0.016}$	...
HIPEQ1052+00	$16.07\pm^{0.011}_{0.011}$	$15.28\pm^{0.002}_{0.002}$	$14.99\pm^{0.003}_{0.003}$	$14.86\pm^{0.003}_{0.003}$	$14.73\pm^{0.014}_{0.014}$	...
HIPEQ1053+02	$15.82\pm^{0.021}_{0.021}$	$15.51\pm^{0.005}_{0.006}$	$15.35\pm^{0.007}_{0.007}$	$15.23\pm^{0.011}_{0.011}$	$15.24\pm^{0.040}_{0.041}$	...
HIPEQ1055+02	$16.61\pm^{0.035}_{0.036}$	$15.95\pm^{0.007}_{0.007}$	$15.80\pm^{0.009}_{0.009}$	$15.80\pm^{0.015}_{0.015}$	$15.80\pm^{0.067}_{0.071}$	...
HIPEQ1101+03	$12.77\pm^{0.005}_{0.005}$	$11.76\pm^{0.001}_{0.001}$	$11.36\pm^{0.001}_{0.001}$	$11.04\pm^{0.001}_{0.001}$	$10.80\pm^{0.002}_{0.002}$	...
HIPEQ1109-00	$15.40\pm^{0.010}_{0.010}$	$14.14\pm^{0.002}_{0.002}$	$13.54\pm^{0.001}_{0.001}$	$13.23\pm^{0.002}_{0.002}$	$13.02\pm^{0.005}_{0.005}$	...
HIPEQ1110+01	$16.44\pm^{0.033}_{0.034}$	$15.62\pm^{0.006}_{0.006}$	$15.35\pm^{0.007}_{0.007}$	$15.30\pm^{0.012}_{0.012}$	$15.25\pm^{0.041}_{0.043}$	...
HIPEQ1113+05	$15.48\pm^{0.020}_{0.021}$	$14.46\pm^{0.004}_{0.004}$	$14.28\pm^{0.004}_{0.004}$	$14.08\pm^{0.005}_{0.005}$	$14.49\pm^{0.018}_{0.018}$	...
HIPEQ1117+04a	$13.70\pm^{0.005}_{0.005}$	$12.52\pm^{0.001}_{0.001}$	$11.96\pm^{0.001}_{0.001}$	$11.68\pm^{0.001}_{0.001}$	$11.48\pm^{0.002}_{0.002}$	...
HIPEQ1119+02	$14.07\pm^{0.017}_{0.017}$	$13.52\pm^{0.003}_{0.003}$	$13.32\pm^{0.004}_{0.004}$	$13.12\pm^{0.006}_{0.006}$	$13.16\pm^{0.029}_{0.029}$	...
HIPEQ1124+03	$13.55\pm^{0.009}_{0.009}$	$12.92\pm^{0.002}_{0.002}$	$12.71\pm^{0.002}_{0.002}$	$12.58\pm^{0.003}_{0.003}$	$12.41\pm^{0.010}_{0.010}$	...
HIPEQ1127-01	$15.19\pm^{0.019}_{0.019}$	$14.36\pm^{0.005}_{0.005}$	$13.99\pm^{0.005}_{0.005}$	$13.79\pm^{0.006}_{0.006}$	$13.43\pm^{0.016}_{0.016}$	...
HIPEQ1131-02	$13.94\pm^{0.011}_{0.011}$	$13.05\pm^{0.002}_{0.002}$	$12.61\pm^{0.002}_{0.002}$	$12.34\pm^{0.002}_{0.002}$	$12.19\pm^{0.009}_{0.009}$	...
HIPEQ1133-03	$15.37\pm^{0.019}_{0.020}$	$14.58\pm^{0.005}_{0.005}$	$14.29\pm^{0.005}_{0.005}$	$14.11\pm^{0.007}_{0.007}$	$13.97\pm^{0.020}_{0.021}$	...
HIPEQ1136+00	$15.47\pm^{0.008}_{0.008}$	$14.71\pm^{0.002}_{0.002}$	$14.61\pm^{0.003}_{0.003}$	$14.58\pm^{0.004}_{0.004}$	$14.59\pm^{0.014}_{0.014}$	...
HIPEQ1138+03	$15.59\pm^{0.022}_{0.023}$	$14.36\pm^{0.003}_{0.003}$	$13.78\pm^{0.002}_{0.002}$	$13.46\pm^{0.003}_{0.003}$	$13.28\pm^{0.009}_{0.009}$	...
HIPEQ1143-01	$18.26\pm^{0.135}_{0.154}$	$17.52\pm^{0.027}_{0.028}$	$17.26\pm^{0.035}_{0.036}$	$17.19\pm^{0.054}_{0.057}$	$17.22\pm^{0.192}_{0.234}$	...
HIPEQ1145+02	$17.50\pm^{0.176}_{0.211}$	$17.00\pm^{0.045}_{0.047}$	$16.74\pm^{0.054}_{0.056}$	$16.87\pm^{0.100}_{0.110}$	$18.89\pm^{1.380}_{8.292}$	...
HIPEQ1148-02	$14.67\pm^{0.022}_{0.023}$	$13.83\pm^{0.004}_{0.004}$	$13.50\pm^{0.005}_{0.005}$	$13.24\pm^{0.006}_{0.006}$	$13.23\pm^{0.021}_{0.022}$	0.16
HIPEQ1151-02	$16.09\pm^{0.015}_{0.015}$	$15.04\pm^{0.003}_{0.003}$	$14.64\pm^{0.003}_{0.003}$	$14.45\pm^{0.004}_{0.004}$	$14.32\pm^{0.013}_{0.013}$	...
HIPEQ1152+01	$14.94\pm^{0.015}_{0.015}$	$14.13\pm^{0.002}_{0.002}$	$13.79\pm^{0.003}_{0.003}$	$13.58\pm^{0.004}_{0.004}$	$13.45\pm^{0.012}_{0.013}$	...
HIPEQ1152-02	$14.85\pm^{0.005}_{0.005}$	$14.32\pm^{0.001}_{0.001}$	$14.29\pm^{0.002}_{0.002}$	$14.47\pm^{0.003}_{0.003}$	$14.46\pm^{0.015}_{0.015}$	...

Table 3.4—Continued

HIPASS Name	u^a	g^a	r^a	i^a	z^a	Edge Correction[b]
HIPEQ1152-03b	$15.22\pm^{0.025}_{0.025}$	$14.35\pm^{0.005}_{0.005}$	$14.09\pm^{0.006}_{0.006}$	$13.93\pm^{0.008}_{0.008}$	$13.84\pm^{0.026}_{0.026}$	...
HIPEQ1155+01	$14.16\pm^{0.013}_{0.013}$	$13.08\pm^{0.002}_{0.002}$	$12.61\pm^{0.002}_{0.002}$	$12.38\pm^{0.003}_{0.003}$	$12.14\pm^{0.007}_{0.007}$	...
HIPEQ1200-00	$15.92\pm^{0.049}_{0.051}$	$15.03\pm^{0.010}_{0.010}$	$14.64\pm^{0.011}_{0.011}$	$14.40\pm^{0.013}_{0.014}$	$14.42\pm^{0.052}_{0.054}$	...
HIPEQ1200-01	$11.75\pm^{0.002}_{0.002}$	$10.62\pm^{0.000}_{0.000}$	$10.03\pm^{0.000}_{0.000}$	$9.69\pm^{0.000}_{0.000}$	$9.46\pm^{0.001}_{0.001}$	...
HIPEQ1202+01	$13.60\pm^{0.010}_{0.010}$	$12.19\pm^{0.001}_{0.001}$	$11.48\pm^{0.001}_{0.001}$	$11.08\pm^{0.001}_{0.001}$	$10.79\pm^{0.002}_{0.002}$	...
HIPEQ1204-01	$15.93\pm^{0.057}_{0.060}$	$15.37\pm^{0.013}_{0.013}$	$15.05\pm^{0.015}_{0.015}$	$14.97\pm^{0.023}_{0.024}$	$14.72\pm^{0.067}_{0.071}$	...
HIPEQ1204-02	$15.70\pm^{0.019}_{0.019}$	$14.30\pm^{0.002}_{0.002}$	$13.67\pm^{0.002}_{0.002}$	$13.34\pm^{0.002}_{0.002}$	$13.10\pm^{0.007}_{0.007}$	...
HIPEQ1210+02	$16.09\pm^{0.089}_{0.097}$	$15.27\pm^{0.014}_{0.015}$	$14.91\pm^{0.016}_{0.016}$	$14.77\pm^{0.023}_{0.023}$	$14.54\pm^{0.072}_{0.077}$	...
HIPEQ1215+04a	$15.71\pm^{0.017}_{0.017}$	$14.74\pm^{0.003}_{0.003}$	$14.47\pm^{0.004}_{0.004}$	$14.33\pm^{0.005}_{0.005}$	$14.29\pm^{0.019}_{0.019}$	...
HIPEQ1216-03	$15.25\pm^{0.017}_{0.018}$	$14.38\pm^{0.004}_{0.004}$	$13.97\pm^{0.003}_{0.003}$	$13.75\pm^{0.005}_{0.005}$	$13.49\pm^{0.013}_{0.013}$	...
HIPEQ1218+00	$16.01\pm^{0.048}_{0.051}$	$15.13\pm^{0.010}_{0.010}$	$14.69\pm^{0.010}_{0.010}$	$14.59\pm^{0.015}_{0.016}$	$14.54\pm^{0.047}_{0.049}$	...
HIPEQ1218-01	$15.49\pm^{0.013}_{0.013}$	$14.23\pm^{0.002}_{0.002}$	$13.65\pm^{0.002}_{0.002}$	$13.34\pm^{0.002}_{0.002}$	$13.16\pm^{0.006}_{0.006}$	...
HIPEQ1219+03	$14.83\pm^{0.010}_{0.010}$	$14.00\pm^{0.002}_{0.002}$	$13.65\pm^{0.002}_{0.002}$	$13.53\pm^{0.003}_{0.003}$	$13.37\pm^{0.010}_{0.010}$	...
HIPEQ1220+00	$16.54\pm^{0.032}_{0.033}$	$15.62\pm^{0.006}_{0.006}$	$15.48\pm^{0.008}_{0.008}$	$15.38\pm^{0.011}_{0.011}$	$15.36\pm^{0.049}_{0.051}$	...
HIPEQ1220+01	$15.82\pm^{0.024}_{0.025}$	$14.75\pm^{0.004}_{0.004}$	$14.34\pm^{0.004}_{0.004}$	$14.13\pm^{0.005}_{0.006}$	$13.96\pm^{0.018}_{0.018}$	0.02
HIPEQ1221+03	$15.10\pm^{0.018}_{0.019}$	$13.96\pm^{0.002}_{0.002}$	$13.21\pm^{0.002}_{0.002}$	$12.77\pm^{0.002}_{0.002}$	$12.42\pm^{0.006}_{0.006}$	...
HIPEQ1223+00	$16.16\pm^{0.050}_{0.052}$	$15.49\pm^{0.012}_{0.012}$	$15.21\pm^{0.014}_{0.014}$	$15.11\pm^{0.022}_{0.022}$	$14.93\pm^{0.059}_{0.063}$	...
HIPEQ1223-03b	$14.11\pm^{0.006}_{0.006}$	$12.70\pm^{0.001}_{0.001}$	$11.99\pm^{0.001}_{0.001}$	$11.59\pm^{0.001}_{0.001}$	$11.32\pm^{0.002}_{0.002}$	...
HIPEQ1224+00	$17.94\pm^{0.116}_{0.130}$	$17.11\pm^{0.023}_{0.024}$	$16.77\pm^{0.026}_{0.027}$	$16.67\pm^{0.037}_{0.039}$	$16.62\pm^{0.156}_{0.182}$	...
HIPEQ1224+03b	$14.75\pm^{0.021}_{0.021}$	$13.87\pm^{0.004}_{0.004}$	$13.55\pm^{0.004}_{0.004}$	$13.36\pm^{0.007}_{0.007}$	$13.28\pm^{0.022}_{0.022}$	...
HIPEQ1225+00	$13.79\pm^{0.005}_{0.005}$	$12.76\pm^{0.001}_{0.001}$	$12.21\pm^{0.001}_{0.001}$	$11.93\pm^{0.001}_{0.001}$	$11.70\pm^{0.003}_{0.003}$	...
HIPEQ1226+02	$13.47\pm^{0.004}_{0.004}$	$12.47\pm^{0.001}_{0.001}$	$12.03\pm^{0.001}_{0.001}$	$11.82\pm^{0.001}_{0.001}$	$11.62\pm^{0.003}_{0.003}$	0.01
HIPEQ1227+01	$16.79\pm^{0.090}_{0.098}$	$16.36\pm^{0.030}_{0.030}$	$16.24\pm^{0.035}_{0.036}$	$16.25\pm^{0.059}_{0.062}$	$16.03\pm^{0.174}_{0.208}$	...
HIPEQ1228+02	$15.28\pm^{0.034}_{0.035}$	$14.45\pm^{0.006}_{0.006}$	$14.14\pm^{0.007}_{0.007}$	$13.96\pm^{0.010}_{0.010}$	$13.83\pm^{0.040}_{0.042}$	...
HIPEQ1228+03	$12.75\pm^{0.003}_{0.003}$	$11.18\pm^{0.000}_{0.000}$	$10.48\pm^{0.000}_{0.000}$	$10.11\pm^{0.000}_{0.000}$	$9.88\pm^{0.001}_{0.001}$	...
HIPEQ1229+00	$17.65\pm^{0.077}_{0.083}$	$16.62\pm^{0.012}_{0.012}$	$16.19\pm^{0.012}_{0.013}$	$16.15\pm^{0.019}_{0.020}$	$16.25\pm^{0.072}_{0.077}$	...
HIPEQ1230+02	$16.19\pm^{0.042}_{0.044}$	$15.32\pm^{0.007}_{0.007}$	$15.13\pm^{0.009}_{0.009}$	$15.03\pm^{0.014}_{0.014}$	$15.02\pm^{0.064}_{0.068}$	...
HIPEQ1230+03	$16.31\pm^{0.022}_{0.022}$	$15.56\pm^{0.004}_{0.004}$	$15.39\pm^{0.005}_{0.005}$	$15.27\pm^{0.008}_{0.008}$	$15.24\pm^{0.028}_{0.029}$	...
HIPEQ1232+00a	$13.78\pm^{0.011}_{0.011}$	$12.80\pm^{0.002}_{0.002}$	$12.41\pm^{0.002}_{0.002}$	$12.20\pm^{0.003}_{0.003}$	$12.17\pm^{0.012}_{0.012}$	0.11
HIPEQ1232+00b	$12.01\pm^{0.003}_{0.003}$	$10.91\pm^{0.000}_{0.000}$	$10.24\pm^{0.000}_{0.000}$	$9.84\pm^{0.000}_{0.000}$	$9.49\pm^{0.001}_{0.001}$	0.03
HIPEQ1233-02	$15.49\pm^{0.040}_{0.042}$	$14.81\pm^{0.009}_{0.010}$	$14.41\pm^{0.011}_{0.011}$	$14.26\pm^{0.016}_{0.016}$	$14.28\pm^{0.064}_{0.067}$	...
HIPEQ1236+03	$16.53\pm^{0.051}_{0.053}$	$15.78\pm^{0.010}_{0.010}$	$15.49\pm^{0.012}_{0.012}$	$15.33\pm^{0.019}_{0.019}$	$15.26\pm^{0.061}_{0.065}$	...
HIPEQ1239-00	$12.83\pm^{0.003}_{0.003}$	$11.98\pm^{0.001}_{0.001}$	$11.64\pm^{0.001}_{0.001}$	$11.47\pm^{0.001}_{0.001}$	$11.35\pm^{0.003}_{0.003}$	0.01
HIPEQ1241+01	$15.65\pm^{0.013}_{0.014}$	$14.63\pm^{0.003}_{0.003}$	$14.18\pm^{0.002}_{0.002}$	$13.93\pm^{0.003}_{0.003}$	$13.75\pm^{0.009}_{0.010}$	...
HIPEQ1241-02	$15.47\pm^{0.017}_{0.018}$	$14.47\pm^{0.003}_{0.003}$	$14.01\pm^{0.003}_{0.003}$	$13.73\pm^{0.004}_{0.004}$	$13.55\pm^{0.011}_{0.012}$	...
HIPEQ1242+03b	$13.64\pm^{0.006}_{0.006}$	$12.64\pm^{0.001}_{0.001}$	$12.09\pm^{0.001}_{0.001}$	$11.80\pm^{0.001}_{0.001}$	$11.63\pm^{0.003}_{0.003}$	...
HIPEQ1242-00	$12.93\pm^{0.003}_{0.003}$	$11.92\pm^{0.001}_{0.001}$	$11.46\pm^{0.001}_{0.001}$	$11.23\pm^{0.001}_{0.001}$	$11.01\pm^{0.002}_{0.002}$	...
HIPEQ1242-01a	$14.53\pm^{0.012}_{0.012}$	$13.76\pm^{0.002}_{0.002}$	$13.45\pm^{0.003}_{0.003}$	$13.24\pm^{0.004}_{0.004}$	$13.05\pm^{0.012}_{0.012}$	...
HIPEQ1242-01b	$14.94\pm^{0.014}_{0.014}$	$13.71\pm^{0.002}_{0.002}$	$13.20\pm^{0.002}_{0.002}$	$12.93\pm^{0.002}_{0.002}$	$12.80\pm^{0.008}_{0.008}$	0.11
HIPEQ1243-00	$13.39\pm^{0.007}_{0.007}$	$12.46\pm^{0.001}_{0.001}$	$12.04\pm^{0.001}_{0.001}$	$11.76\pm^{0.002}_{0.002}$	$11.56\pm^{0.004}_{0.004}$	...
HIPEQ1244+00	$14.31\pm^{0.014}_{0.014}$	$13.42\pm^{0.003}_{0.003}$	$13.17\pm^{0.003}_{0.003}$	$13.51\pm^{0.008}_{0.008}$	$12.95\pm^{0.015}_{0.015}$	...
HIPEQ1244-02	$15.59\pm^{0.038}_{0.039}$	$14.88\pm^{0.008}_{0.008}$	$14.63\pm^{0.010}_{0.010}$	$14.54\pm^{0.015}_{0.015}$	$14.38\pm^{0.058}_{0.061}$	...
HIPEQ1245-00	$12.28\pm^{0.002}_{0.002}$	$11.00\pm^{0.000}_{0.000}$	$10.27\pm^{0.000}_{0.000}$	$9.85\pm^{0.000}_{0.000}$	$9.55\pm^{0.001}_{0.001}$	...
HIPEQ1249+03	$13.42\pm^{0.004}_{0.004}$	$12.50\pm^{0.001}_{0.001}$	$12.11\pm^{0.001}_{0.001}$	$11.91\pm^{0.001}_{0.001}$	$11.79\pm^{0.003}_{0.003}$	...
HIPEQ1249+04	$16.01\pm^{0.037}_{0.039}$	$15.08\pm^{0.008}_{0.008}$	$14.85\pm^{0.009}_{0.009}$	$14.72\pm^{0.013}_{0.014}$	$15.35\pm^{0.063}_{0.067}$	...

Table 3.4—Continued

HIPASS Name	u^a	g^a	r^a	i^a	z^a	Edge Correction[b]
HIPEQ1250+05	$12.55\pm^{0.003}_{0.003}$	$11.84\pm^{0.001}_{0.001}$	$11.54\pm^{0.001}_{0.001}$	$11.41\pm^{0.001}_{0.001}$	$11.22\pm^{0.003}_{0.003}$	...
HIPEQ1253+01	$13.60\pm^{0.007}_{0.007}$	$12.33\pm^{0.001}_{0.001}$	$11.69\pm^{0.001}_{0.001}$	$11.31\pm^{0.001}_{0.001}$	$11.04\pm^{0.003}_{0.003}$	...
HIPEQ1253+02	$13.10\pm^{0.008}_{0.008}$	$11.58\pm^{0.001}_{0.001}$	$10.87\pm^{0.001}_{0.001}$	$10.47\pm^{0.001}_{0.001}$	$10.20\pm^{0.002}_{0.002}$	...
HIPEQ1253+04	$13.89\pm^{0.004}_{0.004}$	$13.07\pm^{0.001}_{0.001}$	$12.77\pm^{0.001}_{0.001}$	$12.65\pm^{0.001}_{0.001}$	$12.59\pm^{0.003}_{0.003}$	...
HIPEQ1255+00	$13.38\pm^{0.007}_{0.007}$	$12.45\pm^{0.001}_{0.001}$	$12.00\pm^{0.001}_{0.001}$	$11.78\pm^{0.002}_{0.002}$	$11.68\pm^{0.006}_{0.006}$	0.10
HIPEQ1255+02	$14.85\pm^{0.007}_{0.007}$	$13.44\pm^{0.001}_{0.001}$	$12.75\pm^{0.001}_{0.001}$	$12.39\pm^{0.001}_{0.001}$	$12.13\pm^{0.002}_{0.002}$	...
HIPEQ1255-00	$16.54\pm^{0.041}_{0.043}$	$15.66\pm^{0.008}_{0.008}$	$15.28\pm^{0.009}_{0.009}$	$15.14\pm^{0.012}_{0.012}$	$15.07\pm^{0.043}_{0.045}$	...
HIPEQ1256+03	$16.76\pm^{0.099}_{0.108}$	$15.85\pm^{0.016}_{0.016}$	$15.77\pm^{0.021}_{0.022}$	$15.77\pm^{0.031}_{0.032}$	$16.07\pm^{0.146}_{0.169}$	...
HIPEQ1257+02	$15.71\pm^{0.038}_{0.040}$	$15.11\pm^{0.008}_{0.008}$	$14.82\pm^{0.010}_{0.010}$	$14.71\pm^{0.015}_{0.015}$	$14.56\pm^{0.060}_{0.064}$	...
HIPEQ1257-01	$14.75\pm^{0.008}_{0.008}$	$13.72\pm^{0.001}_{0.001}$	$13.22\pm^{0.001}_{0.001}$	$12.95\pm^{0.002}_{0.002}$	$12.79\pm^{0.006}_{0.006}$	...
HIPEQ1258+02	$15.11\pm^{0.031}_{0.032}$	$14.14\pm^{0.005}_{0.005}$	$13.81\pm^{0.005}_{0.005}$	$13.59\pm^{0.007}_{0.007}$	$13.45\pm^{0.031}_{0.032}$	...
HIPEQ1300+02a	$15.65\pm^{0.031}_{0.032}$	$14.53\pm^{0.004}_{0.004}$	$14.13\pm^{0.005}_{0.005}$	$13.93\pm^{0.006}_{0.006}$	$13.80\pm^{0.024}_{0.024}$	0.03
HIPEQ1300+02b	$12.36\pm^{0.003}_{0.003}$	$11.49\pm^{0.001}_{0.001}$	$11.08\pm^{0.001}_{0.001}$	$10.80\pm^{0.001}_{0.001}$	$10.55\pm^{0.003}_{0.003}$	...
HIPEQ1303+03	$15.17\pm^{0.025}_{0.026}$	$14.30\pm^{0.006}_{0.006}$	$14.03\pm^{0.005}_{0.005}$	$13.86\pm^{0.007}_{0.007}$	$13.82\pm^{0.022}_{0.022}$	...
HIPEQ1304-02	$16.87\pm^{0.041}_{0.043}$	$16.00\pm^{0.007}_{0.007}$	$15.55\pm^{0.008}_{0.008}$	$15.41\pm^{0.012}_{0.012}$	$15.50\pm^{0.047}_{0.049}$	0.34
HIPEQ1304-03	$13.61\pm^{0.011}_{0.011}$	$12.76\pm^{0.002}_{0.002}$	$12.52\pm^{0.003}_{0.003}$	$12.41\pm^{0.004}_{0.004}$	$12.44\pm^{0.014}_{0.014}$	0.27
HIPEQ1307-00	$14.54\pm^{0.006}_{0.007}$	$13.64\pm^{0.002}_{0.002}$	$13.30\pm^{0.001}_{0.001}$	$13.12\pm^{0.002}_{0.002}$	$12.99\pm^{0.006}_{0.006}$	...
HIPEQ1308-02	$15.01\pm^{0.013}_{0.013}$	$14.00\pm^{0.002}_{0.002}$	$13.57\pm^{0.002}_{0.002}$	$13.37\pm^{0.003}_{0.003}$	$13.11\pm^{0.012}_{0.012}$	0.03
HIPEQ1311+03a	$16.46\pm^{0.026}_{0.027}$	$15.51\pm^{0.004}_{0.004}$	$15.19\pm^{0.004}_{0.004}$	$15.06\pm^{0.007}_{0.007}$	$14.91\pm^{0.022}_{0.022}$	...
HIPEQ1312+03	$16.18\pm^{0.022}_{0.023}$	$14.75\pm^{0.003}_{0.003}$	$14.19\pm^{0.002}_{0.002}$	$13.89\pm^{0.003}_{0.003}$	$13.72\pm^{0.009}_{0.009}$	...
HIPEQ1312+05	$17.46\pm^{0.091}_{0.099}$	$16.43\pm^{0.016}_{0.016}$	$16.21\pm^{0.019}_{0.020}$	$16.07\pm^{0.029}_{0.029}$	$16.47\pm^{0.132}_{0.151}$	...
HIPEQ1313+06	$15.10\pm^{0.016}_{0.016}$	$13.86\pm^{0.002}_{0.002}$	$13.30\pm^{0.002}_{0.002}$	$13.02\pm^{0.002}_{0.002}$	$12.81\pm^{0.005}_{0.005}$	...
HIPEQ1317-00	$16.32\pm^{0.020}_{0.020}$	$15.65\pm^{0.006}_{0.006}$	$15.56\pm^{0.007}_{0.007}$	$15.60\pm^{0.011}_{0.011}$	$15.53\pm^{0.036}_{0.037}$	...
HIPEQ1318-01	$14.74\pm^{0.013}_{0.013}$	$13.81\pm^{0.002}_{0.002}$	$13.30\pm^{0.002}_{0.002}$	$13.00\pm^{0.003}_{0.003}$	$12.72\pm^{0.008}_{0.008}$	...
HIPEQ1320+05	$15.52\pm^{0.027}_{0.028}$	$14.87\pm^{0.005}_{0.005}$	$14.43\pm^{0.005}_{0.005}$	$14.30\pm^{0.007}_{0.007}$	$13.62\pm^{0.022}_{0.022}$	...
HIPEQ1327+02	$17.09\pm^{0.070}_{0.075}$	$16.30\pm^{0.013}_{0.013}$	$16.12\pm^{0.017}_{0.017}$	$16.10\pm^{0.028}_{0.028}$	$16.09\pm^{0.111}_{0.123}$	...
HIPEQ1329-00	$16.67\pm^{0.042}_{0.044}$	$15.83\pm^{0.009}_{0.009}$	$15.46\pm^{0.009}_{0.009}$	$15.31\pm^{0.013}_{0.013}$	$15.12\pm^{0.042}_{0.043}$	...
HIPEQ1332+01	$14.87\pm^{0.014}_{0.014}$	$13.62\pm^{0.002}_{0.002}$	$13.02\pm^{0.001}_{0.001}$	$12.68\pm^{0.002}_{0.002}$	$12.46\pm^{0.005}_{0.005}$	...
HIPEQ1335+01	$14.65\pm^{0.015}_{0.015}$	$13.48\pm^{0.002}_{0.002}$	$12.95\pm^{0.002}_{0.002}$	$12.65\pm^{0.002}_{0.002}$	$12.47\pm^{0.008}_{0.008}$	...
HIPEQ1341+05	$15.67\pm^{0.025}_{0.025}$	$14.65\pm^{0.003}_{0.003}$	$14.28\pm^{0.004}_{0.004}$	$14.08\pm^{0.004}_{0.004}$	$13.98\pm^{0.019}_{0.019}$	0.05
HIPEQ1348+03	$13.05\pm^{0.006}_{0.006}$	$11.99\pm^{0.001}_{0.001}$	$11.54\pm^{0.001}_{0.001}$	$11.28\pm^{0.001}_{0.001}$	$10.89\pm^{0.004}_{0.004}$	0.04
HIPEQ1352+02a	$14.34\pm^{0.018}_{0.018}$	$13.07\pm^{0.002}_{0.002}$	$12.41\pm^{0.002}_{0.002}$	$12.06\pm^{0.002}_{0.002}$	$11.82\pm^{0.006}_{0.006}$	...
HIPEQ1352-01	$13.00\pm^{0.006}_{0.006}$	$11.98\pm^{0.001}_{0.001}$	$11.54\pm^{0.001}_{0.001}$	$11.25\pm^{0.001}_{0.001}$	$11.15\pm^{0.004}_{0.004}$	...
HIPEQ1400+02	$15.64\pm^{0.022}_{0.023}$	$14.59\pm^{0.003}_{0.003}$	$14.18\pm^{0.003}_{0.003}$	$13.95\pm^{0.004}_{0.004}$	$13.75\pm^{0.014}_{0.014}$	...
HIPEQ1411-01	$13.61\pm^{0.007}_{0.007}$	$12.63\pm^{0.001}_{0.001}$	$12.31\pm^{0.001}_{0.001}$	$12.21\pm^{0.002}_{0.002}$	$12.04\pm^{0.005}_{0.005}$	...
HIPEQ1415+04	$15.49\pm^{0.016}_{0.016}$	$15.01\pm^{0.003}_{0.004}$	$14.68\pm^{0.004}_{0.004}$	$14.44\pm^{0.005}_{0.005}$	$14.02\pm^{0.013}_{0.013}$	...
HIPEQ1416+03	$16.81\pm^{0.095}_{0.104}$	$16.06\pm^{0.017}_{0.017}$	$15.69\pm^{0.019}_{0.019}$	$15.69\pm^{0.027}_{0.028}$	$15.45\pm^{0.106}_{0.118}$	...
HIPEQ1422-00	$12.83\pm^{0.005}_{0.005}$	$11.89\pm^{0.001}_{0.001}$	$11.50\pm^{0.001}_{0.001}$	$11.33\pm^{0.001}_{0.001}$	$11.14\pm^{0.004}_{0.004}$	...
HIPEQ1429-00	$14.82\pm^{0.011}_{0.011}$	$14.02\pm^{0.002}_{0.002}$	$13.75\pm^{0.003}_{0.003}$	$13.61\pm^{0.004}_{0.004}$	$13.51\pm^{0.013}_{0.013}$	0.10
HIPEQ1432+00	$15.19\pm^{0.012}_{0.012}$	$14.04\pm^{0.002}_{0.002}$	$13.53\pm^{0.002}_{0.002}$	$13.25\pm^{0.002}_{0.002}$	$13.06\pm^{0.008}_{0.008}$	...
HIPEQ1433+01	$17.78\pm^{0.189}_{0.229}$	$16.83\pm^{0.027}_{0.028}$	$16.71\pm^{0.038}_{0.040}$	$16.44\pm^{0.048}_{0.050}$	$16.80\pm^{0.240}_{0.309}$	...
HIPEQ1433+02	$15.32\pm^{0.016}_{0.016}$	$14.51\pm^{0.003}_{0.003}$	$14.27\pm^{0.004}_{0.004}$	$14.24\pm^{0.006}_{0.006}$	$14.15\pm^{0.021}_{0.021}$	...
HIPEQ1437+02	$12.88\pm^{0.005}_{0.005}$	$12.16\pm^{0.001}_{0.001}$	$11.41\pm^{0.001}_{0.001}$	$11.13\pm^{0.001}_{0.001}$	$10.74\pm^{0.003}_{0.003}$	0.02
HIPEQ1437-00	$13.54\pm^{0.004}_{0.004}$	$12.45\pm^{0.001}_{0.001}$	$12.02\pm^{0.001}_{0.001}$	$11.78\pm^{0.001}_{0.001}$	$11.68\pm^{0.003}_{0.003}$	...
HIPEQ1439+02	$16.50\pm^{0.077}_{0.083}$	$15.40\pm^{0.015}_{0.015}$	$14.98\pm^{0.014}_{0.014}$	$14.72\pm^{0.017}_{0.017}$	$14.69\pm^{0.059}_{0.062}$	...

Table 3.4—Continued

HIPASS Name	u^a	g^a	r^a	i^a	z^a	Edge Correction[b]
HIPEQ1439-00	$13.81\pm^{0.010}_{0.010}$	$12.94\pm^{0.002}_{0.002}$	$12.55\pm^{0.002}_{0.002}$	$12.27\pm^{0.002}_{0.002}$	$12.22\pm^{0.007}_{0.007}$	...
HIPEQ1440+02	$15.00\pm^{0.014}_{0.014}$	$13.96\pm^{0.002}_{0.002}$	$13.69\pm^{0.002}_{0.002}$	$13.44\pm^{0.003}_{0.003}$	$13.85\pm^{0.012}_{0.012}$	...
HIPEQ1444+01a	$13.47\pm^{0.007}_{0.007}$	$12.17\pm^{0.001}_{0.001}$	$11.58\pm^{0.001}_{0.001}$	$11.25\pm^{0.001}_{0.001}$	$10.98\pm^{0.002}_{0.002}$	...
HIPEQ1500+01	$13.13\pm^{0.006}_{0.006}$	$11.77\pm^{0.001}_{0.001}$	$11.08\pm^{0.001}_{0.001}$	$10.72\pm^{0.001}_{0.001}$	$10.44\pm^{0.002}_{0.002}$	...
HIPEQ1504+02	$15.99\pm^{0.032}_{0.033}$	$14.95\pm^{0.005}_{0.005}$	$14.63\pm^{0.005}_{0.005}$	$14.48\pm^{0.007}_{0.007}$	$14.50\pm^{0.025}_{0.025}$	...
HIPEQ1504-00	$15.65\pm^{0.024}_{0.025}$	$14.62\pm^{0.005}_{0.005}$	$14.23\pm^{0.004}_{0.004}$	$14.04\pm^{0.006}_{0.006}$	$14.03\pm^{0.020}_{0.020}$	...
HIPEQ1507+01	$12.90\pm^{0.010}_{0.011}$	$11.41\pm^{0.001}_{0.001}$	$10.76\pm^{0.001}_{0.001}$	$10.38\pm^{0.001}_{0.001}$	$10.08\pm^{0.003}_{0.003}$	...
HIPEQ1542+00	$14.81\pm^{0.017}_{0.017}$	$13.61\pm^{0.002}_{0.002}$	$13.06\pm^{0.002}_{0.002}$	$12.77\pm^{0.002}_{0.002}$	$12.56\pm^{0.006}_{0.007}$	0.09
HIPEQ1544+02	$15.78\pm^{0.034}_{0.036}$	$14.57\pm^{0.004}_{0.004}$	$14.06\pm^{0.003}_{0.003}$	$14.02\pm^{0.005}_{0.005}$	$13.46\pm^{0.013}_{0.013}$	...
HIPEQ1545+00	$15.60\pm^{0.044}_{0.046}$	$14.93\pm^{0.010}_{0.010}$	$14.52\pm^{0.011}_{0.011}$	$14.33\pm^{0.016}_{0.016}$	$13.86\pm^{0.035}_{0.036}$	...
HIPEQ1601+01a	$13.52\pm^{0.016}_{0.016}$	$12.59\pm^{0.002}_{0.002}$	$12.25\pm^{0.002}_{0.002}$	$11.83\pm^{0.002}_{0.002}$	$11.77\pm^{0.007}_{0.007}$	0.14
HIPEQ1609-00	$16.60\pm^{0.063}_{0.067}$	$15.78\pm^{0.012}_{0.012}$	$15.76\pm^{0.017}_{0.018}$	$15.73\pm^{0.027}_{0.028}$	$15.71\pm^{0.100}_{0.111}$	...
HIPEQ1613-00	$15.26\pm^{0.023}_{0.023}$	$14.35\pm^{0.003}_{0.003}$	$14.25\pm^{0.004}_{0.004}$	$14.15\pm^{0.006}_{0.006}$	$13.80\pm^{0.018}_{0.018}$	...
HIPEQ1614+00	$14.58\pm^{0.021}_{0.022}$	$13.82\pm^{0.004}_{0.004}$	$13.56\pm^{0.005}_{0.005}$	$13.49\pm^{0.009}_{0.009}$	$13.36\pm^{0.025}_{0.026}$	...
HIPEQ1614-00	$14.90\pm^{0.024}_{0.024}$	$13.36\pm^{0.002}_{0.002}$	$12.66\pm^{0.002}_{0.002}$	$12.25\pm^{0.002}_{0.002}$	$11.97\pm^{0.004}_{0.005}$	0.04
HIPEQ2036-04	$14.92\pm^{0.017}_{0.018}$	$13.34\pm^{0.002}_{0.002}$	$12.55\pm^{0.002}_{0.002}$	$12.12\pm^{0.002}_{0.002}$	$11.98\pm^{0.005}_{0.005}$	...
HIPEQ2314+00	$15.14\pm^{0.013}_{0.013}$	$14.15\pm^{0.002}_{0.002}$	$13.77\pm^{0.002}_{0.002}$	$13.56\pm^{0.002}_{0.002}$	$13.40\pm^{0.009}_{0.009}$	...
HIPEQ2324-00	$14.79\pm^{0.020}_{0.021}$	$14.21\pm^{0.004}_{0.004}$	$14.05\pm^{0.006}_{0.006}$	$13.99\pm^{0.008}_{0.008}$	$13.81\pm^{0.029}_{0.030}$	...
HIPEQ2335+01	$16.40\pm^{0.103}_{0.114}$	$15.74\pm^{0.019}_{0.019}$	$15.25\pm^{0.018}_{0.019}$	$15.09\pm^{0.027}_{0.028}$	$14.81\pm^{0.075}_{0.080}$	...
HIPEQ2336+00	$13.66\pm^{0.007}_{0.007}$	$12.45\pm^{0.001}_{0.001}$	$11.88\pm^{0.001}_{0.001}$	$11.53\pm^{0.001}_{0.001}$	$11.24\pm^{0.003}_{0.003}$	...
HIPEQ2337+00	$15.04\pm^{0.042}_{0.043}$	$14.18\pm^{0.006}_{0.006}$	$13.81\pm^{0.007}_{0.007}$	$13.62\pm^{0.009}_{0.009}$	$13.59\pm^{0.041}_{0.043}$	...
HIPEQ2340+01	$15.74\pm^{0.026}_{0.027}$	$14.66\pm^{0.003}_{0.003}$	$14.15\pm^{0.003}_{0.003}$	$13.89\pm^{0.004}_{0.004}$	$13.78\pm^{0.014}_{0.014}$	...

[a]Uncertainties are based on the photometric errors described in §3.5 and *do not* account for calibration errors or other uncertainties.

[b]Edge corrections are determined using the r-band images of galaxies that are close to the edges of SDSS `fields`

3.6 Photometric Corrections

Various photometric corrections need to be made to responsibly use the aforementioned photometry for science. Variations in extinction, cosmic redshift and SDSS field boundaries can lead to significant offsets in the observed colors and magnitudes of galaxies. In this section we outline the photometric corrections that were are applied to the original photometry in Tables 3.3 and 3.4.

3.6.1 Edge Corrections

Of the 200 galaxies in the HI selected sample, 34 galaxies were close to the edge of an SDSS field, but were included in the sample because the majority of their light falls within their SDSS field. The flux lost beyond the edge boundary should not drastically affect the color of a galaxy, but it can change the derived absolute magnitude and therefore the stellar mass and other derived quantities. The optimal way to correct for this would be to mosaic the adjacent fields and redo the photometry on the mosaicked images. At the time of writing,we have just begun the process of properly mosaicking SDSS fields and have decided to leave that optimal correction for a later date. However, utilizing the Sérsic fit models allows for a reasonable alternative for estimating the 'flux 'lost" across the field edge.

To correct for the "lost" flux we overlay the Sérsic models for each of the 34 galaxies and mask out any regions that overlap (leaving only model flux that crosses the SDSS field boundaries). Using the same Petrosian apertures described in Section 3.5, we calculate the total remaining flux in the Sérsic models and convert the additional flux to a magnitude corrections. Only 23 of the 34 galaxies have any significant model flux that is lost across the field edge. Because the Sérsic models are only calculated in the r-band, we assume that a similar fraction of flux is lost in the other bands and use the r-band value as a universal magnitude correction. This assumption is reasonable for small corrections but may be incorrect for larger amounts of lost flux. The values for the edge correction are listed in Tables 3.3 and 3.4 for the elliptical and circular apertures respectively. The magnitudes in Tables 3.3 and 3.4 have not been corrected for the edge effects. However, the photometric quantities derived in Table 3.13 below include these edge corrections.

3.6.2 Extinction

The photometric magnitudes listed in Tables 3.3 and 3.4 must be corrected for both extinction from the Milky Way as well as the internal extinction from the extragalactic object itself. The former is provided by Schlegel, Finkbeiner, & Davis (1998) using dust maps of the Milky Way. The SDSS database provides the extinction values in all five bands at every SDSS pointing. All of the photometry reported in this thesis (including Tables 3.3 and 3.4) have had the Milky Way extinction corrections applied.

The internal extinction of a galaxy is a little more complicated. The literature gives examples of extinction corrections that have been applied on the basis Hubble type (Gavazzi & Boselli 1996), rotation speed (Tully et al. 1998), and a type-independent "sandwich-model" (Matthews et al. 1998). We follow the method of Tully et al. (1998) and calculate the internal extinction of a face-on galaxy in the I-band (γ_I), using the equation:

$$\gamma_I = 0.92 + 1.63(\log(2V_{rot}) - 2.5) \tag{3.10}$$

where V_{rot} is the inclination corrected W_{20} derived in Chapter 2. Several of the galaxies do not have well-measured axis ratios and thus do not have well measured inclinations, making the appropriate value of V_{rot} uncertain. An inclination of 60 degrees (the average inclination in a randomly aligned sample) has been assigned to all of these galaxies.

The γ_I value is corrected for inclination using:

$$A_I = \gamma_I \log\left(\frac{1}{b/a}\right) \tag{3.11}$$

where b/a is the axis ratio of the galaxy calculated from the Sérsic fits in §4.4.

Tully et al. (1998) also does not include equations for SDSS colors so we convert the I band extinction to the SDSS bands from the relations in Schlegel et al. (1998). The extinction values relative to I-band for u, g, r, i, and z are: 2.66, 1.95, 1.42, 1.07, and 0.763 respectively. Negative extinction values were converted to 0 before the application to the galaxy photometry. Many of the calculated extinction values for galaxies with uncertain axis ratios were negative and all of them had values below 0.09 in the I-band. Thus, the uncertain

inclinations are unlikely to have produced significant errors in the final photometry. All measured extinction values are reported in Table 3.5.

3.6.3 k-Corrections

Although this sample of galaxies is nearby, k-corrections are important for precise photometry of the more distant galaxies in the sample. We use Blanton et al.'s (2003b) kcorrect_v3.2 to k-correct all of the galaxies in the sample to z=0. These corrections are reported in Table 3.5 and are included in all reported photometric values except for the magnitudes and surface brightnesses. The median and the maximum r-band k-corrections are 0.008 and 0.031 respectively. For all science results in the remainder of this thesis, the photometric corrections will be applied unless specifically stated otherwise.

Table 3.5. Photometric Corrections

	Internal Extinction					K-correction				
HIPASS name	u	g	r	i	z	u	g	r	i	z
HIPEQ0014−00	0.848	0.623	0.453	0.343	0.243	0.038	-0.002	0.007	-0.014	-0.023
HIPEQ0027−01a	0.780	0.574	0.417	0.316	0.224	0.038	-0.001	0.008	-0.014	-0.029
HIPEQ0033-01	0.304	0.223	0.162	0.123	0.087	0.014	0.001	0.007	-0.004	-0.020
HIPEQ0043−00	0.476	0.350	0.254	0.193	0.137	0.042	0.009	0.010	0.001	-0.004
HIPEQ0051−00	0.447	0.329	0.239	0.181	0.128	0.010	-0.001	0.008	-0.001	-0.004
HIPEQ0058+00	0.015	0.011	0.008	0.006	0.004	0.053	0.012	0.017	0.004	-0.016
HIPEQ0107+01	0.000	0.000	0.000	0.000	0.000	0.004	-0.000	0.001	-0.002	-0.010
HIPEQ0119+00	0.053	0.039	0.028	0.021	0.015	0.041	-0.003	0.010	-0.008	0.006
HIPEQ0120−00	0.387	0.284	0.206	0.156	0.111	0.010	-0.001	0.008	-0.003	-0.007
HIPEQ0122+00	1.346	0.990	0.719	0.545	0.386	0.017	0.002	0.008	-0.008	-0.032
HIPEQ0123−00	0.000	0.000	0.000	0.000	0.000	0.070	0.009	0.024	-0.004	0.019
HIPEQ0126+00a	0.087	0.064	0.046	0.035	0.025	0.057	0.022	0.017	0.010	-0.016
HIPEQ0126-00b	0.134	0.098	0.071	0.054	0.038	0.012	-0.001	0.008	-0.007	-0.019
HIPEQ0154−00	0.028	0.021	0.015	0.011	0.008	0.075	0.045	0.019	0.021	-0.008
HIPEQ0222−00	0.786	0.578	0.420	0.318	0.225	0.008	-0.004	0.009	-0.004	-0.003
HIPEQ0228-01	0.017	0.012	0.009	0.007	0.005	0.010	-0.001	0.008	-0.001	-0.003
HIPEQ0230+00	0.000	0.000	0.000	0.000	0.000	0.016	0.008	0.005	0.005	-0.005
HIPEQ0230-01	1.023	0.752	0.546	0.414	0.293	0.012	0.004	0.006	0.003	-0.004
HIPEQ0231+00	0.253	0.186	0.135	0.102	0.073	0.060	0.002	0.016	-0.003	-0.023
HIPEQ0236+00	1.242	0.913	0.663	0.503	0.356	0.063	-0.001	0.015	-0.006	-0.030
HIPEQ0238+00	0.347	0.255	0.185	0.141	0.100	0.022	0.002	0.005	-0.008	-0.018
HIPEQ0240+01	0.000	0.000	0.000	0.000	0.000	0.006	-0.002	0.007	-0.002	-0.003
HIPEQ0241+00	1.366	1.004	0.729	0.553	0.392	0.006	0.000	0.004	0.000	-0.006
HIPEQ0244+00	0.000	0.000	0.000	0.000	0.000	0.025	0.006	0.004	-0.000	-0.004
HIPEQ0246-00a	0.785	0.577	0.419	0.318	0.225	0.025	0.007	0.005	0.001	-0.003
HIPEQ0246-00b	0.128	0.094	0.068	0.052	0.037	0.009	-0.000	0.008	0.000	-0.003
HIPEQ0249−00	0.151	0.111	0.081	0.061	0.043	0.069	0.015	0.017	0.007	-0.027
HIPEQ0249-00a	0.302	0.222	0.161	0.122	0.087	0.022	0.002	0.005	-0.008	-0.017
HIPEQ0249-00b	0.384	0.282	0.205	0.155	0.110	0.073	0.017	0.022	0.005	-0.007
HIPEQ0251-01	0.205	0.151	0.109	0.083	0.059	0.008	-0.004	0.009	-0.004	0.000
HIPEQ0300+00	0.911	0.669	0.486	0.368	0.261	0.025	0.002	0.001	-0.009	-0.006
HIPEQ0301−00	0.198	0.146	0.106	0.080	0.057	0.022	0.002	0.005	-0.008	-0.017
HIPEQ0306−00	0.125	0.092	0.067	0.051	0.036	0.041	0.026	0.008	0.012	-0.012
HIPEQ0316−00	0.000	0.000	0.000	0.000	0.000	0.081	0.040	0.022	0.019	-0.002
HIPEQ0320-06	0.601	0.442	0.321	0.243	0.172	0.018	0.005	0.007	-0.001	-0.021
HIPEQ0351−00	0.202	0.149	0.108	0.082	0.058	0.090	0.018	0.031	0.002	-0.026
HIPEQ0809+00	0.313	0.230	0.167	0.127	0.090	0.011	-0.001	0.008	-0.004	-0.010
HIPEQ0821+03b	0.442	0.325	0.236	0.179	0.127	0.044	0.015	0.010	0.005	-0.013
HIPEQ0821−00	0.000	0.000	0.000	0.000	0.000	0.011	-0.002	0.008	-0.006	-0.013
HIPEQ0822−00	0.328	0.241	0.175	0.133	0.094	0.042	-0.001	0.013	-0.005	0.008
HIPEQ0825−00	1.315	0.967	0.702	0.532	0.377	0.046	0.008	0.018	0.003	0.000
HIPEQ0855+02	0.276	0.203	0.148	0.112	0.079	0.038	0.004	0.009	-0.007	-0.028
HIPEQ0856+00	0.096	0.070	0.051	0.039	0.027	0.020	0.004	0.008	-0.003	-0.011
HIPEQ0923−00	0.910	0.669	0.486	0.368	0.261	0.034	0.001	0.005	-0.012	-0.032
HIPEQ0930+04	0.000	0.000	0.000	0.000	0.000	0.048	0.004	0.018	-0.002	0.009
HIPEQ0936+01	1.080	0.794	0.576	0.437	0.310	0.043	-0.012	0.017	-0.019	-0.019
HIPEQ0942+00	0.058	0.043	0.031	0.024	0.017	0.013	0.003	0.007	0.002	-0.004
HIPEQ0944-00b	0.247	0.182	0.132	0.100	0.071	0.006	-0.004	0.008	-0.004	-0.005
HIPEQ0945+01	1.219	0.896	0.651	0.493	0.350	0.012	-0.002	0.008	-0.006	-0.016
HIPEQ0946+02	0.727	0.535	0.388	0.294	0.209	0.013	-0.001	0.007	-0.006	-0.019
HIPEQ0947+00a	0.710	0.522	0.379	0.287	0.204	0.011	-0.002	0.008	-0.004	-0.008
HIPEQ0947+00b	0.221	0.163	0.118	0.089	0.063	0.012	-0.002	0.008	-0.007	-0.016
HIPEQ0953+01	2.414	1.775	1.289	0.977	0.693	0.007	-0.004	0.009	-0.005	-0.004
HIPEQ0954+01a	0.025	0.018	0.013	0.010	0.007	0.011	-0.003	0.008	-0.006	-0.013
HIPEQ0954+02a	0.000	0.000	0.000	0.000	0.000	0.070	0.003	0.021	-0.012	-0.013
HIPEQ0955+04a	0.657	0.483	0.351	0.266	0.188	0.012	-0.001	0.008	-0.003	-0.011
HIPEQ0958+01	0.216	0.159	0.116	0.088	0.062	0.011	-0.002	0.008	-0.006	-0.013
HIPEQ1000+03	1.477	1.086	0.788	0.598	0.424	0.015	0.003	0.007	-0.001	-0.019

Table 3.5—Continued

	Internal Extinction					K-correction				
HIPASS name	u	g	r	i	z	u	g	r	i	z
HIPEQ1010+05	0.223	0.164	0.119	0.090	0.064	0.043	0.012	0.010	0.003	-0.013
HIPEQ1014+03	0.520	0.382	0.277	0.210	0.149	0.010	0.004	0.005	0.003	-0.002
HIPEQ1015+02	0.453	0.333	0.242	0.183	0.130	0.007	-0.004	0.009	-0.005	-0.005
HIPEQ1026+03	0.678	0.498	0.362	0.274	0.194	0.015	0.003	0.008	-0.003	-0.019
HIPEQ1028+03	0.347	0.255	0.185	0.141	0.100	0.006	-0.003	0.007	-0.004	-0.008
HIPEQ1031+04	1.076	0.791	0.575	0.436	0.309	0.006	-0.004	0.007	-0.004	-0.009
HIPEQ1039+01	0.000	0.000	0.000	0.000	0.000	0.005	0.000	0.001	-0.001	-0.008
HIPEQ1041+00	0.052	0.038	0.028	0.021	0.015	0.049	-0.001	0.018	-0.007	0.011
HIPEQ1046+01	1.394	1.025	0.744	0.564	0.400	0.005	-0.002	0.004	-0.003	-0.013
HIPEQ1050+01	0.295	0.217	0.157	0.119	0.085	0.009	-0.003	0.009	-0.004	-0.003
HIPEQ1051+04a	0.460	0.338	0.245	0.186	0.132	0.005	-0.003	0.005	-0.004	-0.014
HIPEQ1052+00	0.092	0.068	0.049	0.037	0.026	0.011	-0.001	0.008	-0.004	-0.009
HIPEQ1053+02	0.070	0.052	0.038	0.028	0.020	0.005	-0.003	0.005	-0.004	-0.014
HIPEQ1055+02	0.060	0.044	0.032	0.024	0.017	0.005	-0.003	0.005	-0.004	-0.014
HIPEQ1101+03	1.546	1.137	0.825	0.626	0.443	0.006	-0.003	0.006	-0.004	-0.011
HIPEQ1109−00	0.982	0.722	0.524	0.397	0.282	0.040	0.009	0.009	0.000	-0.022
HIPEQ1110+01	0.000	0.000	0.000	0.000	0.000	0.005	-0.002	0.004	-0.003	-0.013
HIPEQ1113+05	0.083	0.061	0.045	0.034	0.024	0.020	0.002	0.007	-0.008	-0.023
HIPEQ1117+04a	0.385	0.283	0.206	0.156	0.111	0.011	0.002	0.007	0.002	-0.005
HIPEQ1119+02	0.408	0.300	0.218	0.165	0.117	0.009	-0.004	0.010	-0.006	-0.003
HIPEQ1124+03	0.237	0.174	0.127	0.096	0.068	0.007	-0.005	0.010	-0.005	-0.002
HIPEQ1127-01	0.017	0.013	0.009	0.007	0.005	0.005	-0.001	0.004	-0.001	-0.004
HIPEQ1131-02	0.011	0.008	0.006	0.004	0.003	0.045	0.005	0.016	0.000	-0.001
HIPEQ1133-03	0.306	0.225	0.164	0.124	0.088	0.009	-0.003	0.009	-0.004	-0.001
HIPEQ1136+00	0.090	0.066	0.048	0.037	0.026	0.005	-0.003	0.006	-0.004	-0.012
HIPEQ1138+03	0.031	0.023	0.016	0.012	0.009	0.058	0.023	0.018	0.011	-0.010
HIPEQ1143-01	0.000	0.000	0.000	0.000	0.000	0.010	-0.004	0.009	-0.006	-0.006
HIPEQ1145+02	0.000	0.000	0.000	0.000	0.000	0.005	-0.003	0.004	-0.004	-0.015
HIPEQ1148-02	0.490	0.360	0.261	0.198	0.140	0.010	-0.003	0.008	-0.005	-0.008
HIPEQ1151-02	0.597	0.439	0.319	0.242	0.171	0.038	0.003	0.008	-0.007	-0.025
HIPEQ1152+01	0.235	0.173	0.126	0.095	0.067	0.055	-0.008	0.016	-0.013	-0.002
HIPEQ1152-02	0.000	0.000	0.000	0.000	0.000	0.005	-0.003	0.005	-0.004	-0.014
HIPEQ1152-03b	0.002	0.001	0.001	0.001	0.000	0.009	-0.002	0.008	-0.002	-0.004
HIPEQ1155+01	0.325	0.239	0.174	0.132	0.093	0.013	0.003	0.007	0.001	-0.009
HIPEQ1200−00	0.000	0.000	0.000	0.000	0.000	0.014	0.002	0.007	-0.001	-0.015
HIPEQ1200-01	0.223	0.164	0.119	0.090	0.064	0.010	0.002	0.007	0.002	0.002
HIPEQ1202+01	0.090	0.066	0.048	0.036	0.026	0.017	0.010	0.006	0.007	0.002
HIPEQ1204-01	0.041	0.030	0.022	0.017	0.012	0.008	-0.004	0.010	-0.004	0.000
HIPEQ1204-02	0.000	0.000	0.000	0.000	0.000	0.067	0.032	0.019	0.016	-0.007
HIPEQ1210+02	0.010	0.007	0.005	0.004	0.003	0.008	-0.002	0.009	-0.001	0.003
HIPEQ1215+04a	0.050	0.037	0.027	0.020	0.014	0.016	0.003	0.007	-0.003	-0.025
HIPEQ1216-03	0.002	0.002	0.001	0.001	0.001	0.046	0.004	0.019	-0.001	0.007
HIPEQ1218+00	0.000	0.000	0.000	0.000	0.000	0.006	-0.001	0.003	-0.001	-0.009
HIPEQ1218-01	0.579	0.426	0.309	0.234	0.166	0.056	0.013	0.017	0.004	-0.013
HIPEQ1219+03	0.000	0.000	0.000	0.000	0.000	0.009	-0.002	0.009	-0.002	-0.000
HIPEQ1220+00	0.000	0.000	0.000	0.000	0.000	0.005	-0.001	0.002	-0.003	-0.014
HIPEQ1220+01	1.216	0.894	0.649	0.492	0.349	0.009	-0.004	0.010	-0.006	-0.003
HIPEQ1221+03	1.499	1.102	0.800	0.607	0.430	0.021	0.006	0.008	0.000	-0.003
HIPEQ1223+00	0.084	0.062	0.045	0.034	0.024	0.014	0.001	0.008	-0.005	-0.021
HIPEQ1223-03b	1.662	1.222	0.887	0.673	0.477	0.015	0.003	0.007	-0.000	-0.016
HIPEQ1224+00	0.020	0.014	0.010	0.008	0.006	0.015	0.002	0.007	-0.003	-0.021
HIPEQ1224+03b	0.000	0.000	0.000	0.000	0.000	0.005	-0.001	0.003	-0.001	-0.010
HIPEQ1225+00	0.133	0.098	0.071	0.054	0.038	0.017	0.006	0.007	0.003	-0.008
HIPEQ1226+02	0.585	0.430	0.312	0.237	0.168	0.010	-0.002	0.008	-0.002	-0.004
HIPEQ1227+01	0.000	0.000	0.000	0.000	0.000	0.007	-0.004	0.009	-0.005	-0.004
HIPEQ1228+02	0.592	0.435	0.316	0.240	0.170	0.008	-0.004	0.010	-0.005	-0.002
HIPEQ1228+03	0.160	0.118	0.085	0.065	0.046	0.008	0.003	0.003	0.002	-0.001
HIPEQ1229+00	0.320	0.235	0.171	0.129	0.092	0.016	0.003	0.008	-0.005	-0.030

Table 3.5—Continued

	Internal Extinction					K-correction				
HIPASS name	u	g	r	i	z	u	g	r	i	z
HIPEQ1230+02	0.000	0.000	0.000	0.000	0.000	0.009	-0.003	0.009	-0.004	-0.003
HIPEQ1230+03	0.200	0.147	0.107	0.081	0.057	0.045	-0.011	0.017	-0.020	-0.019
HIPEQ1232+00a	0.370	0.272	0.197	0.150	0.106	0.009	-0.002	0.009	-0.002	-0.003
HIPEQ1232+00b	2.121	1.559	1.132	0.858	0.608	0.006	-0.003	0.006	-0.004	-0.010
HIPEQ1233-02	0.000	0.000	0.000	0.000	0.000	0.020	0.004	0.007	-0.004	-0.021
HIPEQ1236+03	0.347	0.255	0.185	0.140	0.099	0.008	-0.004	0.010	-0.005	-0.001
HIPEQ1239−00	0.860	0.632	0.459	0.348	0.247	0.005	-0.003	0.005	-0.004	-0.013
HIPEQ1241+01	0.293	0.215	0.156	0.118	0.084	0.011	0.000	0.007	0.000	-0.004
HIPEQ1241-02	0.157	0.116	0.084	0.064	0.045	0.009	-0.000	0.008	0.001	0.000
HIPEQ1242+03b	0.273	0.201	0.146	0.110	0.078	0.005	0.001	0.001	-0.000	-0.006
HIPEQ1242−00	0.788	0.579	0.420	0.319	0.226	0.010	-0.002	0.008	-0.003	-0.004
HIPEQ1242-01a	0.216	0.159	0.115	0.087	0.062	0.006	-0.002	0.006	-0.002	-0.006
HIPEQ1242-01b	1.326	0.975	0.708	0.537	0.380	0.031	0.003	0.000	-0.007	-0.014
HIPEQ1243−00	0.297	0.218	0.159	0.120	0.085	0.022	0.006	0.007	-0.000	-0.004
HIPEQ1244+00	0.178	0.131	0.095	0.072	0.051	0.006	-0.004	0.007	-0.004	-0.009
HIPEQ1244-02	0.178	0.131	0.095	0.072	0.051	0.009	-0.004	0.009	-0.005	-0.002
HIPEQ1245−00	1.344	0.988	0.718	0.544	0.386	0.009	0.000	0.008	0.001	-0.001
HIPEQ1249+03	0.231	0.170	0.123	0.094	0.066	0.005	0.000	0.001	-0.002	-0.010
HIPEQ1249+04	0.018	0.013	0.010	0.007	0.005	0.022	0.002	0.005	-0.008	-0.016
HIPEQ1250+05	0.261	0.192	0.139	0.106	0.075	0.004	-0.000	0.001	-0.003	-0.012
HIPEQ1253+01	1.308	0.961	0.698	0.529	0.375	0.007	-0.001	0.005	-0.000	-0.006
HIPEQ1253+02	0.165	0.122	0.088	0.067	0.047	0.009	0.003	0.004	0.003	0.001
HIPEQ1253+04	0.004	0.003	0.002	0.001	0.001	0.005	-0.000	0.001	-0.002	-0.013
HIPEQ1255+00	0.068	0.050	0.036	0.027	0.019	0.008	-0.001	0.008	-0.000	-0.003
HIPEQ1255+02	1.239	0.911	0.662	0.502	0.356	0.026	0.009	0.005	0.003	-0.009
HIPEQ1255−00	0.090	0.066	0.048	0.036	0.026	0.006	-0.002	0.005	-0.002	-0.008
HIPEQ1256+03	0.327	0.241	0.175	0.133	0.094	0.004	-0.000	0.000	-0.003	-0.015
HIPEQ1257+02	0.146	0.107	0.078	0.059	0.042	0.005	-0.002	0.003	-0.004	-0.014
HIPEQ1257-01	1.427	1.049	0.762	0.578	0.409	0.025	0.002	0.001	-0.009	-0.006
HIPEQ1258+02	0.346	0.254	0.185	0.140	0.099	0.024	0.005	0.004	-0.003	-0.009
HIPEQ1300+02a	0.000	0.000	0.000	0.000	0.000	0.006	0.000	0.002	-0.000	-0.007
HIPEQ1300+02b	0.134	0.098	0.071	0.054	0.038	0.005	-0.001	0.004	-0.001	-0.003
HIPEQ1303+03	0.014	0.010	0.007	0.006	0.004	0.026	0.005	0.002	-0.003	-0.007
HIPEQ1304-02	0.042	0.031	0.022	0.017	0.012	0.007	-0.002	0.008	-0.002	-0.004
HIPEQ1304-03	0.156	0.114	0.083	0.063	0.045	0.008	-0.004	0.010	-0.004	-0.002
HIPEQ1307−00	0.271	0.199	0.145	0.110	0.078	0.048	-0.004	0.017	-0.011	-0.011
HIPEQ1308-02	0.118	0.087	0.063	0.048	0.034	0.048	0.006	0.018	0.000	0.008
HIPEQ1311+03a	0.642	0.472	0.343	0.260	0.184	0.028	0.002	-0.000	-0.009	-0.008
HIPEQ1312+03	0.199	0.147	0.106	0.081	0.057	0.090	0.037	0.027	0.013	-0.027
HIPEQ1312+05	0.024	0.018	0.013	0.010	0.007	0.005	-0.002	0.003	-0.004	-0.016
HIPEQ1313+06	0.103	0.075	0.055	0.041	0.029	0.077	0.025	0.021	0.011	-0.018
HIPEQ1317−00	0.235	0.173	0.126	0.095	0.068	0.006	-0.004	0.008	-0.005	-0.007
HIPEQ1318-01	0.054	0.039	0.029	0.022	0.015	0.052	0.011	0.020	0.005	0.021
HIPEQ1320+05	0.023	0.017	0.012	0.009	0.007	0.005	-0.000	0.004	-0.001	-0.003
HIPEQ1327+02	0.000	0.000	0.000	0.000	0.000	0.005	-0.003	0.004	-0.004	-0.014
HIPEQ1329−00	0.511	0.375	0.273	0.207	0.147	0.031	0.002	0.001	-0.008	-0.012
HIPEQ1332+01	0.065	0.047	0.034	0.026	0.019	0.035	0.018	0.007	0.009	-0.007
HIPEQ1335+01	0.400	0.294	0.213	0.162	0.115	0.051	0.011	0.017	0.004	-0.018
HIPEQ1341+05	0.329	0.242	0.175	0.133	0.094	0.067	-0.001	0.019	-0.011	-0.019
HIPEQ1348+03	0.365	0.268	0.195	0.148	0.105	0.007	-0.000	0.006	0.000	0.001
HIPEQ1352+02a	0.444	0.326	0.237	0.180	0.127	0.049	0.018	0.015	0.008	-0.008
HIPEQ1352-01	0.325	0.239	0.173	0.131	0.093	0.009	-0.001	0.008	-0.000	-0.003
HIPEQ1400+02	1.273	0.936	0.680	0.515	0.365	0.035	0.001	0.006	-0.012	-0.033
HIPEQ1411-01	1.430	1.051	0.763	0.579	0.410	0.008	-0.004	0.010	-0.006	-0.002
HIPEQ1415+04	0.000	0.000	0.000	0.000	0.000	0.051	-0.001	0.018	-0.007	0.012
HIPEQ1416+03	0.292	0.215	0.156	0.118	0.084	0.008	-0.004	0.010	-0.004	-0.001
HIPEQ1422−00	0.380	0.279	0.203	0.154	0.109	0.009	-0.002	0.009	-0.002	-0.001
HIPEQ1429−00	0.493	0.362	0.263	0.200	0.141	0.008	-0.004	0.010	-0.006	-0.002

Table 3.5—Continued

	Internal Extinction					K-correction				
HIPASS name	u	g	r	i	z	u	g	r	i	z
HIPEQ1432+00	1.045	0.768	0.558	0.423	0.300	0.010	-0.002	0.008	-0.002	-0.005
HIPEQ1433+01	0.000	0.000	0.000	0.000	0.000	0.011	-0.002	0.008	-0.007	-0.014
HIPEQ1433+02	0.090	0.066	0.048	0.036	0.026	0.008	-0.004	0.010	-0.005	-0.002
HIPEQ1437+02	1.445	1.063	0.772	0.585	0.415	0.011	-0.002	0.008	-0.004	-0.005
HIPEQ1437−00	0.396	0.291	0.211	0.160	0.114	0.013	0.002	0.007	-0.000	-0.013
HIPEQ1439+02	0.123	0.091	0.066	0.050	0.035	0.010	0.000	0.007	0.001	-0.004
HIPEQ1439−00	0.597	0.439	0.319	0.242	0.171	0.011	-0.002	0.008	-0.004	-0.009
HIPEQ1440+02	0.205	0.150	0.109	0.083	0.059	0.009	-0.004	0.009	-0.005	-0.003
HIPEQ1444+01a	0.585	0.430	0.312	0.237	0.168	0.011	0.002	0.007	0.002	-0.002
HIPEQ1500+01	0.685	0.504	0.366	0.277	0.197	0.010	0.002	0.007	0.002	-0.001
HIPEQ1504+02	0.136	0.100	0.073	0.055	0.039	0.084	-0.008	0.030	-0.024	-0.023
HIPEQ1504−00	0.935	0.688	0.499	0.379	0.268	0.011	-0.003	0.008	-0.006	-0.012
HIPEQ1507+01	0.037	0.027	0.020	0.015	0.011	0.025	0.015	0.008	0.009	0.003
HIPEQ1542+00	1.546	1.137	0.825	0.626	0.443	0.013	-0.001	0.007	-0.005	-0.018
HIPEQ1544+02	0.039	0.029	0.021	0.016	0.011	0.039	0.015	0.012	0.006	0.008
HIPEQ1545+00	0.038	0.028	0.020	0.015	0.011	0.038	0.008	0.010	-0.001	-0.006
HIPEQ1601+01a	0.565	0.416	0.302	0.229	0.162	0.013	0.001	0.007	-0.002	-0.016
HIPEQ1609−00	0.141	0.103	0.075	0.057	0.040	0.008	-0.004	0.010	-0.005	-0.002
HIPEQ1613−00	0.238	0.175	0.127	0.096	0.068	0.015	0.001	0.008	-0.006	-0.023
HIPEQ1614+00	0.056	0.041	0.030	0.023	0.016	0.013	-0.000	0.007	-0.005	-0.019
HIPEQ1614−00	2.380	1.750	1.270	0.963	0.683	0.014	0.001	0.007	-0.005	-0.022
HIPEQ2036-04	0.624	0.459	0.333	0.253	0.179	0.071	0.033	0.018	0.017	-0.023
HIPEQ2314+00	0.000	0.000	0.000	0.000	0.000	0.043	0.006	0.011	-0.000	-0.003
HIPEQ2324−00	0.264	0.194	0.141	0.107	0.076	0.023	0.002	0.004	-0.008	-0.014
HIPEQ2335+01	0.080	0.059	0.043	0.033	0.023	0.022	0.006	0.007	-0.001	-0.004
HIPEQ2336+00	0.420	0.309	0.224	0.170	0.121	0.023	0.010	0.008	0.005	-0.000
HIPEQ2337+00	0.167	0.123	0.089	0.068	0.048	0.023	0.005	0.005	-0.003	-0.013
HIPEQ2340+01	0.529	0.389	0.282	0.214	0.152	0.013	0.002	0.007	-0.000	-0.012

3.7 Other Measured Petrosian Properties

In addition to providing a measurement of flux that is robust to changes in surface brightness and distance, Petrosian quantities can be use to calculate robust measurements of size and surface brightness. In this section, we describe the method used to derive the Petrosian sizes and surface brightness.

Once a Petrosian flux has been measured (see above), we compute the 50% (R50)and 90% (R90) radii for both the elliptical apertures and circular apertures. These values correspond to the `PetroR50` and `PetroR90` parameters in the SDSS `tsObj` files. They are converted to arcseconds using the SDSS pixel scale of 0.396 $''$/pixel. The R90 and R590 values and there uncertainties are reported in Tables 3.6 and 3.7. For an exponential disk galaxy, the R50 and R90 values correspond to 1.668 and 3.816 times the scale length respectively. For a de Vaucouleurs model the R50 and R90 correspond to 0.7124 and 2.387 times the effective half-light radius (r_e).

For this study we report four different values of surface brightness for every galaxy. Each surface brightness value reported below has been corrected for Milky Way extinction but has not been corrected for internal extinction, or k-corrections. The four methods are as follows, with values tabulated in Tables 3.8 and 3.9:

- *Observed elliptical Petrosian surface brightness* - This quantity is the measured surface brightness within R50. It is defined by taking half of the Petrosian flux and dividing by the elliptical aperture area with a semi-major axis equal to the elliptical R50. For galaxies with well defined elliptical apertures, this is the most reliable measure of the average surface brightness of the galaxy as it appears in the image. For an exponential disk, the Petrosian surface brightness is 1.118 times the central surface brightness in mag/$\Box''$.

- *Observed circular Petrosian surface brightness* - An integrated surface brightness that is defined by taking half of the circular Petrosian flux and dividing by the area enclosed by a circle with a radius equal to the circular R50. This surface brightness is the default defined by SDSS and is used for selecting targets for SDSS spectroscopy (Strauss et

al. 2002). This surface brightness is adopted when a a circular aperture is used for photometry. However, due to the effects discussed in Appendix A, it is not a robust measure of the apparent surface brightness.

- *Intrinsic face-on surface brightness (optically thin)* - Many of the galaxies in this sample are optically thin due to the prevalence of late-type, low mass galaxies in the HIPASS/SDSS sample. We have therefore computed an intrinsic surface brightness that corresponds to the expected surface brightness of the galaxy if it were seen face-on. To calculate this quantity, we assume that *all* of the light from the galaxy is detected but that the apparent surface brightness has been amplified due to the inclination of the galaxy, which produces a larger line of sight through the galaxy. For the galaxies with well defined elliptical apertures, we de-project the galaxy and divide half of the Petrosian flux by a circle with the elliptical R50 radius[1] Although this quantity should reproduce the face-on surface brightness for an optically thin galaxy, it will overestimate the face-on surface brightness of optically thick galaxies in our sample. For these systems, the apparent surface brightness is likely to be constant at all inclinations and thus the observed elliptical Petrosian Surface brightness is the more appropriate measure of the intrinsic face-on surface brightness.

- *Fiber surface brightness (central)* - Following SDSS, we define a surface brightness within a $3''$ circular radius that is placed at the center of each galaxy. The positions are not the SDSS defined fiber positions but instead the centers determined for the Sérsic fits for each galaxy. We did not make any corrections for inclination and simply measured the flux inside the "fiber" and divide by the circular fiber area. These are more robust than the SDSS fiber quantities because they are specifically placed at the center of each galaxy rather than occasionally ending up on an HII region as happens in spectral targeting. Given the large angular extent of the galaxies in the HIPASS/SDSS sample, the resulting surface brightness is an approximate measure of the apparent central surface brightness of the galaxy image.

[1]Note that this radius is distinct from the circular Petrosian surface brightness because the elliptical R50 is always larger than the circular R50 (as described in Appendix A).

Table 3.6. Measured Elliptical Petrosian Sizes

	R50 (″)					R90 (″)				
HIPASS Name	u	g	r	i	z	u	g	r	i	z
HIPEQ0014-00	30.5±5.9	25.3±0.4	21.4±0.4	19.8±0.4	18.6±0.4	69.7±5.9	61.8±0.4	59.0±0.8	58.2±0.8	63.0±4.4
HIPEQ0027-01a	24.9±6.3	22.2±0.4	21.4±0.4	21.0±0.4	19.8±0.8	63.4±6.3	45.1±1.2	43.6±0.8	44.0±2.0	60.2±5.9
HIPEQ0033-01	34.8±0.4	29.7±0.4	26.9±0.4	29.7±1.2	29.7±2.8	65.3±0.4	61.8±0.4	60.6±2.0	63.8±2.8	63.0±0.4
HIPEQ0043-00	16.6±1.6	15.0±0.4	13.9±0.4	13.5±0.4	13.1±0.4	41.6±1.6	38.0±0.4	36.4±0.4	36.4±0.4	36.4±1.2
HIPEQ0051-00	5.5±2.4	5.5±0.4	6.3±0.4	6.7±0.4	6.7±0.4	16.6±2.4	16.6±0.4	17.4±0.4	18.6±0.4	18.6±1.2
HIPEQ0058+00	12.3±2.8	11.1±0.4	10.7±0.4	10.3±0.4	9.9±0.4	30.5±2.8	23.4±0.4	23.0±0.4	23.0±0.4	23.8±1.2
HIPEQ0107+01	7.9±5.1	10.3±0.4	11.5±0.4	12.7±0.4	12.3±0.8	25.7±5.1	25.3±0.4	27.3±0.8	29.3±1.6	30.1±6.7
HIPEQ0119+00	13.1±50.3	9.5±0.4	8.7±0.4	8.3±0.4	9.5±1.2	25.3±50.3	20.6±2.4	18.2±2.0	16.2±2.0	17.0±17.0
HIPEQ0120-00	19.0±11.5	17.8±0.4	18.2±0.4	18.6±0.4	19.4±0.8	39.2±11.5	33.3±0.4	35.6±0.8	37.6±1.2	48.7±6.3
HIPEQ0122+00	68.9±4.8	56.6±0.4	53.5±0.4	53.1±0.4	56.2±0.4	149.7±4.8	108.1±0.8	105.7±0.8	109.3±1.2	137.4±4.8
HIPEQ0123-00	17.0±2.4	14.3±0.4	13.1±0.4	13.1±0.4	13.1±0.4	44.7±2.4	32.1±0.4	31.3±0.4	31.3±0.8	34.8±4.0
HIPEQ0126+00a	12.3±19.4	11.5±0.8	10.7±0.4	10.7±0.4	9.1±1.6	24.2±19.4	24.2±3.6	23.0±2.0	23.4±3.2	26.5±13.1
HIPEQ0126-00b	4.8±1.6	4.8±0.4	5.1±0.4	5.5±0.4	5.1±0.4	11.1±1.6	10.7±0.4	11.5±0.4	11.9±0.4	10.3±1.6
HIPEQ0154-00	9.9±3.2	8.7±0.4	8.3±0.4	8.3±0.4	7.5±0.4	30.1±3.2	26.9±0.4	26.5±0.4	26.5±0.4	25.3±0.4
HIPEQ0222-00	36.0±14.7	32.9±0.4	32.5±0.4	31.3±0.4	30.9±1.2	74.8±14.7	63.8±1.2	63.0±1.6	59.0±1.6	59.8±9.5
HIPEQ0228-01	31.3±2.4	27.3±0.4	26.1±0.4	26.1±0.4	26.9±0.4	74.1±2.4	66.9±0.4	64.9±0.4	66.5±0.4	71.7±1.6
HIPEQ0230+00	32.5±118.8	24.2±0.4	25.3±0.4	24.9±0.4	26.1±2.4	79.6±118.8	55.8±4.8	57.8±2.4	59.0±2.8	68.1±9.5
HIPEQ0230-01	19.0±0.8	16.2±0.4	15.4±0.4	15.4±0.4	14.7±0.4	54.3±0.8	48.7±0.4	46.7±0.4	46.3±0.4	43.2±0.4
HIPEQ0231+00	18.6±7.1	15.4±0.4	15.0±0.4	14.7±0.4	15.8±1.6	49.1±7.1	32.9±1.6	34.5±2.4	34.8±2.4	43.2±5.5
HIPEQ0236+00	18.6±6.3	16.2±0.4	15.0±0.4	14.3±0.4	13.5±0.4	40.4±6.3	32.5±0.8	31.7±0.8	31.3±0.8	29.7±2.0
HIPEQ0238+00	17.8±44.4	18.6±0.4	17.8±0.8	17.8±1.2	17.4±2.0	30.5±44.4	36.0±2.4	33.7±3.6	36.8±4.4	37.6±17.0
HIPEQ0240+01	21.8±28.1	22.6±0.8	23.4±1.2	23.8±1.6	26.5±3.6	57.8±28.1	55.8±3.2	60.6±4.8	61.8±5.9	66.5±13.5
HIPEQ0241+00	120.8±4.4	106.5±0.4	101.4±0.4	95.8±0.4	91.5±0.4	248.3±4.4	247.1±0.4	245.1±0.4	236.8±0.4	236.0±1.6
HIPEQ0244+00	26.1±10.3	21.8±0.4	22.2±0.4	23.4±0.4	23.8±1.2	78.8±10.3	47.5±1.6	50.7±2.4	63.0±4.0	71.3±6.7
HIPEQ0246-00a	56.6±3.6	44.4±0.4	40.8±0.4	38.8±0.4	40.0±0.4	123.2±3.6	102.6±0.4	96.6±0.4	95.8±0.4	108.5±1.6
HIPEQ0246-00b	39.2±1.6	40.0±0.4	40.0±0.4	40.4±0.4	40.4±0.4	94.2±1.6	90.7±0.4	91.9±0.4	93.9±0.4	95.8±0.8
HIPEQ0249-00	16.2±5.1	13.1±0.4	12.3±0.4	12.3±0.4	11.5±0.4	38.0±5.1	31.3±0.8	28.9±0.4	28.9±0.8	30.5±2.0
HIPEQ0249-00a	23.8±12.3	19.4±0.4	18.2±0.4	16.2±0.8	19.4±3.6	49.5±12.3	38.8±2.0	36.0±27.7	33.7±11.9	49.1±53.1
HIPEQ0249-00b	18.6±3.2	15.0±0.4	13.9±0.4	13.9±0.4	13.5±0.4	51.9±3.2	41.6±0.4	39.6±0.4	40.4±0.4	42.0±0.8
HIPEQ0251-01	47.5±8.3	44.0±0.8	43.6±0.4	43.6±0.8	44.4±1.6	93.5±8.3	86.7±2.0	86.3±1.6	87.5±2.8	86.3±5.9
HIPEQ0300+00	20.2±20.2	19.8±0.4	18.6±0.4	18.2±0.4	19.4±0.8	59.4±20.2	39.6±0.8	37.6±0.8	38.0±1.6	47.9±11.5
HIPEQ0301-00	22.2±5.5	17.8±0.4	17.0±0.4	17.8±0.4	19.0±1.6	57.0±5.5	47.1±1.2	47.1±2.0	49.1±2.0	51.1±4.0
HIPEQ0306-00	14.3±2.0	11.5±0.4	11.1±0.4	11.5±0.4	10.7±0.4	43.6±2.0	40.4±0.4	39.6±0.4	40.0±0.4	38.8±0.4
HIPEQ0316-00	20.2±5.5	19.8±0.4	17.4±0.4	16.6±0.4	16.2±0.4	39.6±5.5	37.6±0.4	36.0±0.4	35.6±0.4	37.2±1.6
HIPEQ0320-06	15.0±0.8	14.7±0.4	14.3±0.4	14.3±0.4	13.9±0.4	32.1±0.8	31.3±0.4	31.7±0.4	32.9±0.4	32.5±0.4
HIPEQ0351-00	5.5±2.0	5.9±0.4	5.9±0.4	5.9±0.4	5.1±0.4	12.7±2.0	13.9±5.1	13.9±0.4	13.9±6.7	13.5±32.5
HIPEQ0809+00	22.2±3.6	19.8±0.4	19.4±0.4	19.0±0.4	20.2±0.4	50.7±3.6	39.6±0.4	40.4±0.4	40.8±0.4	51.1±2.8
HIPEQ0821+03b	13.1±1.6	12.7±0.4	11.9±0.4	11.5±0.4	10.7±0.4	33.3±1.6	30.1±0.4	27.7±0.4	27.7±0.4	27.3±0.8
HIPEQ0821-00	11.5±2.4	13.5±0.4	13.9±0.4	13.1±0.4	15.4±1.6	36.0±2.4	36.0±0.8	36.0±0.8	32.9±1.2	48.7±14.3
HIPEQ0822-00	23.4±3.2	19.4±0.4	18.6±0.4	18.2±0.4	19.4±0.8	55.8±3.2	37.6±0.8	37.2±0.4	38.0±0.4	49.5±2.8

Table 3.6—Continued

	R50 (″)					R90 (″)				
HIPASS Name	u	g	r	i	z	u	g	r	i	z
HIPEQ0825-00	34.8±2.0	23.0±0.4	20.6±0.4	20.2±0.4	19.4±0.4	75.2±2.0	53.9±0.4	48.7±0.4	50.7±0.4	54.3±1.2
HIPEQ0855+02	35.2±13.1	34.8±0.4	32.5±0.4	33.7±1.2	38.0±3.6	72.1±13.1	71.3±1.2	70.1±2.0	73.3±2.8	75.2±6.7
HIPEQ0856+00	26.5±2.4	21.0±0.4	20.2±0.4	24.6±0.4	24.9±0.8	60.2±2.4	56.6±1.2	58.6±0.8	63.4±0.4	61.8±2.4
HIPEQ0923-00	22.2±4.4	19.4±0.4	18.2±0.4	17.8±0.4	17.4±0.4	47.1±4.4	36.4±0.4	36.0±0.4	37.6±0.4	45.1±5.9
HIPEQ0930+04	30.5±4.4	25.3±0.4	23.8±0.4	23.8±0.4	23.8±0.4	79.6±4.4	66.5±0.8	64.9±0.8	67.3±1.2	72.9±2.8
HIPEQ0942+00	35.2±1.6	30.5±0.4	28.5±0.4	28.1±0.4	29.7±0.4	85.1±1.6	76.0±0.4	72.1±0.4	73.3±0.4	82.4±1.2
HIPEQ0944-00b	12.7±10.3	12.3±0.4	11.5±0.4	9.9±0.4	12.3±1.2	31.3±10.3	29.7±1.2	27.3±0.8	23.4±1.6	33.7±5.5
HIPEQ0945+01	36.8±9.1	34.8±0.4	34.1±0.4	34.1±0.4	35.2±0.4	82.0±9.1	72.5±0.8	72.9±0.8	75.6±0.8	93.5±3.2
HIPEQ0946+02	41.2±9.5	34.5±0.4	32.9±0.4	32.1±0.4	35.6±1.6	90.3±9.5	85.1±2.8	82.0±2.8	86.7±2.8	91.1±7.1
HIPEQ0947+00a	37.6±5.9	30.9±0.4	29.3±0.4	28.9±0.4	30.9±0.8	77.2±5.9	65.7±1.2	63.8±1.6	67.3±1.6	76.4±5.1
HIPEQ0947+00b	33.3±8.3	25.3±0.4	23.8±0.8	22.2±0.8	23.0±2.8	64.2±8.3	56.2±2.8	53.5±3.6	56.6±27.3	58.2±34.5
HIPEQ0953+01	76.4±3.6	72.1±0.4	68.5±0.4	68.9±0.4	64.2±0.8	166.7±3.6	150.5±0.4	148.9±0.4	155.6±0.8	154.4±2.8
HIPEQ0954+02a	18.6±2.0	15.0±0.4	14.3±0.4	14.3±0.4	14.3±0.4	48.3±2.0	30.5±0.4	30.9±0.4	33.3±1.2	42.8±3.6
HIPEQ0955+04a	30.1±3.2	29.3±0.4	28.5±0.4	28.5±0.4	28.9±0.4	78.0±3.2	64.2±0.4	63.8±0.4	64.9±0.4	74.1±1.6
HIPEQ0958+01	20.2±17.0	17.0±0.4	16.2±0.8	15.4±2.0	20.2±32.9	36.4±17.0	31.7±5.5	32.5±10.3	43.2±53.9	34.8±90.3
HIPEQ1000+03	24.6±2.8	22.2±0.4	19.0±0.4	18.2±0.4	15.0±0.4	60.2±2.8	58.2±0.4	55.0±0.4	57.0±0.4	53.1±0.8
HIPEQ1010+05	7.1±4.4	7.5±0.4	7.9±0.4	8.3±0.4	7.9±0.4	24.9±4.4	23.8±0.8	24.9±0.4	24.2±0.8	24.9±2.4
HIPEQ1014+03	80.4±2.8	61.8±0.4	53.1±0.4	49.1±0.4	43.6±0.4	188.5±2.8	179.8±0.4	173.1±0.4	170.3±0.4	167.1±0.8
HIPEQ1015+02	42.4±24.6	38.8±0.8	35.6±0.8	40.0±1.6	33.3±4.0	97.4±24.6	102.6±4.8	96.2±5.5	106.9±7.5	76.8±15.4
HIPEQ1026+03	40.0±4.0	33.3±0.4	30.9±0.4	30.5±0.4	30.9±0.4	88.3±4.0	75.2±0.4	73.7±0.4	72.9±0.8	84.0±2.4
HIPEQ1028+03	24.9±17.0	25.3±0.4	25.7±0.4	25.7±0.4	27.3±0.8	56.6±17.0	52.3±2.0	52.7±2.4	56.6±3.2	65.3±7.9
HIPEQ1039+01	14.7±2.8	14.3±0.4	15.0±0.4	16.2±0.4	17.0±0.4	47.9±2.8	38.8±0.8	41.2±0.8	44.4±1.2	49.5±3.2
HIPEQ1041+00	19.0±3.6	15.4±0.4	15.4±0.4	16.6±0.4	16.6±0.4	48.3±3.6	32.5±0.8	35.2±0.8	40.8±1.2	47.9±2.4
HIPEQ1046+01	72.9±9.5	62.6±0.4	60.6±0.4	61.0±0.4	62.2±0.8	177.4±9.5	131.1±1.2	130.7±1.2	135.8±1.6	169.1±6.3
HIPEQ1050+01	10.7±43.6	10.3±0.4	10.7±0.4	10.3±0.4	8.3±1.6	15.4±43.6	17.4±1.2	19.0±1.2	18.2±2.4	14.3±51.5
HIPEQ1051+04a	30.9±4.8	26.1±0.4	24.9±0.4	24.6±0.4	24.9±1.2	77.2±4.8	63.8±0.8	63.4±0.8	64.2±1.2	77.6±5.5
HIPEQ1052+00	4.0±1.2	4.8±0.4	5.1±0.4	5.9±0.4	5.9±0.4	12.7±1.2	13.9±0.4	14.7±0.4	15.4±0.4	15.4±1.2
HIPEQ1053+02	11.9±5.1	12.3±0.4	13.1±0.4	13.5±0.4	14.7±1.2	28.9±5.1	25.7±0.8	28.1±1.2	29.3±2.0	31.3±6.7
HIPEQ1055+02	7.5±3.2	7.9±0.4	8.7±0.4	9.1±0.4	8.7±0.8	20.6±3.2	19.0±0.8	19.4±0.8	21.0±1.6	17.4±7.9
HIPEQ1101+03	86.3±4.4	76.4±0.4	73.3±0.4	72.1±0.4	72.9±0.4	188.9±4.4	152.5±0.8	145.3±0.8	148.5±0.8	166.3±1.6
HIPEQ1109-00	15.0±1.2	13.5±0.4	11.9±0.4	11.5±0.4	10.3±0.4	42.8±1.2	40.0±0.4	37.6±0.4	36.0±0.4	32.1±0.8
HIPEQ1110+01	15.0±11.5	16.2±0.4	17.0±0.4	17.4±0.4	18.2±1.2	40.4±11.5	31.3±0.8	34.5±1.2	34.8±2.0	36.8±8.3
HIPEQ1113+05	16.2±7.1	15.0±0.4	15.0±0.4	14.7±0.4	16.2±0.8	40.8±7.1	32.1±0.8	33.3±0.8	32.1±0.8	46.3±4.4
HIPEQ1117+04a	10.7±1.2	12.3±0.4	13.1±0.4	13.9±0.4	13.1±0.4	44.4±1.2	41.6±0.4	41.6±0.4	42.0±0.4	42.4±0.8
HIPEQ1119+02	45.5±2.8	35.2±0.4	34.1±0.4	36.0±0.4	40.8±2.4	99.0±2.8	90.3±1.2	89.9±1.6	90.3±2.0	85.9±6.3
HIPEQ1124+03	58.2±7.5	54.3±0.8	54.6±0.4	57.0±0.4	61.8±1.2	152.9±7.5	150.9±0.4	151.7±2.0	155.6±2.0	153.6±7.5
HIPEQ1127-01	22.2±7.1	19.4±0.4	20.6±0.4	21.8±0.4	31.7±1.2	66.1±7.1	61.8±1.2	64.5±1.6	66.5±2.0	75.6±4.4
HIPEQ1131-02	35.6±2.8	28.1±0.4	26.1±0.4	25.7±0.4	28.1±0.4	72.1±2.8	61.4±0.4	60.6±0.8	63.8±0.8	71.7±2.8
HIPEQ1133-03	25.7±4.0	22.2±0.4	21.4±0.4	21.8±0.4	24.6±0.8	59.0±4.0	48.7±1.6	47.5±1.6	51.1±2.0	62.6±5.1
HIPEQ1136+00	7.5±1.2	8.3±0.4	9.5±0.4	10.7±0.4	10.3±0.4	19.8±1.2	23.0±0.4	24.6±0.4	26.1±0.4	26.5±2.4

Table 3.6—Continued

HIPASS Name	R50 (″)					R90 (″)				
	u	g	r	i	z	u	g	r	i	z
HIPEQ1138+03	14.7±3.2	12.7±0.4	11.1±0.4	10.7±0.4	9.1±0.4	34.8±3.2	30.1±0.8	28.9±0.4	28.5±0.8	28.5±2.8
HIPEQ1143-01	11.1±15.8	11.1±0.4	11.1±0.4	11.5±0.8	10.7±4.4	32.5±15.8	21.4±3.2	28.5±4.8	25.3±8.7	22.2±18.2
HIPEQ1145+02	24.2±10.3	20.2±1.6	22.6±1.6	19.0±2.0	75.6±37.2	57.0±10.3	51.9±0.4	49.1±11.5	42.4±36.0	84.3±48.3
HIPEQ1148-02	42.8±7.1	37.2±0.4	34.8±0.4	38.4±0.4	35.6±1.6	95.8±7.1	91.1±1.2	91.9±2.0	99.4±2.0	90.7±8.7
HIPEQ1151-02	9.1±1.6	9.1±0.4	8.3±0.4	7.9±0.4	7.5±0.4	23.4±1.6	24.2±0.4	23.0±0.4	22.2±0.4	19.8±2.0
HIPEQ1152+01	17.8±4.4	16.2±0.4	16.2±0.4	16.2±0.4	16.2±0.4	40.8±4.4	32.5±0.4	34.1±0.8	36.8±0.8	40.8±2.4
HIPEQ1152-02	6.3±0.4	6.7±0.4	7.5±0.4	8.3±0.4	8.3±0.4	15.4±0.4	17.8±0.4	19.8±0.4	21.4±0.4	20.6±2.4
HIPEQ1152-03b	24.6±4.0	22.6±0.4	23.0±0.4	23.8±0.4	24.6±1.2	61.0±4.0	53.1±1.2	53.1±1.2	55.8±2.0	59.0±6.7
HIPEQ1155+01	51.9±2.8	46.7±0.4	45.1±0.4	43.6±0.4	45.1±0.4	89.5±2.8	84.0±0.4	83.6±0.4	82.8±0.8	87.9±2.0
HIPEQ1200-00	40.0±8.7	32.9±0.4	32.1±0.4	31.7±1.2	43.6±4.4	80.8±8.7	74.8±2.8	73.3±2.8	74.1±3.2	91.9±13.1
HIPEQ1200-01	45.9±1.2	38.8±0.4	34.8±0.4	34.1±0.4	32.1±0.4	113.7±1.2	100.2±0.4	97.8±0.4	100.2±0.4	102.6±0.4
HIPEQ1202+01	28.9±3.6	24.6±0.4	23.0±0.4	22.6±0.4	21.8±0.4	84.0±3.6	75.2±0.4	72.9±0.4	73.3±0.4	76.0±1.2
HIPEQ1204-01	30.1±9.9	25.7±0.4	25.7±0.8	24.2±0.8	25.7±2.4	55.0±9.9	48.7±2.4	49.1±2.0	46.3±3.6	48.3±13.9
HIPEQ1204-02	15.8±2.4	13.9±0.4	11.9±0.4	11.1±0.4	10.7±0.4	40.0±2.4	35.6±0.4	34.1±0.4	33.7±0.8	32.9±2.0
HIPEQ1210+02	31.3±11.1	24.9±0.8	24.2±0.8	23.8±1.2	24.6±3.6	55.0±11.1	51.9±2.4	52.7±2.4	51.1±3.6	54.6±11.5
HIPEQ1215+04a	13.5±5.1	13.1±0.4	13.9±0.4	13.9±0.4	13.9±0.4	34.5±5.1	31.3±0.4	32.1±0.8	32.1±0.8	35.6±4.8
HIPEQ1216-03	19.4±2.0	14.7±0.4	13.5±0.4	13.1±0.4	14.3±0.4	46.3±2.0	34.5±1.2	33.7±1.2	34.8±1.2	44.4±2.4
HIPEQ1218+00	38.8±9.1	31.7±0.8	31.3±0.4	30.5±0.4	29.7±2.4	71.3±9.1	69.7±2.4	67.7±2.8	71.3±3.2	72.1±13.5
HIPEQ1218-01	13.9±3.6	12.7±0.4	11.9±0.4	11.5±0.4	10.7±0.4	35.2±3.6	32.5±0.4	29.7±0.4	29.3±0.4	28.5±1.2
HIPEQ1219+03	10.3±2.4	12.3±0.4	13.5±0.4	14.7±0.4	15.0±0.4	32.9±2.4	32.1±0.4	33.3±0.4	34.8±0.8	38.8±2.4
HIPEQ1220+00	18.2±14.7	19.0±0.4	18.6±0.4	19.0±0.4	19.0±1.2	40.8±14.7	40.4±1.6	39.6±2.0	40.4±2.8	52.3±17.8
HIPEQ1220+01	32.5±6.7	29.7±0.4	28.9±0.4	28.5±0.4	28.5±0.8	68.5±6.7	58.2±1.2	59.0±0.8	58.2±1.6	65.3±4.8
HIPEQ1221+03	44.7±4.4	27.7±0.4	24.6±0.4	22.6±0.4	21.0±0.4	95.4±4.4	72.9±0.8	68.5±0.8	65.7±0.8	67.3±2.4
HIPEQ1223+00	26.1±9.9	22.6±0.8	23.4±0.8	23.0±1.2	26.5±2.4	62.6±9.9	55.4±2.0	57.8±2.8	57.0±5.9	59.0±10.7
HIPEQ1223-03b	33.7±2.8	30.5±0.4	28.1±0.4	28.1±0.4	26.5±0.4	80.0±2.8	70.1±0.4	66.9±0.4	67.7±0.4	66.9±1.2
HIPEQ1224+00	11.9±9.5	10.3±0.4	10.7±0.8	10.7±0.4	10.3±2.0	19.8±9.5	17.8±1.2	19.4±1.2	19.4±1.6	16.2±83.2
HIPEQ1224+03b	24.6±5.9	23.8±0.4	23.4±0.4	24.6±0.4	24.6±1.2	63.4±5.9	59.4±0.8	59.4±1.2	62.2±1.6	63.0±5.5
HIPEQ1225+00	21.4±1.6	22.2±0.4	21.0±0.4	21.8±0.4	22.2±0.4	61.8±1.6	54.6±0.8	53.5±0.4	54.6±0.4	61.4±0.8
HIPEQ1226+02	23.8±1.6	23.0±0.4	22.6±0.4	22.6±0.4	22.2±0.4	51.1±1.6	47.1±0.4	47.1±0.4	47.9±0.4	49.9±0.8
HIPEQ1227+01	19.4±9.1	17.4±1.2	19.0±1.2	21.0±1.6	21.8±5.1	44.7±9.1	40.8±3.6	43.6±3.2	43.2±7.1	44.4±19.0
HIPEQ1228+02	47.1±9.5	40.8±0.4	39.6±0.8	39.2±0.8	42.0±3.6	92.3±9.5	82.8±1.6	83.2±1.6	83.6±2.4	92.7±11.5
HIPEQ1228+03	22.6±0.8	20.6±0.4	19.8±0.4	19.8±0.4	19.0±0.4	69.7±0.8	68.1±0.4	66.9±0.4	66.9±0.4	66.1±0.4
HIPEQ1229+00	15.4±6.3	16.2±0.4	17.4±0.4	17.0±0.4	15.0±1.6	26.1±6.3	28.5±1.2	34.8±1.6	34.5±4.4	26.1±7.5
HIPEQ1230+02	21.4±6.7	18.6±0.4	17.8±0.4	17.8±0.4	17.0±1.6	38.8±6.7	35.2±0.8	33.7±1.2	34.8±3.2	36.0±9.1
HIPEQ1230+03	6.3±2.4	6.7±0.4	6.7±0.4	6.7±0.4	6.7±0.4	14.3±2.4	13.9±0.4	13.9±0.4	14.3±0.4	13.1±1.6
HIPEQ1232+00a	64.5±2.8	61.4±0.4	60.2±0.4	59.0±0.4	63.8±1.6	114.4±2.8	111.3±0.8	111.3±0.8	110.9±0.8	113.7±3.2
HIPEQ1232+00b	204.3±0.4	179.8±0.4	173.8±0.4	169.9±0.4	172.7±0.4	356.8±0.4	356.8±0.4	356.8±0.4	356.8±0.4	356.8±0.4
HIPEQ1233-02	44.4±9.1	39.6±0.8	40.8±0.8	40.8±1.6	47.5±4.0	78.4±9.1	75.6±2.8	77.6±2.4	81.2±3.6	88.7±9.1
HIPEQ1236+03	23.0±9.1	21.0±0.4	21.0±0.4	21.4±0.4	21.8±2.4	49.1±9.1	44.4±2.0	46.3±2.4	47.5±4.8	49.1±15.0
HIPEQ1239-00	53.1±2.4	51.5±0.4	50.7±0.4	50.3±0.4	49.9±0.4	140.2±2.4	129.5±0.4	128.7±0.4	129.5±0.8	137.0±1.6

Table 3.6—Continued

HIPASS Name	R50 (″)					R90 (″)				
	u	g	r	i	z	u	g	r	i	z
HIPEQ1241+01	8.3±2.4	8.3±0.4	8.7±0.4	9.1±0.4	9.5±0.4	22.6±2.4	22.2±0.4	22.6±0.4	24.2±0.4	24.6±1.2
HIPEQ1241-02	14.7±3.6	15.4±0.4	15.8±0.4	17.0±0.4	17.0±0.4	42.4±3.6	39.6±0.8	39.2±0.8	41.2±0.8	47.1±4.8
HIPEQ1242+03b	27.7±2.4	26.9±0.4	27.3±0.4	28.5±0.4	29.3±0.4	87.9±2.4	73.3±0.8	71.3±0.4	73.3±0.8	82.4±1.6
HIPEQ1242-00	42.4±2.0	40.8±0.4	40.4±0.4	40.0±0.4	40.8±0.4	93.5±2.0	84.0±0.4	85.1±0.4	85.1±0.4	98.6±1.2
HIPEQ1242-01a	23.4±3.2	19.0±0.4	19.0±0.4	19.4±0.4	21.4±0.4	63.0±3.2	47.9±0.8	48.3±0.8	51.1±1.2	60.6±3.6
HIPEQ1242-01b	35.6±6.3	33.3±0.4	31.3±0.4	30.1±0.4	28.1±0.4	70.1±6.3	61.0±0.4	59.4±0.4	58.2±0.4	55.8±1.6
HIPEQ1243-00	49.5±3.2	40.8±0.4	37.6±0.4	36.4±0.4	38.0±0.4	110.1±3.2	98.6±0.8	96.6±0.8	93.5±0.4	102.6±2.0
HIPEQ1244+00	59.8±5.1	55.4±0.4	50.3±0.4	33.3±0.4	47.5±1.6	119.2±5.1	110.9±0.8	102.2±1.2	61.4±4.8	90.7±3.6
HIPEQ1244-02	29.3±9.5	24.6±0.4	24.6±0.4	23.0±0.8	24.2±3.6	63.4±9.5	56.6±2.0	59.4±2.4	56.6±4.0	56.6±14.7
HIPEQ1245-00	66.5±1.6	56.2±0.4	50.3±0.4	47.1±0.4	42.4±0.4	153.6±1.6	136.2±0.4	129.5±0.4	127.5±0.4	121.6±0.4
HIPEQ1249+03	20.2±0.8	18.6±0.4	17.4±0.4	17.4±0.4	16.6±0.4	55.0±0.8	51.9±0.4	49.9±0.4	49.1±0.4	49.1±0.8
HIPEQ1249+04	23.0±7.1	21.0±0.4	21.0±0.4	21.0±0.4	19.0±2.0	44.4±7.1	41.6±1.2	42.8±1.6	42.8±2.4	42.8±14.3
HIPEQ1250+05	36.8±1.6	33.3±0.4	32.1±0.4	31.3±0.4	33.3±0.4	79.6±1.6	64.5±0.4	63.4±0.4	63.8±0.4	81.6±1.6
HIPEQ1253+01	54.3±4.0	46.3±0.4	43.6±0.4	43.2±0.4	43.2±0.4	133.1±4.0	104.9±0.8	101.0±0.4	100.6±0.8	114.4±2.0
HIPEQ1253+02	45.5±2.8	34.5±0.4	32.5±0.4	31.7±0.4	31.7±0.4	105.3±2.8	98.2±0.4	97.0±0.4	96.6±0.4	97.0±1.2
HIPEQ1253+04	8.3±0.8	9.5±0.4	9.9±0.4	10.7±0.4	10.3±0.4	21.8±0.8	26.1±0.4	27.7±0.4	29.3±0.4	28.1±0.4
HIPEQ1255+00	47.9±2.8	44.4±0.4	44.7±0.4	44.7±0.4	44.0±0.4	92.7±2.8	88.3±0.4	91.1±0.4	90.7±0.4	87.1±2.4
HIPEQ1255+02	13.1±1.2	12.3±0.4	11.1±0.4	10.7±0.4	10.3±0.4	32.9±1.2	30.9±0.4	29.7±0.4	29.7±0.4	28.1±0.4
HIPEQ1255-00	27.7±22.6	28.5±0.4	30.5±0.4	30.9±0.8	31.3±2.4	64.9±22.6	64.5±4.4	70.5±4.4	73.3±6.3	70.1±8.7
HIPEQ1256+03	21.0±9.9	18.6±0.8	18.2±0.8	17.8±1.2	19.0±7.5	39.2±9.9	37.6±1.6	38.4±2.4	38.4±3.2	42.0±12.3
HIPEQ1257+02	23.0±5.1	19.4±0.4	19.4±0.4	19.4±0.8	20.2±2.0	50.7±5.1	43.6±1.6	44.4±2.0	45.5±2.8	46.7±14.7
HIPEQ1257-01	28.1±3.6	25.3±0.4	23.4±0.4	23.0±0.4	21.4±0.4	68.1±3.6	57.8±0.4	55.0±0.4	55.4±0.4	56.2±2.4
HIPEQ1258+02	42.0±6.7	36.4±0.4	35.6±0.4	36.4±0.4	41.6±2.4	83.6±6.7	77.6±1.2	77.6±1.6	79.6±2.4	85.9±6.7
HIPEQ1300+02a	11.1±9.5	14.7±0.4	16.2±0.4	18.6±0.4	19.0±1.2	47.9±9.5	41.6±1.2	41.6±1.2	45.1±1.6	49.9±4.4
HIPEQ1300+02b	39.2±1.6	37.2±0.4	37.2±0.4	38.4±0.4	41.2±0.4	90.7±1.6	75.6±0.4	77.6±0.4	82.0±0.4	96.6±1.6
HIPEQ1303+03	26.1±4.8	23.8±0.4	22.6±0.4	22.2±0.4	22.6±0.8	51.9±4.8	48.3±1.2	46.7±1.2	48.7±1.2	49.5±4.8
HIPEQ1304-02	11.9±10.3	9.5±0.4	9.9±0.4	9.5±0.4	8.7±0.4	26.5±10.3	19.0±0.4	22.6±1.2	21.4±1.2	23.0±9.5
HIPEQ1304-03	57.8±3.2	57.8±0.4	55.4±0.4	54.3±0.8	54.3±1.2	96.6±3.2	97.0±1.2	96.6±0.4	95.8±0.8	94.2±3.2
HIPEQ1307-00	16.6±1.2	15.4±0.4	14.7±0.4	14.3±0.4	13.9±0.4	40.4±1.2	36.0±0.4	34.8±0.4	34.5±0.4	35.6±1.6
HIPEQ1308-02	19.4±2.4	17.0±0.4	16.2±0.4	15.4±0.4	17.0±0.4	48.3±2.4	39.6±0.4	39.6±0.8	40.0±0.8	48.7±1.6
HIPEQ1311+03a	10.3±2.4	10.7±0.4	9.9±0.4	9.9±0.4	9.9±0.4	33.7±2.4	28.1±0.8	26.1±0.8	25.3±0.8	25.3±2.8
HIPEQ1312+03	8.3±3.6	8.3±0.4	8.3±0.4	7.9±0.4	7.5±0.4	21.8±3.6	22.6±0.4	22.6±0.4	22.6±0.4	21.0±1.2
HIPEQ1312+05	18.2±10.7	16.6±0.4	15.8±0.8	15.8±0.8	16.2±4.0	35.6±10.7	30.9±2.4	28.9±2.8	31.3±3.6	36.0±22.2
HIPEQ1313+06	16.2±5.5	14.7±0.4	13.5±0.4	13.1±0.4	12.7±0.4	43.6±5.5	33.7±0.4	32.1±0.4	31.3±0.4	33.7±0.8
HIPEQ1317-00	18.2±2.4	17.8±0.4	17.0±0.4	16.2±0.4	17.4±1.2	29.3±2.4	28.5±0.8	28.1±0.8	30.1±1.2	35.6±6.7
HIPEQ1318-01	28.5±2.4	21.4±0.4	20.6±0.4	20.2±0.4	21.4±0.4	64.2±2.4	41.6±0.4	42.0±0.4	43.6±0.8	58.2±2.4
HIPEQ1320+05	22.6±10.7	22.2±0.4	23.8±0.4	24.9±0.4	26.1±1.2	57.8±10.7	53.9±1.6	57.0±1.6	59.8±3.2	68.1±9.1
HIPEQ1327+02	17.4±14.3	15.4±0.4	15.0±0.4	14.3±0.8	14.7±4.0	40.0±14.3	32.9±2.8	31.7±2.4	28.9±4.0	45.9±20.6
HIPEQ1329-00	21.8±9.5	17.8±0.4	17.4±0.4	17.0±0.4	19.0±1.6	50.7±9.5	45.1±2.0	45.9±2.0	49.1±5.1	59.0±13.5
HIPEQ1332+01	12.7±3.2	12.3±0.4	11.9±0.4	11.9±0.4	11.5±0.4	34.8±3.2	30.1±0.4	29.3±0.4	30.1±0.4	29.7±0.8

Table 3.6—Continued

HIPASS Name	R50 (″)					R90 (″)				
	u	g	r	i	z	u	g	r	i	z
HIPEQ1335+01	28.5±4.0	21.0±0.4	18.2±0.4	17.0±0.4	16.2±0.4	68.5±4.0	57.8±0.8	54.6±0.4	53.9±0.8	57.4±3.6
HIPEQ1341+05	15.8±2.8	13.5±0.4	11.1±0.4	10.3±0.4	8.7±0.4	37.2±2.8	33.3±0.8	32.5±0.4	32.5±0.8	32.1±4.8
HIPEQ1348+03	61.4±2.8	54.3±0.4	51.9±0.4	52.3±0.4	53.1±0.4	121.2±2.8	107.7±0.4	106.1±0.4	110.1±0.4	113.3±1.6
HIPEQ1352+02a	42.4±3.2	32.9±0.4	28.9±0.4	26.9±0.4	27.3±0.8	78.4±3.2	70.9±0.4	68.1±0.4	67.3±0.8	69.7±2.0
HIPEQ1352-01	61.4±2.0	57.0±0.4	54.3±0.4	54.6±0.4	54.3±0.4	106.1±2.0	103.8±0.4	102.2±0.4	104.5±0.4	104.5±1.2
HIPEQ1400+02	22.2±4.0	21.0±0.4	20.2±0.4	19.8±0.4	19.8±0.8	44.7±4.0	42.0±0.8	41.6±0.8	41.2±0.4	44.7±3.2
HIPEQ1411-01	74.8±5.9	68.9±0.4	64.5±0.4	63.4±0.4	62.2±0.4	171.1±5.9	131.1±1.2	125.5±0.8	141.0±2.4	160.0±5.5
HIPEQ1415+04	8.7±2.4	7.5±0.4	7.9±0.4	8.7±0.4	9.5±0.4	21.4±2.4	17.4±0.4	19.0±0.4	20.2±0.8	18.2±1.2
HIPEQ1416+03	82.4±0.4	85.5±4.0	91.9±3.6	104.9±5.9	111.3±40.4	135.0±0.4	135.4±0.4	135.4±0.4	135.4±0.4	135.4±0.4
HIPEQ1422-00	58.6±1.6	55.4±0.4	54.3±0.4	53.1±0.4	54.6±0.4	105.3±1.6	101.0±0.4	101.0±0.4	102.2±0.4	108.1±1.6
HIPEQ1429-00	24.6±0.4	23.0±0.4	21.8±0.4	21.8±0.4	21.8±0.8	59.8±0.4	49.9±1.2	47.9±0.8	50.3±1.2	55.0±3.6
HIPEQ1432+00	23.0±5.5	23.8±0.4	24.2±0.4	24.2±0.4	23.4±0.4	59.8±5.5	53.5±0.8	54.6±0.4	55.0±0.8	57.8±2.8
HIPEQ1433+01	22.6±52.7	23.4±1.2	22.2±1.2	22.6±1.2	21.4±23.0	38.0±52.7	45.1±8.3	40.8±9.9	38.0±4.8	49.9±84.7
HIPEQ1433+02	12.7±4.0	13.5±0.4	13.1±0.4	12.3±0.4	12.3±0.8	34.1±4.0	33.7±0.4	33.7±0.8	29.3±1.6	33.7±4.4
HIPEQ1437+02	82.8±0.4	53.5±0.4	59.8±0.4	60.6±0.4	61.8±0.4	144.9±0.4	144.9±1.6	144.9±0.4	144.9±0.4	144.9±0.4
HIPEQ1437-00	19.0±1.6	22.6±0.4	24.2±0.4	25.3±0.4	24.9±0.4	59.8±1.6	63.4±0.4	66.9±0.4	69.7±0.4	71.3±1.2
HIPEQ1439-00	61.8±3.6	53.9±0.4	52.3±0.4	53.1±0.4	50.7±0.4	113.7±3.6	104.1±0.8	104.9±0.8	107.3±0.8	110.5±4.0
HIPEQ1440+02	13.9±4.8	13.5±0.4	13.1±0.4	13.1±0.4	13.1±0.4	35.6±4.8	29.7±0.4	29.7±0.4	30.5±0.4	33.7±2.4
HIPEQ1444+01a	35.2±2.0	28.9±0.4	26.1±0.4	24.9±0.4	24.6±0.4	85.5±2.0	70.5±0.4	66.5±0.4	65.3±0.4	69.3±0.8
HIPEQ1500+01	38.4±2.4	34.8±0.4	33.7±0.4	32.5±0.4	32.5±0.4	104.1±2.4	88.7±1.6	87.5±0.4	86.7±0.4	94.6±1.2
HIPEQ1504+02	12.3±3.6	10.7±0.4	10.3±0.4	10.3±0.4	9.5±0.4	34.8±3.6	23.4±0.4	23.0±0.8	24.6±1.2	30.9±5.5
HIPEQ1504-00	31.7±10.3	30.5±0.4	30.1±0.4	30.1±0.4	28.1±1.2	65.7±10.3	57.0±0.8	57.4±0.8	58.6±1.6	63.0±6.7
HIPEQ1507+01	61.8±4.4	50.7±0.4	43.2±0.4	41.6±0.4	42.8±0.4	118.0±4.4	116.4±0.4	112.9±0.4	112.1±0.4	114.0±1.2
HIPEQ1542+00	54.3±0.4	51.5±0.4	49.1±0.4	47.1±0.4	46.3±0.4	135.0±0.4	98.2±0.4	96.6±0.8	95.4±1.2	104.1±0.4
HIPEQ1544+02	13.9±5.5	11.9±0.4	11.1±0.4	10.7±0.4	10.3±0.4	36.0±5.5	27.7±0.4	28.5±0.4	26.1±0.8	28.9±4.8
HIPEQ1545+00	24.9±6.7	20.2±0.4	22.6±0.4	24.6±0.8	21.8±1.6	59.0±6.7	50.3±2.4	53.1±2.8	55.8±3.2	54.6±6.7
HIPEQ1601+01a	49.9±7.9	42.8±0.4	42.4±0.4	42.8±0.4	45.1±0.4	103.8±7.9	94.2±0.8	93.5±1.2	97.8±1.2	101.0±2.8
HIPEQ1609-00	24.2±11.9	19.8±0.4	18.2±0.4	18.6±1.2	19.4±4.0	53.9±11.9	48.3±3.2	48.7±4.8	50.7±9.5	61.4±84.0
HIPEQ1613-00	12.3±7.9	12.3±0.4	12.3±0.4	11.9±0.4	12.3±0.4	31.3±7.9	27.3±0.8	27.7±0.8	26.5±1.2	29.7±3.6
HIPEQ1614+00	37.2±4.4	34.5±0.4	33.3±0.4	32.1±0.4	34.8±1.6	71.7±4.4	69.3±0.8	68.9±0.8	66.5±2.0	71.3±4.8
HIPEQ1614-00	63.4±6.3	63.4±0.4	58.2±0.4	55.4±0.4	51.1±0.8	106.1±6.3	115.6±0.8	110.1±0.8	107.7±0.8	102.6±1.2
HIPEQ2036-04	39.2±5.5	28.9±0.4	25.7±0.4	25.7±0.4	26.1±0.4	87.5±5.5	69.7±1.2	65.3±0.4	69.3±0.8	78.4±2.4
HIPEQ2314+00	9.9±1.2	9.1±0.4	9.1±0.4	8.7±0.4	9.1±0.4	19.4±1.2	17.4±0.4	17.0±0.4	17.8±0.4	19.8±0.8
HIPEQ2324-00	31.7±6.3	29.7±0.4	28.9±0.4	28.5±0.4	31.3±2.0	78.4±6.3	71.3±1.6	73.3±1.6	73.7±2.8	81.2±5.1
HIPEQ2335+01	34.5±15.0	23.0±1.2	24.2±0.8	23.4±1.2	30.5±4.8	62.2±15.0	55.0±2.8	54.6±2.8	55.8±5.5	57.4±10.3
HIPEQ2336+00	31.7±2.0	23.0±0.4	19.4±0.4	18.6±0.4	19.4±0.4	76.4±2.0	59.4±0.4	55.0±0.4	55.4±0.4	66.9±1.6
HIPEQ2337+00	44.0±8.7	40.0±0.4	39.2±0.4	38.8±0.8	37.2±2.8	77.6±8.7	72.1±1.2	72.5±1.2	72.9±2.0	75.2±7.9
HIPEQ2340+01	14.7±5.1	13.9±0.4	13.9±0.4	13.9±0.4	12.7±0.4	37.2±5.1	33.7±0.8	32.9±0.8	33.3±0.8	31.3±2.8

Table 3.7. Measured Circular Petrosian Sizes

	R50 (″)					R90 (″)				
HIPASS Name	u	g	r	i	z	u	g	r	i	z
HIPEQ0014-00	21.8±1.2	17.8±0.4	15.0±0.4	14.3±0.4	13.5±0.4	49.1±2.4	45.5±0.4	43.6±0.4	42.8±0.8	42.8±2.4
HIPEQ0027-01a	17.0±0.8	15.0±0.4	14.3±0.4	14.3±0.4	13.9±0.8	44.4±3.6	33.7±0.8	32.9±1.2	32.5±1.2	38.4±4.4
HIPEQ0033-01	26.1±2.8	22.6±0.8	20.2±0.4	22.2±0.8	23.0±2.0	48.3±0.4	48.3±0.4	45.9±1.6	51.1±2.8	48.3±0.4
HIPEQ0043-00	14.3±0.4	12.7±0.4	11.9±0.4	11.5±0.4	11.1±0.4	35.6±0.8	32.1±0.4	30.5±0.4	30.9±0.4	30.9±0.8
HIPEQ0051-00	4.4±0.4	4.4±0.4	4.8±0.4	5.1±0.4	5.1±0.4	12.7±1.2	13.1±0.4	13.9±0.4	14.3±0.4	14.7±1.2
HIPEQ0058+00	12.3±0.4	11.1±0.4	10.3±0.4	10.3±0.4	9.5±0.4	30.1±2.4	23.0±0.4	22.6±0.4	23.0±0.4	23.4±1.2
HIPEQ0107+01	7.5±0.8	9.9±0.4	10.7±0.4	11.9±0.4	11.9±0.8	24.9±5.1	24.2±0.4	26.5±0.8	28.1±1.2	28.9±5.9
HIPEQ0119+00	9.9±2.0	7.9±0.4	7.1±0.4	6.7±0.4	7.5±1.2	17.8±44.0	16.2±1.6	15.4±2.0	13.5±2.0	14.3±18.6
HIPEQ0120-00	13.1±1.2	11.9±0.4	12.3±0.4	12.3±0.4	13.1±1.2	32.5±4.8	28.1±0.8	28.9±0.8	30.1±1.2	31.3±4.4
HIPEQ0122+00	44.0±0.8	35.2±0.4	32.9±0.4	32.5±0.4	35.6±0.4	84.0±2.4	77.2±0.4	75.6±0.4	75.2±0.8	80.0±2.0
HIPEQ0123-00	16.6±0.4	13.5±0.4	12.7±0.4	12.7±0.4	12.7±0.4	43.2±2.8	30.9±0.4	30.1±0.4	30.5±0.4	34.5±4.4
HIPEQ0126+00a	10.3±4.0	9.9±0.4	9.1±0.4	9.5±0.4	7.9±1.2	23.0±42.0	21.0±2.0	19.4±2.4	19.8±2.8	23.4±22.2
HIPEQ0126-00b	4.0±0.4	4.0±0.4	4.4±0.4	4.4±0.4	4.4±0.4	9.1±1.2	9.1±0.4	10.3±0.4	10.3±0.4	9.1±2.0
HIPEQ0154-00	9.1±0.4	7.9±0.4	7.5±0.4	7.5±0.4	7.1±0.4	27.7±3.2	24.9±0.4	24.6±0.4	24.6±0.4	23.8±0.8
HIPEQ0222-00	21.4±3.6	19.8±0.4	18.6±0.4	17.8±0.4	17.4±1.6	49.5±17.0	46.7±1.6	46.3±1.2	42.8±2.4	41.6±5.5
HIPEQ0228-01	30.5±0.4	26.9±0.4	25.7±0.4	26.1±0.4	26.5±0.4	72.9±2.4	65.7±0.4	63.8±0.4	65.3±0.4	70.1±2.0
HIPEQ0230+00	24.2±4.8	19.0±0.4	19.8±0.4	19.8±0.4	20.6±2.0	51.5±90.3	43.6±3.2	44.4±2.0	44.4±2.0	50.3±4.4
HIPEQ0230-01	15.4±0.4	12.3±0.4	11.9±0.4	11.9±0.4	11.1±0.4	44.7±0.8	38.0±0.4	36.0±0.4	36.0±0.4	35.2±0.4
HIPEQ0231+00	13.9±2.0	12.3±0.4	11.9±0.4	11.5±0.4	12.3±0.8	38.0±6.7	28.1±1.6	28.1±1.2	28.1±1.2	32.5±5.5
HIPEQ0236+00	13.1±0.8	10.7±0.4	9.9±0.4	9.5±0.4	8.7±0.4	28.5±3.6	24.2±0.8	23.0±0.4	23.0±0.4	21.8±1.6
HIPEQ0238+00	13.5±2.4	14.3±0.4	13.5±0.4	13.9±1.2	13.5±2.4	25.7±29.3	27.7±1.6	27.3±2.0	28.1±2.4	26.9±41.6
HIPEQ0240+01	19.0±4.4	20.6±1.2	20.6±0.8	21.4±1.2	22.6±2.0	52.7±55.4	51.1±3.6	52.3±4.8	53.5±5.9	55.8±15.0
HIPEQ0241+00	73.3±0.8	64.2±0.4	61.4±0.4	58.2±0.4	56.2±0.4	160.8±3.6	156.4±0.4	151.7±0.4	146.5±0.4	143.0±0.8
HIPEQ0244+00	18.6±2.0	14.7±0.4	15.0±0.4	16.2±0.8	17.4±1.2	50.3±7.9	36.4±1.2	37.6±1.6	42.0±2.0	44.4±4.4
HIPEQ0246-00a	41.6±0.8	33.3±0.4	30.5±0.4	28.9±0.4	30.1±0.4	91.9±2.4	76.8±0.4	72.9±0.4	71.7±0.4	78.0±1.2
HIPEQ0246-00b	36.4±0.4	37.2±0.4	37.2±0.4	37.6±0.4	37.6±0.4	87.9±2.0	85.5±0.4	86.7±0.4	88.7±0.4	89.9±0.8
HIPEQ0249-00	14.7±1.2	11.9±0.4	11.1±0.4	11.1±0.4	10.7±0.4	35.2±4.0	28.1±0.4	26.1±0.4	25.7±0.4	27.3±2.4
HIPEQ0249-00a	17.4±2.4	15.0±0.4	13.9±0.4	12.7±0.4	14.3±1.2	35.2±10.7	28.5±1.2	26.1±1.2	24.6±10.3	30.1±15.4
HIPEQ0249-00b	18.2±0.8	13.5±0.4	12.7±0.4	12.7±0.4	12.3±0.4	50.7±2.8	36.4±0.4	34.8±0.4	36.0±0.4	39.2±1.6
HIPEQ0251-01	32.1±1.6	29.3±0.4	28.1±0.4	28.1±0.4	28.1±1.2	53.1±3.6	51.1±0.8	50.3±0.8	50.7±1.2	51.9±2.4
HIPEQ0300+00	13.9±2.0	12.7±0.4	11.9±0.4	11.9±0.4	11.9±1.2	35.6±5.9	30.1±0.8	28.5±0.8	28.5±1.6	31.3±5.1
HIPEQ0301-00	17.4±1.2	14.3±0.4	13.5±0.4	13.9±0.4	14.7±1.6	44.0±10.3	32.1±1.6	32.1±1.2	34.5±1.2	36.4±6.3
HIPEQ0306-00	13.9±0.4	11.1±0.4	10.7±0.4	11.1±0.4	10.3±0.4	41.6±1.6	38.4±0.4	38.0±0.4	38.0±0.4	37.2±0.4
HIPEQ0316-00	13.9±2.0	12.7±0.4	11.5±0.4	10.7±0.4	10.7±0.4	32.9±32.5	31.7±0.8	30.5±0.4	29.7±0.4	30.1±1.6
HIPEQ0320-06	11.5±0.4	11.1±0.4	10.7±0.4	10.7±0.4	10.7±0.4	26.9±1.2	25.7±0.4	25.7±0.4	26.5±0.4	26.9±0.8
HIPEQ0351-00	4.8±0.4	5.1±0.4	5.1±0.4	4.8±0.4	4.8±0.4	10.7±1.2	11.5±0.4	11.5±0.4	11.5±0.4	11.5±0.4
HIPEQ0809+00	18.6±0.4	15.8±0.4	15.4±0.4	15.0±0.4	16.2±0.4	42.4±2.0	36.0±0.4	36.4±0.4	35.6±0.8	43.2±2.4
HIPEQ0821+03b	11.9±0.4	11.1±0.4	10.3±0.4	9.9±0.4	9.5±0.4	27.7±2.4	24.6±0.4	23.0±0.4	22.6±0.4	22.6±0.4
HIPEQ0821-00	9.1±0.8	9.9±0.4	10.3±0.4	9.9±0.4	11.5±1.2	32.1±0.4	32.1±0.4	32.1±0.4	29.7±1.2	32.5±3.2
HIPEQ0822-00	17.8±0.4	14.3±0.4	13.5±0.4	13.5±0.4	14.7±0.8	40.8±2.0	29.7±0.4	29.7±0.4	30.5±0.4	36.8±1.2

Table 3.7—Continued

HIPASS Name	R50 (″)					R90 (″)				
	u	g	r	i	z	u	g	r	i	z
HIPEQ0825-00	29.7±0.4	16.2±0.4	14.7±0.4	14.7±0.4	14.7±0.4	60.6±1.6	46.3±0.8	42.0±0.4	44.0±0.4	47.5±1.2
HIPEQ0855+02	24.9±2.0	24.6±0.4	23.4±0.4	24.2±0.4	26.1±2.0	54.3±8.7	54.3±1.6	53.9±1.6	55.4±2.0	57.0±4.8
HIPEQ0856+00	26.1±0.8	19.0±0.4	17.8±0.4	23.4±0.4	23.0±1.2	61.0±0.4	49.9±0.8	47.9±0.8	56.2±0.8	55.0±2.4
HIPEQ0923-00	15.8±0.4	13.5±0.4	12.3±0.4	11.9±0.4	11.9±0.4	36.4±3.2	29.3±0.4	28.9±0.8	29.7±0.4	35.2±2.8
HIPEQ0930+04	21.8±0.4	18.2±0.4	17.0±0.4	17.0±0.4	17.0±0.4	51.1±2.4	42.0±0.8	40.4±0.4	42.8±0.8	48.7±1.6
HIPEQ0942+00	32.9±0.4	28.5±0.4	26.9±0.4	26.5±0.4	27.7±0.4	79.6±1.6	70.9±0.4	67.7±0.4	68.5±0.4	77.2±0.8
HIPEQ0944-00b	10.3±0.8	9.5±0.4	9.1±0.4	7.5±0.4	9.5±0.4	22.2±6.3	21.8±0.8	20.6±0.8	17.4±1.6	28.9±7.5
HIPEQ0945+01	24.9±1.6	21.4±0.4	21.0±0.4	21.0±0.4	23.4±0.4	194.0±45.9	55.8±0.8	55.4±0.8	56.6±0.8	60.2±2.0
HIPEQ0946+02	24.9±1.2	21.8±0.4	20.6±0.4	20.2±0.4	22.2±1.2	52.3±6.3	47.1±0.8	44.4±0.8	45.1±1.2	50.7±3.2
HIPEQ0947+00a	26.1±1.6	20.6±0.4	19.4±0.4	19.4±0.4	20.6±0.8	52.7±4.4	49.1±1.2	48.7±1.2	49.9±1.6	53.5±2.8
HIPEQ0947+00b	25.7±2.0	19.0±0.8	17.4±0.4	16.6±0.8	17.0±3.2	47.1±6.7	39.6±0.8	39.2±1.6	40.0±2.4	44.7±9.5
HIPEQ0953+01	48.3±0.4	43.6±0.4	40.4±0.4	40.8±0.4	39.6±0.4	112.1±1.6	106.5±0.4	102.6±0.4	103.8±0.8	103.8±1.6
HIPEQ0954+02a	18.6±0.8	14.7±0.4	14.3±0.4	13.9±0.4	14.3±0.4	47.9±2.0	30.5±0.4	30.9±0.8	33.3±1.2	42.8±3.6
HIPEQ0955+04a	23.4±0.4	21.4±0.4	20.6±0.4	21.0±0.4	21.8±0.4	57.0±2.0	45.9±0.4	46.3±0.4	47.1±0.4	54.6±1.2
HIPEQ0958+01	17.0±4.8	13.1±0.8	13.1±1.2	11.9±2.0	17.4±10.7	28.1±62.6	26.5±4.8	25.3±5.1	27.3±53.1	25.3±104.5
HIPEQ1000+03	17.0±0.4	15.0±0.4	12.7±0.4	12.3±0.4	10.7±0.4	41.6±1.6	40.4±0.4	37.6±0.4	38.4±0.4	37.6±0.4
HIPEQ1010+05	5.9±0.4	6.3±0.4	6.7±0.4	6.7±0.4	6.7±0.4	18.6±2.8	18.2±0.4	18.6±0.4	18.6±0.8	19.8±1.6
HIPEQ1014+03	61.0±0.4	47.5±0.4	40.4±0.4	37.6±0.4	33.3±0.4	138.6±2.4	138.6±0.4	133.5±0.4	131.1±0.4	128.3±0.4
HIPEQ1015+02	27.3±2.8	24.6±0.8	23.4±0.4	26.9±1.2	24.6±3.6	57.8±5.9	60.6±2.0	57.4±2.4	64.5±3.6	50.3±47.1
HIPEQ1026+03	30.1±0.8	24.2±0.4	22.2±0.4	21.8±0.4	22.6±0.4	64.5±2.4	57.0±0.4	55.4±0.4	54.6±0.8	59.4±1.6
HIPEQ1028+03	15.4±1.2	13.9±0.4	14.3±0.4	13.9±0.4	14.3±0.8	31.7±2.8	32.1±1.2	32.5±0.8	30.9±1.2	34.8±3.6
HIPEQ1039+01	13.5±0.4	13.1±0.4	13.9±0.4	14.7±0.4	15.0±0.8	42.4±3.2	34.8±1.2	36.8±0.8	40.0±1.2	44.0±2.4
HIPEQ1041+00	17.4±0.8	14.3±0.4	14.3±0.4	15.0±0.4	15.0±0.4	44.0±3.2	28.1±0.4	31.3±0.4	36.8±1.2	43.6±2.4
HIPEQ1046+01	43.6±1.2	38.8±0.4	37.2±0.4	36.8±0.4	37.6±0.8	100.2±4.4	92.3±0.8	89.5±0.8	88.7±0.8	89.1±3.2
HIPEQ1050+01	6.7±1.6	7.1±0.4	7.5±0.4	7.1±0.4	5.9±1.2	12.7±23.8	13.1±1.2	14.3±1.2	13.5±2.0	10.7±53.5
HIPEQ1051+04a	22.6±0.8	17.8±0.4	17.0±0.4	16.6±0.4	17.0±0.8	53.9±2.8	48.3±0.8	47.5±0.8	46.7±0.8	48.7±4.0
HIPEQ1052+00	3.2±0.4	4.0±0.4	4.4±0.4	4.8±0.4	4.8±0.4	10.7±0.8	10.7±0.4	11.5±0.4	12.3±0.4	12.7±1.2
HIPEQ1053+02	8.7±0.4	9.1±0.4	9.5±0.4	9.9±0.4	10.3±0.8	21.0±3.6	19.4±0.8	20.6±0.8	22.2±1.6	25.7±6.7
HIPEQ1055+02	6.3±0.4	6.3±0.4	6.7±0.4	7.1±0.4	6.7±0.8	17.8±2.4	15.4±0.8	15.8±1.2	16.2±0.8	15.0±5.1
HIPEQ1101+03	49.5±0.4	45.9±0.4	44.0±0.4	43.2±0.4	43.6±0.4	97.0±1.6	95.4±0.4	92.7±0.4	92.7±0.4	93.9±0.8
HIPEQ1109-00	11.9±0.4	10.3±0.4	9.1±0.4	8.7±0.4	7.5±0.4	34.5±1.6	30.5±0.4	28.5±0.4	27.3±0.4	25.3±1.6
HIPEQ1110+01	9.1±0.8	9.9±0.4	10.7±0.4	10.3±0.4	10.7±0.4	28.9±5.1	24.2±0.8	24.6±1.2	22.6±1.2	26.1±6.3
HIPEQ1113+05	13.9±0.4	13.1±0.4	12.7±0.4	12.7±0.4	13.9±0.4	33.7±5.5	27.3±0.4	27.7±0.8	27.3±0.4	40.8±2.4
HIPEQ1117+04a	9.9±0.4	11.1±0.4	11.5±0.4	12.3±0.4	11.9±0.4	41.6±0.8	38.0±0.4	38.4±0.4	38.8±0.4	39.6±0.8
HIPEQ1119+02	38.0±2.0	30.5±0.4	28.9±0.4	30.5±0.4	32.5±2.0	78.8±4.0	73.3±1.2	72.5±1.2	72.9±1.6	68.5±5.9
HIPEQ1124+03	35.2±0.8	32.1±0.4	31.7±0.4	32.5±0.4	35.2±0.8	68.5±3.2	60.2±0.4	61.4±0.4	64.2±0.8	70.5±3.6
HIPEQ1127-01	19.0±0.8	17.4±0.4	18.2±0.4	19.4±0.4	26.9±0.8	55.4±5.1	53.5±1.2	54.6±1.2	57.0±1.6	65.7±3.6
HIPEQ1131-02	34.8±0.8	27.7±0.4	25.7±0.4	24.9±0.4	27.7±0.8	70.5±2.4	60.2±0.4	59.4±0.4	62.6±0.8	70.5±2.8
HIPEQ1133-03	19.4±0.8	17.4±0.4	16.6±0.4	16.6±0.4	18.6±0.8	43.6±3.2	37.6±0.8	37.2±1.2	39.2±1.2	42.8±3.6
HIPEQ1136+00	5.5±0.4	5.9±0.4	6.7±0.4	7.5±0.4	7.1±0.4	14.7±0.8	16.2±0.4	17.4±0.4	18.2±0.4	17.8±2.0

Table 3.7—Continued

HIPASS Name	R50 (″)					R90 (″)				
	u	g	r	i	z	u	g	r	i	z
HIPEQ1138+03	14.3±0.4	12.3±0.4	10.7±0.4	10.3±0.4	8.7±0.4	34.1±3.6	30.1±0.8	28.5±0.4	28.1±0.4	28.5±2.4
HIPEQ1143-01	9.5±1.2	9.1±0.4	9.5±0.8	9.9±1.2	10.7±4.8	27.3±17.0	19.0±2.8	24.9±5.5	26.9±9.5	22.6±31.3
HIPEQ1145+02	18.6±5.5	16.6±1.2	17.8±1.2	15.4±2.0	35.6±26.9	53.5±2.0	43.6±0.4	38.4±6.3	29.7±10.3	66.9±36.0
HIPEQ1148-02	36.8±1.2	31.7±0.4	29.3±0.4	32.1±0.4	30.1±1.2	82.8±4.8	81.2±1.2	80.8±1.6	91.9±2.0	76.8±4.8
HIPEQ1151-02	7.1±0.4	6.7±0.4	6.3±0.4	5.9±0.4	5.5±0.4	18.2±1.6	18.2±0.4	17.0±0.4	16.6±0.4	15.8±1.2
HIPEQ1152+01	14.3±0.4	13.1±0.4	13.1±0.4	13.1±0.4	13.1±0.4	29.3±3.2	25.7±0.4	27.3±0.4	28.9±0.8	32.5±2.4
HIPEQ1152-02	5.1±0.4	5.1±0.4	5.9±0.4	6.3±0.4	6.3±0.4	11.9±0.4	13.1±0.4	14.7±0.4	15.8±0.4	14.7±0.8
HIPEQ1152-03b	21.4±0.4	19.4±0.4	19.8±0.4	20.2±0.4	20.6±0.8	52.3±3.6	44.0±1.2	44.0±1.2	45.9±1.6	50.3±4.8
HIPEQ1155+01	42.4±0.8	38.0±0.4	36.4±0.4	35.2±0.4	36.8±0.4	71.7±2.8	67.3±0.8	67.3±0.4	66.5±0.4	70.5±1.2
HIPEQ1200-00	30.5±2.8	26.5±0.4	25.7±0.4	25.3±0.8	33.7±2.8	66.9±8.3	58.6±2.0	56.6±1.6	57.0±2.4	78.4±10.3
HIPEQ1200-01	42.0±0.4	35.2±0.4	32.1±0.4	30.9±0.4	29.3±0.4	103.4±0.4	91.5±0.4	89.5±0.4	91.5±0.4	93.5±0.4
HIPEQ1202+01	27.7±0.8	23.8±0.4	22.2±0.4	21.8±0.4	21.0±0.4	80.4±3.6	72.1±0.4	69.7±0.4	70.1±0.4	72.9±0.8
HIPEQ1204-01	26.9±2.0	23.4±0.4	23.4±0.4	21.8±0.8	23.4±2.0	48.7±8.7	44.7±1.6	44.7±1.6	42.8±2.8	44.4±11.1
HIPEQ1204-02	15.4±0.8	13.1±0.4	11.5±0.4	10.7±0.4	10.3±0.4	38.8±1.6	34.8±0.4	33.7±0.4	32.9±0.4	32.5±1.6
HIPEQ1210+02	28.9±4.8	23.0±0.8	22.6±0.4	22.2±0.8	22.6±3.6	52.7±10.7	49.5±2.0	50.7±2.4	48.3±3.2	51.9±11.5
HIPEQ1215+04a	9.9±0.4	9.5±0.4	9.9±0.4	9.9±0.4	9.9±0.4	26.1±2.8	23.4±0.4	24.2±0.4	24.6±0.8	29.7±2.8
HIPEQ1216-03	19.4±0.8	14.7±0.4	13.5±0.4	13.1±0.4	14.3±0.4	46.3±2.0	34.5±1.2	33.7±0.8	34.8±1.2	44.4±2.4
HIPEQ1218+00	31.7±2.8	26.1±0.4	25.7±0.4	25.3±0.8	24.9±2.0	56.2±5.5	54.6±1.6	53.5±1.6	55.4±2.8	56.6±7.9
HIPEQ1218-01	11.5±0.4	10.7±0.4	9.5±0.4	9.5±0.4	8.7±0.4	31.7±2.4	26.5±0.4	25.3±0.4	25.3±0.4	25.7±1.2
HIPEQ1219+03	9.5±0.4	11.5±0.4	12.7±0.4	13.9±0.4	14.3±0.4	30.1±2.0	29.7±0.4	31.3±0.4	32.9±0.8	36.0±2.0
HIPEQ1220+00	12.3±0.8	11.9±0.4	11.5±0.4	11.5±0.4	11.5±1.2	25.7±5.1	27.3±0.8	26.5±1.6	27.3±2.4	27.7±7.5
HIPEQ1220+01	21.8±1.6	17.8±0.4	16.6±0.4	15.4±0.4	15.4±1.6	48.7±5.1	44.7±1.2	44.0±1.2	42.8±15.0	43.6±29.3
HIPEQ1221+03	24.6±1.2	14.7±0.4	13.1±0.4	12.3±0.4	12.3±0.4	51.5±1.6	43.6±0.8	40.8±0.4	40.4±0.4	43.2±1.2
HIPEQ1223+00	24.2±1.6	19.0±0.8	19.8±0.8	19.0±0.8	22.2±2.8	49.5±6.7	44.7±2.8	46.3±2.4	45.5±4.4	49.1±9.5
HIPEQ1223-03b	25.7±0.8	20.6±0.4	18.6±0.4	18.6±0.4	18.2±0.4	64.9±2.4	57.0±0.4	54.3±0.4	54.3±0.4	56.2±0.4
HIPEQ1224+00	10.7±2.0	9.5±0.4	9.9±0.4	9.9±0.4	9.5±2.0	17.8±9.1	15.8±0.8	17.4±1.2	17.4±2.0	15.0±64.2
HIPEQ1224+03b	21.8±1.6	21.4±0.4	21.0±0.4	22.2±0.4	22.2±1.2	57.0±4.8	53.5±0.8	53.5±0.8	56.2±1.6	56.6±4.8
HIPEQ1225+00	19.0±0.4	19.4±0.4	18.2±0.4	19.0±0.4	19.4±0.4	52.7±1.6	47.9±0.4	47.1±0.4	48.3±0.4	52.3±0.8
HIPEQ1226+02	18.2±0.4	17.0±0.4	16.6±0.4	16.2±0.4	16.2±0.4	40.4±0.4	36.4±0.4	36.8±0.4	37.2±0.4	39.6±0.4
HIPEQ1227+01	16.2±4.8	14.3±0.8	15.0±0.8	15.4±1.2	15.0±5.5	30.9±5.5	28.9±2.8	30.1±2.0	29.7±4.8	30.5±38.0
HIPEQ1228+02	28.1±1.2	26.5±0.4	25.3±0.4	25.3±0.4	26.5±1.2	57.0±6.3	54.6±0.8	52.7±1.2	53.9±1.6	60.2±5.1
HIPEQ1228+03	20.6±0.4	18.6±0.4	17.8±0.4	18.2±0.4	17.4±0.4	64.5±0.8	63.0±0.4	61.8±0.4	61.8±0.4	61.4±0.4
HIPEQ1229+00	9.9±2.0	9.5±0.4	10.3±0.4	9.9±0.4	9.1±1.6	21.4±47.5	21.4±1.2	24.9±2.0	23.4±2.8	17.8±82.4
HIPEQ1230+02	15.4±1.2	14.3±0.4	13.5±0.4	13.1±0.4	13.1±1.2	31.3±4.8	27.3±0.8	26.5±1.2	26.1±1.6	26.1±7.1
HIPEQ1230+03	5.1±0.4	5.5±0.4	5.5±0.4	5.5±0.4	5.5±0.4	11.5±1.6	12.3±0.4	12.3±0.4	12.7±0.8	11.5±1.2
HIPEQ1232+00a	47.9±1.2	45.9±0.4	45.1±0.4	44.4±0.4	47.9±0.8	95.0±2.8	92.7±0.4	92.3±0.4	90.7±0.4	90.7±2.8
HIPEQ1232+00b	97.8±0.8	94.2±0.8	91.5±0.4	88.7±0.4	90.7±0.4	216.6±3.2	209.9±0.4	207.1±0.4	205.1±0.4	211.1±1.2
HIPEQ1233-02	35.2±2.8	31.7±0.4	32.1±0.8	32.1±0.8	38.0±4.4	61.0±8.3	58.6±1.6	60.6±1.6	62.2±2.8	63.0±10.3
HIPEQ1236+03	15.8±2.0	13.5±0.4	13.5±0.4	13.5±0.8	13.9±2.4	39.6±5.5	38.0±1.6	38.0±2.4	37.6±2.4	37.6±7.5
HIPEQ1239-00	35.2±0.8	33.3±0.4	32.1±0.4	32.1±0.4	32.1±0.4	86.3±1.6	85.1±0.4	83.2±0.4	81.2±0.4	82.8±1.6

Table 3.7—Continued

HIPASS Name	R50 (″)					R90 (″)				
	u	g	r	i	z	u	g	r	i	z
HIPEQ1241+01	6.7±0.4	6.7±0.4	6.7±0.4	7.1±0.4	7.5±0.4	18.2±1.6	17.4±0.4	17.8±0.4	19.4±0.4	19.0±1.2
HIPEQ1241-02	10.7±0.4	10.7±0.4	11.1±0.4	11.9±0.4	12.3±0.4	32.1±3.2	29.3±0.4	29.7±0.4	31.3±0.4	34.8±1.2
HIPEQ1242+03b	22.6±0.4	21.8±0.4	22.2±0.4	23.0±0.4	23.8±0.4	67.3±2.0	57.8±0.8	56.6±0.4	57.8±0.4	63.4±1.2
HIPEQ1242-00	28.1±0.4	27.3±0.4	27.3±0.4	26.9±0.4	28.5±0.4	66.5±1.2	63.4±0.4	63.4±0.4	63.0±0.4	70.9±0.8
HIPEQ1242-01a	20.2±0.4	16.6±0.4	16.6±0.4	17.0±0.4	18.6±0.4	53.9±2.4	40.8±0.4	40.8±0.8	44.0±1.2	51.9±2.8
HIPEQ1242-01b	23.8±0.8	21.0±0.4	19.4±0.4	18.6±0.4	17.8±0.4	48.7±2.4	47.5±0.4	45.9±0.4	44.7±0.8	43.2±2.0
HIPEQ1243-00	43.6±0.4	35.6±0.4	32.9±0.4	31.7±0.4	32.9±0.4	92.7±2.0	84.0±0.4	81.6±0.4	79.2±0.8	86.7±1.6
HIPEQ1244+00	40.4±1.2	38.8±0.4	36.0±0.4	26.1±0.4	34.5±0.8	72.5±2.8	69.7±0.4	65.3±0.8	190.9±4.0	62.2±24.2
HIPEQ1244-02	24.6±2.0	19.8±0.4	19.8±0.4	19.0±0.8	18.6±2.0	50.3±5.5	47.1±1.2	47.9±2.0	46.3±3.2	49.5±10.3
HIPEQ1245-00	48.7±0.4	40.0±0.4	34.8±0.4	32.5±0.4	28.9±0.4	106.9±1.2	101.0±0.4	95.8±0.4	93.1±0.4	89.9±0.4
HIPEQ1249+03	18.2±0.4	16.6±0.4	15.4±0.4	15.0±0.4	14.7±0.4	50.3±0.4	46.7±0.4	44.4±0.4	43.6±0.4	44.0±0.8
HIPEQ1249+04	17.8±0.8	16.2±0.4	16.2±0.4	16.6±0.4	15.0±2.0	32.5±3.6	29.7±0.8	30.5±1.2	31.7±1.6	32.9±9.9
HIPEQ1250+05	31.3±0.4	28.5±0.4	27.7±0.4	26.9±0.4	28.9±0.4	69.3±1.2	58.2±0.4	57.0±0.4	57.4±0.4	71.3±1.2
HIPEQ1253+01	36.4±0.8	30.5±0.4	28.5±0.4	28.1±0.4	28.9±0.4	85.9±2.4	79.6±0.8	76.0±0.4	74.8±0.8	77.2±1.2
HIPEQ1253+02	43.6±0.8	32.5±0.4	30.9±0.4	30.1±0.4	30.1±0.4	102.6±2.8	95.0±0.4	93.9±0.4	93.1±0.4	93.5±1.2
HIPEQ1253+04	6.7±0.4	7.1±0.4	7.9±0.4	8.3±0.4	7.9±0.4	17.0±0.4	19.8±0.4	21.4±0.4	23.0±0.4	22.2±0.4
HIPEQ1255+00	45.5±0.4	42.4±0.4	43.2±0.4	42.8±0.4	42.0±0.4	88.3±2.0	84.3±0.4	86.7±0.4	86.3±0.8	82.8±2.0
HIPEQ1255+02	9.9±0.4	8.7±0.4	7.9±0.4	7.9±0.4	7.5±0.4	27.7±1.2	24.6±0.4	23.8±0.4	23.8±0.4	23.4±0.4
HIPEQ1255-00	20.2±2.4	18.6±0.8	19.0±0.4	19.0±0.4	22.6±3.2	44.4±50.7	42.4±1.6	43.6±2.0	45.5±2.8	54.6±6.7
HIPEQ1256+03	18.2±2.4	16.2±0.8	15.4±0.4	15.0±1.2	16.6±5.9	33.3±11.9	31.3±1.2	32.1±2.0	31.7±3.2	33.3±30.1
HIPEQ1257+02	19.0±1.2	16.2±0.4	16.2±0.4	15.8±0.4	16.6±1.6	40.8±4.0	34.8±0.8	35.2±1.6	36.4±2.8	37.6±8.3
HIPEQ1257-01	19.0±0.4	16.2±0.4	14.7±0.4	14.3±0.4	13.9±0.4	46.7±2.0	42.0±0.4	40.0±0.8	39.6±0.8	39.2±1.6
HIPEQ1258+02	26.5±2.0	24.2±0.4	23.4±0.4	23.8±0.4	26.9±1.6	52.3±4.8	48.3±0.8	48.7±0.8	49.5±1.2	51.9±3.6
HIPEQ1300+02a	9.9±0.8	13.1±0.4	14.7±0.4	16.2±0.4	16.6±0.8	41.2±9.1	37.2±0.8	36.8±1.2	39.6±1.2	44.0±4.0
HIPEQ1300+02b	32.9±0.4	30.9±0.4	30.9±0.4	32.1±0.4	34.1±0.4	73.3±1.2	59.8±0.4	61.8±0.4	65.7±0.4	78.0±0.8
HIPEQ1303+03	25.7±1.2	23.4±0.4	22.2±0.4	21.8±0.4	22.2±0.8	50.7±4.4	47.1±0.8	45.9±1.2	47.9±1.6	48.3±4.8
HIPEQ1304-02	9.5±0.4	7.9±0.4	7.9±0.4	7.5±0.4	6.7±0.4	18.2±6.3	15.0±0.4	17.0±0.8	17.0±0.8	17.8±6.7
HIPEQ1304-03	51.1±0.8	51.1±0.4	49.1±0.4	47.9±0.4	47.5±1.2	85.5±2.8	86.7±0.4	85.9±0.8	84.7±0.8	83.6±3.6
HIPEQ1307-00	15.0±0.4	13.9±0.4	13.1±0.4	12.7±0.4	12.3±0.4	35.6±1.2	31.7±0.4	30.5±0.4	30.1±0.4	31.3±1.6
HIPEQ1308-02	17.8±0.4	15.4±0.4	14.7±0.4	14.3±0.4	15.4±0.4	45.1±2.0	36.4±0.4	36.4±0.4	36.4±0.8	45.5±2.0
HIPEQ1311+03a	6.7±0.4	6.3±0.4	5.9±0.4	5.9±0.4	5.9±0.4	17.4±3.6	17.4±0.4	16.2±0.8	16.6±0.8	16.6±2.0
HIPEQ1312+03	7.1±0.4	7.1±0.4	7.1±0.4	7.1±0.4	6.3±0.4	19.4±2.8	19.4±0.4	19.4±0.4	19.0±0.4	18.6±1.2
HIPEQ1312+05	13.9±2.8	12.3±0.4	11.5±0.4	11.5±0.4	12.3±3.6	26.5±16.2	24.2±1.2	23.0±2.0	23.8±3.2	24.9±57.0
HIPEQ1313+06	15.0±0.4	13.9±0.4	12.7±0.4	12.3±0.4	11.9±0.4	38.0±4.0	31.3±0.4	29.7±0.4	28.9±0.4	30.5±1.2
HIPEQ1317-00	12.3±0.4	10.7±0.4	9.9±0.4	9.1±0.4	9.9±1.2	19.8±1.6	19.4±0.4	19.0±0.4	18.6±0.8	26.9±8.7
HIPEQ1318-01	25.7±0.4	19.4±0.4	18.6±0.4	18.2±0.4	19.4±0.4	57.4±3.2	36.8±0.4	37.2±0.4	39.2±0.8	51.5±2.0
HIPEQ1320+05	14.7±0.8	14.3±0.4	15.0±0.4	15.8±0.4	16.6±0.8	36.8±4.0	33.3±1.2	34.5±1.2	36.0±1.6	40.8±4.4
HIPEQ1327+02	11.1±1.6	10.3±0.4	9.9±0.4	9.5±0.4	9.5±1.6	22.6±9.9	22.2±1.2	21.0±1.6	18.2±2.8	28.1±56.2
HIPEQ1329-00	15.4±1.6	12.7±0.4	12.3±0.4	11.9±0.4	12.7±1.6	32.5±6.3	26.9±1.2	28.1±1.6	27.7±1.6	33.3±5.5
HIPEQ1332+01	11.9±0.4	11.5±0.4	11.1±0.4	11.1±0.4	10.3±0.4	30.5±3.2	26.1±0.4	25.7±0.4	26.1±0.4	26.1±0.8

Table 3.7—Continued

HIPASS Name	R50 (″)					R90 (″)				
	u	g	r	i	z	u	g	r	i	z
HIPEQ1335+01	24.2±0.8	18.6±0.4	15.8±0.4	15.0±0.4	13.9±0.4	55.0±2.8	46.3±0.4	43.2±0.4	42.4±0.8	45.5±2.4
HIPEQ1341+05	13.9±0.8	11.9±0.4	9.9±0.4	8.7±0.4	7.5±0.4	32.5±3.2	28.1±0.4	27.3±0.4	26.9±0.8	28.9±4.4
HIPEQ1348+03	50.7±0.4	45.1±0.4	43.2±0.4	43.6±0.4	44.0±0.4	102.2±2.8	90.7±0.4	89.9±0.4	92.7±0.4	93.5±1.2
HIPEQ1352+02a	34.8±0.8	27.3±0.4	24.2±0.4	23.0±0.4	23.0±0.4	64.2±3.2	57.0±0.4	54.6±0.4	54.3±0.8	57.0±1.6
HIPEQ1352-01	52.3±0.4	48.7±0.4	46.3±0.4	46.3±0.4	45.9±0.4	93.1±1.6	89.9±0.4	88.7±0.4	90.3±0.4	89.9±0.8
HIPEQ1400+02	15.0±0.8	13.5±0.4	12.7±0.4	11.9±0.4	12.3±0.4	37.2±4.4	33.7±0.8	32.9±0.8	31.7±0.8	34.5±2.8
HIPEQ1411-01	44.4±0.8	42.0±0.4	38.0±0.4	38.4±0.4	37.2±0.8	94.6±2.4	98.2±0.8	94.2±0.4	95.8±1.2	90.7±2.4
HIPEQ1415+04	8.3±0.4	7.5±0.4	7.9±0.4	8.3±0.4	9.1±0.4	20.6±2.4	17.0±0.4	18.6±0.4	19.4±0.8	17.8±1.2
HIPEQ1416+03	15.0±2.4	15.4±0.4	15.8±0.4	16.6±0.4	17.4±3.2	33.7±7.5	31.7±1.6	32.9±2.0	34.5±2.0	36.0±8.7
HIPEQ1422-00	47.9±0.4	44.7±0.4	44.0±0.4	42.8±0.4	44.4±0.4	84.7±1.6	82.4±0.4	82.8±0.4	83.6±0.4	86.7±1.2
HIPEQ1429-00	19.8±0.4	17.8±0.4	16.6±0.4	16.6±0.4	17.0±0.4	48.7±2.8	42.0±0.4	40.4±0.8	41.6±1.2	45.1±4.4
HIPEQ1432+00	15.8±0.4	15.0±0.4	14.7±0.4	14.7±0.4	14.7±0.4	40.4±2.4	37.2±0.4	37.2±0.4	37.2±0.4	39.2±1.6
HIPEQ1433+01	19.0±12.3	17.0±1.2	15.4±1.6	15.0±1.6	11.1±7.5	41.2±49.9	33.3±3.2	30.5±4.0	30.1±4.4	29.7±57.4
HIPEQ1433+02	10.7±0.4	11.1±0.4	11.1±0.4	10.3±0.4	10.3±0.4	27.3±2.4	25.7±0.4	26.1±0.4	23.0±0.4	28.5±6.3
HIPEQ1437+02	47.5±0.4	32.1±0.4	35.2±0.4	34.1±0.4	36.4±0.4	89.1±1.6	74.4±0.4	82.4±0.4	82.8±0.4	84.3±0.8
HIPEQ1437-00	13.9±0.4	16.2±0.4	17.0±0.4	18.2±0.4	17.8±0.4	42.0±1.2	44.4±0.4	46.3±0.4	48.7±0.4	51.9±0.8
HIPEQ1439-00	40.8±0.8	35.2±0.4	34.1±0.4	34.8±0.4	33.3±0.8	72.5±2.0	66.5±0.4	66.9±0.4	68.1±0.8	68.5±1.2
HIPEQ1440+02	11.5±0.4	11.1±0.4	10.7±0.4	10.7±0.4	10.7±0.4	29.3±3.2	24.9±0.4	24.9±0.4	25.3±0.4	28.1±2.8
HIPEQ1444+01a	30.1±0.4	23.8±0.4	21.8±0.4	20.6±0.4	20.6±0.4	71.3±2.0	60.2±0.4	57.0±0.4	55.0±0.4	57.4±0.8
HIPEQ1500+01	32.9±0.4	28.5±0.4	27.3±0.4	26.5±0.4	26.5±0.4	78.4±2.8	72.5±0.8	71.3±0.4	71.3±0.4	74.8±0.8
HIPEQ1504+02	11.5±1.2	9.9±0.4	9.1±0.4	9.1±0.4	8.7±0.4	32.1±5.1	21.8±0.8	21.0±0.8	23.0±1.6	27.3±5.1
HIPEQ1504-00	19.0±1.2	19.0±0.4	18.6±0.4	18.6±0.4	17.8±1.2	43.2±3.6	42.4±1.2	42.0±0.8	40.4±0.8	38.4±3.6
HIPEQ1507+01	60.6±0.8	49.5±0.4	42.4±0.4	40.8±0.4	42.0±0.4	114.8±4.4	113.7±0.4	110.1±0.4	109.3±0.4	111.3±1.2
HIPEQ1542+00	36.0±2.0	32.1±0.4	30.1±0.4	27.7±0.4	27.7±1.2	78.8±6.3	80.0±1.2	78.4±1.2	75.6±1.6	78.4±4.0
HIPEQ1544+02	13.1±0.8	11.1±0.4	10.3±0.4	9.9±0.4	9.9±0.4	32.9±5.1	25.7±0.8	26.5±0.4	24.6±0.8	29.3±4.4
HIPEQ1545+00	24.2±2.4	19.4±0.4	21.4±0.4	23.0±0.8	21.0±2.0	55.4±5.5	47.1±2.4	50.3±2.4	52.7±3.2	51.9±7.5
HIPEQ1601+01a	38.0±0.8	33.3±0.4	32.5±0.4	32.9±0.4	34.5±0.8	73.7±4.8	68.1±0.4	68.1±0.4	69.3±0.4	71.7±2.0
HIPEQ1609-00	18.6±2.4	15.8±0.4	14.3±0.8	13.9±1.6	13.9±4.0	40.0±11.1	37.6±3.6	37.6±5.1	34.8±17.8	43.6±85.9
HIPEQ1613-00	10.3±0.8	10.3±0.4	10.3±0.4	10.3±0.4	10.7±0.4	26.1±5.9	24.9±0.8	24.9±0.8	24.2±1.2	28.1±3.6
HIPEQ1614+00	34.5±1.2	32.1±0.4	30.9±0.4	29.7±0.4	32.1±1.6	66.5±3.6	64.9±1.2	64.2±1.2	62.2±2.0	66.5±5.1
HIPEQ1614-00	33.7±2.4	34.5±0.4	31.3±0.4	29.7±0.4	27.7±0.4	73.3±6.3	85.9±1.2	79.2±0.8	76.0±0.8	68.1±1.6
HIPEQ2036-04	32.5±1.2	23.0±0.4	21.0±0.4	20.6±0.4	21.4±0.4	71.3±4.4	57.0±0.8	53.9±0.8	56.6±0.4	62.6±1.2
HIPEQ2314+00	9.5±0.4	8.7±0.4	8.7±0.4	8.7±0.4	8.7±0.4	18.2±1.6	16.6±0.4	16.6±0.4	17.0±0.4	19.0±1.2
HIPEQ2324-00	23.8±1.2	20.2±0.4	19.0±0.4	18.6±0.4	20.2±1.6	42.8±1.2	41.2±0.4	41.2±0.4	41.2±1.2	45.5±4.4
HIPEQ2335+01	28.9±5.9	20.2±0.8	20.6±0.4	19.8±1.2	24.6±3.6	59.8±11.9	45.9±2.4	45.5±3.2	45.9±3.2	46.3±7.1
HIPEQ2336+00	26.9±0.4	19.8±0.4	17.0±0.4	15.8±0.4	17.0±0.4	64.2±1.6	51.1±0.4	47.1±0.4	47.5±0.4	57.4±1.2
HIPEQ2337+00	36.8±2.4	34.1±0.4	33.7±0.4	32.9±0.4	32.1±2.8	64.9±5.1	61.8±0.8	61.4±0.8	61.8±1.6	61.8±5.9
HIPEQ2340+01	10.7±0.8	10.3±0.4	10.3±0.4	9.9±0.4	9.5±0.4	29.7±3.6	27.3±0.4	26.5±0.4	26.5±0.8	26.1±2.4

Table 3.8. Observed Petrosian Surface Brightness

	$\Sigma_{Elliptical}$					$\Sigma_{Circular}$				
HIPASS Name	u	g	r	i	z	u	g	r	i	z
HIPEQ0014-00	$23.10\pm^{0.089}_{0.084}$	$21.90\pm^{0.037}_{0.036}$	$21.16\pm^{0.043}_{0.042}$	$20.77\pm^{0.047}_{0.046}$	$20.46\pm^{0.056}_{0.055}$	$23.23\pm^{0.114}_{0.104}$	$22.02\pm^{0.051}_{0.050}$	$21.27\pm^{0.060}_{0.059}$	$20.93\pm^{0.064}_{0.063}$	$20.63\pm^{0.073}_{0.071}$
HIPEQ0027-01a	$23.36\pm^{0.074}_{0.071}$	$22.36\pm^{0.044}_{0.043}$	$21.90\pm^{0.044}_{0.044}$	$21.67\pm^{0.047}_{0.046}$	$21.43\pm^{0.094}_{0.089}$	$23.50\pm^{0.099}_{0.091}$	$22.53\pm^{0.063}_{0.061}$	$22.03\pm^{0.065}_{0.064}$	$21.85\pm^{0.067}_{0.065}$	$21.61\pm^{0.124}_{0.113}$
HIPEQ0033-01	$24.20\pm^{0.100}_{0.071}$	$23.76\pm^{0.033}_{0.032}$	$23.26\pm^{0.037}_{0.036}$	$23.20\pm^{0.080}_{0.075}$	$22.45\pm^{0.087}_{0.066}$	$24.18\pm^{0.099}_{0.072}$	$23.72\pm^{0.075}_{0.071}$	$23.19\pm^{0.047}_{0.046}$	$23.14\pm^{0.074}_{0.070}$	$22.45\pm^{0.081}_{0.063}$
HIPEQ0043-00	$22.08\pm^{0.058}_{0.057}$	$20.76\pm^{0.059}_{0.057}$	$20.06\pm^{0.064}_{0.062}$	$19.72\pm^{0.066}_{0.064}$	$19.42\pm^{0.070}_{0.068}$	$22.16\pm^{0.067}_{0.065}$	$20.82\pm^{0.070}_{0.068}$	$20.15\pm^{0.075}_{0.072}$	$19.80\pm^{0.077}_{0.075}$	$19.48\pm^{0.083}_{0.080}$
HIPEQ0051-00	$20.88\pm^{0.175}_{0.164}$	$19.93\pm^{0.163}_{0.152}$	$19.77\pm^{0.142}_{0.134}$	$19.66\pm^{0.134}_{0.127}$	$19.53\pm^{0.140}_{0.132}$	$21.05\pm^{0.222}_{0.204}$	$20.10\pm^{0.209}_{0.191}$	$19.84\pm^{0.191}_{0.176}$	$19.78\pm^{0.176}_{0.164}$	$19.65\pm^{0.182}_{0.169}$
HIPEQ0058+00	$22.36\pm^{0.080}_{0.078}$	$21.13\pm^{0.081}_{0.078}$	$20.57\pm^{0.084}_{0.081}$	$20.23\pm^{0.088}_{0.084}$	$20.00\pm^{0.095}_{0.091}$	$22.39\pm^{0.080}_{0.078}$	$21.16\pm^{0.081}_{0.078}$	$20.52\pm^{0.087}_{0.084}$	$20.26\pm^{0.088}_{0.084}$	$19.94\pm^{0.099}_{0.095}$
HIPEQ0107+01	$22.19\pm^{0.254}_{0.231}$	$21.92\pm^{0.090}_{0.086}$	$21.88\pm^{0.081}_{0.079}$	$21.94\pm^{0.076}_{0.073}$	$21.70\pm^{0.138}_{0.123}$	$22.17\pm^{0.267}_{0.241}$	$21.93\pm^{0.093}_{0.090}$	$21.82\pm^{0.087}_{0.084}$	$21.89\pm^{0.080}_{0.078}$	$21.71\pm^{0.141}_{0.125}$
HIPEQ0119+00	$24.12\pm^{0.287}_{0.140}$	$23.39\pm^{0.101}_{0.096}$	$22.91\pm^{0.114}_{0.109}$	$22.63\pm^{0.126}_{0.120}$	$22.29\pm^{0.186}_{0.132}$	$24.09\pm^{0.248}_{0.138}$	$23.48\pm^{0.117}_{0.110}$	$22.96\pm^{0.137}_{0.128}$	$22.68\pm^{0.151}_{0.141}$	$22.28\pm^{0.239}_{0.155}$
HIPEQ0120-00	$23.23\pm^{0.144}_{0.131}$	$22.30\pm^{0.053}_{0.052}$	$21.96\pm^{0.053}_{0.052}$	$21.80\pm^{0.053}_{0.052}$	$21.63\pm^{0.094}_{0.088}$	$23.45\pm^{0.189}_{0.159}$	$22.55\pm^{0.079}_{0.076}$	$22.23\pm^{0.077}_{0.075}$	$22.02\pm^{0.078}_{0.076}$	$21.84\pm^{0.178}_{0.148}$
HIPEQ0122+00	$23.04\pm^{0.029}_{0.029}$	$21.86\pm^{0.017}_{0.016}$	$21.37\pm^{0.017}_{0.017}$	$21.07\pm^{0.018}_{0.018}$	$20.95\pm^{0.019}_{0.019}$	$23.51\pm^{0.037}_{0.036}$	$22.40\pm^{0.026}_{0.026}$	$21.89\pm^{0.028}_{0.028}$	$21.57\pm^{0.029}_{0.029}$	$21.48\pm^{0.027}_{0.026}$
HIPEQ0123-00	$23.00\pm^{0.106}_{0.099}$	$21.83\pm^{0.064}_{0.062}$	$21.23\pm^{0.069}_{0.067}$	$21.00\pm^{0.070}_{0.068}$	$20.76\pm^{0.075}_{0.073}$	$23.02\pm^{0.060}_{0.058}$	$21.78\pm^{0.067}_{0.065}$	$21.23\pm^{0.071}_{0.069}$	$21.00\pm^{0.072}_{0.070}$	$20.77\pm^{0.077}_{0.074}$
HIPEQ0126+00a	$24.31\pm^{0.385}_{0.106}$	$23.74\pm^{0.150}_{0.134}$	$23.27\pm^{0.093}_{0.088}$	$23.06\pm^{0.098}_{0.093}$	$22.27\pm^{0.277}_{0.173}$	$24.29\pm^{0.411}_{0.115}$	$23.71\pm^{0.094}_{0.088}$	$23.22\pm^{0.107}_{0.101}$	$23.09\pm^{0.105}_{0.099}$	$22.27\pm^{0.242}_{0.161}$
HIPEQ0126-00b	$21.30\pm^{0.211}_{0.196}$	$20.69\pm^{0.193}_{0.178}$	$20.68\pm^{0.179}_{0.166}$	$20.84\pm^{0.168}_{0.157}$	$20.68\pm^{0.196}_{0.182}$	$21.34\pm^{0.251}_{0.229}$	$20.71\pm^{0.233}_{0.211}$	$20.73\pm^{0.212}_{0.194}$	$20.73\pm^{0.214}_{0.196}$	$20.72\pm^{0.227}_{0.207}$
HIPEQ0154-00	$22.53\pm^{0.193}_{0.176}$	$20.59\pm^{0.103}_{0.098}$	$19.71\pm^{0.107}_{0.102}$	$19.31\pm^{0.107}_{0.102}$	$18.85\pm^{0.121}_{0.115}$	$22.52\pm^{0.112}_{0.107}$	$20.56\pm^{0.113}_{0.108}$	$19.66\pm^{0.119}_{0.113}$	$19.26\pm^{0.119}_{0.113}$	$18.91\pm^{0.128}_{0.121}$
HIPEQ0222-00	$23.60\pm^{0.190}_{0.154}$	$22.54\pm^{0.031}_{0.031}$	$22.10\pm^{0.032}_{0.031}$	$21.86\pm^{0.033}_{0.033}$	$21.69\pm^{0.085}_{0.079}$	$24.05\pm^{0.201}_{0.125}$	$23.45\pm^{0.048}_{0.046}$	$22.93\pm^{0.053}_{0.051}$	$22.65\pm^{0.055}_{0.053}$	$22.21\pm^{0.129}_{0.102}$
HIPEQ0228-01	$22.89\pm^{0.057}_{0.055}$	$21.80\pm^{0.033}_{0.033}$	$21.33\pm^{0.034}_{0.034}$	$21.12\pm^{0.035}_{0.034}$	$21.04\pm^{0.035}_{0.034}$	$22.87\pm^{0.033}_{0.032}$	$21.80\pm^{0.034}_{0.033}$	$21.33\pm^{0.035}_{0.034}$	$21.15\pm^{0.035}_{0.034}$	$21.04\pm^{0.036}_{0.035}$
HIPEQ0230+00	$24.42\pm^{0.062}_{0.032}$	$23.91\pm^{0.039}_{0.038}$	$23.37\pm^{0.037}_{0.036}$	$22.91\pm^{0.039}_{0.038}$	$22.49\pm^{0.075}_{0.057}$	$24.41\pm^{0.067}_{0.035}$	$23.89\pm^{0.047}_{0.045}$	$23.33\pm^{0.046}_{0.044}$	$22.90\pm^{0.047}_{0.046}$	$22.48\pm^{0.081}_{0.061}$
HIPEQ0230-01	$21.50\pm^{0.051}_{0.050}$	$19.53\pm^{0.054}_{0.053}$	$18.66\pm^{0.057}_{0.055}$	$18.25\pm^{0.057}_{0.055}$	$17.91\pm^{0.061}_{0.059}$	$21.94\pm^{0.062}_{0.060}$	$19.88\pm^{0.072}_{0.070}$	$19.05\pm^{0.074}_{0.072}$	$18.63\pm^{0.074}_{0.072}$	$18.25\pm^{0.080}_{0.077}$
HIPEQ0231+00	$23.80\pm^{0.218}_{0.161}$	$22.59\pm^{0.061}_{0.059}$	$22.18\pm^{0.063}_{0.062}$	$21.93\pm^{0.066}_{0.064}$	$21.75\pm^{0.201}_{0.167}$	$23.77\pm^{0.257}_{0.185}$	$22.64\pm^{0.076}_{0.073}$	$22.22\pm^{0.079}_{0.077}$	$21.96\pm^{0.083}_{0.080}$	$21.75\pm^{0.136}_{0.121}$
HIPEQ0236+00	$23.16\pm^{0.104}_{0.098}$	$21.71\pm^{0.057}_{0.055}$	$20.92\pm^{0.061}_{0.059}$	$20.46\pm^{0.064}_{0.063}$	$20.14\pm^{0.073}_{0.071}$	$23.52\pm^{0.125}_{0.111}$	$22.09\pm^{0.086}_{0.082}$	$21.31\pm^{0.092}_{0.089}$	$20.87\pm^{0.096}_{0.093}$	$20.47\pm^{0.109}_{0.105}$
HIPEQ0238+00	$24.12\pm^{0.145}_{0.096}$	$24.01\pm^{0.049}_{0.047}$	$23.75\pm^{0.089}_{0.081}$	$23.51\pm^{0.120}_{0.103}$	$22.53\pm^{0.094}_{0.065}$	$24.12\pm^{0.196}_{0.114}$	$24.03\pm^{0.060}_{0.057}$	$23.75\pm^{0.066}_{0.062}$	$23.54\pm^{0.148}_{0.121}$	$22.54\pm^{0.142}_{0.082}$
HIPEQ0240+01	$24.21\pm^{6.181}_{0.097}$	$24.25\pm^{0.060}_{0.056}$	$24.09\pm^{0.077}_{0.067}$	$23.82\pm^{0.083}_{0.069}$	$22.62\pm^{0.066}_{0.043}$	$24.22\pm^{0.205}_{0.100}$	$24.33\pm^{0.086}_{0.074}$	$24.13\pm^{0.058}_{0.053}$	$23.86\pm^{0.066}_{0.056}$	$22.63\pm^{0.045}_{0.034}$
HIPEQ0241+00	$23.43\pm^{0.020}_{0.019}$	$21.96\pm^{0.009}_{0.009}$	$21.07\pm^{0.009}_{0.009}$	$20.54\pm^{0.009}_{0.009}$	$20.17\pm^{0.010}_{0.010}$	$23.50\pm^{0.021}_{0.020}$	$22.03\pm^{0.014}_{0.014}$	$21.15\pm^{0.014}_{0.014}$	$20.63\pm^{0.015}_{0.015}$	$20.28\pm^{0.016}_{0.016}$
HIPEQ0244+00	$23.63\pm^{0.168}_{0.138}$	$22.66\pm^{0.045}_{0.044}$	$22.30\pm^{0.045}_{0.044}$	$22.20\pm^{0.044}_{0.043}$	$21.90\pm^{0.094}_{0.085}$	$23.84\pm^{0.164}_{0.126}$	$22.93\pm^{0.065}_{0.063}$	$22.59\pm^{0.064}_{0.062}$	$22.51\pm^{0.112}_{0.105}$	$22.15\pm^{0.101}_{0.085}$
HIPEQ0246-00a	$23.25\pm^{0.031}_{0.030}$	$21.72\pm^{0.020}_{0.020}$	$20.97\pm^{0.022}_{0.022}$	$20.58\pm^{0.023}_{0.023}$	$20.37\pm^{0.024}_{0.024}$	$23.32\pm^{0.040}_{0.039}$	$21.85\pm^{0.027}_{0.027}$	$21.09\pm^{0.029}_{0.029}$	$20.69\pm^{0.031}_{0.031}$	$20.49\pm^{0.031}_{0.031}$
HIPEQ0246-00b	$21.90\pm^{0.025}_{0.025}$	$20.97\pm^{0.022}_{0.022}$	$20.55\pm^{0.022}_{0.022}$	$20.34\pm^{0.022}_{0.022}$	$20.19\pm^{0.023}_{0.023}$	$21.90\pm^{0.027}_{0.027}$	$20.97\pm^{0.024}_{0.023}$	$20.55\pm^{0.024}_{0.023}$	$20.35\pm^{0.024}_{0.023}$	$20.19\pm^{0.024}_{0.024}$
HIPEQ0249-00	$23.26\pm^{0.153}_{0.135}$	$21.80\pm^{0.070}_{0.068}$	$21.16\pm^{0.074}_{0.072}$	$20.87\pm^{0.074}_{0.072}$	$20.53\pm^{0.083}_{0.080}$	$23.28\pm^{0.168}_{0.145}$	$21.85\pm^{0.077}_{0.074}$	$21.19\pm^{0.082}_{0.079}$	$20.90\pm^{0.082}_{0.079}$	$20.62\pm^{0.089}_{0.085}$
HIPEQ0249-00a	$23.96\pm^{0.157}_{0.107}$	$23.54\pm^{0.051}_{0.049}$	$23.24\pm^{0.056}_{0.055}$	$22.96\pm^{0.114}_{0.106}$	$22.39\pm^{0.205}_{0.120}$	$23.98\pm^{0.155}_{0.104}$	$23.67\pm^{0.059}_{0.057}$	$23.34\pm^{0.068}_{0.065}$	$23.10\pm^{0.076}_{0.072}$	$22.40\pm^{0.092}_{0.071}$
HIPEQ0249-00b	$22.58\pm^{0.099}_{0.095}$	$21.02\pm^{0.060}_{0.058}$	$20.27\pm^{0.064}_{0.063}$	$19.94\pm^{0.064}_{0.063}$	$19.68\pm^{0.069}_{0.067}$	$22.79\pm^{0.099}_{0.093}$	$21.10\pm^{0.067}_{0.065}$	$20.41\pm^{0.071}_{0.068}$	$20.08\pm^{0.071}_{0.069}$	$19.79\pm^{0.075}_{0.073}$
HIPEQ0251-01	$23.77\pm^{0.048}_{0.043}$	$23.35\pm^{0.042}_{0.041}$	$23.06\pm^{0.024}_{0.024}$	$22.88\pm^{0.042}_{0.041}$	$22.24\pm^{0.046}_{0.041}$	$23.88\pm^{0.053}_{0.046}$	$23.56\pm^{0.032}_{0.031}$	$23.20\pm^{0.033}_{0.032}$	$23.02\pm^{0.033}_{0.032}$	$22.29\pm^{0.048}_{0.043}$
HIPEQ0300+00	$23.21\pm^{0.241}_{0.189}$	$22.33\pm^{0.049}_{0.048}$	$21.86\pm^{0.052}_{0.051}$	$21.62\pm^{0.055}_{0.054}$	$21.53\pm^{0.099}_{0.092}$	$23.51\pm^{0.234}_{0.162}$	$22.67\pm^{0.074}_{0.071}$	$22.19\pm^{0.079}_{0.077}$	$21.99\pm^{0.081}_{0.078}$	$21.72\pm^{0.202}_{0.166}$

Table 3.8—Continued

	$\Sigma_{Elliptical}$					$\Sigma_{Circular}$				
HIPASS Name	u	g	r	i	z	u	g	r	i	z
HIPEQ0301-00	$23.19\pm^{0.165}_{0.136}$	$22.42\pm^{0.054}_{0.053}$	$22.13\pm^{0.057}_{0.055}$	$22.08\pm^{0.055}_{0.054}$	$21.88\pm^{0.141}_{0.117}$	$23.27\pm^{0.125}_{0.107}$	$22.58\pm^{0.066}_{0.064}$	$22.25\pm^{0.071}_{0.068}$	$22.17\pm^{0.069}_{0.067}$	$21.92\pm^{0.178}_{0.138}$
HIPEQ0306-00	$21.98\pm^{0.071}_{0.069}$	$19.85\pm^{0.077}_{0.074}$	$19.05\pm^{0.080}_{0.077}$	$18.72\pm^{0.077}_{0.074}$	$18.33\pm^{0.084}_{0.081}$	$22.07\pm^{0.073}_{0.071}$	$19.93\pm^{0.080}_{0.077}$	$19.13\pm^{0.083}_{0.080}$	$18.81\pm^{0.080}_{0.077}$	$18.41\pm^{0.087}_{0.084}$
HIPEQ0316-00	$23.09\pm^{0.141}_{0.128}$	$21.68\pm^{0.047}_{0.046}$	$20.80\pm^{0.053}_{0.052}$	$20.36\pm^{0.055}_{0.054}$	$20.01\pm^{0.060}_{0.059}$	$23.37\pm^{0.286}_{0.213}$	$21.97\pm^{0.073}_{0.070}$	$21.14\pm^{0.080}_{0.077}$	$20.64\pm^{0.085}_{0.082}$	$20.34\pm^{0.090}_{0.087}$
HIPEQ0320-06	$21.30\pm^{0.063}_{0.062}$	$20.16\pm^{0.060}_{0.059}$	$19.64\pm^{0.062}_{0.060}$	$19.38\pm^{0.062}_{0.061}$	$19.15\pm^{0.066}_{0.064}$	$21.42\pm^{0.081}_{0.079}$	$20.27\pm^{0.080}_{0.077}$	$19.73\pm^{0.083}_{0.080}$	$19.47\pm^{0.083}_{0.080}$	$19.30\pm^{0.085}_{0.082}$
HIPEQ0351-00	$21.14\pm^{0.189}_{0.178}$	$20.17\pm^{0.153}_{0.143}$	$19.66\pm^{0.152}_{0.143}$	$19.39\pm^{0.152}_{0.143}$	$18.90\pm^{0.181}_{0.168}$	$21.30\pm^{0.218}_{0.203}$	$20.35\pm^{0.177}_{0.164}$	$19.85\pm^{0.177}_{0.164}$	$19.40\pm^{0.192}_{0.176}$	$19.21\pm^{0.196}_{0.181}$
HIPEQ0809+00	$22.82\pm^{0.045}_{0.044}$	$21.79\pm^{0.046}_{0.045}$	$21.39\pm^{0.047}_{0.046}$	$21.18\pm^{0.049}_{0.048}$	$21.13\pm^{0.047}_{0.046}$	$22.95\pm^{0.051}_{0.050}$	$21.84\pm^{0.057}_{0.055}$	$21.42\pm^{0.059}_{0.057}$	$21.21\pm^{0.061}_{0.059}$	$21.18\pm^{0.057}_{0.056}$
HIPEQ0821+03b	$22.22\pm^{0.074}_{0.072}$	$20.92\pm^{0.070}_{0.068}$	$20.21\pm^{0.075}_{0.072}$	$19.81\pm^{0.078}_{0.075}$	$19.44\pm^{0.085}_{0.082}$	$22.43\pm^{0.081}_{0.078}$	$21.06\pm^{0.080}_{0.078}$	$20.32\pm^{0.086}_{0.083}$	$19.91\pm^{0.090}_{0.087}$	$19.60\pm^{0.096}_{0.092}$
HIPEQ0821-00	$22.42\pm^{0.178}_{0.167}$	$22.07\pm^{0.071}_{0.069}$	$21.98\pm^{0.070}_{0.069}$	$21.91\pm^{0.079}_{0.077}$	$21.87\pm^{0.200}_{0.162}$	$22.72\pm^{0.207}_{0.186}$	$22.23\pm^{0.093}_{0.090}$	$22.16\pm^{0.090}_{0.087}$	$22.09\pm^{0.096}_{0.092}$	$21.99\pm^{0.179}_{0.142}$
HIPEQ0822-00	$22.98\pm^{0.043}_{0.042}$	$21.76\pm^{0.048}_{0.047}$	$21.24\pm^{0.049}_{0.048}$	$20.95\pm^{0.051}_{0.050}$	$20.87\pm^{0.094}_{0.090}$	$23.13\pm^{0.051}_{0.050}$	$21.89\pm^{0.064}_{0.062}$	$21.34\pm^{0.067}_{0.065}$	$21.09\pm^{0.068}_{0.066}$	$21.03\pm^{0.121}_{0.113}$
HIPEQ0825-00	$23.19\pm^{0.029}_{0.028}$	$21.16\pm^{0.039}_{0.039}$	$20.15\pm^{0.043}_{0.042}$	$19.67\pm^{0.044}_{0.043}$	$19.25\pm^{0.047}_{0.047}$	$23.58\pm^{0.026}_{0.026}$	$21.39\pm^{0.055}_{0.054}$	$20.40\pm^{0.061}_{0.059}$	$19.95\pm^{0.061}_{0.059}$	$19.60\pm^{0.062}_{0.061}$
HIPEQ0855+02	$23.91\pm^{0.127}_{0.096}$	$23.48\pm^{0.028}_{0.028}$	$23.03\pm^{0.032}_{0.032}$	$22.88\pm^{0.077}_{0.073}$	$22.37\pm^{0.094}_{0.072}$	$23.88\pm^{0.108}_{0.087}$	$23.41\pm^{0.038}_{0.037}$	$23.00\pm^{0.042}_{0.041}$	$22.84\pm^{0.042}_{0.041}$	$22.33\pm^{0.086}_{0.069}$
HIPEQ0856+00	$23.42\pm^{0.035}_{0.034}$	$22.32\pm^{0.044}_{0.043}$	$21.95\pm^{0.046}_{0.045}$	$22.08\pm^{0.038}_{0.038}$	$21.82\pm^{0.061}_{0.057}$	$23.48\pm^{0.062}_{0.059}$	$22.30\pm^{0.050}_{0.049}$	$21.91\pm^{0.054}_{0.053}$	$22.14\pm^{0.042}_{0.041}$	$21.83\pm^{0.099}_{0.089}$
HIPEQ0923-00	$22.75\pm^{0.049}_{0.048}$	$21.64\pm^{0.047}_{0.046}$	$21.20\pm^{0.050}_{0.049}$	$20.97\pm^{0.052}_{0.051}$	$20.80\pm^{0.058}_{0.056}$	$23.09\pm^{0.062}_{0.060}$	$21.99\pm^{0.067}_{0.065}$	$21.49\pm^{0.074}_{0.072}$	$21.24\pm^{0.077}_{0.075}$	$21.07\pm^{0.080}_{0.077}$
HIPEQ0930+04	$22.84\pm^{0.061}_{0.059}$	$22.12\pm^{0.036}_{0.036}$	$21.48\pm^{0.039}_{0.038}$	$21.28\pm^{0.039}_{0.039}$	$20.73\pm^{0.042}_{0.042}$	$22.92\pm^{0.044}_{0.043}$	$22.22\pm^{0.050}_{0.048}$	$21.58\pm^{0.053}_{0.052}$	$21.39\pm^{0.054}_{0.052}$	$20.83\pm^{0.056}_{0.054}$
HIPEQ0942+00	$22.18\pm^{0.027}_{0.027}$	$20.89\pm^{0.029}_{0.029}$	$20.27\pm^{0.031}_{0.030}$	$19.98\pm^{0.031}_{0.031}$	$19.87\pm^{0.031}_{0.031}$	$22.17\pm^{0.029}_{0.028}$	$20.88\pm^{0.031}_{0.031}$	$20.28\pm^{0.033}_{0.032}$	$19.99\pm^{0.033}_{0.033}$	$19.86\pm^{0.033}_{0.033}$
HIPEQ0944-00b	$23.37\pm^{0.190}_{0.157}$	$22.55\pm^{0.076}_{0.074}$	$22.14\pm^{0.083}_{0.081}$	$21.89\pm^{0.101}_{0.097}$	$21.85\pm^{0.186}_{0.152}$	$23.47\pm^{0.148}_{0.125}$	$22.59\pm^{0.097}_{0.093}$	$22.23\pm^{0.103}_{0.098}$	$21.90\pm^{0.128}_{0.122}$	$21.88\pm^{0.089}_{0.081}$
HIPEQ0945+01	$22.30\pm^{0.077}_{0.074}$	$21.20\pm^{0.027}_{0.026}$	$20.69\pm^{0.027}_{0.027}$	$20.47\pm^{0.027}_{0.027}$	$20.32\pm^{0.030}_{0.030}$	$22.70\pm^{0.128}_{0.114}$	$21.54\pm^{0.043}_{0.042}$	$21.03\pm^{0.044}_{0.043}$	$20.80\pm^{0.044}_{0.043}$	$20.75\pm^{0.043}_{0.042}$
HIPEQ0946+02	$23.83\pm^{0.089}_{0.074}$	$23.10\pm^{0.031}_{0.030}$	$22.61\pm^{0.031}_{0.031}$	$22.37\pm^{0.033}_{0.032}$	$22.08\pm^{0.068}_{0.061}$	$23.92\pm^{0.058}_{0.051}$	$23.36\pm^{0.044}_{0.043}$	$22.87\pm^{0.046}_{0.045}$	$22.64\pm^{0.047}_{0.046}$	$22.21\pm^{0.069}_{0.060}$
HIPEQ0947+00a	$23.24\pm^{0.039}_{0.036}$	$22.48\pm^{0.031}_{0.030}$	$21.96\pm^{0.033}_{0.032}$	$21.68\pm^{0.034}_{0.033}$	$21.51\pm^{0.052}_{0.050}$	$23.31\pm^{0.062}_{0.052}$	$22.56\pm^{0.045}_{0.044}$	$22.03\pm^{0.048}_{0.047}$	$21.78\pm^{0.049}_{0.048}$	$21.58\pm^{0.075}_{0.069}$
HIPEQ0947+00b	$23.57\pm^{0.055}_{0.044}$	$23.26\pm^{0.036}_{0.036}$	$22.88\pm^{0.075}_{0.072}$	$22.69\pm^{0.081}_{0.077}$	$22.18\pm^{0.139}_{0.099}$	$23.60\pm^{0.054}_{0.042}$	$23.33\pm^{0.084}_{0.079}$	$22.91\pm^{0.055}_{0.053}$	$22.76\pm^{0.105}_{0.097}$	$22.20\pm^{0.218}_{0.128}$
HIPEQ0953+01	$22.07\pm^{0.014}_{0.014}$	$20.96\pm^{0.012}_{0.013}$	$20.43\pm^{0.013}_{0.013}$	$20.26\pm^{0.013}_{0.013}$	$19.71\pm^{0.029}_{0.029}$	$23.23\pm^{0.019}_{0.018}$	$22.17\pm^{0.021}_{0.020}$	$21.61\pm^{0.022}_{0.022}$	$21.43\pm^{0.022}_{0.022}$	$20.92\pm^{0.024}_{0.024}$
HIPEQ0954+02a	$23.56\pm^{0.074}_{0.067}$	$22.15\pm^{0.060}_{0.059}$	$21.74\pm^{0.064}_{0.062}$	$21.43\pm^{0.065}_{0.063}$	$21.69\pm^{0.060}_{0.058}$	$23.58\pm^{0.073}_{0.067}$	$22.11\pm^{0.062}_{0.060}$	$21.76\pm^{0.064}_{0.062}$	$21.39\pm^{0.067}_{0.065}$	$21.70\pm^{0.060}_{0.057}$
HIPEQ0955+04a	$21.76\pm^{0.033}_{0.032}$	$20.76\pm^{0.030}_{0.030}$	$20.26\pm^{0.031}_{0.031}$	$20.05\pm^{0.031}_{0.031}$	$19.90\pm^{0.033}_{0.032}$	$22.01\pm^{0.041}_{0.040}$	$20.91\pm^{0.041}_{0.041}$	$20.39\pm^{0.043}_{0.042}$	$20.22\pm^{0.042}_{0.041}$	$20.09\pm^{0.042}_{0.042}$
HIPEQ0958+01	$24.35\pm^{0.155}_{0.077}$	$24.21\pm^{0.052}_{0.049}$	$23.99\pm^{0.094}_{0.084}$	$23.87\pm^{0.174}_{0.121}$	$22.73\pm^{0.161}_{0.061}$	$24.40\pm^{0.175}_{0.069}$	$24.29\pm^{0.108}_{0.094}$	$24.12\pm^{0.149}_{0.118}$	$23.92\pm^{0.220}_{0.135}$	$22.75\pm^{0.405}_{0.038}$
HIPEQ1000+03	$22.41\pm^{0.043}_{0.043}$	$20.98\pm^{0.040}_{0.040}$	$20.00\pm^{0.047}_{0.046}$	$19.50\pm^{0.049}_{0.048}$	$18.82\pm^{0.060}_{0.059}$	$22.87\pm^{0.057}_{0.055}$	$21.44\pm^{0.059}_{0.058}$	$20.42\pm^{0.070}_{0.068}$	$19.95\pm^{0.072}_{0.070}$	$19.37\pm^{0.085}_{0.082}$
HIPEQ1010+05	$22.22\pm^{0.144}_{0.136}$	$21.04\pm^{0.121}_{0.115}$	$20.70\pm^{0.115}_{0.109}$	$20.59\pm^{0.110}_{0.105}$	$20.46\pm^{0.121}_{0.116}$	$22.30\pm^{0.170}_{0.159}$	$21.13\pm^{0.144}_{0.136}$	$20.81\pm^{0.135}_{0.127}$	$20.58\pm^{0.136}_{0.128}$	$20.55\pm^{0.141}_{0.133}$
HIPEQ1014+03	$23.01\pm^{0.022}_{0.022}$	$21.00\pm^{0.014}_{0.014}$	$19.95\pm^{0.017}_{0.016}$	$19.36\pm^{0.018}_{0.018}$	$18.86\pm^{0.021}_{0.020}$	$23.02\pm^{0.016}_{0.016}$	$21.03\pm^{0.019}_{0.018}$	$19.97\pm^{0.022}_{0.021}$	$19.39\pm^{0.023}_{0.023}$	$18.89\pm^{0.027}_{0.026}$
HIPEQ1015+02	$23.94\pm^{0.107}_{0.085}$	$23.55\pm^{0.046}_{0.045}$	$23.16\pm^{0.053}_{0.052}$	$23.14\pm^{0.082}_{0.077}$	$22.32\pm^{0.148}_{0.106}$	$23.96\pm^{0.125}_{0.094}$	$23.58\pm^{0.070}_{0.067}$	$23.26\pm^{0.043}_{0.042}$	$23.26\pm^{0.087}_{0.080}$	$22.42\pm^{0.146}_{0.095}$
HIPEQ1026+03	$23.34\pm^{0.042}_{0.041}$	$22.02\pm^{0.028}_{0.027}$	$21.53\pm^{0.030}_{0.029}$	$21.35\pm^{0.030}_{0.030}$	$20.94\pm^{0.032}_{0.031}$	$23.46\pm^{0.051}_{0.049}$	$22.11\pm^{0.037}_{0.037}$	$21.60\pm^{0.041}_{0.040}$	$21.40\pm^{0.042}_{0.041}$	$21.03\pm^{0.042}_{0.041}$
HIPEQ1028+03	$23.23\pm^{0.111}_{0.104}$	$22.41\pm^{0.040}_{0.040}$	$22.34\pm^{0.040}_{0.039}$	$22.16\pm^{0.041}_{0.040}$	$21.87\pm^{0.060}_{0.057}$	$23.80\pm^{0.122}_{0.101}$	$22.96\pm^{0.069}_{0.067}$	$22.91\pm^{0.066}_{0.064}$	$22.65\pm^{0.068}_{0.066}$	$22.15\pm^{0.085}_{0.074}$
HIPEQ1039+01	$23.02\pm^{0.127}_{0.118}$	$22.07\pm^{0.064}_{0.062}$	$21.82\pm^{0.061}_{0.060}$	$21.74\pm^{0.057}_{0.056}$	$21.59\pm^{0.055}_{0.053}$	$23.04\pm^{0.076}_{0.073}$	$22.09\pm^{0.070}_{0.068}$	$21.85\pm^{0.066}_{0.064}$	$21.73\pm^{0.063}_{0.061}$	$21.56\pm^{0.110}_{0.101}$

Table 3.8—Continued

	$\Sigma_{Elliptical}$					$\Sigma_{Circular}$				
HIPASS Name	u	g	r	i	z	u	g	r	i	z
HIPEQ1041+00	$23.32\pm^{0.082}_{0.076}$	$22.28\pm^{0.059}_{0.057}$	$21.91\pm^{0.060}_{0.058}$	$21.82\pm^{0.056}_{0.055}$	$21.57\pm^{0.054}_{0.052}$	$23.33\pm^{0.088}_{0.081}$	$22.31\pm^{0.064}_{0.062}$	$21.94\pm^{0.064}_{0.062}$	$21.80\pm^{0.062}_{0.060}$	$21.56\pm^{0.059}_{0.056}$
HIPEQ1046+01	$23.21\pm^{0.046}_{0.044}$	$21.98\pm^{0.015}_{0.015}$	$21.42\pm^{0.016}_{0.015}$	$21.23\pm^{0.016}_{0.016}$	$20.80\pm^{0.033}_{0.032}$	$23.69\pm^{0.044}_{0.041}$	$22.77\pm^{0.024}_{0.023}$	$22.20\pm^{0.025}_{0.025}$	$21.97\pm^{0.026}_{0.025}$	$21.45\pm^{0.047}_{0.046}$
HIPEQ1050+01	$23.85\pm^{0.189}_{0.140}$	$23.18\pm^{0.101}_{0.097}$	$22.82\pm^{0.096}_{0.093}$	$22.61\pm^{0.105}_{0.101}$	$22.12\pm^{0.373}_{0.232}$	$23.85\pm^{0.411}_{0.219}$	$23.33\pm^{0.137}_{0.128}$	$23.00\pm^{0.129}_{0.121}$	$22.76\pm^{0.142}_{0.132}$	$22.22\pm^{0.359}_{0.210}$
HIPEQ1051+04a	$23.17\pm^{0.060}_{0.058}$	$22.22\pm^{0.036}_{0.035}$	$21.74\pm^{0.038}_{0.037}$	$21.60\pm^{0.039}_{0.038}$	$21.42\pm^{0.105}_{0.098}$	$23.37\pm^{0.074}_{0.070}$	$22.32\pm^{0.052}_{0.050}$	$21.84\pm^{0.054}_{0.053}$	$21.68\pm^{0.056}_{0.055}$	$21.51\pm^{0.102}_{0.095}$
HIPEQ1052+00	$20.46\pm^{0.240}_{0.218}$	$20.07\pm^{0.191}_{0.176}$	$19.95\pm^{0.176}_{0.164}$	$20.12\pm^{0.153}_{0.143}$	$20.00\pm^{0.162}_{0.152}$	$20.55\pm^{0.301}_{0.267}$	$20.26\pm^{0.231}_{0.209}$	$20.18\pm^{0.210}_{0.192}$	$20.22\pm^{0.192}_{0.177}$	$20.09\pm^{0.201}_{0.185}$
HIPEQ1053+02	$22.28\pm^{0.091}_{0.089}$	$22.06\pm^{0.076}_{0.074}$	$22.03\pm^{0.073}_{0.071}$	$21.97\pm^{0.074}_{0.072}$	$21.92\pm^{0.154}_{0.130}$	$22.49\pm^{0.118}_{0.113}$	$22.29\pm^{0.101}_{0.097}$	$22.22\pm^{0.099}_{0.095}$	$22.18\pm^{0.097}_{0.093}$	$22.00\pm^{0.142}_{0.119}$
HIPEQ1055+02	$22.24\pm^{0.148}_{0.142}$	$21.71\pm^{0.118}_{0.112}$	$21.76\pm^{0.109}_{0.105}$	$21.86\pm^{0.109}_{0.104}$	$21.63\pm^{0.224}_{0.194}$	$22.57\pm^{0.166}_{0.156}$	$21.95\pm^{0.146}_{0.137}$	$21.94\pm^{0.139}_{0.131}$	$22.06\pm^{0.135}_{0.128}$	$21.73\pm^{0.267}_{0.216}$
HIPEQ1101+03	$22.77\pm^{0.022}_{0.022}$	$21.54\pm^{0.012}_{0.012}$	$21.05\pm^{0.012}_{0.012}$	$20.70\pm^{0.012}_{0.013}$	$20.46\pm^{0.013}_{0.013}$	$23.10\pm^{0.020}_{0.020}$	$22.04\pm^{0.020}_{0.019}$	$21.55\pm^{0.020}_{0.020}$	$21.20\pm^{0.021}_{0.021}$	$20.93\pm^{0.021}_{0.021}$
HIPEQ1109-00	$22.35\pm^{0.065}_{0.064}$	$20.88\pm^{0.066}_{0.064}$	$20.01\pm^{0.075}_{0.073}$	$19.62\pm^{0.078}_{0.075}$	$19.18\pm^{0.090}_{0.087}$	$22.65\pm^{0.079}_{0.076}$	$21.17\pm^{0.087}_{0.083}$	$20.31\pm^{0.098}_{0.094}$	$19.90\pm^{0.103}_{0.098}$	$19.37\pm^{0.123}_{0.117}$
HIPEQ1110+01	$22.97\pm^{0.190}_{0.172}$	$22.38\pm^{0.059}_{0.057}$	$22.20\pm^{0.057}_{0.056}$	$22.20\pm^{0.060}_{0.058}$	$21.98\pm^{0.124}_{0.107}$	$23.15\pm^{0.202}_{0.178}$	$22.58\pm^{0.093}_{0.089}$	$22.47\pm^{0.087}_{0.084}$	$22.33\pm^{0.094}_{0.090}$	$22.07\pm^{0.076}_{0.070}$
HIPEQ1113+05	$23.09\pm^{0.106}_{0.098}$	$22.01\pm^{0.061}_{0.059}$	$21.84\pm^{0.061}_{0.060}$	$21.58\pm^{0.064}_{0.062}$	$21.93\pm^{0.082}_{0.074}$	$23.08\pm^{0.069}_{0.066}$	$22.03\pm^{0.070}_{0.068}$	$21.79\pm^{0.072}_{0.070}$	$21.58\pm^{0.073}_{0.071}$	$21.91\pm^{0.053}_{0.049}$
HIPEQ1117+04a	$20.56\pm^{0.086}_{0.083}$	$19.68\pm^{0.072}_{0.070}$	$19.26\pm^{0.067}_{0.065}$	$19.11\pm^{0.064}_{0.062}$	$18.78\pm^{0.069}_{0.067}$	$20.65\pm^{0.093}_{0.090}$	$19.73\pm^{0.080}_{0.077}$	$19.25\pm^{0.077}_{0.074}$	$19.11\pm^{0.072}_{0.070}$	$18.84\pm^{0.076}_{0.073}$
HIPEQ1119+02	$23.59\pm^{0.071}_{0.065}$	$22.76\pm^{0.027}_{0.027}$	$22.49\pm^{0.029}_{0.028}$	$22.40\pm^{0.028}_{0.028}$	$22.23\pm^{0.075}_{0.064}$	$23.64\pm^{0.081}_{0.072}$	$22.91\pm^{0.030}_{0.030}$	$22.59\pm^{0.033}_{0.033}$	$22.50\pm^{0.032}_{0.032}$	$22.21\pm^{0.081}_{0.069}$
HIPEQ1124+03	$23.03\pm^{0.033}_{0.033}$	$22.32\pm^{0.033}_{0.033}$	$22.12\pm^{0.018}_{0.018}$	$22.07\pm^{0.018}_{0.018}$	$21.87\pm^{0.036}_{0.035}$	$23.14\pm^{0.049}_{0.047}$	$22.42\pm^{0.028}_{0.028}$	$22.18\pm^{0.029}_{0.029}$	$22.09\pm^{0.029}_{0.029}$	$21.88\pm^{0.041}_{0.039}$
HIPEQ1127-01	$23.50\pm^{0.103}_{0.093}$	$22.55\pm^{0.049}_{0.048}$	$22.31\pm^{0.046}_{0.045}$	$22.22\pm^{0.044}_{0.043}$	$22.23\pm^{0.049}_{0.044}$	$23.44\pm^{0.085}_{0.078}$	$22.56\pm^{0.053}_{0.052}$	$22.29\pm^{0.051}_{0.050}$	$22.21\pm^{0.049}_{0.048}$	$22.18\pm^{0.041}_{0.038}$
HIPEQ1131-02	$23.47\pm^{0.044}_{0.042}$	$22.24\pm^{0.032}_{0.032}$	$21.65\pm^{0.035}_{0.034}$	$21.34\pm^{0.036}_{0.035}$	$21.32\pm^{0.035}_{0.034}$	$23.47\pm^{0.045}_{0.043}$	$22.25\pm^{0.033}_{0.032}$	$21.65\pm^{0.035}_{0.035}$	$21.32\pm^{0.037}_{0.036}$	$21.33\pm^{0.063}_{0.061}$
HIPEQ1133-03	$23.56\pm^{0.085}_{0.078}$	$22.66\pm^{0.043}_{0.042}$	$22.30\pm^{0.045}_{0.044}$	$22.15\pm^{0.045}_{0.044}$	$21.99\pm^{0.058}_{0.054}$	$23.57\pm^{0.077}_{0.071}$	$22.76\pm^{0.053}_{0.052}$	$22.38\pm^{0.056}_{0.055}$	$22.19\pm^{0.057}_{0.056}$	$22.01\pm^{0.073}_{0.066}$
HIPEQ1136+00	$20.95\pm^{0.125}_{0.119}$	$20.42\pm^{0.108}_{0.103}$	$20.61\pm^{0.095}_{0.091}$	$20.83\pm^{0.086}_{0.083}$	$20.73\pm^{0.095}_{0.092}$	$21.17\pm^{0.169}_{0.157}$	$20.57\pm^{0.152}_{0.142}$	$20.74\pm^{0.134}_{0.127}$	$20.94\pm^{0.121}_{0.115}$	$20.81\pm^{0.132}_{0.124}$
HIPEQ1138+03	$23.19\pm^{0.122}_{0.113}$	$21.74\pm^{0.071}_{0.069}$	$20.87\pm^{0.081}_{0.078}$	$20.47\pm^{0.085}_{0.082}$	$19.93\pm^{0.104}_{0.100}$	$23.24\pm^{0.070}_{0.068}$	$21.79\pm^{0.074}_{0.071}$	$20.91\pm^{0.084}_{0.081}$	$20.52\pm^{0.088}_{0.085}$	$19.96\pm^{0.109}_{0.105}$
HIPEQ1143-01	$24.23\pm^{0.127}_{0.091}$	$24.14\pm^{0.074}_{0.069}$	$23.87\pm^{0.079}_{0.073}$	$23.70\pm^{0.116}_{0.098}$	$22.62\pm^{0.406}_{0.106}$	$24.22\pm^{0.153}_{0.104}$	$24.10\pm^{0.092}_{0.085}$	$23.89\pm^{0.160}_{0.134}$	$23.71\pm^{0.192}_{0.142}$	$22.67\pm^{0.371}_{0.082}$
HIPEQ1145+02	$24.35\pm^{0.236}_{0.081}$	$24.48\pm^{0.110}_{0.089}$	$24.31\pm^{0.086}_{0.070}$	$23.95\pm^{0.125}_{0.092}$	$22.79\pm^{0.012}_{0.002}$	$24.35\pm^{0.211}_{0.080}$	$24.53\pm^{0.093}_{0.077}$	$24.31\pm^{0.081}_{0.067}$	$23.97\pm^{0.142}_{0.096}$	$22.79\pm^{0.145}_{0.004}$
HIPEQ1148-02	$23.87\pm^{0.058}_{0.053}$	$23.08\pm^{0.026}_{0.026}$	$22.62\pm^{0.028}_{0.028}$	$22.55\pm^{0.027}_{0.027}$	$22.08\pm^{0.072}_{0.065}$	$23.99\pm^{0.044}_{0.040}$	$23.28\pm^{0.029}_{0.029}$	$22.80\pm^{0.032}_{0.032}$	$22.71\pm^{0.030}_{0.029}$	$22.19\pm^{0.057}_{0.051}$
HIPEQ1151-02	$22.14\pm^{0.109}_{0.104}$	$21.11\pm^{0.099}_{0.095}$	$20.50\pm^{0.109}_{0.104}$	$20.21\pm^{0.115}_{0.110}$	$19.96\pm^{0.129}_{0.123}$	$22.36\pm^{0.135}_{0.128}$	$21.21\pm^{0.134}_{0.127}$	$20.67\pm^{0.143}_{0.134}$	$20.33\pm^{0.154}_{0.144}$	$20.04\pm^{0.173}_{0.161}$
HIPEQ1152+01	$22.74\pm^{0.059}_{0.058}$	$21.76\pm^{0.056}_{0.055}$	$21.42\pm^{0.056}_{0.055}$	$21.20\pm^{0.057}_{0.056}$	$21.04\pm^{0.061}_{0.060}$	$22.70\pm^{0.071}_{0.069}$	$21.71\pm^{0.069}_{0.067}$	$21.37\pm^{0.069}_{0.067}$	$21.16\pm^{0.070}_{0.068}$	$21.00\pm^{0.073}_{0.071}$
HIPEQ1152-02	$20.14\pm^{0.145}_{0.137}$	$19.74\pm^{0.133}_{0.125}$	$19.95\pm^{0.119}_{0.113}$	$20.35\pm^{0.109}_{0.104}$	$20.33\pm^{0.118}_{0.113}$	$20.38\pm^{0.179}_{0.166}$	$19.84\pm^{0.175}_{0.162}$	$20.11\pm^{0.152}_{0.142}$	$20.42\pm^{0.144}_{0.135}$	$20.44\pm^{0.153}_{0.144}$
HIPEQ1152-03b	$23.59\pm^{0.093}_{0.084}$	$22.74\pm^{0.043}_{0.042}$	$22.52\pm^{0.042}_{0.041}$	$22.42\pm^{0.042}_{0.041}$	$22.09\pm^{0.079}_{0.070}$	$23.62\pm^{0.044}_{0.042}$	$22.76\pm^{0.048}_{0.048}$	$22.55\pm^{0.048}_{0.047}$	$22.42\pm^{0.048}_{0.047}$	$22.07\pm^{0.066}_{0.060}$
HIPEQ1155+01	$23.89\pm^{0.025}_{0.024}$	$22.96\pm^{0.020}_{0.019}$	$22.43\pm^{0.021}_{0.020}$	$22.12\pm^{0.022}_{0.021}$	$21.79\pm^{0.019}_{0.019}$	$23.89\pm^{0.029}_{0.028}$	$22.95\pm^{0.024}_{0.023}$	$22.40\pm^{0.025}_{0.025}$	$22.09\pm^{0.026}_{0.026}$	$21.79\pm^{0.023}_{0.022}$
HIPEQ1200-00	$24.27\pm^{0.066}_{0.048}$	$23.94\pm^{0.028}_{0.027}$	$23.53\pm^{0.031}_{0.030}$	$23.23\pm^{0.075}_{0.070}$	$22.63\pm^{0.047}_{0.034}$	$24.26\pm^{0.065}_{0.049}$	$23.98\pm^{0.032}_{0.031}$	$23.56\pm^{0.036}_{0.035}$	$23.25\pm^{0.063}_{0.059}$	$22.62\pm^{0.041}_{0.032}$
HIPEQ1200-01	$21.85\pm^{0.020}_{0.020}$	$20.36\pm^{0.023}_{0.022}$	$19.53\pm^{0.025}_{0.025}$	$19.14\pm^{0.026}_{0.025}$	$18.78\pm^{0.028}_{0.027}$	$21.86\pm^{0.022}_{0.022}$	$20.35\pm^{0.025}_{0.025}$	$19.56\pm^{0.027}_{0.027}$	$19.13\pm^{0.028}_{0.028}$	$18.79\pm^{0.030}_{0.030}$
HIPEQ1202+01	$22.77\pm^{0.065}_{0.063}$	$21.05\pm^{0.036}_{0.036}$	$20.20\pm^{0.038}_{0.038}$	$19.76\pm^{0.039}_{0.039}$	$19.39\pm^{0.042}_{0.041}$	$22.77\pm^{0.067}_{0.065}$	$21.06\pm^{0.037}_{0.037}$	$20.21\pm^{0.040}_{0.039}$	$19.77\pm^{0.041}_{0.040}$	$19.40\pm^{0.044}_{0.043}$
HIPEQ1204-01	$24.20\pm^{0.053}_{0.045}$	$24.02\pm^{0.034}_{0.033}$	$23.71\pm^{0.062}_{0.059}$	$23.43\pm^{0.066}_{0.062}$	$22.53\pm^{0.075}_{0.056}$	$24.20\pm^{0.070}_{0.056}$	$24.03\pm^{0.037}_{0.036}$	$23.71\pm^{0.039}_{0.038}$	$23.42\pm^{0.072}_{0.067}$	$22.53\pm^{0.069}_{0.053}$

Table 3.8—Continued

	$\Sigma_{Elliptical}$					$\Sigma_{Circular}$				
HIPASS Name	u	g	r	i	z	u	g	r	i	z
HIPEQ1204-02	$23.36\pm^{0.104}_{0.095}$	$21.82\pm^{0.065}_{0.063}$	$20.86\pm^{0.075}_{0.073}$	$20.37\pm^{0.081}_{0.078}$	$20.04\pm^{0.088}_{0.085}$	$23.43\pm^{0.103}_{0.093}$	$21.86\pm^{0.069}_{0.067}$	$20.95\pm^{0.078}_{0.075}$	$20.46\pm^{0.084}_{0.081}$	$20.13\pm^{0.091}_{0.088}$
HIPEQ1210+02	$24.27\pm^{0.144}_{0.080}$	$23.96\pm^{0.064}_{0.061}$	$23.56\pm^{0.071}_{0.067}$	$23.33\pm^{0.099}_{0.090}$	$22.47\pm^{0.138}_{0.089}$	$24.26\pm^{0.127}_{0.076}$	$23.91\pm^{0.070}_{0.066}$	$23.55\pm^{0.044}_{0.042}$	$23.31\pm^{0.075}_{0.070}$	$22.46\pm^{0.158}_{0.099}$
HIPEQ1215+04a	$22.43\pm^{0.143}_{0.135}$	$21.41\pm^{0.070}_{0.068}$	$21.27\pm^{0.066}_{0.064}$	$21.13\pm^{0.067}_{0.066}$	$21.05\pm^{0.076}_{0.074}$	$22.63\pm^{0.101}_{0.097}$	$21.62\pm^{0.095}_{0.092}$	$21.43\pm^{0.092}_{0.089}$	$21.29\pm^{0.093}_{0.090}$	$21.17\pm^{0.099}_{0.095}$
HIPEQ1216-03	$23.48\pm^{0.045}_{0.043}$	$22.19\pm^{0.063}_{0.061}$	$21.60\pm^{0.068}_{0.066}$	$21.32\pm^{0.071}_{0.069}$	$21.19\pm^{0.067}_{0.064}$	$23.48\pm^{0.078}_{0.072}$	$22.20\pm^{0.063}_{0.061}$	$21.61\pm^{0.068}_{0.066}$	$21.32\pm^{0.071}_{0.069}$	$21.19\pm^{0.067}_{0.064}$
HIPEQ1218+00	$24.28\pm^{0.046}_{0.037}$	$23.97\pm^{0.049}_{0.047}$	$23.55\pm^{0.030}_{0.030}$	$23.32\pm^{0.032}_{0.031}$	$22.48\pm^{0.068}_{0.054}$	$24.29\pm^{0.054}_{0.041}$	$24.02\pm^{0.032}_{0.031}$	$23.60\pm^{0.034}_{0.034}$	$23.39\pm^{0.060}_{0.056}$	$22.51\pm^{0.062}_{0.049}$
HIPEQ1218-01	$22.63\pm^{0.071}_{0.069}$	$21.21\pm^{0.071}_{0.069}$	$20.49\pm^{0.075}_{0.073}$	$20.11\pm^{0.078}_{0.076}$	$19.76\pm^{0.087}_{0.084}$	$22.72\pm^{0.084}_{0.080}$	$21.36\pm^{0.084}_{0.081}$	$20.52\pm^{0.094}_{0.090}$	$20.21\pm^{0.094}_{0.091}$	$19.83\pm^{0.106}_{0.102}$
HIPEQ1219+03	$21.73\pm^{0.094}_{0.091}$	$21.29\pm^{0.074}_{0.071}$	$21.14\pm^{0.067}_{0.065}$	$21.20\pm^{0.062}_{0.061}$	$21.06\pm^{0.063}_{0.061}$	$21.72\pm^{0.101}_{0.097}$	$21.30\pm^{0.079}_{0.076}$	$21.16\pm^{0.071}_{0.069}$	$21.23\pm^{0.066}_{0.064}$	$21.09\pm^{0.066}_{0.064}$
HIPEQ1220+00	$23.32\pm^{0.104}_{0.098}$	$22.61\pm^{0.050}_{0.049}$	$22.42\pm^{0.053}_{0.052}$	$22.35\pm^{0.054}_{0.053}$	$22.04\pm^{0.119}_{0.103}$	$23.69\pm^{0.123}_{0.106}$	$22.99\pm^{0.078}_{0.075}$	$22.76\pm^{0.082}_{0.079}$	$22.65\pm^{0.083}_{0.079}$	$22.22\pm^{0.160}_{0.122}$
HIPEQ1220+01	$23.13\pm^{0.115}_{0.108}$	$21.95\pm^{0.033}_{0.033}$	$21.48\pm^{0.033}_{0.034}$	$21.24\pm^{0.035}_{0.035}$	$21.03\pm^{0.073}_{0.072}$	$23.96\pm^{0.105}_{0.086}$	$22.96\pm^{0.055}_{0.053}$	$22.41\pm^{0.058}_{0.057}$	$22.04\pm^{0.065}_{0.063}$	$21.73\pm^{0.213}_{0.177}$
HIPEQ1221+03	$23.68\pm^{0.079}_{0.072}$	$21.74\pm^{0.033}_{0.033}$	$20.73\pm^{0.037}_{0.036}$	$20.12\pm^{0.041}_{0.040}$	$19.61\pm^{0.047}_{0.046}$	$23.80\pm^{0.078}_{0.070}$	$21.89\pm^{0.062}_{0.060}$	$20.88\pm^{0.069}_{0.067}$	$20.29\pm^{0.073}_{0.071}$	$19.89\pm^{0.076}_{0.074}$
HIPEQ1223+00	$24.10\pm^{0.071}_{0.059}$	$23.70\pm^{0.076}_{0.072}$	$23.48\pm^{0.074}_{0.070}$	$23.28\pm^{0.104}_{0.094}$	$22.53\pm^{0.068}_{0.052}$	$24.18\pm^{0.061}_{0.050}$	$23.76\pm^{0.087}_{0.082}$	$23.56\pm^{0.084}_{0.078}$	$23.31\pm^{0.086}_{0.079}$	$22.55\pm^{0.090}_{0.061}$
HIPEQ1223-03b	$22.23\pm^{0.031}_{0.031}$	$20.62\pm^{0.029}_{0.029}$	$19.74\pm^{0.031}_{0.031}$	$19.33\pm^{0.031}_{0.031}$	$18.93\pm^{0.035}_{0.034}$	$22.96\pm^{0.067}_{0.064}$	$21.22\pm^{0.043}_{0.043}$	$20.30\pm^{0.048}_{0.047}$	$19.89\pm^{0.048}_{0.047}$	$19.54\pm^{0.050}_{0.049}$
HIPEQ1224+00	$24.18\pm^{0.175}_{0.105}$	$23.83\pm^{0.088}_{0.083}$	$23.56\pm^{0.157}_{0.139}$	$23.38\pm^{0.085}_{0.079}$	$22.50\pm^{0.208}_{0.114}$	$24.18\pm^{0.197}_{0.112}$	$23.86\pm^{0.092}_{0.086}$	$23.60\pm^{0.091}_{0.085}$	$23.41\pm^{0.087}_{0.081}$	$22.51\pm^{0.219}_{0.114}$
HIPEQ1224+03b	$23.36\pm^{0.105}_{0.097}$	$22.53\pm^{0.039}_{0.039}$	$22.17\pm^{0.041}_{0.040}$	$22.08\pm^{0.041}_{0.040}$	$21.83\pm^{0.095}_{0.087}$	$23.32\pm^{0.154}_{0.137}$	$22.50\pm^{0.044}_{0.043}$	$22.14\pm^{0.045}_{0.044}$	$22.06\pm^{0.044}_{0.044}$	$21.81\pm^{0.105}_{0.095}$
HIPEQ1225+00	$22.02\pm^{0.045}_{0.044}$	$21.08\pm^{0.040}_{0.039}$	$20.41\pm^{0.042}_{0.041}$	$20.21\pm^{0.041}_{0.040}$	$20.02\pm^{0.041}_{0.041}$	$22.15\pm^{0.050}_{0.049}$	$21.18\pm^{0.046}_{0.045}$	$20.50\pm^{0.049}_{0.048}$	$20.31\pm^{0.047}_{0.046}$	$20.12\pm^{0.047}_{0.046}$
HIPEQ1226+02	$21.43\pm^{0.040}_{0.039}$	$20.36\pm^{0.038}_{0.038}$	$19.89\pm^{0.039}_{0.038}$	$19.67\pm^{0.039}_{0.039}$	$19.44\pm^{0.042}_{0.041}$	$21.72\pm^{0.051}_{0.050}$	$20.60\pm^{0.052}_{0.051}$	$20.11\pm^{0.053}_{0.052}$	$19.84\pm^{0.054}_{0.053}$	$19.64\pm^{0.056}_{0.055}$
HIPEQ1227+01	$24.06\pm^{0.331}_{0.178}$	$23.85\pm^{0.150}_{0.134}$	$23.83\pm^{0.125}_{0.110}$	$23.78\pm^{0.115}_{0.094}$	$22.64\pm^{0.156}_{0.072}$	$24.13\pm^{0.408}_{0.177}$	$23.96\pm^{0.119}_{0.108}$	$23.88\pm^{0.104}_{0.093}$	$23.74\pm^{0.123}_{0.100}$	$22.60\pm^{0.352}_{0.107}$
HIPEQ1228+02	$24.02\pm^{0.069}_{0.060}$	$23.36\pm^{0.025}_{0.024}$	$22.99\pm^{0.047}_{0.046}$	$22.77\pm^{0.048}_{0.047}$	$22.30\pm^{0.109}_{0.087}$	$24.01\pm^{0.061}_{0.055}$	$23.49\pm^{0.034}_{0.034}$	$23.09\pm^{0.037}_{0.037}$	$22.89\pm^{0.038}_{0.038}$	$22.34\pm^{0.060}_{0.052}$
HIPEQ1228+03	$21.26\pm^{0.041}_{0.041}$	$19.50\pm^{0.042}_{0.042}$	$18.72\pm^{0.044}_{0.043}$	$18.35\pm^{0.044}_{0.043}$	$18.02\pm^{0.047}_{0.046}$	$21.30\pm^{0.045}_{0.044}$	$19.52\pm^{0.047}_{0.046}$	$18.73\pm^{0.049}_{0.048}$	$18.40\pm^{0.048}_{0.047}$	$18.07\pm^{0.051}_{0.050}$
HIPEQ1229+00	$23.60\pm^{0.282}_{0.219}$	$22.88\pm^{0.063}_{0.062}$	$22.60\pm^{0.060}_{0.059}$	$22.50\pm^{0.066}_{0.065}$	$22.05\pm^{0.205}_{0.161}$	$24.01\pm^{0.317}_{0.184}$	$23.44\pm^{0.100}_{0.095}$	$23.19\pm^{0.093}_{0.088}$	$23.02\pm^{0.098}_{0.092}$	$22.36\pm^{0.237}_{0.145}$
HIPEQ1230+02	$23.80\pm^{0.103}_{0.091}$	$22.93\pm^{0.052}_{0.050}$	$22.65\pm^{0.056}_{0.055}$	$22.53\pm^{0.058}_{0.057}$	$22.10\pm^{0.170}_{0.136}$	$23.80\pm^{0.138}_{0.116}$	$23.06\pm^{0.065}_{0.063}$	$22.75\pm^{0.071}_{0.069}$	$22.57\pm^{0.076}_{0.074}$	$22.18\pm^{0.157}_{0.124}$
HIPEQ1230+03	$21.88\pm^{0.160}_{0.151}$	$21.28\pm^{0.135}_{0.128}$	$21.10\pm^{0.136}_{0.129}$	$20.98\pm^{0.139}_{0.131}$	$20.92\pm^{0.151}_{0.142}$	$21.88\pm^{0.194}_{0.181}$	$21.28\pm^{0.165}_{0.154}$	$21.09\pm^{0.166}_{0.155}$	$20.98\pm^{0.168}_{0.157}$	$20.92\pm^{0.180}_{0.167}$
HIPEQ1232+00a	$23.82\pm^{0.029}_{0.028}$	$23.06\pm^{0.015}_{0.015}$	$22.63\pm^{0.016}_{0.016}$	$22.37\pm^{0.016}_{0.016}$	$22.15\pm^{0.036}_{0.034}$	$23.82\pm^{0.038}_{0.036}$	$23.08\pm^{0.020}_{0.020}$	$22.65\pm^{0.020}_{0.020}$	$22.40\pm^{0.021}_{0.021}$	$22.16\pm^{0.026}_{0.025}$
HIPEQ1232+00b	$23.20\pm^{0.010}_{0.009}$	$21.92\pm^{0.005}_{0.005}$	$21.18\pm^{0.006}_{0.005}$	$20.73\pm^{0.006}_{0.005}$	$20.41\pm^{0.006}_{0.006}$	$23.69\pm^{0.014}_{0.013}$	$22.76\pm^{0.018}_{0.018}$	$22.04\pm^{0.010}_{0.010}$	$21.56\pm^{0.010}_{0.010}$	$21.22\pm^{0.010}_{0.010}$
HIPEQ1233-02	$24.18\pm^{0.049}_{0.040}$	$24.04\pm^{0.038}_{0.036}$	$23.72\pm^{0.039}_{0.038}$	$23.48\pm^{0.066}_{0.060}$	$22.62\pm^{0.041}_{0.031}$	$24.19\pm^{0.058}_{0.046}$	$24.08\pm^{0.026}_{0.025}$	$23.73\pm^{0.048}_{0.046}$	$23.50\pm^{0.045}_{0.043}$	$22.63\pm^{0.053}_{0.037}$
HIPEQ1236+03	$23.72\pm^{0.164}_{0.136}$	$23.04\pm^{0.049}_{0.048}$	$22.75\pm^{0.051}_{0.050}$	$22.61\pm^{0.055}_{0.054}$	$22.19\pm^{0.174}_{0.132}$	$24.00\pm^{0.178}_{0.127}$	$23.38\pm^{0.071}_{0.068}$	$23.08\pm^{0.073}_{0.071}$	$22.90\pm^{0.136}_{0.126}$	$22.35\pm^{0.226}_{0.140}$
HIPEQ1239-00	$22.11\pm^{0.019}_{0.019}$	$21.20\pm^{0.017}_{0.017}$	$20.83\pm^{0.018}_{0.018}$	$20.64\pm^{0.018}_{0.018}$	$20.49\pm^{0.019}_{0.019}$	$22.54\pm^{0.051}_{0.049}$	$21.59\pm^{0.027}_{0.026}$	$21.17\pm^{0.028}_{0.027}$	$20.99\pm^{0.028}_{0.028}$	$20.84\pm^{0.029}_{0.028}$
HIPEQ1241+01	$21.69\pm^{0.118}_{0.113}$	$20.68\pm^{0.109}_{0.104}$	$20.34\pm^{0.103}_{0.099}$	$20.18\pm^{0.099}_{0.095}$	$20.08\pm^{0.101}_{0.097}$	$21.80\pm^{0.144}_{0.136}$	$20.78\pm^{0.134}_{0.127}$	$20.34\pm^{0.134}_{0.126}$	$20.20\pm^{0.127}_{0.120}$	$20.13\pm^{0.125}_{0.119}$
HIPEQ1241-02	$22.24\pm^{0.075}_{0.073}$	$21.37\pm^{0.059}_{0.058}$	$20.96\pm^{0.058}_{0.056}$	$20.84\pm^{0.055}_{0.053}$	$20.64\pm^{0.060}_{0.059}$	$22.55\pm^{0.096}_{0.092}$	$21.60\pm^{0.085}_{0.082}$	$21.22\pm^{0.082}_{0.079}$	$21.07\pm^{0.077}_{0.075}$	$20.92\pm^{0.079}_{0.076}$
HIPEQ1242+03b	$22.31\pm^{0.036}_{0.036}$	$21.27\pm^{0.033}_{0.033}$	$20.75\pm^{0.033}_{0.032}$	$20.56\pm^{0.031}_{0.031}$	$20.43\pm^{0.032}_{0.031}$	$22.38\pm^{0.043}_{0.042}$	$21.32\pm^{0.041}_{0.040}$	$20.82\pm^{0.040}_{0.039}$	$20.60\pm^{0.039}_{0.038}$	$20.49\pm^{0.038}_{0.038}$
HIPEQ1242-00	$21.98\pm^{0.023}_{0.023}$	$20.90\pm^{0.022}_{0.022}$	$20.42\pm^{0.022}_{0.022}$	$20.16\pm^{0.022}_{0.022}$	$19.98\pm^{0.023}_{0.023}$	$22.14\pm^{0.034}_{0.033}$	$21.09\pm^{0.032}_{0.032}$	$20.63\pm^{0.032}_{0.032}$	$20.37\pm^{0.033}_{0.032}$	$20.23\pm^{0.032}_{0.032}$

Table 3.8—Continued

	$\Sigma_{Elliptical}$					$\Sigma_{Circular}$				
HIPASS Name	u	g	r	i	z	u	g	r	i	z
HIPEQ1242-01a	$22.98\pm^{0.043}_{0.042}$	$21.83\pm^{0.048}_{0.047}$	$21.52\pm^{0.048}_{0.047}$	$21.35\pm^{0.048}_{0.047}$	$21.30\pm^{0.046}_{0.045}$	$22.98\pm^{0.048}_{0.047}$	$21.86\pm^{0.054}_{0.053}$	$21.55\pm^{0.055}_{0.054}$	$21.38\pm^{0.054}_{0.053}$	$21.32\pm^{0.051}_{0.050}$
HIPEQ1242-01b	$23.17\pm^{0.052}_{0.050}$	$21.90\pm^{0.028}_{0.027}$	$21.26\pm^{0.029}_{0.029}$	$20.90\pm^{0.031}_{0.031}$	$20.60\pm^{0.037}_{0.037}$	$23.53\pm^{0.064}_{0.060}$	$22.30\pm^{0.043}_{0.042}$	$21.62\pm^{0.047}_{0.046}$	$21.26\pm^{0.050}_{0.049}$	$20.99\pm^{0.055}_{0.054}$
HIPEQ1243-00	$23.38\pm^{0.033}_{0.032}$	$22.16\pm^{0.022}_{0.022}$	$21.57\pm^{0.024}_{0.024}$	$21.22\pm^{0.025}_{0.025}$	$21.07\pm^{0.025}_{0.025}$	$23.42\pm^{0.021}_{0.020}$	$22.21\pm^{0.025}_{0.025}$	$21.61\pm^{0.027}_{0.027}$	$21.25\pm^{0.029}_{0.028}$	$21.09\pm^{0.028}_{0.028}$
HIPEQ1244+00	$23.91\pm^{0.038}_{0.035}$	$23.25\pm^{0.017}_{0.017}$	$22.79\pm^{0.019}_{0.019}$	$22.24\pm^{0.032}_{0.032}$	$22.11\pm^{0.051}_{0.047}$	$23.92\pm^{0.041}_{0.038}$	$23.31\pm^{0.023}_{0.023}$	$22.89\pm^{0.026}_{0.025}$	$22.43\pm^{0.038}_{0.037}$	$22.17\pm^{0.035}_{0.033}$
HIPEQ1244-02	$23.91\pm^{0.115}_{0.093}$	$23.24\pm^{0.040}_{0.039}$	$22.99\pm^{0.042}_{0.041}$	$22.74\pm^{0.082}_{0.079}$	$22.24\pm^{0.214}_{0.145}$	$23.98\pm^{0.104}_{0.083}$	$23.31\pm^{0.048}_{0.047}$	$23.06\pm^{0.050}_{0.048}$	$22.85\pm^{0.095}_{0.090}$	$22.23\pm^{0.159}_{0.120}$
HIPEQ1245-00	$22.13\pm^{0.015}_{0.015}$	$20.50\pm^{0.016}_{0.016}$	$19.52\pm^{0.017}_{0.017}$	$18.97\pm^{0.019}_{0.018}$	$18.43\pm^{0.021}_{0.021}$	$22.64\pm^{0.019}_{0.019}$	$20.98\pm^{0.022}_{0.022}$	$19.96\pm^{0.025}_{0.025}$	$19.39\pm^{0.027}_{0.027}$	$18.83\pm^{0.031}_{0.030}$
HIPEQ1249+03	$21.62\pm^{0.047}_{0.046}$	$20.53\pm^{0.047}_{0.046}$	$20.01\pm^{0.051}_{0.050}$	$19.80\pm^{0.051}_{0.050}$	$19.57\pm^{0.055}_{0.054}$	$21.70\pm^{0.052}_{0.051}$	$20.59\pm^{0.053}_{0.052}$	$20.05\pm^{0.057}_{0.056}$	$19.79\pm^{0.059}_{0.057}$	$19.60\pm^{0.062}_{0.061}$
HIPEQ1249+04	$23.82\pm^{0.107}_{0.090}$	$23.07\pm^{0.046}_{0.045}$	$22.84\pm^{0.047}_{0.046}$	$22.69\pm^{0.050}_{0.049}$	$22.40\pm^{0.113}_{0.083}$	$23.84\pm^{0.072}_{0.065}$	$23.10\pm^{0.058}_{0.056}$	$22.87\pm^{0.058}_{0.057}$	$22.76\pm^{0.058}_{0.057}$	$22.43\pm^{0.133}_{0.090}$
HIPEQ1250+05	$22.04\pm^{0.026}_{0.026}$	$21.11\pm^{0.027}_{0.026}$	$20.73\pm^{0.028}_{0.027}$	$20.55\pm^{0.028}_{0.028}$	$20.47\pm^{0.028}_{0.028}$	$22.01\pm^{0.030}_{0.030}$	$21.11\pm^{0.031}_{0.030}$	$20.74\pm^{0.032}_{0.031}$	$20.55\pm^{0.033}_{0.032}$	$20.49\pm^{0.032}_{0.032}$
HIPEQ1253+01	$22.76\pm^{0.036}_{0.035}$	$21.19\pm^{0.020}_{0.019}$	$20.41\pm^{0.021}_{0.020}$	$20.01\pm^{0.021}_{0.021}$	$19.74\pm^{0.022}_{0.022}$	$23.25\pm^{0.047}_{0.046}$	$21.73\pm^{0.030}_{0.029}$	$20.94\pm^{0.031}_{0.031}$	$20.53\pm^{0.032}_{0.031}$	$20.30\pm^{0.033}_{0.032}$
HIPEQ1253+02	$23.17\pm^{0.039}_{0.038}$	$21.13\pm^{0.026}_{0.026}$	$20.29\pm^{0.027}_{0.027}$	$19.84\pm^{0.028}_{0.028}$	$19.58\pm^{0.029}_{0.029}$	$23.19\pm^{0.040}_{0.039}$	$21.13\pm^{0.027}_{0.027}$	$20.31\pm^{0.029}_{0.028}$	$19.86\pm^{0.029}_{0.029}$	$19.59\pm^{0.031}_{0.031}$
HIPEQ1253+04	$19.82\pm^{0.110}_{0.105}$	$19.28\pm^{0.093}_{0.089}$	$19.07\pm^{0.089}_{0.086}$	$19.12\pm^{0.083}_{0.080}$	$18.98\pm^{0.088}_{0.084}$	$20.02\pm^{0.135}_{0.128}$	$19.31\pm^{0.125}_{0.118}$	$19.24\pm^{0.112}_{0.107}$	$19.22\pm^{0.107}_{0.102}$	$19.05\pm^{0.114}_{0.108}$
HIPEQ1255+00	$23.50\pm^{0.018}_{0.018}$	$22.57\pm^{0.020}_{0.020}$	$22.15\pm^{0.020}_{0.020}$	$21.91\pm^{0.020}_{0.020}$	$21.65\pm^{0.020}_{0.020}$	$23.49\pm^{0.019}_{0.019}$	$22.57\pm^{0.021}_{0.021}$	$22.17\pm^{0.021}_{0.021}$	$21.91\pm^{0.021}_{0.021}$	$21.65\pm^{0.021}_{0.021}$
HIPEQ1255+02	$21.32\pm^{0.074}_{0.072}$	$19.77\pm^{0.072}_{0.070}$	$18.87\pm^{0.080}_{0.077}$	$18.42\pm^{0.083}_{0.080}$	$18.09\pm^{0.087}_{0.084}$	$21.74\pm^{0.096}_{0.093}$	$20.09\pm^{0.102}_{0.098}$	$19.20\pm^{0.112}_{0.107}$	$18.83\pm^{0.112}_{0.107}$	$18.47\pm^{0.120}_{0.114}$
HIPEQ1255-00	$23.75\pm^{0.107}_{0.093}$	$23.20\pm^{0.036}_{0.035}$	$22.97\pm^{0.035}_{0.034}$	$22.83\pm^{0.061}_{0.058}$	$22.30\pm^{0.099}_{0.080}$	$24.16\pm^{0.117}_{0.082}$	$23.83\pm^{0.087}_{0.081}$	$23.51\pm^{0.048}_{0.047}$	$23.27\pm^{0.047}_{0.046}$	$22.55\pm^{0.100}_{0.065}$
HIPEQ1256+03	$24.13\pm^{0.109}_{0.081}$	$23.69\pm^{0.094}_{0.088}$	$23.54\pm^{0.096}_{0.089}$	$23.39\pm^{0.128}_{0.112}$	$22.61\pm^{0.339}_{0.093}$	$24.16\pm^{0.134}_{0.090}$	$23.77\pm^{0.103}_{0.095}$	$23.57\pm^{0.062}_{0.059}$	$23.41\pm^{0.148}_{0.125}$	$22.63\pm^{0.259}_{0.081}$
HIPEQ1257+02	$23.76\pm^{0.094}_{0.084}$	$23.08\pm^{0.050}_{0.049}$	$22.80\pm^{0.051}_{0.050}$	$22.67\pm^{0.096}_{0.091}$	$22.20\pm^{0.153}_{0.119}$	$23.76\pm^{0.109}_{0.094}$	$23.12\pm^{0.058}_{0.056}$	$22.84\pm^{0.059}_{0.058}$	$22.65\pm^{0.064}_{0.062}$	$22.21\pm^{0.148}_{0.116}$
HIPEQ1257-01	$22.43\pm^{0.037}_{0.037}$	$21.20\pm^{0.036}_{0.035}$	$20.52\pm^{0.039}_{0.038}$	$20.21\pm^{0.040}_{0.039}$	$19.90\pm^{0.046}_{0.045}$	$23.05\pm^{0.049}_{0.048}$	$21.78\pm^{0.055}_{0.054}$	$21.05\pm^{0.061}_{0.060}$	$20.70\pm^{0.064}_{0.062}$	$20.45\pm^{0.069}_{0.067}$
HIPEQ1258+02	$23.89\pm^{0.109}_{0.090}$	$23.02\pm^{0.027}_{0.027}$	$22.65\pm^{0.028}_{0.028}$	$22.45\pm^{0.029}_{0.029}$	$22.19\pm^{0.083}_{0.072}$	$23.84\pm^{0.115}_{0.096}$	$23.02\pm^{0.039}_{0.038}$	$22.63\pm^{0.041}_{0.040}$	$22.43\pm^{0.042}_{0.041}$	$22.17\pm^{0.089}_{0.076}$
HIPEQ1300+02a	$22.58\pm^{0.183}_{0.170}$	$22.10\pm^{0.063}_{0.062}$	$21.92\pm^{0.058}_{0.056}$	$22.01\pm^{0.052}_{0.051}$	$21.76\pm^{0.125}_{0.111}$	$22.59\pm^{0.202}_{0.186}$	$22.10\pm^{0.070}_{0.068}$	$21.94\pm^{0.063}_{0.062}$	$21.96\pm^{0.058}_{0.057}$	$21.73\pm^{0.100}_{0.091}$
HIPEQ1300+02b	$21.90\pm^{0.025}_{0.025}$	$20.93\pm^{0.024}_{0.023}$	$20.52\pm^{0.024}_{0.024}$	$20.31\pm^{0.023}_{0.023}$	$20.20\pm^{0.023}_{0.023}$	$21.93\pm^{0.029}_{0.029}$	$20.94\pm^{0.029}_{0.028}$	$20.53\pm^{0.029}_{0.028}$	$20.33\pm^{0.028}_{0.027}$	$20.20\pm^{0.027}_{0.027}$
HIPEQ1303+03	$23.83\pm^{0.051}_{0.047}$	$23.09\pm^{0.040}_{0.039}$	$22.72\pm^{0.042}_{0.041}$	$22.50\pm^{0.043}_{0.042}$	$22.14\pm^{0.055}_{0.050}$	$23.83\pm^{0.071}_{0.064}$	$23.10\pm^{0.040}_{0.040}$	$22.72\pm^{0.042}_{0.042}$	$22.51\pm^{0.044}_{0.043}$	$22.14\pm^{0.055}_{0.050}$
HIPEQ1304-02	$23.50\pm^{0.208}_{0.172}$	$22.33\pm^{0.098}_{0.094}$	$21.96\pm^{0.096}_{0.092}$	$21.74\pm^{0.102}_{0.099}$	$21.53\pm^{0.124}_{0.117}$	$23.55\pm^{0.099}_{0.092}$	$22.49\pm^{0.117}_{0.111}$	$22.03\pm^{0.119}_{0.113}$	$21.77\pm^{0.128}_{0.121}$	$21.53\pm^{0.153}_{0.141}$
HIPEQ1304-03	$23.77\pm^{0.023}_{0.023}$	$23.22\pm^{0.016}_{0.016}$	$22.90\pm^{0.017}_{0.017}$	$22.72\pm^{0.032}_{0.032}$	$22.27\pm^{0.028}_{0.026}$	$23.79\pm^{0.025}_{0.024}$	$23.25\pm^{0.018}_{0.018}$	$22.93\pm^{0.019}_{0.019}$	$22.75\pm^{0.020}_{0.019}$	$22.28\pm^{0.031}_{0.029}$
HIPEQ1307-00	$22.33\pm^{0.057}_{0.056}$	$21.28\pm^{0.058}_{0.056}$	$20.82\pm^{0.061}_{0.059}$	$20.59\pm^{0.063}_{0.061}$	$20.39\pm^{0.067}_{0.065}$	$22.39\pm^{0.062}_{0.061}$	$21.34\pm^{0.064}_{0.063}$	$20.87\pm^{0.068}_{0.066}$	$20.63\pm^{0.071}_{0.069}$	$20.41\pm^{0.075}_{0.073}$
HIPEQ1308-02	$23.16\pm^{0.048}_{0.047}$	$21.97\pm^{0.053}_{0.052}$	$21.43\pm^{0.056}_{0.054}$	$21.12\pm^{0.059}_{0.058}$	$21.03\pm^{0.058}_{0.057}$	$23.15\pm^{0.052}_{0.050}$	$21.94\pm^{0.058}_{0.057}$	$21.39\pm^{0.062}_{0.060}$	$21.13\pm^{0.064}_{0.062}$	$21.00\pm^{0.063}_{0.062}$
HIPEQ1311+03a	$22.19\pm^{0.195}_{0.182}$	$21.33\pm^{0.086}_{0.083}$	$20.85\pm^{0.093}_{0.090}$	$20.71\pm^{0.095}_{0.092}$	$20.55\pm^{0.107}_{0.104}$	$22.60\pm^{0.155}_{0.146}$	$21.57\pm^{0.144}_{0.136}$	$21.10\pm^{0.155}_{0.145}$	$20.95\pm^{0.157}_{0.147}$	$20.79\pm^{0.169}_{0.157}$
HIPEQ1312+03	$22.26\pm^{0.124}_{0.119}$	$20.85\pm^{0.108}_{0.103}$	$20.29\pm^{0.108}_{0.103}$	$19.88\pm^{0.114}_{0.109}$	$19.59\pm^{0.126}_{0.120}$	$22.40\pm^{0.143}_{0.135}$	$20.99\pm^{0.127}_{0.120}$	$20.43\pm^{0.126}_{0.120}$	$20.13\pm^{0.127}_{0.121}$	$19.69\pm^{0.149}_{0.140}$
HIPEQ1312+05	$24.13\pm^{0.179}_{0.106}$	$23.68\pm^{0.057}_{0.055}$	$23.37\pm^{0.112}_{0.104}$	$23.17\pm^{0.111}_{0.102}$	$22.56\pm^{0.201}_{0.093}$	$24.17\pm^{0.190}_{0.103}$	$23.75\pm^{0.073}_{0.070}$	$23.40\pm^{0.083}_{0.079}$	$23.20\pm^{0.084}_{0.080}$	$22.58\pm^{0.233}_{0.092}$
HIPEQ1313+06	$22.94\pm^{0.062}_{0.060}$	$21.53\pm^{0.061}_{0.060}$	$20.80\pm^{0.066}_{0.064}$	$20.45\pm^{0.069}_{0.067}$	$20.16\pm^{0.073}_{0.071}$	$22.93\pm^{0.066}_{0.064}$	$21.56\pm^{0.065}_{0.063}$	$20.82\pm^{0.070}_{0.068}$	$20.46\pm^{0.073}_{0.071}$	$20.18\pm^{0.078}_{0.075}$
HIPEQ1317-00	$23.11\pm^{0.058}_{0.057}$	$22.47\pm^{0.054}_{0.053}$	$22.27\pm^{0.057}_{0.056}$	$22.20\pm^{0.062}_{0.061}$	$22.01\pm^{0.123}_{0.105}$	$23.55\pm^{0.072}_{0.067}$	$22.77\pm^{0.088}_{0.084}$	$22.51\pm^{0.096}_{0.092}$	$22.37\pm^{0.108}_{0.103}$	$22.13\pm^{0.198}_{0.148}$

Table 3.8—Continued

	$\Sigma_{Elliptical}$					$\Sigma_{Circular}$				
HIPASS Name	u	g	r	i	z	u	g	r	i	z
HIPEQ1318-01	$23.57\pm^{0.052}_{0.049}$	$22.22\pm^{0.042}_{0.041}$	$21.63\pm^{0.044}_{0.043}$	$21.29\pm^{0.046}_{0.045}$	$21.09\pm^{0.045}_{0.044}$	$23.57\pm^{0.033}_{0.032}$	$22.24\pm^{0.046}_{0.045}$	$21.64\pm^{0.049}_{0.048}$	$21.29\pm^{0.050}_{0.049}$	$21.11\pm^{0.049}_{0.048}$
HIPEQ1320+05	$22.99\pm^{0.165}_{0.150}$	$22.37\pm^{0.043}_{0.043}$	$22.08\pm^{0.041}_{0.040}$	$22.05\pm^{0.041}_{0.040}$	$21.39\pm^{0.107}_{0.100}$	$23.22\pm^{0.126}_{0.116}$	$22.63\pm^{0.065}_{0.063}$	$22.30\pm^{0.062}_{0.061}$	$22.27\pm^{0.060}_{0.059}$	$21.58\pm^{0.107}_{0.099}$
HIPEQ1327+02	$23.88\pm^{0.227}_{0.161}$	$23.20\pm^{0.065}_{0.063}$	$22.97\pm^{0.070}_{0.068}$	$22.80\pm^{0.136}_{0.127}$	$22.32\pm^{0.428}_{0.203}$	$23.90\pm^{0.236}_{0.164}$	$23.31\pm^{0.092}_{0.088}$	$23.05\pm^{0.099}_{0.094}$	$22.92\pm^{0.107}_{0.101}$	$22.33\pm^{0.246}_{0.154}$
HIPEQ1329-00	$23.92\pm^{0.109}_{0.091}$	$23.06\pm^{0.054}_{0.053}$	$22.65\pm^{0.057}_{0.056}$	$22.43\pm^{0.060}_{0.059}$	$22.13\pm^{0.134}_{0.109}$	$24.03\pm^{0.131}_{0.099}$	$23.30\pm^{0.073}_{0.070}$	$22.87\pm^{0.077}_{0.075}$	$22.64\pm^{0.081}_{0.078}$	$22.19\pm^{0.190}_{0.138}$
HIPEQ1332+01	$22.13\pm^{0.081}_{0.079}$	$20.83\pm^{0.073}_{0.070}$	$20.15\pm^{0.075}_{0.073}$	$19.81\pm^{0.075}_{0.073}$	$19.52\pm^{0.081}_{0.078}$	$22.23\pm^{0.085}_{0.083}$	$20.92\pm^{0.078}_{0.075}$	$20.24\pm^{0.080}_{0.078}$	$19.90\pm^{0.081}_{0.078}$	$19.52\pm^{0.090}_{0.087}$
HIPEQ1335+01	$23.38\pm^{0.085}_{0.079}$	$21.68\pm^{0.044}_{0.043}$	$20.84\pm^{0.050}_{0.049}$	$20.40\pm^{0.054}_{0.052}$	$20.11\pm^{0.061}_{0.059}$	$23.42\pm^{0.067}_{0.064}$	$21.82\pm^{0.049}_{0.048}$	$20.95\pm^{0.057}_{0.055}$	$20.53\pm^{0.060}_{0.059}$	$20.17\pm^{0.070}_{0.068}$
HIPEQ1341+05	$23.23\pm^{0.163}_{0.144}$	$21.97\pm^{0.068}_{0.066}$	$21.18\pm^{0.082}_{0.080}$	$20.82\pm^{0.089}_{0.086}$	$20.35\pm^{0.117}_{0.113}$	$23.25\pm^{0.125}_{0.114}$	$22.02\pm^{0.076}_{0.074}$	$21.26\pm^{0.092}_{0.088}$	$20.78\pm^{0.105}_{0.100}$	$20.35\pm^{0.133}_{0.126}$
HIPEQ1348+03	$23.40\pm^{0.016}_{0.015}$	$22.21\pm^{0.017}_{0.017}$	$21.66\pm^{0.017}_{0.017}$	$21.42\pm^{0.018}_{0.017}$	$21.02\pm^{0.018}_{0.018}$	$23.42\pm^{0.018}_{0.018}$	$22.25\pm^{0.020}_{0.020}$	$21.70\pm^{0.021}_{0.021}$	$21.46\pm^{0.021}_{0.021}$	$21.06\pm^{0.021}_{0.021}$
HIPEQ1352+02a	$23.75\pm^{0.035}_{0.034}$	$22.24\pm^{0.028}_{0.028}$	$21.32\pm^{0.032}_{0.031}$	$20.81\pm^{0.034}_{0.034}$	$20.58\pm^{0.068}_{0.066}$	$23.73\pm^{0.041}_{0.039}$	$22.24\pm^{0.033}_{0.033}$	$21.32\pm^{0.037}_{0.037}$	$20.86\pm^{0.040}_{0.039}$	$20.60\pm^{0.042}_{0.041}$
HIPEQ1352-01	$23.40\pm^{0.025}_{0.025}$	$22.39\pm^{0.016}_{0.016}$	$21.84\pm^{0.017}_{0.017}$	$21.57\pm^{0.017}_{0.017}$	$21.37\pm^{0.017}_{0.017}$	$23.40\pm^{0.017}_{0.016}$	$22.40\pm^{0.019}_{0.019}$	$21.85\pm^{0.019}_{0.019}$	$21.57\pm^{0.020}_{0.019}$	$21.36\pm^{0.020}_{0.019}$
HIPEQ1400+02	$22.67\pm^{0.095}_{0.091}$	$21.55\pm^{0.045}_{0.044}$	$21.05\pm^{0.046}_{0.045}$	$20.79\pm^{0.048}_{0.047}$	$20.57\pm^{0.099}_{0.095}$	$23.32\pm^{0.120}_{0.110}$	$22.22\pm^{0.069}_{0.067}$	$21.67\pm^{0.073}_{0.071}$	$21.31\pm^{0.079}_{0.077}$	$21.10\pm^{0.084}_{0.081}$
HIPEQ1411-01	$23.02\pm^{0.025}_{0.025}$	$21.96\pm^{0.014}_{0.014}$	$21.49\pm^{0.015}_{0.015}$	$21.35\pm^{0.015}_{0.015}$	$21.10\pm^{0.017}_{0.017}$	$23.51\pm^{0.032}_{0.031}$	$22.70\pm^{0.022}_{0.022}$	$22.17\pm^{0.024}_{0.024}$	$22.08\pm^{0.024}_{0.024}$	$21.67\pm^{0.041}_{0.040}$
HIPEQ1415+04	$22.12\pm^{0.115}_{0.110}$	$21.34\pm^{0.121}_{0.115}$	$21.12\pm^{0.115}_{0.110}$	$21.08\pm^{0.106}_{0.101}$	$20.83\pm^{0.100}_{0.096}$	$22.07\pm^{0.120}_{0.114}$	$21.38\pm^{0.121}_{0.115}$	$21.17\pm^{0.115}_{0.110}$	$21.03\pm^{0.111}_{0.106}$	$20.79\pm^{0.105}_{0.100}$
HIPEQ1416+03	$24.27\pm^{0.215}_{0.091}$	$24.40\pm^{0.063}_{0.055}$	$24.15\pm^{0.052}_{0.047}$	$23.99\pm^{0.045}_{0.038}$	$22.70\pm^{0.144}_{0.044}$	$24.04\pm^{0.207}_{0.132}$	$23.85\pm^{0.057}_{0.054}$	$23.55\pm^{0.058}_{0.055}$	$23.50\pm^{0.049}_{0.046}$	$22.54\pm^{0.147}_{0.084}$
HIPEQ1422-00	$23.10\pm^{0.016}_{0.016}$	$22.13\pm^{0.016}_{0.016}$	$21.69\pm^{0.017}_{0.017}$	$21.48\pm^{0.017}_{0.017}$	$21.28\pm^{0.017}_{0.017}$	$23.12\pm^{0.019}_{0.019}$	$22.13\pm^{0.020}_{0.020}$	$21.70\pm^{0.020}_{0.020}$	$21.48\pm^{0.021}_{0.021}$	$21.29\pm^{0.021}_{0.020}$
HIPEQ1429-00	$23.01\pm^{0.040}_{0.039}$	$22.14\pm^{0.040}_{0.039}$	$21.77\pm^{0.042}_{0.041}$	$21.62\pm^{0.043}_{0.042}$	$21.43\pm^{0.080}_{0.076}$	$23.17\pm^{0.046}_{0.045}$	$22.26\pm^{0.051}_{0.049}$	$21.85\pm^{0.055}_{0.053}$	$21.69\pm^{0.056}_{0.054}$	$21.53\pm^{0.054}_{0.052}$
HIPEQ1432+00	$22.27\pm^{0.048}_{0.047}$	$21.22\pm^{0.038}_{0.038}$	$20.74\pm^{0.037}_{0.037}$	$20.46\pm^{0.038}_{0.037}$	$20.19\pm^{0.044}_{0.044}$	$23.03\pm^{0.062}_{0.060}$	$21.90\pm^{0.060}_{0.058}$	$21.33\pm^{0.062}_{0.060}$	$21.04\pm^{0.062}_{0.061}$	$20.81\pm^{0.067}_{0.065}$
HIPEQ1433+01	$24.18\pm^{0.267}_{0.109}$	$24.19\pm^{0.087}_{0.077}$	$23.95\pm^{0.097}_{0.085}$	$23.63\pm^{0.091}_{0.080}$	$22.63\pm^{4.225}_{0.109}$	$24.29\pm^{0.859}_{0.080}$	$24.43\pm^{0.092}_{0.076}$	$24.13\pm^{0.147}_{0.111}$	$23.77\pm^{0.148}_{0.111}$	$22.59\pm^{1.418}_{0.130}$
HIPEQ1433+02	$22.30\pm^{0.082}_{0.080}$	$21.63\pm^{0.067}_{0.066}$	$21.33\pm^{0.070}_{0.068}$	$21.17\pm^{0.077}_{0.075}$	$21.04\pm^{0.154}_{0.143}$	$22.42\pm^{0.095}_{0.091}$	$21.71\pm^{0.082}_{0.079}$	$21.48\pm^{0.082}_{0.080}$	$21.27\pm^{0.091}_{0.088}$	$21.13\pm^{0.098}_{0.093}$
HIPEQ1437+02	$22.84\pm^{0.023}_{0.023}$	$21.23\pm^{0.017}_{0.017}$	$20.73\pm^{0.015}_{0.015}$	$20.47\pm^{0.015}_{0.015}$	$20.12\pm^{0.017}_{0.017}$	$23.15\pm^{0.019}_{0.019}$	$21.68\pm^{0.028}_{0.027}$	$21.14\pm^{0.025}_{0.025}$	$20.78\pm^{0.026}_{0.026}$	$20.53\pm^{0.026}_{0.026}$
HIPEQ1437-00	$21.15\pm^{0.050}_{0.049}$	$20.44\pm^{0.039}_{0.038}$	$20.15\pm^{0.037}_{0.036}$	$20.02\pm^{0.035}_{0.034}$	$19.88\pm^{0.037}_{0.037}$	$21.24\pm^{0.067}_{0.065}$	$20.50\pm^{0.054}_{0.053}$	$20.16\pm^{0.052}_{0.051}$	$20.07\pm^{0.048}_{0.047}$	$19.91\pm^{0.051}_{0.050}$
HIPEQ1439-00	$23.56\pm^{0.026}_{0.025}$	$22.61\pm^{0.017}_{0.017}$	$22.16\pm^{0.018}_{0.018}$	$21.92\pm^{0.018}_{0.018}$	$21.64\pm^{0.019}_{0.019}$	$23.60\pm^{0.035}_{0.034}$	$22.65\pm^{0.026}_{0.026}$	$22.19\pm^{0.027}_{0.027}$	$21.96\pm^{0.027}_{0.026}$	$21.67\pm^{0.047}_{0.045}$
HIPEQ1440+02	$22.24\pm^{0.074}_{0.072}$	$21.16\pm^{0.067}_{0.065}$	$20.82\pm^{0.069}_{0.067}$	$20.58\pm^{0.070}_{0.068}$	$20.95\pm^{0.074}_{0.072}$	$22.27\pm^{0.087}_{0.084}$	$21.17\pm^{0.081}_{0.078}$	$20.83\pm^{0.084}_{0.081}$	$20.58\pm^{0.085}_{0.082}$	$20.96\pm^{0.088}_{0.084}$
HIPEQ1444+01a	$22.66\pm^{0.029}_{0.029}$	$20.97\pm^{0.031}_{0.030}$	$20.17\pm^{0.034}_{0.033}$	$19.73\pm^{0.035}_{0.035}$	$19.42\pm^{0.037}_{0.037}$	$22.78\pm^{0.033}_{0.033}$	$21.03\pm^{0.037}_{0.037}$	$20.26\pm^{0.041}_{0.040}$	$19.81\pm^{0.043}_{0.042}$	$19.53\pm^{0.044}_{0.044}$
HIPEQ1500+01	$22.41\pm^{0.049}_{0.048}$	$20.87\pm^{0.025}_{0.025}$	$20.11\pm^{0.026}_{0.026}$	$19.66\pm^{0.027}_{0.027}$	$19.39\pm^{0.029}_{0.028}$	$22.65\pm^{0.030}_{0.030}$	$21.03\pm^{0.031}_{0.031}$	$20.26\pm^{0.032}_{0.032}$	$19.83\pm^{0.033}_{0.033}$	$19.55\pm^{0.035}_{0.034}$
HIPEQ1504+02	$23.10\pm^{0.149}_{0.135}$	$21.87\pm^{0.086}_{0.083}$	$21.46\pm^{0.090}_{0.087}$	$21.31\pm^{0.092}_{0.088}$	$21.11\pm^{0.107}_{0.102}$	$23.15\pm^{0.226}_{0.191}$	$21.92\pm^{0.093}_{0.089}$	$21.41\pm^{0.101}_{0.097}$	$21.26\pm^{0.103}_{0.099}$	$21.14\pm^{0.115}_{0.109}$
HIPEQ1504-00	$23.44\pm^{0.094}_{0.084}$	$22.54\pm^{0.032}_{0.032}$	$22.13\pm^{0.032}_{0.032}$	$21.94\pm^{0.034}_{0.033}$	$21.64\pm^{0.080}_{0.082}$	$23.66\pm^{0.099}_{0.085}$	$22.97\pm^{0.050}_{0.048}$	$22.55\pm^{0.050}_{0.049}$	$22.35\pm^{0.052}_{0.051}$	$21.97\pm^{0.113}_{0.097}$
HIPEQ1507+01	$23.53\pm^{0.025}_{0.024}$	$21.88\pm^{0.018}_{0.018}$	$20.88\pm^{0.021}_{0.021}$	$20.42\pm^{0.022}_{0.021}$	$20.18\pm^{0.022}_{0.022}$	$23.53\pm^{0.025}_{0.024}$	$21.87\pm^{0.018}_{0.018}$	$20.89\pm^{0.021}_{0.021}$	$20.42\pm^{0.022}_{0.022}$	$20.18\pm^{0.023}_{0.023}$
HIPEQ1542+00	$23.25\pm^{0.052}_{0.049}$	$22.22\pm^{0.018}_{0.019}$	$21.57\pm^{0.019}_{0.019}$	$21.18\pm^{0.020}_{0.021}$	$20.90\pm^{0.023}_{0.023}$	$23.72\pm^{0.049}_{0.042}$	$23.08\pm^{0.028}_{0.028}$	$22.42\pm^{0.031}_{0.031}$	$21.95\pm^{0.035}_{0.034}$	$21.59\pm^{0.083}_{0.077}$
HIPEQ1544+02	$23.12\pm^{0.118}_{0.106}$	$21.78\pm^{0.077}_{0.074}$	$21.12\pm^{0.082}_{0.079}$	$21.00\pm^{0.086}_{0.083}$	$20.34\pm^{0.096}_{0.092}$	$23.14\pm^{0.124}_{0.110}$	$21.78\pm^{0.082}_{0.079}$	$21.11\pm^{0.088}_{0.085}$	$20.98\pm^{0.093}_{0.089}$	$20.40\pm^{0.099}_{0.095}$
HIPEQ1545+00	$23.76\pm^{0.120}_{0.087}$	$23.27\pm^{0.047}_{0.046}$	$23.09\pm^{0.043}_{0.042}$	$23.02\pm^{0.070}_{0.066}$	$22.04\pm^{0.114}_{0.095}$	$23.78\pm^{0.103}_{0.077}$	$23.29\pm^{0.048}_{0.047}$	$23.09\pm^{0.045}_{0.044}$	$23.00\pm^{0.075}_{0.071}$	$22.06\pm^{0.143}_{0.113}$

Table 3.8—Continued

	$\Sigma_{Elliptical}$					$\Sigma_{Circular}$				
HIPASS Name	u	g	r	i	z	u	g	r	i	z
HIPEQ1601+01a	$23.13\pm^{0.047}_{0.045}$	$22.09\pm^{0.022}_{0.022}$	$21.73\pm^{0.022}_{0.022}$	$21.32\pm^{0.022}_{0.022}$	$21.30\pm^{0.022}_{0.022}$	$23.17\pm^{0.042}_{0.041}$	$22.19\pm^{0.028}_{0.027}$	$21.80\pm^{0.028}_{0.028}$	$21.41\pm^{0.028}_{0.028}$	$21.35\pm^{0.049}_{0.047}$
HIPEQ1609-00	$23.76\pm^{0.055}_{0.044}$	$23.43\pm^{0.045}_{0.044}$	$23.23\pm^{0.054}_{0.052}$	$23.16\pm^{0.125}_{0.110}$	$22.39\pm^{0.182}_{0.097}$	$23.79\pm^{0.093}_{0.063}$	$23.59\pm^{0.053}_{0.051}$	$23.35\pm^{0.116}_{0.106}$	$23.21\pm^{0.217}_{0.171}$	$22.39\pm^{0.292}_{0.120}$
HIPEQ1613-00	$22.31\pm^{0.086}_{0.083}$	$21.45\pm^{0.074}_{0.072}$	$21.34\pm^{0.075}_{0.073}$	$21.17\pm^{0.079}_{0.076}$	$20.86\pm^{0.083}_{0.080}$	$22.27\pm^{0.183}_{0.167}$	$21.40\pm^{0.088}_{0.085}$	$21.30\pm^{0.089}_{0.086}$	$21.20\pm^{0.090}_{0.087}$	$20.88\pm^{0.093}_{0.089}$
HIPEQ1614+00	$23.66\pm^{0.049}_{0.044}$	$23.25\pm^{0.026}_{0.025}$	$22.93\pm^{0.028}_{0.028}$	$22.75\pm^{0.031}_{0.030}$	$22.24\pm^{0.051}_{0.044}$	$23.66\pm^{0.041}_{0.037}$	$23.27\pm^{0.027}_{0.027}$	$22.94\pm^{0.030}_{0.029}$	$22.76\pm^{0.033}_{0.032}$	$22.24\pm^{0.055}_{0.047}$
HIPEQ1614-00	$23.29\pm^{0.051}_{0.048}$	$22.13\pm^{0.015}_{0.016}$	$21.25\pm^{0.016}_{0.017}$	$20.74\pm^{0.017}_{0.017}$	$20.27\pm^{0.037}_{0.037}$	$23.61\pm^{0.061}_{0.049}$	$22.97\pm^{0.026}_{0.025}$	$22.10\pm^{0.029}_{0.029}$	$21.59\pm^{0.031}_{0.030}$	$21.10\pm^{0.033}_{0.033}$
HIPEQ2036-04	$23.82\pm^{0.037}_{0.034}$	$22.15\pm^{0.032}_{0.031}$	$21.11\pm^{0.035}_{0.035}$	$20.68\pm^{0.035}_{0.035}$	$20.55\pm^{0.037}_{0.036}$	$23.84\pm^{0.042}_{0.038}$	$22.13\pm^{0.040}_{0.039}$	$21.15\pm^{0.043}_{0.042}$	$20.67\pm^{0.044}_{0.043}$	$20.59\pm^{0.044}_{0.043}$
HIPEQ2314+00	$22.00\pm^{0.099}_{0.096}$	$20.85\pm^{0.098}_{0.094}$	$20.47\pm^{0.098}_{0.094}$	$20.16\pm^{0.103}_{0.099}$	$20.09\pm^{0.104}_{0.100}$	$22.01\pm^{0.103}_{0.099}$	$20.84\pm^{0.103}_{0.098}$	$20.46\pm^{0.103}_{0.098}$	$20.26\pm^{0.103}_{0.099}$	$20.09\pm^{0.109}_{0.104}$
HIPEQ2324-00	$23.14\pm^{0.062}_{0.060}$	$22.52\pm^{0.033}_{0.032}$	$22.30\pm^{0.035}_{0.034}$	$22.19\pm^{0.037}_{0.037}$	$21.96\pm^{0.112}_{0.098}$	$23.46\pm^{0.096}_{0.087}$	$22.72\pm^{0.046}_{0.045}$	$22.43\pm^{0.050}_{0.049}$	$22.30\pm^{0.053}_{0.052}$	$22.01\pm^{0.131}_{0.110}$
HIPEQ2335+01	$24.23\pm^{0.147}_{0.068}$	$23.95\pm^{0.099}_{0.090}$	$23.60\pm^{0.070}_{0.066}$	$23.32\pm^{0.101}_{0.092}$	$22.56\pm^{0.100}_{0.061}$	$24.23\pm^{0.118}_{0.061}$	$24.03\pm^{0.074}_{0.068}$	$23.64\pm^{0.045}_{0.044}$	$23.35\pm^{0.115}_{0.102}$	$22.54\pm^{0.098}_{0.062}$
HIPEQ2336+00	$22.77\pm^{0.032}_{0.031}$	$20.90\pm^{0.039}_{0.038}$	$19.97\pm^{0.046}_{0.045}$	$19.54\pm^{0.048}_{0.047}$	$19.33\pm^{0.048}_{0.047}$	$22.76\pm^{0.036}_{0.036}$	$20.92\pm^{0.045}_{0.044}$	$20.03\pm^{0.052}_{0.051}$	$19.53\pm^{0.056}_{0.054}$	$19.39\pm^{0.054}_{0.053}$
HIPEQ2337+00	$24.08\pm^{0.055}_{0.047}$	$23.69\pm^{0.023}_{0.023}$	$23.30\pm^{0.025}_{0.025}$	$23.05\pm^{0.044}_{0.043}$	$22.36\pm^{0.082}_{0.066}$	$24.08\pm^{0.064}_{0.053}$	$23.72\pm^{0.026}_{0.025}$	$23.35\pm^{0.028}_{0.027}$	$23.07\pm^{0.029}_{0.028}$	$22.38\pm^{0.090}_{0.070}$
HIPEQ2340+01	$22.73\pm^{0.136}_{0.128}$	$21.58\pm^{0.066}_{0.064}$	$21.07\pm^{0.066}_{0.064}$	$20.80\pm^{0.067}_{0.065}$	$20.49\pm^{0.081}_{0.078}$	$22.83\pm^{0.177}_{0.162}$	$21.72\pm^{0.088}_{0.085}$	$21.22\pm^{0.088}_{0.085}$	$20.87\pm^{0.093}_{0.089}$	$20.64\pm^{0.103}_{0.098}$

Table 3.9. Other Surface Brightness Measures

	$\Sigma_{face-on}$					Σ_{fiber}				
HIPASS Name	u^a	g^a	r^a	i^a	z^a	u^a	g^a	r^a	i^a	z^a
HIPEQ0014-00	$23.71\pm^{0.061}_{0.056}$	$22.75\pm^{0.036}_{0.035}$	$22.01\pm^{0.043}_{0.042}$	$21.62\pm^{0.047}_{0.046}$	$21.26\pm^{0.051}_{0.050}$	$21.77\pm^{0.468}_{0.825}$	$20.30\pm^{0.048}_{0.050}$	$19.54\pm^{0.035}_{0.036}$	$19.17\pm^{0.038}_{0.039}$	$18.86\pm^{0.105}_{0.116}$
HIPEQ0027-01a	$23.99\pm^{0.043}_{0.039}$	$23.34\pm^{0.041}_{0.040}$	$22.88\pm^{0.042}_{0.041}$	$22.65\pm^{0.043}_{0.042}$	$22.15\pm^{0.060}_{0.054}$	$22.13\pm^{0.461}_{0.797}$	$20.95\pm^{0.092}_{0.101}$	$20.40\pm^{0.066}_{0.071}$	$20.14\pm^{0.088}_{0.096}$	$19.95\pm^{0.241}_{0.309}$
HIPEQ0033-01	$24.33\pm^{0.062}_{0.044}$	$24.17\pm^{0.027}_{0.026}$	$23.71\pm^{0.031}_{0.030}$	$23.58\pm^{0.062}_{0.056}$	$22.58\pm^{0.055}_{0.041}$	$23.15\pm^{0.904}_{2.126}$	$22.05\pm^{0.234}_{0.297}$	$21.63\pm^{0.190}_{0.230}$	$21.35\pm^{0.242}_{0.310}$	$21.36\pm^{0.673}_{1.358}$
HIPEQ0043-00	$22.49\pm^{0.057}_{0.056}$	$21.19\pm^{0.059}_{0.057}$	$20.49\pm^{0.064}_{0.062}$	$20.14\pm^{0.066}_{0.064}$	$19.84\pm^{0.070}_{0.068}$	$20.66\pm^{0.134}_{0.153}$	$19.24\pm^{0.016}_{0.016}$	$18.49\pm^{0.013}_{0.013}$	$18.14\pm^{0.014}_{0.014}$	$17.85\pm^{0.043}_{0.044}$
HIPEQ0051-00	$21.59\pm^{0.174}_{0.163}$	$20.64\pm^{0.163}_{0.152}$	$20.48\pm^{0.142}_{0.134}$	$20.37\pm^{0.134}_{0.126}$	$20.24\pm^{0.138}_{0.130}$	$19.84\pm^{0.084}_{0.091}$	$19.06\pm^{0.015}_{0.015}$	$18.83\pm^{0.018}_{0.018}$	$18.68\pm^{0.022}_{0.022}$	$18.56\pm^{0.075}_{0.081}$
HIPEQ0058+00	$22.39\pm^{0.080}_{0.078}$	$21.16\pm^{0.081}_{0.078}$	$20.60\pm^{0.084}_{0.081}$	$20.26\pm^{0.088}_{0.084}$	$20.03\pm^{0.095}_{0.091}$	$20.65\pm^{0.148}_{0.171}$	$19.58\pm^{0.024}_{0.024}$	$18.94\pm^{0.019}_{0.019}$	$18.65\pm^{0.025}_{0.026}$	$18.41\pm^{0.069}_{0.073}$
HIPEQ0107+01	$22.28\pm^{0.253}_{0.229}$	$22.01\pm^{0.090}_{0.086}$	$21.97\pm^{0.081}_{0.078}$	$22.03\pm^{0.075}_{0.073}$	$21.77\pm^{0.133}_{0.118}$	$21.41\pm^{0.284}_{0.384}$	$20.94\pm^{0.070}_{0.075}$	$20.81\pm^{0.093}_{0.102}$	$20.87\pm^{0.158}_{0.185}$	$20.85\pm^{0.484}_{0.840}$
HIPEQ0119+00	$24.24\pm^{0.195}_{0.092}$	$23.80\pm^{0.090}_{0.084}$	$23.34\pm^{0.106}_{0.099}$	$23.05\pm^{0.114}_{0.106}$	$22.46\pm^{0.129}_{0.088}$	$23.40\pm^{1.016}_{2.052}$	$22.71\pm^{0.307}_{0.425}$	$22.23\pm^{0.302}_{0.416}$	$21.92\pm^{0.377}_{0.572}$	$21.80\pm^{0.853}_{1.549}$
HIPEQ0120-00	$23.95\pm^{0.081}_{0.068}$	$23.39\pm^{0.049}_{0.048}$	$23.05\pm^{0.049}_{0.048}$	$22.87\pm^{0.047}_{0.046}$	$22.31\pm^{0.050}_{0.044}$	$22.85\pm^{0.775}_{1.885}$	$21.85\pm^{0.156}_{0.182}$	$21.44\pm^{0.165}_{0.195}$	$21.19\pm^{0.197}_{0.241}$	$20.99\pm^{0.570}_{1.106}$
HIPEQ0122+00	$24.04\pm^{0.013}_{0.012}$	$23.38\pm^{0.015}_{0.015}$	$22.91\pm^{0.016}_{0.016}$	$22.60\pm^{0.016}_{0.016}$	$22.15\pm^{0.011}_{0.010}$	$22.43\pm^{0.662}_{1.604}$	$21.00\pm^{0.077}_{0.083}$	$20.42\pm^{0.065}_{0.069}$	$20.10\pm^{0.083}_{0.090}$	$19.88\pm^{0.229}_{0.289}$
HIPEQ0123-00	$23.06\pm^{0.104}_{0.097}$	$21.90\pm^{0.064}_{0.062}$	$21.30\pm^{0.069}_{0.067}$	$21.07\pm^{0.070}_{0.068}$	$20.83\pm^{0.074}_{0.072}$	$20.62\pm^{0.152}_{0.176}$	$19.77\pm^{0.028}_{0.028}$	$19.24\pm^{0.024}_{0.025}$	$18.99\pm^{0.031}_{0.032}$	$18.77\pm^{0.094}_{0.103}$
HIPEQ0126+00a	$24.35\pm^{0.302}_{0.081}$	$23.96\pm^{0.136}_{0.120}$	$23.51\pm^{0.086}_{0.081}$	$23.28\pm^{0.088}_{0.083}$	$22.39\pm^{0.226}_{0.136}$	$23.83\pm^{1.304}_{2.052}$	$22.89\pm^{0.370}_{0.551}$	$22.60\pm^{0.398}_{0.618}$	$22.31\pm^{0.525}_{0.978}$	$21.72\pm^{0.814}_{1.528}$
HIPEQ0126-00b	$21.71\pm^{0.210}_{0.194}$	$21.10\pm^{0.193}_{0.178}$	$21.09\pm^{0.178}_{0.166}$	$21.25\pm^{0.167}_{0.156}$	$21.07\pm^{0.189}_{0.173}$	$20.47\pm^{0.153}_{0.178}$	$19.92\pm^{0.031}_{0.032}$	$19.89\pm^{0.043}_{0.044}$	$20.09\pm^{0.075}_{0.081}$	$20.06\pm^{0.258}_{0.337}$
HIPEQ0154-00	$22.69\pm^{0.189}_{0.172}$	$20.76\pm^{0.103}_{0.098}$	$19.88\pm^{0.107}_{0.102}$	$19.47\pm^{0.107}_{0.102}$	$19.02\pm^{0.121}_{0.115}$	$20.35\pm^{0.113}_{0.126}$	$18.46\pm^{0.009}_{0.009}$	$17.57\pm^{0.006}_{0.006}$	$17.15\pm^{0.006}_{0.006}$	$16.85\pm^{0.015}_{0.016}$
HIPEQ0222-00	$24.31\pm^{0.039}_{0.029}$	$24.28\pm^{0.018}_{0.018}$	$23.90\pm^{0.020}_{0.020}$	$23.59\pm^{0.019}_{0.019}$	$22.59\pm^{0.020}_{0.017}$	$22.92\pm^{0.917}_{2.374}$	$21.97\pm^{0.181}_{0.217}$	$21.46\pm^{0.174}_{0.207}$	$21.17\pm^{0.175}_{0.209}$	$21.30\pm^{0.582}_{1.067}$
HIPEQ0228-01	$22.92\pm^{0.057}_{0.055}$	$21.83\pm^{0.033}_{0.033}$	$21.36\pm^{0.034}_{0.034}$	$21.15\pm^{0.035}_{0.034}$	$21.07\pm^{0.035}_{0.034}$	$20.85\pm^{0.167}_{0.197}$	$19.76\pm^{0.033}_{0.034}$	$19.30\pm^{0.024}_{0.025}$	$19.06\pm^{0.031}_{0.032}$	$18.88\pm^{0.084}_{0.091}$
HIPEQ0230+00	$24.45\pm^{0.040}_{0.020}$	$24.25\pm^{0.031}_{0.030}$	$23.75\pm^{0.031}_{0.030}$	$23.30\pm^{0.033}_{0.033}$	$22.60\pm^{0.049}_{0.037}$	$24.40\pm^{1.218}_{1.299}$	$23.68\pm^{0.616}_{1.124}$	$22.97\pm^{0.434}_{0.688}$	$22.70\pm^{0.554}_{1.012}$	$22.31\pm^{0.894}_{1.205}$
HIPEQ0230-01	$22.43\pm^{0.049}_{0.048}$	$20.49\pm^{0.054}_{0.053}$	$19.61\pm^{0.057}_{0.055}$	$19.20\pm^{0.057}_{0.055}$	$18.87\pm^{0.060}_{0.059}$	$19.49\pm^{0.054}_{0.057}$	$17.62\pm^{0.006}_{0.006}$	$16.77\pm^{0.004}_{0.004}$	$16.38\pm^{0.004}_{0.004}$	$16.10\pm^{0.008}_{0.008}$
HIPEQ0231+00	$24.06\pm^{0.152}_{0.106}$	$23.12\pm^{0.059}_{0.057}$	$22.72\pm^{0.061}_{0.060}$	$22.46\pm^{0.063}_{0.061}$	$22.11\pm^{0.155}_{0.122}$	$22.49\pm^{0.657}_{1.569}$	$21.36\pm^{0.101}_{0.111}$	$20.81\pm^{0.097}_{0.106}$	$20.56\pm^{0.110}_{0.123}$	$20.31\pm^{0.350}_{0.515}$
HIPEQ0236+00	$23.99\pm^{0.054}_{0.048}$	$22.98\pm^{0.054}_{0.053}$	$22.21\pm^{0.060}_{0.058}$	$21.74\pm^{0.063}_{0.062}$	$21.36\pm^{0.064}_{0.062}$	$22.64\pm^{0.663}_{1.522}$	$20.95\pm^{0.073}_{0.078}$	$19.98\pm^{0.046}_{0.049}$	$19.49\pm^{0.047}_{0.049}$	$19.09\pm^{0.100}_{0.110}$
HIPEQ0238+00	$24.25\pm^{0.087}_{0.056}$	$24.37\pm^{0.034}_{0.033}$	$24.11\pm^{0.063}_{0.056}$	$23.81\pm^{0.081}_{0.067}$	$22.63\pm^{0.055}_{0.038}$	$23.33\pm^{1.024}_{2.125}$	$22.99\pm^{0.405}_{0.628}$	$22.94\pm^{0.498}_{0.863}$	$22.79\pm^{0.681}_{1.420}$	$22.33\pm^{1.041}_{1.396}$
HIPEQ0240+01	$24.28\pm^{0.130}_{0.068}$	$24.45\pm^{0.047}_{0.043}$	$24.26\pm^{0.058}_{0.050}$	$23.95\pm^{0.061}_{0.050}$	$22.67\pm^{0.047}_{0.030}$	$23.88\pm^{1.473}_{2.190}$	$23.73\pm^{0.669}_{1.245}$	$23.90\pm^{0.987}_{1.672}$	$23.70\pm^{1.123}_{1.672}$	$22.59\pm^{1.227}_{1.390}$
HIPEQ0241+00	$24.07\pm^{0.009}_{0.009}$	$23.10\pm^{0.008}_{0.008}$	$22.23\pm^{0.009}_{0.009}$	$21.70\pm^{0.009}_{0.009}$	$21.28\pm^{0.009}_{0.009}$	$21.89\pm^{0.381}_{0.584}$	$20.03\pm^{0.034}_{0.035}$	$19.11\pm^{0.020}_{0.021}$	$18.66\pm^{0.023}_{0.024}$	$18.33\pm^{0.052}_{0.055}$
HIPEQ0244+00	$24.16\pm^{0.075}_{0.057}$	$23.74\pm^{0.038}_{0.037}$	$23.40\pm^{0.039}_{0.038}$	$23.23\pm^{0.035}_{0.034}$	$22.45\pm^{0.042}_{0.036}$	$23.30\pm^{1.005}_{2.157}$	$22.03\pm^{0.185}_{0.222}$	$21.63\pm^{0.195}_{0.237}$	$21.49\pm^{0.262}_{0.345}$	$21.38\pm^{0.612}_{1.135}$
HIPEQ0246-00a	$23.76\pm^{0.022}_{0.021}$	$22.46\pm^{0.020}_{0.020}$	$21.71\pm^{0.022}_{0.022}$	$21.32\pm^{0.023}_{0.023}$	$21.07\pm^{0.023}_{0.022}$	$21.19\pm^{0.229}_{0.291}$	$19.51\pm^{0.021}_{0.022}$	$18.71\pm^{0.015}_{0.015}$	$18.30\pm^{0.016}_{0.016}$	$17.99\pm^{0.043}_{0.044}$
HIPEQ0246-00b	$22.05\pm^{0.025}_{0.025}$	$21.13\pm^{0.022}_{0.022}$	$20.70\pm^{0.022}_{0.022}$	$20.50\pm^{0.022}_{0.022}$	$20.34\pm^{0.023}_{0.022}$	$19.46\pm^{0.063}_{0.067}$	$18.71\pm^{0.012}_{0.012}$	$18.25\pm^{0.011}_{0.011}$	$18.12\pm^{0.013}_{0.013}$	$17.87\pm^{0.035}_{0.037}$
HIPEQ0249-00	$23.44\pm^{0.139}_{0.119}$	$22.06\pm^{0.069}_{0.067}$	$21.41\pm^{0.074}_{0.072}$	$21.12\pm^{0.074}_{0.072}$	$20.77\pm^{0.082}_{0.079}$	$20.16\pm^{0.126}_{0.142}$	$19.14\pm^{0.017}_{0.018}$	$18.60\pm^{0.016}_{0.016}$	$18.34\pm^{0.016}_{0.016}$	$18.10\pm^{0.044}_{0.046}$
HIPEQ0249-00a	$24.15\pm^{0.088}_{0.058}$	$24.08\pm^{0.039}_{0.037}$	$23.79\pm^{0.044}_{0.042}$	$23.48\pm^{0.085}_{0.076}$	$22.56\pm^{0.114}_{0.064}$	$23.44\pm^{1.157}_{2.164}$	$22.62\pm^{0.310}_{0.430}$	$22.41\pm^{0.352}_{0.515}$	$22.37\pm^{0.486}_{0.841}$	$22.04\pm^{0.992}_{1.577}$
HIPEQ0249-00b	$22.89\pm^{0.094}_{0.089}$	$21.37\pm^{0.060}_{0.058}$	$20.62\pm^{0.064}_{0.063}$	$20.30\pm^{0.064}_{0.063}$	$20.03\pm^{0.068}_{0.066}$	$19.86\pm^{0.081}_{0.088}$	$18.56\pm^{0.012}_{0.012}$	$17.96\pm^{0.009}_{0.009}$	$17.65\pm^{0.010}_{0.010}$	$17.43\pm^{0.025}_{0.026}$
HIPEQ0251-01	$24.08\pm^{0.019}_{0.017}$	$24.18\pm^{0.026}_{0.025}$	$23.90\pm^{0.015}_{0.015}$	$23.64\pm^{0.024}_{0.023}$	$22.54\pm^{0.018}_{0.016}$	$23.75\pm^{1.357}_{1.940}$	$22.70\pm^{0.431}_{0.702}$	$22.37\pm^{0.354}_{0.519}$	$22.27\pm^{0.492}_{0.864}$	$22.09\pm^{0.971}_{1.463}$
HIPEQ0300+00	$23.80\pm^{0.102}_{0.071}$	$23.52\pm^{0.041}_{0.039}$	$23.09\pm^{0.046}_{0.045}$	$22.83\pm^{0.047}_{0.045}$	$22.27\pm^{0.046}_{0.041}$	$22.96\pm^{1.125}_{2.419}$	$21.62\pm^{0.157}_{0.184}$	$21.08\pm^{0.130}_{0.148}$	$20.80\pm^{0.151}_{0.175}$	$20.71\pm^{0.524}_{0.972}$

Table 3.9—Continued

	$\Sigma_{face-on}$					Σ_{fiber}				
HIPASS Name	u^a	g^a	r^a	i^a	z^a	u^a	g^a	r^a	i^a	z^a
HIPEQ0301-00	$23.53\pm^{0.112}_{0.088}$	$23.02\pm^{0.051}_{0.049}$	$22.73\pm^{0.054}_{0.052}$	$22.66\pm^{0.050}_{0.049}$	$22.20\pm^{0.094}_{0.074}$	$22.11\pm^{0.733}_{1.935}$	$21.19\pm^{0.120}_{0.135}$	$20.92\pm^{0.120}_{0.135}$	$20.80\pm^{0.150}_{0.174}$	$20.78\pm^{0.444}_{0.723}$
HIPEQ0306-00	$22.15\pm^{0.070}_{0.069}$	$20.02\pm^{0.077}_{0.074}$	$19.22\pm^{0.080}_{0.077}$	$18.89\pm^{0.077}_{0.074}$	$18.51\pm^{0.083}_{0.081}$	$19.64\pm^{0.088}_{0.096}$	$17.80\pm^{0.007}_{0.007}$	$17.00\pm^{0.004}_{0.005}$	$16.61\pm^{0.004}_{0.004}$	$16.30\pm^{0.010}_{0.010}$
HIPEQ0316-00	$23.83\pm^{0.070}_{0.060}$	$22.91\pm^{0.045}_{0.044}$	$22.04\pm^{0.052}_{0.051}$	$21.60\pm^{0.054}_{0.053}$	$21.20\pm^{0.054}_{0.053}$	$21.96\pm^{0.559}_{1.145}$	$20.33\pm^{0.050}_{0.052}$	$19.43\pm^{0.033}_{0.034}$	$19.02\pm^{0.030}_{0.030}$	$18.70\pm^{0.079}_{0.085}$
HIPEQ0320-06	$22.01\pm^{0.062}_{0.060}$	$20.88\pm^{0.060}_{0.059}$	$20.36\pm^{0.062}_{0.060}$	$20.11\pm^{0.062}_{0.061}$	$19.87\pm^{0.066}_{0.064}$	$20.32\pm^{0.110}_{0.123}$	$18.87\pm^{0.013}_{0.013}$	$18.28\pm^{0.012}_{0.012}$	$17.96\pm^{0.014}_{0.014}$	$17.72\pm^{0.038}_{0.040}$
HIPEQ0351-00	$21.62\pm^{0.186}_{0.174}$	$20.66\pm^{0.153}_{0.143}$	$20.15\pm^{0.152}_{0.143}$	$19.88\pm^{0.152}_{0.143}$	$19.39\pm^{0.180}_{0.167}$	$19.68\pm^{0.131}_{0.149}$	$18.81\pm^{0.018}_{0.018}$	$18.30\pm^{0.015}_{0.016}$	$18.05\pm^{0.015}_{0.015}$	$17.77\pm^{0.039}_{0.040}$
HIPEQ0809+00	$23.28\pm^{0.039}_{0.038}$	$22.32\pm^{0.045}_{0.044}$	$21.92\pm^{0.046}_{0.045}$	$21.71\pm^{0.048}_{0.047}$	$21.59\pm^{0.042}_{0.041}$	$20.97\pm^{0.147}_{0.169}$	$20.29\pm^{0.035}_{0.036}$	$19.99\pm^{0.041}_{0.043}$	$19.84\pm^{0.058}_{0.062}$	$19.77\pm^{0.170}_{0.201}$
HIPEQ0821+03b	$22.63\pm^{0.072}_{0.070}$	$21.35\pm^{0.070}_{0.068}$	$20.63\pm^{0.075}_{0.072}$	$20.24\pm^{0.078}_{0.075}$	$19.86\pm^{0.085}_{0.082}$	$20.11\pm^{0.074}_{0.079}$	$19.10\pm^{0.014}_{0.014}$	$18.37\pm^{0.010}_{0.010}$	$18.05\pm^{0.012}_{0.012}$	$17.73\pm^{0.028}_{0.028}$
HIPEQ0821-00	$23.13\pm^{0.158}_{0.142}$	$22.84\pm^{0.069}_{0.067}$	$22.75\pm^{0.068}_{0.065}$	$22.66\pm^{0.073}_{0.070}$	$22.30\pm^{0.125}_{0.094}$	$21.25\pm^{0.232}_{0.295}$	$20.64\pm^{0.061}_{0.065}$	$20.63\pm^{0.082}_{0.089}$	$20.72\pm^{0.136}_{0.155}$	$20.60\pm^{0.396}_{0.614}$
HIPEQ0822-00	$23.59\pm^{0.031}_{0.030}$	$22.57\pm^{0.047}_{0.046}$	$22.05\pm^{0.048}_{0.047}$	$21.76\pm^{0.050}_{0.049}$	$21.59\pm^{0.080}_{0.075}$	$21.12\pm^{0.198}_{0.242}$	$19.86\pm^{0.036}_{0.037}$	$19.30\pm^{0.026}_{0.027}$	$19.06\pm^{0.033}_{0.034}$	$18.88\pm^{0.094}_{0.103}$
HIPEQ0825-00	$23.83\pm^{0.017}_{0.017}$	$22.15\pm^{0.039}_{0.038}$	$21.15\pm^{0.043}_{0.042}$	$20.66\pm^{0.044}_{0.043}$	$20.24\pm^{0.047}_{0.046}$	$21.29\pm^{0.242}_{0.311}$	$19.28\pm^{0.019}_{0.020}$	$18.22\pm^{0.010}_{0.011}$	$17.66\pm^{0.010}_{0.010}$	$17.22\pm^{0.023}_{0.023}$
HIPEQ0855+02	$24.13\pm^{0.074}_{0.054}$	$24.02\pm^{0.022}_{0.022}$	$23.60\pm^{0.027}_{0.026}$	$23.40\pm^{0.060}_{0.056}$	$22.55\pm^{0.053}_{0.040}$	$22.48\pm^{0.709}_{1.793}$	$21.43\pm^{0.127}_{0.143}$	$20.95\pm^{0.128}_{0.145}$	$20.76\pm^{0.167}_{0.198}$	$20.55\pm^{0.452}_{0.763}$
HIPEQ0856+00	$23.55\pm^{0.032}_{0.031}$	$22.50\pm^{0.044}_{0.043}$	$22.14\pm^{0.046}_{0.045}$	$22.26\pm^{0.038}_{0.037}$	$21.95\pm^{0.055}_{0.052}$	$21.76\pm^{0.368}_{0.556}$	$20.63\pm^{0.072}_{0.077}$	$20.16\pm^{0.064}_{0.068}$	$19.92\pm^{0.081}_{0.087}$	$19.77\pm^{0.241}_{0.310}$
HIPEQ0923-00	$23.66\pm^{0.033}_{0.032}$	$22.78\pm^{0.046}_{0.045}$	$22.34\pm^{0.049}_{0.048}$	$22.11\pm^{0.050}_{0.049}$	$21.79\pm^{0.044}_{0.042}$	$21.82\pm^{0.357}_{0.531}$	$20.54\pm^{0.047}_{0.049}$	$20.05\pm^{0.045}_{0.047}$	$19.80\pm^{0.053}_{0.056}$	$19.62\pm^{0.150}_{0.174}$
HIPEQ0930+04	$23.50\pm^{0.046}_{0.043}$	$22.94\pm^{0.035}_{0.034}$	$22.31\pm^{0.038}_{0.037}$	$22.11\pm^{0.038}_{0.038}$	$21.49\pm^{0.037}_{0.036}$	$20.99\pm^{0.204}_{0.251}$	$20.28\pm^{0.037}_{0.039}$	$19.67\pm^{0.033}_{0.034}$	$19.47\pm^{0.041}_{0.043}$	$18.88\pm^{0.094}_{0.103}$
HIPEQ0942+00	$22.31\pm^{0.027}_{0.026}$	$21.03\pm^{0.029}_{0.029}$	$20.41\pm^{0.031}_{0.030}$	$20.12\pm^{0.031}_{0.031}$	$20.01\pm^{0.031}_{0.031}$	$20.38\pm^{0.132}_{0.150}$	$18.88\pm^{0.015}_{0.015}$	$18.26\pm^{0.012}_{0.012}$	$17.93\pm^{0.013}_{0.013}$	$17.71\pm^{0.044}_{0.046}$
HIPEQ0944-00b	$23.72\pm^{0.137}_{0.108}$	$23.12\pm^{0.073}_{0.070}$	$22.71\pm^{0.081}_{0.077}$	$22.46\pm^{0.096}_{0.092}$	$22.19\pm^{0.132}_{0.102}$	$22.73\pm^{0.656}_{1.364}$	$21.65\pm^{0.124}_{0.140}$	$21.35\pm^{0.148}_{0.171}$	$21.23\pm^{0.197}_{0.240}$	$21.02\pm^{0.494}_{0.846}$
HIPEQ0945+01	$23.27\pm^{0.040}_{0.037}$	$22.59\pm^{0.025}_{0.025}$	$22.09\pm^{0.026}_{0.026}$	$21.86\pm^{0.026}_{0.026}$	$21.57\pm^{0.023}_{0.023}$	$21.20\pm^{0.423}_{0.692}$	$20.22\pm^{0.065}_{0.069}$	$19.53\pm^{0.048}_{0.051}$	$19.28\pm^{0.055}_{0.058}$	$18.99\pm^{0.157}_{0.183}$
HIPEQ0946+02	$24.19\pm^{0.031}_{0.025}$	$24.13\pm^{0.021}_{0.020}$	$23.72\pm^{0.023}_{0.022}$	$23.43\pm^{0.023}_{0.022}$	$22.53\pm^{0.025}_{0.022}$	$22.78\pm^{0.651}_{1.350}$	$21.70\pm^{0.163}_{0.191}$	$21.31\pm^{0.133}_{0.152}$	$21.13\pm^{0.165}_{0.195}$	$21.05\pm^{0.422}_{0.654}$
HIPEQ0947+00a	$23.51\pm^{0.017}_{0.016}$	$23.32\pm^{0.025}_{0.024}$	$22.86\pm^{0.029}_{0.029}$	$22.58\pm^{0.030}_{0.029}$	$22.08\pm^{0.030}_{0.028}$	$22.46\pm^{0.736}_{1.442}$	$21.14\pm^{0.115}_{0.129}$	$20.60\pm^{0.098}_{0.108}$	$20.38\pm^{0.123}_{0.139}$	$20.25\pm^{0.304}_{0.419}$
HIPEQ0947+00b	$23.69\pm^{0.030}_{0.023}$	$23.77\pm^{0.027}_{0.026}$	$23.44\pm^{0.060}_{0.056}$	$23.22\pm^{0.062}_{0.057}$	$22.37\pm^{0.078}_{0.054}$	$22.27\pm^{0.673}_{1.425}$	$21.87\pm^{0.197}_{0.239}$	$21.58\pm^{0.213}_{0.265}$	$21.43\pm^{0.273}_{0.364}$	$21.18\pm^{0.603}_{1.115}$
HIPEQ0953+01	$23.98\pm^{0.006}_{0.006}$	$23.32\pm^{0.011}_{0.011}$	$22.81\pm^{0.012}_{0.012}$	$22.63\pm^{0.012}_{0.012}$	$21.89\pm^{0.020}_{0.020}$	$21.33\pm^{0.184}_{0.221}$	$20.14\pm^{0.031}_{0.032}$	$19.55\pm^{0.028}_{0.029}$	$19.32\pm^{0.037}_{0.039}$	$18.80\pm^{0.100}_{0.110}$
HIPEQ0954+02a	$23.58\pm^{0.073}_{0.066}$	$22.17\pm^{0.060}_{0.059}$	$21.77\pm^{0.064}_{0.062}$	$21.45\pm^{0.065}_{0.063}$	$21.71\pm^{0.060}_{0.057}$	$22.29\pm^{0.404}_{0.630}$	$20.66\pm^{0.055}_{0.058}$	$20.11\pm^{0.048}_{0.050}$	$19.69\pm^{0.060}_{0.064}$	$20.04\pm^{0.207}_{0.255}$
HIPEQ0955+04a	$22.56\pm^{0.031}_{0.031}$	$21.59\pm^{0.030}_{0.030}$	$21.09\pm^{0.031}_{0.031}$	$20.88\pm^{0.031}_{0.031}$	$20.71\pm^{0.031}_{0.031}$	$18.91\pm^{0.034}_{0.035}$	$18.37\pm^{0.008}_{0.008}$	$17.73\pm^{0.007}_{0.007}$	$17.74\pm^{0.009}_{0.009}$	$17.55\pm^{0.030}_{0.031}$
HIPEQ0958+01	$24.44\pm^{0.084}_{0.041}$	$24.57\pm^{0.033}_{0.031}$	$24.33\pm^{0.059}_{0.051}$	$24.08\pm^{0.100}_{0.067}$	$22.76\pm^{0.086}_{0.032}$	$24.25\pm^{1.608}_{1.959}$	$24.05\pm^{0.805}_{1.447}$	$23.80\pm^{0.958}_{1.769}$	$23.86\pm^{1.299}_{1.794}$	$23.06\pm^{1.750}_{1.460}$
HIPEQ1000+03	$23.57\pm^{0.032}_{0.031}$	$22.32\pm^{0.040}_{0.039}$	$21.34\pm^{0.047}_{0.046}$	$20.84\pm^{0.048}_{0.047}$	$20.16\pm^{0.060}_{0.058}$	$21.25\pm^{0.215}_{0.269}$	$19.54\pm^{0.020}_{0.020}$	$18.48\pm^{0.011}_{0.011}$	$17.92\pm^{0.009}_{0.009}$	$17.43\pm^{0.021}_{0.021}$
HIPEQ1010+05	$22.67\pm^{0.139}_{0.131}$	$21.51\pm^{0.121}_{0.115}$	$21.17\pm^{0.114}_{0.109}$	$21.05\pm^{0.110}_{0.105}$	$20.91\pm^{0.118}_{0.111}$	$21.00\pm^{0.137}_{0.157}$	$19.74\pm^{0.027}_{0.028}$	$19.36\pm^{0.023}_{0.024}$	$19.17\pm^{0.030}_{0.031}$	$19.11\pm^{0.085}_{0.093}$
HIPEQ1014+03	$23.51\pm^{0.018}_{0.018}$	$21.63\pm^{0.014}_{0.014}$	$20.59\pm^{0.017}_{0.016}$	$19.99\pm^{0.018}_{0.018}$	$19.50\pm^{0.020}_{0.020}$	$20.07\pm^{0.082}_{0.089}$	$18.28\pm^{0.008}_{0.008}$	$17.50\pm^{0.005}_{0.005}$	$17.13\pm^{0.005}_{0.005}$	$16.83\pm^{0.013}_{0.013}$
HIPEQ1015+02	$24.23\pm^{0.045}_{0.035}$	$24.30\pm^{0.030}_{0.028}$	$23.95\pm^{0.036}_{0.034}$	$23.78\pm^{0.046}_{0.042}$	$22.59\pm^{0.062}_{0.043}$	$22.82\pm^{0.776}_{1.890}$	$21.92\pm^{0.178}_{0.213}$	$21.59\pm^{0.199}_{0.243}$	$21.48\pm^{0.298}_{0.411}$	$21.15\pm^{0.644}_{1.340}$
HIPEQ1026+03	$23.84\pm^{0.028}_{0.026}$	$22.79\pm^{0.027}_{0.026}$	$22.31\pm^{0.029}_{0.029}$	$22.12\pm^{0.029}_{0.029}$	$21.63\pm^{0.027}_{0.026}$	$21.86\pm^{0.326}_{0.465}$	$20.36\pm^{0.041}_{0.042}$	$19.82\pm^{0.035}_{0.036}$	$19.61\pm^{0.039}_{0.041}$	$19.18\pm^{0.102}_{0.113}$
HIPEQ1028+03	$24.18\pm^{0.033}_{0.029}$	$24.07\pm^{0.028}_{0.027}$	$23.93\pm^{0.025}_{0.024}$	$23.65\pm^{0.022}_{0.022}$	$22.59\pm^{0.015}_{0.013}$	$23.11\pm^{0.777}_{1.645}$	$22.10\pm^{0.221}_{0.278}$	$22.02\pm^{0.237}_{0.303}$	$21.90\pm^{0.302}_{0.416}$	$21.49\pm^{0.559}_{0.941}$
HIPEQ1039+01	$23.20\pm^{0.121}_{0.111}$	$22.28\pm^{0.064}_{0.062}$	$22.03\pm^{0.061}_{0.059}$	$21.95\pm^{0.057}_{0.055}$	$21.76\pm^{0.050}_{0.048}$	$22.49\pm^{0.589}_{1.224}$	$21.57\pm^{0.117}_{0.131}$	$21.26\pm^{0.138}_{0.158}$	$21.11\pm^{0.174}_{0.208}$	$20.87\pm^{0.485}_{0.840}$

Table 3.9—Continued

	$\Sigma_{face-on}$					Σ_{fiber}				
HIPASS Name	u^a	g^a	r^a	i^a	z^a	u^a	g^a	r^a	i^a	z^a
HIPEQ1041+00	$23.47\pm^{0.075}_{0.069}$	$22.48\pm^{0.059}_{0.057}$	$22.11\pm^{0.059}_{0.058}$	$22.02\pm^{0.056}_{0.054}$	$21.73\pm^{0.050}_{0.048}$	$21.91\pm^{0.325}_{0.460}$	$20.91\pm^{0.064}_{0.068}$	$20.48\pm^{0.067}_{0.071}$	$20.31\pm^{0.094}_{0.103}$	$20.12\pm^{0.243}_{0.312}$
HIPEQ1046+01	$24.14\pm^{0.014}_{0.013}$	$23.72\pm^{0.012}_{0.012}$	$23.21\pm^{0.014}_{0.014}$	$22.99\pm^{0.013}_{0.013}$	$22.20\pm^{0.016}_{0.016}$	$21.61\pm^{0.301}_{0.415}$	$20.45\pm^{0.045}_{0.047}$	$19.90\pm^{0.044}_{0.045}$	$19.74\pm^{0.058}_{0.061}$	$19.24\pm^{0.174}_{0.208}$
HIPEQ1050+01	$24.15\pm^{0.088}_{0.062}$	$23.98\pm^{0.078}_{0.072}$	$23.64\pm^{0.077}_{0.072}$	$23.38\pm^{0.079}_{0.073}$	$22.48\pm^{0.189}_{0.105}$	$23.62\pm^{1.068}_{1.766}$	$22.82\pm^{0.405}_{0.632}$	$22.41\pm^{0.369}_{0.552}$	$22.28\pm^{0.502}_{0.901}$	$22.11\pm^{1.047}_{1.604}$
HIPEQ1051+04a	$23.81\pm^{0.039}_{0.037}$	$23.12\pm^{0.034}_{0.033}$	$22.65\pm^{0.036}_{0.036}$	$22.50\pm^{0.037}_{0.036}$	$22.08\pm^{0.071}_{0.064}$	$22.12\pm^{0.440}_{0.734}$	$21.15\pm^{0.078}_{0.085}$	$20.70\pm^{0.079}_{0.086}$	$20.53\pm^{0.094}_{0.103}$	$20.36\pm^{0.323}_{0.457}$
HIPEQ1052+00	$21.05\pm^{0.239}_{0.217}$	$20.66\pm^{0.191}_{0.176}$	$20.55\pm^{0.176}_{0.163}$	$20.72\pm^{0.153}_{0.143}$	$20.58\pm^{0.159}_{0.148}$	$20.06\pm^{0.071}_{0.076}$	$19.54\pm^{0.019}_{0.019}$	$19.33\pm^{0.023}_{0.024}$	$19.30\pm^{0.033}_{0.034}$	$19.19\pm^{0.130}_{0.148}$
HIPEQ1053+02	$23.09\pm^{0.081}_{0.077}$	$22.93\pm^{0.073}_{0.071}$	$22.89\pm^{0.069}_{0.067}$	$22.80\pm^{0.067}_{0.065}$	$22.37\pm^{0.087}_{0.069}$	$22.12\pm^{0.473}_{0.830}$	$21.82\pm^{0.145}_{0.167}$	$21.78\pm^{0.213}_{0.264}$	$21.70\pm^{0.321}_{0.454}$	$21.87\pm^{0.921}_{1.634}$
HIPEQ1055+02	$22.92\pm^{0.137}_{0.129}$	$22.43\pm^{0.116}_{0.111}$	$22.48\pm^{0.107}_{0.102}$	$22.55\pm^{0.103}_{0.098}$	$22.11\pm^{0.162}_{0.130}$	$21.02\pm^{0.215}_{0.268}$	$20.67\pm^{0.059}_{0.063}$	$20.75\pm^{0.095}_{0.104}$	$21.04\pm^{0.191}_{0.231}$	$20.94\pm^{0.649}_{1.451}$
HIPEQ1101+03	$23.90\pm^{0.011}_{0.010}$	$23.13\pm^{0.011}_{0.011}$	$22.65\pm^{0.012}_{0.012}$	$22.30\pm^{0.012}_{0.012}$	$21.87\pm^{0.009}_{0.009}$	$21.69\pm^{0.364}_{0.548}$	$20.17\pm^{0.038}_{0.040}$	$19.56\pm^{0.029}_{0.030}$	$19.17\pm^{0.027}_{0.028}$	$18.91\pm^{0.072}_{0.077}$
HIPEQ1109-00	$23.16\pm^{0.057}_{0.054}$	$21.78\pm^{0.066}_{0.064}$	$20.91\pm^{0.075}_{0.072}$	$20.52\pm^{0.078}_{0.075}$	$20.07\pm^{0.089}_{0.086}$	$21.16\pm^{0.166}_{0.196}$	$19.59\pm^{0.020}_{0.020}$	$18.75\pm^{0.014}_{0.015}$	$18.34\pm^{0.016}_{0.016}$	$18.01\pm^{0.044}_{0.046}$
HIPEQ1110+01	$23.88\pm^{0.113}_{0.092}$	$23.59\pm^{0.052}_{0.050}$	$23.40\pm^{0.049}_{0.048}$	$23.31\pm^{0.045}_{0.043}$	$22.51\pm^{0.049}_{0.040}$	$22.09\pm^{0.381}_{0.582}$	$21.64\pm^{0.109}_{0.121}$	$21.55\pm^{0.157}_{0.183}$	$21.53\pm^{0.249}_{0.322}$	$21.46\pm^{0.668}_{1.280}$
HIPEQ1113+05	$23.33\pm^{0.095}_{0.086}$	$22.33\pm^{0.060}_{0.059}$	$22.15\pm^{0.061}_{0.059}$	$21.89\pm^{0.063}_{0.061}$	$22.12\pm^{0.068}_{0.060}$	$22.29\pm^{0.484}_{0.847}$	$21.08\pm^{0.087}_{0.095}$	$20.80\pm^{0.089}_{0.097}$	$20.52\pm^{0.106}_{0.117}$	$20.95\pm^{0.329}_{0.458}$
HIPEQ1117+04a	$20.83\pm^{0.086}_{0.083}$	$19.96\pm^{0.072}_{0.070}$	$19.54\pm^{0.067}_{0.065}$	$19.38\pm^{0.064}_{0.062}$	$19.06\pm^{0.069}_{0.067}$	$18.15\pm^{0.019}_{0.019}$	$17.15\pm^{0.004}_{0.004}$	$16.67\pm^{0.003}_{0.003}$	$16.46\pm^{0.004}_{0.004}$	$16.43\pm^{0.013}_{0.013}$
HIPEQ1119+02	$23.84\pm^{0.053}_{0.047}$	$23.20\pm^{0.026}_{0.025}$	$22.93\pm^{0.027}_{0.027}$	$22.82\pm^{0.026}_{0.026}$	$22.40\pm^{0.053}_{0.044}$	$23.05\pm^{0.976}_{2.277}$	$21.81\pm^{0.165}_{0.195}$	$21.49\pm^{0.186}_{0.225}$	$21.35\pm^{0.256}_{0.335}$	$21.18\pm^{0.775}_{1.859}$
HIPEQ1124+03	$23.87\pm^{0.018}_{0.017}$	$23.51\pm^{0.029}_{0.029}$	$23.30\pm^{0.015}_{0.015}$	$23.19\pm^{0.014}_{0.014}$	$22.45\pm^{0.015}_{0.014}$	$21.71\pm^{0.389}_{0.606}$	$20.82\pm^{0.070}_{0.075}$	$20.52\pm^{0.079}_{0.085}$	$20.37\pm^{0.113}_{0.126}$	$20.26\pm^{0.341}_{0.494}$
HIPEQ1127-01	$23.66\pm^{0.093}_{0.083}$	$22.77\pm^{0.048}_{0.047}$	$22.53\pm^{0.045}_{0.044}$	$22.44\pm^{0.043}_{0.042}$	$22.33\pm^{0.041}_{0.037}$	$21.59\pm^{0.220}_{0.275}$	$21.01\pm^{0.077}_{0.083}$	$20.84\pm^{0.086}_{0.094}$	$20.81\pm^{0.134}_{0.153}$	$20.77\pm^{0.393}_{0.601}$
HIPEQ1131-02	$23.50\pm^{0.043}_{0.041}$	$22.28\pm^{0.032}_{0.032}$	$21.69\pm^{0.035}_{0.034}$	$21.38\pm^{0.036}_{0.035}$	$21.35\pm^{0.035}_{0.034}$	$21.48\pm^{0.263}_{0.347}$	$19.83\pm^{0.026}_{0.027}$	$19.05\pm^{0.020}_{0.020}$	$18.65\pm^{0.022}_{0.022}$	$18.35\pm^{0.071}_{0.076}$
HIPEQ1133-03	$23.92\pm^{0.059}_{0.052}$	$23.26\pm^{0.041}_{0.040}$	$22.90\pm^{0.043}_{0.042}$	$22.74\pm^{0.042}_{0.041}$	$22.31\pm^{0.038}_{0.035}$	$23.12\pm^{0.762}_{1.601}$	$21.90\pm^{0.175}_{0.209}$	$21.47\pm^{0.160}_{0.187}$	$21.21\pm^{0.199}_{0.243}$	$21.09\pm^{0.515}_{0.904}$
HIPEQ1136+00	$21.84\pm^{0.124}_{0.118}$	$21.31\pm^{0.108}_{0.103}$	$21.50\pm^{0.095}_{0.091}$	$21.71\pm^{0.085}_{0.082}$	$21.53\pm^{0.083}_{0.078}$	$20.77\pm^{0.112}_{0.125}$	$20.28\pm^{0.034}_{0.035}$	$20.26\pm^{0.051}_{0.053}$	$20.33\pm^{0.089}_{0.096}$	$20.34\pm^{0.270}_{0.357}$
HIPEQ1138+03	$23.30\pm^{0.118}_{0.108}$	$21.87\pm^{0.071}_{0.069}$	$21.00\pm^{0.081}_{0.078}$	$20.60\pm^{0.085}_{0.082}$	$20.06\pm^{0.104}_{0.100}$	$20.08\pm^{0.099}_{0.109}$	$18.92\pm^{0.014}_{0.014}$	$18.22\pm^{0.011}_{0.011}$	$17.89\pm^{0.013}_{0.013}$	$17.59\pm^{0.034}_{0.036}$
HIPEQ1143-01	$24.32\pm^{0.093}_{0.066}$	$24.37\pm^{0.061}_{0.056}$	$24.10\pm^{0.064}_{0.059}$	$23.87\pm^{0.090}_{0.074}$	$22.67\pm^{0.298}_{0.076}$	$24.18\pm^{1.381}_{1.789}$	$23.85\pm^{0.618}_{1.077}$	$23.36\pm^{0.655}_{1.275}$	$23.19\pm^{0.833}_{1.651}$	$22.25\pm^{1.068}_{1.543}$
HIPEQ1145+02	$24.41\pm^{0.148}_{0.050}$	$24.68\pm^{0.073}_{0.058}$	$24.47\pm^{0.055}_{0.045}$	$24.08\pm^{0.080}_{0.058}$	$22.79\pm^{0.007}_{0.001}$	$24.58\pm^{1.803}_{1.706}$	$24.30\pm^{0.940}_{1.488}$	$23.75\pm^{0.911}_{1.695}$	$23.69\pm^{1.202}_{1.847}$	$22.58\pm^{1.466}_{1.699}$
HIPEQ1148-02	$24.12\pm^{0.039}_{0.035}$	$23.60\pm^{0.024}_{0.024}$	$23.15\pm^{0.027}_{0.026}$	$23.05\pm^{0.024}_{0.024}$	$22.35\pm^{0.049}_{0.043}$	$21.43\pm^{0.234}_{0.299}$	$20.56\pm^{0.048}_{0.051}$	$20.14\pm^{0.050}_{0.052}$	$19.94\pm^{0.070}_{0.075}$	$19.81\pm^{0.196}_{0.238}$
HIPEQ1151-02	$22.84\pm^{0.103}_{0.097}$	$21.83\pm^{0.099}_{0.094}$	$21.23\pm^{0.108}_{0.104}$	$20.93\pm^{0.115}_{0.109}$	$20.67\pm^{0.126}_{0.119}$	$21.57\pm^{0.230}_{0.292}$	$20.37\pm^{0.038}_{0.039}$	$19.78\pm^{0.036}_{0.037}$	$19.50\pm^{0.044}_{0.046}$	$19.25\pm^{0.133}_{0.151}$
HIPEQ1152+01	$23.11\pm^{0.056}_{0.054}$	$22.18\pm^{0.056}_{0.054}$	$21.83\pm^{0.056}_{0.055}$	$21.62\pm^{0.056}_{0.055}$	$21.41\pm^{0.057}_{0.055}$	$20.05\pm^{0.098}_{0.107}$	$19.45\pm^{0.021}_{0.021}$	$19.08\pm^{0.022}_{0.023}$	$18.98\pm^{0.032}_{0.033}$	$18.84\pm^{0.103}_{0.114}$
HIPEQ1152-02	$20.85\pm^{0.145}_{0.136}$	$20.45\pm^{0.133}_{0.125}$	$20.67\pm^{0.119}_{0.113}$	$21.06\pm^{0.109}_{0.104}$	$21.02\pm^{0.113}_{0.107}$	$20.04\pm^{0.076}_{0.082}$	$19.53\pm^{0.019}_{0.020}$	$19.66\pm^{0.033}_{0.034}$	$20.03\pm^{0.072}_{0.077}$	$20.09\pm^{0.307}_{0.427}$
HIPEQ1152-03b	$23.81\pm^{0.077}_{0.069}$	$23.08\pm^{0.041}_{0.041}$	$22.85\pm^{0.041}_{0.040}$	$22.74\pm^{0.040}_{0.039}$	$22.26\pm^{0.063}_{0.055}$	$22.96\pm^{0.737}_{1.665}$	$22.04\pm^{0.204}_{0.252}$	$21.73\pm^{0.201}_{0.246}$	$21.68\pm^{0.297}_{0.408}$	$21.31\pm^{0.627}_{1.218}$
HIPEQ1155+01	$24.09\pm^{0.018}_{0.017}$	$23.37\pm^{0.019}_{0.018}$	$22.84\pm^{0.020}_{0.020}$	$22.53\pm^{0.021}_{0.021}$	$22.08\pm^{0.015}_{0.015}$	$21.86\pm^{0.307}_{0.427}$	$20.63\pm^{0.046}_{0.049}$	$20.10\pm^{0.044}_{0.046}$	$19.84\pm^{0.055}_{0.058}$	$19.59\pm^{0.147}_{0.170}$
HIPEQ1200-00	$24.36\pm^{0.042}_{0.031}$	$24.29\pm^{0.022}_{0.021}$	$23.90\pm^{0.025}_{0.024}$	$23.58\pm^{0.058}_{0.054}$	$22.69\pm^{0.030}_{0.022}$	$22.33\pm^{0.398}_{0.619}$	$21.86\pm^{0.137}_{0.156}$	$21.59\pm^{0.163}_{0.191}$	$21.47\pm^{0.218}_{0.272}$	$21.50\pm^{0.659}_{1.236}$
HIPEQ1200-01	$22.05\pm^{0.020}_{0.020}$	$20.56\pm^{0.023}_{0.022}$	$19.74\pm^{0.025}_{0.025}$	$19.34\pm^{0.026}_{0.025}$	$18.99\pm^{0.028}_{0.027}$	$19.73\pm^{0.049}_{0.051}$	$17.97\pm^{0.007}_{0.007}$	$17.16\pm^{0.004}_{0.004}$	$16.73\pm^{0.004}_{0.004}$	$16.41\pm^{0.010}_{0.010}$
HIPEQ1202+01	$22.85\pm^{0.064}_{0.062}$	$21.13\pm^{0.036}_{0.036}$	$20.28\pm^{0.038}_{0.038}$	$19.84\pm^{0.039}_{0.039}$	$19.48\pm^{0.042}_{0.041}$	$19.91\pm^{0.087}_{0.095}$	$18.15\pm^{0.008}_{0.008}$	$17.28\pm^{0.005}_{0.005}$	$16.80\pm^{0.005}_{0.005}$	$16.38\pm^{0.012}_{0.013}$
HIPEQ1204-01	$24.26\pm^{0.044}_{0.037}$	$24.17\pm^{0.031}_{0.030}$	$23.86\pm^{0.057}_{0.053}$	$23.57\pm^{0.059}_{0.055}$	$22.57\pm^{0.062}_{0.047}$	$24.10\pm^{1.441}_{1.924}$	$23.45\pm^{0.509}_{0.870}$	$23.07\pm^{0.558}_{1.040}$	$22.81\pm^{0.693}_{1.470}$	$22.48\pm^{1.226}_{1.524}$

Table 3.9—Continued

	$\Sigma_{face-on}$					Σ_{fiber}				
HIPASS Name	u^a	g^a	r^a	i^a	z^a	u^a	g^a	r^a	i^a	z^a
HIPEQ1204-02	$23.50\pm^{0.097}_{0.088}$	$22.00\pm^{0.065}_{0.063}$	$21.04\pm^{0.075}_{0.073}$	$20.56\pm^{0.081}_{0.078}$	$20.23\pm^{0.088}_{0.085}$	$20.51\pm^{0.112}_{0.124}$	$19.03\pm^{0.014}_{0.014}$	$18.27\pm^{0.010}_{0.010}$	$17.85\pm^{0.011}_{0.011}$	$17.54\pm^{0.032}_{0.032}$
HIPEQ1210+02	$24.29\pm^{0.129}_{0.071}$	$24.05\pm^{0.061}_{0.057}$	$23.66\pm^{0.068}_{0.064}$	$23.41\pm^{0.094}_{0.084}$	$22.51\pm^{0.125}_{0.080}$	$23.97\pm^{1.534}_{2.207}$	$23.01\pm^{0.409}_{0.640}$	$22.63\pm^{0.441}_{0.727}$	$22.38\pm^{0.540}_{1.025}$	$21.88\pm^{1.003}_{1.827}$
HIPEQ1215+04a	$23.25\pm^{0.126}_{0.115}$	$22.31\pm^{0.069}_{0.067}$	$22.16\pm^{0.065}_{0.064}$	$22.02\pm^{0.066}_{0.064}$	$21.80\pm^{0.060}_{0.057}$	$21.66\pm^{0.274}_{0.366}$	$20.61\pm^{0.050}_{0.052}$	$20.38\pm^{0.062}_{0.065}$	$20.27\pm^{0.086}_{0.093}$	$20.19\pm^{0.294}_{0.402}$
HIPEQ1216-03	$23.48\pm^{0.045}_{0.043}$	$22.20\pm^{0.063}_{0.061}$	$21.61\pm^{0.068}_{0.066}$	$21.32\pm^{0.071}_{0.069}$	$21.19\pm^{0.067}_{0.064}$	$21.81\pm^{0.337}_{0.488}$	$20.42\pm^{0.053}_{0.055}$	$19.79\pm^{0.039}_{0.041}$	$19.43\pm^{0.046}_{0.048}$	$19.24\pm^{0.130}_{0.148}$
HIPEQ1218+00	$24.36\pm^{0.030}_{0.024}$	$24.29\pm^{0.038}_{0.036}$	$23.90\pm^{0.024}_{0.024}$	$23.64\pm^{0.024}_{0.024}$	$22.59\pm^{0.045}_{0.035}$	$23.78\pm^{1.025}_{1.649}$	$23.02\pm^{0.350}_{0.507}$	$22.61\pm^{0.362}_{0.535}$	$22.50\pm^{0.511}_{0.911}$	$22.07\pm^{0.859}_{1.337}$
HIPEQ1218-01	$23.11\pm^{0.065}_{0.063}$	$21.73\pm^{0.071}_{0.069}$	$21.02\pm^{0.075}_{0.073}$	$20.64\pm^{0.078}_{0.075}$	$20.29\pm^{0.086}_{0.083}$	$21.30\pm^{0.184}_{0.221}$	$19.88\pm^{0.030}_{0.031}$	$19.09\pm^{0.019}_{0.019}$	$18.72\pm^{0.021}_{0.021}$	$18.41\pm^{0.052}_{0.055}$
HIPEQ1219+03	$21.88\pm^{0.094}_{0.090}$	$21.44\pm^{0.074}_{0.071}$	$21.29\pm^{0.067}_{0.065}$	$21.35\pm^{0.062}_{0.061}$	$21.20\pm^{0.062}_{0.060}$	$19.82\pm^{0.056}_{0.059}$	$19.34\pm^{0.020}_{0.020}$	$19.18\pm^{0.022}_{0.022}$	$19.74\pm^{0.056}_{0.059}$	$19.55\pm^{0.160}_{0.188}$
HIPEQ1220+00	$24.11\pm^{0.047}_{0.041}$	$23.87\pm^{0.041}_{0.039}$	$23.66\pm^{0.042}_{0.040}$	$23.49\pm^{0.037}_{0.035}$	$22.57\pm^{0.042}_{0.034}$	$23.32\pm^{0.832}_{1.692}$	$22.33\pm^{0.200}_{0.244}$	$22.21\pm^{0.269}_{0.357}$	$22.04\pm^{0.340}_{0.490}$	$22.06\pm^{1.032}_{1.679}$
HIPEQ1220+01	$24.27\pm^{0.031}_{0.027}$	$23.95\pm^{0.026}_{0.025}$	$23.52\pm^{0.028}_{0.027}$	$23.24\pm^{0.027}_{0.027}$	$22.44\pm^{0.026}_{0.024}$	$22.46\pm^{0.570}_{1.159}$	$21.20\pm^{0.108}_{0.119}$	$20.67\pm^{0.087}_{0.094}$	$20.37\pm^{0.112}_{0.124}$	$20.19\pm^{0.328}_{0.469}$
HIPEQ1221+03	$24.28\pm^{0.028}_{0.025}$	$23.13\pm^{0.032}_{0.031}$	$22.15\pm^{0.037}_{0.036}$	$21.53\pm^{0.040}_{0.039}$	$20.99\pm^{0.044}_{0.043}$	$21.76\pm^{0.369}_{0.558}$	$19.93\pm^{0.030}_{0.031}$	$18.94\pm^{0.019}_{0.019}$	$18.43\pm^{0.020}_{0.020}$	$17.98\pm^{0.050}_{0.053}$
HIPEQ1223+00	$24.23\pm^{0.049}_{0.041}$	$24.05\pm^{0.065}_{0.061}$	$23.82\pm^{0.062}_{0.058}$	$23.58\pm^{0.084}_{0.074}$	$22.62\pm^{0.046}_{0.035}$	$22.95\pm^{0.624}_{1.237}$	$22.35\pm^{0.206}_{0.254}$	$22.17\pm^{0.254}_{0.330}$	$22.15\pm^{0.393}_{0.606}$	$21.91\pm^{0.779}_{1.294}$
HIPEQ1223-03b	$23.52\pm^{0.022}_{0.022}$	$22.11\pm^{0.029}_{0.029}$	$21.23\pm^{0.031}_{0.031}$	$20.83\pm^{0.031}_{0.031}$	$20.42\pm^{0.034}_{0.033}$	$21.06\pm^{0.164}_{0.193}$	$19.32\pm^{0.019}_{0.020}$	$18.40\pm^{0.012}_{0.012}$	$18.01\pm^{0.013}_{0.014}$	$17.64\pm^{0.033}_{0.034}$
HIPEQ1224+00	$24.24\pm^{0.147}_{0.087}$	$23.99\pm^{0.081}_{0.076}$	$23.73\pm^{0.146}_{0.127}$	$23.52\pm^{0.076}_{0.070}$	$22.55\pm^{0.175}_{0.095}$	$23.96\pm^{1.185}_{1.702}$	$23.38\pm^{0.454}_{0.727}$	$23.08\pm^{0.517}_{0.906}$	$23.00\pm^{0.683}_{1.321}$	$22.22\pm^{1.132}_{1.667}$
HIPEQ1224+03b	$23.52\pm^{0.097}_{0.089}$	$22.73\pm^{0.039}_{0.039}$	$22.37\pm^{0.040}_{0.040}$	$22.28\pm^{0.040}_{0.039}$	$21.97\pm^{0.087}_{0.078}$	$21.71\pm^{0.316}_{0.445}$	$20.63\pm^{0.053}_{0.056}$	$20.24\pm^{0.057}_{0.060}$	$20.04\pm^{0.085}_{0.092}$	$19.98\pm^{0.264}_{0.349}$
HIPEQ1225+00	$22.41\pm^{0.044}_{0.043}$	$21.48\pm^{0.040}_{0.039}$	$20.82\pm^{0.042}_{0.041}$	$20.61\pm^{0.041}_{0.040}$	$20.42\pm^{0.041}_{0.040}$	$17.99\pm^{0.013}_{0.013}$	$17.51\pm^{0.004}_{0.004}$	$16.96\pm^{0.004}_{0.004}$	$17.12\pm^{0.006}_{0.006}$	$16.84\pm^{0.013}_{0.013}$
HIPEQ1226+02	$22.32\pm^{0.039}_{0.038}$	$21.27\pm^{0.038}_{0.038}$	$20.79\pm^{0.039}_{0.038}$	$20.58\pm^{0.039}_{0.038}$	$20.34\pm^{0.041}_{0.040}$	$20.97\pm^{0.185}_{0.222}$	$19.63\pm^{0.023}_{0.024}$	$19.04\pm^{0.020}_{0.021}$	$18.73\pm^{0.025}_{0.026}$	$18.48\pm^{0.081}_{0.088}$
HIPEQ1227+01	$24.25\pm^{0.216}_{0.109}$	$24.26\pm^{0.118}_{0.101}$	$24.17\pm^{0.090}_{0.077}$	$23.99\pm^{0.074}_{0.059}$	$22.70\pm^{0.093}_{0.043}$	$23.69\pm^{1.184}_{2.104}$	$23.40\pm^{0.612}_{1.222}$	$23.13\pm^{0.620}_{1.246}$	$23.12\pm^{0.894}_{1.889}$	$22.24\pm^{1.206}_{1.766}$
HIPEQ1228+02	$24.35\pm^{0.028}_{0.024}$	$24.23\pm^{0.017}_{0.017}$	$23.88\pm^{0.034}_{0.033}$	$23.59\pm^{0.032}_{0.031}$	$22.61\pm^{0.045}_{0.034}$	$23.38\pm^{1.068}_{2.306}$	$22.37\pm^{0.236}_{0.300}$	$22.00\pm^{0.262}_{0.344}$	$21.75\pm^{0.337}_{0.488}$	$21.82\pm^{1.111}_{2.150}$
HIPEQ1228+03	$21.51\pm^{0.041}_{0.041}$	$19.75\pm^{0.042}_{0.042}$	$18.96\pm^{0.044}_{0.043}$	$18.59\pm^{0.044}_{0.043}$	$18.27\pm^{0.046}_{0.046}$	$18.14\pm^{0.019}_{0.020}$	$16.41\pm^{0.002}_{0.002}$	$15.65\pm^{0.002}_{0.002}$	$15.27\pm^{0.002}_{0.002}$	$14.94\pm^{0.004}_{0.004}$
HIPEQ1229+00	$24.32\pm^{0.082}_{0.055}$	$24.32\pm^{0.039}_{0.036}$	$24.04\pm^{0.036}_{0.034}$	$23.79\pm^{0.033}_{0.031}$	$22.64\pm^{0.052}_{0.037}$	$23.31\pm^{0.857}_{1.796}$	$22.54\pm^{0.235}_{0.298}$	$22.13\pm^{0.244}_{0.313}$	$22.08\pm^{0.353}_{0.517}$	$21.95\pm^{0.809}_{1.339}$
HIPEQ1230+02	$24.13\pm^{0.063}_{0.054}$	$23.59\pm^{0.047}_{0.046}$	$23.31\pm^{0.051}_{0.049}$	$23.15\pm^{0.050}_{0.049}$	$22.42\pm^{0.104}_{0.079}$	$23.48\pm^{1.133}_{2.310}$	$22.69\pm^{0.307}_{0.424}$	$22.35\pm^{0.349}_{0.511}$	$22.26\pm^{0.498}_{0.896}$	$22.28\pm^{1.394}_{1.997}$
HIPEQ1230+03	$22.30\pm^{0.157}_{0.148}$	$21.70\pm^{0.135}_{0.127}$	$21.52\pm^{0.136}_{0.128}$	$21.40\pm^{0.138}_{0.130}$	$21.30\pm^{0.142}_{0.132}$	$21.09\pm^{0.224}_{0.282}$	$20.46\pm^{0.048}_{0.050}$	$20.32\pm^{0.063}_{0.066}$	$20.28\pm^{0.102}_{0.112}$	$20.17\pm^{0.318}_{0.448}$
HIPEQ1232+00a	$24.11\pm^{0.018}_{0.017}$	$23.65\pm^{0.014}_{0.014}$	$23.23\pm^{0.015}_{0.014}$	$22.96\pm^{0.015}_{0.015}$	$22.42\pm^{0.022}_{0.021}$	$23.32\pm^{0.830}_{1.696}$	$21.60\pm^{0.106}_{0.118}$	$21.10\pm^{0.107}_{0.118}$	$20.88\pm^{0.133}_{0.151}$	$20.72\pm^{0.449}_{0.748}$
HIPEQ1232+00b	$24.31\pm^{0.002}_{0.002}$	$24.00\pm^{0.004}_{0.004}$	$23.35\pm^{0.005}_{0.005}$	$22.90\pm^{0.005}_{0.005}$	$22.22\pm^{0.003}_{0.003}$	$22.75\pm^{0.580}_{1.140}$	$21.15\pm^{0.073}_{0.078}$	$20.30\pm^{0.052}_{0.054}$	$19.82\pm^{0.052}_{0.055}$	$19.43\pm^{0.160}_{0.188}$
HIPEQ1233-02	$24.29\pm^{0.030}_{0.025}$	$24.37\pm^{0.028}_{0.026}$	$24.06\pm^{0.029}_{0.028}$	$23.77\pm^{0.047}_{0.042}$	$22.68\pm^{0.025}_{0.019}$	$23.91\pm^{1.166}_{1.694}$	$23.39\pm^{0.487}_{0.811}$	$22.77\pm^{0.476}_{0.817}$	$22.67\pm^{0.643}_{1.337}$	$22.03\pm^{1.085}_{1.788}$
HIPEQ1236+03	$24.26\pm^{0.063}_{0.049}$	$24.15\pm^{0.035}_{0.034}$	$23.86\pm^{0.036}_{0.035}$	$23.62\pm^{0.034}_{0.033}$	$22.61\pm^{0.061}_{0.043}$	$23.26\pm^{0.950}_{2.119}$	$22.48\pm^{0.266}_{0.351}$	$22.25\pm^{0.323}_{0.457}$	$22.08\pm^{0.466}_{0.805}$	$21.80\pm^{0.943}_{1.781}$
HIPEQ1239-00	$23.32\pm^{0.016}_{0.015}$	$22.52\pm^{0.017}_{0.017}$	$22.15\pm^{0.017}_{0.017}$	$21.96\pm^{0.018}_{0.017}$	$21.68\pm^{0.015}_{0.015}$	$21.35\pm^{0.200}_{0.245}$	$20.29\pm^{0.035}_{0.036}$	$19.88\pm^{0.037}_{0.038}$	$19.66\pm^{0.045}_{0.047}$	$19.50\pm^{0.132}_{0.150}$
HIPEQ1241+01	$22.23\pm^{0.116}_{0.111}$	$21.22\pm^{0.108}_{0.103}$	$20.88\pm^{0.103}_{0.099}$	$20.72\pm^{0.099}_{0.095}$	$20.61\pm^{0.099}_{0.094}$	$21.01\pm^{0.179}_{0.215}$	$19.96\pm^{0.037}_{0.038}$	$19.62\pm^{0.035}_{0.036}$	$19.44\pm^{0.049}_{0.051}$	$19.31\pm^{0.155}_{0.181}$
HIPEQ1241-02	$23.19\pm^{0.064}_{0.062}$	$22.40\pm^{0.058}_{0.057}$	$22.00\pm^{0.057}_{0.056}$	$21.87\pm^{0.054}_{0.052}$	$21.57\pm^{0.051}_{0.049}$	$21.25\pm^{0.218}_{0.273}$	$20.39\pm^{0.041}_{0.043}$	$20.03\pm^{0.050}_{0.052}$	$19.83\pm^{0.065}_{0.070}$	$19.65\pm^{0.195}_{0.237}$
HIPEQ1242+03b	$22.80\pm^{0.034}_{0.034}$	$21.79\pm^{0.033}_{0.033}$	$21.27\pm^{0.033}_{0.032}$	$21.07\pm^{0.031}_{0.031}$	$20.93\pm^{0.031}_{0.030}$	$19.54\pm^{0.047}_{0.049}$	$19.18\pm^{0.018}_{0.018}$	$18.70\pm^{0.014}_{0.014}$	$18.87\pm^{0.023}_{0.023}$	$18.69\pm^{0.062}_{0.065}$
HIPEQ1242-00	$23.00\pm^{0.021}_{0.020}$	$21.97\pm^{0.022}_{0.021}$	$21.49\pm^{0.022}_{0.022}$	$21.23\pm^{0.022}_{0.022}$	$21.02\pm^{0.022}_{0.021}$	$21.63\pm^{0.233}_{0.296}$	$20.45\pm^{0.040}_{0.041}$	$19.93\pm^{0.038}_{0.039}$	$19.66\pm^{0.045}_{0.047}$	$19.43\pm^{0.131}_{0.149}$

Table 3.9—Continued

	$\Sigma_{face-on}$					Σ_{fiber}				
HIPASS Name	u^a	g^a	r^a	i^a	z^a	u^a	g^a	r^a	i^a	z^a
HIPEQ1242-01a	$23.25\pm^{0.040}_{0.039}$	$22.15\pm^{0.047}_{0.047}$	$21.84\pm^{0.048}_{0.047}$	$21.66\pm^{0.048}_{0.047}$	$21.57\pm^{0.042}_{0.041}$	$21.80\pm^{0.344}_{0.503}$	$20.74\pm^{0.057}_{0.060}$	$20.44\pm^{0.071}_{0.076}$	$20.32\pm^{0.105}_{0.116}$	$20.19\pm^{0.308}_{0.427}$
HIPEQ1242-01b	$24.01\pm^{0.024}_{0.022}$	$23.27\pm^{0.025}_{0.025}$	$22.65\pm^{0.028}_{0.028}$	$22.29\pm^{0.030}_{0.029}$	$21.83\pm^{0.027}_{0.026}$	$22.33\pm^{0.513}_{0.947}$	$20.73\pm^{0.056}_{0.060}$	$20.02\pm^{0.049}_{0.052}$	$19.65\pm^{0.058}_{0.062}$	$19.29\pm^{0.148}_{0.171}$
HIPEQ1243-00	$23.62\pm^{0.029}_{0.028}$	$22.49\pm^{0.022}_{0.022}$	$21.90\pm^{0.024}_{0.024}$	$21.55\pm^{0.025}_{0.025}$	$21.37\pm^{0.024}_{0.023}$	$21.52\pm^{0.233}_{0.297}$	$20.08\pm^{0.029}_{0.030}$	$19.40\pm^{0.025}_{0.025}$	$19.04\pm^{0.026}_{0.027}$	$18.80\pm^{0.071}_{0.076}$
HIPEQ1244+00	$24.23\pm^{0.019}_{0.018}$	$23.97\pm^{0.014}_{0.014}$	$23.55\pm^{0.016}_{0.016}$	$23.01\pm^{0.028}_{0.028}$	$22.47\pm^{0.027}_{0.024}$	$22.57\pm^{0.478}_{0.822}$	$21.70\pm^{0.117}_{0.131}$	$21.36\pm^{0.128}_{0.145}$	$21.15\pm^{0.175}_{0.208}$	$21.16\pm^{0.481}_{0.799}$
HIPEQ1244-02	$24.12\pm^{0.077}_{0.060}$	$23.72\pm^{0.036}_{0.035}$	$23.47\pm^{0.037}_{0.036}$	$23.19\pm^{0.072}_{0.067}$	$22.45\pm^{0.144}_{0.093}$	$22.69\pm^{0.631}_{1.352}$	$21.79\pm^{0.136}_{0.156}$	$21.53\pm^{0.171}_{0.202}$	$21.44\pm^{0.252}_{0.328}$	$21.36\pm^{0.796}_{1.801}$
HIPEQ1245-00	$23.27\pm^{0.012}_{0.012}$	$21.74\pm^{0.016}_{0.015}$	$20.77\pm^{0.017}_{0.017}$	$20.21\pm^{0.019}_{0.018}$	$19.68\pm^{0.021}_{0.021}$	$20.72\pm^{0.121}_{0.136}$	$19.02\pm^{0.012}_{0.013}$	$18.16\pm^{0.009}_{0.009}$	$17.73\pm^{0.009}_{0.009}$	$17.38\pm^{0.021}_{0.021}$
HIPEQ1249+03	$21.93\pm^{0.047}_{0.046}$	$20.84\pm^{0.047}_{0.046}$	$20.32\pm^{0.051}_{0.050}$	$20.11\pm^{0.051}_{0.050}$	$19.88\pm^{0.055}_{0.054}$	$20.13\pm^{0.102}_{0.112}$	$18.99\pm^{0.014}_{0.014}$	$18.45\pm^{0.013}_{0.013}$	$18.20\pm^{0.017}_{0.017}$	$17.92\pm^{0.046}_{0.048}$
HIPEQ1249+04	$24.07\pm^{0.070}_{0.058}$	$23.60\pm^{0.042}_{0.041}$	$23.36\pm^{0.043}_{0.042}$	$23.18\pm^{0.043}_{0.041}$	$22.55\pm^{0.070}_{0.050}$	$22.91\pm^{0.684}_{1.458}$	$21.73\pm^{0.147}_{0.170}$	$21.48\pm^{0.168}_{0.198}$	$21.34\pm^{0.241}_{0.309}$	$21.60\pm^{0.636}_{1.117}$
HIPEQ1250+05	$22.36\pm^{0.025}_{0.025}$	$21.45\pm^{0.027}_{0.026}$	$21.06\pm^{0.028}_{0.027}$	$20.88\pm^{0.028}_{0.028}$	$20.79\pm^{0.028}_{0.027}$	$20.59\pm^{0.128}_{0.145}$	$19.40\pm^{0.018}_{0.018}$	$18.94\pm^{0.017}_{0.017}$	$18.71\pm^{0.019}_{0.020}$	$18.54\pm^{0.071}_{0.076}$
HIPEQ1253+01	$23.88\pm^{0.021}_{0.020}$	$22.64\pm^{0.019}_{0.019}$	$21.87\pm^{0.020}_{0.020}$	$21.47\pm^{0.021}_{0.020}$	$21.16\pm^{0.021}_{0.020}$	$21.66\pm^{0.303}_{0.420}$	$20.01\pm^{0.038}_{0.039}$	$19.23\pm^{0.025}_{0.025}$	$18.84\pm^{0.028}_{0.029}$	$18.60\pm^{0.084}_{0.091}$
HIPEQ1253+02	$23.27\pm^{0.038}_{0.037}$	$21.26\pm^{0.026}_{0.026}$	$20.42\pm^{0.027}_{0.027}$	$19.97\pm^{0.028}_{0.028}$	$19.70\pm^{0.029}_{0.029}$	$19.87\pm^{0.077}_{0.083}$	$17.85\pm^{0.006}_{0.006}$	$16.87\pm^{0.004}_{0.004}$	$16.40\pm^{0.004}_{0.004}$	$16.02\pm^{0.010}_{0.010}$
HIPEQ1253+04	$20.49\pm^{0.109}_{0.105}$	$19.95\pm^{0.093}_{0.089}$	$19.75\pm^{0.089}_{0.086}$	$19.79\pm^{0.083}_{0.080}$	$19.65\pm^{0.087}_{0.084}$	$18.86\pm^{0.034}_{0.035}$	$18.14\pm^{0.007}_{0.007}$	$17.99\pm^{0.008}_{0.008}$	$17.97\pm^{0.010}_{0.010}$	$17.86\pm^{0.030}_{0.031}$
HIPEQ1255+00	$23.57\pm^{0.017}_{0.017}$	$22.67\pm^{0.020}_{0.020}$	$22.24\pm^{0.020}_{0.020}$	$22.01\pm^{0.020}_{0.020}$	$21.73\pm^{0.020}_{0.019}$	$20.88\pm^{0.135}_{0.154}$	$19.87\pm^{0.024}_{0.025}$	$19.45\pm^{0.025}_{0.025}$	$19.24\pm^{0.031}_{0.032}$	$19.04\pm^{0.114}_{0.127}$
HIPEQ1255+02	$22.40\pm^{0.071}_{0.069}$	$20.88\pm^{0.072}_{0.070}$	$19.97\pm^{0.080}_{0.077}$	$19.53\pm^{0.083}_{0.080}$	$19.19\pm^{0.087}_{0.084}$	$20.36\pm^{0.114}_{0.127}$	$18.45\pm^{0.010}_{0.010}$	$17.56\pm^{0.006}_{0.006}$	$17.13\pm^{0.007}_{0.007}$	$16.82\pm^{0.018}_{0.018}$
HIPEQ1255-00	$24.33\pm^{0.029}_{0.024}$	$24.45\pm^{0.019}_{0.018}$	$24.19\pm^{0.017}_{0.017}$	$23.90\pm^{0.025}_{0.024}$	$22.68\pm^{0.023}_{0.018}$	$23.63\pm^{0.954}_{1.673}$	$22.66\pm^{0.260}_{0.339}$	$22.34\pm^{0.290}_{0.393}$	$22.27\pm^{0.398}_{0.615}$	$21.88\pm^{0.814}_{1.401}$
HIPEQ1256+03	$24.23\pm^{0.078}_{0.057}$	$24.00\pm^{0.082}_{0.076}$	$23.83\pm^{0.082}_{0.075}$	$23.64\pm^{0.104}_{0.088}$	$22.66\pm^{0.241}_{0.065}$	$23.74\pm^{1.328}_{2.206}$	$22.76\pm^{0.348}_{0.507}$	$22.65\pm^{0.426}_{0.686}$	$22.77\pm^{0.620}_{1.210}$	$22.18\pm^{1.020}_{1.514}$
HIPEQ1257+02	$23.97\pm^{0.072}_{0.062}$	$23.47\pm^{0.047}_{0.046}$	$23.19\pm^{0.048}_{0.047}$	$23.04\pm^{0.088}_{0.082}$	$22.38\pm^{0.113}_{0.085}$	$23.36\pm^{1.078}_{2.284}$	$22.28\pm^{0.223}_{0.280}$	$21.92\pm^{0.250}_{0.324}$	$21.71\pm^{0.342}_{0.497}$	$21.37\pm^{0.883}_{2.107}$
HIPEQ1257-01	$23.72\pm^{0.025}_{0.024}$	$22.72\pm^{0.035}_{0.034}$	$22.05\pm^{0.038}_{0.037}$	$21.74\pm^{0.039}_{0.038}$	$21.36\pm^{0.041}_{0.040}$	$21.56\pm^{0.225}_{0.284}$	$20.29\pm^{0.035}_{0.036}$	$19.43\pm^{0.027}_{0.028}$	$19.05\pm^{0.034}_{0.035}$	$18.76\pm^{0.086}_{0.093}$
HIPEQ1258+02	$24.22\pm^{0.054}_{0.043}$	$23.82\pm^{0.023}_{0.022}$	$23.46\pm^{0.024}_{0.024}$	$23.23\pm^{0.024}_{0.023}$	$22.52\pm^{0.041}_{0.035}$	$21.68\pm^{0.349}_{0.513}$	$20.91\pm^{0.069}_{0.074}$	$20.62\pm^{0.083}_{0.090}$	$20.44\pm^{0.119}_{0.134}$	$20.22\pm^{0.401}_{0.635}$
HIPEQ1300+02a	$22.82\pm^{0.178}_{0.164}$	$22.35\pm^{0.063}_{0.061}$	$22.16\pm^{0.057}_{0.056}$	$22.25\pm^{0.051}_{0.050}$	$21.94\pm^{0.112}_{0.098}$	$21.87\pm^{0.389}_{0.606}$	$21.19\pm^{0.091}_{0.099}$	$20.93\pm^{0.109}_{0.121}$	$21.02\pm^{0.190}_{0.231}$	$20.83\pm^{0.558}_{1.096}$
HIPEQ1300+02b	$22.30\pm^{0.024}_{0.024}$	$21.34\pm^{0.024}_{0.023}$	$20.93\pm^{0.024}_{0.023}$	$20.71\pm^{0.023}_{0.023}$	$20.60\pm^{0.023}_{0.023}$	$19.47\pm^{0.057}_{0.060}$	$18.43\pm^{0.009}_{0.009}$	$18.11\pm^{0.010}_{0.010}$	$17.93\pm^{0.013}_{0.013}$	$17.74\pm^{0.049}_{0.051}$
HIPEQ1303+03	$23.85\pm^{0.050}_{0.046}$	$23.14\pm^{0.040}_{0.039}$	$22.76\pm^{0.042}_{0.041}$	$22.54\pm^{0.043}_{0.042}$	$22.16\pm^{0.053}_{0.048}$	$22.70\pm^{0.597}_{1.209}$	$21.35\pm^{0.113}_{0.127}$	$20.82\pm^{0.085}_{0.093}$	$20.60\pm^{0.103}_{0.114}$	$20.56\pm^{0.295}_{0.401}$
HIPEQ1304-02	$23.85\pm^{0.158}_{0.124}$	$22.87\pm^{0.096}_{0.092}$	$22.50\pm^{0.094}_{0.090}$	$22.27\pm^{0.100}_{0.095}$	$21.94\pm^{0.100}_{0.091}$	$22.67\pm^{0.621}_{1.324}$	$21.68\pm^{0.122}_{0.137}$	$21.29\pm^{0.146}_{0.169}$	$21.03\pm^{0.184}_{0.222}$	$21.03\pm^{0.565}_{1.082}$
HIPEQ1304-03	$23.93\pm^{0.019}_{0.018}$	$23.50\pm^{0.015}_{0.015}$	$23.17\pm^{0.016}_{0.016}$	$22.98\pm^{0.030}_{0.029}$	$22.39\pm^{0.022}_{0.021}$	$23.51\pm^{0.991}_{1.876}$	$22.46\pm^{0.285}_{0.385}$	$22.01\pm^{0.255}_{0.333}$	$21.82\pm^{0.341}_{0.495}$	$21.41\pm^{0.676}_{1.332}$
HIPEQ1307-00	$22.61\pm^{0.056}_{0.054}$	$21.58\pm^{0.058}_{0.056}$	$21.12\pm^{0.061}_{0.059}$	$20.89\pm^{0.063}_{0.061}$	$20.68\pm^{0.066}_{0.064}$	$21.14\pm^{0.154}_{0.180}$	$20.02\pm^{0.032}_{0.033}$	$19.49\pm^{0.026}_{0.027}$	$19.20\pm^{0.031}_{0.032}$	$19.03\pm^{0.088}_{0.095}$
HIPEQ1308-02	$23.30\pm^{0.046}_{0.044}$	$22.15\pm^{0.053}_{0.051}$	$21.61\pm^{0.056}_{0.054}$	$21.30\pm^{0.059}_{0.058}$	$21.20\pm^{0.056}_{0.055}$	$21.34\pm^{0.214}_{0.267}$	$20.22\pm^{0.035}_{0.036}$	$19.68\pm^{0.037}_{0.038}$	$19.45\pm^{0.048}_{0.050}$	$19.19\pm^{0.160}_{0.188}$
HIPEQ1311+03a	$23.38\pm^{0.160}_{0.140}$	$22.64\pm^{0.084}_{0.081}$	$22.16\pm^{0.092}_{0.088}$	$22.02\pm^{0.093}_{0.089}$	$21.72\pm^{0.085}_{0.079}$	$21.45\pm^{0.301}_{0.417}$	$20.67\pm^{0.058}_{0.061}$	$20.20\pm^{0.057}_{0.061}$	$20.03\pm^{0.083}_{0.089}$	$19.92\pm^{0.259}_{0.340}$
HIPEQ1312+03	$22.73\pm^{0.119}_{0.113}$	$21.35\pm^{0.108}_{0.103}$	$20.78\pm^{0.108}_{0.103}$	$20.38\pm^{0.114}_{0.109}$	$20.09\pm^{0.125}_{0.118}$	$20.44\pm^{0.120}_{0.134}$	$19.09\pm^{0.015}_{0.016}$	$18.50\pm^{0.013}_{0.013}$	$18.19\pm^{0.017}_{0.017}$	$17.93\pm^{0.046}_{0.048}$
HIPEQ1312+05	$24.29\pm^{0.095}_{0.055}$	$24.22\pm^{0.042}_{0.040}$	$23.92\pm^{0.084}_{0.075}$	$23.65\pm^{0.077}_{0.068}$	$22.66\pm^{0.105}_{0.047}$	$23.86\pm^{1.201}_{1.801}$	$23.03\pm^{0.398}_{0.612}$	$22.56\pm^{0.390}_{0.598}$	$22.09\pm^{0.427}_{0.694}$	$21.71\pm^{0.793}_{1.472}$
HIPEQ1313+06	$23.06\pm^{0.060}_{0.058}$	$21.68\pm^{0.061}_{0.060}$	$20.94\pm^{0.066}_{0.064}$	$20.59\pm^{0.069}_{0.067}$	$20.30\pm^{0.073}_{0.070}$	$20.85\pm^{0.165}_{0.195}$	$19.45\pm^{0.019}_{0.019}$	$18.79\pm^{0.015}_{0.015}$	$18.37\pm^{0.015}_{0.015}$	$18.09\pm^{0.038}_{0.039}$
HIPEQ1317-00	$24.02\pm^{0.028}_{0.026}$	$23.78\pm^{0.045}_{0.043}$	$23.57\pm^{0.046}_{0.044}$	$23.42\pm^{0.044}_{0.042}$	$22.56\pm^{0.042}_{0.034}$	$22.83\pm^{0.584}_{1.128}$	$21.90\pm^{0.165}_{0.194}$	$21.69\pm^{0.177}_{0.211}$	$21.64\pm^{0.260}_{0.340}$	$21.58\pm^{0.659}_{1.195}$

Table 3.9—Continued

	$\Sigma_{face-on}$					Σ_{fiber}				
HIPASS Name	u^a	g^a	r^a	i^a	z^a	u^a	g^a	r^a	i^a	z^a
HIPEQ1318-01	$23.72\pm^{0.047}_{0.044}$	$22.45\pm^{0.042}_{0.041}$	$21.86\pm^{0.044}_{0.043}$	$21.52\pm^{0.045}_{0.045}$	$21.30\pm^{0.043}_{0.042}$	$21.50\pm^{0.249}_{0.322}$	$20.08\pm^{0.030}_{0.031}$	$19.42\pm^{0.028}_{0.028}$	$19.02\pm^{0.033}_{0.034}$	$18.73\pm^{0.089}_{0.097}$
HIPEQ1320+05	$23.85\pm^{0.100}_{0.083}$	$23.52\pm^{0.039}_{0.038}$	$23.23\pm^{0.037}_{0.036}$	$23.14\pm^{0.033}_{0.032}$	$22.22\pm^{0.061}_{0.054}$	$22.22\pm^{0.543}_{1.073}$	$21.77\pm^{0.143}_{0.165}$	$21.49\pm^{0.173}_{0.206}$	$21.40\pm^{0.242}_{0.310}$	$20.74\pm^{0.620}_{1.383}$
HIPEQ1327+02	$24.24\pm^{0.108}_{0.071}$	$24.04\pm^{0.050}_{0.048}$	$23.79\pm^{0.053}_{0.051}$	$23.55\pm^{0.095}_{0.084}$	$22.60\pm^{0.200}_{0.085}$	$23.87\pm^{1.352}_{2.092}$	$22.83\pm^{0.348}_{0.506}$	$22.67\pm^{0.445}_{0.736}$	$22.46\pm^{0.573}_{1.132}$	$22.41\pm^{1.358}_{1.768}$
HIPEQ1329-00	$24.26\pm^{0.050}_{0.040}$	$23.93\pm^{0.044}_{0.043}$	$23.53\pm^{0.048}_{0.046}$	$23.28\pm^{0.048}_{0.046}$	$22.51\pm^{0.064}_{0.049}$	$23.32\pm^{0.797}_{1.589}$	$22.08\pm^{0.159}_{0.186}$	$21.60\pm^{0.157}_{0.184}$	$21.42\pm^{0.204}_{0.251}$	$21.32\pm^{0.590}_{1.093}$
HIPEQ1332+01	$22.36\pm^{0.080}_{0.078}$	$21.06\pm^{0.073}_{0.070}$	$20.39\pm^{0.075}_{0.073}$	$20.05\pm^{0.075}_{0.073}$	$19.75\pm^{0.081}_{0.078}$	$19.36\pm^{0.054}_{0.057}$	$18.28\pm^{0.008}_{0.008}$	$17.63\pm^{0.007}_{0.007}$	$17.37\pm^{0.008}_{0.008}$	$17.10\pm^{0.022}_{0.023}$
HIPEQ1335+01	$23.67\pm^{0.072}_{0.066}$	$22.08\pm^{0.043}_{0.043}$	$21.25\pm^{0.050}_{0.049}$	$20.80\pm^{0.053}_{0.052}$	$20.50\pm^{0.060}_{0.058}$	$20.81\pm^{0.156}_{0.182}$	$18.95\pm^{0.016}_{0.016}$	$18.06\pm^{0.009}_{0.009}$	$17.64\pm^{0.010}_{0.010}$	$17.36\pm^{0.028}_{0.029}$
HIPEQ1341+05	$23.47\pm^{0.146}_{0.127}$	$22.29\pm^{0.067}_{0.065}$	$21.50\pm^{0.082}_{0.079}$	$21.13\pm^{0.089}_{0.086}$	$20.66\pm^{0.116}_{0.111}$	$21.41\pm^{0.256}_{0.335}$	$19.71\pm^{0.023}_{0.023}$	$18.91\pm^{0.016}_{0.017}$	$18.58\pm^{0.017}_{0.018}$	$18.29\pm^{0.058}_{0.061}$
HIPEQ1348+03	$23.71\pm^{0.013}_{0.013}$	$22.64\pm^{0.016}_{0.016}$	$22.10\pm^{0.017}_{0.017}$	$21.85\pm^{0.017}_{0.017}$	$21.42\pm^{0.017}_{0.017}$	$21.63\pm^{0.272}_{0.362}$	$20.19\pm^{0.036}_{0.037}$	$19.54\pm^{0.029}_{0.030}$	$19.25\pm^{0.035}_{0.036}$	$18.78\pm^{0.094}_{0.103}$
HIPEQ1352+02a	$23.95\pm^{0.027}_{0.026}$	$22.63\pm^{0.028}_{0.027}$	$21.71\pm^{0.032}_{0.031}$	$21.20\pm^{0.034}_{0.034}$	$20.96\pm^{0.066}_{0.063}$	$20.58\pm^{0.140}_{0.161}$	$18.68\pm^{0.011}_{0.012}$	$17.84\pm^{0.008}_{0.008}$	$17.44\pm^{0.009}_{0.009}$	$17.14\pm^{0.022}_{0.023}$
HIPEQ1352-01	$23.63\pm^{0.021}_{0.021}$	$22.74\pm^{0.016}_{0.016}$	$22.19\pm^{0.017}_{0.017}$	$21.92\pm^{0.017}_{0.017}$	$21.66\pm^{0.015}_{0.015}$	$22.32\pm^{0.446}_{0.741}$	$20.78\pm^{0.068}_{0.072}$	$20.11\pm^{0.046}_{0.048}$	$19.77\pm^{0.053}_{0.056}$	$19.57\pm^{0.143}_{0.165}$
HIPEQ1400+02	$23.89\pm^{0.050}_{0.046}$	$23.16\pm^{0.042}_{0.041}$	$22.67\pm^{0.044}_{0.043}$	$22.40\pm^{0.045}_{0.044}$	$21.96\pm^{0.067}_{0.061}$	$22.01\pm^{0.469}_{0.824}$	$20.83\pm^{0.071}_{0.076}$	$20.19\pm^{0.059}_{0.063}$	$19.86\pm^{0.068}_{0.073}$	$19.54\pm^{0.194}_{0.236}$
HIPEQ1411-01	$24.04\pm^{0.008}_{0.008}$	$23.69\pm^{0.011}_{0.011}$	$23.26\pm^{0.013}_{0.012}$	$23.08\pm^{0.012}_{0.012}$	$22.33\pm^{0.007}_{0.007}$	$22.08\pm^{0.389}_{0.600}$	$20.94\pm^{0.081}_{0.087}$	$20.36\pm^{0.059}_{0.063}$	$20.08\pm^{0.071}_{0.076}$	$19.79\pm^{0.176}_{0.210}$
HIPEQ1415+04	$22.17\pm^{0.114}_{0.110}$	$21.38\pm^{0.121}_{0.115}$	$21.17\pm^{0.115}_{0.110}$	$21.13\pm^{0.106}_{0.101}$	$20.88\pm^{0.100}_{0.095}$	$20.76\pm^{0.177}_{0.212}$	$20.08\pm^{0.034}_{0.035}$	$19.67\pm^{0.036}_{0.037}$	$19.47\pm^{0.050}_{0.052}$	$19.23\pm^{0.136}_{0.156}$
HIPEQ1416+03	$24.46\pm^{0.016}_{0.007}$	$24.95\pm^{0.005}_{0.004}$	$24.68\pm^{0.004}_{0.004}$	$24.28\pm^{0.003}_{0.003}$	$22.78\pm^{0.010}_{0.003}$	$24.22\pm^{1.484}_{1.774}$	$23.84\pm^{0.621}_{1.065}$	$23.29\pm^{0.605}_{1.128}$	$23.34\pm^{0.798}_{1.397}$	$22.30\pm^{1.197}_{1.665}$
HIPEQ1422-00	$23.46\pm^{0.014}_{0.014}$	$22.59\pm^{0.016}_{0.016}$	$22.15\pm^{0.016}_{0.016}$	$21.94\pm^{0.017}_{0.017}$	$21.67\pm^{0.015}_{0.015}$	$20.96\pm^{0.147}_{0.170}$	$19.94\pm^{0.027}_{0.027}$	$19.62\pm^{0.029}_{0.030}$	$19.39\pm^{0.036}_{0.037}$	$19.05\pm^{0.098}_{0.108}$
HIPEQ1429-00	$23.53\pm^{0.031}_{0.030}$	$22.80\pm^{0.038}_{0.038}$	$22.42\pm^{0.041}_{0.040}$	$22.27\pm^{0.041}_{0.041}$	$21.93\pm^{0.062}_{0.057}$	$21.74\pm^{0.272}_{0.361}$	$20.78\pm^{0.053}_{0.055}$	$20.42\pm^{0.058}_{0.062}$	$20.24\pm^{0.078}_{0.084}$	$20.13\pm^{0.257}_{0.335}$
HIPEQ1432+00	$23.68\pm^{0.030}_{0.029}$	$22.89\pm^{0.037}_{0.036}$	$22.42\pm^{0.036}_{0.036}$	$22.14\pm^{0.037}_{0.036}$	$21.73\pm^{0.034}_{0.033}$	$21.58\pm^{0.249}_{0.322}$	$20.30\pm^{0.034}_{0.035}$	$19.69\pm^{0.031}_{0.032}$	$19.39\pm^{0.037}_{0.039}$	$19.10\pm^{0.128}_{0.145}$
HIPEQ1433+01	$24.32\pm^{0.097}_{0.038}$	$24.66\pm^{0.037}_{0.032}$	$24.41\pm^{0.041}_{0.035}$	$24.04\pm^{0.037}_{0.031}$	$22.71\pm^{3.157}_{0.038}$	$24.31\pm^{1.809}_{1.922}$	$23.75\pm^{0.693}_{1.286}$	$23.94\pm^{1.058}_{1.726}$	$23.96\pm^{1.374}_{1.707}$	$22.48\pm^{1.376}_{1.667}$
HIPEQ1433+02	$22.78\pm^{0.078}_{0.075}$	$22.14\pm^{0.067}_{0.065}$	$21.84\pm^{0.070}_{0.068}$	$21.67\pm^{0.076}_{0.074}$	$21.49\pm^{0.140}_{0.127}$	$21.02\pm^{0.193}_{0.235}$	$20.23\pm^{0.039}_{0.040}$	$19.92\pm^{0.045}_{0.047}$	$19.82\pm^{0.071}_{0.076}$	$19.75\pm^{0.223}_{0.280}$
HIPEQ1437+02	$23.93\pm^{0.012}_{0.011}$	$22.77\pm^{0.017}_{0.016}$	$22.28\pm^{0.015}_{0.015}$	$22.02\pm^{0.015}_{0.015}$	$21.57\pm^{0.014}_{0.014}$	$21.90\pm^{0.431}_{0.714}$	$20.38\pm^{0.045}_{0.047}$	$19.52\pm^{0.033}_{0.034}$	$19.06\pm^{0.036}_{0.037}$	$18.63\pm^{0.109}_{0.121}$
HIPEQ1437-00	$21.92\pm^{0.049}_{0.048}$	$21.22\pm^{0.039}_{0.038}$	$20.93\pm^{0.036}_{0.036}$	$20.80\pm^{0.035}_{0.034}$	$20.64\pm^{0.036}_{0.035}$	$19.29\pm^{0.037}_{0.038}$	$18.56\pm^{0.009}_{0.009}$	$18.30\pm^{0.010}_{0.010}$	$18.19\pm^{0.013}_{0.013}$	$18.07\pm^{0.041}_{0.043}$
HIPEQ1439-00	$24.04\pm^{0.013}_{0.013}$	$23.51\pm^{0.016}_{0.015}$	$23.08\pm^{0.017}_{0.016}$	$22.82\pm^{0.016}_{0.016}$	$22.23\pm^{0.011}_{0.011}$	$21.98\pm^{0.370}_{0.558}$	$20.80\pm^{0.057}_{0.060}$	$20.51\pm^{0.065}_{0.069}$	$20.28\pm^{0.080}_{0.086}$	$20.11\pm^{0.220}_{0.275}$
HIPEQ1440+02	$22.66\pm^{0.071}_{0.069}$	$21.59\pm^{0.067}_{0.065}$	$21.26\pm^{0.069}_{0.067}$	$21.02\pm^{0.070}_{0.068}$	$21.35\pm^{0.069}_{0.066}$	$21.44\pm^{0.291}_{0.398}$	$20.28\pm^{0.047}_{0.050}$	$19.90\pm^{0.046}_{0.048}$	$19.60\pm^{0.058}_{0.062}$	$19.96\pm^{0.198}_{0.241}$
HIPEQ1444+01a	$23.10\pm^{0.027}_{0.026}$	$21.47\pm^{0.031}_{0.030}$	$20.66\pm^{0.034}_{0.033}$	$20.23\pm^{0.035}_{0.035}$	$19.92\pm^{0.037}_{0.037}$	$19.70\pm^{0.075}_{0.080}$	$18.14\pm^{0.008}_{0.008}$	$17.31\pm^{0.005}_{0.005}$	$16.88\pm^{0.005}_{0.005}$	$16.48\pm^{0.014}_{0.014}$
HIPEQ1500+01	$22.96\pm^{0.044}_{0.043}$	$21.48\pm^{0.025}_{0.025}$	$20.71\pm^{0.026}_{0.026}$	$20.27\pm^{0.027}_{0.027}$	$19.99\pm^{0.028}_{0.028}$	$19.84\pm^{0.081}_{0.088}$	$18.00\pm^{0.007}_{0.007}$	$17.08\pm^{0.005}_{0.005}$	$16.62\pm^{0.005}_{0.005}$	$16.26\pm^{0.013}_{0.013}$
HIPEQ1504+02	$23.27\pm^{0.140}_{0.125}$	$22.09\pm^{0.086}_{0.083}$	$21.68\pm^{0.090}_{0.086}$	$21.53\pm^{0.091}_{0.088}$	$21.31\pm^{0.103}_{0.098}$	$21.62\pm^{0.369}_{0.558}$	$20.38\pm^{0.052}_{0.054}$	$19.80\pm^{0.045}_{0.047}$	$19.52\pm^{0.055}_{0.058}$	$19.37\pm^{0.159}_{0.186}$
HIPEQ1504-00	$24.06\pm^{0.032}_{0.028}$	$23.86\pm^{0.025}_{0.024}$	$23.48\pm^{0.026}_{0.025}$	$23.24\pm^{0.025}_{0.025}$	$22.41\pm^{0.035}_{0.031}$	$22.71\pm^{0.596}_{1.154}$	$21.59\pm^{0.140}_{0.160}$	$21.16\pm^{0.118}_{0.133}$	$20.95\pm^{0.158}_{0.185}$	$20.69\pm^{0.385}_{0.585}$
HIPEQ1507+01	$23.56\pm^{0.024}_{0.023}$	$21.93\pm^{0.018}_{0.018}$	$20.93\pm^{0.021}_{0.021}$	$20.46\pm^{0.022}_{0.021}$	$20.22\pm^{0.022}_{0.022}$	$19.94\pm^{0.099}_{0.109}$	$17.94\pm^{0.007}_{0.007}$	$17.02\pm^{0.005}_{0.005}$	$16.57\pm^{0.004}_{0.004}$	$16.20\pm^{0.012}_{0.012}$
HIPEQ1542+00	$23.90\pm^{0.011}_{0.010}$	$23.88\pm^{0.012}_{0.012}$	$23.37\pm^{0.015}_{0.015}$	$22.99\pm^{0.016}_{0.016}$	$22.23\pm^{0.010}_{0.009}$	$22.55\pm^{0.637}_{1.258}$	$21.19\pm^{0.093}_{0.102}$	$20.35\pm^{0.065}_{0.069}$	$20.04\pm^{0.080}_{0.087}$	$19.74\pm^{0.185}_{0.223}$
HIPEQ1544+02	$23.23\pm^{0.110}_{0.097}$	$21.93\pm^{0.077}_{0.074}$	$21.28\pm^{0.082}_{0.079}$	$21.16\pm^{0.086}_{0.083}$	$20.49\pm^{0.095}_{0.091}$	$22.05\pm^{0.586}_{1.220}$	$20.56\pm^{0.067}_{0.072}$	$19.88\pm^{0.051}_{0.053}$	$19.73\pm^{0.061}_{0.065}$	$19.13\pm^{0.159}_{0.187}$
HIPEQ1545+00	$23.80\pm^{0.110}_{0.079}$	$23.37\pm^{0.046}_{0.044}$	$23.19\pm^{0.042}_{0.041}$	$23.11\pm^{0.067}_{0.063}$	$22.10\pm^{0.106}_{0.088}$	$22.68\pm^{0.664}_{1.353}$	$21.41\pm^{0.111}_{0.124}$	$20.93\pm^{0.115}_{0.128}$	$20.75\pm^{0.172}_{0.204}$	$20.25\pm^{0.335}_{0.481}$

Table 3.9—Continued

	$\Sigma_{face-on}$					Σ_{fiber}				
HIPASS Name	u^a	g^a	r^a	i^a	z^a	u^a	g^a	r^a	i^a	z^a
HIPEQ1601+01a	$23.50\pm^{0.032}_{0.030}$	$22.71\pm^{0.021}_{0.021}$	$22.36\pm^{0.021}_{0.021}$	$21.96\pm^{0.021}_{0.021}$	$21.79\pm^{0.017}_{0.017}$	$21.47\pm^{0.477}_{0.853}$	$20.41\pm^{0.069}_{0.074}$	$19.89\pm^{0.055}_{0.058}$	$19.44\pm^{0.057}_{0.060}$	$19.34\pm^{0.166}_{0.196}$
HIPEQ1609-00	$23.88\pm^{0.029}_{0.023}$	$23.93\pm^{0.033}_{0.032}$	$23.73\pm^{0.039}_{0.037}$	$23.57\pm^{0.083}_{0.070}$	$22.51\pm^{0.099}_{0.051}$	$22.83\pm^{0.798}_{1.597}$	$22.23\pm^{0.242}_{0.310}$	$22.09\pm^{0.317}_{0.445}$	$22.00\pm^{0.437}_{0.716}$	$21.48\pm^{0.835}_{1.682}$
HIPEQ1613-00	$22.61\pm^{0.081}_{0.077}$	$21.79\pm^{0.074}_{0.071}$	$21.68\pm^{0.074}_{0.072}$	$21.51\pm^{0.078}_{0.076}$	$21.16\pm^{0.078}_{0.075}$	$21.34\pm^{0.380}_{0.583}$	$20.61\pm^{0.074}_{0.080}$	$20.53\pm^{0.092}_{0.101}$	$20.48\pm^{0.135}_{0.154}$	$20.16\pm^{0.380}_{0.583}$
HIPEQ1614+00	$23.73\pm^{0.043}_{0.038}$	$23.41\pm^{0.025}_{0.024}$	$23.09\pm^{0.027}_{0.027}$	$22.90\pm^{0.029}_{0.029}$	$22.31\pm^{0.044}_{0.039}$	$23.06\pm^{0.852}_{1.636}$	$21.90\pm^{0.173}_{0.206}$	$21.50\pm^{0.185}_{0.223}$	$21.27\pm^{0.257}_{0.336}$	$21.12\pm^{0.608}_{1.183}$
HIPEQ1614-00	$23.85\pm^{0.008}_{0.007}$	$23.96\pm^{0.008}_{0.008}$	$23.33\pm^{0.013}_{0.013}$	$22.85\pm^{0.014}_{0.014}$	$22.05\pm^{0.019}_{0.018}$	$22.46\pm^{0.678}_{1.406}$	$20.81\pm^{0.077}_{0.083}$	$19.86\pm^{0.046}_{0.049}$	$19.33\pm^{0.041}_{0.043}$	$18.94\pm^{0.101}_{0.112}$
HIPEQ2036-04	$23.99\pm^{0.025}_{0.023}$	$22.63\pm^{0.031}_{0.031}$	$21.60\pm^{0.035}_{0.034}$	$21.16\pm^{0.035}_{0.035}$	$21.01\pm^{0.035}_{0.035}$	$21.13\pm^{0.175}_{0.209}$	$19.06\pm^{0.017}_{0.017}$	$18.04\pm^{0.009}_{0.009}$	$17.58\pm^{0.010}_{0.010}$	$17.39\pm^{0.027}_{0.028}$
HIPEQ2314+00	$22.10\pm^{0.099}_{0.095}$	$20.94\pm^{0.098}_{0.094}$	$20.56\pm^{0.098}_{0.094}$	$20.26\pm^{0.103}_{0.099}$	$20.18\pm^{0.104}_{0.100}$	$21.32\pm^{0.290}_{0.397}$	$20.03\pm^{0.032}_{0.033}$	$19.47\pm^{0.030}_{0.031}$	$19.19\pm^{0.036}_{0.037}$	$19.00\pm^{0.133}_{0.152}$
HIPEQ2324-00	$23.83\pm^{0.037}_{0.035}$	$23.49\pm^{0.029}_{0.029}$	$23.27\pm^{0.031}_{0.030}$	$23.12\pm^{0.031}_{0.030}$	$22.43\pm^{0.054}_{0.045}$	$21.55\pm^{0.320}_{0.453}$	$21.07\pm^{0.081}_{0.088}$	$20.98\pm^{0.115}_{0.128}$	$20.96\pm^{0.172}_{0.205}$	$20.76\pm^{0.497}_{0.886}$
HIPEQ2335+01	$24.28\pm^{0.103}_{0.047}$	$24.21\pm^{0.082}_{0.072}$	$23.88\pm^{0.058}_{0.054}$	$23.58\pm^{0.082}_{0.073}$	$22.62\pm^{0.070}_{0.043}$	$23.55\pm^{1.250}_{2.233}$	$22.85\pm^{0.352}_{0.512}$	$22.41\pm^{0.363}_{0.539}$	$22.21\pm^{0.479}_{0.835}$	$21.94\pm^{0.997}_{1.703}$
HIPEQ2336+00	$23.07\pm^{0.030}_{0.029}$	$21.25\pm^{0.039}_{0.038}$	$20.31\pm^{0.046}_{0.045}$	$19.88\pm^{0.048}_{0.047}$	$19.67\pm^{0.047}_{0.047}$	$19.60\pm^{0.066}_{0.071}$	$17.78\pm^{0.005}_{0.005}$	$16.94\pm^{0.004}_{0.004}$	$16.54\pm^{0.004}_{0.004}$	$16.21\pm^{0.012}_{0.012}$
HIPEQ2337+00	$24.18\pm^{0.040}_{0.034}$	$23.99\pm^{0.020}_{0.020}$	$23.61\pm^{0.022}_{0.022}$	$23.34\pm^{0.038}_{0.037}$	$22.48\pm^{0.060}_{0.048}$	$23.61\pm^{1.282}_{2.259}$	$22.71\pm^{0.303}_{0.416}$	$22.13\pm^{0.291}_{0.396}$	$21.86\pm^{0.352}_{0.519}$	$21.54\pm^{0.904}_{1.951}$
HIPEQ2340+01	$23.39\pm^{0.112}_{0.102}$	$22.36\pm^{0.065}_{0.063}$	$21.85\pm^{0.065}_{0.064}$	$21.59\pm^{0.066}_{0.064}$	$21.23\pm^{0.074}_{0.071}$	$21.11\pm^{0.234}_{0.298}$	$20.18\pm^{0.037}_{0.038}$	$19.77\pm^{0.038}_{0.040}$	$19.59\pm^{0.054}_{0.057}$	$19.36\pm^{0.153}_{0.178}$

[a]Uncertainties are based on the photometric errors described in §3.5 and *do not* account for calibration errors or other uncertainties.

3.8 Other Photometric Quantities

To facilitate comparisons with the 2MASS[2] survey, we calculate Kron (1980) radii and magnitudes for every galaxy in the sample. We follow the 2MASS prescription (Bertin & Arnouts 1996) for Kron photometry and use the sample elliptical and circular apertures discussed above. Kron magnitudes are similar to Petrosian magnitudes in that the photometric aperture changes with the surface brightness profile of the galaxy. However, unlike the SDSS Petrosian magnitudes, Kron magnitudes utilize a Kron radius to determine the aperture size that is defined as the radius at which the flux enclosed is equal to the mean integrated flux. We derive Kron radii for the HIPASS/SDSS sample using the equation:

$$r_K \equiv \frac{\int_0^\infty 2\pi r'^2 dr'}{\int_0^\infty 2\pi r' dr'} \tag{3.12}$$

where r is defined by Equation (3.2) for the elliptical aperture.

The Kron flux is defined by 2MASS to be:

$$f_K \equiv \int_0^{2.5r_K} 2\pi r' I(r') dr'. \tag{3.13}$$

where an upper bound on the Kron aperture is fixed by the sky subtraction mask (the same as Petrosian photometry). As in the Petrosian case, the aperture rarely crosses the mask boundaries. The photometric uncertainties are calculated using Equation (3.9) and all of the Kron photometry is reported in Table 3.10. The Kron radii are given in Tables 3.11 and . 3.12

To allow comparison of our galaxy sizes with previous work, we also compute r_{25}, the size of the sample galaxies at a limiting isophote of μ_r=25 mag/$\Box''$. These values are given in Tables 3.11 and 3.12. For some of the galaxies, the r_{25} occurs almost immediately and in others, the values is never reached because of their irregular LSB nature. The r_{25} values for these latter cases have been omitted from Tables 3.11 and 3.12.

---

[2]http://www.ipac.caltech.edu/2mass/

Table 3.10. Kron Photometry

	Elliptical					Circular				
HIPASS Name	u^a	g^a	r^a	i^a	z^a	u^a	g^a	r^a	i^a	z^a
HIPEQ0014-00	$14.79\pm^{0.019}_{0.019}$	$13.83\pm^{0.003}_{0.003}$	$13.44\pm^{0.003}_{0.003}$	$13.22\pm^{0.003}_{0.003}$	$13.08\pm^{0.011}_{0.011}$	$14.78\pm^{0.019}_{0.020}$	$13.84\pm^{0.003}_{0.003}$	$13.45\pm^{0.003}_{0.003}$	$13.22\pm^{0.003}_{0.003}$	$13.07\pm^{0.011}_{0.011}$
HIPEQ0027-01a	$15.65\pm^{0.023}_{0.023}$	$14.70\pm^{0.005}_{0.005}$	$14.32\pm^{0.004}_{0.004}$	$14.14\pm^{0.006}_{0.006}$	$14.16\pm^{0.020}_{0.021}$	$15.64\pm^{0.027}_{0.028}$	$14.70\pm^{0.006}_{0.006}$	$14.31\pm^{0.005}_{0.005}$	$14.13\pm^{0.007}_{0.007}$	$14.11\pm^{0.024}_{0.025}$
HIPEQ0033-01	$15.95\pm^{0.048}_{0.050}$	$15.08\pm^{0.011}_{0.011}$	$14.74\pm^{0.009}_{0.009}$	$14.57\pm^{0.013}_{0.013}$	$14.45\pm^{0.042}_{0.044}$	$15.97\pm^{0.048}_{0.050}$	$15.11\pm^{0.011}_{0.011}$	$14.76\pm^{0.009}_{0.009}$	$14.60\pm^{0.013}_{0.013}$	$14.48\pm^{0.042}_{0.044}$
HIPEQ0043-00	$14.45\pm^{0.007}_{0.007}$	$13.33\pm^{0.001}_{0.001}$	$12.80\pm^{0.001}_{0.001}$	$12.52\pm^{0.001}_{0.001}$	$12.29\pm^{0.004}_{0.004}$	$14.45\pm^{0.007}_{0.007}$	$13.33\pm^{0.001}_{0.001}$	$12.80\pm^{0.001}_{0.001}$	$12.52\pm^{0.001}_{0.001}$	$12.29\pm^{0.004}_{0.004}$
HIPEQ0051-00	$15.84\pm^{0.015}_{0.015}$	$14.91\pm^{0.002}_{0.002}$	$14.46\pm^{0.002}_{0.002}$	$14.22\pm^{0.002}_{0.002}$	$14.10\pm^{0.009}_{0.009}$	$15.86\pm^{0.016}_{0.017}$	$14.91\pm^{0.002}_{0.002}$	$14.46\pm^{0.002}_{0.002}$	$14.22\pm^{0.003}_{0.003}$	$14.09\pm^{0.009}_{0.010}$
HIPEQ0058+00	$15.07\pm^{0.012}_{0.012}$	$13.97\pm^{0.002}_{0.002}$	$13.49\pm^{0.002}_{0.002}$	$13.23\pm^{0.002}_{0.002}$	$13.11\pm^{0.007}_{0.007}$	$15.06\pm^{0.012}_{0.012}$	$13.97\pm^{0.002}_{0.002}$	$13.49\pm^{0.002}_{0.002}$	$13.23\pm^{0.002}_{0.002}$	$13.11\pm^{0.007}_{0.007}$
HIPEQ0107+01	$15.87\pm^{0.031}_{0.032}$	$15.00\pm^{0.005}_{0.005}$	$14.74\pm^{0.006}_{0.006}$	$14.60\pm^{0.009}_{0.009}$	$14.59\pm^{0.031}_{0.032}$	$15.87\pm^{0.031}_{0.032}$	$15.00\pm^{0.005}_{0.005}$	$14.74\pm^{0.006}_{0.006}$	$14.60\pm^{0.009}_{0.009}$	$14.59\pm^{0.031}_{0.031}$
HIPEQ0119+00	$17.99\pm^{0.097}_{0.107}$	$17.10\pm^{0.019}_{0.019}$	$16.78\pm^{0.021}_{0.021}$	$16.62\pm^{0.031}_{0.032}$	$16.44\pm^{0.092}_{0.100}$	$17.90\pm^{0.105}_{0.116}$	$17.11\pm^{0.020}_{0.020}$	$16.78\pm^{0.022}_{0.023}$	$16.63\pm^{0.034}_{0.035}$	$16.50\pm^{0.097}_{0.107}$
HIPEQ0120-00	$16.17\pm^{0.033}_{0.034}$	$15.21\pm^{0.005}_{0.005}$	$14.83\pm^{0.006}_{0.006}$	$14.65\pm^{0.007}_{0.007}$	$14.58\pm^{0.027}_{0.028}$	$16.15\pm^{0.041}_{0.042}$	$15.22\pm^{0.007}_{0.007}$	$14.84\pm^{0.007}_{0.007}$	$14.65\pm^{0.009}_{0.009}$	$14.54\pm^{0.035}_{0.036}$
HIPEQ0122+00	$13.63\pm^{0.008}_{0.008}$	$12.73\pm^{0.001}_{0.001}$	$12.36\pm^{0.001}_{0.001}$	$12.08\pm^{0.002}_{0.002}$	$11.91\pm^{0.005}_{0.005}$	$13.56\pm^{0.013}_{0.013}$	$12.71\pm^{0.002}_{0.002}$	$12.35\pm^{0.002}_{0.002}$	$12.05\pm^{0.003}_{0.003}$	$11.87\pm^{0.008}_{0.008}$
HIPEQ0123-00	$15.17\pm^{0.017}_{0.017}$	$14.18\pm^{0.003}_{0.003}$	$13.77\pm^{0.003}_{0.003}$	$13.54\pm^{0.004}_{0.004}$	$13.37\pm^{0.012}_{0.012}$	$15.17\pm^{0.017}_{0.017}$	$14.18\pm^{0.003}_{0.003}$	$13.77\pm^{0.003}_{0.003}$	$13.54\pm^{0.004}_{0.004}$	$13.37\pm^{0.012}_{0.012}$
HIPEQ0126+00a	$18.60\pm^{0.254}_{0.333}$	$16.88\pm^{0.022}_{0.023}$	$16.53\pm^{0.023}_{0.024}$	$16.36\pm^{0.036}_{0.037}$	$16.36\pm^{0.111}_{0.124}$	$18.58\pm^{0.255}_{0.334}$	$16.88\pm^{0.022}_{0.023}$	$16.52\pm^{0.023}_{0.024}$	$16.36\pm^{0.036}_{0.037}$	$16.37\pm^{0.111}_{0.124}$
HIPEQ0126-00b	$16.36\pm^{0.023}_{0.023}$	$15.74\pm^{0.004}_{0.004}$	$15.57\pm^{0.005}_{0.005}$	$15.58\pm^{0.007}_{0.008}$	$15.60\pm^{0.029}_{0.030}$	$16.36\pm^{0.023}_{0.024}$	$15.75\pm^{0.004}_{0.004}$	$15.58\pm^{0.005}_{0.005}$	$15.59\pm^{0.008}_{0.008}$	$15.60\pm^{0.029}_{0.030}$
HIPEQ0154-00	$15.81\pm^{0.021}_{0.021}$	$14.08\pm^{0.002}_{0.002}$	$13.30\pm^{0.001}_{0.001}$	$12.90\pm^{0.001}_{0.001}$	$12.66\pm^{0.004}_{0.004}$	$15.79\pm^{0.021}_{0.021}$	$14.08\pm^{0.002}_{0.002}$	$13.30\pm^{0.001}_{0.001}$	$12.90\pm^{0.001}_{0.001}$	$12.66\pm^{0.004}_{0.004}$
HIPEQ0222-00	$16.20\pm^{0.045}_{0.047}$	$15.08\pm^{0.005}_{0.005}$	$14.66\pm^{0.006}_{0.006}$	$14.48\pm^{0.006}_{0.006}$	$14.53\pm^{0.024}_{0.024}$	$16.17\pm^{0.076}_{0.082}$	$15.09\pm^{0.009}_{0.010}$	$14.68\pm^{0.010}_{0.010}$	$14.49\pm^{0.011}_{0.011}$	$14.52\pm^{0.042}_{0.043}$
HIPEQ0228-01	$13.60\pm^{0.008}_{0.008}$	$12.71\pm^{0.002}_{0.002}$	$12.33\pm^{0.001}_{0.001}$	$12.12\pm^{0.002}_{0.002}$	$12.04\pm^{0.006}_{0.006}$	$13.60\pm^{0.008}_{0.008}$	$12.71\pm^{0.002}_{0.002}$	$12.32\pm^{0.001}_{0.001}$	$12.12\pm^{0.002}_{0.002}$	$12.04\pm^{0.006}_{0.006}$
HIPEQ0230+00	$17.72\pm^{0.133}_{0.151}$	$15.69\pm^{0.014}_{0.015}$	$14.98\pm^{0.009}_{0.009}$	$14.55\pm^{0.011}_{0.011}$	$14.90\pm^{0.045}_{0.047}$	$17.62\pm^{0.131}_{0.149}$	$15.67\pm^{0.014}_{0.014}$	$14.96\pm^{0.009}_{0.009}$	$14.53\pm^{0.011}_{0.011}$	$14.85\pm^{0.044}_{0.046}$
HIPEQ0230-01	$14.13\pm^{0.006}_{0.006}$	$12.48\pm^{0.001}_{0.001}$	$11.71\pm^{0.000}_{0.000}$	$11.29\pm^{0.000}_{0.000}$	$11.07\pm^{0.001}_{0.001}$	$14.09\pm^{0.006}_{0.006}$	$12.48\pm^{0.001}_{0.001}$	$11.71\pm^{0.000}_{0.000}$	$11.30\pm^{0.000}_{0.000}$	$11.07\pm^{0.001}_{0.001}$
HIPEQ0231+00	$16.51\pm^{0.048}_{0.050}$	$15.27\pm^{0.006}_{0.006}$	$14.92\pm^{0.006}_{0.006}$	$14.73\pm^{0.008}_{0.008}$	$14.58\pm^{0.029}_{0.030}$	$16.53\pm^{0.055}_{0.058}$	$15.27\pm^{0.006}_{0.006}$	$14.91\pm^{0.007}_{0.007}$	$14.72\pm^{0.009}_{0.009}$	$14.55\pm^{0.033}_{0.034}$
HIPEQ0236+00	$16.27\pm^{0.027}_{0.028}$	$14.98\pm^{0.003}_{0.003}$	$14.36\pm^{0.003}_{0.003}$	$14.02\pm^{0.003}_{0.003}$	$13.82\pm^{0.009}_{0.009}$	$16.21\pm^{0.033}_{0.034}$	$14.99\pm^{0.004}_{0.004}$	$14.37\pm^{0.004}_{0.004}$	$14.02\pm^{0.004}_{0.004}$	$13.81\pm^{0.011}_{0.011}$
HIPEQ0238+00	$17.39\pm^{0.119}_{0.134}$	$16.51\pm^{0.021}_{0.021}$	$16.34\pm^{0.024}_{0.025}$	$16.20\pm^{0.037}_{0.038}$	$16.10\pm^{0.101}_{0.112}$	$17.39\pm^{0.129}_{0.147}$	$16.50\pm^{0.023}_{0.023}$	$16.34\pm^{0.026}_{0.027}$	$16.18\pm^{0.040}_{0.041}$	$16.08\pm^{0.110}_{0.122}$
HIPEQ0240+01	$17.03\pm^{0.134}_{0.152}$	$16.22\pm^{0.022}_{0.022}$	$16.09\pm^{0.030}_{0.031}$	$15.95\pm^{0.039}_{0.041}$	$15.49\pm^{0.087}_{0.094}$	$17.00\pm^{0.139}_{0.159}$	$16.19\pm^{0.023}_{0.023}$	$16.08\pm^{0.031}_{0.032}$	$15.90\pm^{0.041}_{0.042}$	$15.49\pm^{0.091}_{0.099}$
HIPEQ0241+00	$12.48\pm^{0.005}_{0.005}$	$11.10\pm^{0.001}_{0.001}$	$10.32\pm^{0.000}_{0.000}$	$9.90\pm^{0.000}_{0.000}$	$9.63\pm^{0.001}_{0.001}$	$12.44\pm^{0.005}_{0.005}$	$11.06\pm^{0.001}_{0.001}$	$10.27\pm^{0.000}_{0.000}$	$9.86\pm^{0.000}_{0.000}$	$9.59\pm^{0.001}_{0.001}$
HIPEQ0244+00	$16.13\pm^{0.036}_{0.037}$	$15.21\pm^{0.006}_{0.006}$	$14.81\pm^{0.007}_{0.007}$	$14.63\pm^{0.009}_{0.009}$	$14.55\pm^{0.025}_{0.026}$	$16.06\pm^{0.043}_{0.044}$	$15.17\pm^{0.008}_{0.008}$	$14.78\pm^{0.008}_{0.008}$	$14.59\pm^{0.011}_{0.011}$	$14.46\pm^{0.030}_{0.031}$
HIPEQ0246-00a	$13.48\pm^{0.007}_{0.007}$	$12.30\pm^{0.001}_{0.001}$	$11.72\pm^{0.001}_{0.001}$	$11.43\pm^{0.001}_{0.001}$	$11.19\pm^{0.003}_{0.003}$	$13.47\pm^{0.008}_{0.009}$	$12.30\pm^{0.001}_{0.001}$	$11.72\pm^{0.001}_{0.001}$	$11.43\pm^{0.001}_{0.001}$	$11.18\pm^{0.003}_{0.003}$
HIPEQ0246-00b	$12.15\pm^{0.004}_{0.004}$	$11.16\pm^{0.000}_{0.000}$	$10.74\pm^{0.001}_{0.001}$	$10.52\pm^{0.001}_{0.001}$	$10.37\pm^{0.002}_{0.002}$	$12.15\pm^{0.004}_{0.004}$	$11.16\pm^{0.000}_{0.000}$	$10.74\pm^{0.001}_{0.001}$	$10.52\pm^{0.001}_{0.001}$	$10.37\pm^{0.002}_{0.002}$
HIPEQ0249-00	$15.74\pm^{0.029}_{0.030}$	$14.54\pm^{0.003}_{0.003}$	$14.01\pm^{0.003}_{0.003}$	$13.72\pm^{0.003}_{0.003}$	$13.56\pm^{0.009}_{0.010}$	$15.75\pm^{0.030}_{0.031}$	$14.53\pm^{0.003}_{0.003}$	$14.01\pm^{0.003}_{0.003}$	$13.72\pm^{0.003}_{0.003}$	$13.56\pm^{0.010}_{0.010}$
HIPEQ0249-00a	$16.60\pm^{0.066}_{0.071}$	$15.94\pm^{0.014}_{0.014}$	$15.75\pm^{0.017}_{0.017}$	$15.73\pm^{0.026}_{0.026}$	$15.55\pm^{0.075}_{0.081}$	$16.61\pm^{0.068}_{0.073}$	$15.94\pm^{0.014}_{0.014}$	$15.74\pm^{0.017}_{0.017}$	$15.73\pm^{0.026}_{0.027}$	$15.48\pm^{0.076}_{0.081}$
HIPEQ0249-00b	$14.75\pm^{0.012}_{0.012}$	$13.54\pm^{0.002}_{0.002}$	$12.96\pm^{0.001}_{0.001}$	$12.64\pm^{0.002}_{0.002}$	$12.45\pm^{0.004}_{0.004}$	$14.74\pm^{0.013}_{0.013}$	$13.53\pm^{0.002}_{0.002}$	$12.95\pm^{0.002}_{0.002}$	$12.63\pm^{0.002}_{0.002}$	$12.44\pm^{0.005}_{0.005}$
HIPEQ0251-01	$15.09\pm^{0.035}_{0.036}$	$14.35\pm^{0.008}_{0.008}$	$14.06\pm^{0.007}_{0.007}$	$13.91\pm^{0.010}_{0.010}$	$13.72\pm^{0.027}_{0.027}$	$15.12\pm^{0.037}_{0.038}$	$14.36\pm^{0.009}_{0.009}$	$14.07\pm^{0.007}_{0.007}$	$13.93\pm^{0.010}_{0.010}$	$13.70\pm^{0.028}_{0.029}$
HIPEQ0300+00	$16.37\pm^{0.058}_{0.061}$	$15.21\pm^{0.006}_{0.006}$	$14.87\pm^{0.006}_{0.006}$	$14.68\pm^{0.008}_{0.008}$	$14.63\pm^{0.033}_{0.034}$	$16.36\pm^{0.074}_{0.079}$	$15.23\pm^{0.008}_{0.008}$	$14.87\pm^{0.008}_{0.008}$	$14.69\pm^{0.010}_{0.010}$	$14.63\pm^{0.042}_{0.044}$

Table 3.10—Continued

	Elliptical					Circular				
HIPASS Name	u^a	g^a	r^a	i^a	z^a	u^a	g^a	r^a	i^a	z^a
HIPEQ0301-00	$15.52\pm^{0.038}_{0.040}$	$14.89\pm^{0.007}_{0.007}$	$14.68\pm^{0.007}_{0.007}$	$14.56\pm^{0.009}_{0.009}$	$14.51\pm^{0.029}_{0.030}$	$15.51\pm^{0.043}_{0.045}$	$14.89\pm^{0.007}_{0.008}$	$14.68\pm^{0.008}_{0.008}$	$14.55\pm^{0.010}_{0.010}$	$14.51\pm^{0.033}_{0.034}$
HIPEQ0306-00	$14.32\pm^{0.012}_{0.012}$	$12.67\pm^{0.001}_{0.001}$	$11.95\pm^{0.001}_{0.001}$	$11.55\pm^{0.001}_{0.001}$	$11.32\pm^{0.002}_{0.002}$	$14.31\pm^{0.012}_{0.012}$	$12.67\pm^{0.001}_{0.001}$	$11.95\pm^{0.001}_{0.001}$	$11.55\pm^{0.001}_{0.001}$	$11.32\pm^{0.002}_{0.002}$
HIPEQ0316-00	$15.95\pm^{0.041}_{0.042}$	$14.47\pm^{0.003}_{0.003}$	$13.86\pm^{0.003}_{0.003}$	$13.52\pm^{0.003}_{0.003}$	$13.27\pm^{0.007}_{0.008}$	$15.94\pm^{0.052}_{0.055}$	$14.51\pm^{0.004}_{0.004}$	$13.88\pm^{0.004}_{0.004}$	$13.54\pm^{0.004}_{0.004}$	$13.26\pm^{0.010}_{0.010}$
HIPEQ0320-06	$14.18\pm^{0.006}_{0.006}$	$13.08\pm^{0.001}_{0.001}$	$12.62\pm^{0.001}_{0.001}$	$12.37\pm^{0.001}_{0.001}$	$12.21\pm^{0.003}_{0.003}$	$14.18\pm^{0.006}_{0.006}$	$13.09\pm^{0.001}_{0.001}$	$12.63\pm^{0.001}_{0.001}$	$12.37\pm^{0.001}_{0.001}$	$12.21\pm^{0.003}_{0.003}$
HIPEQ0351-00	$15.94\pm^{0.030}_{0.031}$	$14.84\pm^{0.003}_{0.003}$	$14.34\pm^{0.003}_{0.003}$	$14.07\pm^{0.003}_{0.003}$	$13.89\pm^{0.007}_{0.008}$	$15.95\pm^{0.033}_{0.034}$	$14.84\pm^{0.003}_{0.003}$	$14.34\pm^{0.003}_{0.003}$	$14.06\pm^{0.003}_{0.003}$	$13.89\pm^{0.008}_{0.008}$
HIPEQ0809+00	$14.77\pm^{0.010}_{0.010}$	$13.87\pm^{0.002}_{0.002}$	$13.52\pm^{0.002}_{0.002}$	$13.36\pm^{0.003}_{0.003}$	$13.29\pm^{0.009}_{0.009}$	$14.76\pm^{0.011}_{0.011}$	$13.88\pm^{0.002}_{0.002}$	$13.52\pm^{0.002}_{0.002}$	$13.36\pm^{0.003}_{0.003}$	$13.27\pm^{0.010}_{0.010}$
HIPEQ0821+03b	$15.16\pm^{0.010}_{0.010}$	$13.88\pm^{0.001}_{0.001}$	$13.29\pm^{0.001}_{0.001}$	$12.97\pm^{0.001}_{0.001}$	$12.75\pm^{0.004}_{0.004}$	$15.17\pm^{0.010}_{0.011}$	$13.88\pm^{0.001}_{0.001}$	$13.29\pm^{0.001}_{0.001}$	$12.97\pm^{0.001}_{0.001}$	$12.75\pm^{0.004}_{0.004}$
HIPEQ0821-00	$15.99\pm^{0.031}_{0.032}$	$15.27\pm^{0.007}_{0.007}$	$15.12\pm^{0.008}_{0.008}$	$15.16\pm^{0.014}_{0.014}$	$15.09\pm^{0.043}_{0.044}$	$15.99\pm^{0.025}_{0.026}$	$15.28\pm^{0.006}_{0.006}$	$15.14\pm^{0.007}_{0.007}$	$15.16\pm^{0.011}_{0.011}$	$15.03\pm^{0.035}_{0.036}$
HIPEQ0822-00	$15.18\pm^{0.013}_{0.013}$	$14.18\pm^{0.003}_{0.003}$	$13.75\pm^{0.002}_{0.002}$	$13.51\pm^{0.003}_{0.003}$	$13.38\pm^{0.009}_{0.009}$	$15.14\pm^{0.014}_{0.014}$	$14.17\pm^{0.003}_{0.003}$	$13.74\pm^{0.003}_{0.003}$	$13.50\pm^{0.003}_{0.003}$	$13.35\pm^{0.010}_{0.010}$
HIPEQ0825-00	$14.75\pm^{0.011}_{0.011}$	$13.39\pm^{0.001}_{0.001}$	$12.61\pm^{0.001}_{0.001}$	$12.18\pm^{0.001}_{0.001}$	$11.86\pm^{0.003}_{0.003}$	$14.66\pm^{0.012}_{0.012}$	$13.39\pm^{0.002}_{0.002}$	$12.61\pm^{0.001}_{0.001}$	$12.18\pm^{0.001}_{0.001}$	$11.83\pm^{0.003}_{0.003}$
HIPEQ0855+02	$15.47\pm^{0.049}_{0.051}$	$14.56\pm^{0.007}_{0.007}$	$14.23\pm^{0.009}_{0.009}$	$14.04\pm^{0.011}_{0.012}$	$13.94\pm^{0.039}_{0.040}$	$15.47\pm^{0.051}_{0.054}$	$14.57\pm^{0.008}_{0.008}$	$14.24\pm^{0.009}_{0.009}$	$14.05\pm^{0.012}_{0.012}$	$13.95\pm^{0.041}_{0.042}$
HIPEQ0856+00	$14.85\pm^{0.015}_{0.015}$	$14.03\pm^{0.003}_{0.003}$	$13.77\pm^{0.004}_{0.004}$	$13.56\pm^{0.004}_{0.004}$	$13.44\pm^{0.015}_{0.015}$	$14.90\pm^{0.020}_{0.021}$	$14.06\pm^{0.005}_{0.005}$	$13.80\pm^{0.006}_{0.006}$	$13.61\pm^{0.006}_{0.007}$	$13.49\pm^{0.022}_{0.022}$
HIPEQ0923-00	$15.32\pm^{0.014}_{0.015}$	$14.38\pm^{0.002}_{0.002}$	$14.08\pm^{0.003}_{0.003}$	$13.91\pm^{0.003}_{0.003}$	$13.88\pm^{0.011}_{0.011}$	$15.30\pm^{0.017}_{0.017}$	$14.40\pm^{0.003}_{0.003}$	$14.09\pm^{0.003}_{0.003}$	$13.91\pm^{0.004}_{0.004}$	$13.85\pm^{0.013}_{0.013}$
HIPEQ0930+04	$14.45\pm^{0.012}_{0.012}$	$14.01\pm^{0.003}_{0.003}$	$13.50\pm^{0.002}_{0.003}$	$13.32\pm^{0.003}_{0.003}$	$12.81\pm^{0.008}_{0.008}$	$14.43\pm^{0.011}_{0.011}$	$13.99\pm^{0.003}_{0.003}$	$13.49\pm^{0.002}_{0.002}$	$13.31\pm^{0.003}_{0.003}$	$12.80\pm^{0.008}_{0.008}$
HIPEQ0942+00	$12.71\pm^{0.004}_{0.004}$	$11.67\pm^{0.001}_{0.001}$	$11.19\pm^{0.001}_{0.001}$	$10.93\pm^{0.001}_{0.001}$	$10.73\pm^{0.002}_{0.002}$	$12.71\pm^{0.004}_{0.004}$	$11.67\pm^{0.001}_{0.001}$	$11.19\pm^{0.001}_{0.001}$	$10.93\pm^{0.001}_{0.001}$	$10.73\pm^{0.002}_{0.002}$
HIPEQ0944-00b	$16.75\pm^{0.044}_{0.046}$	$15.79\pm^{0.007}_{0.007}$	$15.50\pm^{0.009}_{0.009}$	$15.55\pm^{0.015}_{0.015}$	$15.36\pm^{0.040}_{0.041}$	$16.76\pm^{0.043}_{0.045}$	$15.79\pm^{0.007}_{0.007}$	$15.50\pm^{0.009}_{0.009}$	$15.58\pm^{0.014}_{0.014}$	$15.40\pm^{0.039}_{0.040}$
HIPEQ0945+01	$14.02\pm^{0.016}_{0.016}$	$12.95\pm^{0.002}_{0.002}$	$12.48\pm^{0.002}_{0.002}$	$12.27\pm^{0.002}_{0.002}$	$12.11\pm^{0.007}_{0.007}$	$13.94\pm^{0.021}_{0.022}$	$12.96\pm^{0.003}_{0.003}$	$12.48\pm^{0.002}_{0.002}$	$12.27\pm^{0.003}_{0.003}$	$12.04\pm^{0.009}_{0.009}$
HIPEQ0946+02	$15.63\pm^{0.031}_{0.032}$	$14.80\pm^{0.008}_{0.008}$	$14.40\pm^{0.006}_{0.006}$	$14.23\pm^{0.008}_{0.008}$	$14.07\pm^{0.021}_{0.021}$	$15.65\pm^{0.036}_{0.037}$	$14.80\pm^{0.009}_{0.009}$	$14.38\pm^{0.007}_{0.007}$	$14.23\pm^{0.009}_{0.009}$	$14.08\pm^{0.024}_{0.025}$
HIPEQ0947+00a	$15.05\pm^{0.026}_{0.027}$	$14.08\pm^{0.004}_{0.004}$	$13.66\pm^{0.004}_{0.004}$	$13.42\pm^{0.005}_{0.005}$	$13.30\pm^{0.013}_{0.013}$	$15.04\pm^{0.034}_{0.035}$	$14.09\pm^{0.005}_{0.005}$	$13.67\pm^{0.005}_{0.005}$	$13.42\pm^{0.006}_{0.006}$	$13.28\pm^{0.016}_{0.017}$
HIPEQ0947+00b	$15.80\pm^{0.054}_{0.057}$	$15.11\pm^{0.010}_{0.010}$	$14.82\pm^{0.011}_{0.011}$	$14.82\pm^{0.016}_{0.016}$	$14.81\pm^{0.053}_{0.056}$	$15.80\pm^{0.062}_{0.066}$	$15.10\pm^{0.011}_{0.011}$	$14.82\pm^{0.012}_{0.013}$	$14.81\pm^{0.018}_{0.019}$	$14.81\pm^{0.061}_{0.065}$
HIPEQ0953+01	$13.18\pm^{0.003}_{0.003}$	$12.15\pm^{0.001}_{0.001}$	$11.73\pm^{0.001}_{0.001}$	$11.56\pm^{0.001}_{0.001}$	$11.17\pm^{0.002}_{0.002}$	$12.99\pm^{0.005}_{0.005}$	$12.05\pm^{0.001}_{0.001}$	$11.64\pm^{0.001}_{0.001}$	$11.44\pm^{0.001}_{0.001}$	$11.02\pm^{0.004}_{0.004}$
HIPEQ0954+02a	$15.62\pm^{0.018}_{0.018}$	$14.32\pm^{0.003}_{0.003}$	$14.03\pm^{0.003}_{0.003}$	$13.73\pm^{0.005}_{0.005}$	$14.17\pm^{0.018}_{0.018}$	$15.62\pm^{0.018}_{0.018}$	$14.32\pm^{0.003}_{0.003}$	$14.03\pm^{0.003}_{0.003}$	$13.73\pm^{0.005}_{0.005}$	$14.17\pm^{0.018}_{0.018}$
HIPEQ0955+04a	$13.30\pm^{0.005}_{0.005}$	$12.30\pm^{0.001}_{0.001}$	$11.86\pm^{0.001}_{0.001}$	$11.66\pm^{0.001}_{0.001}$	$11.51\pm^{0.003}_{0.003}$	$13.26\pm^{0.005}_{0.005}$	$12.29\pm^{0.001}_{0.001}$	$11.85\pm^{0.001}_{0.001}$	$11.65\pm^{0.001}_{0.001}$	$11.49\pm^{0.003}_{0.003}$
HIPEQ0958+01	$17.92\pm^{0.156}_{0.182}$	$17.05\pm^{0.028}_{0.028}$	$16.97\pm^{0.041}_{0.043}$	$17.35\pm^{0.087}_{0.095}$	$17.27\pm^{0.326}_{0.467}$	$17.95\pm^{0.201}_{0.246}$	$17.05\pm^{0.036}_{0.038}$	$16.95\pm^{0.054}_{0.057}$	$17.27\pm^{0.113}_{0.127}$	$17.23\pm^{0.412}_{0.672}$
HIPEQ1000+03	$14.85\pm^{0.010}_{0.010}$	$13.62\pm^{0.001}_{0.001}$	$12.96\pm^{0.001}_{0.001}$	$12.56\pm^{0.001}_{0.001}$	$12.30\pm^{0.003}_{0.003}$	$14.82\pm^{0.011}_{0.011}$	$13.60\pm^{0.001}_{0.001}$	$12.95\pm^{0.001}_{0.001}$	$12.54\pm^{0.001}_{0.001}$	$12.27\pm^{0.003}_{0.003}$
HIPEQ1010+05	$16.52\pm^{0.023}_{0.024}$	$15.19\pm^{0.004}_{0.004}$	$14.75\pm^{0.003}_{0.003}$	$14.52\pm^{0.004}_{0.004}$	$14.52\pm^{0.013}_{0.013}$	$16.53\pm^{0.025}_{0.026}$	$15.17\pm^{0.004}_{0.004}$	$14.73\pm^{0.004}_{0.004}$	$14.50\pm^{0.004}_{0.004}$	$14.50\pm^{0.014}_{0.014}$
HIPEQ1014+03	$12.34\pm^{0.004}_{0.004}$	$10.80\pm^{0.000}_{0.000}$	$10.07\pm^{0.000}_{0.000}$	$9.64\pm^{0.000}_{0.000}$	$9.40\pm^{0.001}_{0.001}$	$12.28\pm^{0.004}_{0.004}$	$10.76\pm^{0.000}_{0.000}$	$10.04\pm^{0.000}_{0.000}$	$9.61\pm^{0.000}_{0.000}$	$9.37\pm^{0.001}_{0.001}$
HIPEQ1015+02	$15.49\pm^{0.042}_{0.043}$	$14.83\pm^{0.009}_{0.009}$	$14.59\pm^{0.011}_{0.011}$	$14.42\pm^{0.016}_{0.016}$	$14.35\pm^{0.058}_{0.061}$	$15.42\pm^{0.046}_{0.048}$	$14.81\pm^{0.010}_{0.010}$	$14.56\pm^{0.012}_{0.012}$	$14.39\pm^{0.017}_{0.017}$	$14.24\pm^{0.060}_{0.064}$
HIPEQ1026+03	$14.38\pm^{0.011}_{0.011}$	$13.26\pm^{0.002}_{0.002}$	$12.93\pm^{0.002}_{0.002}$	$12.77\pm^{0.002}_{0.002}$	$12.41\pm^{0.006}_{0.006}$	$14.36\pm^{0.012}_{0.013}$	$13.26\pm^{0.002}_{0.002}$	$12.93\pm^{0.002}_{0.002}$	$12.77\pm^{0.002}_{0.002}$	$12.38\pm^{0.007}_{0.007}$
HIPEQ1028+03	$16.32\pm^{0.030}_{0.031}$	$15.32\pm^{0.007}_{0.007}$	$15.23\pm^{0.007}_{0.007}$	$15.05\pm^{0.009}_{0.009}$	$14.89\pm^{0.023}_{0.023}$	$16.33\pm^{0.042}_{0.044}$	$15.33\pm^{0.009}_{0.009}$	$15.23\pm^{0.010}_{0.010}$	$15.05\pm^{0.012}_{0.012}$	$14.87\pm^{0.032}_{0.033}$
HIPEQ1039+01	$15.60\pm^{0.023}_{0.023}$	$14.58\pm^{0.003}_{0.003}$	$14.22\pm^{0.004}_{0.004}$	$14.00\pm^{0.005}_{0.005}$	$13.92\pm^{0.016}_{0.017}$	$15.59\pm^{0.022}_{0.023}$	$14.58\pm^{0.003}_{0.003}$	$14.22\pm^{0.004}_{0.004}$	$14.00\pm^{0.004}_{0.004}$	$13.92\pm^{0.016}_{0.017}$

Table 3.10—Continued

	Elliptical					Circular				
HIPASS Name	u^a	g^a	r^a	i^a	z^a	u^a	g^a	r^a	i^a	z^a
HIPEQ1041+00	$15.45\pm^{0.016}_{0.016}$	$14.59\pm^{0.003}_{0.003}$	$14.23\pm^{0.004}_{0.004}$	$14.01\pm^{0.005}_{0.005}$	$13.95\pm^{0.015}_{0.015}$	$15.45\pm^{0.016}_{0.016}$	$14.59\pm^{0.003}_{0.003}$	$14.23\pm^{0.004}_{0.004}$	$14.01\pm^{0.005}_{0.005}$	$13.95\pm^{0.015}_{0.015}$
HIPEQ1046+01	$14.03\pm^{0.010}_{0.010}$	$12.92\pm^{0.001}_{0.001}$	$12.43\pm^{0.001}_{0.001}$	$12.25\pm^{0.002}_{0.002}$	$11.84\pm^{0.006}_{0.006}$	$13.92\pm^{0.015}_{0.015}$	$12.90\pm^{0.002}_{0.002}$	$12.41\pm^{0.002}_{0.002}$	$12.21\pm^{0.003}_{0.003}$	$11.73\pm^{0.010}_{0.010}$
HIPEQ1050+01	$18.14\pm^{0.114}_{0.128}$	$17.14\pm^{0.023}_{0.024}$	$16.68\pm^{0.020}_{0.021}$	$16.59\pm^{0.030}_{0.031}$	$16.82\pm^{0.136}_{0.155}$	$18.20\pm^{0.134}_{0.153}$	$17.15\pm^{0.027}_{0.027}$	$16.67\pm^{0.023}_{0.023}$	$16.58\pm^{0.034}_{0.035}$	$16.94\pm^{0.150}_{0.175}$
HIPEQ1051+04a	$14.88\pm^{0.015}_{0.015}$	$14.13\pm^{0.003}_{0.003}$	$13.75\pm^{0.003}_{0.003}$	$13.66\pm^{0.004}_{0.004}$	$13.58\pm^{0.016}_{0.016}$	$14.87\pm^{0.018}_{0.018}$	$14.14\pm^{0.003}_{0.003}$	$13.75\pm^{0.004}_{0.004}$	$13.65\pm^{0.005}_{0.005}$	$13.56\pm^{0.019}_{0.019}$
HIPEQ1052+00	$16.11\pm^{0.011}_{0.011}$	$15.32\pm^{0.002}_{0.002}$	$15.04\pm^{0.003}_{0.003}$	$14.92\pm^{0.003}_{0.003}$	$14.78\pm^{0.014}_{0.014}$	$16.11\pm^{0.012}_{0.012}$	$15.32\pm^{0.002}_{0.002}$	$15.04\pm^{0.003}_{0.003}$	$14.92\pm^{0.004}_{0.004}$	$14.79\pm^{0.014}_{0.014}$
HIPEQ1053+02	$15.89\pm^{0.021}_{0.021}$	$15.54\pm^{0.005}_{0.006}$	$15.38\pm^{0.007}_{0.007}$	$15.28\pm^{0.011}_{0.011}$	$15.31\pm^{0.040}_{0.041}$	$15.87\pm^{0.023}_{0.024}$	$15.53\pm^{0.006}_{0.006}$	$15.39\pm^{0.008}_{0.008}$	$15.27\pm^{0.012}_{0.013}$	$15.32\pm^{0.044}_{0.046}$
HIPEQ1055+02	$16.63\pm^{0.035}_{0.036}$	$15.97\pm^{0.007}_{0.007}$	$15.84\pm^{0.009}_{0.009}$	$15.86\pm^{0.015}_{0.015}$	$15.84\pm^{0.067}_{0.071}$	$16.66\pm^{0.035}_{0.036}$	$16.00\pm^{0.007}_{0.007}$	$15.85\pm^{0.009}_{0.009}$	$15.86\pm^{0.015}_{0.015}$	$15.79\pm^{0.065}_{0.069}$
HIPEQ1101+03	$12.86\pm^{0.005}_{0.005}$	$11.80\pm^{0.001}_{0.001}$	$11.40\pm^{0.001}_{0.001}$	$11.09\pm^{0.001}_{0.001}$	$10.86\pm^{0.002}_{0.002}$	$12.77\pm^{0.007}_{0.007}$	$11.77\pm^{0.001}_{0.001}$	$11.37\pm^{0.001}_{0.001}$	$11.06\pm^{0.001}_{0.001}$	$10.81\pm^{0.002}_{0.002}$
HIPEQ1109-00	$15.35\pm^{0.010}_{0.010}$	$14.11\pm^{0.002}_{0.002}$	$13.52\pm^{0.001}_{0.001}$	$13.20\pm^{0.002}_{0.002}$	$13.00\pm^{0.005}_{0.005}$	$15.31\pm^{0.011}_{0.012}$	$14.10\pm^{0.002}_{0.002}$	$13.51\pm^{0.002}_{0.002}$	$13.19\pm^{0.002}_{0.002}$	$12.98\pm^{0.006}_{0.006}$
HIPEQ1110+01	$16.50\pm^{0.033}_{0.034}$	$15.63\pm^{0.006}_{0.006}$	$15.37\pm^{0.007}_{0.007}$	$15.33\pm^{0.012}_{0.012}$	$15.31\pm^{0.041}_{0.043}$	$16.51\pm^{0.036}_{0.038}$	$15.64\pm^{0.007}_{0.007}$	$15.37\pm^{0.008}_{0.008}$	$15.34\pm^{0.013}_{0.013}$	$15.32\pm^{0.046}_{0.048}$
HIPEQ1113+05	$15.57\pm^{0.020}_{0.021}$	$14.50\pm^{0.004}_{0.004}$	$14.33\pm^{0.004}_{0.004}$	$14.12\pm^{0.005}_{0.005}$	$14.61\pm^{0.018}_{0.018}$	$15.57\pm^{0.021}_{0.021}$	$14.49\pm^{0.004}_{0.004}$	$14.32\pm^{0.004}_{0.004}$	$14.12\pm^{0.005}_{0.005}$	$14.62\pm^{0.018}_{0.018}$
HIPEQ1117+04a	$13.74\pm^{0.005}_{0.005}$	$12.55\pm^{0.001}_{0.001}$	$11.99\pm^{0.001}_{0.001}$	$11.71\pm^{0.001}_{0.001}$	$11.52\pm^{0.002}_{0.002}$	$13.74\pm^{0.005}_{0.005}$	$12.55\pm^{0.001}_{0.001}$	$11.99\pm^{0.001}_{0.001}$	$11.71\pm^{0.001}_{0.001}$	$11.52\pm^{0.002}_{0.002}$
HIPEQ1119+02	$14.15\pm^{0.017}_{0.017}$	$13.57\pm^{0.003}_{0.003}$	$13.36\pm^{0.004}_{0.004}$	$13.17\pm^{0.006}_{0.006}$	$13.16\pm^{0.029}_{0.029}$	$14.13\pm^{0.017}_{0.018}$	$13.56\pm^{0.004}_{0.004}$	$13.35\pm^{0.005}_{0.005}$	$13.16\pm^{0.006}_{0.006}$	$13.13\pm^{0.030}_{0.030}$
HIPEQ1124+03	$13.70\pm^{0.009}_{0.009}$	$13.06\pm^{0.002}_{0.002}$	$12.85\pm^{0.002}_{0.002}$	$12.73\pm^{0.003}_{0.003}$	$12.57\pm^{0.010}_{0.010}$	$13.56\pm^{0.010}_{0.010}$	$12.92\pm^{0.002}_{0.002}$	$12.70\pm^{0.002}_{0.002}$	$12.57\pm^{0.004}_{0.004}$	$12.43\pm^{0.011}_{0.011}$
HIPEQ1127-01	$15.28\pm^{0.019}_{0.019}$	$14.43\pm^{0.005}_{0.005}$	$14.07\pm^{0.005}_{0.005}$	$13.87\pm^{0.006}_{0.006}$	$13.58\pm^{0.016}_{0.016}$	$15.28\pm^{0.018}_{0.018}$	$14.42\pm^{0.004}_{0.004}$	$14.07\pm^{0.004}_{0.004}$	$13.87\pm^{0.006}_{0.006}$	$13.59\pm^{0.015}_{0.015}$
HIPEQ1131-02	$14.03\pm^{0.011}_{0.011}$	$13.10\pm^{0.002}_{0.002}$	$12.66\pm^{0.002}_{0.002}$	$12.40\pm^{0.002}_{0.002}$	$12.29\pm^{0.009}_{0.009}$	$14.03\pm^{0.010}_{0.011}$	$13.10\pm^{0.002}_{0.002}$	$12.66\pm^{0.002}_{0.002}$	$12.40\pm^{0.002}_{0.002}$	$12.29\pm^{0.009}_{0.009}$
HIPEQ1133-03	$15.46\pm^{0.019}_{0.020}$	$14.63\pm^{0.005}_{0.005}$	$14.34\pm^{0.005}_{0.005}$	$14.17\pm^{0.007}_{0.007}$	$14.09\pm^{0.020}_{0.021}$	$15.45\pm^{0.021}_{0.021}$	$14.62\pm^{0.005}_{0.005}$	$14.34\pm^{0.005}_{0.005}$	$14.16\pm^{0.007}_{0.007}$	$14.05\pm^{0.022}_{0.022}$
HIPEQ1136+00	$15.48\pm^{0.008}_{0.008}$	$14.74\pm^{0.002}_{0.002}$	$14.65\pm^{0.003}_{0.003}$	$14.62\pm^{0.004}_{0.004}$	$14.62\pm^{0.014}_{0.014}$	$15.49\pm^{0.008}_{0.008}$	$14.74\pm^{0.002}_{0.002}$	$14.65\pm^{0.003}_{0.003}$	$14.62\pm^{0.004}_{0.004}$	$14.63\pm^{0.014}_{0.014}$
HIPEQ1138+03	$15.69\pm^{0.022}_{0.023}$	$14.42\pm^{0.003}_{0.003}$	$13.83\pm^{0.002}_{0.002}$	$13.52\pm^{0.003}_{0.003}$	$13.34\pm^{0.009}_{0.009}$	$15.69\pm^{0.023}_{0.023}$	$14.42\pm^{0.003}_{0.003}$	$13.83\pm^{0.002}_{0.002}$	$13.52\pm^{0.003}_{0.003}$	$13.33\pm^{0.009}_{0.009}$
HIPEQ1143-01	$18.37\pm^{0.135}_{0.154}$	$17.53\pm^{0.027}_{0.028}$	$17.31\pm^{0.035}_{0.036}$	$17.23\pm^{0.054}_{0.057}$	$17.21\pm^{0.192}_{0.234}$	$18.23\pm^{0.143}_{0.164}$	$17.52\pm^{0.030}_{0.031}$	$17.31\pm^{0.039}_{0.041}$	$17.26\pm^{0.060}_{0.063}$	$17.10\pm^{0.210}_{0.260}$
HIPEQ1145+02	$17.55\pm^{0.176}_{0.211}$	$17.01\pm^{0.045}_{0.047}$	$16.77\pm^{0.054}_{0.056}$	$16.91\pm^{0.100}_{0.110}$	$19.59\pm^{1.380}_{8.292}$	$17.66\pm^{0.177}_{0.212}$	$17.07\pm^{0.045}_{0.047}$	$16.76\pm^{0.054}_{0.057}$	$16.87\pm^{0.100}_{0.111}$	$24.95\pm^{1.384}_{8.302}$
HIPEQ1148-02	$14.73\pm^{0.022}_{0.023}$	$13.87\pm^{0.004}_{0.004}$	$13.56\pm^{0.005}_{0.005}$	$13.32\pm^{0.006}_{0.006}$	$13.28\pm^{0.021}_{0.022}$	$14.75\pm^{0.021}_{0.021}$	$13.89\pm^{0.004}_{0.004}$	$13.58\pm^{0.005}_{0.005}$	$13.36\pm^{0.006}_{0.006}$	$13.29\pm^{0.020}_{0.021}$
HIPEQ1151-02	$16.14\pm^{0.015}_{0.015}$	$15.07\pm^{0.003}_{0.003}$	$14.67\pm^{0.003}_{0.003}$	$14.48\pm^{0.004}_{0.004}$	$14.33\pm^{0.013}_{0.013}$	$16.13\pm^{0.015}_{0.016}$	$15.10\pm^{0.003}_{0.003}$	$14.68\pm^{0.003}_{0.003}$	$14.48\pm^{0.004}_{0.004}$	$14.35\pm^{0.014}_{0.014}$
HIPEQ1152+01	$15.04\pm^{0.015}_{0.015}$	$14.17\pm^{0.002}_{0.002}$	$13.83\pm^{0.003}_{0.003}$	$13.64\pm^{0.004}_{0.004}$	$13.53\pm^{0.012}_{0.013}$	$15.04\pm^{0.014}_{0.014}$	$14.17\pm^{0.002}_{0.002}$	$13.83\pm^{0.003}_{0.003}$	$13.64\pm^{0.003}_{0.003}$	$13.55\pm^{0.012}_{0.012}$
HIPEQ1152-02	$14.86\pm^{0.005}_{0.005}$	$14.33\pm^{0.001}_{0.001}$	$14.31\pm^{0.002}_{0.002}$	$14.49\pm^{0.003}_{0.003}$	$14.50\pm^{0.015}_{0.015}$	$14.85\pm^{0.006}_{0.006}$	$14.32\pm^{0.001}_{0.001}$	$14.29\pm^{0.002}_{0.002}$	$14.47\pm^{0.004}_{0.004}$	$14.47\pm^{0.017}_{0.017}$
HIPEQ1152-03b	$15.28\pm^{0.025}_{0.025}$	$14.38\pm^{0.005}_{0.005}$	$14.12\pm^{0.006}_{0.006}$	$13.97\pm^{0.008}_{0.008}$	$13.90\pm^{0.026}_{0.026}$	$15.28\pm^{0.024}_{0.024}$	$14.38\pm^{0.005}_{0.005}$	$14.12\pm^{0.005}_{0.005}$	$13.97\pm^{0.008}_{0.008}$	$13.89\pm^{0.025}_{0.025}$
HIPEQ1155+01	$14.17\pm^{0.013}_{0.013}$	$13.08\pm^{0.002}_{0.002}$	$12.61\pm^{0.002}_{0.002}$	$12.38\pm^{0.003}_{0.003}$	$12.15\pm^{0.007}_{0.007}$	$14.17\pm^{0.013}_{0.013}$	$13.08\pm^{0.002}_{0.002}$	$12.61\pm^{0.002}_{0.002}$	$12.38\pm^{0.003}_{0.003}$	$12.15\pm^{0.007}_{0.007}$
HIPEQ1200-00	$15.95\pm^{0.049}_{0.051}$	$15.05\pm^{0.010}_{0.010}$	$14.66\pm^{0.011}_{0.011}$	$14.42\pm^{0.013}_{0.014}$	$14.53\pm^{0.052}_{0.054}$	$16.00\pm^{0.049}_{0.051}$	$15.08\pm^{0.010}_{0.010}$	$14.67\pm^{0.011}_{0.011}$	$14.44\pm^{0.013}_{0.014}$	$14.58\pm^{0.052}_{0.054}$
HIPEQ1200-01	$11.86\pm^{0.002}_{0.002}$	$10.69\pm^{0.000}_{0.000}$	$10.09\pm^{0.000}_{0.000}$	$9.76\pm^{0.000}_{0.000}$	$9.54\pm^{0.001}_{0.001}$	$11.86\pm^{0.002}_{0.002}$	$10.69\pm^{0.000}_{0.000}$	$10.09\pm^{0.000}_{0.000}$	$9.76\pm^{0.000}_{0.000}$	$9.54\pm^{0.001}_{0.001}$
HIPEQ1202+01	$13.75\pm^{0.010}_{0.010}$	$12.29\pm^{0.001}_{0.001}$	$11.57\pm^{0.001}_{0.001}$	$11.17\pm^{0.001}_{0.001}$	$10.90\pm^{0.002}_{0.002}$	$13.75\pm^{0.010}_{0.010}$	$12.29\pm^{0.001}_{0.001}$	$11.57\pm^{0.001}_{0.001}$	$11.17\pm^{0.001}_{0.001}$	$10.90\pm^{0.002}_{0.002}$
HIPEQ1204-01	$15.95\pm^{0.057}_{0.060}$	$15.38\pm^{0.013}_{0.013}$	$15.05\pm^{0.015}_{0.015}$	$14.98\pm^{0.023}_{0.024}$	$14.73\pm^{0.067}_{0.071}$	$15.94\pm^{0.057}_{0.060}$	$15.38\pm^{0.013}_{0.013}$	$15.05\pm^{0.015}_{0.015}$	$14.97\pm^{0.023}_{0.024}$	$14.74\pm^{0.066}_{0.071}$

Table 3.10—Continued

	Elliptical					Circular				
HIPASS Name	u^a	g^a	r^a	i^a	z^a	u^a	g^a	r^a	i^a	z^a
HIPEQ1204-02	$15.45\pm^{0.019}_{0.019}$	$14.19\pm^{0.002}_{0.002}$	$13.57\pm^{0.002}_{0.002}$	$13.24\pm^{0.002}_{0.002}$	$13.00\pm^{0.007}_{0.007}$	$15.44\pm^{0.019}_{0.019}$	$14.19\pm^{0.002}_{0.002}$	$13.57\pm^{0.002}_{0.002}$	$13.24\pm^{0.002}_{0.002}$	$12.99\pm^{0.007}_{0.007}$
HIPEQ1210+02	$16.12\pm^{0.089}_{0.097}$	$15.28\pm^{0.014}_{0.015}$	$14.93\pm^{0.016}_{0.016}$	$14.78\pm^{0.023}_{0.023}$	$14.56\pm^{0.072}_{0.077}$	$16.13\pm^{0.087}_{0.095}$	$15.29\pm^{0.014}_{0.014}$	$14.93\pm^{0.016}_{0.016}$	$14.79\pm^{0.022}_{0.023}$	$14.56\pm^{0.070}_{0.075}$
HIPEQ1215+04a	$15.78\pm^{0.017}_{0.017}$	$14.77\pm^{0.003}_{0.003}$	$14.50\pm^{0.004}_{0.004}$	$14.37\pm^{0.005}_{0.005}$	$14.36\pm^{0.019}_{0.019}$	$15.75\pm^{0.018}_{0.018}$	$14.77\pm^{0.003}_{0.003}$	$14.50\pm^{0.004}_{0.004}$	$14.37\pm^{0.005}_{0.005}$	$14.34\pm^{0.020}_{0.021}$
HIPEQ1216-03	$15.42\pm^{0.017}_{0.018}$	$14.44\pm^{0.004}_{0.004}$	$14.03\pm^{0.003}_{0.003}$	$13.82\pm^{0.005}_{0.005}$	$13.62\pm^{0.013}_{0.013}$	$15.42\pm^{0.017}_{0.018}$	$14.44\pm^{0.004}_{0.004}$	$14.03\pm^{0.003}_{0.003}$	$13.82\pm^{0.005}_{0.005}$	$13.62\pm^{0.013}_{0.013}$
HIPEQ1218+00	$16.01\pm^{0.048}_{0.051}$	$15.12\pm^{0.010}_{0.010}$	$14.69\pm^{0.010}_{0.010}$	$14.59\pm^{0.015}_{0.016}$	$14.54\pm^{0.047}_{0.049}$	$16.02\pm^{0.050}_{0.052}$	$15.14\pm^{0.010}_{0.010}$	$14.70\pm^{0.010}_{0.010}$	$14.61\pm^{0.016}_{0.016}$	$14.56\pm^{0.048}_{0.051}$
HIPEQ1218-01	$15.52\pm^{0.013}_{0.013}$	$14.24\pm^{0.002}_{0.002}$	$13.66\pm^{0.002}_{0.002}$	$13.35\pm^{0.002}_{0.002}$	$13.17\pm^{0.006}_{0.006}$	$15.50\pm^{0.014}_{0.014}$	$14.23\pm^{0.002}_{0.002}$	$13.65\pm^{0.002}_{0.002}$	$13.34\pm^{0.002}_{0.002}$	$13.16\pm^{0.006}_{0.006}$
HIPEQ1219+03	$14.89\pm^{0.010}_{0.010}$	$14.04\pm^{0.002}_{0.002}$	$13.70\pm^{0.002}_{0.002}$	$13.58\pm^{0.003}_{0.003}$	$13.45\pm^{0.010}_{0.010}$	$14.89\pm^{0.010}_{0.010}$	$14.04\pm^{0.002}_{0.002}$	$13.70\pm^{0.002}_{0.002}$	$13.58\pm^{0.003}_{0.003}$	$13.44\pm^{0.010}_{0.010}$
HIPEQ1220+00	$16.62\pm^{0.032}_{0.033}$	$15.66\pm^{0.006}_{0.006}$	$15.52\pm^{0.008}_{0.008}$	$15.41\pm^{0.011}_{0.011}$	$15.44\pm^{0.049}_{0.051}$	$16.56\pm^{0.040}_{0.041}$	$15.68\pm^{0.007}_{0.007}$	$15.54\pm^{0.010}_{0.010}$	$15.45\pm^{0.014}_{0.014}$	$15.44\pm^{0.063}_{0.067}$
HIPEQ1220+01	$15.87\pm^{0.024}_{0.025}$	$14.77\pm^{0.004}_{0.004}$	$14.36\pm^{0.004}_{0.004}$	$14.15\pm^{0.005}_{0.006}$	$14.03\pm^{0.018}_{0.018}$	$15.86\pm^{0.044}_{0.046}$	$14.80\pm^{0.008}_{0.008}$	$14.39\pm^{0.007}_{0.007}$	$14.17\pm^{0.010}_{0.011}$	$14.02\pm^{0.034}_{0.036}$
HIPEQ1221+03	$15.27\pm^{0.018}_{0.019}$	$14.01\pm^{0.002}_{0.002}$	$13.26\pm^{0.002}_{0.002}$	$12.82\pm^{0.002}_{0.002}$	$12.48\pm^{0.006}_{0.006}$	$15.18\pm^{0.019}_{0.020}$	$14.07\pm^{0.003}_{0.003}$	$13.31\pm^{0.002}_{0.002}$	$12.85\pm^{0.002}_{0.002}$	$12.46\pm^{0.006}_{0.006}$
HIPEQ1223+00	$16.21\pm^{0.050}_{0.052}$	$15.51\pm^{0.012}_{0.012}$	$15.25\pm^{0.014}_{0.014}$	$15.15\pm^{0.022}_{0.022}$	$14.97\pm^{0.059}_{0.063}$	$16.19\pm^{0.052}_{0.054}$	$15.50\pm^{0.013}_{0.013}$	$15.23\pm^{0.015}_{0.015}$	$15.13\pm^{0.023}_{0.023}$	$14.97\pm^{0.062}_{0.065}$
HIPEQ1223-03b	$14.16\pm^{0.006}_{0.006}$	$12.73\pm^{0.001}_{0.001}$	$12.01\pm^{0.001}_{0.001}$	$11.61\pm^{0.001}_{0.001}$	$11.35\pm^{0.002}_{0.002}$	$14.10\pm^{0.008}_{0.008}$	$12.73\pm^{0.001}_{0.001}$	$12.01\pm^{0.001}_{0.001}$	$11.60\pm^{0.001}_{0.001}$	$11.32\pm^{0.003}_{0.003}$
HIPEQ1224+00	$17.95\pm^{0.116}_{0.130}$	$17.10\pm^{0.023}_{0.024}$	$16.77\pm^{0.026}_{0.027}$	$16.66\pm^{0.037}_{0.039}$	$16.60\pm^{0.156}_{0.182}$	$17.94\pm^{0.114}_{0.127}$	$17.11\pm^{0.023}_{0.023}$	$16.77\pm^{0.026}_{0.026}$	$16.67\pm^{0.037}_{0.038}$	$16.61\pm^{0.153}_{0.178}$
HIPEQ1224+03b	$14.82\pm^{0.021}_{0.021}$	$13.92\pm^{0.004}_{0.004}$	$13.59\pm^{0.004}_{0.004}$	$13.41\pm^{0.007}_{0.007}$	$13.35\pm^{0.022}_{0.022}$	$14.81\pm^{0.021}_{0.022}$	$13.92\pm^{0.004}_{0.004}$	$13.59\pm^{0.004}_{0.004}$	$13.41\pm^{0.007}_{0.007}$	$13.35\pm^{0.022}_{0.023}$
HIPEQ1225+00	$13.91\pm^{0.005}_{0.005}$	$12.84\pm^{0.001}_{0.001}$	$12.29\pm^{0.001}_{0.001}$	$12.01\pm^{0.001}_{0.001}$	$11.82\pm^{0.003}_{0.003}$	$13.89\pm^{0.005}_{0.005}$	$12.84\pm^{0.001}_{0.001}$	$12.29\pm^{0.001}_{0.001}$	$12.01\pm^{0.001}_{0.001}$	$11.81\pm^{0.003}_{0.003}$
HIPEQ1226+02	$13.52\pm^{0.004}_{0.004}$	$12.50\pm^{0.001}_{0.001}$	$12.06\pm^{0.001}_{0.001}$	$11.85\pm^{0.001}_{0.001}$	$11.68\pm^{0.003}_{0.003}$	$13.48\pm^{0.004}_{0.004}$	$12.49\pm^{0.001}_{0.001}$	$12.04\pm^{0.001}_{0.001}$	$11.83\pm^{0.001}_{0.001}$	$11.64\pm^{0.003}_{0.003}$
HIPEQ1227+01	$16.81\pm^{0.090}_{0.098}$	$16.37\pm^{0.030}_{0.030}$	$16.26\pm^{0.035}_{0.036}$	$16.26\pm^{0.059}_{0.062}$	$16.05\pm^{0.174}_{0.208}$	$16.79\pm^{0.087}_{0.094}$	$16.36\pm^{0.028}_{0.029}$	$16.24\pm^{0.033}_{0.034}$	$16.25\pm^{0.057}_{0.060}$	$16.03\pm^{0.168}_{0.198}$
HIPEQ1228+02	$15.30\pm^{0.034}_{0.035}$	$14.45\pm^{0.006}_{0.006}$	$14.14\pm^{0.007}_{0.007}$	$13.96\pm^{0.010}_{0.010}$	$13.84\pm^{0.040}_{0.042}$	$15.32\pm^{0.034}_{0.036}$	$14.48\pm^{0.006}_{0.006}$	$14.16\pm^{0.007}_{0.007}$	$13.98\pm^{0.010}_{0.010}$	$13.89\pm^{0.041}_{0.043}$
HIPEQ1228+03	$12.71\pm^{0.003}_{0.003}$	$11.15\pm^{0.000}_{0.000}$	$10.45\pm^{0.000}_{0.000}$	$10.09\pm^{0.000}_{0.000}$	$9.85\pm^{0.001}_{0.001}$	$12.71\pm^{0.003}_{0.003}$	$11.15\pm^{0.000}_{0.000}$	$10.45\pm^{0.000}_{0.000}$	$10.08\pm^{0.000}_{0.000}$	$9.85\pm^{0.001}_{0.001}$
HIPEQ1229+00	$17.59\pm^{0.077}_{0.083}$	$16.61\pm^{0.012}_{0.012}$	$16.21\pm^{0.012}_{0.013}$	$16.20\pm^{0.019}_{0.020}$	$16.19\pm^{0.072}_{0.077}$	$17.56\pm^{0.102}_{0.112}$	$16.61\pm^{0.017}_{0.017}$	$16.24\pm^{0.018}_{0.018}$	$16.19\pm^{0.027}_{0.028}$	$16.20\pm^{0.099}_{0.109}$
HIPEQ1230+02	$16.22\pm^{0.042}_{0.044}$	$15.34\pm^{0.007}_{0.007}$	$15.15\pm^{0.009}_{0.009}$	$15.06\pm^{0.014}_{0.014}$	$15.04\pm^{0.064}_{0.068}$	$16.23\pm^{0.046}_{0.048}$	$15.35\pm^{0.008}_{0.008}$	$15.15\pm^{0.010}_{0.010}$	$15.06\pm^{0.015}_{0.015}$	$15.05\pm^{0.070}_{0.074}$
HIPEQ1230+03	$16.36\pm^{0.022}_{0.022}$	$15.59\pm^{0.004}_{0.004}$	$15.42\pm^{0.005}_{0.005}$	$15.31\pm^{0.008}_{0.008}$	$15.26\pm^{0.028}_{0.029}$	$16.37\pm^{0.023}_{0.023}$	$15.60\pm^{0.004}_{0.004}$	$15.42\pm^{0.005}_{0.005}$	$15.31\pm^{0.008}_{0.008}$	$15.23\pm^{0.029}_{0.030}$
HIPEQ1232+00a	$13.79\pm^{0.011}_{0.011}$	$12.80\pm^{0.002}_{0.002}$	$12.41\pm^{0.002}_{0.002}$	$12.20\pm^{0.003}_{0.003}$	$12.17\pm^{0.012}_{0.012}$	$13.81\pm^{0.012}_{0.012}$	$12.82\pm^{0.002}_{0.002}$	$12.43\pm^{0.002}_{0.002}$	$12.22\pm^{0.003}_{0.003}$	$12.18\pm^{0.013}_{0.013}$
HIPEQ1232+00b	$12.24\pm^{0.003}_{0.003}$	$11.06\pm^{0.000}_{0.000}$	$10.38\pm^{0.000}_{0.000}$	$9.98\pm^{0.000}_{0.000}$	$9.66\pm^{0.001}_{0.001}$	$12.05\pm^{0.004}_{0.004}$	$10.94\pm^{0.001}_{0.001}$	$10.27\pm^{0.000}_{0.000}$	$9.86\pm^{0.001}_{0.001}$	$9.53\pm^{0.002}_{0.002}$
HIPEQ1233-02	$15.49\pm^{0.040}_{0.042}$	$14.81\pm^{0.009}_{0.010}$	$14.41\pm^{0.011}_{0.011}$	$14.27\pm^{0.016}_{0.016}$	$14.28\pm^{0.064}_{0.067}$	$15.49\pm^{0.042}_{0.044}$	$14.81\pm^{0.010}_{0.010}$	$14.41\pm^{0.012}_{0.012}$	$14.26\pm^{0.016}_{0.017}$	$14.28\pm^{0.066}_{0.071}$
HIPEQ1236+03	$16.54\pm^{0.051}_{0.053}$	$15.80\pm^{0.010}_{0.010}$	$15.51\pm^{0.012}_{0.012}$	$15.37\pm^{0.019}_{0.019}$	$15.30\pm^{0.061}_{0.065}$	$16.60\pm^{0.063}_{0.066}$	$15.85\pm^{0.013}_{0.013}$	$15.57\pm^{0.015}_{0.015}$	$15.41\pm^{0.024}_{0.024}$	$15.34\pm^{0.076}_{0.082}$
HIPEQ1239-00	$12.90\pm^{0.003}_{0.003}$	$12.03\pm^{0.001}_{0.001}$	$11.69\pm^{0.001}_{0.001}$	$11.53\pm^{0.001}_{0.001}$	$11.42\pm^{0.003}_{0.003}$	$12.90\pm^{0.004}_{0.004}$	$12.04\pm^{0.001}_{0.001}$	$11.69\pm^{0.001}_{0.001}$	$11.52\pm^{0.001}_{0.001}$	$11.39\pm^{0.003}_{0.003}$
HIPEQ1241+01	$15.67\pm^{0.013}_{0.014}$	$14.65\pm^{0.003}_{0.003}$	$14.20\pm^{0.002}_{0.002}$	$13.95\pm^{0.003}_{0.003}$	$13.77\pm^{0.009}_{0.010}$	$15.68\pm^{0.014}_{0.014}$	$14.66\pm^{0.003}_{0.003}$	$14.21\pm^{0.002}_{0.002}$	$13.96\pm^{0.003}_{0.003}$	$13.78\pm^{0.010}_{0.010}$
HIPEQ1241-02	$15.52\pm^{0.017}_{0.018}$	$14.50\pm^{0.003}_{0.003}$	$14.04\pm^{0.003}_{0.003}$	$13.77\pm^{0.004}_{0.004}$	$13.62\pm^{0.011}_{0.012}$	$15.50\pm^{0.019}_{0.019}$	$14.50\pm^{0.003}_{0.003}$	$14.04\pm^{0.003}_{0.003}$	$13.75\pm^{0.004}_{0.004}$	$13.60\pm^{0.012}_{0.013}$
HIPEQ1242+03b	$13.76\pm^{0.006}_{0.006}$	$12.71\pm^{0.001}_{0.001}$	$12.15\pm^{0.001}_{0.001}$	$11.87\pm^{0.001}_{0.001}$	$11.73\pm^{0.003}_{0.003}$	$13.74\pm^{0.006}_{0.006}$	$12.70\pm^{0.001}_{0.001}$	$12.15\pm^{0.001}_{0.001}$	$11.86\pm^{0.001}_{0.001}$	$11.72\pm^{0.003}_{0.003}$
HIPEQ1242-00	$13.00\pm^{0.003}_{0.003}$	$11.96\pm^{0.001}_{0.001}$	$11.50\pm^{0.001}_{0.001}$	$11.27\pm^{0.001}_{0.001}$	$11.08\pm^{0.002}_{0.002}$	$12.96\pm^{0.004}_{0.004}$	$11.94\pm^{0.001}_{0.001}$	$11.48\pm^{0.001}_{0.001}$	$11.25\pm^{0.001}_{0.001}$	$11.05\pm^{0.002}_{0.002}$

Table 3.10—Continued

	Elliptical					Circular				
HIPASS Name	u^a	g^a	r^a	i^a	z^a	u^a	g^a	r^a	i^a	z^a
HIPEQ1242-01a	$14.68\pm^{0.012}_{0.012}$	$13.82\pm^{0.002}_{0.002}$	$13.51\pm^{0.003}_{0.003}$	$13.31\pm^{0.004}_{0.004}$	$13.17\pm^{0.012}_{0.012}$	$14.67\pm^{0.012}_{0.012}$	$13.81\pm^{0.002}_{0.002}$	$13.51\pm^{0.003}_{0.003}$	$13.31\pm^{0.004}_{0.004}$	$13.17\pm^{0.012}_{0.012}$
HIPEQ1242-01b	$15.02\pm^{0.014}_{0.014}$	$13.73\pm^{0.002}_{0.002}$	$13.22\pm^{0.002}_{0.002}$	$12.95\pm^{0.002}_{0.002}$	$12.83\pm^{0.008}_{0.008}$	$14.93\pm^{0.019}_{0.019}$	$13.75\pm^{0.002}_{0.002}$	$13.23\pm^{0.002}_{0.003}$	$12.96\pm^{0.003}_{0.003}$	$12.80\pm^{0.010}_{0.011}$
HIPEQ1243-00	$13.48\pm^{0.007}_{0.007}$	$12.52\pm^{0.001}_{0.001}$	$12.09\pm^{0.001}_{0.001}$	$11.80\pm^{0.002}_{0.002}$	$11.63\pm^{0.004}_{0.004}$	$13.48\pm^{0.007}_{0.007}$	$12.52\pm^{0.001}_{0.001}$	$12.09\pm^{0.001}_{0.001}$	$11.80\pm^{0.002}_{0.002}$	$11.63\pm^{0.004}_{0.004}$
HIPEQ1244+00	$14.35\pm^{0.014}_{0.014}$	$13.44\pm^{0.003}_{0.003}$	$13.15\pm^{0.003}_{0.003}$	$13.28\pm^{0.008}_{0.008}$	$12.88\pm^{0.015}_{0.015}$	$14.38\pm^{0.014}_{0.014}$	$13.45\pm^{0.003}_{0.003}$	$13.14\pm^{0.003}_{0.003}$	$13.14\pm^{0.007}_{0.007}$	$12.86\pm^{0.014}_{0.015}$
HIPEQ1244-02	$15.65\pm^{0.038}_{0.039}$	$14.92\pm^{0.008}_{0.008}$	$14.68\pm^{0.010}_{0.010}$	$14.57\pm^{0.015}_{0.015}$	$14.40\pm^{0.058}_{0.061}$	$15.63\pm^{0.040}_{0.041}$	$14.92\pm^{0.008}_{0.008}$	$14.68\pm^{0.010}_{0.010}$	$14.57\pm^{0.016}_{0.016}$	$14.41\pm^{0.061}_{0.065}$
HIPEQ1245-00	$12.38\pm^{0.002}_{0.002}$	$11.07\pm^{0.000}_{0.000}$	$10.33\pm^{0.000}_{0.000}$	$9.91\pm^{0.000}_{0.000}$	$9.60\pm^{0.001}_{0.001}$	$12.33\pm^{0.003}_{0.003}$	$11.05\pm^{0.000}_{0.000}$	$10.31\pm^{0.000}_{0.000}$	$9.89\pm^{0.000}_{0.000}$	$9.58\pm^{0.001}_{0.001}$
HIPEQ1249+03	$13.43\pm^{0.004}_{0.004}$	$12.51\pm^{0.001}_{0.001}$	$12.12\pm^{0.001}_{0.001}$	$11.92\pm^{0.001}_{0.001}$	$11.80\pm^{0.003}_{0.003}$	$13.42\pm^{0.004}_{0.005}$	$12.51\pm^{0.001}_{0.001}$	$12.12\pm^{0.001}_{0.001}$	$11.92\pm^{0.001}_{0.001}$	$11.79\pm^{0.003}_{0.003}$
HIPEQ1249+04	$16.02\pm^{0.037}_{0.039}$	$15.10\pm^{0.008}_{0.008}$	$14.87\pm^{0.009}_{0.009}$	$14.74\pm^{0.013}_{0.014}$	$15.37\pm^{0.063}_{0.067}$	$16.03\pm^{0.036}_{0.037}$	$15.09\pm^{0.007}_{0.007}$	$14.87\pm^{0.009}_{0.009}$	$14.75\pm^{0.013}_{0.013}$	$15.38\pm^{0.061}_{0.064}$
HIPEQ1250+05	$12.64\pm^{0.003}_{0.003}$	$11.88\pm^{0.001}_{0.001}$	$11.57\pm^{0.001}_{0.001}$	$11.44\pm^{0.001}_{0.001}$	$11.31\pm^{0.003}_{0.003}$	$12.63\pm^{0.003}_{0.003}$	$11.88\pm^{0.001}_{0.001}$	$11.57\pm^{0.001}_{0.001}$	$11.44\pm^{0.001}_{0.001}$	$11.30\pm^{0.003}_{0.003}$
HIPEQ1253+01	$13.71\pm^{0.007}_{0.007}$	$12.38\pm^{0.001}_{0.001}$	$11.73\pm^{0.001}_{0.001}$	$11.35\pm^{0.001}_{0.001}$	$11.11\pm^{0.003}_{0.003}$	$13.65\pm^{0.009}_{0.009}$	$12.39\pm^{0.001}_{0.001}$	$11.73\pm^{0.001}_{0.001}$	$11.35\pm^{0.001}_{0.001}$	$11.08\pm^{0.003}_{0.004}$
HIPEQ1253+02	$13.21\pm^{0.008}_{0.008}$	$11.66\pm^{0.001}_{0.001}$	$10.95\pm^{0.001}_{0.001}$	$10.55\pm^{0.001}_{0.001}$	$10.28\pm^{0.002}_{0.002}$	$13.22\pm^{0.008}_{0.008}$	$11.66\pm^{0.001}_{0.001}$	$10.95\pm^{0.001}_{0.001}$	$10.55\pm^{0.001}_{0.001}$	$10.28\pm^{0.002}_{0.002}$
HIPEQ1253+04	$13.88\pm^{0.004}_{0.004}$	$13.06\pm^{0.001}_{0.001}$	$12.76\pm^{0.001}_{0.001}$	$12.64\pm^{0.001}_{0.001}$	$12.58\pm^{0.003}_{0.003}$	$13.89\pm^{0.004}_{0.004}$	$13.06\pm^{0.001}_{0.001}$	$12.76\pm^{0.001}_{0.001}$	$12.64\pm^{0.001}_{0.001}$	$12.57\pm^{0.003}_{0.003}$
HIPEQ1255+00	$13.41\pm^{0.007}_{0.007}$	$12.47\pm^{0.001}_{0.001}$	$12.03\pm^{0.001}_{0.001}$	$11.80\pm^{0.002}_{0.002}$	$11.69\pm^{0.006}_{0.006}$	$13.41\pm^{0.007}_{0.007}$	$12.47\pm^{0.001}_{0.001}$	$12.03\pm^{0.001}_{0.001}$	$11.80\pm^{0.002}_{0.002}$	$11.69\pm^{0.006}_{0.006}$
HIPEQ1255+02	$14.83\pm^{0.007}_{0.007}$	$13.42\pm^{0.001}_{0.001}$	$12.73\pm^{0.001}_{0.001}$	$12.37\pm^{0.001}_{0.001}$	$12.12\pm^{0.002}_{0.002}$	$14.79\pm^{0.009}_{0.009}$	$13.40\pm^{0.001}_{0.001}$	$12.72\pm^{0.001}_{0.001}$	$12.35\pm^{0.001}_{0.001}$	$12.09\pm^{0.003}_{0.003}$
HIPEQ1255-00	$16.54\pm^{0.041}_{0.043}$	$15.69\pm^{0.008}_{0.008}$	$15.33\pm^{0.009}_{0.009}$	$15.19\pm^{0.012}_{0.012}$	$15.12\pm^{0.043}_{0.045}$	$16.50\pm^{0.060}_{0.063}$	$15.65\pm^{0.012}_{0.012}$	$15.28\pm^{0.013}_{0.013}$	$15.11\pm^{0.017}_{0.018}$	$15.01\pm^{0.057}_{0.061}$
HIPEQ1256+03	$16.76\pm^{0.099}_{0.108}$	$15.85\pm^{0.016}_{0.016}$	$15.77\pm^{0.021}_{0.022}$	$15.77\pm^{0.031}_{0.032}$	$16.08\pm^{0.146}_{0.169}$	$16.76\pm^{0.099}_{0.109}$	$15.85\pm^{0.016}_{0.017}$	$15.77\pm^{0.021}_{0.022}$	$15.77\pm^{0.031}_{0.032}$	$16.07\pm^{0.147}_{0.169}$
HIPEQ1257+02	$15.75\pm^{0.038}_{0.040}$	$15.13\pm^{0.008}_{0.008}$	$14.85\pm^{0.010}_{0.010}$	$14.75\pm^{0.015}_{0.015}$	$14.62\pm^{0.060}_{0.064}$	$15.77\pm^{0.038}_{0.039}$	$15.13\pm^{0.008}_{0.008}$	$14.85\pm^{0.009}_{0.010}$	$14.75\pm^{0.015}_{0.015}$	$14.62\pm^{0.060}_{0.063}$
HIPEQ1257-01	$14.83\pm^{0.008}_{0.008}$	$13.76\pm^{0.001}_{0.001}$	$13.25\pm^{0.001}_{0.001}$	$12.98\pm^{0.002}_{0.002}$	$12.84\pm^{0.006}_{0.006}$	$14.80\pm^{0.010}_{0.010}$	$13.78\pm^{0.002}_{0.002}$	$13.27\pm^{0.002}_{0.002}$	$12.98\pm^{0.003}_{0.003}$	$12.80\pm^{0.008}_{0.008}$
HIPEQ1258+02	$15.16\pm^{0.031}_{0.032}$	$14.17\pm^{0.005}_{0.005}$	$13.84\pm^{0.005}_{0.005}$	$13.62\pm^{0.007}_{0.007}$	$13.49\pm^{0.031}_{0.032}$	$15.16\pm^{0.033}_{0.034}$	$14.16\pm^{0.005}_{0.005}$	$13.84\pm^{0.006}_{0.006}$	$13.61\pm^{0.008}_{0.008}$	$13.48\pm^{0.032}_{0.033}$
HIPEQ1300+02a	$15.73\pm^{0.031}_{0.032}$	$14.58\pm^{0.004}_{0.004}$	$14.18\pm^{0.005}_{0.005}$	$13.99\pm^{0.006}_{0.006}$	$13.90\pm^{0.024}_{0.024}$	$15.73\pm^{0.031}_{0.032}$	$14.58\pm^{0.004}_{0.004}$	$14.17\pm^{0.005}_{0.005}$	$13.99\pm^{0.006}_{0.006}$	$13.89\pm^{0.023}_{0.024}$
HIPEQ1300+02b	$12.42\pm^{0.003}_{0.003}$	$11.52\pm^{0.001}_{0.001}$	$11.11\pm^{0.001}_{0.001}$	$10.84\pm^{0.001}_{0.001}$	$10.63\pm^{0.003}_{0.003}$	$12.42\pm^{0.003}_{0.003}$	$11.52\pm^{0.001}_{0.001}$	$11.11\pm^{0.001}_{0.001}$	$10.84\pm^{0.001}_{0.001}$	$10.62\pm^{0.003}_{0.003}$
HIPEQ1303+03	$15.21\pm^{0.025}_{0.026}$	$14.32\pm^{0.006}_{0.006}$	$14.04\pm^{0.005}_{0.005}$	$13.89\pm^{0.007}_{0.007}$	$13.84\pm^{0.022}_{0.022}$	$15.21\pm^{0.025}_{0.026}$	$14.32\pm^{0.006}_{0.006}$	$14.05\pm^{0.005}_{0.005}$	$13.89\pm^{0.007}_{0.007}$	$13.84\pm^{0.022}_{0.022}$
HIPEQ1304-02	$16.97\pm^{0.041}_{0.043}$	$16.02\pm^{0.007}_{0.007}$	$15.59\pm^{0.008}_{0.008}$	$15.45\pm^{0.012}_{0.012}$	$15.56\pm^{0.047}_{0.049}$	$16.97\pm^{0.044}_{0.046}$	$16.02\pm^{0.008}_{0.008}$	$15.58\pm^{0.009}_{0.009}$	$15.44\pm^{0.012}_{0.012}$	$15.56\pm^{0.050}_{0.052}$
HIPEQ1304-03	$13.62\pm^{0.011}_{0.011}$	$12.76\pm^{0.002}_{0.002}$	$12.53\pm^{0.003}_{0.003}$	$12.41\pm^{0.004}_{0.004}$	$12.45\pm^{0.014}_{0.014}$	$13.62\pm^{0.011}_{0.011}$	$12.76\pm^{0.002}_{0.002}$	$12.53\pm^{0.003}_{0.003}$	$12.41\pm^{0.004}_{0.004}$	$12.45\pm^{0.014}_{0.014}$
HIPEQ1307-00	$14.60\pm^{0.006}_{0.007}$	$13.67\pm^{0.002}_{0.002}$	$13.32\pm^{0.001}_{0.001}$	$13.15\pm^{0.002}_{0.002}$	$13.03\pm^{0.006}_{0.006}$	$14.60\pm^{0.007}_{0.007}$	$13.67\pm^{0.002}_{0.002}$	$13.32\pm^{0.002}_{0.002}$	$13.15\pm^{0.002}_{0.002}$	$13.03\pm^{0.006}_{0.006}$
HIPEQ1308-02	$15.10\pm^{0.013}_{0.013}$	$14.05\pm^{0.002}_{0.002}$	$13.61\pm^{0.002}_{0.002}$	$13.41\pm^{0.003}_{0.003}$	$13.21\pm^{0.012}_{0.012}$	$15.11\pm^{0.013}_{0.013}$	$14.05\pm^{0.002}_{0.002}$	$13.62\pm^{0.002}_{0.002}$	$13.42\pm^{0.003}_{0.003}$	$13.22\pm^{0.012}_{0.012}$
HIPEQ1311+03a	$16.54\pm^{0.026}_{0.027}$	$15.55\pm^{0.004}_{0.004}$	$15.22\pm^{0.004}_{0.004}$	$15.09\pm^{0.007}_{0.007}$	$14.93\pm^{0.022}_{0.022}$	$16.50\pm^{0.031}_{0.032}$	$15.58\pm^{0.005}_{0.005}$	$15.25\pm^{0.005}_{0.005}$	$15.10\pm^{0.008}_{0.008}$	$14.96\pm^{0.026}_{0.027}$
HIPEQ1312+03	$16.21\pm^{0.022}_{0.023}$	$14.78\pm^{0.003}_{0.003}$	$14.22\pm^{0.002}_{0.002}$	$13.92\pm^{0.003}_{0.003}$	$13.74\pm^{0.009}_{0.009}$	$16.19\pm^{0.024}_{0.025}$	$14.76\pm^{0.003}_{0.003}$	$14.20\pm^{0.002}_{0.002}$	$13.90\pm^{0.003}_{0.003}$	$13.73\pm^{0.010}_{0.010}$
HIPEQ1312+05	$17.50\pm^{0.091}_{0.099}$	$16.44\pm^{0.016}_{0.016}$	$16.22\pm^{0.019}_{0.020}$	$16.11\pm^{0.029}_{0.029}$	$16.51\pm^{0.132}_{0.151}$	$17.52\pm^{0.103}_{0.114}$	$16.45\pm^{0.018}_{0.018}$	$16.23\pm^{0.022}_{0.022}$	$16.09\pm^{0.033}_{0.034}$	$16.50\pm^{0.150}_{0.174}$
HIPEQ1313+06	$15.22\pm^{0.016}_{0.016}$	$13.90\pm^{0.002}_{0.002}$	$13.34\pm^{0.002}_{0.002}$	$13.05\pm^{0.002}_{0.002}$	$12.87\pm^{0.005}_{0.005}$	$15.21\pm^{0.016}_{0.016}$	$13.90\pm^{0.002}_{0.002}$	$13.34\pm^{0.002}_{0.002}$	$13.06\pm^{0.002}_{0.002}$	$12.88\pm^{0.005}_{0.005}$
HIPEQ1317-00	$16.35\pm^{0.020}_{0.020}$	$15.67\pm^{0.006}_{0.006}$	$15.57\pm^{0.007}_{0.007}$	$15.62\pm^{0.011}_{0.011}$	$15.57\pm^{0.036}_{0.037}$	$16.36\pm^{0.029}_{0.030}$	$15.66\pm^{0.008}_{0.008}$	$15.56\pm^{0.010}_{0.010}$	$15.63\pm^{0.017}_{0.017}$	$15.65\pm^{0.053}_{0.056}$

Table 3.10—Continued

	Elliptical					Circular				
HIPASS Name	u^a	g^a	r^a	i^a	z^a	u^a	g^a	r^a	i^a	z^a
HIPEQ1318-01	$14.91\pm^{0.013}_{0.013}$	$13.85\pm^{0.002}_{0.002}$	$13.34\pm^{0.002}_{0.002}$	$13.05\pm^{0.003}_{0.003}$	$12.84\pm^{0.008}_{0.008}$	$14.91\pm^{0.013}_{0.013}$	$13.85\pm^{0.002}_{0.002}$	$13.34\pm^{0.002}_{0.002}$	$13.05\pm^{0.003}_{0.003}$	$12.83\pm^{0.008}_{0.008}$
HIPEQ1320+05	$15.59\pm^{0.027}_{0.028}$	$14.91\pm^{0.005}_{0.005}$	$14.48\pm^{0.005}_{0.005}$	$14.37\pm^{0.007}_{0.007}$	$13.72\pm^{0.022}_{0.022}$	$15.57\pm^{0.031}_{0.032}$	$14.91\pm^{0.006}_{0.006}$	$14.47\pm^{0.006}_{0.006}$	$14.35\pm^{0.008}_{0.008}$	$13.68\pm^{0.025}_{0.025}$
HIPEQ1327+02	$17.21\pm^{0.070}_{0.075}$	$16.35\pm^{0.013}_{0.013}$	$16.16\pm^{0.017}_{0.017}$	$16.11\pm^{0.028}_{0.028}$	$16.25\pm^{0.111}_{0.123}$	$17.13\pm^{0.078}_{0.084}$	$16.32\pm^{0.014}_{0.014}$	$16.15\pm^{0.018}_{0.019}$	$16.13\pm^{0.030}_{0.031}$	$16.18\pm^{0.116}_{0.130}$
HIPEQ1329-00	$16.75\pm^{0.042}_{0.044}$	$15.89\pm^{0.009}_{0.009}$	$15.52\pm^{0.009}_{0.009}$	$15.39\pm^{0.013}_{0.013}$	$15.26\pm^{0.042}_{0.043}$	$16.71\pm^{0.048}_{0.050}$	$15.86\pm^{0.010}_{0.010}$	$15.51\pm^{0.011}_{0.011}$	$15.36\pm^{0.015}_{0.015}$	$15.20\pm^{0.048}_{0.050}$
HIPEQ1332+01	$14.94\pm^{0.014}_{0.014}$	$13.66\pm^{0.002}_{0.002}$	$13.05\pm^{0.001}_{0.001}$	$12.72\pm^{0.002}_{0.002}$	$12.51\pm^{0.005}_{0.005}$	$14.94\pm^{0.014}_{0.014}$	$13.66\pm^{0.002}_{0.002}$	$13.05\pm^{0.001}_{0.001}$	$12.72\pm^{0.002}_{0.002}$	$12.51\pm^{0.005}_{0.005}$
HIPEQ1335+01	$14.83\pm^{0.015}_{0.015}$	$13.57\pm^{0.002}_{0.002}$	$13.03\pm^{0.002}_{0.002}$	$12.73\pm^{0.002}_{0.002}$	$12.56\pm^{0.008}_{0.008}$	$14.83\pm^{0.015}_{0.015}$	$13.56\pm^{0.002}_{0.002}$	$13.02\pm^{0.002}_{0.002}$	$12.72\pm^{0.002}_{0.002}$	$12.56\pm^{0.008}_{0.008}$
HIPEQ1341+05	$15.80\pm^{0.025}_{0.025}$	$14.73\pm^{0.003}_{0.003}$	$14.35\pm^{0.004}_{0.004}$	$14.15\pm^{0.004}_{0.004}$	$14.07\pm^{0.019}_{0.019}$	$15.81\pm^{0.023}_{0.024}$	$14.74\pm^{0.003}_{0.003}$	$14.35\pm^{0.004}_{0.004}$	$14.15\pm^{0.004}_{0.004}$	$14.07\pm^{0.018}_{0.018}$
HIPEQ1348+03	$13.10\pm^{0.006}_{0.006}$	$12.01\pm^{0.001}_{0.001}$	$11.56\pm^{0.001}_{0.001}$	$11.31\pm^{0.001}_{0.001}$	$10.92\pm^{0.004}_{0.004}$	$13.10\pm^{0.006}_{0.006}$	$12.02\pm^{0.001}_{0.001}$	$11.57\pm^{0.001}_{0.001}$	$11.31\pm^{0.001}_{0.001}$	$10.92\pm^{0.004}_{0.004}$
HIPEQ1352+02a	$14.44\pm^{0.018}_{0.018}$	$13.12\pm^{0.002}_{0.002}$	$12.46\pm^{0.002}_{0.002}$	$12.11\pm^{0.002}_{0.002}$	$11.88\pm^{0.006}_{0.006}$	$14.44\pm^{0.017}_{0.017}$	$13.12\pm^{0.002}_{0.002}$	$12.46\pm^{0.002}_{0.002}$	$12.10\pm^{0.002}_{0.002}$	$11.87\pm^{0.006}_{0.006}$
HIPEQ1352-01	$13.00\pm^{0.006}_{0.006}$	$11.98\pm^{0.001}_{0.001}$	$11.54\pm^{0.001}_{0.001}$	$11.26\pm^{0.001}_{0.001}$	$11.15\pm^{0.004}_{0.004}$	$13.01\pm^{0.006}_{0.006}$	$11.99\pm^{0.001}_{0.001}$	$11.55\pm^{0.001}_{0.001}$	$11.27\pm^{0.001}_{0.001}$	$11.16\pm^{0.004}_{0.004}$
HIPEQ1400+02	$15.69\pm^{0.022}_{0.023}$	$14.61\pm^{0.003}_{0.003}$	$14.19\pm^{0.003}_{0.003}$	$13.98\pm^{0.004}_{0.004}$	$13.80\pm^{0.014}_{0.014}$	$15.69\pm^{0.032}_{0.033}$	$14.65\pm^{0.005}_{0.005}$	$14.22\pm^{0.005}_{0.005}$	$13.99\pm^{0.006}_{0.006}$	$13.79\pm^{0.020}_{0.021}$
HIPEQ1411-01	$13.72\pm^{0.007}_{0.007}$	$12.69\pm^{0.001}_{0.001}$	$12.35\pm^{0.001}_{0.001}$	$12.28\pm^{0.002}_{0.002}$	$12.13\pm^{0.005}_{0.005}$	$13.59\pm^{0.010}_{0.010}$	$12.66\pm^{0.002}_{0.002}$	$12.33\pm^{0.002}_{0.002}$	$12.23\pm^{0.003}_{0.003}$	$12.03\pm^{0.008}_{0.008}$
HIPEQ1415+04	$15.55\pm^{0.016}_{0.016}$	$15.03\pm^{0.003}_{0.004}$	$14.72\pm^{0.004}_{0.004}$	$14.49\pm^{0.005}_{0.005}$	$14.05\pm^{0.013}_{0.013}$	$15.55\pm^{0.016}_{0.016}$	$15.03\pm^{0.003}_{0.003}$	$14.72\pm^{0.004}_{0.004}$	$14.49\pm^{0.005}_{0.005}$	$14.05\pm^{0.013}_{0.013}$
HIPEQ1416+03	$17.22\pm^{0.095}_{0.104}$	$16.48\pm^{0.017}_{0.017}$	$16.15\pm^{0.019}_{0.019}$	$16.22\pm^{0.027}_{0.028}$	$16.02\pm^{0.106}_{0.118}$	$16.82\pm^{0.084}_{0.091}$	$16.07\pm^{0.015}_{0.015}$	$15.71\pm^{0.017}_{0.017}$	$15.72\pm^{0.024}_{0.025}$	$15.47\pm^{0.094}_{0.103}$
HIPEQ1422-00	$12.83\pm^{0.005}_{0.005}$	$11.90\pm^{0.001}_{0.001}$	$11.50\pm^{0.001}_{0.001}$	$11.34\pm^{0.001}_{0.001}$	$11.15\pm^{0.004}_{0.004}$	$12.83\pm^{0.005}_{0.005}$	$11.89\pm^{0.001}_{0.001}$	$11.50\pm^{0.001}_{0.001}$	$11.33\pm^{0.001}_{0.001}$	$11.14\pm^{0.004}_{0.004}$
HIPEQ1429-00	$14.91\pm^{0.011}_{0.011}$	$14.07\pm^{0.002}_{0.002}$	$13.80\pm^{0.003}_{0.003}$	$13.66\pm^{0.004}_{0.004}$	$13.58\pm^{0.013}_{0.013}$	$14.91\pm^{0.012}_{0.012}$	$14.07\pm^{0.002}_{0.002}$	$13.80\pm^{0.003}_{0.003}$	$13.66\pm^{0.004}_{0.004}$	$13.57\pm^{0.015}_{0.015}$
HIPEQ1432+00	$15.24\pm^{0.012}_{0.012}$	$14.07\pm^{0.002}_{0.002}$	$13.56\pm^{0.002}_{0.002}$	$13.28\pm^{0.002}_{0.002}$	$13.10\pm^{0.008}_{0.008}$	$15.20\pm^{0.017}_{0.017}$	$14.07\pm^{0.002}_{0.002}$	$13.56\pm^{0.002}_{0.002}$	$13.27\pm^{0.003}_{0.003}$	$13.08\pm^{0.011}_{0.011}$
HIPEQ1433+01	$17.73\pm^{0.189}_{0.229}$	$16.87\pm^{0.027}_{0.028}$	$16.73\pm^{0.038}_{0.040}$	$16.45\pm^{0.048}_{0.050}$	$16.91\pm^{0.240}_{0.309}$	$17.84\pm^{0.247}_{0.320}$	$16.85\pm^{0.037}_{0.038}$	$16.71\pm^{0.053}_{0.055}$	$16.43\pm^{0.067}_{0.071}$	$16.83\pm^{0.322}_{0.459}$
HIPEQ1433+02	$15.38\pm^{0.016}_{0.016}$	$14.56\pm^{0.003}_{0.003}$	$14.32\pm^{0.004}_{0.004}$	$14.28\pm^{0.006}_{0.006}$	$14.21\pm^{0.021}_{0.021}$	$15.37\pm^{0.017}_{0.017}$	$14.54\pm^{0.003}_{0.003}$	$14.31\pm^{0.004}_{0.004}$	$14.28\pm^{0.007}_{0.007}$	$14.21\pm^{0.021}_{0.022}$
HIPEQ1437+02	$13.32\pm^{0.005}_{0.005}$	$12.32\pm^{0.001}_{0.001}$	$11.68\pm^{0.001}_{0.001}$	$11.42\pm^{0.001}_{0.001}$	$11.06\pm^{0.003}_{0.003}$	$12.92\pm^{0.005}_{0.005}$	$12.17\pm^{0.001}_{0.001}$	$11.45\pm^{0.001}_{0.001}$	$11.16\pm^{0.001}_{0.001}$	$10.78\pm^{0.003}_{0.003}$
HIPEQ1437-00	$13.57\pm^{0.004}_{0.004}$	$12.49\pm^{0.001}_{0.001}$	$12.06\pm^{0.001}_{0.001}$	$11.83\pm^{0.001}_{0.001}$	$11.74\pm^{0.003}_{0.003}$	$13.57\pm^{0.004}_{0.004}$	$12.48\pm^{0.001}_{0.001}$	$12.05\pm^{0.001}_{0.001}$	$11.82\pm^{0.001}_{0.001}$	$11.72\pm^{0.003}_{0.003}$
HIPEQ1439+02	$16.58\pm^{0.077}_{0.083}$	$15.44\pm^{0.015}_{0.015}$	$15.01\pm^{0.014}_{0.014}$	$14.77\pm^{0.017}_{0.017}$	$14.79\pm^{0.059}_{0.062}$	$16.57\pm^{0.077}_{0.082}$	$15.44\pm^{0.015}_{0.015}$	$15.01\pm^{0.014}_{0.014}$	$14.76\pm^{0.017}_{0.017}$	$14.79\pm^{0.059}_{0.062}$
HIPEQ1439-00	$13.84\pm^{0.010}_{0.010}$	$12.95\pm^{0.002}_{0.002}$	$12.56\pm^{0.002}_{0.002}$	$12.29\pm^{0.002}_{0.002}$	$12.24\pm^{0.007}_{0.007}$	$13.83\pm^{0.011}_{0.012}$	$12.95\pm^{0.002}_{0.002}$	$12.56\pm^{0.002}_{0.002}$	$12.28\pm^{0.002}_{0.002}$	$12.23\pm^{0.008}_{0.008}$
HIPEQ1440+02	$15.09\pm^{0.014}_{0.014}$	$13.98\pm^{0.002}_{0.002}$	$13.72\pm^{0.002}_{0.002}$	$13.48\pm^{0.003}_{0.003}$	$13.92\pm^{0.012}_{0.012}$	$15.07\pm^{0.014}_{0.014}$	$13.99\pm^{0.002}_{0.002}$	$13.72\pm^{0.002}_{0.002}$	$13.48\pm^{0.003}_{0.003}$	$13.92\pm^{0.012}_{0.012}$
HIPEQ1444+01a	$13.59\pm^{0.007}_{0.007}$	$12.22\pm^{0.001}_{0.001}$	$11.63\pm^{0.001}_{0.001}$	$11.29\pm^{0.001}_{0.001}$	$11.04\pm^{0.002}_{0.002}$	$13.56\pm^{0.007}_{0.007}$	$12.21\pm^{0.001}_{0.001}$	$11.62\pm^{0.001}_{0.001}$	$11.28\pm^{0.001}_{0.001}$	$11.02\pm^{0.003}_{0.003}$
HIPEQ1500+01	$13.23\pm^{0.006}_{0.006}$	$11.83\pm^{0.001}_{0.001}$	$11.14\pm^{0.001}_{0.001}$	$10.77\pm^{0.001}_{0.001}$	$10.52\pm^{0.002}_{0.002}$	$13.19\pm^{0.007}_{0.007}$	$11.82\pm^{0.001}_{0.001}$	$11.13\pm^{0.001}_{0.001}$	$10.77\pm^{0.001}_{0.001}$	$10.50\pm^{0.002}_{0.002}$
HIPEQ1504+02	$16.14\pm^{0.032}_{0.033}$	$15.00\pm^{0.005}_{0.005}$	$14.67\pm^{0.005}_{0.005}$	$14.54\pm^{0.007}_{0.007}$	$14.61\pm^{0.025}_{0.025}$	$16.14\pm^{0.032}_{0.033}$	$14.99\pm^{0.005}_{0.005}$	$14.67\pm^{0.005}_{0.005}$	$14.54\pm^{0.007}_{0.007}$	$14.60\pm^{0.025}_{0.026}$
HIPEQ1504-00	$15.72\pm^{0.024}_{0.025}$	$14.63\pm^{0.005}_{0.005}$	$14.25\pm^{0.004}_{0.004}$	$14.07\pm^{0.006}_{0.006}$	$14.08\pm^{0.020}_{0.020}$	$15.67\pm^{0.034}_{0.035}$	$14.64\pm^{0.007}_{0.007}$	$14.25\pm^{0.006}_{0.006}$	$14.04\pm^{0.008}_{0.008}$	$14.02\pm^{0.028}_{0.029}$
HIPEQ1507+01	$12.97\pm^{0.010}_{0.011}$	$11.48\pm^{0.001}_{0.001}$	$10.83\pm^{0.001}_{0.001}$	$10.44\pm^{0.001}_{0.001}$	$10.15\pm^{0.003}_{0.003}$	$12.97\pm^{0.010}_{0.011}$	$11.48\pm^{0.001}_{0.001}$	$10.82\pm^{0.001}_{0.001}$	$10.44\pm^{0.001}_{0.001}$	$10.15\pm^{0.003}_{0.003}$
HIPEQ1542+00	$14.92\pm^{0.017}_{0.017}$	$13.65\pm^{0.002}_{0.002}$	$13.10\pm^{0.002}_{0.002}$	$12.80\pm^{0.002}_{0.002}$	$12.62\pm^{0.006}_{0.007}$	$14.83\pm^{0.032}_{0.033}$	$13.67\pm^{0.004}_{0.004}$	$13.11\pm^{0.004}_{0.004}$	$12.81\pm^{0.005}_{0.005}$	$12.59\pm^{0.012}_{0.012}$
HIPEQ1544+02	$15.88\pm^{0.034}_{0.036}$	$14.60\pm^{0.004}_{0.004}$	$14.10\pm^{0.003}_{0.003}$	$14.05\pm^{0.005}_{0.005}$	$13.51\pm^{0.013}_{0.013}$	$15.87\pm^{0.035}_{0.036}$	$14.60\pm^{0.004}_{0.004}$	$14.10\pm^{0.004}_{0.004}$	$14.05\pm^{0.005}_{0.005}$	$13.52\pm^{0.013}_{0.013}$
HIPEQ1545+00	$15.65\pm^{0.044}_{0.046}$	$14.96\pm^{0.010}_{0.010}$	$14.55\pm^{0.011}_{0.011}$	$14.36\pm^{0.016}_{0.016}$	$13.89\pm^{0.035}_{0.036}$	$15.65\pm^{0.045}_{0.047}$	$14.96\pm^{0.010}_{0.010}$	$14.55\pm^{0.011}_{0.011}$	$14.36\pm^{0.016}_{0.017}$	$13.89\pm^{0.036}_{0.037}$

Table 3.10—Continued

HIPASS Name	Elliptical					Circular				
	u^a	g^a	r^a	i^a	z^a	u^a	g^a	r^a	i^a	z^a
HIPEQ1601+01a	$13.58\pm^{0.016}_{0.016}$	$12.63\pm^{0.002}_{0.002}$	$12.30\pm^{0.002}_{0.002}$	$11.88\pm^{0.002}_{0.002}$	$11.82\pm^{0.007}_{0.007}$	$13.54\pm^{0.017}_{0.017}$	$12.62\pm^{0.002}_{0.002}$	$12.28\pm^{0.002}_{0.002}$	$11.87\pm^{0.002}_{0.002}$	$11.79\pm^{0.007}_{0.007}$
HIPEQ1609-00	$16.68\pm^{0.063}_{0.067}$	$15.82\pm^{0.012}_{0.012}$	$15.80\pm^{0.017}_{0.018}$	$15.80\pm^{0.027}_{0.028}$	$15.87\pm^{0.100}_{0.111}$	$16.65\pm^{0.080}_{0.087}$	$15.82\pm^{0.015}_{0.015}$	$15.80\pm^{0.022}_{0.022}$	$15.78\pm^{0.035}_{0.036}$	$15.85\pm^{0.133}_{0.151}$
HIPEQ1613-00	$15.33\pm^{0.023}_{0.023}$	$14.39\pm^{0.003}_{0.003}$	$14.29\pm^{0.004}_{0.004}$	$14.18\pm^{0.006}_{0.006}$	$13.86\pm^{0.018}_{0.018}$	$15.33\pm^{0.023}_{0.024}$	$14.40\pm^{0.003}_{0.003}$	$14.30\pm^{0.004}_{0.004}$	$14.19\pm^{0.006}_{0.006}$	$13.85\pm^{0.018}_{0.018}$
HIPEQ1614+00	$14.59\pm^{0.021}_{0.022}$	$13.83\pm^{0.004}_{0.004}$	$13.57\pm^{0.005}_{0.005}$	$13.49\pm^{0.009}_{0.009}$	$13.37\pm^{0.025}_{0.026}$	$14.59\pm^{0.021}_{0.022}$	$13.83\pm^{0.004}_{0.004}$	$13.57\pm^{0.005}_{0.005}$	$13.49\pm^{0.009}_{0.009}$	$13.37\pm^{0.025}_{0.026}$
HIPEQ1614-00	$14.85\pm^{0.024}_{0.024}$	$13.36\pm^{0.002}_{0.002}$	$12.66\pm^{0.002}_{0.002}$	$12.25\pm^{0.002}_{0.002}$	$11.97\pm^{0.004}_{0.005}$	$14.81\pm^{0.031}_{0.032}$	$13.43\pm^{0.003}_{0.003}$	$12.70\pm^{0.002}_{0.002}$	$12.29\pm^{0.002}_{0.002}$	$11.96\pm^{0.006}_{0.006}$
HIPEQ2036-04	$15.06\pm^{0.017}_{0.018}$	$13.41\pm^{0.002}_{0.002}$	$12.60\pm^{0.002}_{0.002}$	$12.18\pm^{0.002}_{0.002}$	$12.07\pm^{0.005}_{0.005}$	$15.03\pm^{0.017}_{0.018}$	$13.40\pm^{0.002}_{0.002}$	$12.60\pm^{0.002}_{0.002}$	$12.18\pm^{0.002}_{0.002}$	$12.05\pm^{0.005}_{0.005}$
HIPEQ2314+00	$15.19\pm^{0.013}_{0.013}$	$14.16\pm^{0.002}_{0.002}$	$13.78\pm^{0.002}_{0.002}$	$13.58\pm^{0.002}_{0.002}$	$13.46\pm^{0.009}_{0.009}$	$15.19\pm^{0.013}_{0.013}$	$14.16\pm^{0.002}_{0.002}$	$13.78\pm^{0.002}_{0.002}$	$13.58\pm^{0.002}_{0.002}$	$13.46\pm^{0.009}_{0.009}$
HIPEQ2324-00	$14.86\pm^{0.020}_{0.021}$	$14.26\pm^{0.004}_{0.004}$	$14.10\pm^{0.006}_{0.006}$	$14.04\pm^{0.008}_{0.008}$	$13.89\pm^{0.029}_{0.030}$	$14.83\pm^{0.021}_{0.022}$	$14.23\pm^{0.004}_{0.004}$	$14.07\pm^{0.006}_{0.006}$	$14.02\pm^{0.009}_{0.009}$	$13.86\pm^{0.031}_{0.032}$
HIPEQ2335+01	$16.45\pm^{0.103}_{0.114}$	$15.75\pm^{0.019}_{0.019}$	$15.26\pm^{0.018}_{0.019}$	$15.10\pm^{0.027}_{0.028}$	$14.81\pm^{0.075}_{0.080}$	$16.52\pm^{0.103}_{0.113}$	$15.76\pm^{0.018}_{0.019}$	$15.28\pm^{0.018}_{0.019}$	$15.12\pm^{0.027}_{0.027}$	$14.84\pm^{0.074}_{0.080}$
HIPEQ2336+00	$13.79\pm^{0.007}_{0.007}$	$12.50\pm^{0.001}_{0.001}$	$11.92\pm^{0.001}_{0.001}$	$11.58\pm^{0.001}_{0.001}$	$11.32\pm^{0.003}_{0.003}$	$13.78\pm^{0.007}_{0.007}$	$12.50\pm^{0.001}_{0.001}$	$11.92\pm^{0.001}_{0.001}$	$11.58\pm^{0.001}_{0.001}$	$11.32\pm^{0.003}_{0.003}$
HIPEQ2337+00	$15.04\pm^{0.042}_{0.043}$	$14.18\pm^{0.006}_{0.006}$	$13.81\pm^{0.007}_{0.007}$	$13.62\pm^{0.009}_{0.009}$	$13.59\pm^{0.041}_{0.043}$	$15.04\pm^{0.043}_{0.044}$	$14.18\pm^{0.006}_{0.006}$	$13.81\pm^{0.007}_{0.007}$	$13.62\pm^{0.009}_{0.009}$	$13.59\pm^{0.042}_{0.044}$
HIPEQ2340+01	$15.81\pm^{0.026}_{0.027}$	$14.71\pm^{0.003}_{0.003}$	$14.19\pm^{0.003}_{0.003}$	$13.93\pm^{0.004}_{0.004}$	$13.82\pm^{0.014}_{0.014}$	$15.82\pm^{0.027}_{0.027}$	$14.72\pm^{0.003}_{0.003}$	$14.21\pm^{0.003}_{0.003}$	$13.95\pm^{0.004}_{0.004}$	$13.84\pm^{0.014}_{0.014}$

[a]Uncertainties are based on the photometric errors described in §3.5 and *do not* account for calibration errors or other uncertainties.

Table 3.11. Other Measured Sizes - Elliptical

	r_{25}					r_K				
HIPASS Name	u	g	r	i	z	u	g	r	i	z
HIPEQ0014-00	38.0	58.2	64.5	66.5	50.7	35.7	29.9	27.1	26.1	26.3
HIPEQ0027-01a	29.7	43.2	45.1	44.7	40.0	34.1	25.9	24.9	24.5	28.2
HIPEQ0033-01	14.7	26.5	32.5	40.8	26.5	34.6	32.1	30.6	32.5	32.2
HIPEQ0043-00	38.0	49.5	52.7	57.8	47.1	27.4	21.5	20.4	21.0	21.9
HIPEQ0051-00	15.8	24.6	24.9	29.7	26.5	13.1	11.4	12.3	12.4	14.0
HIPEQ0058+00	22.6	27.7	30.5	31.3	29.3	19.1	13.6	13.2	13.3	13.9
HIPEQ0107+01	15.8	24.9	28.5	28.5	24.2	11.3	12.5	13.6	14.7	14.8
HIPEQ0119+00	7.1	15.4	16.6	16.2	17.4	13.2	10.8	9.9	9.4	9.5
HIPEQ0120-00	28.5	36.0	40.0	40.4	38.8	24.2	18.9	20.0	20.7	22.8
HIPEQ0122+00	102.6	113.3	114.8	125.5	111.3	76.2	61.3	59.0	59.6	65.1
HIPEQ0123-00	24.9	34.5	36.0	36.4	34.8	21.8	16.8	15.9	16.1	17.6
HIPEQ0126+00a	2.0	15.0	15.4	16.6	13.1	11.8	12.5	11.9	11.9	11.6
HIPEQ0126-00b	12.3	13.9	14.7	15.4	12.3	6.1	5.7	5.9	6.4	6.7
HIPEQ0154-00	16.6	32.5	39.2	42.8	53.9	22.5	16.0	15.0	15.3	15.7
HIPEQ0222-00	35.2	61.0	67.3	68.5	55.8	40.9	36.3	35.6	32.7	35.2
HIPEQ0228-01	48.3	70.5	72.9	77.2	82.0	36.7	32.6	31.5	31.9	33.5
HIPEQ0230+00	0.8	33.3	38.4	44.0	27.3	38.5	28.7	29.4	29.5	32.5
HIPEQ0230-01	51.5	82.8	90.7	97.4	100.6	39.2	26.9	24.8	24.8	23.5
HIPEQ0231+00	15.8	29.3	30.9	31.3	30.5	23.0	18.1	18.1	17.6	20.7
HIPEQ0236+00	27.3	35.6	39.2	42.0	36.8	27.0	19.0	18.7	18.3	17.0
HIPEQ0238+00	3.6	23.8	23.4	21.4	22.6	17.9	20.0	18.8	19.4	19.5
HIPEQ0240+01	...	21.8	...	0.8	...	27.9	30.3	31.5	32.2	36.6
HIPEQ0241+00	157.2	...	...	...	157.2	122.6	112.7	107.8	104.2	101.4
HIPEQ0244+00	26.1	41.6	44.4	45.5	40.4	41.2	29.0	29.0	32.9	35.7
HIPEQ0246-00a	79.2	110.5	115.2	123.9	138.6	64.4	51.5	47.8	46.6	49.0
HIPEQ0246-00b	87.9	111.3	123.6	131.9	132.7	49.8	47.8	47.7	48.4	46.4
HIPEQ0249-00	22.2	29.7	34.5	35.2	29.7	21.3	16.1	15.2	14.8	16.4
HIPEQ0249-00a	15.0	26.5	27.7	27.7	18.2	25.9	21.3	19.8	18.1	23.0
HIPEQ0249-00b	31.7	47.5	51.1	55.0	57.4	30.8	21.7	20.3	20.8	22.2
HIPEQ0251-01	...	64.9	66.5	75.6	56.2	51.1	47.1	46.6	47.3	47.9
HIPEQ0300+00	23.4	40.8	41.2	42.4	34.5	26.1	22.1	20.8	20.7	23.4
HIPEQ0301-00	20.6	32.1	34.1	38.0	22.2	27.2	22.2	21.5	22.7	24.6
HIPEQ0306-00	30.1	73.7	82.0	89.9	93.9	37.9	26.7	25.0	25.1	26.1
HIPEQ0316-00	33.3	45.9	46.7	47.1	48.7	21.6	22.3	20.6	19.5	21.8
HIPEQ0320-06	37.2	46.3	50.7	53.9	50.7	21.5	18.4	18.0	18.9	20.7
HIPEQ0351-00	15.0	19.0	19.8	21.4	20.2	9.2	6.1	6.6	6.3	6.2
HIPEQ0809+00	38.4	44.4	46.7	48.7	50.7	27.4	22.5	22.7	22.3	26.5
HIPEQ0821+03b	27.7	37.6	39.2	40.0	38.0	19.4	16.6	15.0	14.7	15.3
HIPEQ0821-00	18.6	36.4	31.3	29.7	25.7	16.4	17.2	17.5	15.7	20.2
HIPEQ0822-00	36.0	43.2	44.0	45.9	44.4	31.0	22.1	21.4	21.8	25.2
HIPEQ0825-00	46.7	62.2	68.1	87.5	94.2	59.5	32.8	28.7	31.8	33.3
HIPEQ0855+02	9.1	53.1	55.4	62.6	36.4	38.5	37.9	36.2	37.6	39.9
HIPEQ0856+00	32.5	37.2	38.4	70.5	54.3	33.4	24.6	22.4	29.6	28.9
HIPEQ0923-00	37.6	42.8	44.0	44.7	43.2	28.9	21.7	21.4	22.9	25.9
HIPEQ0930+04	37.2	57.0	61.0	65.7	69.7	40.6	33.2	31.9	32.2	34.5
HIPEQ0942+00	79.2	92.3	101.8	110.9	122.8	44.3	38.7	36.6	36.5	39.6
HIPEQ0944-00b	16.2	23.0	25.3	23.8	25.3	15.5	14.5	13.7	11.7	15.6
HIPEQ0945+01	66.9	85.1	89.1	95.4	106.1	37.0	40.3	40.8	42.3	49.7
HIPEQ0946+02	26.1	55.4	57.0	59.4	50.3	45.8	40.8	38.9	39.9	42.8
HIPEQ0947+00a	26.9	56.6	58.6	62.6	64.5	40.6	33.3	32.4	32.9	35.6
HIPEQ0947+00b	11.5	41.6	42.4	41.6	21.0	34.4	28.0	26.7	26.6	28.1
HIPEQ0953+01	152.1	194.0	194.0	194.0	200.0	78.8	76.3	73.9	74.1	70.3
HIPEQ0954+02a	21.0	30.9	31.3	33.3	30.1	29.2	20.1	19.5	20.2	22.9
HIPEQ0955+04a	68.5	78.0	83.2	91.9	108.9	41.6	34.6	34.8	36.1	40.0
HIPEQ0958+01	0.8	17.4	...	...	...	22.3	18.1	17.8	18.1	21.8
HIPEQ1000+03	43.2	72.9	85.9	93.1	82.4	40.4	35.0	31.3	32.2	30.8
HIPEQ1010+05	18.2	26.1	28.9	27.7	24.2	13.7	11.2	11.7	11.5	12.7
HIPEQ1014+03	135.8	215.8	252.6	215.8	282.7	92.3	80.9	74.4	72.2	68.7

Table 3.11—Continued

	r_{25}					r_K				
HIPASS Name	u	g	r	i	z	u	g	r	i	z
HIPEQ1015+02	23.0	50.3	51.9	53.1	37.6	46.7	47.3	44.1	48.9	36.1
HIPEQ1026+03	55.0	77.6	78.8	80.4	89.5	44.6	38.0	36.2	35.2	37.3
HIPEQ1028+03	...	...	...	...	...	30.1	29.1	29.1	30.1	33.4
HIPEQ1039+01	18.6	29.7	34.8	37.6	32.9	20.8	18.2	19.1	20.6	22.7
HIPEQ1041+00	24.6	33.3	34.1	35.2	36.0	23.6	17.6	18.4	20.3	22.1
HIPEQ1046+01	103.0	130.3	140.2	141.8	160.8	92.6	74.3	72.8	75.2	84.3
HIPEQ1050+01	...	16.6	20.2	19.0	14.3	9.1	10.4	11.1	10.8	7.3
HIPEQ1051+04a	42.8	56.6	57.8	60.2	59.0	37.0	30.9	30.3	30.1	32.6
HIPEQ1052+00	13.1	19.0	19.8	21.8	19.4	6.9	7.1	7.3	8.3	8.4
HIPEQ1053+02	21.4	26.1	27.7	28.9	30.5	14.9	14.1	15.1	15.7	16.9
HIPEQ1055+02	12.3	19.8	22.2	19.8	15.4	9.2	9.2	9.8	10.6	9.7
HIPEQ1101+03	129.5	163.5	193.6	210.7	228.1	97.1	83.9	80.6	80.1	83.6
HIPEQ1109-00	28.1	50.3	54.6	57.0	46.7	32.6	26.3	22.8	21.6	19.7
HIPEQ1110+01	22.6	32.5	35.2	34.8	32.1	18.9	17.7	19.2	19.2	21.0
HIPEQ1113+05	25.7	31.3	32.1	33.7	32.1	20.9	18.0	18.0	17.5	22.1
HIPEQ1117+04a	42.8	69.7	75.6	81.6	81.6	25.0	21.5	21.6	22.1	23.6
HIPEQ1119+02	45.1	61.0	63.4	74.4	53.1	51.8	43.5	42.6	43.8	43.9
HIPEQ1124+03	76.4	99.8	107.7	115.6	117.2	67.3	64.0	64.1	65.8	68.7
HIPEQ1127-01	22.2	35.6	40.4	43.6	53.5	30.1	27.1	28.6	30.0	38.4
HIPEQ1131-02	51.9	57.8	63.8	70.1	77.2	38.6	31.5	30.0	30.2	33.7
HIPEQ1133-03	32.9	42.0	40.8	44.4	41.2	29.4	25.6	24.6	25.5	29.2
HIPEQ1136+00	21.4	27.7	27.7	32.1	24.9	11.1	12.2	13.6	15.2	15.5
HIPEQ1138+03	19.8	30.1	36.4	38.8	32.1	19.2	15.5	14.3	14.0	14.0
HIPEQ1143-01	...	13.5	13.5	13.1	6.7	15.0	11.8	13.0	13.6	13.4
HIPEQ1145+02	...	...	1.6	...	1.2	28.2	25.1	26.0	21.7	95.2
HIPEQ1148-02	42.8	54.6	62.6	71.3	60.2	48.8	44.3	42.8	47.3	42.7
HIPEQ1151-02	20.6	28.9	29.3	29.3	24.6	14.9	12.9	12.2	12.1	11.8
HIPEQ1152+01	29.7	34.8	38.0	43.6	36.0	20.2	17.6	17.7	18.7	19.6
HIPEQ1152-02	21.4	28.5	30.5	32.1	26.1	9.0	9.4	10.9	12.6	13.3
HIPEQ1152-03b	26.9	40.0	43.6	46.7	38.4	29.8	26.5	26.7	27.7	29.4
HIPEQ1155+01	57.8	85.1	92.3	93.1	95.0	52.6	48.0	46.7	45.5	47.8
HIPEQ1200-00	9.1	34.8	38.4	41.6	28.9	43.4	37.8	37.0	36.8	47.9
HIPEQ1200-01	109.7	135.4	154.4	167.5	169.5	56.2	49.0	46.6	46.6	46.0
HIPEQ1202+01	40.4	80.8	96.2	104.1	104.5	38.1	33.0	31.3	31.1	31.6
HIPEQ1204-01	0.8	31.7	34.1	34.8	29.3	31.3	27.2	27.3	25.9	27.4
HIPEQ1204-02	12.3	32.9	45.9	53.5	40.0	36.2	25.1	23.8	23.0	24.4
HIPEQ1210+02	...	26.1	28.1	30.5	26.1	33.0	27.9	27.7	27.1	28.1
HIPEQ1215+04a	24.2	33.3	37.2	37.6	36.4	18.5	16.9	17.8	18.1	21.9
HIPEQ1216-03	23.0	30.1	31.3	32.5	36.8	24.5	18.2	17.1	17.2	20.3
HIPEQ1218+00	4.0	31.3	40.4	37.6	38.0	40.3	36.1	35.2	35.2	35.0
HIPEQ1218-01	25.7	36.8	37.2	37.6	33.3	27.9	21.8	19.8	20.3	21.4
HIPEQ1219+03	23.8	33.7	36.8	40.0	35.6	15.9	16.5	17.6	19.3	21.2
HIPEQ1220+00	26.5	35.2	36.4	35.6	21.4	23.3	21.8	22.0	22.5	25.1
HIPEQ1220+01	51.1	64.5	68.5	68.5	64.5	39.9	33.5	32.9	32.9	35.7
HIPEQ1221+03	36.4	67.7	78.4	83.6	74.4	71.4	37.3	34.7	33.4	35.0
HIPEQ1223+00	13.1	27.3	29.3	28.9	28.9	30.9	26.6	27.8	27.2	30.2
HIPEQ1223-03b	64.9	89.9	97.8	108.5	105.7	52.4	43.8	41.0	41.5	48.3
HIPEQ1224+00	1.2	15.4	15.8	16.6	12.3	12.0	10.5	11.1	11.0	9.7
HIPEQ1224+03b	28.9	50.7	54.3	56.6	48.7	29.9	28.2	27.9	29.2	29.2
HIPEQ1225+00	44.7	64.9	73.7	77.6	86.3	23.5	25.4	24.3	24.7	25.4
HIPEQ1226+02	56.6	69.3	95.0	103.8	100.6	29.6	26.9	27.0	27.0	28.2
HIPEQ1227+01	...	17.8	19.0	11.5	7.5	21.2	19.9	21.2	22.0	23.5
HIPEQ1228+02	35.2	67.7	70.9	66.5	57.8	50.8	45.0	44.0	43.9	47.5
HIPEQ1228+03	72.9	122.8	148.5	165.9	161.2	40.5	40.3	38.9	39.8	39.5
HIPEQ1229+00	20.2	30.5	34.5	30.1	22.6	15.0	16.6	19.1	19.2	14.0
HIPEQ1230+02	17.8	34.1	33.7	33.3	...	22.5	20.2	19.3	19.4	19.4
HIPEQ1230+03	12.3	16.6	16.6	17.8	15.8	7.2	7.8	7.9	8.0	8.2
HIPEQ1232+00a	64.5	111.7	123.6	124.3	123.9	66.1	63.2	62.4	61.7	64.3

Table 3.11—Continued

	r_{25}					r_K				
HIPASS Name	u	g	r	i	z	u	g	r	i	z
HIPEQ1232+00b	318.4	123.9	123.9	123.9	318.4	176.1	163.6	159.4	156.6	156.7
HIPEQ1233-02	16.2	36.8	52.7	49.5	22.2	44.9	41.8	42.9	44.0	48.1
HIPEQ1236+03	25.7	36.0	35.6	38.8	30.5	25.5	23.4	23.8	24.3	24.9
HIPEQ1239-00	103.0	142.6	165.1	171.9	162.4	67.7	63.4	62.6	62.7	64.1
HIPEQ1241+01	20.6	27.7	29.7	35.6	32.5	14.2	12.9	13.2	14.2	13.9
HIPEQ1241-02	24.6	42.4	45.5	48.7	47.5	22.2	21.4	21.7	23.5	26.7
HIPEQ1242+03b	53.9	74.8	84.3	95.0	105.3	39.7	35.2	35.0	36.5	38.4
HIPEQ1242-00	84.3	106.1	116.0	127.9	144.1	51.6	47.6	47.3	47.0	53.0
HIPEQ1242-01a	28.9	45.5	48.3	52.3	50.3	30.1	23.6	23.6	24.6	28.0
HIPEQ1242-01b	57.8	72.1	72.5	76.0	66.9	39.6	35.2	33.3	32.4	30.9
HIPEQ1243-00	65.7	89.5	97.8	105.7	113.3	56.4	48.5	46.1	44.3	47.7
HIPEQ1244+00	45.1	92.3	99.4	89.1	97.4	63.6	59.0	52.8	14.7	46.1
HIPEQ1244-02	22.6	36.4	39.6	41.6	28.9	32.0	28.0	28.4	27.4	28.3
HIPEQ1245-00	135.4	186.9	213.8	229.3	252.6	83.4	70.8	65.0	62.6	59.8
HIPEQ1249+03	58.6	74.4	77.2	85.9	86.7	33.5	28.6	26.9	26.6	27.0
HIPEQ1249+04	28.5	34.1	34.8	38.4	27.7	24.0	22.0	22.2	22.5	21.1
HIPEQ1250+05	75.2	78.0	79.6	83.6	108.5	42.1	36.1	34.9	34.2	38.5
HIPEQ1253+01	89.9	120.0	134.2	144.9	175.8	68.8	57.7	54.7	54.5	59.2
HIPEQ1253+02	68.1	108.9	123.6	130.7	131.5	51.6	44.0	42.8	42.3	42.4
HIPEQ1253+04	31.3	47.1	55.8	65.3	57.8	16.2	16.3	18.0	19.5	20.2
HIPEQ1255+00	74.4	91.9	103.4	106.5	98.6	50.9	48.1	48.8	48.5	46.7
HIPEQ1255+02	34.8	55.4	61.4	74.1	60.2	33.1	22.6	21.8	22.1	22.1
HIPEQ1255-00	30.9	45.9	48.7	51.5	36.4	34.8	37.2	39.8	42.5	46.9
HIPEQ1256+03	7.5	18.6	24.9	19.0	13.1	21.1	19.7	19.7	19.8	21.9
HIPEQ1257+02	24.9	30.1	32.1	36.4	26.9	26.5	22.1	22.2	22.4	23.6
HIPEQ1257-01	51.9	64.9	70.1	71.7	64.9	43.8	32.9	30.6	31.1	31.8
HIPEQ1258+02	30.5	64.2	69.7	78.4	72.1	43.8	39.8	39.3	40.3	43.9
HIPEQ1300+02a	18.2	32.9	38.4	41.6	34.8	19.3	19.8	20.6	22.5	24.7
HIPEQ1300+02b	85.9	96.6	106.5	123.9	133.5	47.8	42.1	42.5	44.5	49.9
HIPEQ1303+03	26.9	41.2	42.0	44.7	31.7	27.9	25.4	24.4	24.7	24.9
HIPEQ1304-02	15.0	20.6	22.2	23.0	16.2	13.7	10.4	11.7	11.4	11.2
HIPEQ1304-03	74.8	99.8	102.2	102.6	99.0	58.1	58.4	56.5	55.4	55.0
HIPEQ1307-00	29.3	43.6	44.7	45.9	42.4	23.7	19.7	19.1	18.9	20.2
HIPEQ1308-02	28.1	37.2	40.8	45.5	57.8	25.9	20.4	19.9	19.6	24.6
HIPEQ1311+03a	18.2	28.9	29.7	28.9	27.7	14.5	15.7	14.1	13.8	12.5
HIPEQ1312+03	14.3	27.7	29.3	35.2	30.1	14.1	11.5	12.0	11.8	11.6
HIPEQ1312+05	0.8	23.4	25.3	23.8	6.7	19.1	17.4	16.7	17.2	17.8
HIPEQ1313+06	23.0	37.6	38.4	39.6	37.2	23.8	18.6	17.4	16.6	18.5
HIPEQ1317-00	26.1	30.5	30.9	30.9	29.7	19.0	17.7	17.3	17.0	18.1
HIPEQ1318-01	34.1	42.0	45.1	44.4	41.6	35.1	23.8	23.4	23.9	28.1
HIPEQ1320+05	33.3	43.6	47.9	53.5	39.6	29.1	27.2	29.1	30.6	33.5
HIPEQ1327+02	...	25.7	24.2	23.8	15.0	19.2	17.8	17.2	15.1	21.7
HIPEQ1329-00	17.8	29.3	29.3	32.1	22.6	24.7	21.5	21.7	22.2	24.8
HIPEQ1332+01	27.7	36.4	39.6	44.0	44.4	22.0	16.8	15.9	16.3	17.7
HIPEQ1335+01	28.9	55.8	59.4	61.8	61.0	33.9	27.1	24.4	23.4	23.8
HIPEQ1341+05	18.2	31.3	32.9	34.8	31.3	18.6	16.2	14.7	14.2	13.6
HIPEQ1348+03	91.1	112.5	125.1	134.6	141.4	67.0	59.2	57.4	58.5	58.7
HIPEQ1352+02a	19.8	74.8	80.8	86.3	91.1	43.1	34.5	31.8	30.7	31.4
HIPEQ1352-01	94.6	118.0	120.0	126.3	127.1	62.7	59.4	57.4	57.9	57.4
HIPEQ1400+02	38.0	51.1	51.5	51.9	50.3	27.6	23.7	23.4	23.2	26.6
HIPEQ1411-01	...	...	...	...	...	88.0	76.3	71.8	73.6	76.4
HIPEQ1415+04	17.0	20.2	22.6	23.4	22.2	11.3	9.6	10.0	10.6	11.0
HIPEQ1416+03	...	...	...	...	...	57.0	56.5	59.4	63.1	60.9
HIPEQ1422-00	90.7	115.6	122.8	126.3	127.1	60.5	57.6	56.6	56.0	58.3
HIPEQ1429-00	37.2	47.5	47.9	49.1	45.1	29.7	26.3	25.3	25.9	26.7
HIPEQ1432+00	...	...	...	...	...	35.6	30.1	30.4	31.0	33.2
HIPEQ1433+01	...	21.8	...	...	1.2	25.6	26.0	24.3	23.3	22.7
HIPEQ1433+02	24.2	32.9	34.1	29.3	30.9	17.5	16.5	16.7	16.0	17.4

Table 3.11—Continued

	r_{25}					r_K				
HIPASS Name	u	g	r	i	z	u	g	r	i	z
HIPEQ1437+02	...	...	...	...	...	62.0	52.7	53.8	53.4	53.9
HIPEQ1437-00	50.3	80.8	97.8	104.1	103.4	31.6	33.5	35.3	37.6	39.6
HIPEQ1439-00	84.3	101.8	111.3	120.0	105.7	63.2	55.8	55.2	56.3	55.4
HIPEQ1440+02	28.9	34.5	36.8	38.0	36.8	22.0	16.6	16.5	17.3	19.7
HIPEQ1444+01a	57.0	86.3	98.2	103.4	109.7	46.8	36.5	33.8	32.6	33.8
HIPEQ1500+01	68.9	108.5	119.2	143.7	145.7	50.0	44.3	43.0	42.5	43.7
HIPEQ1504+02	16.2	23.8	24.6	24.6	25.3	17.2	12.7	12.5	12.8	14.3
HIPEQ1504-00	40.8	58.2	61.4	61.8	52.3	36.6	32.4	32.4	32.9	32.6
HIPEQ1507+01	80.8	128.7	139.4	143.4	145.3	61.3	54.9	50.6	49.5	50.9
HIPEQ1542+00	74.1	105.3	110.1	113.7	112.9	62.6	55.5	53.8	52.3	53.4
HIPEQ1544+02	20.2	28.1	33.3	29.7	26.1	20.3	15.3	14.8	14.6	15.7
HIPEQ1545+00	19.8	25.3	36.8	39.2	38.4	29.2	24.1	25.7	27.5	25.6
HIPEQ1601+01a	60.2	88.7	101.8	112.1	117.2	55.7	48.8	48.5	49.5	51.8
HIPEQ1609-00	8.7	25.7	27.3	24.9	17.0	28.2	24.4	23.4	22.9	24.8
HIPEQ1613-00	22.2	28.1	29.3	29.7	26.5	16.2	15.2	14.9	14.9	16.4
HIPEQ1614+00	36.8	53.9	55.8	60.2	59.4	39.6	37.0	36.0	34.4	37.6
HIPEQ1614-00	...	...	...	...	137.0	67.0	66.8	62.4	59.9	56.7
HIPEQ2036-04	46.7	64.2	71.3	89.1	99.0	46.9	36.4	33.3	34.6	35.8
HIPEQ2314+00	19.8	23.0	23.4	24.6	24.6	13.8	10.4	10.4	10.8	12.6
HIPEQ2324-00	44.0	49.5	60.2	60.2	51.9	37.0	34.2	34.4	34.6	38.3
HIPEQ2335+01	2.8	21.4	26.9	28.1	23.0	33.9	27.3	27.6	27.2	30.5
HIPEQ2336+00	51.5	70.1	74.8	94.6	114.0	46.7	34.7	29.8	30.4	34.8
HIPEQ2337+00	2.4	55.0	62.2	68.1	41.2	46.3	41.0	40.4	40.2	40.0
HIPEQ2340+01	24.6	35.6	39.6	41.6	34.8	19.0	17.2	16.8	17.2	16.7

Note. — For some of the galaxies, the r_{25} occurs almost immediately and in others, the values is never reached because of their irregular LSB nature. The r_{25} values for these latter cases have been omitted from the table

Table 3.12. Other Measured Sizes - Circular

	r_{25}					r_K				
HIPASS Name	u	g	r	i	z	u	g	r	i	z
HIPEQ0014-00	24.6	39.2	46.3	47.1	45.1	26.1	22.3	20.3	19.4	19.2
HIPEQ0027-01a	20.2	31.3	31.7	32.9	31.7	24.2	18.4	17.7	17.3	19.1
HIPEQ0033-01	14.3	24.9	25.7	34.5	24.6	26.7	24.9	23.3	25.5	24.9
HIPEQ0043-00	30.5	42.0	44.7	48.3	53.1	23.0	18.3	17.3	17.8	18.5
HIPEQ0051-00	11.1	17.8	20.2	22.6	21.8	9.4	8.5	9.1	9.2	10.2
HIPEQ0058+00	22.2	27.7	30.1	30.5	30.1	18.8	13.4	13.0	13.1	13.7
HIPEQ0107+01	12.3	24.6	26.9	28.9	23.4	10.8	12.0	13.1	14.1	14.1
HIPEQ0119+00	2.4	11.5	13.1	12.7	9.9	10.6	8.9	8.2	8.0	8.1
HIPEQ0120-00	14.3	24.2	27.7	30.1	30.5	16.7	13.6	14.2	14.4	15.5
HIPEQ0122+00	59.4	79.2	83.6	87.5	86.7	45.6	39.4	37.8	37.6	40.8
HIPEQ0123-00	23.8	32.9	34.1	34.5	32.5	21.0	16.2	15.4	15.5	17.0
HIPEQ0126+00a	1.6	12.3	13.1	15.0	11.5	10.5	11.0	10.4	10.4	10.1
HIPEQ0126-00b	12.3	11.9	12.3	13.1	10.3	5.4	4.9	5.1	5.5	5.7
HIPEQ0154-00	17.8	30.5	36.8	41.6	45.5	21.0	15.0	14.1	14.3	14.7
HIPEQ0222-00	12.3	26.5	30.5	36.0	29.3	21.8	23.2	22.2	19.4	22.6
HIPEQ0228-01	47.9	69.7	74.4	75.6	80.4	36.1	32.1	31.0	31.4	33.0
HIPEQ0230+00	0.8	25.3	31.3	32.5	24.2	27.9	22.3	22.7	22.8	24.8
HIPEQ0230-01	37.2	58.6	64.5	70.1	70.1	28.1	20.6	19.1	19.0	17.6
HIPEQ0231+00	12.7	23.4	24.6	25.3	25.3	19.4	14.8	14.8	14.3	16.7
HIPEQ0236+00	16.6	23.4	26.1	25.7	25.7	17.2	12.9	12.8	12.4	11.2
HIPEQ0238+00	2.8	15.0	14.7	17.4	14.3	14.1	15.5	14.7	15.0	15.2
HIPEQ0240+01	...	17.4	16.6	...	...	23.5	24.8	26.1	26.2	29.9
HIPEQ0241+00	98.2	159.6	198.8	209.1	205.5	82.4	76.6	73.7	70.3	68.4
HIPEQ0244+00	14.3	24.9	29.7	30.5	31.3	25.7	18.6	18.3	20.3	21.2
HIPEQ0246-00a	59.0	77.2	81.6	86.7	97.4	48.4	40.0	37.1	36.1	37.1
HIPEQ0246-00b	80.8	105.7	112.9	121.6	123.6	46.9	45.1	45.1	45.7	43.5
HIPEQ0249-00	20.6	26.9	29.7	31.7	27.7	19.2	14.6	13.7	13.4	14.8
HIPEQ0249-00a	13.1	22.6	23.8	20.2	17.4	19.8	15.8	14.6	13.1	16.0
HIPEQ0249-00b	25.7	39.2	41.2	47.5	43.6	26.5	18.7	17.4	17.9	19.2
HIPEQ0251-01	...	45.5	46.7	47.1	48.3	33.0	29.5	28.5	28.7	27.6
HIPEQ0300+00	12.7	22.6	26.1	26.9	23.8	17.2	15.2	14.3	14.1	15.7
HIPEQ0301-00	17.8	29.3	30.1	30.9	23.8	21.6	17.0	16.3	17.2	18.4
HIPEQ0306-00	26.1	66.9	71.3	83.6	86.7	35.2	24.8	23.2	23.2	24.2
HIPEQ0316-00	14.3	31.3	35.2	36.4	33.3	13.8	16.9	15.3	14.1	15.6
HIPEQ0320-06	28.1	36.0	40.0	43.6	44.4	16.2	14.1	13.7	14.2	15.6
HIPEQ0351-00	13.1	15.8	17.4	17.0	19.4	8.2	5.2	5.7	5.3	5.2
HIPEQ0809+00	30.5	38.8	40.4	42.8	45.1	22.8	18.9	18.8	18.3	21.3
HIPEQ0821+03b	22.6	28.9	30.9	32.9	34.8	16.3	14.0	12.7	12.4	12.9
HIPEQ0821-00	13.9	17.4	18.6	20.6	17.0	14.0	14.7	14.8	12.6	15.4
HIPEQ0822-00	25.3	31.7	34.8	35.6	47.5	21.4	15.9	15.4	15.7	17.3
HIPEQ0825-00	31.7	46.3	52.3	68.9	74.1	44.2	26.2	22.7	25.5	25.6
HIPEQ0855+02	17.4	34.1	37.2	40.8	33.3	27.5	27.4	26.5	27.6	29.0
HIPEQ0856+00	29.3	36.4	45.9	64.9	58.2	30.0	21.7	18.7	25.1	24.8
HIPEQ0923-00	23.4	30.9	32.5	34.1	26.5	19.9	15.6	15.0	16.2	17.3
HIPEQ0930+04	29.7	38.0	39.6	43.6	51.9	26.3	21.2	20.3	20.6	22.3
HIPEQ0942+00	73.3	88.3	94.6	104.9	108.9	41.4	36.1	34.1	34.1	37.0
HIPEQ0944-00b	13.5	18.6	19.8	16.2	15.8	11.9	11.1	10.5	9.3	12.3
HIPEQ0945+01	36.4	58.2	62.6	65.7	64.9	15.1	26.3	26.3	26.9	28.6
HIPEQ0946+02	16.2	35.6	40.8	40.0	33.7	28.1	24.6	23.1	24.2	26.9
HIPEQ0947+00a	23.8	42.0	45.5	44.4	44.4	28.1	24.6	23.7	24.0	25.3
HIPEQ0947+00b	9.9	32.1	32.5	28.5	18.2	25.8	21.1	20.2	20.0	21.3
HIPEQ0953+01	76.0	116.0	118.4	122.4	122.8	55.7	51.9	49.0	49.7	48.7
HIPEQ0954+02a	20.6	30.5	31.7	31.7	26.1	28.9	19.9	19.3	20.0	22.6
HIPEQ0955+04a	49.9	59.0	61.4	65.3	78.4	29.0	25.5	25.4	26.4	28.0
HIPEQ0958+01	0.8	11.9	...	...	...	18.0	14.5	14.0	13.6	18.4
HIPEQ1000+03	27.3	44.0	50.7	53.5	52.3	25.4	22.1	19.5	19.7	18.9
HIPEQ1010+05	14.3	20.2	21.4	23.0	22.2	11.1	8.7	9.2	9.0	9.7
HIPEQ1014+03	103.8	158.4	182.6	190.1	189.3	68.4	60.9	55.9	54.2	52.6

Table 3.12—Continued

HIPASS Name	r_{25}					r_K				
	u	g	r	i	z	u	g	r	i	z
HIPEQ1015+02	16.6	27.3	28.5	36.0	24.2	25.2	29.1	26.1	28.4	12.6
HIPEQ1026+03	40.8	57.4	59.8	61.0	63.0	32.2	27.9	26.7	25.6	26.5
HIPEQ1028+03	14.3	24.9	24.2	26.9	21.8	17.9	16.5	16.6	16.1	17.0
HIPEQ1039+01	19.0	28.1	30.1	32.1	28.1	18.8	16.4	17.2	18.5	20.5
HIPEQ1041+00	23.0	28.5	30.1	32.9	32.5	21.3	15.9	16.6	18.2	19.9
HIPEQ1046+01	48.3	71.7	79.6	87.9	90.3	48.0	44.4	42.8	43.4	42.8
HIPEQ1050+01	6.7	11.9	13.1	13.1	8.3	7.8	7.3	7.7	7.6	5.6
HIPEQ1051+04a	25.3	38.0	42.8	42.4	31.7	26.7	22.8	22.1	21.7	23.7
HIPEQ1052+00	11.5	15.0	15.8	19.0	14.3	5.3	5.5	5.6	6.4	6.3
HIPEQ1053+02	14.3	18.6	20.2	19.8	16.6	10.6	10.2	11.0	11.3	12.2
HIPEQ1055+02	11.1	13.9	15.4	15.0	13.1	7.4	7.3	7.8	8.3	7.3
HIPEQ1101+03	74.4	98.2	108.5	114.8	115.2	50.0	50.5	48.3	47.9	47.8
HIPEQ1109-00	21.0	32.9	40.4	42.0	25.7	24.7	19.8	17.0	16.0	14.0
HIPEQ1110+01	11.1	20.2	21.4	21.0	17.4	12.8	11.8	12.3	12.0	13.3
HIPEQ1113+05	23.0	27.3	29.7	29.7	26.5	17.7	15.3	15.4	14.9	18.8
HIPEQ1117+04a	35.2	59.8	68.1	72.5	78.8	22.1	19.2	19.2	19.7	21.0
HIPEQ1119+02	37.2	52.7	51.9	60.2	55.0	41.9	35.5	34.6	35.6	34.0
HIPEQ1124+03	55.4	63.8	67.3	68.1	72.1	37.7	34.0	34.0	35.0	38.1
HIPEQ1127-01	21.0	31.3	34.8	39.6	48.7	26.7	24.2	25.6	26.8	34.7
HIPEQ1131-02	49.1	56.6	62.6	69.3	70.5	37.9	30.8	29.4	29.6	33.0
HIPEQ1133-03	23.4	32.1	33.3	36.4	39.6	22.6	19.6	19.0	19.6	21.9
HIPEQ1136+00	15.0	19.4	19.4	21.8	18.2	7.6	8.4	9.1	10.1	10.4
HIPEQ1138+03	20.2	28.5	33.3	38.8	36.4	18.5	14.9	13.8	13.4	13.4
HIPEQ1143-01	...	9.9	9.9	10.3	5.5	12.6	10.2	11.3	12.0	11.9
HIPEQ1145+02	...	...	1.2	...	1.2	23.6	20.7	20.5	16.1	72.8
HIPEQ1148-02	23.0	44.4	48.3	53.5	52.3	41.5	38.2	36.8	41.1	36.3
HIPEQ1151-02	13.1	19.0	21.0	20.6	19.4	11.9	10.3	9.7	9.7	9.5
HIPEQ1152+01	23.0	28.9	32.1	36.0	29.3	16.4	14.1	14.3	15.1	15.9
HIPEQ1152-02	15.8	19.8	20.6	21.0	17.0	6.4	6.6	7.5	8.5	8.9
HIPEQ1152-03b	26.1	35.2	37.2	40.4	26.9	25.3	22.3	22.5	23.3	24.9
HIPEQ1155+01	49.9	66.9	75.2	76.4	79.6	42.4	38.9	37.9	37.0	38.7
HIPEQ1200-00	8.7	28.5	32.9	33.3	14.3	34.8	30.1	29.3	29.1	39.4
HIPEQ1200-01	103.8	123.9	142.6	153.3	156.0	51.5	44.9	42.8	42.7	42.1
HIPEQ1202+01	36.4	78.8	91.1	100.6	103.0	36.5	31.6	30.0	29.8	30.3
HIPEQ1204-01	0.8	28.1	29.3	30.1	19.0	28.1	24.8	24.8	23.5	24.7
HIPEQ1204-02	19.8	31.3	45.1	48.3	38.8	33.7	23.2	22.1	21.2	22.6
HIPEQ1210+02	4.8	26.1	26.1	25.7	23.4	31.3	26.4	26.3	25.6	26.6
HIPEQ1215+04a	19.0	24.2	25.3	26.1	25.3	13.1	12.2	12.6	13.0	15.3
HIPEQ1216-03	22.2	30.1	31.3	32.1	32.9	24.4	18.1	17.1	17.2	20.3
HIPEQ1218+00	5.1	27.3	33.3	32.9	30.5	32.2	29.0	27.9	28.3	28.2
HIPEQ1218-01	22.2	27.7	32.5	34.1	32.5	22.4	17.8	16.3	16.5	17.4
HIPEQ1219+03	22.6	30.9	34.8	38.8	38.4	14.8	15.4	16.5	18.1	19.7
HIPEQ1220+00	13.5	20.6	20.6	20.2	17.8	14.8	14.9	14.7	15.1	16.0
HIPEQ1220+01	13.9	28.1	32.9	38.8	32.9	23.9	21.4	20.2	19.3	20.5
HIPEQ1221+03	19.0	36.4	45.9	53.9	57.0	36.3	22.3	22.1	20.6	18.9
HIPEQ1223+00	9.9	21.8	27.3	22.6	26.5	25.4	21.8	22.5	22.0	24.4
HIPEQ1223-03b	39.2	63.0	68.9	75.2	78.0	27.3	27.6	25.8	25.3	29.5
HIPEQ1224+00	1.2	14.3	15.4	14.3	11.9	10.8	9.5	10.1	10.0	8.8
HIPEQ1224+03b	22.6	47.5	49.1	53.1	48.7	27.1	25.6	25.2	26.4	26.4
HIPEQ1225+00	40.4	55.0	61.4	67.7	73.3	19.5	21.8	20.8	20.9	21.2
HIPEQ1226+02	44.4	54.6	59.8	61.0	60.2	21.1	19.5	19.3	19.2	20.1
HIPEQ1227+01	7.5	11.5	15.4	16.2	7.5	15.9	14.8	15.7	15.9	16.9
HIPEQ1228+02	11.5	36.8	39.6	41.2	33.3	31.2	28.4	27.2	27.2	30.5
HIPEQ1228+03	61.0	115.2	135.0	146.5	143.4	36.3	36.3	35.0	35.8	35.6
HIPEQ1229+00	6.7	13.9	15.4	16.2	12.3	8.1	10.6	12.4	11.4	8.3
HIPEQ1230+02	17.4	25.7	24.9	24.9	19.0	16.8	15.3	14.6	14.5	14.5
HIPEQ1230+03	10.3	14.3	14.3	14.7	14.3	6.0	6.6	6.7	6.8	7.1
HIPEQ1232+00a	54.6	78.0	87.9	89.9	83.2	51.9	49.8	49.1	48.2	49.8

Table 3.12—Continued

	r_{25}					r_K				
HIPASS Name	u	g	r	i	z	u	g	r	i	z
HIPEQ1232+00b	112.1	187.7	238.8	249.1	281.2	112.2	107.0	104.6	102.5	105.0
HIPEQ1233-02	11.1	28.5	35.6	38.8	23.4	35.6	32.6	33.3	34.0	36.7
HIPEQ1236+03	11.5	16.6	20.6	22.2	12.7	19.2	17.8	17.5	17.6	17.8
HIPEQ1239-00	64.5	85.9	91.1	93.5	94.2	44.3	42.8	41.5	40.4	40.3
HIPEQ1241+01	15.0	21.4	23.0	30.5	26.1	11.8	10.6	10.9	11.5	11.2
HIPEQ1241-02	17.8	27.7	32.1	36.8	40.4	14.8	14.9	15.1	15.9	18.1
HIPEQ1242+03b	44.0	59.4	69.7	74.8	82.8	31.4	27.9	27.7	28.9	30.0
HIPEQ1242-00	66.5	76.8	82.0	85.1	91.9	33.7	32.1	31.8	31.3	35.2
HIPEQ1242-01a	28.9	40.0	42.0	45.1	43.6	25.8	20.5	20.4	21.3	24.0
HIPEQ1242-01b	26.9	51.5	55.0	56.6	51.1	24.2	23.8	22.5	21.4	19.8
HIPEQ1243-00	59.4	78.0	84.3	90.3	96.6	48.6	41.7	39.5	37.8	40.9
HIPEQ1244+00	29.7	67.3	68.9	66.9	70.5	42.1	37.6	31.6	-7.5	25.1
HIPEQ1244-02	17.0	29.3	29.7	34.1	22.6	26.3	23.1	23.3	22.3	22.9
HIPEQ1245-00	94.2	122.4	133.5	138.6	140.2	56.3	48.9	44.8	42.5	40.9
HIPEQ1249+03	55.8	66.5	68.1	72.1	72.5	29.4	25.2	23.6	23.4	23.7
HIPEQ1249+04	22.2	26.9	29.3	28.9	23.4	18.1	16.8	16.9	17.2	16.0
HIPEQ1250+05	69.3	71.3	75.2	75.6	93.1	36.3	31.4	30.3	29.6	32.9
HIPEQ1253+01	50.3	78.4	87.5	95.0	102.6	40.0	38.0	36.0	35.5	37.0
HIPEQ1253+02	64.2	102.2	119.6	125.9	128.7	49.7	42.4	41.3	40.8	40.8
HIPEQ1253+04	22.2	36.0	43.2	46.7	38.8	12.0	12.0	13.2	14.2	14.7
HIPEQ1255+00	70.5	87.9	99.4	101.8	95.4	48.6	46.0	46.6	46.3	44.6
HIPEQ1255+02	24.9	36.4	48.3	53.5	55.8	21.4	14.5	14.5	14.2	13.7
HIPEQ1255-00	11.1	21.0	26.5	25.7	13.5	17.9	21.6	22.1	22.0	24.7
HIPEQ1256+03	6.7	15.0	20.6	16.2	10.3	17.9	16.7	16.6	16.4	17.6
HIPEQ1257+02	20.2	25.3	28.9	29.7	23.0	21.9	18.3	18.3	18.4	19.7
HIPEQ1257-01	28.1	40.8	44.0	49.5	40.8	28.7	22.4	20.6	20.0	19.4
HIPEQ1258+02	19.8	44.0	47.9	51.5	43.6	27.8	25.5	25.3	25.8	27.9
HIPEQ1300+02a	16.6	29.3	32.9	36.8	28.1	17.1	17.5	18.2	19.8	21.7
HIPEQ1300+02b	66.9	78.4	85.9	94.6	113.3	39.1	34.2	34.6	36.4	40.8
HIPEQ1303+03	27.3	40.4	42.0	42.0	34.1	27.4	24.9	23.9	24.2	24.4
HIPEQ1304-02	11.1	16.2	19.0	19.0	13.9	10.7	8.3	9.0	8.7	8.5
HIPEQ1304-03	63.0	85.9	87.1	90.7	84.0	51.0	51.6	49.8	48.8	48.1
HIPEQ1307-00	28.5	37.6	39.6	38.8	39.2	20.7	17.2	16.6	16.5	17.5
HIPEQ1308-02	24.9	33.7	37.2	39.2	56.2	23.6	18.6	18.2	18.0	22.5
HIPEQ1311+03a	11.5	16.2	17.4	19.4	18.6	8.9	11.1	10.0	9.3	8.7
HIPEQ1312+03	12.7	23.4	24.6	25.7	23.4	11.4	9.3	9.6	9.5	9.3
HIPEQ1312+05	4.4	15.0	16.2	16.6	7.9	14.9	13.1	12.5	12.6	13.0
HIPEQ1313+06	24.2	34.5	35.2	37.6	34.8	22.3	17.3	16.2	15.5	17.3
HIPEQ1317-00	19.4	20.2	20.6	19.8	17.4	12.9	11.5	10.7	10.3	12.0
HIPEQ1318-01	30.1	37.2	40.4	41.6	41.2	31.3	21.2	20.9	21.3	25.1
HIPEQ1320+05	17.4	26.5	30.5	31.7	28.5	18.7	17.2	18.2	18.6	20.0
HIPEQ1327+02	···	15.4	15.8	15.8	12.7	12.7	11.8	11.3	10.5	12.9
HIPEQ1329-00	11.1	19.8	23.8	24.2	19.0	16.3	14.3	14.6	15.0	15.8
HIPEQ1332+01	24.2	31.7	34.8	38.4	34.5	19.9	15.1	14.3	14.6	16.0
HIPEQ1335+01	31.3	45.9	49.5	52.7	49.9	28.4	22.5	20.2	19.3	19.9
HIPEQ1341+05	15.8	26.5	28.1	27.3	23.4	15.8	13.9	12.6	12.2	11.6
HIPEQ1348+03	77.6	92.7	103.8	112.9	116.4	55.3	49.6	48.2	48.9	49.2
HIPEQ1352+02a	13.9	61.4	67.3	69.7	70.9	35.5	28.4	26.3	25.4	26.1
HIPEQ1352-01	82.0	97.4	103.4	108.1	108.5	54.3	51.5	49.7	50.2	49.6
HIPEQ1400+02	21.0	30.9	32.1	33.3	32.9	16.1	15.9	15.3	15.1	15.9
HIPEQ1411-01	51.9	80.4	88.3	89.1	90.3	46.6	48.9	45.4	45.8	41.4
HIPEQ1415+04	17.0	19.8	21.0	22.6	23.8	11.0	9.4	9.8	10.4	10.7
HIPEQ1416+03	···	18.6	21.8	22.6	2.4	18.0	17.6	18.0	18.7	19.5
HIPEQ1422-00	82.0	95.0	101.8	103.0	107.3	49.4	47.0	46.2	45.6	47.3
HIPEQ1429-00	26.5	37.2	38.8	40.0	38.8	23.5	20.9	20.0	20.4	20.6
HIPEQ1432+00	25.3	36.8	40.4	43.6	40.4	19.8	18.0	18.1	17.9	18.1
HIPEQ1433+01	···	9.1	···	···	0.8	20.9	18.4	16.7	16.2	13.8
HIPEQ1433+02	19.0	26.9	28.1	24.6	25.3	13.9	12.9	13.0	12.3	13.5

Table 3.12—Continued

	r_{25}					r_K				
HIPASS Name	u	g	r	i	z	u	g	r	i	z
HIPEQ1437+02	87.5	85.9	107.7	113.7	120.8	49.8	37.6	41.5	41.1	42.7
HIPEQ1437-00	38.4	58.6	67.7	76.8	79.6	22.3	23.2	24.5	25.9	26.9
HIPEQ1439-00	57.8	69.7	72.9	77.6	78.0	40.8	36.5	36.2	36.7	35.8
HIPEQ1440+02	24.2	29.3	31.3	31.7	33.7	18.0	13.7	13.7	14.3	16.3
HIPEQ1444+01a	50.7	71.3	77.6	79.6	82.4	38.6	30.6	28.4	27.3	28.2
HIPEQ1500+01	53.1	86.3	98.6	103.4	109.7	38.8	35.5	34.4	34.1	34.6
HIPEQ1504+02	17.8	21.8	22.2	23.0	20.2	15.7	11.6	11.4	11.7	12.9
HIPEQ1504-00	16.6	34.1	38.0	38.0	36.8	21.7	20.9	20.8	19.7	18.4
HIPEQ1507+01	74.4	127.1	135.4	140.6	141.8	59.9	53.7	49.4	48.4	49.7
HIPEQ1542+00	23.0	53.1	62.6	66.5	72.9	41.2	38.5	37.0	35.2	35.8
HIPEQ1544+02	19.0	26.1	30.5	30.1	24.9	18.8	14.2	13.7	13.5	14.6
HIPEQ1545+00	18.2	26.9	35.6	34.5	34.8	27.6	22.7	24.4	26.0	24.3
HIPEQ1601+01a	47.9	70.9	76.4	79.2	84.7	40.4	37.3	37.1	38.5	38.8
HIPEQ1609-00	7.5	21.0	17.4	17.4	12.3	21.0	18.5	18.0	17.8	18.7
HIPEQ1613-00	17.8	23.8	26.9	25.7	24.6	14.3	13.4	13.1	13.1	14.3
HIPEQ1614+00	38.4	47.9	51.5	48.7	50.3	36.6	34.1	33.2	31.7	34.7
HIPEQ1614-00	28.1	71.7	85.5	98.6	100.6	28.5	39.9	36.0	34.6	29.9
HIPEQ2036-04	40.4	53.5	61.8	74.4	79.2	35.5	29.1	26.7	27.7	28.3
HIPEQ2314+00	18.6	21.8	22.6	23.4	23.0	13.2	9.9	10.0	10.3	12.0
HIPEQ2324-00	23.0	43.6	43.6	43.2	38.8	23.8	21.8	21.5	21.5	23.4
HIPEQ2335+01	5.9	17.4	23.4	24.2	16.2	29.7	23.2	23.3	23.0	25.6
HIPEQ2336+00	44.4	60.6	65.7	82.0	96.2	40.0	29.9	25.5	26.2	29.8
HIPEQ2337+00	2.4	44.0	51.5	55.8	43.2	38.9	34.6	34.1	33.9	33.4
HIPEQ2340+01	18.6	24.9	30.1	30.1	27.7	14.4	13.1	13.0	13.2	13.0

Note. — For some of the galaxies, the r_{25} occurs almost immediately and in others, the values is never reached because of their irregular LSB nature. The r_{25} values for these latter cases have been omitted from the table

3.9 Photometric Sample

3.9.1 Derived Quantities

With excellent five-band photometry, it is possible to explore the photometric properties of this HI selected sample with unprecedented uniformity. In this section we derive several quantities from the photometric data, give an overview of the sample properties. and highlight some empirical results from the photometry.

Using the distances derived from the Virgo infall model described in Chapter 2, we compute physical sizes and absolute magnitudes for every galaxy, given in Table 3.13. Absolute magnitudes are computed using the standard distance modulus formula including all photometric corrections (foreground extinction, internal extinction, k-corrections). Luminosities can be computed from the tabulated values of absolute magnitude using the solar absolute *ugriz* magnitudes (6.41, 5.15, 4.67, 4.56, and 4.53 respectively), provided by Bell et al. (2003) but are not explicitly calculated in this section. We also tabulate the physical R50 and R90 size (kpc) of each galaxy in the r-band.

To aid in Tully-Fisher and other dynamical studies, we include the inclination corrected circular velocity in Table 3.13. We correct for inclination effects in the HI line widths using the equation:

$$W_{20,c} = \frac{W_{20}}{2}\left(\frac{1-(b/a)^2}{1-0.19^2}\right)^{-1/2} \tag{3.14}$$

where b/a is the optically derived axis ratio, and 0.19 is typical intrinsic axis ratio for spiral galaxies (Pizagno et al. 2005). Because of the large uncertainties in several of the derived inclinations (galaxies with circular aperture photometry), not all of the velocities were properly corrected. The incorrectly corrected velocities are excluded from the dynamical studies of this thesis.

In order to compute stellar mass, we use the method of Bell et al. (2003) to calculate the mass-to-light ratio in the i-band. Specifically we use the relation:

$$\log(M_*/L_i) = -0.222 + 0.864(g-r) + log(0.71) \tag{3.15}$$

where the factor of 0.71 comes from the conversion between Bell et al.'s (2003) "diet Salpeter" and a Kroupa IMF (Pizagno et al. 2005).

Assuming an i-band solar absolute magnitude of 4.56 (Bell et al. 2003), we derive a stellar mass using:

$$M_* = M_*/L_i(10.^{(-(M_i-4.56)/2.51)}). \tag{3.16}$$

The stellar mass values are given in Table 3.13.

Table 3.13. Derived Quantities

HIPASS Name	Distance (Mpc)	Rotational Velocity (km/s)[a]	Log(Stellar Mass) ($M_\odot$)	Absolute Magnitude u	g	r	i	z	R50 (kpc) r-band	R90 (kpc) r-band
HIPEQ0014-00	56.5±1.5	159.6±14.0	10.0±0.6	-19.99±0.09	-20.63±0.06	-20.84±0.15	-20.93±0.01	-20.99±0.09	5.85	16.15
HIPEQ0027-01a	55.4±1.5	119.1±13.6	9.6±0.6	-19.00±0.10	-19.63±0.06	-19.87±0.12	-19.92±0.02	-19.85±0.10	5.74	11.70
HIPEQ0033-01	27.9±1.5	··· ···	8.8±0.6	-16.58±0.17	-17.37±0.13	-17.65±0.28	-17.79±0.01	-17.83±0.17	2.73	6.21
HIPEQ0043-00	59.5±1.6	191.6±17.0	10.4±0.6	-19.98±0.09	-20.92±0.06	-21.35±0.27	-21.57±0.14	-21.74±0.09	4.00	10.50
HIPEQ0051-00	22.7±1.5	99.1±14.6	8.8±0.6	-16.36±0.17	-17.18±0.14	-17.55±0.32	-17.72±0.01	-17.79±0.17	0.70	1.92
HIPEQ0058+00	77.5±1.6	··· ···	10.3±0.6	-19.54±0.08	-20.53±0.05	-21.01±0.29	-21.26±0.18	-21.37±0.07	4.02	8.63
HIPEQ0107+01	8.5±1.5	··· ···	7.7±0.6	-13.84±0.40	-14.68±0.36	-14.95±0.51	-15.10±0.23	-15.12±0.40	0.44	1.09
HIPEQ0119+00	62.1±1.6	··· ···	8.6±0.6	-16.15±0.16	-16.92±0.07	-17.24±0.21	-17.36±0.04	-17.52±0.16	2.14	4.65
HIPEQ0120-00	24.0±1.5	67.8±13.3	8.7±0.6	-16.21±0.18	-16.99±0.14	-17.32±0.28	-17.46±0.01	-17.54±0.17	2.12	4.14
HIPEQ0122+00	33.0±1.5	134.2±12.9	9.9±0.6	-20.44±0.13	-20.90±0.10	-21.00±0.20	-21.10±0.02	-21.12±0.13	8.54	16.89
HIPEQ0123-00	106.6±1.6	··· ···	10.4±0.6	-20.21±0.07	-21.01±0.04	-21.44±0.24	-21.64±0.15	-21.88±0.06	6.75	16.17
HIPEQ0126+00a	77.3±1.6	··· ···	9.0±0.6	-15.95±0.30	-17.64±0.07	-17.98±0.24	-18.14±0.09	-18.12±0.16	3.41	7.27
HIPEQ0126-00b	26.6±1.5	··· ···	8.2±0.6	-15.86±0.16	-16.46±0.12	-16.64±0.10	-16.62±0.17	-16.58±0.16	0.56	1.33
HIPEQ0154-00	82.0±1.6	··· ···	10.8±0.6	-18.91±0.08	-20.57±0.04	-21.32±0.44	-21.72±0.34	-21.92±0.07	3.31	10.55
HIPEQ0222-00	21.1±1.5	71.3±12.6	8.7±0.6	-16.38±0.20	-17.26±0.16	-17.53±0.20	-17.57±0.13	-17.48±0.19	3.33	6.45
HIPEQ0228-01	22.1±1.5	··· ···	9.6±0.6	-18.23±0.18	-19.07±0.15	-19.46±0.34	-19.66±0.03	-19.76±0.17	2.76	6.83
HIPEQ0230-01	20.6±1.5	178.8±13.7	10.2±0.6	-18.53±0.19	-19.88±0.16	-20.45±0.43	-20.72±0.10	-20.82±0.18	1.54	4.67
HIPEQ0231+00	90.7±1.6	96.5±15.6	9.8±0.6	-18.83±0.09	-19.81±0.04	-20.12±0.17	-20.25±0.07	-20.38±0.08	6.62	15.15
HIPEQ0236+00	93.8±1.6	154.0±13.1	10.3±0.6	-19.96±0.08	-20.82±0.04	-21.20±0.20	-21.37±0.11	-21.39±0.07	6.85	14.41
HIPEQ0238+00	20.1±1.5	··· ···	7.7±0.6	-14.32±0.29	-15.16±0.18	-15.30±0.31	-15.41±0.08	-15.52±0.27	1.31	2.66
HIPEQ0240+01	16.0±1.5	··· ···	7.6±0.6	-14.07±0.34	-14.88±0.22	-15.00±0.39	-15.15±0.08	-15.62±0.29	1.60	4.07
HIPEQ0241+00	13.3±1.5	202.5±13.3	10.4±0.6	-19.67±0.26	-20.67±0.23	-21.18±0.46	-21.41±0.02	-21.51±0.26	6.55	15.83
HIPEQ0244+00	39.2±1.5	36.6±13.3	9.1±0.6	-17.01±0.13	-17.80±0.09	-18.20±0.30	-18.40±0.10	-18.51±0.12	4.21	9.62
HIPEQ0246-00a	38.7±1.5	175.6±14.5	10.5±0.6	-20.40±0.12	-21.28±0.09	-21.69±0.27	-21.88±0.08	-22.04±0.11	7.65	18.12
HIPEQ0246-00b	20.7±1.5	··· ···	10.2±0.6	-19.61±0.18	-20.55±0.15	-20.96±0.35	-21.16±0.03	-21.28±0.18	4.01	9.22
HIPEQ0249-00	94.3±1.6	94.9±20.4	10.3±0.6	-19.47±0.08	-20.51±0.04	-21.00±0.30	-21.26±0.20	-21.38±0.07	5.61	13.22
HIPEQ0249-00a	37.0±1.5	··· ···	8.4±0.6	-16.66±0.16	-17.16±0.10	-17.28±0.07	-17.23±0.16	-17.47±0.17	2.49	4.69
HIPEQ0249-00b	101.3±1.6	183.8±18.1	10.9±0.6	-20.86±0.07	-21.84±0.04	-22.33±0.30	-22.59±0.21	-22.74±0.06	6.80	19.44
HIPEQ0251-01	20.5±1.5	54.9±13.4	8.7±0.6	-16.69±0.20	-17.36±0.16	-17.62±0.27	-17.72±0.07	-17.90±0.20	4.33	8.57
HIPEQ0300+00	39.9±1.5	109.1±13.1	9.0±0.6	-17.72±0.15	-18.51±0.09	-18.67±0.15	-18.73±0.04	-18.72±0.13	3.60	7.29
HIPEQ0301-00	36.9±1.5	65.4±15.1	8.9±0.6	-17.69±0.14	-18.16±0.10	-18.32±0.20	-18.42±0.01	-18.45±0.13	3.04	8.42
HIPEQ0306-00	45.1±1.5	··· ···	10.7±0.6	-19.03±0.11	-20.66±0.07	-21.35±0.46	-21.74±0.30	-21.93±0.10	2.42	8.65
HIPEQ0316-00	99.3±1.6	38.7±13.2	10.5±0.6	-19.11±0.09	-20.56±0.04	-21.15±0.37	-21.49±0.28	-21.76±0.07	8.39	17.34
HIPEQ0320-06	31.9±1.5	130.0±14.6	9.9±0.6	-18.99±0.13	-19.91±0.10	-20.25±0.27	-20.42±0.05	-20.50±0.13	2.20	4.90
HIPEQ0351-00	132.9±1.6	74.4±16.2	10.5±0.6	-19.99±0.07	-20.99±0.03	-21.46±0.25	-21.68±0.17	-21.81±0.06	3.83	8.93
HIPEQ0809+00	25.1±1.5	93.8±15.8	9.2±0.6	-17.64±0.16	-18.38±0.13	-18.68±0.24	-18.80±0.04	-18.88±0.16	2.36	4.92
HIPEQ0821+03b	58.4±1.6	169.4±16.9	10.3±0.6	-19.23±0.09	-20.33±0.06	-20.81±0.32	-21.07±0.18	-21.22±0.09	3.37	7.85
HIPEQ0821-00	25.1±1.5	··· ···	8.3±0.6	-16.04±0.17	-16.74±0.13	-16.90±0.10	-16.86±0.19	-17.00±0.17	1.26	3.91
HIPEQ0822-00	64.1±1.6	73.4±14.2	10.0±0.6	-19.39±0.08	-20.15±0.06	-20.53±0.24	-20.71±0.11	-20.87±0.08	5.78	11.56
HIPEQ0825-00	70.9±1.6	249.9±13.6	10.9±0.6	-21.02±0.08	-21.88±0.05	-22.39±0.31	-22.65±0.19	-22.82±0.08	7.08	16.74
HIPEQ0855+02	54.4±1.5	73.8±14.8	9.6±0.6	-18.54±0.12	-19.35±0.07	-19.62±0.22	-19.77±0.06	-19.82±0.11	8.57	18.49
HIPEQ0856+00	35.4±1.5	··· ···	9.4±0.6	-18.18±0.13	-18.91±0.09	-19.18±0.36	-19.44±0.15	-19.52±0.13	3.47	10.06
HIPEQ0923-00	49.8±1.5	122.4±13.3	9.5±0.6	-19.20±0.10	-19.79±0.07	-19.92±0.12	-19.96±0.04	-19.92±0.10	4.39	8.69
HIPEQ0930+04	76.4±1.6	37.9±14.1	10.3±0.6	-20.13±0.08	-20.47±0.05	-20.99±0.22	-21.16±0.11	-21.70±0.08	8.80	24.07
HIPEQ0942+00	26.7±1.5	··· ···	10.3±0.6	-19.58±0.15	-20.56±0.12	-21.03±0.37	-21.27±0.10	-21.49±0.15	3.69	9.32
HIPEQ0944-00b	17.1±1.5	75.0±15.3	7.9±0.6	-14.74±0.24	-15.62±0.19	-15.85±0.08	-15.73±0.33	-15.98±0.23	0.95	2.26
HIPEQ0945+01	26.4±1.5	135.3±13.0	9.8±0.6	-19.37±0.16	-20.09±0.12	-20.32±0.17	-20.37±0.09	-20.42±0.15	4.36	9.33
HIPEQ0946+02	27.6±1.5	91.4±13.1	9.0±0.6	-17.39±0.16	-17.99±0.12	-18.25±0.20	-18.33±0.06	-18.41±0.15	4.39	10.96
HIPEQ0947+00a	25.0±1.5	114.0±13.7	9.2±0.6	-17.75±0.17	-18.48±0.13	-18.77±0.28	-18.91±0.01	-18.98±0.16	3.56	7.74
HIPEQ0947+00b	26.3±1.5	65.2±14.6	8.6±0.6	-16.61±0.18	-17.20±0.13	-17.44±0.11	-17.42±0.17	-17.39±0.18	3.03	6.82
HIPEQ0953+01	18.2±1.5	162.7±12.6	9.7±0.6	-20.69±0.20	-21.03±0.17	-20.98±0.03	-20.83±0.34	-20.94±0.20	6.04	13.14
HIPEQ0954+02a	105.7±1.6	··· ···	10.2±0.6	-19.68±0.07	-20.83±0.04	-21.14±0.32	-21.42±0.23	-21.00±0.07	7.31	15.84
HIPEQ0955+04a	26.1±1.5	122.7±14.1	10.0±0.6	-19.54±0.15	-20.30±0.12	-20.62±0.23	-20.73±0.03	-20.82±0.15	3.60	8.06
HIPEQ0958+01	25.8±1.5	··· ···	7.4±0.6	-14.40±0.33	-15.19±0.16	-15.23±0.12	-14.88±0.54	-14.87±0.54	1.63	3.17
HIPEQ1000+03	29.5±1.5	185.4±13.1	9.9±0.6	-19.01±0.14	-19.83±0.11	-20.19±0.31	-20.40±0.07	-20.47±0.14	2.72	7.87
HIPEQ1010+05	59.2±1.6	··· ···	9.6±0.6	-17.64±0.10	-18.89±0.06	-19.30±0.25	-19.49±0.12	-19.47±0.09	1.93	5.34
HIPEQ1014+03	17.5±1.5	256.6±15.0	10.7±0.6	-19.88±0.21	-21.16±0.18	-21.70±0.49	-22.02±0.11	-22.14±0.21	4.49	14.65

Table 3.13—Continued

HIPASS Name	Distance (Mpc)	Rotational Velocity (km/s)[a]	Log(Stellar Mass) ($M_\odot$)	Absolute Magnitude u	g	r	i	z	R50 (kpc) r-band	R90 (kpc) r-band
HIPEQ1015+02	18.2±1.5	76.7±13.5	8.4±0.6	-16.35±0.23	-16.90±0.18	-17.03±0.32	-17.16±0.07	-17.04±0.24	3.15	8.50
HIPEQ1026+03	31.0±1.5	135.3±14.3	9.6±0.6	-18.87±0.14	-19.75±0.11	-19.94±0.16	-20.00±0.07	-20.31±0.14	4.64	11.05
HIPEQ1028+03	16.5±1.5	55.1±12.7	7.9±0.6	-15.19±0.23	-16.06±0.20	-16.09±0.32	-16.22±0.09	-16.38±0.23	2.06	4.22
HIPEQ1039+01	10.1±1.5	··· ···	8.7±0.6	-15.86±0.34	-16.81±0.30	-17.18±0.55	-17.42±0.08	-17.53±0.34	0.68	1.81
HIPEQ1041+00	81.0±1.6	··· ···	10.0±0.6	-19.33±0.08	-20.02±0.04	-20.41±0.26	-20.62±0.15	-20.75±0.08	6.06	13.84
HIPEQ1046+01	14.1±1.5	116.4±12.7	9.3±0.6	-18.25±0.25	-18.91±0.22	-19.12±0.23	-19.13±0.23	-19.41±0.25	4.15	8.95
HIPEQ1050+01	22.9±1.5	64.7±13.7	7.9±0.6	-13.90±0.26	-14.88±0.16	-15.29±0.23	-15.35±0.11	-14.98±0.28	1.19	2.11
HIPEQ1051+04a	15.2±1.5	83.3±13.8	8.7±0.6	-16.61±0.24	-17.16±0.21	-17.46±0.25	-17.49±0.19	-17.56±0.24	1.83	4.66
HIPEQ1052+00	26.0±1.5	52.9±15.3	8.6±0.6	-16.10±0.16	-16.86±0.13	-17.14±0.24	-17.25±0.03	-17.36±0.16	0.65	1.84
HIPEQ1053+02	15.1±1.5	··· ···	7.8±0.6	-15.19±0.24	-15.47±0.21	-15.61±0.31	-15.71±0.13	-15.68±0.26	0.70	1.51
HIPEQ1055+02	15.0±1.5	··· ···	7.6±0.6	-14.36±0.25	-14.98±0.22	-15.12±0.20	-15.09±0.26	-15.13±0.28	0.49	1.16
HIPEQ1101+03	16.3±1.5	152.4±12.8	9.8±0.6	-19.85±0.22	-20.44±0.19	-20.54±0.30	-20.64±0.11	-20.70±0.22	5.81	11.52
HIPEQ1109-00	55.3±1.5	183.6±13.9	10.1±0.6	-19.34±0.09	-20.30±0.06	-20.71±0.24	-20.89±0.10	-20.95±0.09	3.19	10.09
HIPEQ1110+01	14.3±1.5	··· ···	7.9±0.6	-14.33±0.26	-15.16±0.22	-15.44±0.26	-15.47±0.21	-15.50±0.27	0.74	1.71
HIPEQ1113+05	36.9±1.5	60.8±18.7	9.1±0.6	-17.46±0.12	-18.44±0.09	-18.60±0.27	-18.78±0.07	-18.35±0.12	2.69	5.95
HIPEQ1117+04a	23.0±1.5	272.0±19.7	9.9±0.6	-18.51±0.17	-19.58±0.14	-20.06±0.37	-20.29±0.07	-20.44±0.17	1.46	4.64
HIPEQ1119+02	22.9±1.5	··· ···	9.1±0.6	-18.11±0.17	-18.55±0.14	-18.69±0.27	-18.82±0.03	-18.74±0.18	3.21	8.05
HIPEQ1124+03	20.0±1.5	··· ···	9.2±0.6	-18.33±0.19	-18.84±0.16	-19.01±0.24	-19.08±0.10	-19.22±0.19	3.07	5.95
HIPEQ1127-01	13.8±1.5	··· ···	8.5±0.6	-15.54±0.26	-16.36±0.23	-16.73±0.43	-16.92±0.05	-17.27±0.26	1.38	4.33
HIPEQ1131-02	68.1±1.6	··· ···	10.5±0.6	-20.28±0.08	-21.13±0.05	-21.58±0.30	-21.83±0.18	-21.97±0.08	8.63	20.01
HIPEQ1133-03	23.0±1.5	82.5±15.1	8.7±0.6	-16.75±0.17	-17.45±0.14	-17.68±0.27	-17.81±0.03	-17.92±0.18	2.38	5.29
HIPEQ1136+00	16.0±1.5	··· ···	8.1±0.6	-15.70±0.23	-16.40±0.20	-16.49±0.21	-16.50±0.21	-16.46±0.23	0.52	1.35
HIPEQ1138+03	80.8±1.6	··· ···	10.3±0.6	-19.03±0.08	-20.22±0.04	-20.79±0.35	-21.10±0.24	-21.26±0.07	4.34	11.32
HIPEQ1143-01	24.5±1.5	··· ···	7.6±0.6	-13.76±0.28	-14.43±0.16	-14.70±0.26	-14.77±0.10	-14.75±0.34	1.13	2.96
HIPEQ1145+02	14.8±1.5	··· ···	7.2±0.6	-13.35±0.39	-13.85±0.26	-14.12±0.17	-13.98±0.41	-11.95±1.60	1.28	2.76
HIPEQ1148-02	24.9±1.5	136.4±15.5	9.3±0.6	-17.97±0.17	-18.67±0.13	-18.91±0.32	-19.09±0.03	-19.05±0.17	4.20	11.08
HIPEQ1151-02	55.7±1.5	128.0±14.5	9.5±0.6	-18.27±0.09	-19.13±0.06	-19.42±0.16	-19.52±0.02	-19.56±0.09	2.25	6.20
HIPEQ1152+01	88.6±1.6	91.3±17.1	10.2±0.6	-20.08±0.07	-20.77±0.04	-21.09±0.20	-21.24±0.09	-21.35±0.07	6.98	14.64
HIPEQ1152-02	15.2±1.5	··· ···	8.1±0.6	-16.08±0.24	-16.62±0.21	-16.66±0.03	-16.49±0.40	-16.45±0.24	0.44	1.08
HIPEQ1152-03b	23.5±1.5	··· ···	8.8±0.6	-16.64±0.17	-17.51±0.14	-17.77±0.29	-17.92±0.01	-18.01±0.18	2.25	5.00
HIPEQ1155+01	27.4±1.5	116.2±16.8	9.7±0.6	-18.36±0.15	-19.35±0.12	-19.76±0.30	-19.94±0.04	-20.13±0.15	6.00	11.10
HIPEQ1200-00	28.1±1.5	34.1±16.0	8.9±0.6	-16.33±0.17	-17.21±0.12	-17.60±0.36	-17.84±0.09	-17.80±0.17	4.36	9.96
HIPEQ1200-01	21.2±1.5	··· ···	10.7±0.6	-20.11±0.18	-21.17±0.15	-21.72±0.46	-22.03±0.14	-22.23±0.18	3.58	10.04
HIPEQ1202+01	28.8±1.5	··· ···	10.5±0.6	-18.80±0.14	-20.18±0.11	-20.87±0.50	-21.26±0.26	-21.53±0.14	3.20	10.16
HIPEQ1204-01	21.3±1.5	··· ···	8.4±0.6	-15.76±0.21	-16.29±0.16	-16.62±0.23	-16.68±0.11	-16.93±0.22	2.41	4.62
HIPEQ1204-02	86.3±1.6	··· ···	10.5±0.6	-19.05±0.07	-20.41±0.04	-21.03±0.38	-21.36±0.27	-21.58±0.07	4.97	14.26
HIPEQ1210+02	19.6±1.5	··· ···	8.4±0.6	-15.39±0.25	-16.20±0.18	-16.56±0.31	-16.69±0.06	-16.92±0.24	2.14	4.82
HIPEQ1215+04a	32.0±1.5	46.4±13.9	8.9±0.6	-16.88±0.14	-17.82±0.10	-18.09±0.23	-18.21±0.00	-18.23±0.14	2.15	4.98
HIPEQ1216-03	73.9±1.6	··· ···	10.0±0.6	-19.14±0.08	-19.97±0.05	-20.39±0.25	-20.59±0.14	-20.86±0.08	4.82	12.06
HIPEQ1218+00	13.8±1.5	··· ···	8.2±0.6	-14.69±0.28	-15.56±0.24	-16.00±0.34	-16.10±0.15	-16.15±0.28	1.72	3.57
HIPEQ1218-01	82.0±1.6	185.2±15.8	10.4±0.6	-19.71±0.07	-20.78±0.04	-21.25±0.26	-21.47±0.16	-21.57±0.07	4.72	11.81
HIPEQ1219+03	22.4±1.5	··· ···	9.0±0.6	-16.93±0.17	-17.75±0.14	-18.11±0.26	-18.23±0.04	-18.38±0.17	1.47	3.62
HIPEQ1220+00	13.2±1.5	36.1±13.0	7.6±0.6	-14.06±0.28	-14.97±0.24	-15.12±0.34	-15.21±0.16	-15.22±0.29	1.19	2.53
HIPEQ1220+01	23.3±1.5	91.2±12.6	8.9±0.6	-17.27±0.18	-18.00±0.14	-18.18±0.18	-18.22±0.12	-18.25±0.17	3.27	6.67
HIPEQ1221+03	37.5±1.5	175.1±13.0	10.1±0.6	-19.29±0.12	-20.02±0.09	-20.47±0.32	-20.70±0.13	-20.87±0.12	4.47	12.46
HIPEQ1223+00	29.8±1.5	··· ···	8.6±0.6	-16.27±0.17	-16.92±0.12	-17.19±0.21	-17.27±0.05	-17.43±0.18	2.86	6.70
HIPEQ1223-03b	28.8±1.5	188.6±12.9	10.3±0.6	-19.86±0.14	-20.82±0.11	-21.20±0.30	-21.38±0.05	-21.44±0.14	3.93	9.34
HIPEQ1224+00	30.0±1.5	··· ···	8.0±0.6	-14.54±0.23	-15.33±0.13	-15.66±0.23	-15.74±0.06	-15.76±0.26	1.44	2.53
HIPEQ1224+03b	13.9±1.5	··· ···	8.6±0.6	-15.97±0.26	-16.84±0.23	-17.17±0.42	-17.35±0.06	-17.42±0.26	1.41	3.60
HIPEQ1225+00	31.1±1.5	67.0±17.3	10.1±0.6	-18.83±0.13	-19.81±0.10	-20.33±0.37	-20.60±0.14	-20.79±0.13	3.17	8.07
HIPEQ1226+02	24.7±1.5	101.7±13.9	9.9±0.6	-19.10±0.16	-19.93±0.13	-20.27±0.26	-20.39±0.02	-20.51±0.16	2.71	5.65
HIPEQ1227+01	19.0±1.5	··· ···	7.6±0.6	-14.61±0.26	-15.03±0.19	-15.16±0.20	-15.14±0.23	-15.36±0.34	1.39	2.77
HIPEQ1228+02	23.0±1.5	88.8±13.4	8.8±0.6	-17.14±0.18	-17.79±0.14	-18.00±0.23	-18.09±0.08	-18.15±0.19	4.42	9.29
HIPEQ1228+03	13.5±1.5	102.1±20.7	10.2±0.6	-18.07±0.26	-19.59±0.23	-20.26±0.58	-20.60±0.10	-20.82±0.26	1.29	4.38
HIPEQ1229+00	32.5±1.5	54.8±12.7	8.4±0.6	-15.25±0.18	-16.18±0.11	-16.55±0.10	-16.53±0.14	-16.38±0.18	2.75	5.50
HIPEQ1230+02	24.0±1.5	··· ···	8.3±0.6	-15.73±0.19	-16.58±0.14	-16.78±0.24	-16.87±0.07	-16.88±0.21	1.57	3.09
HIPEQ1230+03	75.7±1.6	··· ···	9.2±0.6	-18.26±0.08	-18.93±0.05	-19.11±0.11	-19.17±0.01	-19.18±0.09	2.03	4.51

Table 3.13—Continued

	Distance	Rotational	Log(Stellar Mass)	Absolute Magnitude					R50 (kpc)	R90 (kpc)
HIPASS Name	(Mpc)	Velocity (km/s)[a]	($M_\odot$)	u	g	r	i	z	r-band	r-band
HIPEQ1232+00a	22.3±1.5	92.4±15.0	9.6±0.6	-18.45±0.18	-19.32±0.15	-19.65±0.30	-19.80±0.01	-19.79±0.18	6.51	12.03
HIPEQ1232+00b	16.6±1.5	150.6±12.6	10.5±0.6	-21.25±0.22	-21.78±0.19	-22.03±0.31	-22.15±0.09	-22.23±0.22	14.00	28.74
HIPEQ1233-02	35.8±1.5	... ...	9.2±0.6	-17.30±0.14	-17.97±0.10	-18.37±0.24	-18.51±0.02	-18.47±0.16	5.56	10.51
HIPEQ1236+03	21.3±1.5	61.1±13.1	8.2±0.6	-15.46±0.21	-16.11±0.16	-16.34±0.27	-16.44±0.08	-16.47±0.22	2.16	4.78
HIPEQ1239-00	15.8±1.5	102.1±13.1	9.5±0.6	-19.03±0.23	-19.65±0.20	-19.82±0.25	-19.87±0.17	-19.88±0.23	3.88	9.85
HIPEQ1241+01	25.0±1.5	88.5±15.7	9.0±0.6	-16.64±0.16	-17.57±0.13	-17.97±0.34	-18.17±0.06	-18.32±0.16	1.05	2.73
HIPEQ1241-02	20.8±1.5	52.7±13.5	9.0±0.6	-16.29±0.19	-17.24±0.16	-17.67±0.41	-17.93±0.08	-18.09±0.18	1.60	3.96
HIPEQ1242+03b	11.4±1.5	86.7±15.9	9.3±0.6	-16.92±0.30	-17.84±0.27	-18.34±0.52	-18.59±0.04	-18.72±0.30	1.51	3.94
HIPEQ1242-00	25.0±1.5	114.4±13.5	10.1±0.6	-19.86±0.16	-20.65±0.13	-20.96±0.25	-21.08±0.03	-21.21±0.16	4.91	10.34
HIPEQ1242-01a	16.2±1.5	106.3±18.8	8.8±0.6	-16.73±0.23	-17.44±0.20	-17.71±0.38	-17.89±0.04	-18.05±0.23	1.49	3.79
HIPEQ1242-01b	46.3±1.5	149.6±13.0	10.0±0.6	-19.86±0.10	-20.70±0.07	-20.95±0.16	-21.04±0.00	-21.00±0.10	7.03	13.34
HIPEQ1243-00	38.1±1.5	139.7±18.4	10.2±0.6	-19.84±0.12	-20.67±0.09	-21.03±0.32	-21.27±0.13	-21.42±0.12	6.94	17.84
HIPEQ1244+00	17.3±1.5	56.9±14.0	8.7±0.6	-17.06±0.22	-17.89±0.19	-18.12±0.18	-17.74±0.58	-18.28±0.22	4.21	8.56
HIPEQ1244-02	23.0±1.5	... ...	8.5±0.6	-16.38±0.19	-17.03±0.15	-17.26±0.22	-17.33±0.10	-17.47±0.21	2.21	5.34
HIPEQ1245-00	22.2±1.5	180.3±13.2	10.8±0.6	-20.81±0.17	-21.72±0.14	-22.18±0.38	-22.42±0.07	-22.56±0.17	5.40	13.92
HIPEQ1249+03	11.1±1.5	116.3±19.0	9.1±0.6	-17.05±0.31	-17.90±0.28	-18.24±0.45	-18.41±0.13	-18.50±0.31	0.94	2.69
HIPEQ1249+04	39.0±1.5	44.9±15.4	8.9±0.6	-16.99±0.13	-17.89±0.09	-18.12±0.21	-18.23±0.01	-17.60±0.15	3.97	8.09
HIPEQ1250+05	10.2±1.5	122.1±18.5	9.1±0.6	-17.75±0.33	-18.39±0.30	-18.64±0.39	-18.73±0.23	-18.88±0.33	1.58	3.13
HIPEQ1253+01	17.0±1.5	141.4±12.9	9.9±0.6	-18.86±0.22	-19.77±0.19	-20.16±0.39	-20.37±0.00	-20.48±0.22	3.58	8.30
HIPEQ1253+02	15.0±1.5	... ...	10.2±0.6	-17.95±0.24	-19.43±0.21	-20.11±0.58	-20.48±0.15	-20.73±0.24	2.36	7.06
HIPEQ1253+04	11.1±1.5	43.4±14.8	8.7±0.6	-16.35±0.31	-17.17±0.28	-17.46±0.39	-17.58±0.18	-17.63±0.31	0.53	1.50
HIPEQ1255+00	19.4±1.5	... ...	9.7±0.6	-18.23±0.19	-19.13±0.16	-19.57±0.38	-19.78±0.03	-19.87±0.19	4.20	8.56
HIPEQ1255+02	40.6±1.5	190.9±13.4	10.2±0.6	-19.46±0.11	-20.53±0.08	-20.96±0.29	-21.16±0.11	-21.26±0.11	2.18	5.85
HIPEQ1255-00	16.5±1.5	46.3±12.8	8.1±0.6	-14.65±0.24	-15.50±0.20	-15.86±0.33	-15.99±0.09	-16.04±0.24	2.44	5.65
HIPEQ1256+03	10.2±1.5	... ...	7.2±0.6	-13.57±0.40	-14.40±0.32	-14.42±0.29	-14.38±0.37	-14.04±0.45	0.76	1.58
HIPEQ1257+02	14.0±1.5	... ...	8.1±0.6	-15.13±0.27	-15.69±0.23	-15.96±0.33	-16.05±0.16	-16.18±0.29	1.10	2.39
HIPEQ1257-01	41.2±1.5	148.3±12.9	9.9±0.6	-19.78±0.11	-20.41±0.08	-20.62±0.16	-20.70±0.02	-20.69±0.11	4.67	11.00
HIPEQ1258+02	40.2±1.5	71.8±13.9	9.5±0.6	-18.28±0.12	-19.14±0.09	-19.40±0.26	-19.57±0.07	-19.67±0.12	6.95	15.14
HIPEQ1300+02a	13.3±1.5	... ...	8.4±0.6	-14.97±0.28	-16.09±0.24	-16.49±0.43	-16.69±0.06	-16.81±0.27	0.94	2.37
HIPEQ1300+02b	14.5±1.5	66.8±17.2	9.8±0.6	-18.59±0.25	-19.41±0.22	-19.80±0.48	-20.06±0.03	-20.29±0.25	2.62	5.46
HIPEQ1303+03	42.0±1.5	... ...	9.3±0.6	-17.98±0.12	-18.83±0.08	-19.10±0.24	-19.26±0.06	-19.29±0.12	4.60	9.51
HIPEQ1304-02	18.5±1.5	47.7±15.7	8.3±0.6	-14.86±0.22	-15.70±0.18	-16.16±0.30	-16.28±0.07	-16.19±0.23	0.89	2.03
HIPEQ1304-03	19.8±1.5	85.8±19.2	9.4±0.6	-18.30±0.19	-19.10±0.16	-19.32±0.24	-19.40±0.10	-19.35±0.19	5.33	9.29
HIPEQ1307-00	78.3±1.6	143.4±19.2	10.3±0.6	-20.24±0.07	-21.02±0.05	-21.34±0.16	-21.45±0.05	-21.54±0.07	5.57	13.24
HIPEQ1308-02	77.3±1.6	... ...	10.2±0.6	-19.63±0.08	-20.56±0.05	-20.98±0.22	-21.15±0.11	-21.40±0.08	6.08	14.84
HIPEQ1311+03a	44.4±1.5	82.4±13.1	8.9±0.6	-17.44±0.11	-18.20±0.08	-18.39±0.12	-18.43±0.05	-18.50±0.11	2.13	5.63
HIPEQ1312+03	120.2±1.6	73.5±16.1	10.5±0.6	-19.51±0.07	-20.83±0.03	-21.34±0.29	-21.61±0.21	-21.71±0.06	4.85	13.15
HIPEQ1312+05	14.0±1.5	... ...	7.5±0.6	-13.31±0.33	-14.33±0.24	-14.54±0.39	-14.68±0.12	-14.25±0.38	0.78	1.56
HIPEQ1313+06	102.7±1.6	... ...	10.7±0.6	-20.14±0.07	-21.30±0.04	-21.83±0.30	-22.09±0.21	-22.26±0.06	6.70	15.97
HIPEQ1317-00	18.1±1.5	53.7±13.0	7.8±0.6	-15.21±0.21	-15.81±0.18	-15.87±0.10	-15.78±0.28	-15.83±0.22	1.50	2.47
HIPEQ1318-01	83.1±1.6	... ...	10.5±0.6	-19.96±0.07	-20.83±0.04	-21.34±0.32	-21.62±0.22	-21.91±0.07	8.29	16.90
HIPEQ1320+05	14.8±1.5	44.2±13.2	8.4±0.6	-15.36±0.25	-16.00±0.22	-16.44±0.34	-16.55±0.11	-17.23±0.25	1.70	4.09
HIPEQ1327+02	15.5±1.5	... ...	7.5±0.6	-13.83±0.29	-14.64±0.22	-14.83±0.23	-14.83±0.23	-14.87±0.32	0.74	1.57
HIPEQ1329-00	47.2±1.5	85.5±13.6	9.0±0.6	-17.24±0.12	-17.92±0.08	-18.18±0.16	-18.26±0.01	-18.38±0.12	3.99	10.51
HIPEQ1332+01	47.7±1.5	... ...	10.2±0.6	-18.62±0.10	-19.83±0.07	-20.42±0.40	-20.75±0.24	-20.94±0.10	2.75	6.78
HIPEQ1335+01	76.2±1.6	162.0±17.3	10.6±0.6	-20.21±0.08	-21.23±0.05	-21.69±0.28	-21.93±0.17	-22.04±0.08	6.73	20.19
HIPEQ1341+05	101.8±1.6	168.2±18.7	10.1±0.6	-19.81±0.07	-20.67±0.04	-21.00±0.17	-21.13±0.08	-21.18±0.07	5.47	16.03
HIPEQ1348+03	17.7±1.5	129.2±16.7	9.8±0.6	-18.59±0.21	-19.55±0.18	-19.94±0.39	-20.14±0.01	-20.49±0.21	4.44	9.08
HIPEQ1352+02a	67.7±1.6	191.5±17.4	10.8±0.6	-20.31±0.08	-21.43±0.05	-21.99±0.34	-22.28±0.22	-22.45±0.08	9.48	22.34
HIPEQ1352-01	20.6±1.5	143.8±18.0	9.9±0.6	-18.90±0.18	-19.83±0.16	-20.22±0.39	-20.45±0.06	-20.52±0.18	5.43	10.22
HIPEQ1400+02	52.6±1.5	120.4±12.8	9.6±0.6	-19.28±0.10	-19.95±0.07	-20.12±0.11	-20.15±0.04	-20.18±0.10	5.15	10.61
HIPEQ1411-01	22.9±1.5	120.2±12.7	9.5±0.6	-19.63±0.17	-20.21±0.14	-20.27±0.04	-20.16±0.26	-20.17±0.17	7.16	13.93
HIPEQ1415+04	84.2±1.6	... ...	9.8±0.6	-19.19±0.07	-19.62±0.04	-19.97±0.26	-20.18±0.16	-20.62±0.07	3.23	7.76
HIPEQ1416+03	22.2±1.5	... ...	8.2±0.6	-15.57±0.23	-16.14±0.16	-16.39±0.07	-16.30±0.27	-16.47±0.24	1.71	3.54
HIPEQ1422-00	24.2±1.5	127.0±16.4	10.0±0.6	-19.48±0.16	-20.31±0.13	-20.64±0.24	-20.74±0.05	-20.89±0.16	6.38	11.87
HIPEQ1429-00	22.9±1.5	114.7±14.8	9.0±0.6	-17.59±0.17	-18.25±0.14	-18.43±0.21	-18.49±0.09	-18.54±0.17	2.42	5.33
HIPEQ1432+00	24.7±1.5	97.5±12.8	9.3±0.6	-17.83±0.16	-18.69±0.13	-19.01±0.26	-19.14±0.02	-19.20±0.16	2.90	6.56

Table 3.13—Continued

HIPASS Name	Distance (Mpc)	Rotational Velocity (km/s)[a]	Log(Stellar Mass) ($M_\odot$)	Absolute Magnitude u	g	r	i	z	R50 (kpc) r-band	R90 (kpc) r-band
HIPEQ1433+01	27.2±1.5	··· ···	7.8±0.6	-14.45±0.37	-15.36±0.16	-15.48±0.43	-15.72±0.07	-15.36±0.44	2.03	4.02
HIPEQ1433+02	22.4±1.5	54.4±16.0	8.6±0.6	-16.53±0.18	-17.31±0.15	-17.54±0.15	-17.54±0.16	-17.63±0.18	1.42	3.66
HIPEQ1437-00	27.9±1.5	84.7±14.3	10.0±0.6	-19.10±0.15	-20.06±0.12	-20.43±0.29	-20.60±0.04	-20.64±0.15	3.26	9.04
HIPEQ1439-00	26.1±1.5	98.4±13.7	9.7±0.6	-18.88±0.15	-19.58±0.13	-19.86±0.31	-20.05±0.04	-20.02±0.15	6.62	13.28
HIPEQ1440+02	24.5±1.5	80.0±16.8	9.1±0.6	-17.17±0.16	-18.14±0.13	-18.38±0.34	-18.58±0.05	-18.15±0.16	1.55	3.53
HIPEQ1444+01a	23.6±1.5	205.1±16.1	10.2±0.6	-18.99±0.17	-20.13±0.14	-20.60±0.39	-20.85±0.10	-21.05±0.17	2.99	7.61
HIPEQ1500+01	20.3±1.5	193.1±15.2	10.3±0.6	-19.11±0.19	-20.28±0.16	-20.83±0.43	-21.11±0.10	-21.30±0.19	3.32	8.63
HIPEQ1504+02	138.8±1.6	··· ···	10.2±0.6	-19.95±0.07	-20.85±0.03	-21.19±0.11	-21.27±0.03	-21.23±0.06	6.93	15.45
HIPEQ1504-00	26.8±1.5	100.0±12.9	9.0±0.6	-17.43±0.16	-18.20±0.13	-18.41±0.18	-18.47±0.09	-18.36±0.16	3.90	7.45
HIPEQ1507+01	37.7±1.5	··· ···	11.0±0.6	-20.05±0.12	-21.51±0.09	-22.15±0.47	-22.53±0.28	-22.81±0.12	7.88	20.61
HIPEQ1542+00	28.7±1.5	124.3±12.7	9.7±0.6	-19.13±0.15	-19.89±0.11	-20.14±0.20	-20.23±0.05	-20.24±0.14	6.82	13.42
HIPEQ1544+02	56.8±1.6	··· ···	9.8±0.6	-18.07±0.10	-19.25±0.06	-19.74±0.09	-19.78±0.05	-20.34±0.09	3.05	7.86
HIPEQ1545+00	56.1±1.5	··· ···	9.5±0.6	-18.22±0.11	-18.85±0.07	-19.25±0.25	-19.43±0.10	-19.89±0.11	6.14	14.43
HIPEQ1601+01a	28.8±1.5	137.8±15.0	9.9±0.6	-19.50±0.15	-20.27±0.11	-20.50±0.46	-20.84±0.21	-20.82±0.14	5.92	13.07
HIPEQ1609-00	22.6±1.5	··· ···	7.9±0.6	-15.32±0.23	-16.11±0.16	-16.12±0.13	-16.08±0.22	-16.05±0.28	1.56	4.11
HIPEQ1613-00	31.1±1.5	··· ···	8.8±0.6	-17.40±0.14	-18.26±0.11	-18.33±0.18	-18.39±0.06	-18.71±0.14	1.55	3.77
HIPEQ1614+00	29.6±1.5	··· ···	9.2±0.6	-17.85±0.15	-18.57±0.11	-18.83±0.17	-18.88±0.08	-19.00±0.15	4.77	9.89
HIPEQ1614-00	30.2±1.5	179.0±12.6	10.1±0.6	-19.94±0.15	-20.83±0.11	-21.06±0.20	-21.15±0.04	-21.13±0.14	8.52	16.12
HIPEQ2036-04	89.8±1.6	236.8±16.2	11.1±0.6	-20.55±0.07	-21.92±0.04	-22.57±0.39	-22.92±0.29	-22.94±0.07	11.20	28.44
HIPEQ2314+00	63.0±1.6	··· ···	9.9±0.6	-18.90±0.09	-19.86±0.05	-20.24±0.25	-20.44±0.12	-20.60±0.08	2.78	5.20
HIPEQ2324-00	38.6±1.5	··· ···	9.1±0.6	-18.49±0.12	-18.96±0.09	-19.06±0.10	-19.07±0.09	-19.21±0.13	3.56	7.71
HIPEQ2335+01	37.1±1.5	··· ···	8.9±0.6	-16.50±0.20	-17.14±0.11	-17.62±0.26	-17.77±0.03	-18.05±0.17	3.71	8.20
HIPEQ2336+00	36.9±1.5	220.4±18.3	10.4±0.6	-19.62±0.12	-20.71±0.09	-21.19±0.38	-21.48±0.18	-21.72±0.12	3.47	9.85
HIPEQ2337+00	38.3±1.5	··· ···	9.4±0.6	-18.01±0.14	-18.83±0.09	-19.17±0.27	-19.34±0.07	-19.35±0.14	6.25	11.39
HIPEQ2340+01	26.6±1.5	105.0±14.3	9.2±0.6	-16.93±0.16	-17.86±0.12	-18.26±0.31	-18.45±0.05	-18.48±0.15	1.79	4.25

[a]Rotational velocities of galaxies without proper inclination corrections have been ommitted.

3.9.2 Sample Properties

With the photometry complete and other photometric quantities derived, it is now possible to examine the global properties of the sample. Whereas the following chapters will discuss various relationships within the data and probe how the HI selection affects the observables, this section simply reports the range of photometric properties that are found in the sample.

Figures 3.4-3.13 show the distributions of various photometric quantities. These distributions are included to give the reader a quick reference for the sample properties. All of the photometric corrections have been applied to the data. Therefore, the distributions shown represent the spread in the intrinsic properties of the sample galaxies themselves and may not indicate true boundaries in the SDSS or HIPASS data. We have included the u-band absolute magnitude distribution (Figure 3.7) because of the u-band's close ties to the star formation rate (Hopkins et al. 2004) and recent work looking at the u-band luminosity function (Baldry et al. 2005). Comparing the r-band (Figure 3.6) and the u-band absolute magnitude distributions shows that this sample has a significant population of blue galaxies. This sample probes a wide range of surface brightnesses (Figures 3.8 and 3.9) and sizes (Figures 3.10 and 3.11). The dotted line in 3.9 is the peak of the Courteau (1996) distribution from an optically selected sample of galaxies. Although our selection methods are very different, the peak of our surface brightness distribution is very close to the same.

The size distribution is somewhat biased because of the selection methods described in Chapter 2; galaxies with large angular extent were often not included in the sample because they were split across SDSS fields. Figure 3.12 shows the axis ratios of the HIPASS/SDSS galaxies (black) and the DR4 main galaxy sample (red). The DR4 sample appears to have a slightly higher fraction of systems at low inclinations. This is opposite to what we might expect of an HI selected sample but it may be due to the effects of seeing for some of the smaller galaxies in the main sample. It does however, demonstrate that the HIPASS/SDSS sample spans a wide range of inclinations and that the inclination problems discussed in Appendix A cannot be ignored.

The velocity distribution (Figure 3.13) also suffers from significant biasing because most of the 39 galaxies that are not included because they cannot be accurately inclination

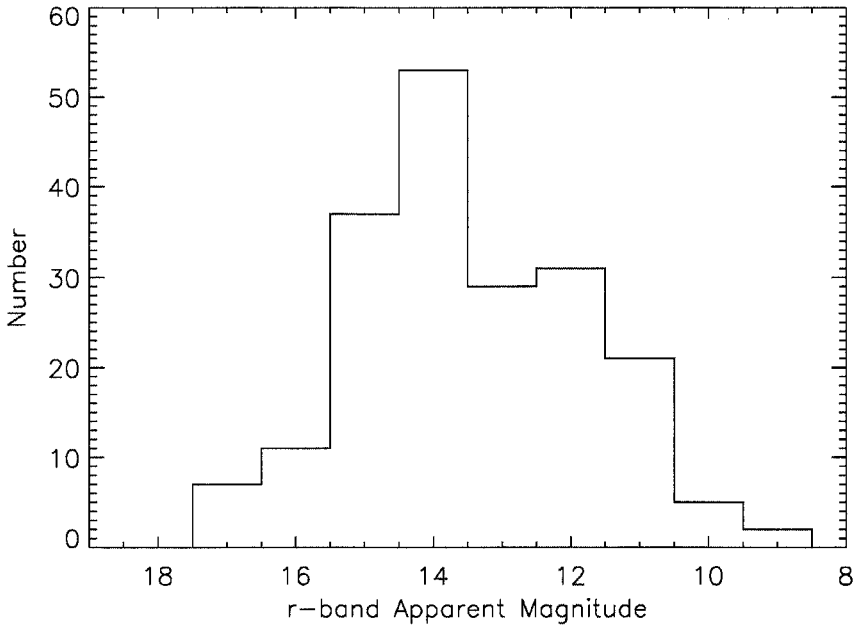

Figure 3.4 Distribution of r-band apparent magnitude for the HIPASS/SDSS galaxies.

corrected have small $V \sin i$ velocities and would most likely contribute to the "low mass" bins.

It is important to note that the large angular extent of the galaxies as well as their close distances are not found in any other SDSS study. The large number of LSB galaxies seen in this thesis also separates this sample from previous SDSS galaxy studies. The low stellar masses derived (Figure 3.14) allow me to examine galaxies with over an order of magnitude fewer stars than previously studied with the SDSS. The following chapters will explore the physical properties of these systems.

We conclude this chapter with a demonstration of the quality of our "SDSS" photometry. Figure 3.15 shows an $r - i$ vs $g - r$ for all of the galaxies in the sample. All of the sample galaxies lie on a well defined locus. The red galaxies, in particular have a very narrow distribution. In the next chapter we will incorporate the HIPASS HI data and investigate how the SDSS photometric trends relate to the galaxy gas content. Chapter 5 will attempt to understand the colors of the galaxies. Chapter 6 will examine the dynamics of the

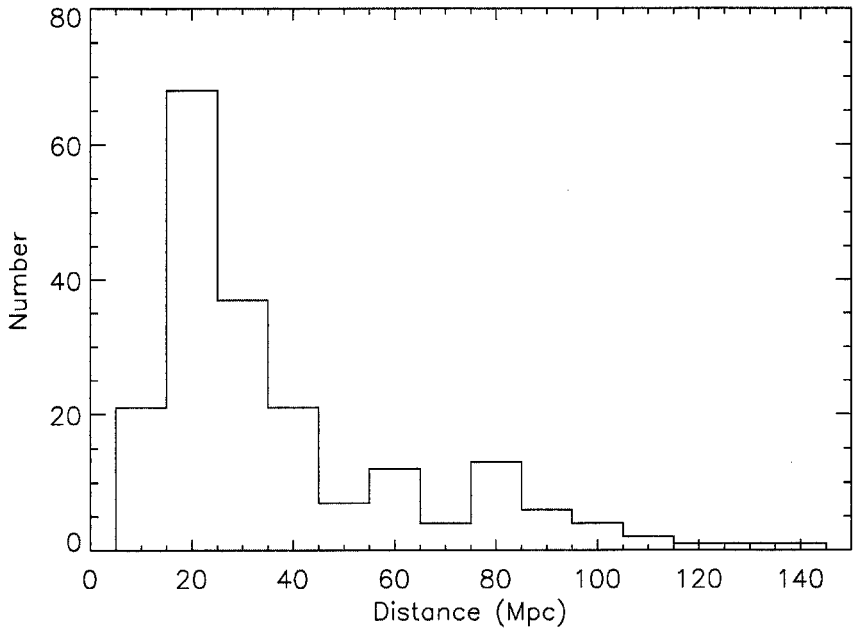

Figure 3.5 Distribution of derived distance (Mpc) for the HIPASS/SDSS galaxies.

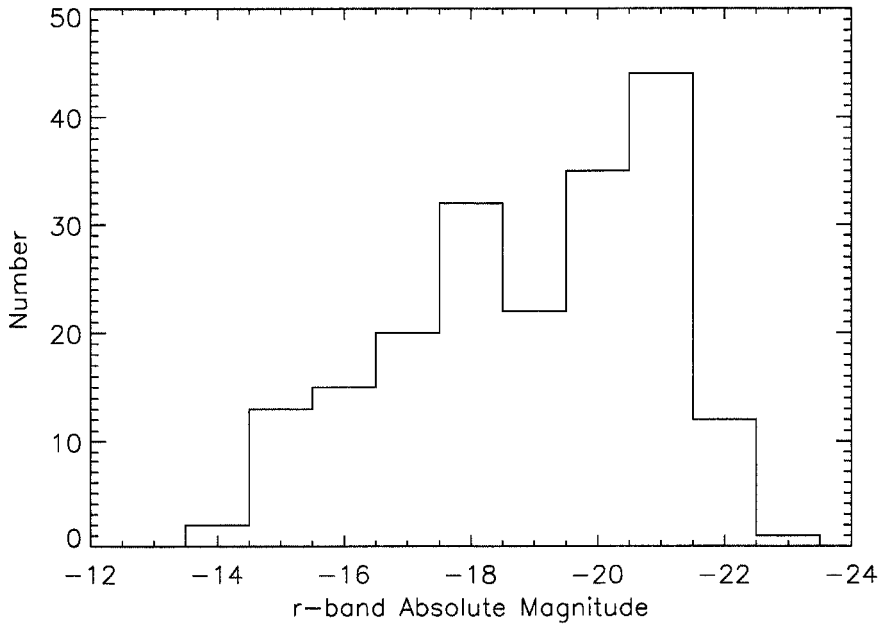

Figure 3.6 Distribution of r-band absolute magnitude for the HIPASS/SDSS galaxies.

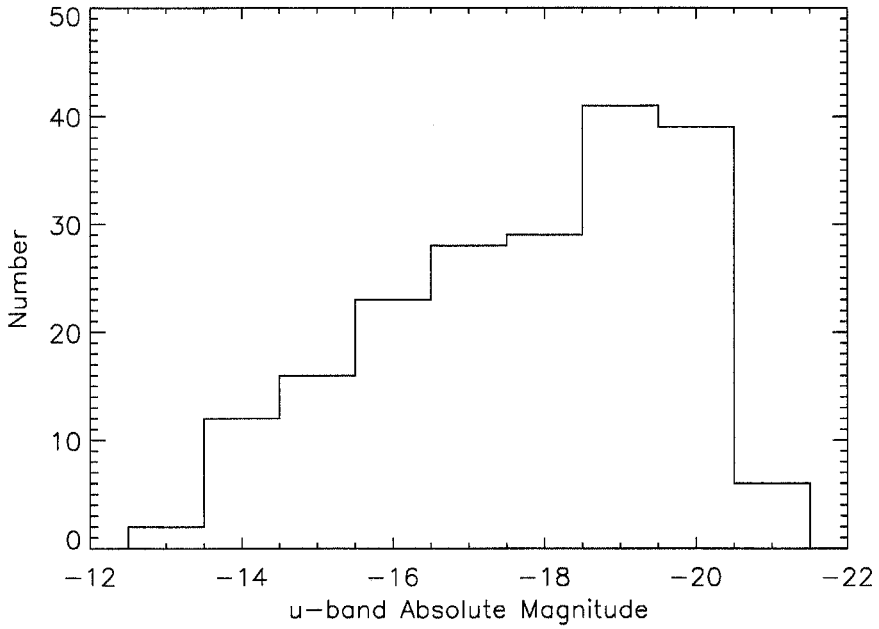

Figure 3.7 Distribution of u-band absolute magnitude for the HIPASS/SDSS galaxies.

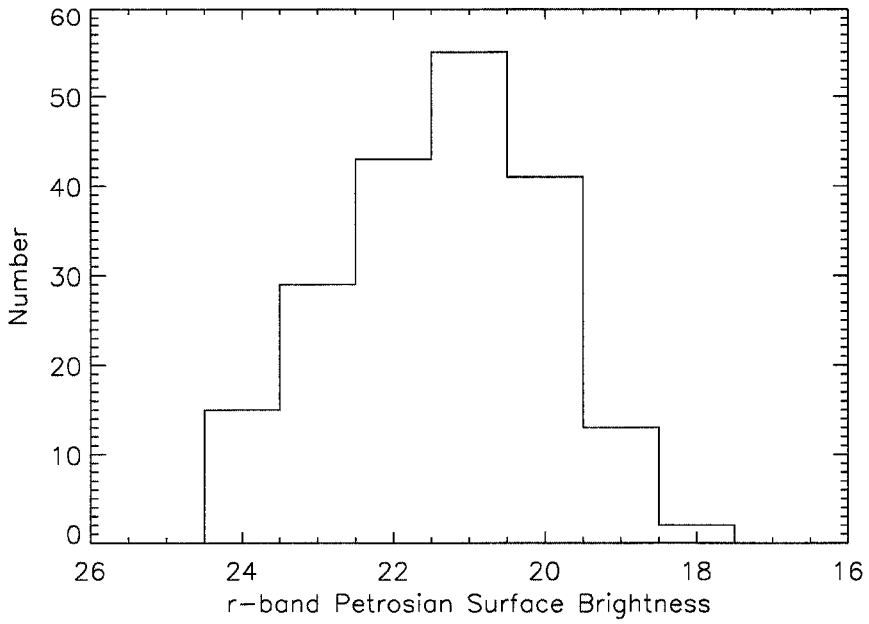

Figure 3.8 Distribution of Petrosian surface brightness for the HIPASS/SDSS sample.

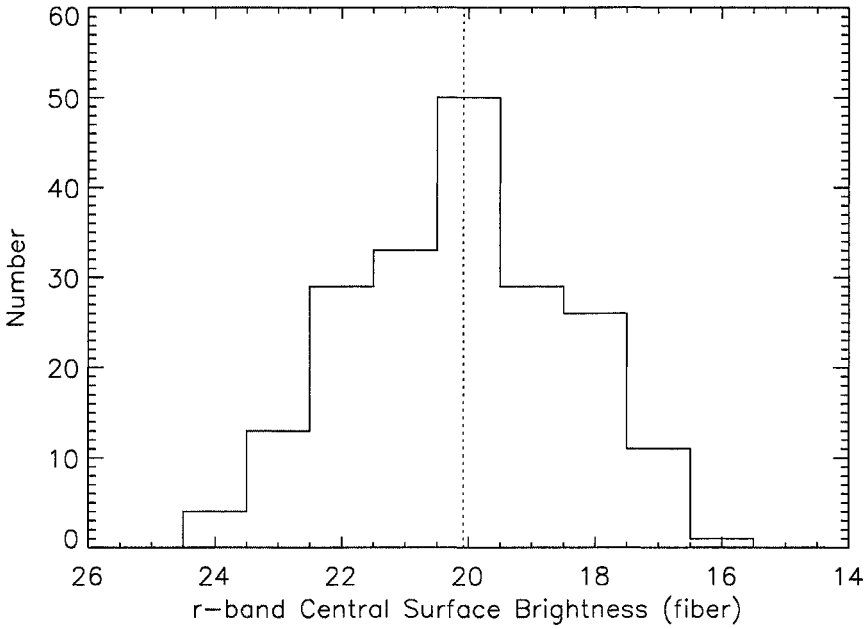

Figure 3.9 Fiber surface brightness (central) distribution for the HIPASS/SDSS galaxies. The dotted line is the peak of the Courteau (1996) distribution from an optically selected sample of galaxies. Although our selection methods are very different, the peak of our surface brightness distribution is very close to Courteau (1996) value.

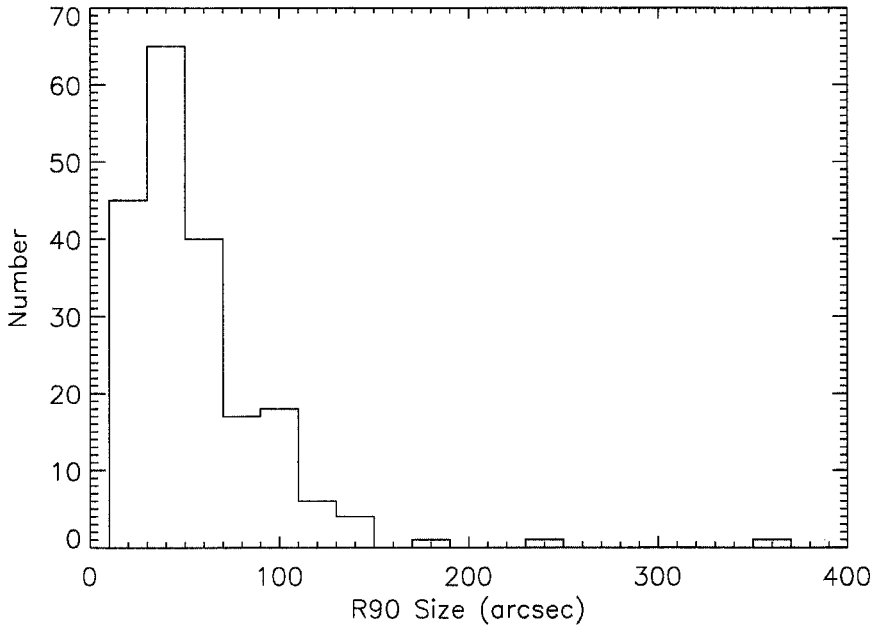

Figure 3.10 Distribution of R90 (arcsec) for all HIPASS/SDSS sample galaxies

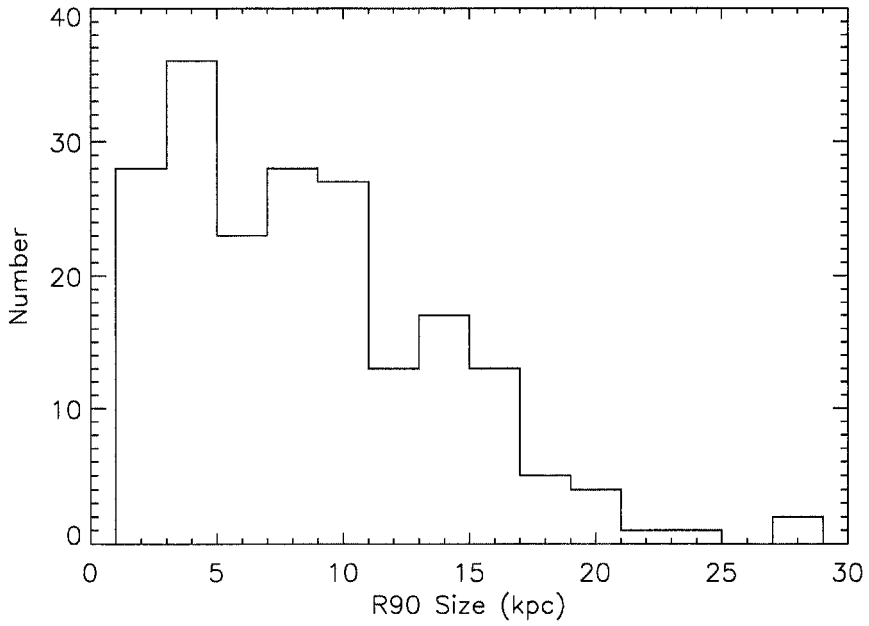

Figure 3.11 Derived size distribution (kpc) for the HIPASS/SDSS galaxies. Sizes were calculated based on the R90 values and the derived distances.

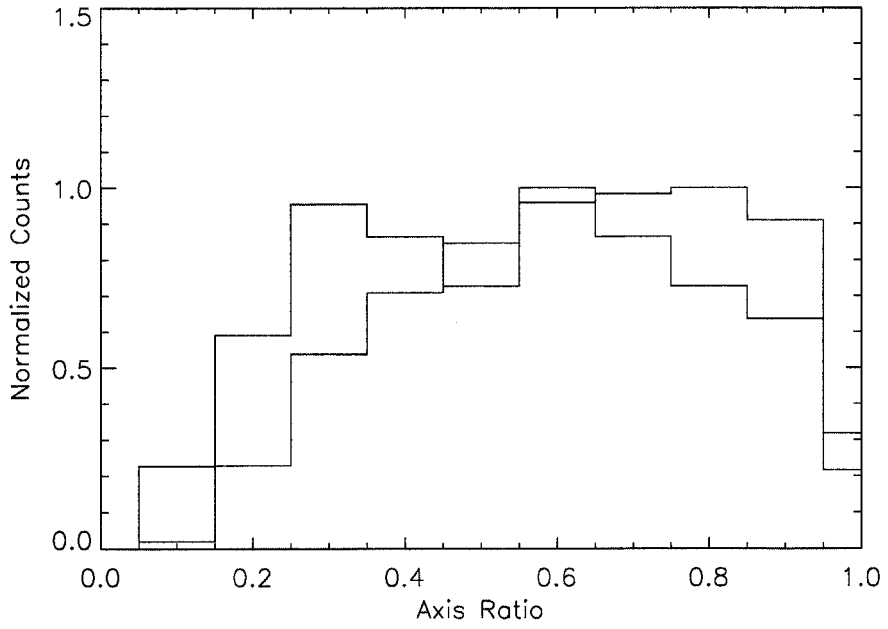

Figure 3.12 Distribution of axis ratios for the HIPASS/SDSS sample (black) and the SDSS DR4 main galaxy sample (red). The distributions are very similar to each other, although the DR4 sample may have a slightly higher fraction of systems at low inclinations. This is the opposite of what one might have expected from an HI selected sample. It does demonstrate that the inclination problems that are large for $b/a < 0.5$ (discussed in Appendix A) cannot be ignored.

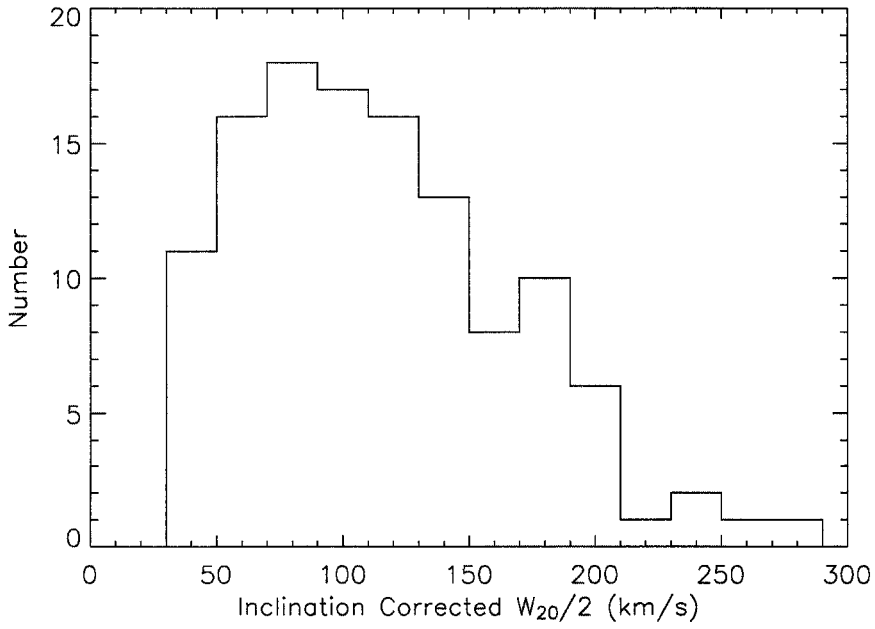

Figure 3.13 Distribution of inclination corrected W_{20} HI line profile widths. Inclinations are based on the Sérsic fit parameters. Galaxies without good ellipticity measures have been omitted from this figure.

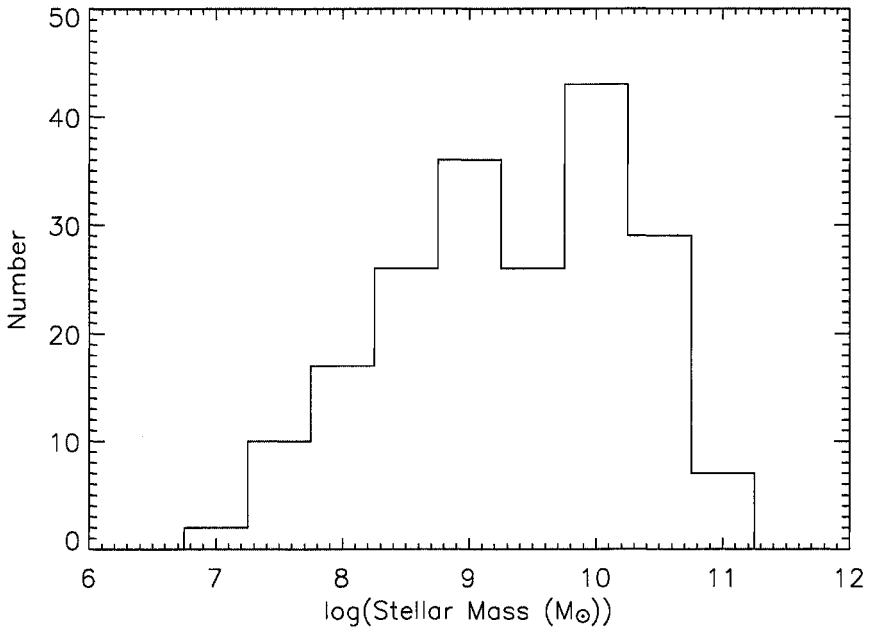

Figure 3.14 Stellar mass distribution of HI selected galaxies. Stellar mass is derived based on the $g-r$ colors, and i-band absolute magnitude based on the prescription of Bell et al. (2003).

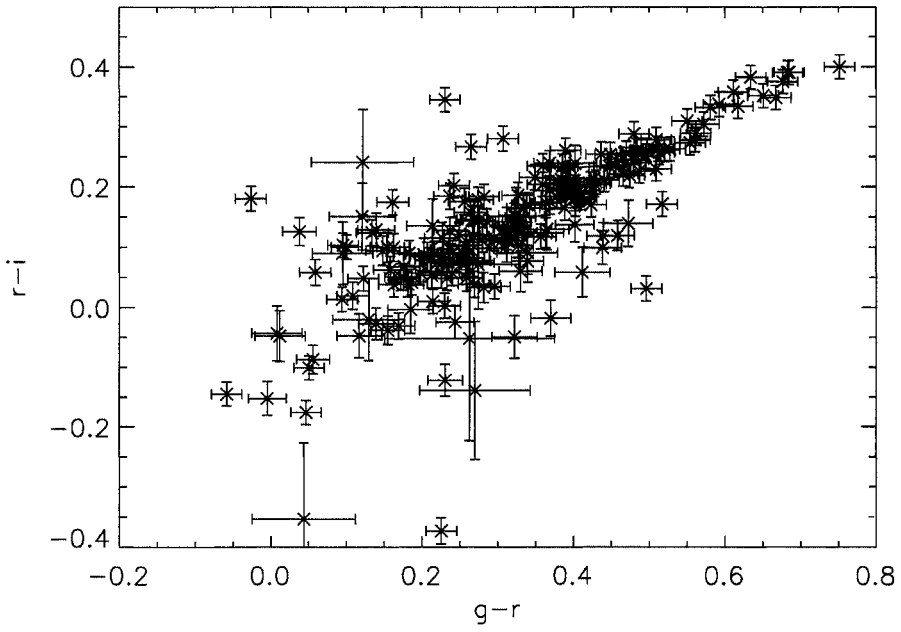

Figure 3.15 $r - i$ vs $g - r$ for HI selected galaxies. All photometric corrections have been applied to these data. Note that the sample galaxies lie on a well defined locus. The red galaxies, in particular have a very narrow distribution in color space. Chapter 5 will discuss this in detail.

HIPASS/SDSS sample and investigate the Tully Fisher relation and its scatter.

Chapter 4

COMPARING PROPERTIES OF GAS, STARS

4.1 Introduction

The combination of the SDSS and HIPASS data allows for a more complete census of the baryons in the nearby Universe. The galaxies in this sample span a wide range of morphological types and gas fractions and will ultimately be a useful database from which to compare simulations of galaxy formation and evolution. These data also give us the opportunity to observe the stars that have formed in a galaxy (optical colors) alongside the gas that may someday turn into stars. In this sense the union of HI and optical data serves to provide a more complete picture of the star formation histories of galaxies. By seeing how the gas content of galaxies changes as a function of stellar properties, we can gain a much deeper understanding for how stars form on the global scale of galaxies. In this chapter, we combine the the HIPASS data discussed in Chapter 2 with the SDSS photometry from Chapter 3 and investigate various trends between the HI and optical data. Can the HI characteristics of a galaxy predict its optical properties? Can the optical properties predict the gas content? Although previous studies have looked at how the HI properties correlate with the stellar population, few data sets have been drawn in a homogeneous and uniform way. The combination of HIPASS and SDSS therefore allows us to probe the gas/star correlations and explore the diverse mix of baryons in nearby galaxies with very little systematic error due to survey inhomogeneity.

In this chapter we first explore in §4.2 how the properties of galaxies change when an HI selection is applied by comparing my sample with a sample of SDSS selected galaxies.[1] Next, in §4.3, we investigate how the fraction of gas varies with the optical properties of

[1]Although the "reverse list" (see Chapter 2), when complete, will be the ideal data with which to study how an HI selected sample differs from an optically selected data set, an SDSS volume limited population (sans gas information) will have to suffice for this chapter.

galaxies and examine the reliability of using either the optical or HI data as a predictor of the other. In §4.4, we use the current global star formation rate to derive the HI mass enclosed in the optical aperture and show that the fraction of gas enclosed is a much better predictor of the optical properties than the total gas fraction. Lastly,in §4.4, we use an estimate of the HI diameter to calculate dynamical masses for the galaxies and compare the baryonic mass to the "total" mass for each galaxy.

It is important to note that for the remainder of this thesis, we will ignore the molecular contribution to the gas mass. Detailed studies of star formation tell us that the molecular phase is important for forming stars (Loren, Vanden Bout, & Davis 1973), and some previous work indicates that it may not be insignificant in some systems (Kennicutt 1989; Kennicutt 1998; Wong & Blitz 2002). However, the challenge of creating a large survey of CO (a common tracer of molecular gas) in galaxies (especially those with low surface brightness), prevents the inclusion of molecular gas in this study. If the neutral/molecular fraction varies significantly from galaxy to galaxy, this omission might explain some of the scatter in the presented relations.

4.2 HI Selection

As seen from the morphological types in Chapter 2, the HI selection identifies a high fraction of late-type galaxies. These are the systems historically known to have significant reservoirs of gas due to their lower star formation efficiencies, which slows the rate at which at which gas is converted into stars. Indeed, many of the latest types in the sample have baryonic components that are almost entirely HI, confirming that one of the qualities of the HI selection is the extraction of galaxies at the gas-rich extreme of the HI/star continuum as we will show in this section. In contrast, although the majority of the galaxies in my sample are late-types, a few have morphologies consistent with Sa, SO and E galaxies. These systems have larger star formation efficiencies that should have exhausted the entirety of their primordial gas supply by the present date. They are likely to have been selected by HIPASS because they have recently accreted gas (see Chapter 5).

Several of the galaxies in this sample are just above the SDSS detection limits and have

surface brightnesses too low to be targeted for spectra (Strauss et al. 2002). Therefore most SDSS studies of the nearby universe do not include these systems and thus to not sample the full range of baryonic properties. Because the photometry of SDSS also is much deeper than previous large surveys, the HI selection identifies faint galaxies in the nearby universe that were previously undetected. There are several "new" galaxies in the HIPASS/SDSS sample.

To quantify the amount of gas in a given galaxy, we define the gas fraction as:

$$f_{gas} = \frac{1.4M_{HI}}{1.4M_{HI} + M_{\star}} \tag{4.1}$$

where the factor of 1.4 accounts for the helium content of the gas and the HI and stellar masses are those derived in Chapters 2 and 3 respectively. The resulting gas fractions are given in Table 4.1.

Figure 4.1 shows the $u-r$ colors as a function of stellar mass for the HI selected sample (colored symbols) and a volume limited sample of galaxies (black dots) from the SDSS Data Release 4 (DR4). The HI selected data have been color coded according to their gas fraction. All photometric corrections have been applied to both data sets. The internal extinction for the DR4 galaxies was computed in the same manner as described in Chapter 3, using rotational velocities estimated from the Pizagno et al. (2005) Tully-Fisher relation. The bimodal galaxy population is easily seen in the DR4 data with a clear color division between the bulge and disk dominated systems.

Figure 4.1 clearly demonstrates that the HI selection identifies a very specific subset of galaxies and although it does manage to select many galaxies that would not otherwise be included, it does exclude most early type galaxies. The majority of the galaxies in the HIPASS/SDSS sample have $u-r < 2.2$ and fall in the blue "disk dominated" color regime described by Strateva et al. (2001). Any results using this HI selected sample will need to address that it is a specific subset of a larger galaxy population. We see that the HI selection also probes a population of low stellar mass galaxies that are missing from the SDSS spectroscopic sample. All of these galaxies have extremely high gas fractions and several of them are at the limit of SDSS detectability. The gas fraction also seems to trace

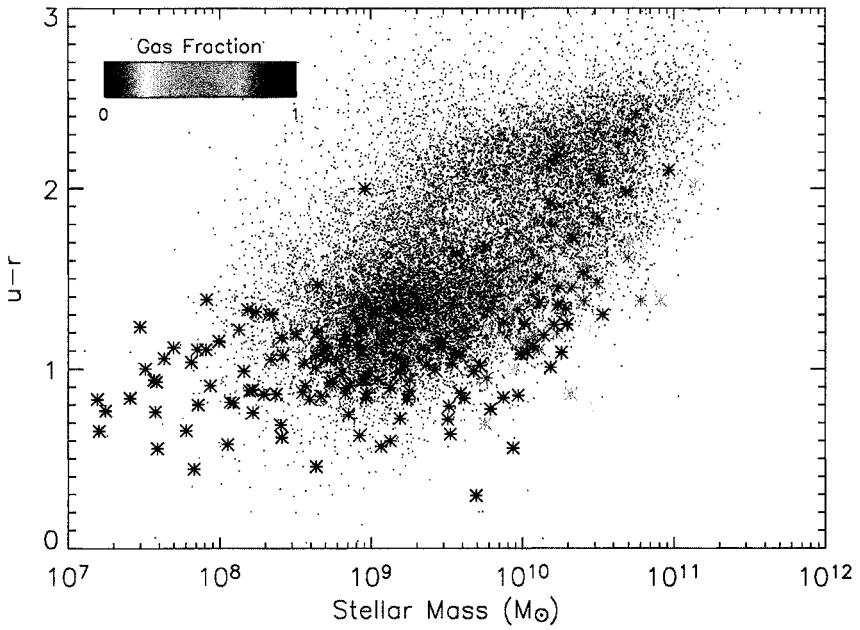

Figure 4.1 $u-r$ color as a function of stellar mass. HI selected galaxies have been color coded according to their gas fraction. The black dots are a volume limited sample from SDSS DR4. All photometric corrections have been applied to the data. The HI selected galaxies are slightly bluer and extend to lower stellar masses than many of their SDSS counterparts.

stellar mass, with the lower gas fractions corresponding to larger stellar masses.

Figure 4.1 also indicates that the HI selected galaxies are slightly bluer than many of their SDSS counterparts. This offset is likely to be due to elevated HI densities (1) making them easier to detect in HI and (2) inducing higher star formation rates, elevating the u-band flux. We will explore this potential offset in more detail in chapter 5.

Another classic way of looking at the HI content of a galaxy is by looking at the mass in HI (M_{HI}) as compared to the optical luminosity L_g. Galaxies that are dominated by gas will have a higher fraction of their mass in HI compared to their optical luminosity. Figure 4.2 shows the ratio M_{HI}/L_g as a function of central i-band surface brightness for the HIPASS/SDSS sample. 123 or 62% of the galaxies in the sample have $M_{HI}/L_g > 1$ and the mean of the sample is 1.72. These are very comparable to the M_{HI}/L_B mean of 1.5

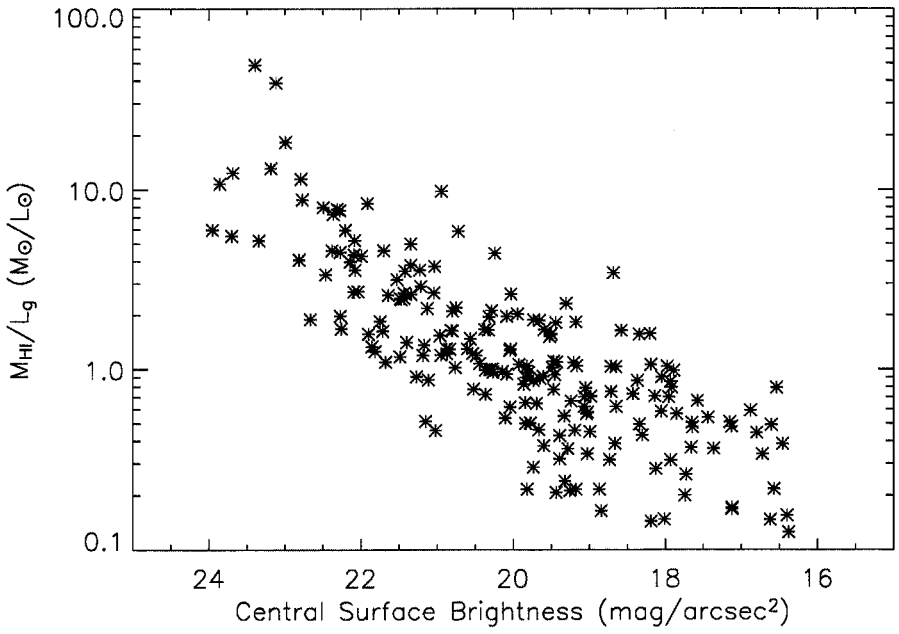

Figure 4.2 M_{HI}/L_g as a function of central i-band surface brightness. 62% of the galaxies in the sample have $M_{HI}/L_g > 1$ and the mean of the sample is 1.72.

found in the late-type dwarf sample of Swaters et al. (2002). However, the HIPASS/SDSS sample contains more early type spirals than the Swaters sample and yet has slightly higher mean M_{HI}/L_g. This would indicate that the HI selection in the HIPASS/SDSS sample is not only selecting a large number of blue, late-type galaxies, often not included in other surveys, but that the early-type galaxies that it does select are more gas rich than their optically selected morphological counterparts. The trend in Figure 4.2 also may indicate a trend in star formation efficiency. If the lower surface brightness disks are low surface density systems, then they may have lower star formation rates. Figure 4.3 suggests that this may be the case.

4.3 Gas Fraction Trends

To determine how well the gas content of a galaxy predicts its stellar properties, we compare the gas fractions for the HI selected sample with several optical quantities. We find trends

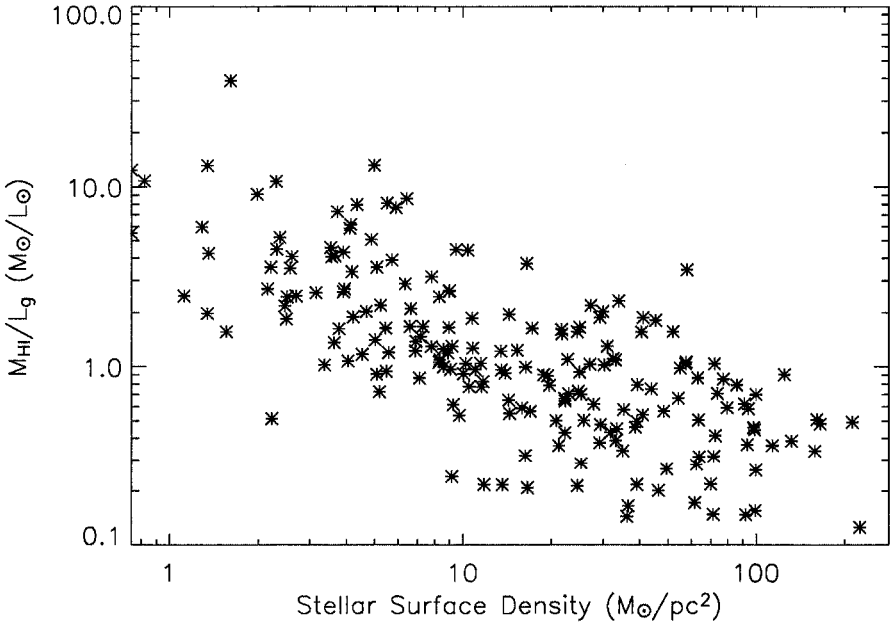

Figure 4.3 M_{HI}/L_g as a function of stellar surface density. If the lower surface brightness disks are low surface density systems, then they may have lower star formation rates and lower M_{HI}/L_g as seen in Figure 4.2.

in the gas fraction with color, absolute magnitude and surface brightness (Figures 4.4-4.6). Although clear trends exist in all three relations, the trend of central surface brightness with gas fraction is the tightest. This is consistent with the results of several past studies including McGaugh & de Blok (1997) and Burkholder, Impey & Sprayberry (2001). All of the relations have significant scatter but clearly show that galaxies with low surface brightnesses, blue colors and large absolute magnitudes have large fractions of their baryonic mass in gas. Figure 4.7 shows the gas fraction versus central surface brightness relation with *gri* composite HIPASS/SDSS sample galaxies as the data symbols. The morphology and color trends with gas fraction are clearly observable in addition to the striking range of surface brightnesses in the HIPASS/SDSS sample.

How well do the gas fractions predict the optical properties? We fit the gas fraction-surface brightness trend with an arctan function and obtain the relation:

$$f_{gas} = 0.52 \arctan(0.28\mu_{0,i} - 5.39) + .49. \tag{4.2}$$

The scatter is large and certainly speaks to the complexity in the gas/star relationship. The mean relation, however, demonstrates that it is possible to approximate the optical properties of a galaxy from just the gas fraction information. The "Universal Rotation Curve" function from Courteau (1997) may prove to be a better function with which to fit this relation and will be explored in the future.

The gas fraction vs. M_i relation (Figure 4.5) reveals a possible turnover at M_i=-21. This could be related to the mass-metallicity turnover seen by Garnett (2002) and Tremonti et al. (2004).

Recent studies have used the optical properties of galaxies to predict their gas fractions (Kannappan 2004). As discussed above, many of the HI selected galaxies appear to have different optical properties than their volume limited SDSS counterparts (see Figure 4.1). This difference is also seen in Figure 4.8, where at the low gas fraction end of the galaxy distribution (red symbols), the HI selected galaxies trace the edge of the distribution defined by the optically selected galaxy distribution. This offset suggests that using the optical properties of galaxies to obtain their gas content is not necessarily a sound technique. For

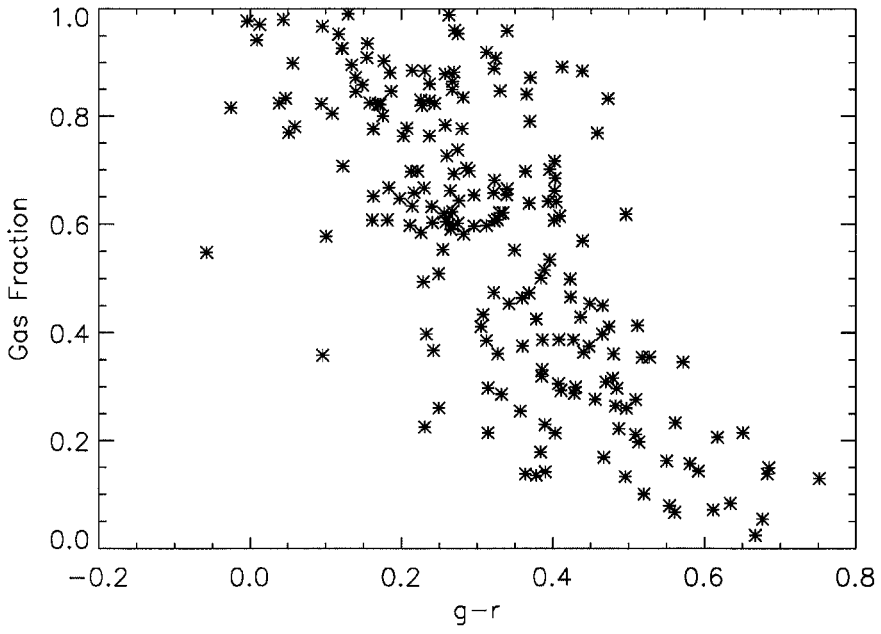

Figure 4.4 Gas fraction as a function of $g - r$ color. Bluer galaxies tend to have higher gas fractions but there is considerable spread in this relation.

very blue galaxies, which have retained much of their primordial gas, this technique is likely acceptable, but as the galaxies get redder, the HI selected galaxies separate from the main galaxy locus. We conclude that galaxies with gas information can predict the colors of galaxies within some scatter but that the reverse is only true for the bluest of systems.

4.4 Deriving HI Surface Density and Radius

The location of the gas within a galactic disk is important for understanding the evolution and formation mechanisms of the galaxy. There is ample evidence that the HI in galactic disks extends well beyond the optical radii (Cayatte et al. 1994; Hunter, Elmegreen & Baker 1998, Swaters et al. 2002; Begum, Chengalur & Karachentsev 2005). Unfortunately, all of the galaxies in the HIPASS/SDSS sample are unresolved by the HIPASS beam, thus constraining only total HI mass without giving any information about the spatial extent of the gas. HI synthesis observations would provide better constraints on how the gas is

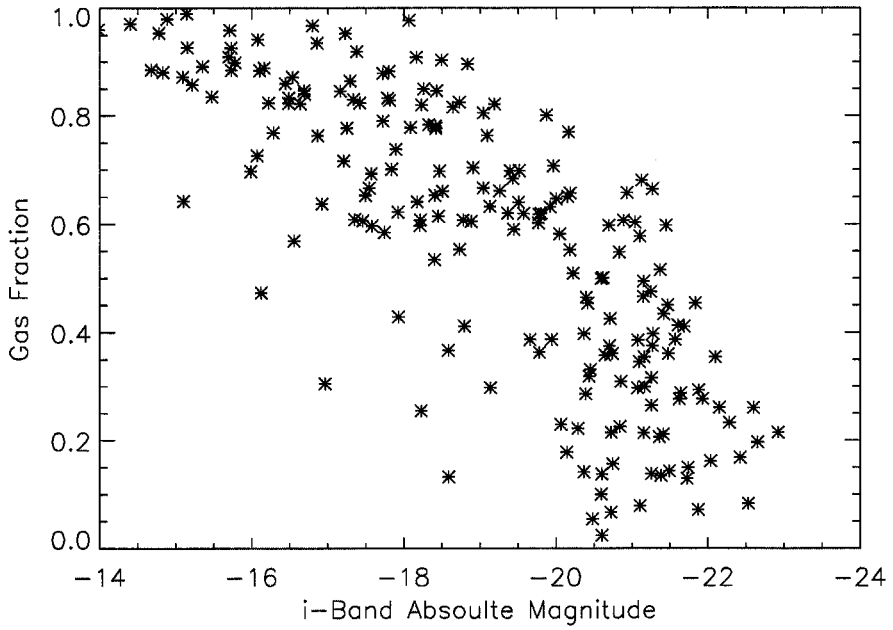

Figure 4.5 Gas fraction as a function of i-band magnitude. Intrinsically fainter galaxies have higher gas fractions. Although the scatter is large, there is evidence for a turnover in the relation around M_i = -21. This may be related to the mass metallicity relation seen by Garnett (2002) and Tremonti et al. (2004).

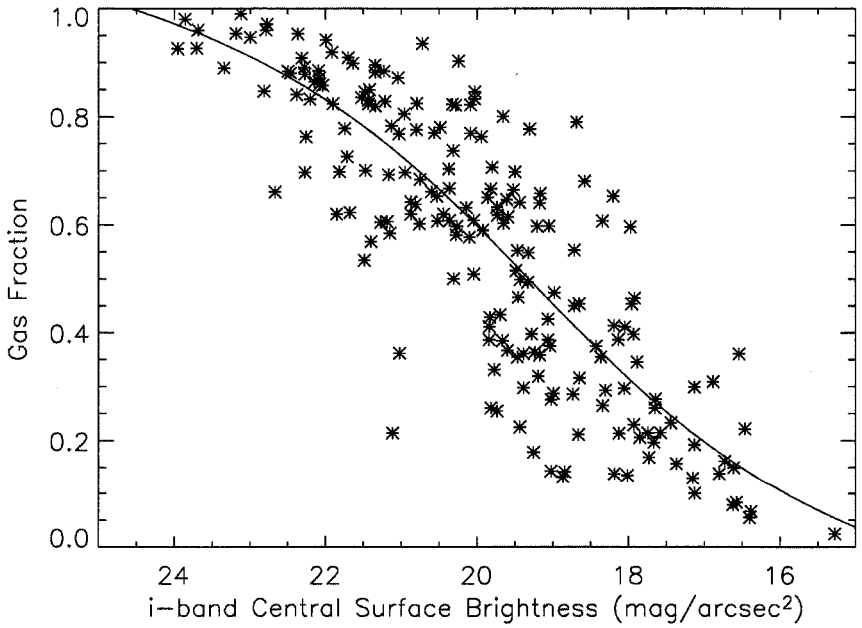

Figure 4.6 Gas fraction as a function of i-band central surface brightness. Red line is a linear fit to this relation. This is the tightest of all of the gas fraction correlations and demonstrates the ability to estimate optical properties from the gas content of galaxies. The fit relation is given in Equation 4.2.

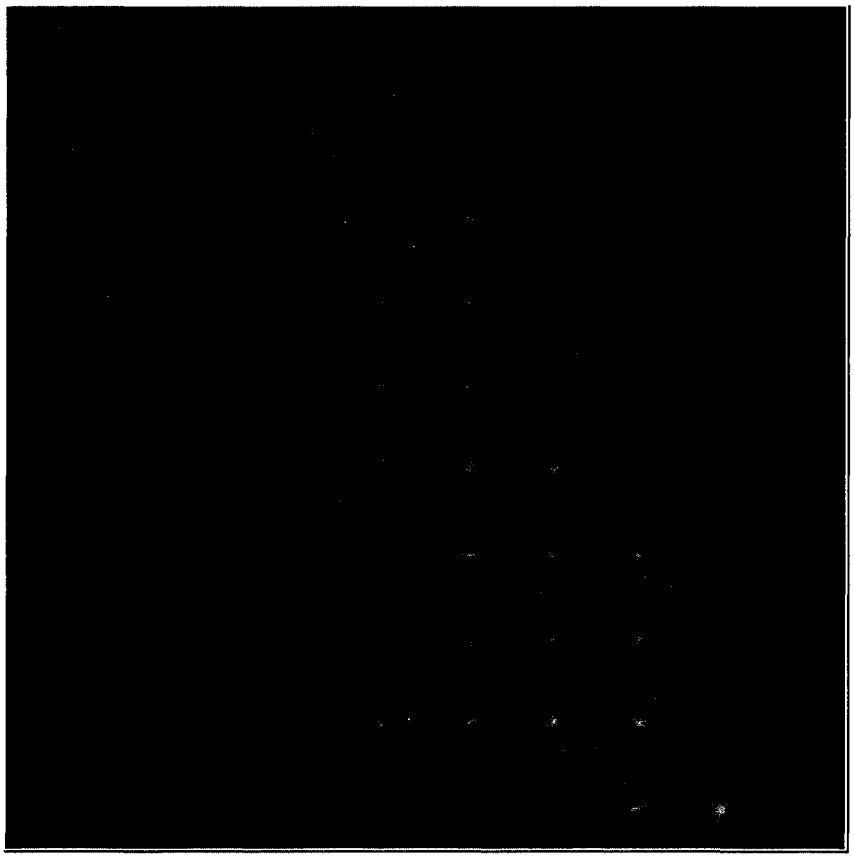

Figure 4.7 HI gas fraction versus i-band central surface brightness relation with gri composite HIPASS/SDSS sample galaxies as the data symbols.

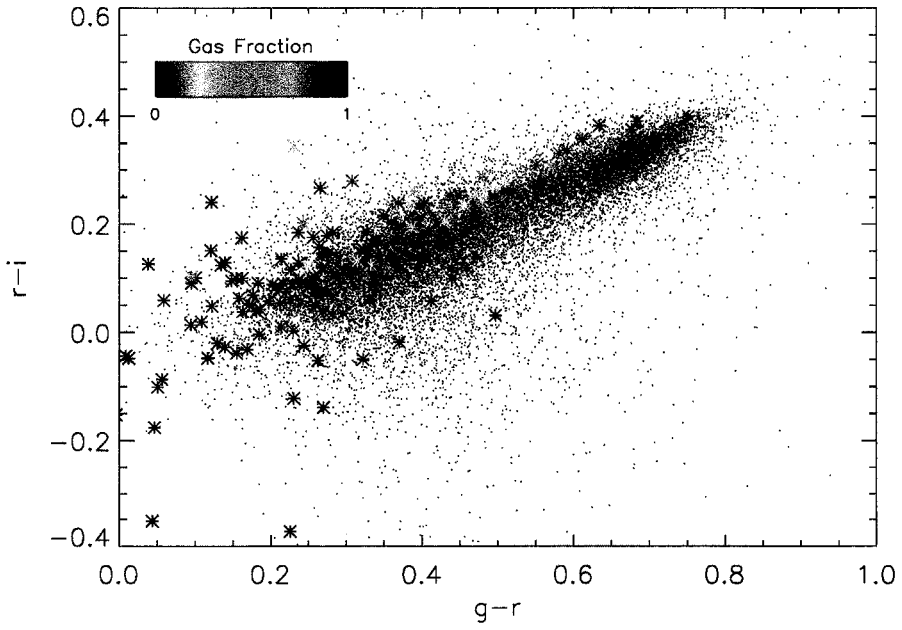

Figure 4.8 $r - i$ vs $g - r$ for HI selected galaxies (colored symbols) plotted with a volume selected sample of galaxies from SDSS (black dots). All photometric corrections have been applied to these data. Galaxies in the HIPASS/SDSS sample have been color coded according to their gas fractions. Note that the HI selected sample appears to have colors that are shifted off of the SDSS galaxy locus and extend to very blue colors.

distributed, but synthesis data are not available for these sources at this time. Although the HIPASS/SDSS data cannot directly probe the HI extent or distribution, some clever tricks can yield significant information about the HI distribution in the HIPASS/SDSS sample galaxies.

We have devised a method for estimating the HI mass inside of the optical radius. This quantity will allow me to examine how concentrated the HI gas is and how this concentration varies with other physical properties. Kennicutt (1998) demonstrates empirically that the SFR density relates to the gas surface density by the equation:

$$\Sigma_{SFR} = 2.5 \times 10^{-4} \left(\frac{\Sigma gas}{1 M_{\odot} pc^{-2}} \right)^{1.4} \mathrm{M_{\odot} yr^{-1} kpc^{-2}}. \tag{4.3}$$

We can estimate the SFR from the u-band luminosity as described by Hopkins et al. (2003) using the relation:

$$SFR_u(\mathrm{M_{\odot} yr^{-1}}) = \left(\frac{10^{-0.4(M_u - 34.10)}}{1.81 \times 10^{21}} \right)^{1.186} \tag{4.4}$$

where the u-band SFR has a one-to-one correlation with the SFR derived from the Hα line luminosity. We use the physical R90 size of the galaxy to determine the physical area of the galaxy and subsequently the average SFR surface density. The HI mass inside the R90 radius is then calculated to be:

$$M_{HI}(r < R_{90}) = (\Sigma_{SFR} \cdot 4 \times 10^9)^{0.714} \pi R_{90}^2 \ (M_{\odot}). \tag{4.5}$$

where the SFR density is in units of $\mathrm{M_{\odot}}/yr/kpc^2$ and R90 is in units of pc. This resulting optically-enclosed HI mass is found in Table 4.1

Figure 4.9 shows the gas fraction of galaxies as a function of enclosed HI mass ratio ($\mathrm{M_{HI}(r< R90)/M_{HI,total}}$). There are two important features of this plot. First, the range of enclosed HI mass ratios is quite large. There are systems whose total HI content is almost entirely found within the optical disk. In contrast, some of the galaxies in the sample have only a few percent of their HI mass within their optical radius. This is consistent with recent observations of a giant HI disk surrounding a dwarf galaxy (Carignan & Beaulieu 1989; Meurer et al. 1996; Begum et al. 2005).

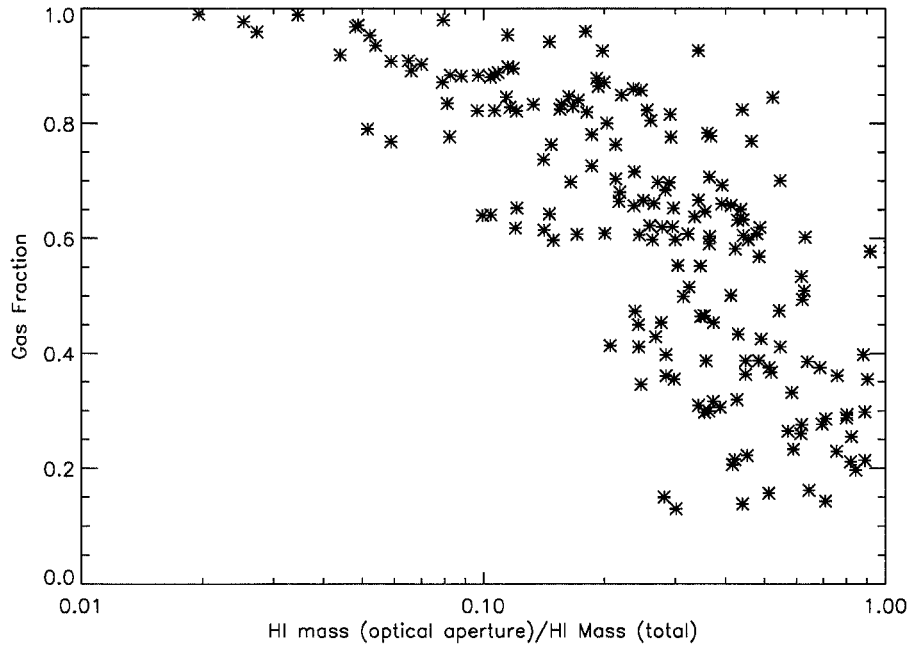

Figure 4.9 Gas fraction as a function of optical to total HI mass fraction. Galaxies with high gas fractions have only small amounts of HI within their optical radii. Galaxies with small gas fractions have almost all of their HI contained in the optical radius.

The second relation of note is the trend with gas fraction. Systems that have their baryonic component dominated by HI have a very small fraction of their HI contained within the optical radius whereas the galaxies with small gas fractions have HI extents that do not go much beyond the optical confines. This suggests that part of the reason for the high gas fractions are not solely inefficiency at turning gas into stars within the optical radius, but the existence of a large untapped reservoir of HI at large radii. Because gas infall may play a significant role in the gas content and subsequent star formation for many of these galaxies, some of the scatter may be caused by infall occurring at large radii in the baryonic disks.

Because many of the HIPASS/SDSS sample galaxies have a large amount of their HI outside of the optical radius, the total HI mass gas fraction is not a good indicator of star formation efficiency within the optical radius. Instead, using the optically-enclosed HI mass, we derive an optically-enclosed gas fraction and use this gas fraction to explain some

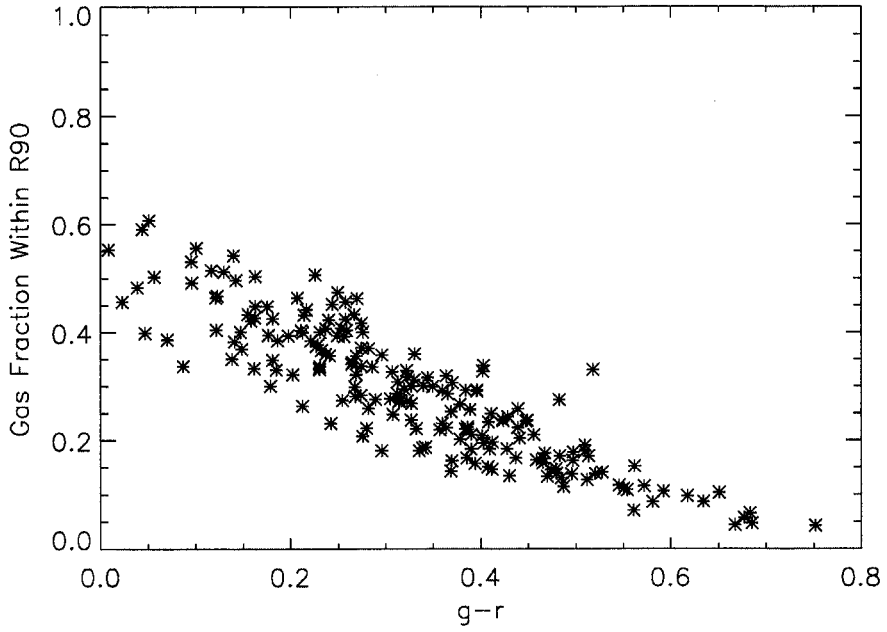

Figure 4.10 Optically-enclosed gas fraction as a function of $g-r$ color. The optically-enclosed gas fraction correlates much more strongly with color than the total mass gas fraction.

of scatter in Figure 4.4. Figure 4.10 plots the optically-enclosed gas fraction as a function of the $g-r$ color. This figure demonstrates that the optically-enclosed gas fraction strongly correlates with the color of the galaxy and is a good measure of the star formation efficiency within the optical radius. In fact, the scatter in 4.10 can be explained by the color and therefore the ability to form stars inside the optical radius. Figure 4.11 again plots the total mass gas fraction as a function of the optically-enclosed HI ratio with the symbols colored according to their $g-r$ color. At a given gas fraction, blue galaxies have lower star formation efficiencies because more of their gas is within the optical radius and yet they can't convert it to stars, whereas red galaxies at the same gas fraction can convert their interior gas into stars but have a reservoir of gas a large radii.

The optically-enclosed HI mass fraction gives us insight into the how the HI mass is distributed in galaxies but does limit the total radial extent of the HI. To constrain the HI radius (R_HI), we use the results of Swaters et al. (2002), who show that the HI radius

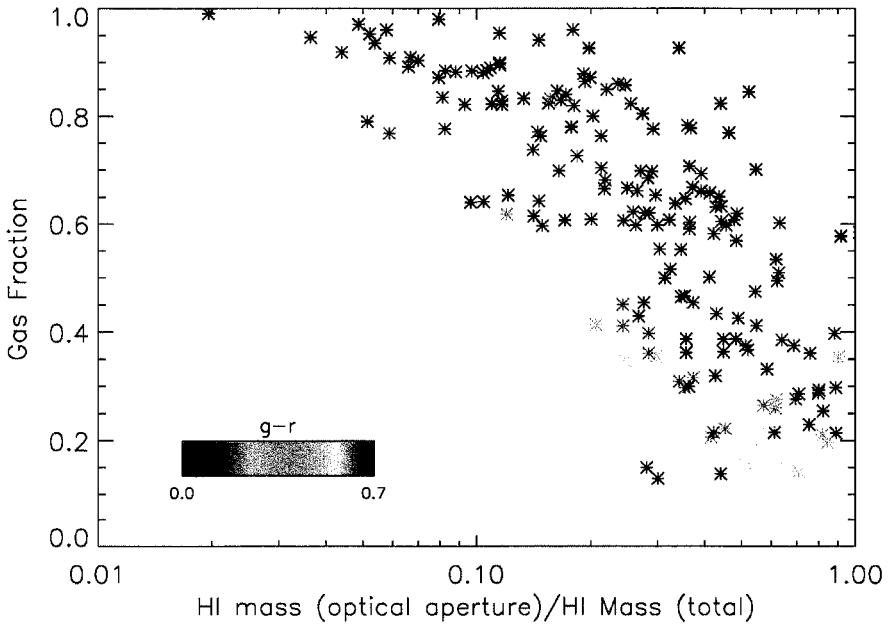

Figure 4.11 Gas fraction as a function of the optically-enclosed HI ratio. Symbols have been colored according to their $g-r$ color. At a given gas fraction, blue galaxies have lower star formation efficiencies because more of their gas is within the optical radius and yet they can't convert it to stars, whereas red galaxies at the same gas fraction can convert their interior gas into stars but have a reservoir of gas a large radii.

(defined to be where the HI surface density drops below 1 $M_{\odot}/pc^2$) is tightly correlated with the total HI mass. Swaters et al. (2002) give the HI diameter as:

$$D_{HI}(kpc) = 10^{(\log(M_{HI})-6.6)/1.86} \tag{4.6}$$

where M_{HI} is in solar units. This relation was derived from a sample of low mass, late-type disks comparable to the majority of the galaxies in our sample. However, it may not be an appropriate relation for some of the earlier morphology types int the HIPASS/SDSS sample. The values of D_{HI} ($2R_{HI}$) calculated from this relation can be found in Table 4.1.

Figure 4.12 shows the distribution of the R_{HI}/r_{25} ratio. We adopt the isophotal optical radius (r_{25}; see Chapter 3) to conform with the surface density limited HI radius. The peak of the HIPASS/SDSS sample is at 1.5, whereas the Swaters (2002) sample peaks around 3. A significant amount of the sample has an HI envelope that extends to more than twice the optical radius. Several of the HIPASS/SDSS galaxies have previous HI synthesis observations that yield robust HI radii. Our derived values are consistent with the few HI radii found in NED.

Figure 4.13 shows the R_{HI}/r_{25} ratio as a function of the enclosed to total HI mass ratio. As expected, these two variables are tightly correlated. Galaxies with large HI extent have only a small amount of their HI within the optical radius

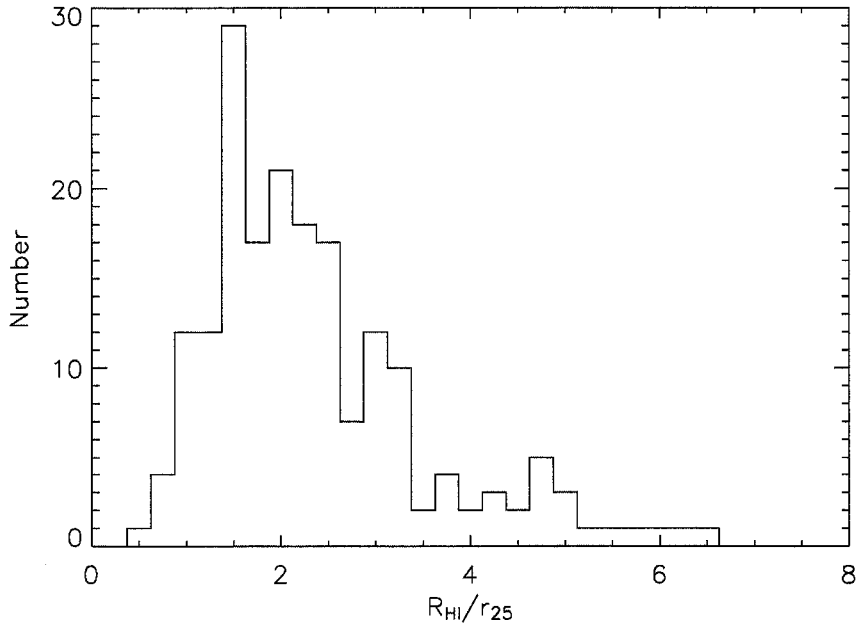

Figure 4.12 The distribution of the R_{HI}/r_{25} ratio. The peak of the HIPASS/SDSS sample is at 1.5, whereas the Swaters (2002) sample peaks around 3. A significant amount of the sample has an HI envelope that extends to more than twice the optical radius.

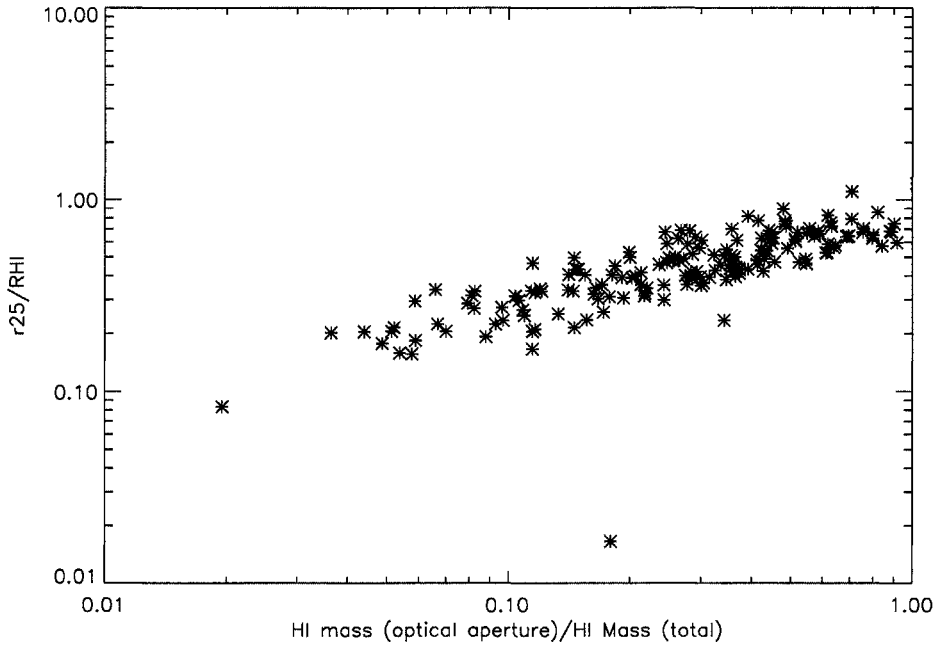

Figure 4.13 The R_{HI}/r_{25} ratio as a function of the enclosed to total HI mass ratio. As expected, these two variables are tightly correlated. This tight correlation gives further credence to our HI parameter approximations.

Table 4.1. Properties Derived from Gas Information

HIPASS Name	Gas Fraction	M_{HI}/L_g	HI Enclosed ($10^9 M_\odot$)	HI Diameter (kpc)	Dynamical Mass[a] ($10^{10} M_\odot$)
HIPEQ0014-00	0.658	0.746	5.33	77.17	45.73
HIPEQ0027-01a	0.632	0.691	2.04	45.20	14.90
HIPEQ0033-01	0.882	3.562	0.28	36.23	6.79
HIPEQ0043-00	0.387	0.506	4.11	72.54	61.89
HIPEQ0051-00	0.790	2.461	0.09	26.77	6.11
HIPEQ0058+00	0.316	0.443	2.62	55.67	...
HIPEQ0107+01	0.642	0.871	0.01	4.46	...
HIPEQ0119+00	0.919	5.995	0.16	38.50	2.22
HIPEQ0120-00	0.606	0.852	0.13	13.81	1.48
HIPEQ0122+00	0.578	0.383	7.78	61.67	25.83
HIPEQ0123-00	0.288	0.322	6.31	59.30	...
HIPEQ0126+00a	0.908	5.567	0.38	53.30	5.11
HIPEQ0126-00b	0.822	1.400	0.05	14.13	1.44
HIPEQ0154-00	0.129	0.363	1.80	50.98	...
HIPEQ0222-00	0.692	0.971	0.30	16.91	2.00
HIPEQ0228-01	0.387	0.443	0.83	27.09	...
HIPEQ0230-01	0.067	0.089	0.84	17.11	12.72
HIPEQ0231+00	0.657	1.053	1.89	59.62	8.71
HIPEQ0236+00	0.515	0.729	4.87	83.69	46.12
HIPEQ0238+00	0.968	8.194	0.17	38.61	7.67
HIPEQ0240+01	0.927	3.939	0.12	11.06	0.36
HIPEQ0241+00	0.211	0.277	4.08	46.30	44.15
HIPEQ0244+00	0.534	0.835	0.67	20.33	0.63
HIPEQ0246-00a	0.293	0.308	7.79	66.29	47.55
HIPEQ0246-00b	0.214	0.201	2.88	36.71	...
HIPEQ0249-00	0.265	0.354	3.16	48.89	10.23
HIPEQ0249-00a	0.953	5.210	0.20	39.70	5.32
HIPEQ0249-00b	0.260	0.361	11.65	94.85	74.47
HIPEQ0251-01	0.879	3.205	0.53	33.72	2.36
HIPEQ0300+00	0.825	1.502	0.58	39.52	10.94
HIPEQ0301-00	0.776	1.161	0.61	28.94	2.88
HIPEQ0306-00	0.150	0.351	1.76	52.33	...
HIPEQ0316-00	0.143	0.242	2.80	40.81	1.42
HIPEQ0320-06	0.454	0.499	1.24	43.61	17.15
HIPEQ0351-00	0.411	0.645	3.79	85.36	11.00
HIPEQ0809+00	0.411	0.358	0.43	17.15	3.51
HIPEQ0821+03b	0.297	0.417	1.95	48.74	32.53
HIPEQ0821-00	0.935	4.184	0.11	28.69	1.09
HIPEQ0822-00	0.425	0.500	2.74	49.23	6.17
HIPEQ0825-00	0.197	0.262	12.08	81.67	118.60
HIPEQ0855+02	0.602	0.729	2.47	40.60	5.14
HIPEQ0856+00	0.590	0.758	0.99	33.38	...
HIPEQ0923-00	0.706	0.684	2.01	48.83	17.02
HIPEQ0930+04	0.354	0.551	7.43	60.65	2.03
HIPEQ0936+01	0.977	7.012	0.34	78.57	36.20
HIPEQ0942+00	0.397	0.608	2.82	67.04	...
HIPEQ0944-00b	0.884	2.547	0.04	12.64	1.65
HIPEQ0945+01	0.398	0.259	2.40	33.46	14.24
HIPEQ0946+02	0.783	1.554	0.87	31.25	6.07
HIPEQ0947+00a	0.703	1.181	0.61	34.26	10.36
HIPEQ0947+00b	0.823	1.763	0.34	22.59	2.24
HIPEQ0953+01	0.548	0.171	8.13	42.76	26.32
HIPEQ0954+01a	0.989	34.852	0.04	19.79	...
HIPEQ0954+02a	0.434	0.461	4.13	65.82	...
HIPEQ0955+04a	0.214	0.143	2.51	27.09	9.49
HIPEQ0958+01	0.980	7.716	0.07	18.55	1.84
HIPEQ1000+03	0.464	0.566	1.64	45.00	35.96
HIPEQ1010+05	0.640	1.305	0.47	44.76	6.86
HIPEQ1014+03	0.071	0.120	3.52	33.12	12.53

Table 4.1—Continued

HIPASS Name	Gas Fraction	M_{HI}/L_g	HI Enclosed ($10^9 M_\odot$)	HI Diameter (kpc)	Dynamical Mass[a] ($10^{10} M_\odot$)
HIPEQ1015+02	0.846	1.763	0.52	19.45	2.66
HIPEQ1026+03	0.646	0.652	1.79	46.51	19.78
HIPEQ1028+03	0.824	1.119	0.13	10.07	0.71
HIPEQ1031+04	0.816	0.922	0.65	30.13	5.65
HIPEQ1039+01	0.473	0.622	0.02	5.62	···
HIPEQ1041+00	0.501	0.709	2.90	55.72	···
HIPEQ1046+01	0.633	0.617	0.97	29.82	9.39
HIPEQ1050+01	0.892	5.480	0.03	13.22	1.29
HIPEQ1051+04a	0.653	0.874	0.19	15.22	2.46
HIPEQ1052+00	0.777	1.656	0.07	18.46	1.20
HIPEQ1053+02	0.909	3.270	0.03	13.22	0.71
HIPEQ1055+02	0.872	1.897	0.01	7.85	0.42
HIPEQ1101+03	0.358	0.154	3.92	30.24	16.33
HIPEQ1109-00	0.607	1.115	2.45	81.70	64.05
HIPEQ1110+01	0.835	2.255	0.02	9.42	0.29
HIPEQ1113+05	0.607	0.553	0.42	22.36	1.92
HIPEQ1117+04a	0.222	0.275	0.82	26.88	46.25
HIPEQ1119+02	0.896	2.710	0.85	56.21	25.10
HIPEQ1124+03	0.667	0.705	0.76	29.92	2.13
HIPEQ1127-01	0.638	1.169	0.14	11.98	···
HIPEQ1131-02	0.454	0.736	7.53	98.19	···
HIPEQ1133-03	0.828	2.060	0.22	27.76	4.40
HIPEQ1136+00	0.823	1.178	0.04	12.12	0.69
HIPEQ1138+03	0.345	0.701	2.06	61.06	···
HIPEQ1143-01	0.954	9.394	0.06	14.16	0.54
HIPEQ1145+02	0.960	8.865	0.05	10.31	0.08
HIPEQ1148-02	0.763	1.447	0.89	41.98	18.15
HIPEQ1151-02	0.698	1.117	0.81	45.78	17.44
HIPEQ1152+01	0.475	0.504	5.41	67.08	12.99
HIPEQ1152-02	0.833	0.927	0.05	11.99	0.33
HIPEQ1152-03b	0.622	0.780	0.20	16.97	0.74
HIPEQ1155+01	0.387	0.465	1.21	31.91	10.02
HIPEQ1200-00	0.700	1.744	0.72	22.56	0.61
HIPEQ1200-01	0.162	0.242	4.45	55.10	···
HIPEQ1202+01	0.138	0.317	1.61	39.16	···
HIPEQ1204-01	0.847	2.907	0.15	18.91	···
HIPEQ1204-02	0.206	0.404	2.38	49.78	···
HIPEQ1210+02	0.841	3.270	0.17	19.21	···
HIPEQ1215+04a	0.597	0.687	0.24	18.52	0.93
HIPEQ1216-03	0.499	0.782	2.32	57.13	···
HIPEQ1218+00	0.884	5.691	0.09	18.94	0.64
HIPEQ1218-01	0.450	0.739	3.58	82.87	66.10
HIPEQ1219+03	0.255	0.205	0.21	9.33	···
HIPEQ1220+00	0.858	1.929	0.05	7.90	0.24
HIPEQ1220+01	0.608	0.518	0.38	17.33	3.35
HIPEQ1221+03	0.375	0.520	2.65	47.16	33.63
HIPEQ1223+00	0.864	2.831	0.32	25.77	1.83
HIPEQ1223-03b	0.135	0.105	3.53	29.62	24.49
HIPEQ1224+00	0.959	13.094	0.05	25.74	···
HIPEQ1224+03b	0.608	0.907	0.10	13.24	···
HIPEQ1225+00	0.100	0.123	1.45	19.56	2.04
HIPEQ1226+02	0.286	0.225	1.46	28.75	6.91
HIPEQ1227+01	0.990	27.775	0.06	34.16	1.17
HIPEQ1228+02	0.778	1.315	0.62	25.88	4.75
HIPEQ1228+03	0.024	0.045	0.56	10.26	2.49
HIPEQ1229+00	0.872	3.726	0.22	20.45	1.43
HIPEQ1230+02	0.763	1.196	0.07	13.49	0.16
HIPEQ1230+03	0.822	1.515	0.69	49.82	7.54
HIPEQ1232+00a	0.620	0.928	1.35	45.66	9.07

Table 4.1—Continued

HIPASS Name	Gas Fraction	M_{HI}/L_g	HI Enclosed ($10^9 M_\odot$)	HI Diameter (kpc)	Dynamical Mass[a] ($10^{10} M_\odot$)
HIPEQ1232+00b	0.261	0.155	19.70	58.46	30.82
HIPEQ1233-02	0.660	1.350	0.80	28.58	1.18
HIPEQ1236+03	0.860	2.548	0.16	16.06	1.39
HIPEQ1239-00	0.800	1.329	1.90	64.92	15.73
HIPEQ1241+01	0.641	1.294	0.14	23.00	4.19
HIPEQ1241-02	0.429	0.643	0.13	13.39	0.86
HIPEQ1242+03b	0.132	0.155	0.22	8.39	1.46
HIPEQ1242-00	0.385	0.329	3.72	50.27	15.29
HIPEQ1242-01a	0.737	1.396	0.18	22.45	5.90
HIPEQ1242-01b	0.603	0.634	4.30	73.43	38.21
HIPEQ1243-00	0.375	0.403	4.99	56.66	25.70
HIPEQ1244+00	0.585	0.367	0.53	13.66	1.03
HIPEQ1244-02	0.830	1.892	0.21	21.82	2.27
HIPEQ1245-00	0.168	0.186	9.23	62.68	47.38
HIPEQ1249+03	0.653	1.121	0.19	24.99	7.86
HIPEQ1249+04	0.820	1.860	0.47	32.69	1.53
HIPEQ1250+05	0.553	0.536	0.36	21.42	7.42
HIPEQ1253+01	0.141	0.118	1.50	18.77	8.72
HIPEQ1253+02	0.054	0.111	0.68	15.32	...
HIPEQ1253+04	0.596	0.739	0.08	13.94	0.61
HIPEQ1255+00	0.363	0.475	0.93	28.95	...
HIPEQ1255+02	0.299	0.343	1.97	48.39	41.00
HIPEQ1255-00	0.697	1.413	0.23	8.67	0.43
HIPEQ1256+03	0.971	6.291	0.02	11.45	4.40
HIPEQ1257+02	0.726	1.158	0.04	8.72	0.94
HIPEQ1257-01	0.598	0.562	3.62	59.41	30.37
HIPEQ1258+02	0.619	0.767	1.65	37.63	4.51
HIPEQ1300+02a	0.305	0.327	0.04	6.04	0.24
HIPEQ1300+02b	0.229	0.224	0.96	22.19	2.30
HIPEQ1303+03	0.661	0.925	0.82	35.79	...
HIPEQ1304-02	0.768	2.672	0.03	13.51	0.71
HIPEQ1304-03	0.698	0.896	1.04	40.13	6.87
HIPEQ1307-00	0.597	0.776	5.79	95.80	45.82
HIPEQ1308-02	0.466	0.664	3.81	69.99	...
HIPEQ1311+03a	0.846	1.871	0.40	38.24	6.04
HIPEQ1312+03	0.413	0.756	3.25	85.90	10.79
HIPEQ1312+05	0.885	3.103	0.02	7.41	0.35
HIPEQ1313+06	0.355	0.617	5.92	97.30	...
HIPEQ1317-00	0.899	1.837	0.04	11.64	0.78
HIPEQ1318-01	0.276	0.412	5.33	62.12	...
HIPEQ1320+05	0.569	1.005	0.12	9.23	0.42
HIPEQ1327+02	0.881	2.402	0.02	7.57	0.15
HIPEQ1329-00	0.850	2.510	0.80	38.92	6.62
HIPEQ1332+01	0.157	0.259	1.11	29.59	...
HIPEQ1335+01	0.277	0.340	7.15	68.30	41.70
HIPEQ1341+05	0.680	1.170	4.61	100.52	66.15
HIPEQ1348+03	0.178	0.152	1.28	19.31	7.49
HIPEQ1352+02a	0.233	0.385	8.21	80.35	68.48
HIPEQ1352-01	0.331	0.359	1.75	35.22	16.93
HIPEQ1400+02	0.651	0.590	2.40	48.79	16.45
HIPEQ1411-01	0.769	0.671	3.69	59.48	19.98
HIPEQ1415+04	0.552	0.790	1.88	48.42	...
HIPEQ1416+03	0.889	3.717	0.09	17.67	1.00
HIPEQ1422-00	0.361	0.306	3.01	40.91	15.33
HIPEQ1429-00	0.903	3.159	0.43	51.89	15.88
HIPEQ1432+00	0.298	0.227	0.59	15.68	3.47
HIPEQ1433+01	0.926	4.262	0.12	14.67	0.40
HIPEQ1433+02	0.666	0.744	0.15	15.02	1.03
HIPEQ1437-00	0.138	0.103	1.90	20.12	3.36

Table 4.1—Continued

HIPASS Name	Gas Fraction	M_{HI}/L_g	HI Enclosed ($10^9 M_\odot$)	HI Diameter (kpc)	Dynamical Mass[a] ($10^{10} M_\odot$)
HIPEQ1439+02	0.716	1.924	0.19	17.33	1.59
HIPEQ1439-00	0.582	0.712	2.00	44.95	10.11
HIPEQ1440+02	0.367	0.269	0.25	13.07	1.94
HIPEQ1444+01a	0.309	0.422	1.58	44.44	43.46
HIPEQ1500+01	0.079	0.105	1.87	22.64	19.62
HIPEQ1504+02	0.664	1.086	5.01	105.40	...
HIPEQ1504-00	0.697	0.854	0.46	25.09	5.84
HIPEQ1507+01	0.083	0.155	6.39	51.39	...
HIPEQ1542+00	0.509	0.440	2.44	40.47	14.53
HIPEQ1544+02	0.618	1.343	0.79	53.60	...
HIPEQ1545+00	0.684	1.567	1.50	47.84	...
HIPEQ1601+01a	0.225	0.148	3.22	27.11	11.97
HIPEQ1609-00	0.942	3.045	0.12	17.73	1.30
HIPEQ1613-00	0.780	0.847	0.32	26.18	7.21
HIPEQ1614+00	0.605	0.647	0.75	25.98	...
HIPEQ1614-00	0.494	0.393	5.10	60.51	45.07
HIPEQ2036-04	0.215	0.477	11.34	114.51	149.25
HIPEQ2314+00	0.319	0.327	1.19	33.86	...
HIPEQ2324-00	0.805	1.096	1.03	40.80	3.46
HIPEQ2335+01	0.832	4.249	0.48	35.84	2.64
HIPEQ2336+00	0.361	0.564	3.00	69.21	78.15
HIPEQ2337+00	0.620	0.954	0.97	36.94	5.00
HIPEQ2340+01	0.614	1.182	0.23	25.20	6.46

[a]Dynamical mass estimates are not available for cases where large inclination uncertainties do not allow for accurate velocity measurements.

4.5 Dynamical Mass

The best measure of the "total" mass of a galaxy comes from the calculation of the dynamical mass. For a spherical distribution, the mass inside a radius R is defined to be:

$$M_{dyn} = \frac{RV_{rot}^2}{G} \tag{4.7}$$

where V_{rot} is the inclination corrected rotational velocity. Equation 5.7 indicates that calculating the dynamical mass requires knowing the characteristic radius of the HI, but as discussed above, the single dish HI data cannot directly constrain the HI radius. As an alternative, we use the HI radius (R_{HI}) derived from Equation 4.6 as a measure of the HI extent (e.g. Swaters 2002) and use it to calculate the dynamical masses. These can be found in Table 4.1. Note that the the dynamical mass only measures the mass within the baryon disk, and is thus a lower limit to the "total" virial mass of the galaxy. The baryonic disk traced by the HI has undoubtedly dissipated and re-collapsed within the dark matter halo (Gunn 1977; Fall & Efstathiou 1980).

Using the results of Equation 5.7, we calculate the mass fraction in the baryonic component compared to the total mass ($(M_\star+M_{HI})/M_{dyn}$). Figure 4.14 shows the resulting baryon fraction as a function of dynamical mass. There is no clear trend between the baryon fraction and dynamical mass. There may be a slight tendency for low mass galaxies to have a higher baryon mass fractions but this has not been statistically tested. To explain their rotation, most galaxies require between 5 and 20 times more mass than is seen in baryons. However, a few of systems have more than 50% of their rotational mass in baryons. Almost all of the galaxies fall below the WMAP Ω_b/Ω_M ratio of 0.16. A few of the galaxies with the highest baryon fractions are earlier type galaxies whose stellar masses might be affected by the presence of AGN.

4.6 Discussion

In this chapter we have shown that the properties of my HI selected sample span a large range of gas fractions, colors, surface brightnesses and baryon distributions. We demonstrate

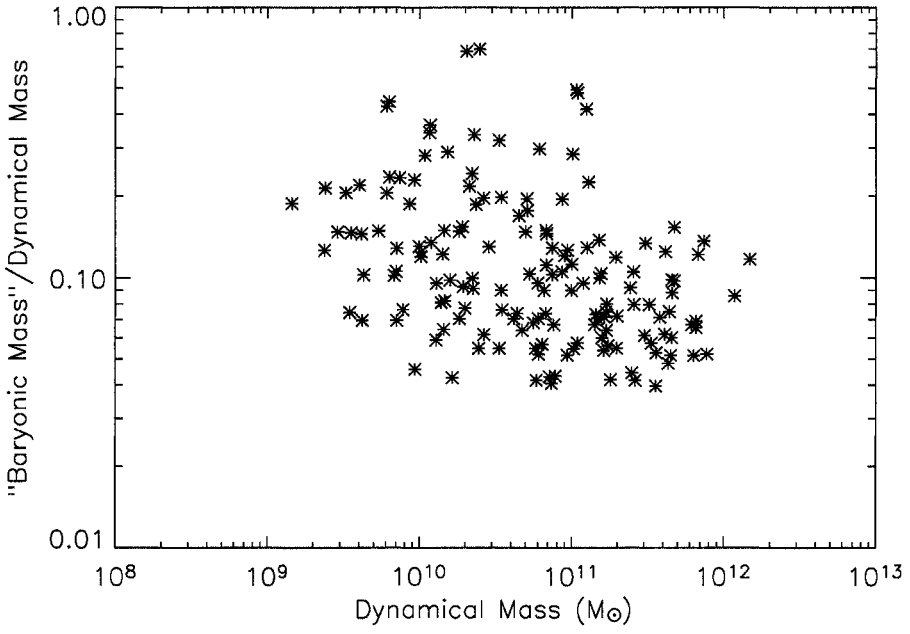

Figure 4.14 The baryonic mass fraction as a function of dynamical mass. Although no clear trends are found, this figure is included to show the range and distribution of mass fractions in the sample.

that the HI selection identifies a unique set of galaxies that may be significantly different than a complete sample of galaxies with similar morphologies. The gas fraction of a galaxy is a decent indicator of its optical properties, in particular the surface brightness, but the reverse is not necessarily true. The gas fraction within the optical radius is an even better predictor of optical properties and serves to indicate a galaxy's star formation efficiency within the optical disk. Caution is required when attempting to infer the gas content of a galaxy from its optical properties. We show that the way in which baryons are distributed in galaxies is quite varied and that some of the systems we see in the optical are truly stellar islands in a vast sea of HI. The total mass derived inside the baryon radius demonstrates that galaxies have a range of baryon fractions.

Although we present many relations that increase our understanding of star formation on the global scales of galaxies, the results from this chapter are arguably most important for those working on simulations of star formation in galaxies. Our results provide an accurate, uniform set of observational constraints that include realistic gas fractions and dynamical relationships that theorists can use to model how star formation proceeds in galaxies.

Chapter 5

UNDERSTANDING COLORS

5.1 Introduction

The star formation history, the metallicity, and the current star formation rate are just a few parameters that contribute to the observed colors of a galaxy. Remarkably, these factors work in concert to yield a fairly well defined locus in galaxy color-color space. Deviations from this locus as well as the morphology of the locus itself can lead to significant insight into the underlying physics in galaxies. In this chapter, we utilize the color information for the HIPASS/SDSS sample to explore the star formation histories and physical conditions that might lead to the observed colors. We show that the HI selection does create a significant offset in the colors of the sample galaxies and that this can be explained by recent bursts of star formation. We demonstrate that the colors of the bluest galaxies in the HIPASS/SDSS sample are dominated by emission lines and that stellar population synthesis models alone (without emission lines) are not adequate for reproducing many of the galaxy colors. Although we find a statistically significant jump in the color dispersion of galaxies, we suggest that the jump is most likely the product of a selection effect and not a tracer of underlying physics.

5.2 Modeling the Colors of Galaxies

Many previous studies have utilized the colors of galaxies to investigate the star formation histories and metallicities of galaxies (e.g. Tinsley 1972; Searle et al. 1973; Tinsley & Gunn 1976; Balcells & Peletier 1994; Roberts & Haynes 1994; de Jong 1996; Bell & de Jong 2000; Galaz et al. 2002; Gavazzi et al. 2002; Bell et al. 2003; MacArthur et al. 2004; Zackrisson, Bergvall & Ostlin 2005). The uniform, well calibrated and low uncertainty nature of the HIPASS/SDSS sample allows for a more detailed explanation of the factors affecting galaxy

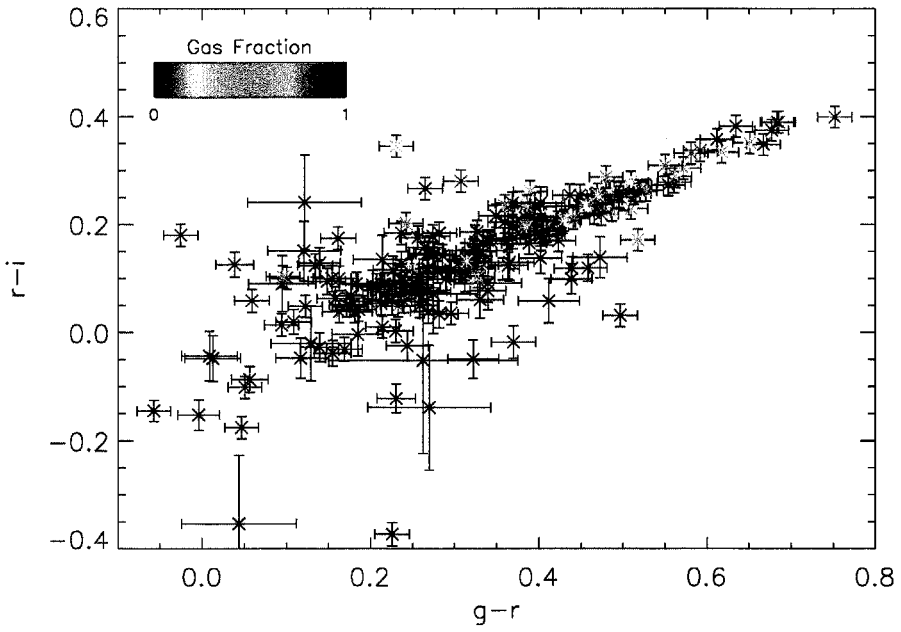

Figure 5.1 $r-i$ vs $g-r$ for HIPASS/SDSS sample galaxies. All photometric corrections have been applied to these data and error bars indicate the photometric and calibration errors of each galaxy. Galaxies have been color coded according to their gas fractions.

color. However, as Bell et al. (2003) explore, there is an unavoidable degeneracy between age and metallicity when using optical colors. Their solution is to use a combination of optical and IR colors; optical color is more sensitive to age while IR color is more sensitive to metallicity. Our sample does not have a complete set of near IR counterpart data and some of our results will reflect this degeneracy. On the other hand, the broad range of optical SDSS colors helps to some degree.

Figure 5.1 shows the $r-i$ colors of the galaxies in my HI selected sample as a function of their $g-r$ color. The error bars indicate the quadrature sum of the photometric and calibration uncertainties. The galaxies are color-coded according to their gas fraction. As discussed in the previous chapter, the gas fraction scales systematically with galaxy color. Figure 5.1 also demonstrates the well defined galaxy locus seen in other SDSS galaxies studies (Strateva et al. 2001; Blanton et al. 2003a).

To compare the colors of the HIPASS/SDSS sample galaxies with theoretical predic-

tions, we ran a series of Bruzual & Charlot (2003) population synthesis models at various metallicities and star formation histories. The models use the Chabrier (2003) initial mass function (IMF) to model the stellar populations with a range of stellar masses of $0.6M_{\odot} \leq m \leq 120M_{\odot}$, at 6 different metallicities (0.005, 0.02, 0.2, 0.4, 1 and 2.5 times solar) and 10 different star formation histories (SFH). The SFHs are modeled as having either (1) an exponentially decreasing star formation rate (SFR; $e^{-t/\tau}$) with e-folding values or τ values of of 8, 4, 2, and 1 Gyr; (2) an exponentially increasing SFR with τ values of 8, 4, 2, and 1 Gyr; (3) a continuous SFR ($\tau = \infty$); or (4) an instantaneous event of star formation ($\tau = 0$). We do not include dust in any of the population models because we have corrected for the internal extinction of the galaxies. Each model is run with gas recycling turned off. For each model we assume that 12 Gyr has elapsed since the first formation of stars and extract the SDSS model colors at that epoch.

Figure 5.2 shows the resulting population grid for the $r-i$ colors as a function of $g-r$. The HIPASS/SDSS sample galaxies have been overplotted and color-coded according to their gas fractions. The "horizontal" lines are lines of constant metallicity and the "vertical" lines are lines of constant τ (a proxy of mean stellar age). The $g-r$ colors are sensitive to age and trace the extent of the models very well. On the other hand, the $r-i$ color is only marginally sensitive to metallicity and the aforementioned degeneracy is apparent at sub-solar metallicities. Metallicity and SFH labels have been included for reference.

At the red end of the galaxy distribution, the colors are well explained by the model grids. The redder galaxies are consistent with having SFHs that have been exponentially decreasing over time and have formed almost all of their stars in the past. The reddest galaxies also have colors indicative of having super-solar metallicities. These results are in agreement with previous work by Bell et al. (2003) as well as with the recent work of Juneau et al. (2005), who demonstrate that galaxies with large stellar masses formed most of their star in the first 3 Gyr after their formation. This story of star formation would suggest that the red galaxies formed almost all of their stars in the distant past and have been undergoing little to no star formation since. We conclude that red galaxies experience disk instabilities that make them extremely efficient at forming stars and that the bulk of their stars were formed several Gyr ago.

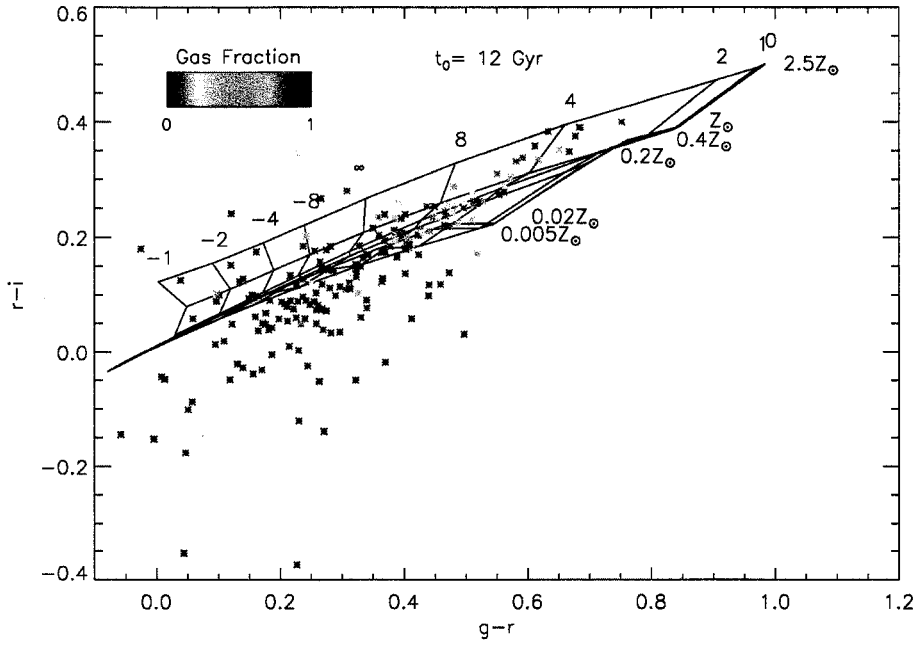

Figure 5.2 $r-i$ vs $g-r$ for HI selected galaxies. All photometric corrections have been applied to these data. Galaxies have been color coded according to their gas fractions. Bruzual & Charlot (2003) population synthesis grids have been overplotted for various SFH and metallicities 12 Gyrs after initial star formation began. The SFH are given by τ values for an exponentially decreasing SFR ($e^{-t/\tau}$) and metallicities are plotted in comparison to solar. Although some of the galaxies are well described by these models, a significant number of systems do not fall on the grids.

The red galaxies have presumably exhausted their entire supply of primordial gas and yet are detected in the HIPASS survey. Some mechanism is responsible for the presence of HI. The cannibalization of gas rich dwarfs or infall from "cold mode" accretion (Katz et al. 2003) might explain the current small reservoir of gas. Regardless of the physical process by which these galaxies acquire gas, the presence of HI suggests that recent star formation has likely to have taken place. As discussed in Chapter 2, the SDSS spectra for these galaxies do not give a representative picture of their spectroscopy properties because of the small fiber apertures. However, all of the galaxies redder than $g - r > 0.5$, have SDSS spectra that contain emission lines. Although some of these spectra may have emission lines due to the presence of an AGN, the majority are strong indicators that current star formation is underway in these galaxies.

As we look to the bluer galaxies in Figure 5.2, the metallicities get lower and the SFHs move toward a constant star formation rate ($\tau = \infty$). This is consistent with a decrease in star formation efficiency and suggests that the reason why these systems have larger gas fractions is due to their inability to convert their primordial gas into stars.

Some of the galaxies are best modeled by SFHs that have increasing SFR. This is an area of the model parameter space that has been ignored by recent galaxy studies (Kauffmann et al. 2003; Brinchmann et al. 2004; Salim et al. 2005). Gas infall might serve to increase the HI surface density and subsequently the SFR in these galaxies. Recent bursts of star formation may contribute some to this effect, however the already blue $g - r$ colors of these galaxies do not change significantly when recent bursts are added to the models.

Many of the bluest galaxies in the HIPASS/SDSS sample have colors that are not predicted by the Bruzual & Charlot models. Most of these galaxies have $r - i$ colors that are too blue to be explained by any iteration of the models. The LSB nature of many of these systems suggests that for even small SFR, emission lines might be able to dominate the broadband colors (Zackrisson et al. 2001; Magris, Binette & Bruzual 2003; Anders & Fritze-v. Alvensleben 2003; Zackrisson, Bervall & Ostlin 2005). We investigate how the colors are affected by the addition of emission lines in §5.5

In addition, there are a five galaxies that seem to be too red in $r - i$ to be explained by any population models. Two of these galaxies have a saturated star nearby that is most

likely affecting their colors, one of the galaxies has very large photometric uncertainties because of its low surface brightness and the other two have very compact cores, which suggests the presence of AGN. We compute the colors for these two galaxies excluding the central region, using a shell with radial boundaries defined to be from half of the Petrosian radius to the Petrosian radius. Both galaxies fall back to or below the model grids when their central core is excluded.

5.3 The Colors of HI vs. Optically Selected Galaxies

The HI selection seems to introduce a systematic shift in the color distribution of the HIPASS/SDSS sample galaxies. Figure 5.3 shows the $r - i$ vs. $g - r$ colors for the HIPASS/SDSS sample plotted on top of a volume limited sample drawn from the SDSS DR4 sample. All galaxies have been k-corrected and corrected for Milky Way extinction. However, no data in Figure 5.3 have been corrected for internal extinction. The reddening vector (derived from Schlegel et al. 1998) has been included to show that any correction to either data set is almost perfectly aligned with the galaxy locus.

It is clear from Figure 5.3 that the HI selected sources fall to one side of the SDSS galaxy distribution. This is particularly pronounced at the red end of the color distribution where the color dispersion is quite small for the HI selected galaxies. As the color coding indicates, these galaxies have small gas fractions but retain enough gas to be detected in HIPASS.

As noted in the previous section, the redder galaxies have SFH that suggest that almost all of the primordial gas in these systems has been converted to stars in the distant past. The presence of HI in these systems may indicate a recent acquisition of HI and a subsequent ignition of star formation. The SDSS spectra for these galaxies confirm that current star formation is underway. A temporary increase in SFR due to late-time accretion would also explain why the red HI selected galaxies are slightly bluer in $g-r$ than the rest of the SDSS galaxy population (Figure 5.3).

To investigate how a recent burst might affect the colors of galaxies, we added a single burst of star formation ranging from 2 Gyr to 100 Myr and producing 1% of the stellar mass of the galaxy to a single Bruzual & Charlot model. We plot the evolutionary track in Figure

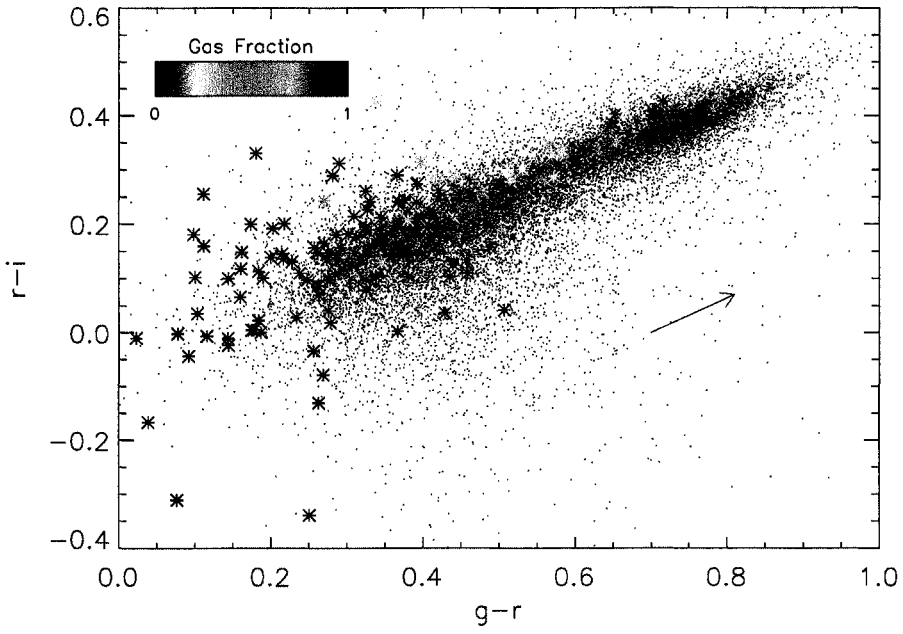

Figure 5.3 $r - i$ vs $g - r$ for HI selected galaxies (colored symbols) plotted with a volume selected sample of galaxies from SDSS (black dots). No internal extinction has been applied to these data but a reddening vector has been plotted for reference. Galaxies in the thesis sample have been color coded according to their gas fractions. Note that the HI selected sample appears to have colors that are shifted off of the SDSS galaxy locus.

5.4 with a colored symbol plotted for model time step since burst (blue to red). Figure 5.5 shows the same burst evolution with symbols plotted every 40 Myr since burst. Figure 5.5 demonstrates that there is a rapid and short-living change in color that occurs in the first few Myrs and is followed by a slow reddening for hundreds of Myrs. This "bottleneck" in the burst evolution suggests that the offset observed in Figure 5.3 may be due to a burst in the past few hundred Myr.

To constrain the amount of recent star formation needed to explain the color offset between the HIPASS/SDSS galaxies and the "main" SDSS sample, we re-ran the same series of Bruzual & Charlot (2003) population synthesis codes as seen in Figure 5.2, but with the addition of a recent burst of star formation. For each model, we added a single burst ranging from 2 Gyr to 100 Myr in the past and varied the burst strength from 1-10% of the integrated star formation. The resulting models were most sensitive to the time at which the burst was placed. The models that most closely match the slight $g - r$ blueing where bursts placed at 300 Myr in the past.

Figure 5.6 shows the HIPASS/SDSS galaxies with the model grids for a 1% burst 300 Myr ago. By comparing the differance between the grids in Figure 5.2 and 5.6 with the offset observed in Figure 5.3, it is clear that the HI selected galaxies in the burst case (Figure 5.6) occupy the same model space as the SDSS "main" galaxies in the burst-free case (Figure 5.2). Unfortunately, our inability to correct for internal extinction in the SDSS "main" sample prohibits us from overlaying the grids on Figure 5.3, which would be highly instructive. The reader will have to settle for a "blinking" back and forth between Figures 5.2 and 5.6 to assure herself that the bursts indeed explain the blueing of the red galaxies. It is important to note that the addition of the burst has little effect on the colors of blue galaxy models. Although degeneracies between age and burst strength in the models prevent an exact characterization of the bursts in the HI selected galaxies, we can safely claim that a new generation of stars has been formed in the last few hundred Myr in these systems. The bursts require no more than 1% of the mass to be involved as long as the burst was in the lat 300 Myr.

The bluer colors are unlikely to be due to main sequence stars, since most blue main sequence stars will have ceased their hydrogen burning after a few hundred Myr. We suggest

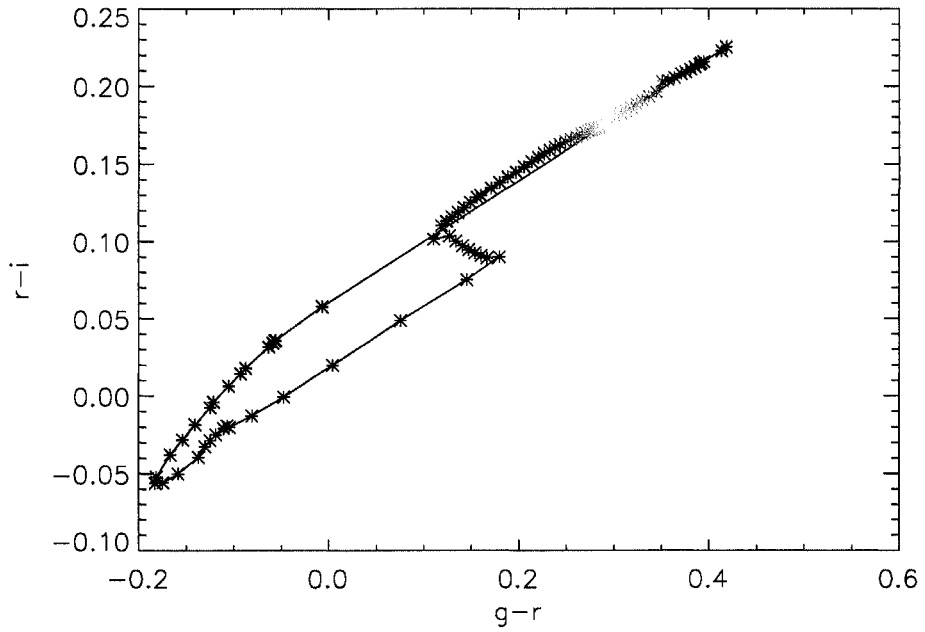

Figure 5.4 The $r-i$ vs. $g-r$ evolution of a single Bruzual & Charlot model with the addition of a burst of star formation that produces 1% of the total stellar mass of the galaxy. Colored symbols are plotted for every model time point since burst (blue to red). The symbols are not uniformly spaced in time but are included to show the direction of the path.

that the blue colors we see in the HI selected galaxies could be specifically due to an elevated level of BHeB stars left over from a recent burst of star formation. These stars are seen several hundred Myr after a star formation event (Dohm-Palmer et al. 2002).

5.4 Modeling Galaxy Colors with Emission Lines

Perhaps the most puzzling aspect of the HIPASS/SDSS galaxy colors is that many of the galaxies don't fall on the model grids. Unlike the red galaxies, which can be easily explained, the majority of the discrepant galaxies are significantly bluer in $r-i$ than any models can predict. They also have high gas fractions and most of them are LSB in nature. No matter what parameters we alter in the Bruzual & Charlot models, we cannot produce a stellar population with those colors. We now show that the discrepant colors can be explains by including the emission lines dominate that the spectra of these outlying galaxies.

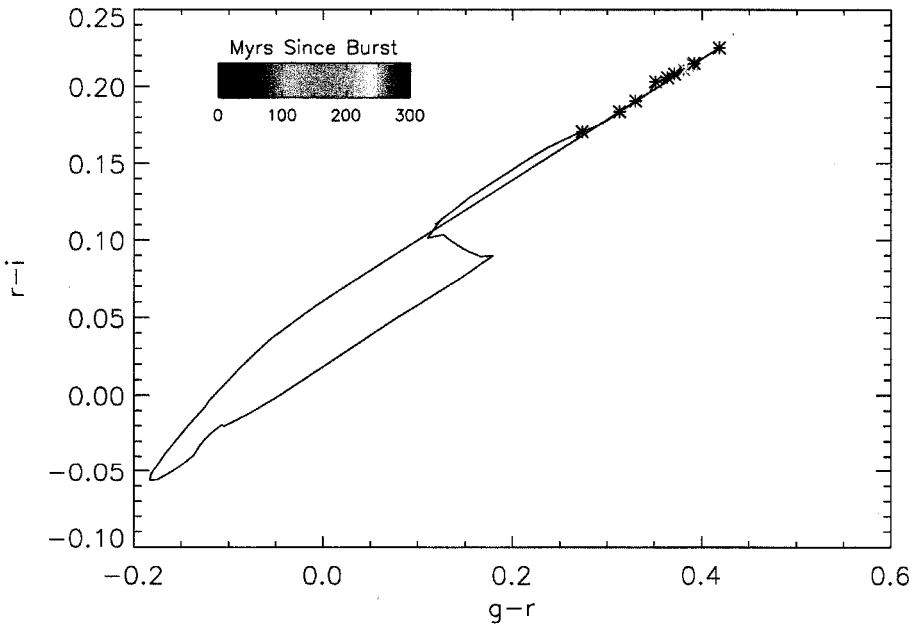

Figure 5.5 The $r-i$ vs. $g-r$ evolution of a single Bruzual & Charlot model with the addition of a burst of star formation that produces 1% of the total stellar mass of the galaxy. Colored symbols are plotted every 40 Myr since burst (blue to red).

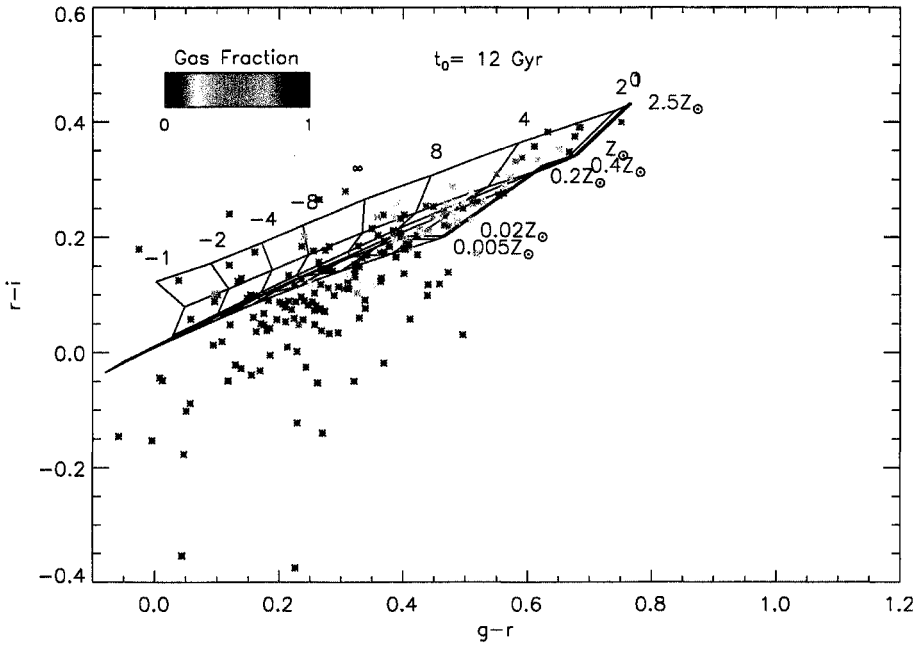

Figure 5.6 $r - i$ vs $g - r$ for HI selected galaxies. All photometric corrections have been applied to these data. Galaxies have been color coded according to their gas fractions. Bruzual & Charlot (2003) population synthesis grids have been overplotted for various SFH and metallicities after 12 Gyrs of star formation. The SFH are given by τ values for an exponentially decreasing SFR ($e^{-t/\tau}$). These grids include a burst of star formation 300 Myr in the past. Galaxies in this Figure have the same metallicities and SFH as the SDSS galaxies would in Figure 5.2 if they had been included. This recent burst of star formation explains the offset observed between the HI selected and "main" SDSS galaxy samples.

A large number of galaxies lie below the model grids in Figure 5.2. Because no stellar populations can explain the integrated colors we observe, we investigate the hypothesis that star formation induced emission lines are significantly affecting the galaxy colors. HII regions produce numerous emission lines in the g and the r bands. Hα dominates the r-band while [OIII] and Hβ dominate the g-band. The i-band has almost no lines. So in an HII region, we would expect the $r-i$ color to be significantly bluer and the $g-r$ color to change only slightly compared to the underlying stellar continuum. Because the SDSS fiber spectra for the HIPASS/SDSS galaxies often fall on HII regions, they can indicate what the colors of emission line regions are in the most extreme cases. By comparing the HII region (spectra) colors with the integrated colors of the galaxies, we can quantify range the colors change when emission lines dominate.

We first select HIPASS/SDSS galaxies with SDSS spectroscopy and require that they have large Hα equivalent widths (> 300 Å). The 10 spectra selected are shown in Figure 5.7. All of the selected spectra have good signal-to-noise (> 10) and are dominated by emission line features. We visually inspect each galaxy to ensure that all of the spectra shown in Figure 5.7 are all from fibers placed on HII regions. We convolve the g, r and i SDSS filters with each spectrum and converts the computed flux density to AB magnitudes using the relation from Oke & Gunn (1983) that a magnitude 0 object has a flux density of 3631 Jy. We then compare the integrated colors of the 10 galaxies derived in Chapter 3 with the HII region colors derived from the spectra.

Figure 5.8 shows the resulting differences between the HII region and the integrated color of each galaxy. The spectra colors are plotted as black symbols and the red diamonds indicate the integrated galaxy colors. Blue lines connect a galaxy's integrated color to its HII color. All of the galaxies get bluer in $r-i$ by $\sim 0.5^m$ and all but 2 get bluer in $g-r$ by $\sim 0.2^m$, and thus the HII region colors are significantly different than the integrated colors. This result confirms the hypothesis that emission lines can make the $r-i$ color blue enough to explain the colors we see in the HIPASS/SDSS sample. However, contrary to our initial explanation, the $g-r$ does change considerably but not always in the same direction.

To further test the emission line hypothesis as well as explore the reason for the $g-r$ color change, we add model emission lines to the computed Bruzual & Charlot model colors.

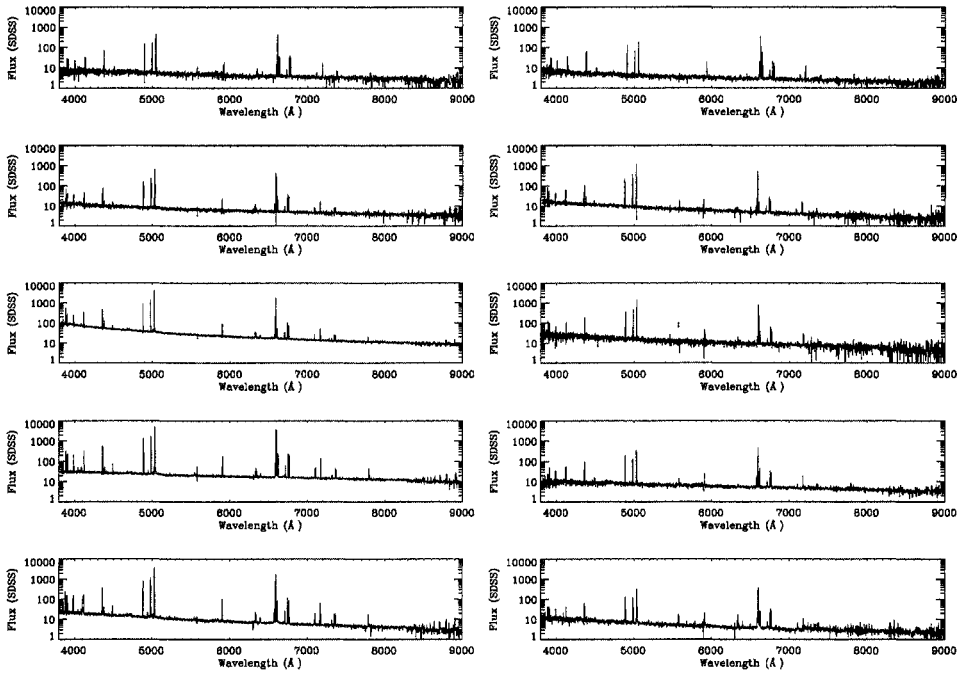

Figure 5.7 SDSS fiber spectra for 10 galaxies in the HIPASS/SDSS sample with strong emission line features. All of the fibers for these spectra were placed on top of HII regions in the galaxies. The flux axis is in units of 10^{-17} ergs/s/cm^{2}Å.

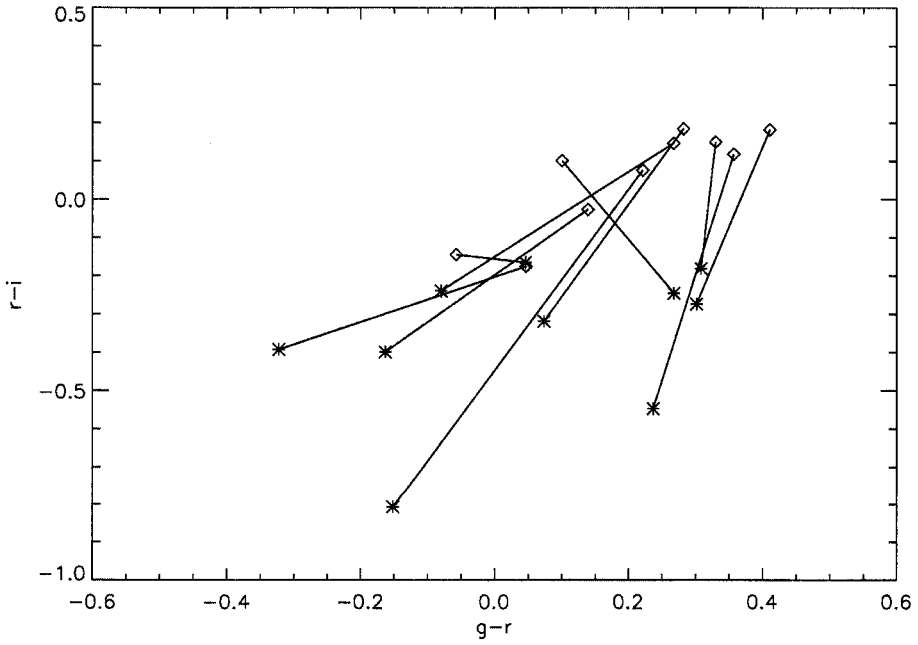

Figure 5.8 $r - i$ vs. $g - r$ color difference between the integrated colors of 10 galaxies (red diamonds) and the "fiber" magnitudes computed from the HII region spectra (black symbols). The blue lines connect each galaxy's integrated color to its HII region color. All of the galaxies get bluer in $r - i$ and all but 2 get bluer in $g - r$

Theoretical models for line emission in galaxies are given by Kewley et al. (2001) using the STARBURST99-MAPPINGS III code. The models cover a range of metallicities, ionization states, electron densities, and assumption about the burst lengths. For each model, the wavelength of every line and its energy are provided. We convolve these energies with the SDSS filters and covert the computed flux densities into AB magnitudes in the same manner as above. We add the emission line output to the Bruzual & Charlot colors using a scaling coefficient that determines the strength of the emission line relative to the true stellar continuum. This coefficient is directly proportional to the SFR and can be used to estimate the range of possible SFR for a galaxy. The final models are not fully self consistent, because the ionizing radiation for the emission line spectrum does not come from the Bruzual & Charlot spectrum. However, because the star formation is highly localized in late-type galaxies, it is possible for the ionizing radiation in isolated HII regions to be different than that of the broader component of stars

When we add the STARBURST99-MAPPINGS III data to the Bruzual & Charlot outputs, we ensure that we are adding same metallicities. Because there are only 3 overlapping metallicities, we limit our analysis to 0.2, 0.4 and 1 times solar populations. In reality most of the galaxies where emission lines dominate do not have significant stellar populations and therefore would not have high metallicities. Even values of 0.2 might be too high for these systems.

Figure 5.9 demonstrates the affect that adding emission lines to an underlying stellar population has on the colors of a single Bruzual & Charlot model. The colored symbols represent different star formation rates. The galaxy's $r-i$ color becomes bluer as star formation is increased, while the $g-r$ color goes almost unchanged. The mean SFR density of the HIPASS/SDSS sample as estimated in Chapter 4 is 0.002 $M_{\odot}/yr/kpc^2$. This is consistent with the star formation rate densities ($\sim$0.002=0.01 $M_{\odot}/yr/kpc^2$) required to blue the galaxies in Figure 5.9.

We also show in Figure 5.10 that the emission lines of varying strength added to stellar populations can explain the all of discrepant blue galaxies. All models that are shown use an 8 Myr continuous burst of star formation. Black lines indicate emission line models with an electron density of 10 cm^{-3} and an ionization parameter of 5×10^6 cm/s. Red lines have

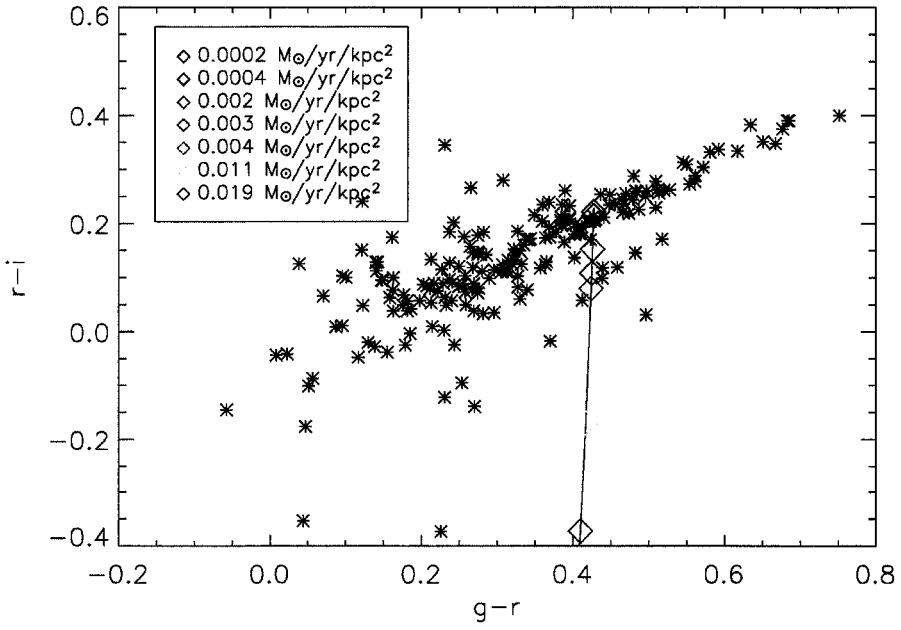

Figure 5.9 The addition of emission lines to an underlying stellar population for a single Bruzual & Charlot model. The colored symbols represent different star formation rates. The galaxy's $r - i$ color becomes bluer as star formation is increased, while the $g - r$ color goes almost unchanged.

the same electron density but an ionization parameter of 8×10^7 cm/s.

We found that varying the electron density and burst length did not have a significant effect on the output models. All significant changes in color are driven by ionization parameter and the global normalization of the emission line spectrum, which should be proportional to the SFR. Solid lines have SFR densities of 1.2×10^{-3} $M_\odot$/yr/kpc^2 and 3.7×10^{-3} $M_\odot$/yr/kpc^2 for the two models (black and red) respectively. The dashed lines have SFRs 3 times larger than the solid lines. For a typical galaxy in the the emission line dominated region, we calculate SFRs of 0.004-0.2 $M_\odot$/yr. These are reasonable SFRs for small, blue galaxies (van Zee 2001). It is clear that the span of these models can easily explain the galaxies that the stellar population models cannot and that many low mass, blue galaxies must have colors that are dominated by emission lines (Zackrisson et al. 2005).

5.5 The Increase in Color Dispersion

The analysis above demonstrates that the observed colors of the HIPASS/SDSS sample can be well explained by stellar population models including emission lines, and that the general trend in color is due to decreasing mean stellar age with increasing gas fraction. However, while this explains most of the general trends seen in the color distribution in Figure 5.1, it does not explain the sharp increase in the dispersion of color at $g-r$ ~0.5. This narrow dispersion from the locus seems to suddenly jump to a much larger value before the photometric uncertainties become large enough to be solely responsible for the discrepancy. We now investigate the mechanisms behind this increased scatter.

To explore how the dispersion in color relates to other physics quantities, we perform a principal component analysis (PCA) on the $r-i$ vs. $g-r$ colors. The result aligns the principal axis (P1) with the galaxy color-color locus and sets the secondary axis (P2) perpendicular to P1. P1 and P2 can be expressed in term of the $g-r$ and $r-i$ colors of the galaxies by

$$P1 = (0.6r - i + 0.8g - r) - \overline{(0.6r - i + 0.8g - r)} \tag{5.1}$$

and

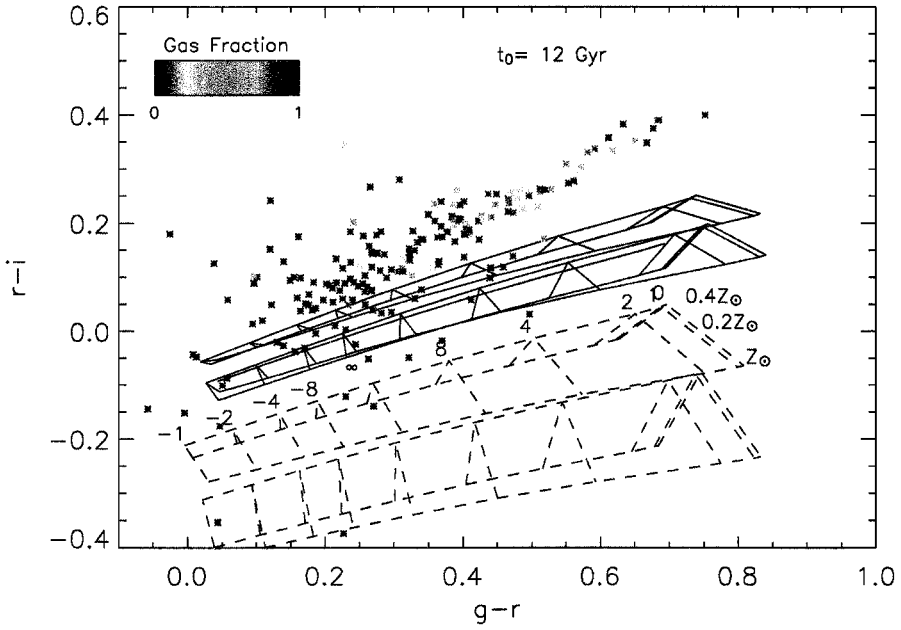

Figure 5.10 $r-i$ vs. $g-r$ colors for the HI selected galaxies. Color coding indicates the gas fractions of the galaxies. The grids represent 2 different linear combinations of the STARBURST99-MAPPINGS III emission line models and the Bruzual & Charlot population synthesis models. The coefficient for the emission line models is a proxy for SFR. The Bruzual & Charlot models are identical to those shown in Figure 5.2. All emission line models use an 8Myr continuous burst of star formation. Black lines indicate emission line models with an electron density of 10 cm^{-3} and an ionization parameter of 5×10^6 cm/s. Red lines have the same electron density but an ionization parameter of 8×10^7 cm/s. Solid lines have SFR densities of 1.2×10^{-3} $M_\odot$/yr/kpc^2 and 3.7×10^{-3} $M_\odot$/yr/kpc^2 for the two models (black and red) respectively. The dashed lines have SFRs 3 times larger than the solid lines. These models clearly describe the colors of all of the galaxies that are not fit by normal populations of stars.

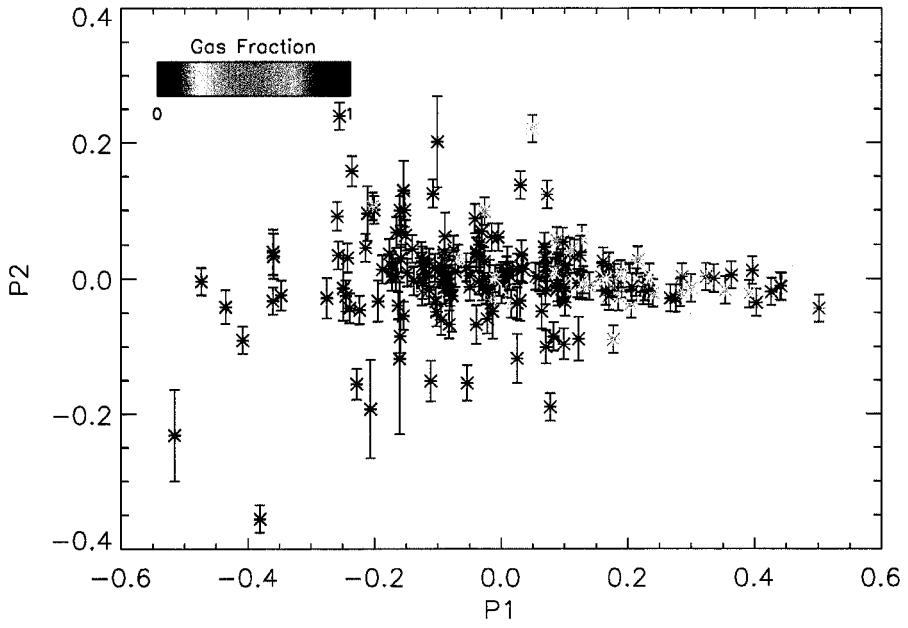

Figure 5.11 Principal axis of the galaxy color-color relation after PCA. Galaxies are color coded according to their gas fraction. Error bars indicate the $g-r$ errors of the sample and are included for reference. The transition between low and high dispersion occurs around a P1 value of 0.1.

$$P2 = (0.8r - i - 0.6g - r) - \overline{(0.8r - i - 0.6g - r)}, \tag{5.2}$$

where the overlined region is the mean of the axis variable.

Figure 5.11 shows the result of the PCA coordinate transformation. Error bars in the P2 direction are the uncertainties in the $g-r$ color and should scale with P2. The P2 axis serves as an indicator of dispersion from the galaxy locus and we compare the P2 values to other physical parameters below. We perform a K-S on the distribution of colors with P1 > 0.1 ad P < 0.1 and find that the two populations are statistically independent.

Recent studies of stellar mass in galaxies have found that various transitions occur at $\sim 10^{10} M_{\odot}$. Kauffmann et al. (2003) show that the stellar populations of galaxies can be divided into young and old bins according to their stellar mass, with the division occurring at $3{\times}10^{10} M_{\odot}$ such that higher stellar mass galaxies have older populations. Baldry et al.

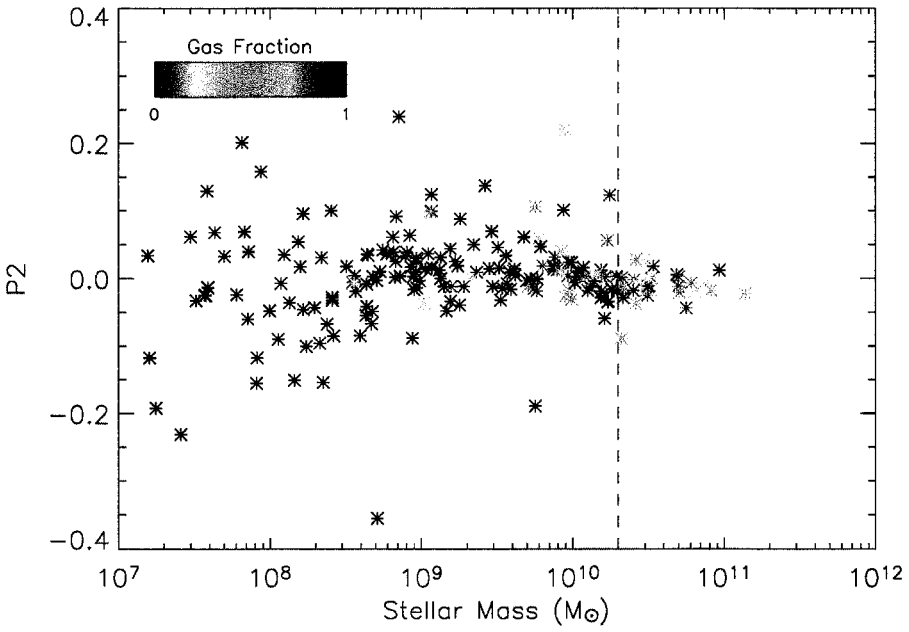

Figure 5.12 P2 PCA axis as a function of stellar mass for the HIPASS/SDSS sample. The galaxies have been color coded according to their gas fraction. The dashed line indicates the $2 \times 10^{10} M_\odot$ transition value from Baldry et al. (2004). Although there is some dispersion around that value, it looks as if the transition may occur at slightly lower values of stellar mass.

(2004) show that the number density per magnitude of red galaxies breaks from that of the blue galaxies at around $3{\times}10^{10} M_\odot$. They claim that this is evidence for the red galaxies being formed by major mergers. Baldry et al. (2004) also show that at a stellar mass of $\sim 2 \times 10^{10} M_\odot$, the $u-r$ colors of galaxies make a significant shift. Because the $u-r$ color is a good indicator of late versus early type morphology (see Strateva et al. 2001; Blanton et al. 2003a), this would imply that a morphological change in galaxies is also happening at $\sim 10^{10} M_\odot$. We find a similar transition point for the dispersion in P2 PCA variable. For the HIPASS/SDSS galaxies, the dispersion in the P2 value gets much larger around a stellar mass of $\sim 10^{10} M_\odot$ (Figure 5.12). The dashed line is the Baldry et al (2004) transition value of $2 \times 10^{10} M_\odot$. These data would indicate that the transition in color dispersion that we are seeing is related to the SFH, color and morphology changes seen in previous studies.

Dalcanton, Yoachim & Bernstein (2004) show that the presence of dust lanes in a sample

of edge-on disk galaxies is related to rotation speed. At $V_c < 120$ km/s, no dust lanes are present in their galaxies. They claim that this is due to disk instabilities occurring at $V_c > 120$ km/s, which act to collapse the dust to a small scale height and produce a larger optical depth (Verde et al. 2002). Star formation efficiency is also increased above this velocity threshold affecting the SFH and colors of the faster rotators. From our analysis of the stellar Tully-Fisher relation in Chapter 6, we find that a V_c of 120 km/s not surprisingly corresponds to a stellar mass of $\sim 10^{10} M_{\odot}$. This suggests that these transitions may be related to the same underlying physical mechanism identified by Dalcanton et al. (2004).

Figure 5.13 shows the P2 PCA variable as a function of inclination corrected HI velocity width (a proxy for rotation speed) for the HIPASS/SDSS sample. The dashed line is at the Dalcanton et al. (2004) transition of 120 km/s. Although our results might argue for a slightly larger transition velocity, it is important to remember that the velocities used are from HI line widths and may have a significant systematic offset. However, it is clear that a transition in the color dispersion does occur at rotation speeds just over 100 km/s and that the mechanism for the color transition is likely related to the onset of disk instability and an increased star formation efficiency.

It is likely that all of the transitions discussed above are evidence for a single significant change in the way stars form in galaxies. Massive galaxies have unstable disks and efficiently convert most of their primordial reservoirs of gas into stars in the first few Gyrs after their formation. These galaxies are bulge dominated and have redder, older and more massive populations of stars. Lower mass galaxies that are disk dominated are less efficient at forming stars because they are stable against disk collapse. This makes star formation much more sporadic and suggests that much of their primordial gas has been retained. This gives a likely explanation for the large color dispersions seen in my SDSS HI selected galaxy colors. The massive galaxies efficiently convert any acquired gas into stars in a well prescribed manner and the resulting colors have small dispersions. However, on the other end of the disk stability transition, star formation proceeds with small sporadic bursts that slowly convert gas into stars. At any moment of observation, a low mass galaxy can be bursting, in a quiescent mode, or somewhere in the middle. The observed star formation mode does not depend on gas fraction, stellar mass or rotation velocity, provided they are

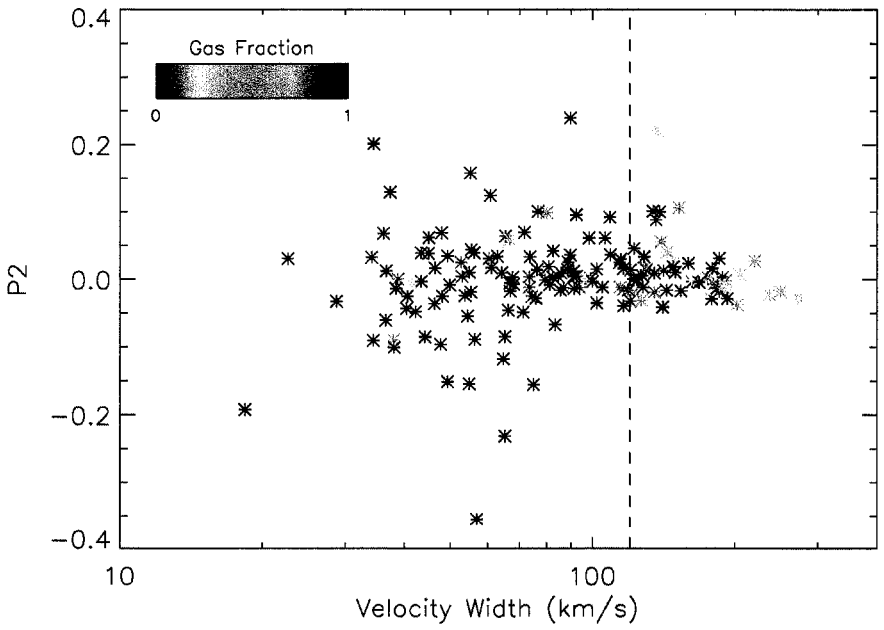

Figure 5.13 P2 PCA variable as a function of inclination corrected HI velocity width (a proxy for rotation speed) for the HIPASS/SDSS sample galaxies. The dashed line is at the Dalcanton et al. (2004) transition of 120 km/s. Although our results might argue for a slightly larger transition velocity, it is important to remember that the velocities used are from HI line widths and may have a significant systematic offset. It is important to note that an offset does appear in these data.

all below their respective stability thresholds. However, the current as well as recent star formation does play an important role in setting the observed colors of the galaxy. Therefore, the stochastic nature of low mass star formation leads to a dispersion in the observed colors.

It is yet unclear if the increase in color dispersion in the HIPASS/SDSS sample is related to the other transitions seen in the literature. It is possible that the change in dispersion is simply a selection effect. As the galaxies get bluer and more gas-rich, their surface brightness decreases. For a high surface brightness galaxy (HSB), a burst of star formation is likely to affect a small predictable change in the colors of a galaxy. However, for an LSB galaxy, a burst of star formation may dominate its colors and drastically change the observed colors. In addition, the LSB galaxies have less massive stellar disks, making them stable against disk collapse and forcing star formation to be a much more sporadic process (see above discussion). Therefore, it is not surprising that at some surface brightness, the combination of the sporadic star formation and the LSB nature of the galaxy combine to increase the dispersion in color.

Figure 5.14 shows that the P2 variable is highly correlated with surface brightness and that as we move into the LSB regime, the P2 dispersion increases. At the low surface brightnesses, the star formation in the galaxies dominates the colors and creates a larger dispersion in the colors.

5.6 Discussion

We use the population synthesis models of Bruzual & Charlot (2003) to model the SFHs and metallicities of galaxies in the HIPASS/SDSS sample. From Figure 5.2 we see that red galaxies have super solar metallicities and have SFHs that are consistent with them forming the bulk of their stars in the distance past. These red galaxies have presumably exhausted their entire primordial gas supply but have acquired gas through mergers and infall.

As galaxies get bluer, their metallicities get smaller and their mean stellar ages are younger (increasing τ values). The mean colors for the blue galaxies falls to the lowest metallicities and off the grids at around the constant SFR model line ($\tau = \infty$). It is also clear that the age-metallicity degeneracy effect is amplified for the blue galaxies. This is

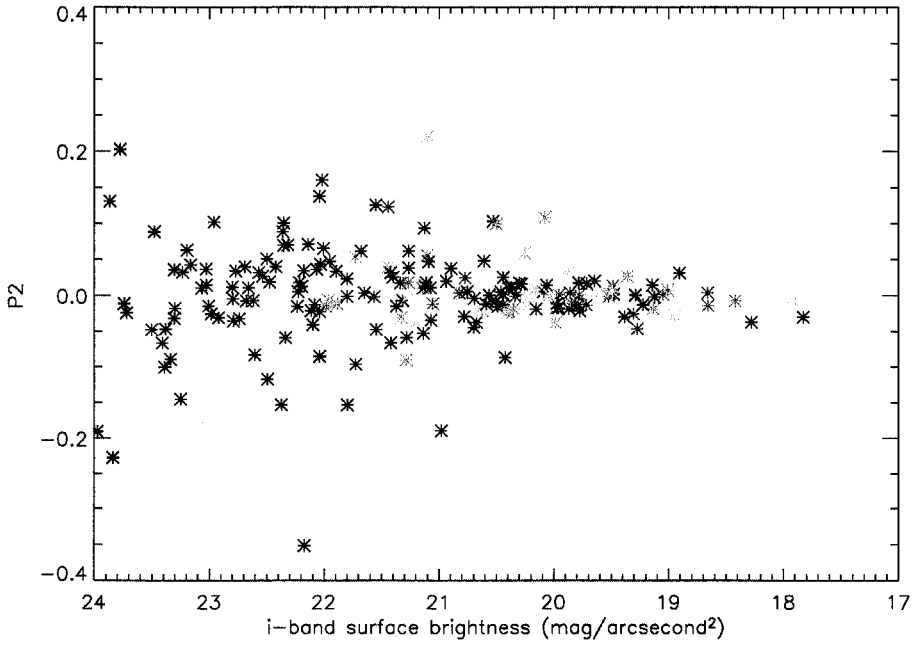

Figure 5.14 The P2 variable as a function of i-band Petrosian surface brightness. The P2 variable is highly correlated with surface brightness. This relations shows that as we move into the LSB regime, the P2 dispersion increases.

seen in the compression of the model grids and makes differentiation between models very difficult. The addition of IR data should resolve this degeneracy and will be left for future work. The gas fraction color coding in Figure 5.2 suggests that these systems have at least as much gas as they do stars. The blue galaxies are less massive and have more stable disks, making their star formation less efficient. They have likely retained much of their initial HI and are slowly converting it into stars as is suggested by the large τ values. As galaxies pass the threshold for disk stability (as discussed above), their star formation becomes sporadic and there is a clear dispersion in the colors. The idealistic Bruzual and Charlot models are likely only loose guides for these systems, as their star formation histories no longer follow smooth exponential functions.

Figure 5.2 indicates that there are only a few galaxies in the regime of exponentially increasing SFR (negative τ values). This is not surprising because there are few mechanisms that will increase the SFR of a galaxy. The likely culprit for these systems is the infall of gas. As gas is accreted, the gas densities in the galaxies will increase and gravitational collapse will become more efficient. This will increase the SFR as well as the metallicity of the galaxy, pushing its $g-r$ colors to the blue (more recent star formation) and its $r-i$ colors slightly to the red (more metals).

We also show that HI selected galaxies are offset from the SDSS galaxy locus, especially at the red end, and that this is likely due to bursts of star formation in the past few hundred Myr. The gas that induces these recent bursts is not primordial and is best explained by the accretion of gas rich dwarfs.

The bluest galaxies in the HI selected sample are not explained by population synthesis models alone. Their colors can be modeled with the inclusion of star formation induced emission lines. We show that emission line spectra with reasonable SFRs can explain the colors of the bluest galaxies in the HIPASS/SDSS sample.

We also show that the distribution of galaxies at the red end of the color-color locus has a very small dispersion that continues until a $g-r$ color of $\sim$0.5 when it suddenly gets larger. This may be explained by a change in the star formation efficiency brought on by a transition in disk stability. Red, higher mass galaxies have unstable disks that easily collapse to form stars. This makes them very efficient star formers that form the majority of

their stars in the distant past. At a rotation velocity of 120 km/s, a stellar mass of $10^{10}M_{\odot}$, a gas fraction of 0.35, and a $g-r$ color of 0.5, the disks of galaxies become more stable and star formation is no longer as efficient. This results in a larger dispersion in color as star formation in these bluer systems is best described by small percolating bursts and not an efficient disk collapse. We also supply further evidence for the suggestion of Dalcanton et al. (2004) that this stability transition occurs at the onset bulge formation and that the two are likely related.

It may be the case that the increase in dispersion is nothing more than an effect of surface brightness. The P2 dispersion axis strongly correlates with i-band surface brightness (Figure 5.14) and as the surface brightness of a system decreases, the effect of a single burst of stars on the color becomes increasingly large, possibly explaining the dispersion in scatter.

It is interesting that the change in color dispersion is not easily seen in the volume selected SDSS data. Applying the HI selection identifies a low dispersion subsample of the SDSS galaxies, most notably at the red end. As mentioned above, the red HI selected galaxies appear to be bluer in $g-r$ than the "main" SDSS sample. These two features are likely related. It is possible that the dispersion at the red end of the SDSS sample is due to gas content and not a symptom of low star formation efficiency. Since most of the red galaxies exhausted their original supply of gas long ago, this dispersion would also be an indication of recent gas infall. We leave further discussion of the "color offset" to future study.

This story, albeit still incomplete, is a significant step toward answering that fundamental question of why galaxies have the colors and morphologies that we observe.

Chapter 6

THE TULLY FISHER RELATION

6.1 Introduction

Since its initial discovery by Tully & Fisher (1977), the tight correlation between luminosity and rotation speed has been used to estimate galaxy distances (Aaronson & Mould 1986; Sakai et al. 2000),to derive peculiar velocities (Haynes et al. 1999), to probe dark matter content (Courteau et al. 2003) and to test formation models of disk galaxies (Courteau & Rix 1999; van den Bosch 2000; Pizagno et al. 2005). At a fundamental level, the tightness and form of the Tully-Fisher (TF) relation directly relate to quantities vital to the understanding of galaxy dynamics and formation such as the concentration of dark matter, the angular momentum of the disk and the ratio of baryons to dark matter (Cole et al. 1994; Dalcanton, Spergel & Summers 1997; Mo, Mao & White 1998; Steinmetz & Navarro 1999; van den Bosch 2000).

The original TF results were derived for massive spirals whose baryonic content was dominated by stars. However, when these studies were extended to lower masses, significant offsets became apparent, due to the much higher gas fractions of low mass, late-type galaxies. These offsets disappeared when the total baryon content was included. Several studies have explored the Baryonic Tully Fisher (BTF) and found that the relation has slightly different properties than the "stellar" TF, including a shallower slope (McGaugh et al. 2000; Bell & De Jong 2001; Gurovich et al. 2004).

Due to its historical use as a distance indicator, many previous studies of the TF relation have been restricted to subsamples of galaxies that meet very narrow selection criteria (Haynes et al. 1999; Courteau et al. 2003; Pizagno et al. 2005). Many of the relevant quantities are compiled from inhomogeneous data sets. These selection effects may play opposing roles in shaping the observed TF relations. The narrow galaxy selection criteria

will tend to produce the narrowest possible TF relation with the smallest degree of scatter, whereas the inhomogeneous nature of some of the data will then to increase the scatter.

HIPASS/SDSS sample an ideal data set with which to test how the slope and spread of the TF and BTF relation changes when an HI selection is applied. The HIPASS/SDSS sample contains galaxies that have been observed in a uniform manner, which should decrease much of the previous scatter caused by catalog inhomogeneities. Bell & de Jong (2001) warn that using HI line widths as velocity indicators for TF studies may yield "ill-defined" rotational velocities. Courteau (1997) and Verheijen (2001) show that although the line width TF relations have slightly more scatter, they yield similar results to those derived by HI rotation curves. Therefore some of the scatter in our TF relations will be due to what part of the rotation curve is being sampled by the line width measurement.

In this section we use the dynamical information provided by the HI spectra to investigate the TF relations from the HIPASS/SDSS sample and show that most of the scatter in our TF relations can be explained by the physical properties of the galaxy systems.

6.2 HIPASS/SDSS Tully-Fisher

Figures 6.1-6.3 show a classic TF relation with the i-band absolute Petrosian magnitude plotted as a function of inclination corrected W_{20}. Figure 6.1 includes the best fit to the TF relation (red), Figure 6.2 overplots the uncertainties and Figure 6.3 displays the fits from previous TF studies. We find a slope of -7.69±0.41 with a scatter of 1.13 magnitudes. The slope is consistent with the results of Courteau et al. (2003) as well as several other previous studies reviewed by Verheijen (2001). On the other hand, our slope is significantly shallower than the Verheijen (2001) adopted slope as well as the Sakai et al. (2000) Hubble Key project TF result. The HIPASS/SDSS sample does have many more sources at the low velocity end that may contribute to the changes in the overall slope. The scatter in our TF is also larger than many of the previous TF relations and may be a result of our small number of selection criteria.

Another way to examine the TF relation is by looking at the the stellar mass as a function of velocity (Figures 6.4-6.6). A fit to the data gives a slope of 3.43±0.19 with a scatter of

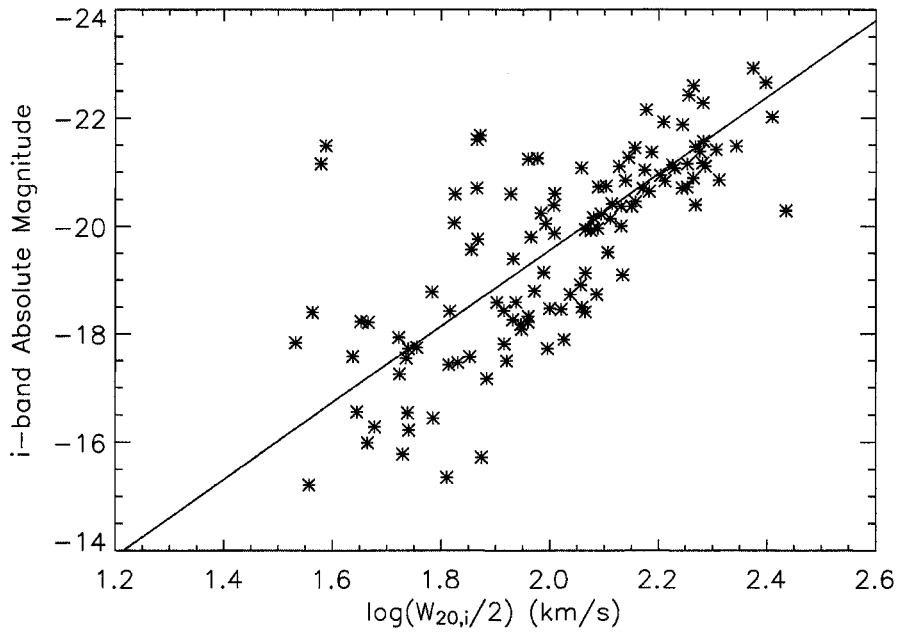

Figure 6.1 i-band Tully-Fisher relation for the HI selected galaxies. The red line is the best fit to the data. This relation has significant scatter that is likely due to the varied morphologies of the galaxies in the HIPASS/SDSS sample but has a slope that is consistent with previous results.

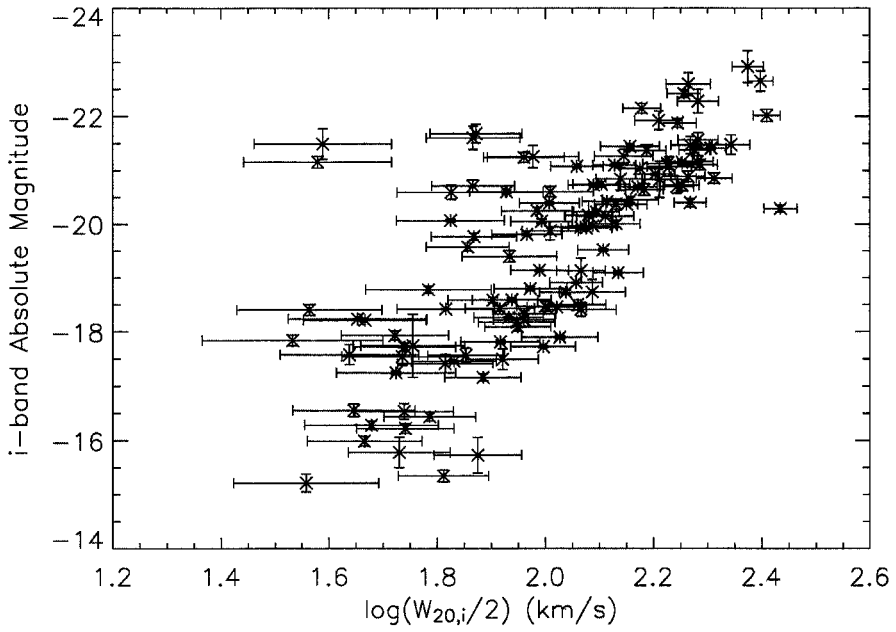

Figure 6.2 i-band Tully-Fisher relation for the HI selected galaxies. The uncertainties have been overplotted for reference.

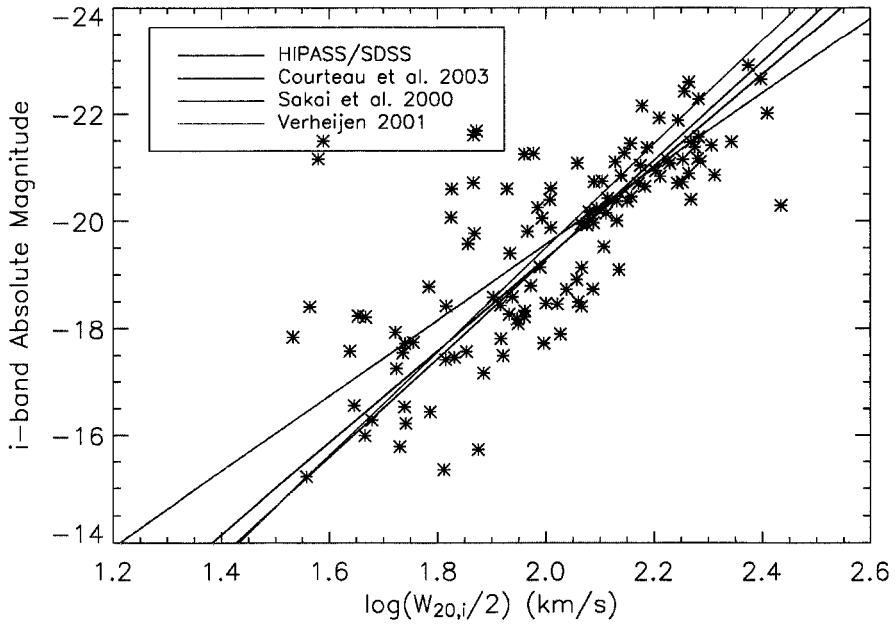

Figure 6.3 i-band Tully-Fisher relation for the HI selected galaxies. The red line is the best fit to the HIPASS/SDSS data. The other colored lines are the fits from previous TF studies.

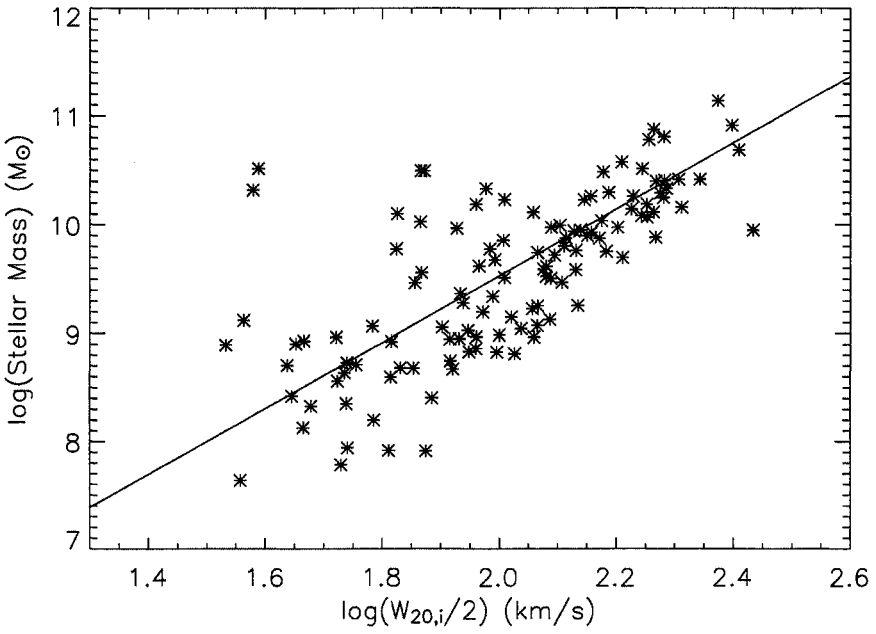

Figure 6.4 Stellar mass Tully-Fisher relation for the HIPASS/SDSS sample. The red line is the best fit to the data.

0.53 $\log(M_{\odot})$ (red line in Figure 6.4). Figure 6.5 overplots the uncertainties for reference. The stellar TF is a much more physical relationship because it tells us how the velocity of the galaxy correlates with the stellar mass. The slope that we measure is much shallower than any of the slopes measured in most previous work (Bell & de Jong 200); McGaugh et al. 2000; Gurovich et al. 2004), including those TF slopes measured in the bluest bands (see Figure 6.6). Although some of the discrepancy may lie in the sample selection, some of the difference is due to the stellar mass calculation. Both the McGaugh et al. (2000) and Gurovich et al. (2004) use fixed mass-to-light ratios that will significantly affect the slope of the stellar TF. Our stellar mass calculation is similar to the Bell & de Jong (2001) prescription but our galaxies extend to much lower velocities and stellar masses due to the HI selection. In a recent study, Pizagno et al. (2005) use SDSS disk dominated galaxies to obtain a shallow stellar TF slope of 2.92. The uniform morphologies of the galaxies in their sample may be the cause of the shallower slope.

If the TF relation is indeed the manifestation of a physical relationship between the

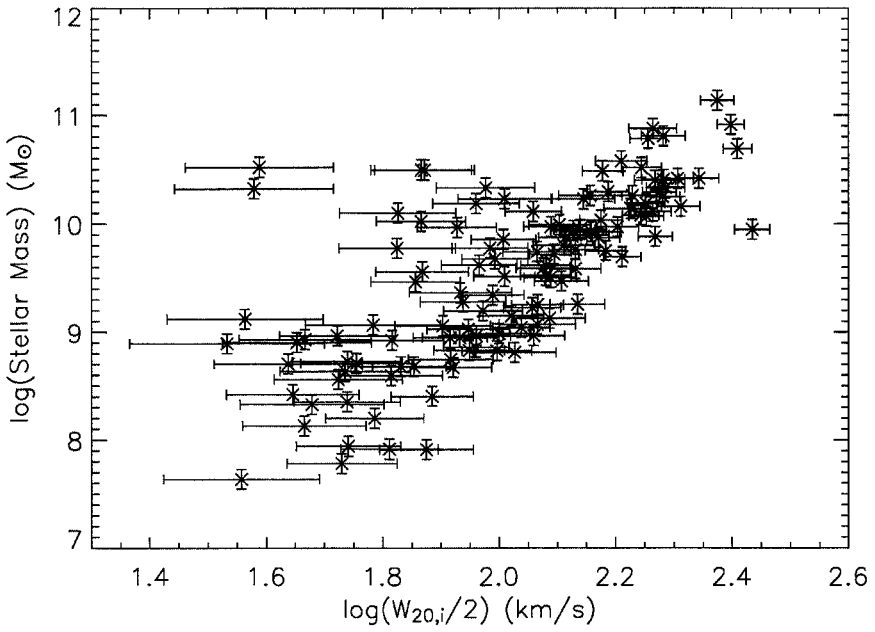

Figure 6.5 Stellar mass Tully-Fisher relation for the HIPASS/SDSS sample. Uncertainties have been overplotted for reference.

disk and the dark matter, then it seems most appropriate to investigate the BTF relation. Figure 6.7 shows the BTF for the HIPASS/SDSS sample with the best fit line plotted in red. For reference, we also include a BTF with overplotted uncertainness (Figure 6.8). As noted above, the BTF does not include any information about the molecular gas content of these systems. We measure a slope of 2.52±0.13 and a scatter of 0.37 $M_{\odot}$. The BTF relation is tighter than the TF relations for stellar properties, as expected if the TF relates to the total disk mass. Our slope is considerably shallower than the McGaugh et al. (2000) slope of ~4 as well as the Bell & de Jong (2001) value of 3.5. However, it agrees well with other HI selected BTF relations (Gurovich et al. 2004). Figure 6.9 compares our fit (red) with the fits from previous BTF studies. Most of this difference may come from an HI selection effect. The HI selected sample includes sources with higher baryon mass for a given velocity and therefore make a BTF slope much shallower. When the "reverse list" sample is complete, it will be an excellent test of the effect of the HI selection as well as the

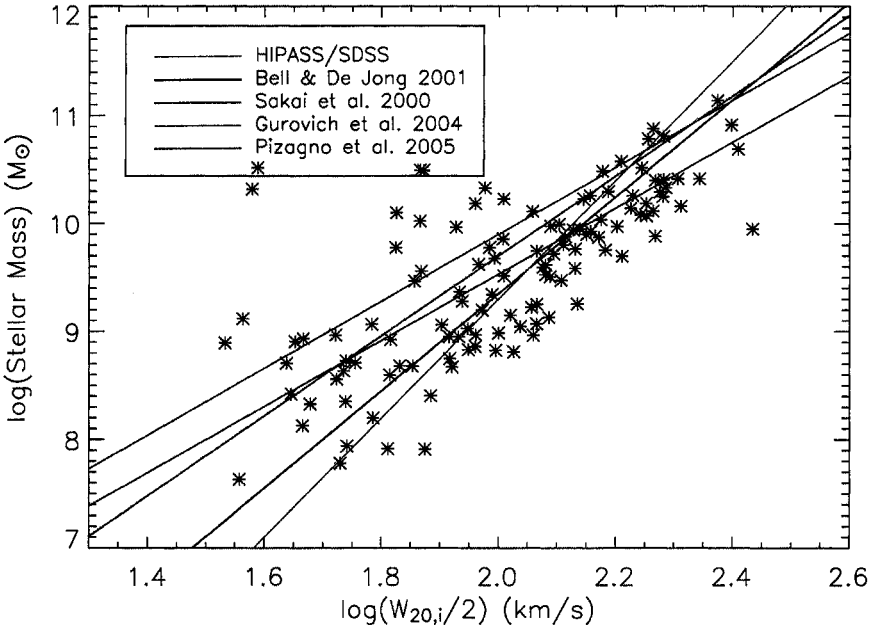

Figure 6.6 Stellar mass Tully-Fisher relation for the HIPASS/SDSS sample. The red line is the best fit to the data. The slope of this relation is significantly shallower than many previous studies (shown in other colors).

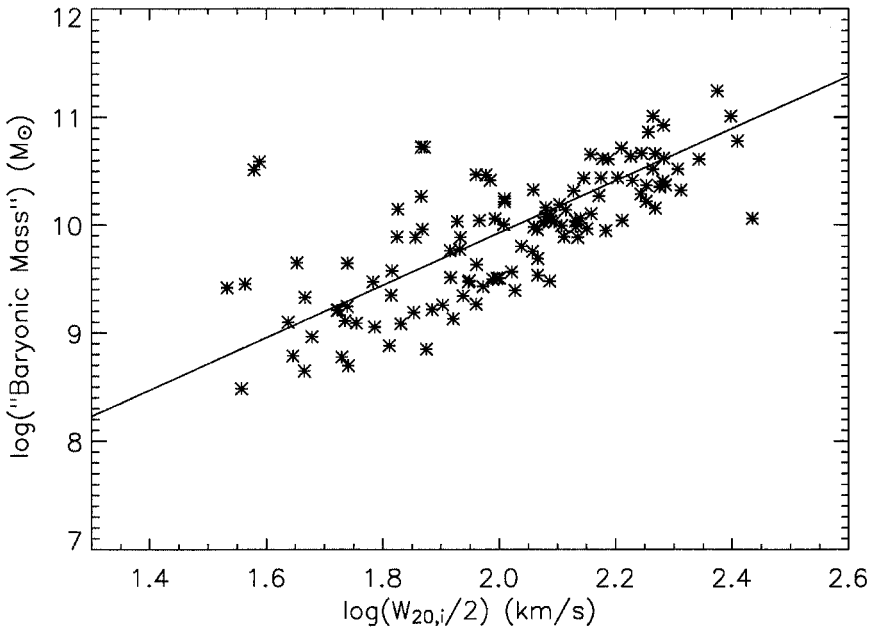

Figure 6.7 Baryonic Tully-Fisher (BTF)relation for the HIPASS/SDSS sample. The red line is the best fit to the relation.

true spread of the BTF relation.

6.3 Scatter in the Tully-Fisher Relation

We now examine the TF residuals as a function of color, gas fraction, surface brightness, inclination, distance and star/baryon mass fraction. We find small trends in the relation between the TF residuals and both the gas fraction and color, which agrees with the results of Verheijen (2001), although there is significant scatter. However, the largest correlation is with the ratio of stellar to dynamical mass as seen in Figure 6.10. Of course it is important to note that our dynamical mass estimate is a lower limit for the true halo mass and that the mass fractions are likely much lower. Figure 6.11 overplots uncertainties on Figure 6.10 and is included for reference.

The baryon mass fraction has an even tighter correlation with BTF residuals (see Figure 6.12 and 6.13). This clear trend explains most of the BTF scatter and brings the residuals

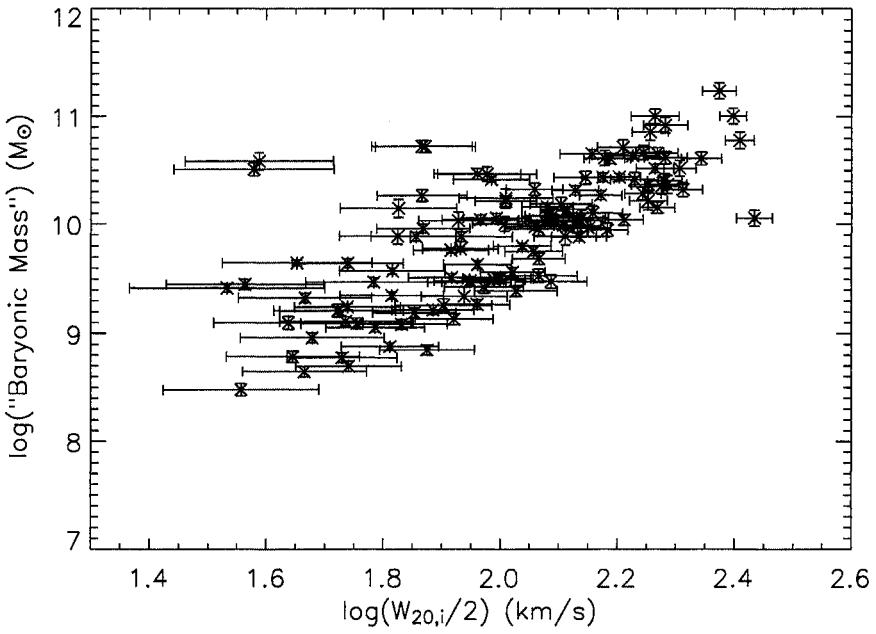

Figure 6.8 Baryonic Tully-Fisher (BTF)relation for the HI selected sample. Uncertainties have been overplotted for reference.

down below the observational errors. This suggests that galaxies with high baryonic mass fractions have more baryons at a given velocity than galaxies with lower mass fractions. Physically, this directly relates to how spread out the baryons are in the dark halo and puts more constraints on disk formation models. A plane fit to the M_{baryon}, M_{dyn} and V_{rot} and data yields a low scatter relation that is plotted in Figure 6.14 and given by:

$$log(V_{rot}) = -1.30 - 0.17\log(M_{baryon}) + 0.46\log(M_{dyn}). \quad (6.1)$$

This result is predicted in Mo et al. (1998), who show that in the formation of disk galaxies, the disk mass relates to the circular velocity (V_c) and the baryonic mass fraction (m_d) by the equation:

$$M_d \approx 1.7 \times 10^{11} h^{-1} \left(\frac{m_d}{0.05}\right) \left(\frac{V_c}{250 kms^{-1}}\right)^3. \quad (6.2)$$

Algebraic manipulation of Equation 6.2 allows us to calculate a velocity using my M_{baryon}

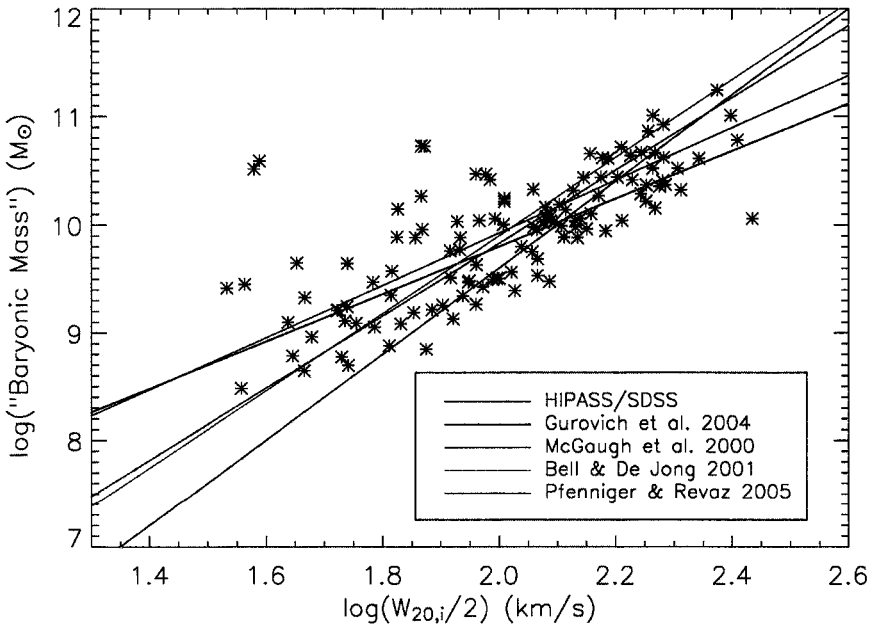

Figure 6.9 Baryonic Tully-Fisher (BTF)relation for the HI selected sample. The red line is the best fit to our relation. The baryonic relation has significantly lower scatter than any of the other TF relations. Although the BTF has shallower slope than most previous results, it does agree with other HI selected samples. This would suggest that the HI selection might act to shallow the slope.

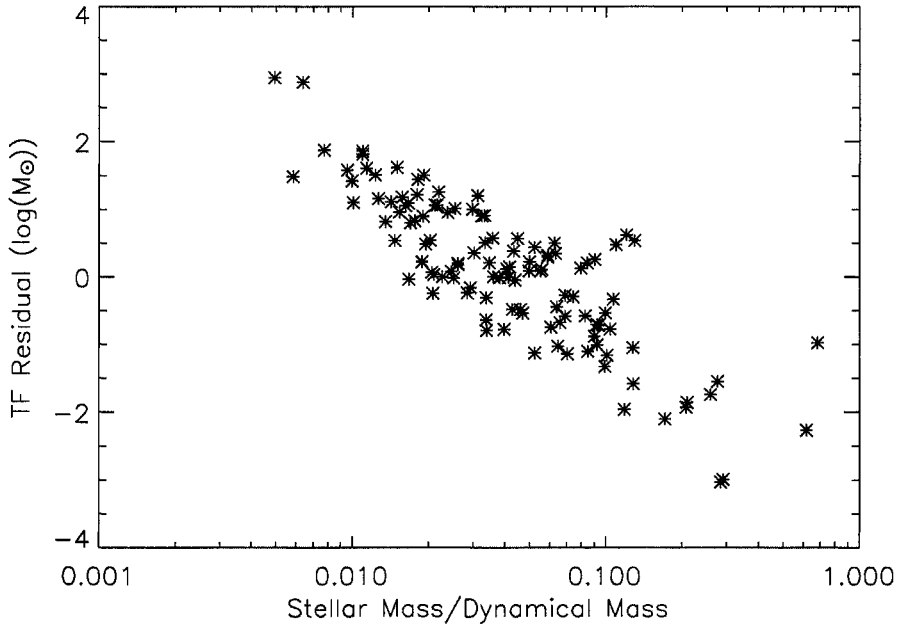

Figure 6.10 Stellar mass Tully-Fisher residuals as a function of stellar mass to dynamical mass. The residuals clearly correlate with the mass fraction. Some of the remaining scatter is due to the exclusion of baryons from the classical TF relation.

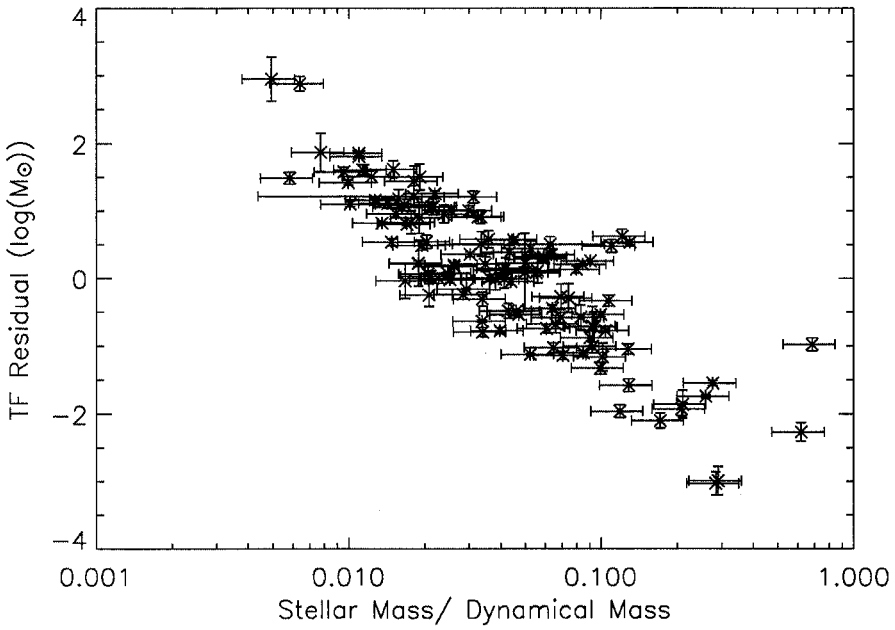

Figure 6.11 Stellar mass Tully-Fisher residuals as a function of stellar mass to dynamical mass. Uncertainties are overplotted for reference.

and M_{dyn}. The results are overplotted on our plane fit in Figure 6.15 (red symbols). The velocities calculated from the Mo et al. (1998) relation are all too low by a constant factor. This offset is likely due to the fact that we have underestimated the total halo mass. However, it is surprising that the same factor of halo mass is missing for all of the sources. A factor of 4 times M_{dyn} brings the velocities into agreement (Figure 6.16). This may suggest that baryon and dark halo extents are very closely related to each other in some uniform way. Regardless of the underlying physics, these data demonstrate that the inclusion of baryonic mass fraction collapses the BTF relation to a "fundamental" plane with very small scatter.

6.4 Discussion

Our TF relations have significantly shallower slopes than most previous TF studies. This may be due to the HI selection or perhaps the uniform quality of our sample. The TF

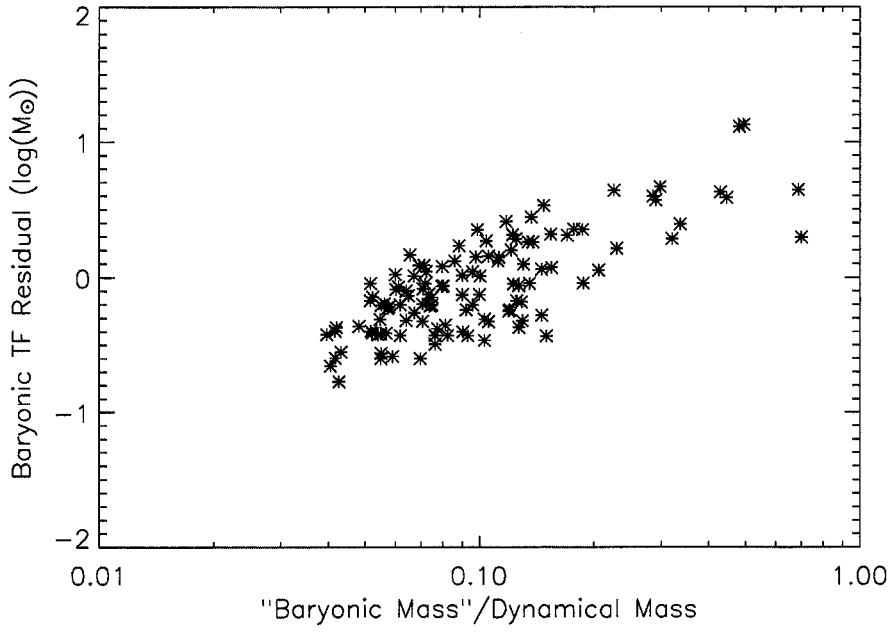

Figure 6.12 Baryonic Tully-Fisher residuals as a function of baryonic mass fraction. The residuals are clearly mapped by the fraction of baryons to dark matter. The small amount of remaining scatter is close to the uncertainties in the derived quantities.

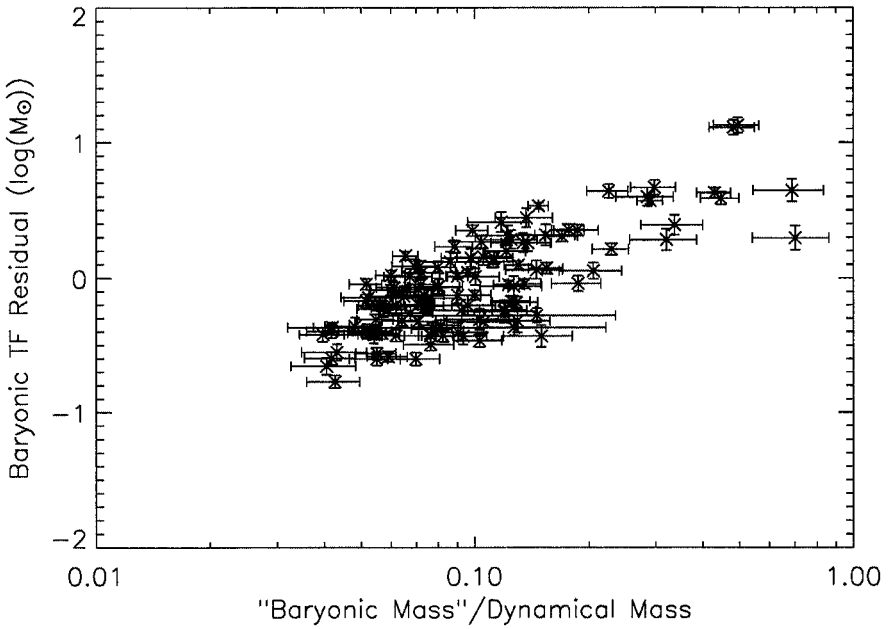

Figure 6.13 Baryonic Tully-Fisher residuals as a function of baryonic mass fraction. Uncertainties are overplotted for reference.

residuals appear to strongly correlate with the stellar/baryonic mass fraction, which is expected from models of galactic disk formation. We derive a new "fundamental plane" for disk galaxies that relates the baryonic and dark matter to the rotation velocity. Further studies will demonstrate the usefulness of this "plane" for deriving properties of galaxies and constraining formation models of late-type systems.

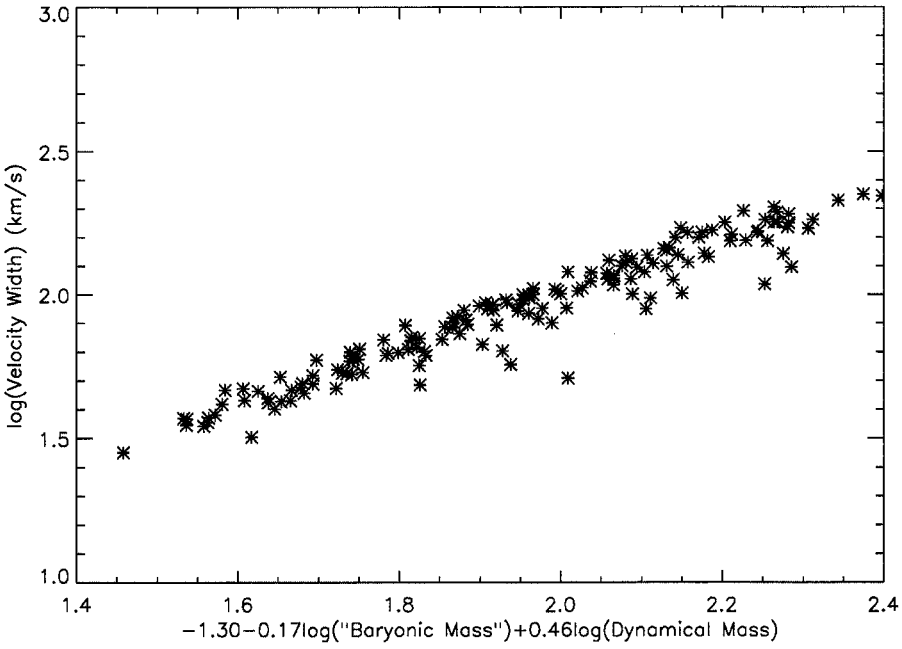

Figure 6.14 Projection of the log(velocity), log(baryonic mass), log(dynamical mass) plane. The scatter is very low and is certainly smaller than the uncertainties in the derived values. The addition of dynamical mass, almost eliminates the scatter of the baryonic Tully-Fisher relation.

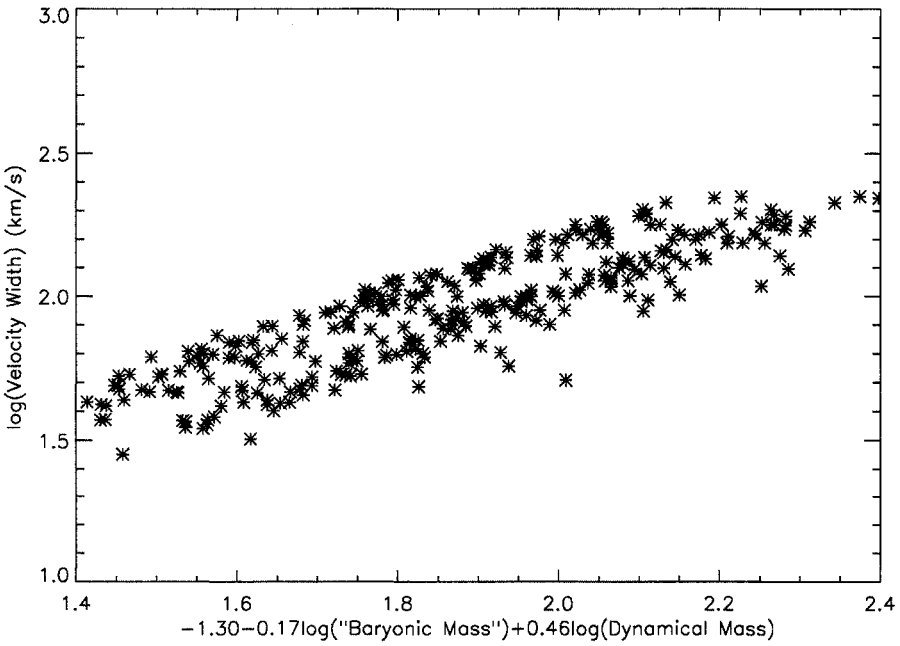

Figure 6.15 Projection of the log(velocity), log(baryonic mass), log(dynamical mass) plane for the HIPASS/SDSS sample (black). The red symbols are the velocities derived from the reformulation of Mo, Mao and White's (1998) disk mass equation (Equation 6.2. The relation appears to be offset by a constant factor.

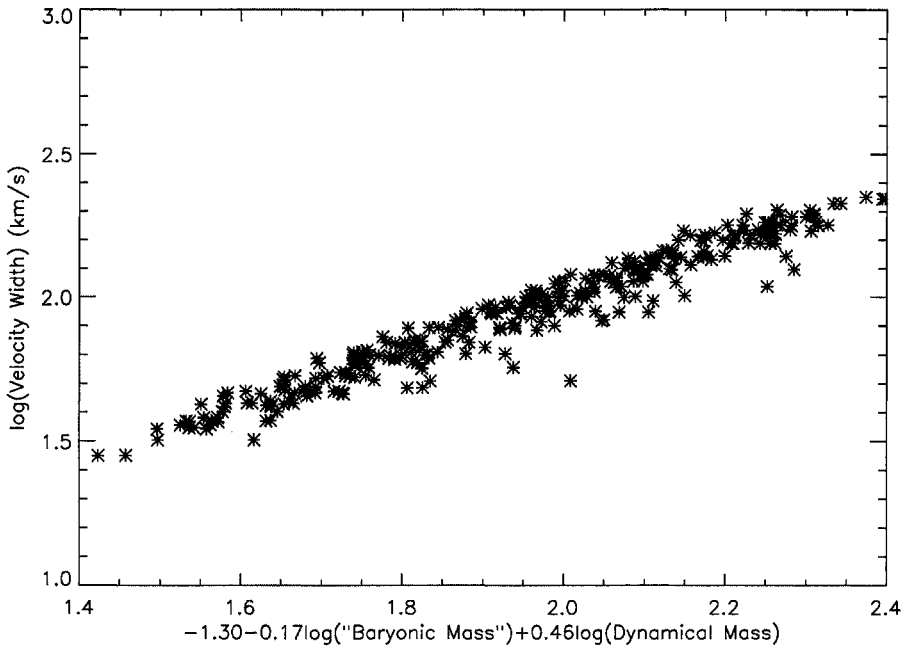

Figure 6.16 Projection of the log(velocity), log(baryonic mass), log(dynamical mass) plane for the HIPASS/SDSSS sample (black). The red symbols are the velocities derived from the reformulation of Mo, Mao and White's (1998) disk mass equation (Equation 6.2. For this figure we have multiplied the dynamical mass by a factor of 4 in calculating the Mo et al. (1998) velocities. This brings the data into alignment.

Chapter 7

CONCLUSIONS

7.1 Introduction

One of the fundamental questions in galaxy evolution is why do galaxies look the way they do? The quality of data coming from large surveys such as SDSS and HIPASS, coupled with the advancements made to star formation models are allowing for a realistic story of star formation in galaxies to be told. One of the goals of this thesis was to provide a uniform observational dataset of the optical and gaseous properties of nearby galaxies that could be used to probe some of these fundamental questions. We have accomplished that goal and provided the first set of scientific results from our HIPASS/SDSS catalog. In this chapter we briefly review the research presented in this thesis and discuss some of the future work that is planned.

7.2 Summary of Thesis

We have created an HI selected catalog using data from the HIPASS and SDSS surveys. These data are uniformly sampled and have well characterized uncertainties and limitations. Our HI selected catalog identifies a large number of blue, LSB galaxies, some of which were previously unidentified. Because LSB galaxies are not allocating SDSS fibers for spectroscopy, many of the galaxies in the HIPASS/SDSS catalog have not been included in previous SDSS nearby galaxy studies. We therefore have uncovered a more complete picture of the baryonic content of the nearby universe.

To account for the fact that the SDSS photometric software was optimized for studying small, distant galaxies, we have created our own software for analyzing large galaxies in the SDSS. In addition, we have explored new ways to correct for SDSS problematic reductions at the catalog level.

We find that the HIPASS/SDSS galaxies span a large range of gas fractions, surface brightnesses and colors, but that as expected, the HI selection identifies a large number of galaxies at the gas-rich extreme of the evolutionary continuum. The different colors and gas fractions of the galaxies in the HIPASS/SDSS sample can be explained by changes in the star formation efficiency and the stability of galactic disks against gravity.

By comparing the colors of the HIPASS/SDSS galaxies to the population synthesis models of Bruzual & Charlot (2003), we confirm that the red, HSB, low gas fraction galaxies in our sample are efficient, high metallicity star formers that formed the bulk of their stars in the distant past. Their current reservoir of gas is likely the product of recent mergers and the infall of gas-rich dwarfs. The colors of the red HIPASS/SDSS galaxies are offset from the SDSS main galaxies. This is explained by a recent burst of stars in the last several hundred Myr and is further bolstered by the observation of emission lines in the SDSS spectra of all of these red, offset sources.

As galaxies get bluer, their metallicities get smaller and their mean stellar ages are younger (increasing τ values). The mean colors for the blue galaxies falls to the lowest metallicities and off the grids at around the constant SFR model line ($\tau = \infty$). It is also clear that the age-metallicity degeneracy effect is amplified for the blue galaxies. This is seen in the compression of the model grids and makes differentiation between models very difficult. The addition of IR data should resolve this degeneracy and will be left for future work. The idealistic Bruzual and Charlot models are likely only loose guides for these systems, as their star formation histories no longer follow smooth exponential functions.

There are only a few galaxies in the HIPASS/SDSS that fall in the regime of exponentially increasing SFR (negative τ values). This is not surprising because there are few mechanisms that will increase the SFR of a galaxy. The likely culprit for these systems is the infall of gas. As gas is accreted, the gas densities in the galaxies will increase and gravitational collapse will become more efficient. This will increase the SFR as well as the metallicity of the galaxy, pushing its $g - r$ colors to the blue (more recent star formation) and its $r - i$ colors slightly to the red (more metals).

We also show that HI selected galaxies are offset from the SDSS galaxy locus, especially at the red end, and that this is likely due to bursts of star formation in the past few hundred

Myr. The gas that induces these recent bursts is not primordial and is best explained by the accretion of gas rich dwarfs.

The bluest galaxies in the HI selected sample are not explained by population synthesis models alone. Their colors can be modeled with the inclusion of star formation induced emission lines. We show that emission line spectra with reasonable SFRs can explain the colors of the bluest galaxies in the HIPASS/SDSS sample.

We observe an increase in the dispersion of the colors in the HIPASS/SDSS galaxies at $g - r \sim 0.5$. Although this may be due to a fundamental and abrupt change in the star formation efficiency, it is most likely a surface brightness effect, where star formation in LSB galaxies makes a significant change in the integrated color of the system, thus increasing the dispersion in the color.

Using the dynamical information provided by the HI spectra, we find that the TF relations for the HIPASS/SDSS galaxies have significantly shallower slopes than most previous TF studies. This may be due to the HI selection or perhaps the uniform quality of our sample. The TF residuals appear to strongly correlate with the stellar/baryonic mass fraction, which is expected from models of galactic disk formation. We derive a new "fundamental plane" for disk galaxies that relates the baryonic and dark matter to the rotation velocity. Further studies will demonstrate the usefulness of this "plane" for deriving properties of galaxies and constraining formation models of late-type systems.

7.3 Future Work

Both the HIPASS and SDSS surveys have increased in sky coverage since we finalized our catalog for this thesis. We plan to augment our current catalog with possibly as many as 200 more sources from these additional survey data.

The northern equivalent of HIPASS, the HI Jodrell Bank All Sky Survey (HIJASS) has direct overlap with SDSS and can provide a number of new sources for our HI selected catalog. In addition to HIJASS, there are a number of previous and current HI programs using the Arecibo observatory. Almost all of the HI sources have SDSS counterparts. The advantage of Arecibo is that its larger dish, creates a smaller beam size, providing less

confusion (see Chapter 2) and its large collecting area allows for lower HI masses to be observed. We plan to use our SDSS data reduction tools to build optical catalogs for several of the Arecibo HI surveys.

As mentioned in Chapter 2, we have begun work on a "reverse list", which is an optically selected, volume-limited sample of SDSS galaxies. This catalog will provide a much more relevant comparison sample to the HI selected HIPASS/SDSS sample. Using both the "forward" and "reverse" lists, we will be able to accurately compare the differences between a classical optically selected sample and an HI selected sample.

Because molecular gas is fundamentally important to the formation of stars, we would like to take CO observations for the entire HIPASS/SDSS sample. Plans are underway to apply for time on single dish and subsequent synthesis telescopes.

The suite of tools that we designed for analyzing large galaxies in SDSS has allowed us to begin building an SDSS Atlas of Nearby Galaxies. We hope to not only create a catalog of art-quality images that can be used by the popular press and the public, but also a set of scientifically useful images and parameters for all large galaxies in the SDSS.

This thesis is a another small step toward understanding the mechanisms behind how galaxies convert their gas into stars. It is also the beginning of a new career and the end of a very long journey.

BIBLIOGRAPHY

Aaronson, M., & Mould, J. 1986, ApJ, 303, 1

Abazajian, K., Adelman-McCarthy, J. K., Agüeros, M. A., Allam, S. S., Anderson, K. S. J., Anderson, S. F., Annis, J., Bahcall, N. A., et al. 2005a, AJ, 129, 1755

Abazajian, K. et al. 2005b, in preparation

Abazajian, K., Adelman-McCarthy, J. K., Agüeros, M. A., Allam, S. S., Anderson, K. S. J., Anderson, S. F., Annis, J., Bahcall, N. A., et al. 2004, AJ, 128, 502

Agüeros, M. A. et al. 2005, AJ, in press

Anders, P., & Fritze-v. Alvensleben, U. 2003, A&A, 401, 1063

Balcells, M., & Peletier, R. F. 1994, AJ, 107, 135

Baldry, I. K., Glazebrook, K., Brinkmann, J., Ivezić, Ž., Lupton, R. H., Nichol, R. C., & Szalay, A. S. 2004, ApJ, 600, 681

Barnes, D. G., Staveley-Smith, L., de Blok, W. J. G., Oosterloo, T., Stewart, I. M., Wright, A. E., Banks, G. D., Bhathal, R., et al. 2001, MNRAS, 322, 486

Barnes, D. G., Staveley-Smith, L., Webster, R. L., & Walsh, W. 1997, MNRAS, 288, 307

Begum, A., Chengalur, J. N., & Karachentsev, I. D. 2005, A&A, 433, L1

Bell, E. F., & de Jong, R. S. 2000, MNRAS, 312, 497

Bell, E. F., McIntosh, D. H., Katz, N., & Weinberg, M. D. 2003, ApJS, 149, 289

Bertin, E., & Arnouts, S. 1996, A&AS, 117, 393

Blanton, M. R., Brinkmann, J., Csabai, I., Doi, M., Eisenstein, D., Fukugita, M., Gunn, J. E., Hogg, D. W., et al. 2003a, AJ, 125, 2348

Blanton, M. R., Dalcanton, J., Eisenstein, D., Loveday, J., Strauss, M. A., SubbaRao, M., Weinberg, D. H., Anderson, J. E., et al. 2001, AJ, 121, 2358

Blanton, M. R., Hogg, D. W., Bahcall, N. A., Baldry, I. K., Brinkmann, J., Csabai, I., Eisenstein, D., Fukugita, M., et al. 2003b, ApJ, 594, 186

Bosma, A. 1978, Ph.D. Thesis

Braun, R. 1997, ApJ, 484, 637

Brinchmann, J., Charlot, S., White, S. D. M., Tremonti, C., Kauffmann, G., Heckman, T., & Brinkmann, J. 2004, MNRAS, 351, 1151

Bruzual, G., & Charlot, S. 2003, MNRAS, 344, 1000

Burkholder, V., Impey, C., & Sprayberry, D. 2001, AJ, 122, 2318

Carignan, C., & Beaulieu, S. 1989, ApJ, 347, 760

Cayatte, V., Kotanyi, C., Balkowski, C., & van Gorkom, J. H. 1994, AJ, 107, 1003

Chabrier, G. 2003, PASP, 115, 763

Cole, S., Aragon-Salamanca, A., Frenk, C. S., Navarro, J. F., & Zepf, S. E. 1994, MNRAS, 271, 781

Courteau, S. 1996, ApJS, 103, 363

—. 1997, AJ, 114, 2402

Courteau, S., Andersen, D. R., Bershady, M. A., MacArthur, L. A., & Rix, H. 2003, ApJ, 594, 208

Courteau, S., & Rix, H. 1999, ApJ, 513, 561

Covey, K. R. et al. 2005, in preparation

Dalcanton, J. J., Spergel, D. N., & Summers, F. J. 1997, ApJ, 482, 659

Dalcanton, J. J., Yoachim, P., & Bernstein, R. A. 2004, ApJ, 608, 189

de Jong, R. S. 1996, Journal of Astronomical Data, 2, 1

Dickey, J. M. 1997, AJ, 113, 1939

Disney, M. J. 1976, Nature, 263, 573

Ewen, H. I.,& Purcell, E. M. 1951, Nature, 168, 356

Fall, S. M., & Efstathiou, G. 1980, MNRAS, 193, 189

Fisher, J. R., & Tully, R. B. 1981, ApJS, 47, 139

Fukugita, M., Ichikawa, T., Gunn, J. E., Doi, M., Shimasaku, K., & Schneider, D. P. 1996, AJ, 111, 1748

Galaz, G., Dalcanton, J. J., Infante, L., & Treister, E. 2002, AJ, 124, 1360

Garcia-Appadoo, D. A., 2005, Ph.D Thesis

Garnett, D. R. 2002, ApJ, 581, 1019

Gavazzi, G., Bonfanti, C., Sanvito, G., Boselli, A., & Scodeggio, M. 2002, ApJ, 576, 135

Gavazzi, G., & Boselli, A. 1996, Astrophysical Letters Communications, 35, 1

Gunn, J. E. 1977, ApJ, 218, 592

Gunn, J. E., Carr, M., Rockosi, C., Sekiguchi, M., Berry, K., Elms, B., de Haas, E., Ivezić, Ž., et al. 1998, AJ, 116, 3040

Gurovich, S., McGaugh, S. S., Freeman, K. C., Jerjen, H., Staveley-Smith, L., & De Blok, W. J. G. 2004, Publications of the Astronomical Society of Australia, 21, 412

Haynes, M. P., Giovanelli, R., Chamaraux, P., da Costa, L. N., Freudling, W., Salzer, J. J., & Wegner, G. 1999, AJ, 117, 2039

Haynes, M. P., & Roberts, M. S. 1979, ApJ, 227, 767

Helmboldt, J. F., Walterbos, R. A. M., Bothun, G. D., O'Neil, K., & de Blok, W. J. G. 2004, ApJ, 613, 914

Henning, P. A. 1992, ApJS, 78, 365

—. 1995, ApJ, 450, 578

Hogg, D. W., Finkbeiner, D. P., Schlegel, D. J., & Gunn, J. E. 2001, AJ, 122, 2129

Hopkins, A. M., Miller, C. J., Nichol, R. C., Connolly, A. J., Bernardi, M., Gómez, P. L., Goto, T., Tremonti, C. A., et al. 2003, ApJ, 599, 971

Hubble, E. 1929, Proceedings of the National Academy of Science, 15, 168

Hunter, D. A., Elmegreen, B. G., & Baker, A. L. 1998, ApJ, 493, 595

Iglesias-Páramo, J., van Driel, W., Duc, P.-A., Papaderos, P., Vílchez, J. M., Cayatte, V., Balkowski, C., O'Neil, K., et al. 2003, A&A, 406, 453

Jarrett, T. H., Chester, T., Cutri, R., Schneider, S., Skrutskie, M., & Huchra, J. P. 2000, AJ, 119, 2498

Juneau, S., Glazebrook, K., Crampton, D., McCarthy, P. J., Savaglio, S., Abraham, R., Carlberg, R. G., Chen, H., et al. 2005, ApJ, 619, L135

Kannappan, S. J. 2004, ApJ, 611, L89

Karachentsev, I. D., Karachentseva, V. E., Huchtmeier, W. K., & Makarov, D. I. 2004, AJ, 127, 2031

Katz, N., Keres, D., Dave, R., & Weinberg, D. H. 2003, in ASSL Vol. 281: The IGM/Galaxy Connection. The Distribution of Baryons at z=0, 185–+

Kauffmann, G., Heckman, T. M., White, S. D. M., Charlot, S., Tremonti, C., Brinchmann, J., Bruzual, G., Peng, E. W., et al. 2003, MNRAS, 341, 33

Kennicutt, R. C. 1989, ApJ, 344, 685

—. 1998, ApJ, 498, 541

Kennicutt, R. C., Tamblyn, P., & Congdon, C. E. 1994, ApJ, 435, 22

Kewley, L. J., Dopita, M. A., Sutherland, R. S., Heisler, C. A., & Trevena, J. 2001, ApJ, 556, 121

Kron, R. G. 1980, ApJS, 43, 305

Krumm, N., & Brosch, N. 1984, AJ, 89, 1461

Lo, K. Y., & Sargent, W. L. W. 1979, ApJ, 227, 756

Loren, R. B., vanden Bout, P. A., & Davis, J. H. 1973, ApJ, 185, L67+

Lupton, R. H., Gunn, J. E., & Szalay, A. S. 1999, AJ, 118, 1406

MacArthur, L. A., Courteau, S., Bell, E., & Holtzman, J. A. 2004, ApJS, 152, 175

MacArthur, L. A., Courteau, S., & Holtzman, J. A. 2003, ApJ, 582, 689

Magris C., G., Binette, L., & Bruzual A., G. 2003, ApJS, 149, 313

Matthews, L. D., Gallagher, J. S., & van Driel, W. 1999, AJ, 118, 2751

McGaugh, S. S., & de Blok, W. J. G. 1997, ApJ, 481, 689

McGaugh, S. S., Schombert, J. M., Bothun, G. D., & de Blok, W. J. G. 2000, ApJ, 533, L99

McMahon, P. M. 1993, Ph.D. Thesis

Meurer, G. R., Carignan, C., Beaulieu, S. F., & Freeman, K. C. 1996, AJ, 111, 1551

Meyer, M. J., Zwaan, M. A., Webster, R. L., Staveley-Smith, L., Ryan-Weber, E., Drinkwater, M. J., Barnes, D. G., Howlett, M., et al. 2004, MNRAS, 350, 1195

Mo, H. J., Mao, S., & White, S. D. M. 1998, MNRAS, 295, 319

Muller, C. A. & Oort, J. H. 1951, Nature, 168, 357

Oke, J. B., & Gunn, J. E. 1983, ApJ, 266, 713

Petrosian, V. 1976, ApJ, 209, L1

Pier, J. R., Munn, J. A., Hindsley, R. B., Hennessy, G. S., Kent, S. M., Lupton, R. H., & Ivezić, Ž. 2003, AJ, 125, 1559

Pizagno, J. et al. 2005, ApJ, in press

Roberts, M. S. 1963, ARA&A, 1, 149

Roberts, M. S., & Haynes, M. P. 1994, ARA&A, 32, 115

Rosenberg, J. L., & Schneider, S. E. 2000, ApJS, 130, 177

—. 2002, ApJ, 567, 247

Rosenberg, J. L., Schneider, S. E., & Posson-Brown, J. 2005, AJ, 129, 1311

Sérsic, J. L. 1968, Boletin de la Asociacion Argentina de Astronomia La Plata Argentina, 13, 20

Sakai, S., Mould, J. R., Hughes, S. M. G., Huchra, J. P., Macri, L. M., Kennicutt, R. C., Gibson, B. K., Ferrarese, L., et al. 2000, ApJ, 529, 698

Salim, S., Charlot, S., Rich, R. M., Kauffmann, G., Heckman, T. M., Barlow, T. A., Bianchi, L., Byun, Y., et al. 2005, ApJ, 619, L39

Schlegel, D. J., Finkbeiner, D. P., & Davis, M. 1998, ApJ, 500, 525

Scodeggio, M., & Gavazzi, G. 1993, ApJ, 409, 110

Searle, L., Sargent, W. L. W., & Bagnuolo, W. G. 1973, ApJ, 179, 427

Shen, S., Mo, H. J., White, S. D. M., Blanton, M. R., Kauffmann, G., Voges, W., Brinkmann, J., & Csabai, I. 2003, MNRAS, 343, 978

Shostak, G. S. 1977, A&A, 54, 919

Smith, J. A., Tucker, D. L., Kent, S., Richmond, M. W., Fukugita, M., Ichikawa, T., Ichikawa, S., Jorgensen, A. M., et al. 2002, AJ, 123, 2121

Spitzak, J. G., & Schneider, S. E. 1998, ApJS, 119, 159

Steinmetz, M., & Navarro, J. F. 1999, ApJ, 513, 555

Strateva, I., Ivezić, Ž., Knapp, G. R., Narayanan, V. K., Strauss, M. A., Gunn, J. E., Lupton, R. H., Schlegel, D., et al. 2001, AJ, 122, 1861

Strauss, M. A., Weinberg, D. H., Lupton, R. H., Narayanan, V. K., Annis, J., Bernardi, M., Blanton, M., Burles, S., et al. 2002, AJ, 124, 1810

Swaters, R. A., van Albada, T. S., van der Hulst, J. M., & Sancisi, R. 2002, A&A, 390, 829

Szomoru, A., van Gorkom, J. H., & Gregg, M. D. 1996, AJ, 111, 2141

Tavarez, M. 2005, Ph.D Thesis

Terry, J. N., Paturel, G., & Ekholm, T. 2002, A&A, 393, 57

Theureau, G., Rauzy, S., Bottinelli, L., & Gouguenheim, L. 1998, A&A, 340, 21

Tinsley, B. M. 1972, A&A, 20, 383

Tinsley, B. M., & Gunn, J. E. 1976, ApJ, 203, 52

Tremonti, C. A., Heckman, T. M., Kauffmann, G., Brinchmann, J., Charlot, S., White, S. D. M., Seibert, M., Peng, E. W., et al. 2004, ApJ, 613, 898

Tully, R. B., & Fisher, J. R. 1977, A&A, 54, 661

Tully, R. B., Pierce, M. J., Huang, J., Saunders, W., Verheijen, M. A. W., & Witchalls, P. L. 1998, AJ, 115, 2264

van Albada, T. S., Bahcall, J. N., Begeman, K., & Sancisi, R. 1985, ApJ, 295, 305

van de Hulst, H. C. 1945, Ned. Tijd. Natuurk., 11, 210

van den Bosch, F. C. 2000, ApJ, 530, 177

van Zee, L. 2001, AJ, 121, 2003

Verde, L., Oh, S. P., & Jimenez, R. 2002, MNRAS, 336, 541

Verheijen, M. A. W. 2001, ApJ, 563, 694

West, A. A. et al. 2005, in preparation

Wong, T., & Blitz, L. 2002, ApJ, 569, 157

Yasuda, N., Fukugita, M., Narayanan, V. K., Lupton, R. H., Strateva, I., Strauss, M. A., Ivezić, Ž., Kim, R. S. J., et al. 2001, AJ, 122, 1104

York, D. G., Adelman, J., Anderson, J. E., Anderson, S. F., Annis, J., Bahcall, N. A., Bakken, J. A., Barkhouser, R., et al. 2000, AJ, 120, 1579

Zackrisson, E., Bergvall, N., & Östlin, G. 2005, A&A, 435, 29

Zackrisson, E., Bergvall, N., Olofsson, K., & Siebert, A. 2001, A&A, 375, 814

Zwaan, M. A., Briggs, F. H., Sprayberry, D., & Sorar, E. 1997, ApJ, 490, 173

Zwaan, M. A., Meyer, M. J., Staveley-Smith, L., & Webster, R. L. 2005, MNRAS, 359, L30

Zwaan, M. A., Meyer, M. J., Webster, R. L., Staveley-Smith, L., Drinkwater, M. J., Barnes, D. G., Bhathal, R., de Blok, W. J. G., et al. 2004, MNRAS, 350, 1210

Appendix A

PHOTOMETRY OF LARGE GALAXIES IN SDSS

A.1 Introduction

The Sloan Digital Sky Survey (SDSS) provides high quality photometry and spectroscopy for millions of astronomical objects. These data have been used to discover the most distant objects in the universe, probe the formation and evolution of galaxies and analyze the properties of low-mass stars. Where the survey has fallen short is in the study of large, nearby galaxies. Because the photometric software used for SDSS was optimized for studying large scale structure traced by marginally resolved galaxies, there are several problems that occur when examining much more extended nearby galaxies. Presently, astronomers either incorrectly include these problematic data in their analysis of nearby galaxies; or completely ignore objects closer than $z < 0.02$, to minimize their impact (Blanton et al. 2003a). The nearby SDSS universe *cannot* be studied at the catalog level. However, the extremely high quality of the SDSS imaging of nearby galaxies is unparalleled and there is much to learn from the large galaxies in SDSS, provided the proper tools can be developed. New techniques are therefore needed to properly analyze these galaxies.

To accurately derive photometric properties from the large galaxies in SDSS, three major problems in the SDSS reductions need to be addressed: deblending, inclination effects and sky subtraction. In this appendix, each of these three problems will be addressed and the extent to which each problem affects a proper analysis of SDSS photometry will be discussed. Perhaps more importantly, several mean relations that will be useful for making corrections to the SDSS catalog data are provided . The detailed discussion of the application of these corrections to the HIPASS/SDSS catalog are left for Chapter 3. However, to demonstrate the promise of the derived corrections, this appendix makes use of the HIPASS/SDSS photometric catalog that is discussed in detail in Chapter 3. Note

that the high signal-to-noise r-band data is used to demonstrate the problems and derive corrections here, but these problems occur in all 5 photometric bands and should each be corrected independently. The correction algorithms for the other filters are equivalent.

A.2 Deblending

The SDSS photometric reduction code, PHOTO[1] has many positive attributes. PHOTO does an excellent job calculating magnitudes for stars and extracting photometry for angularly small galaxies. PHOTO also cleanly deblends foreground stars from large galaxies. When one object falls in front of another on an SDSS `field`, the `parent` image is sent to the deblender. The deblender separates the two objects into `children` and photometry is performed on both images independently. For most objects in the SDSS this process works very well; stars are deblended from background galaxies and individual galaxies are separated from galaxy clusters.

In galaxies with large angular extent however, PHOTO often deblends more `children` than it should; HII regions and spiral arms of galaxies are frequently separated from their `parent` galaxies. The deblender also frequently shreds galaxies into multiple pieces, prohibiting accurate photometry. The problematic deblending occurs as a function of angular size of the object. Although small galaxies are not affected, large galaxies can have a significant amount ($> 10\%$) of their flux removed.

The HIPASS/SDSS sample demonstrates the amplitude of deblending problems in the SDSS catalog. When deblending is complete, an atlas image of each `child` is created and photometry is performed on that `child`. By examining all of the `children` for each galaxy, the degree of deblending that has occurred in the HIPASS/SDSS galaxies is assessed. Some of the galaxies are deblended perfectly. No significant amount of flux has been removed and the foreground stars have been correctly deblended. Figure A.1 shows an atlas image for HIPEQ0120-00 and demonstrates an example of good deblending. A few foreground stars were correctly removed from the outskirts of the galaxy but the galaxy remains essentially

[1]In this thesis all mentions of photo are specifically referring to PHOTO 5_4_25, which is the version used for SDSS Data Releases 3 and 4.

intact and no other `children` contained galaxy flux.

Figure A.2 shows the most common deblending problem, demonstrated for the galaxy HIPEQ0947+00b. As is typical for many large galaxies, HIPEQ0947+00b has been shredded into a large number of pieces (11 in this case), but one `brightest child` retains most of the flux (86%). This typical deblending has a significant impact on the resulting galaxy photometry, reducing the apparent r-band magnitude by ~ 0.14 magnitudes, and making the SDSS catalog photometry for HIPEQ0947+00b only marginally useful.

Figure A.3 shows an extreme example of `PHOTO's` deblending problem for HIPEQ1124+03. The irregular nature of this galaxy makes it an obvious shredding candidate. The aggressive deblending of such objects results in 50% of the total galaxy flux being contained in the `brightest child`. The catalog photometry for HIPEQ1124+03 is therefore completely unreliable.

As described in Chapter 3, using visual inspection, the galaxies in the HIPASS/SDSS sample are reconstructed by hand. This corrected catalog allows for an empirical assessment of the deblending problems. The majority of the galaxies in the HIPASS/SDSS sample indeed have some amount of deblending problems. In only 69 of the 196 cases did all of the galaxy flux fall in a single object. In the remaining cases, the flux from each galaxy was distributed among several children.

Figure A.4 shows the cumulative distribution of the fraction of flux contained in the brightest child for the reconstructed HIPASS/SDSS sample of galaxies. The 90% point has been marked with a dashed line indicating that ~75% of the galaxies have more than 90% of their flux contained in the brightest child. Most of the galaxies that lie below the 90% line have irregular morphologies, are flocculent (leading HII regions to be removed as stars) or have low surface brightness. The dotted line shows the median value of the sample. Half of the objects in the sample have brightest children with more than 96% of the total galaxy flux. It is not clear if the level of deblending correlates strongly with angular size or inclination because of the complexity introduced by irregular morphologies and HII regions. Figure A.4 suggests that in most cases, deblending has a ~10% effect on the flux of a galaxy in a single filter. Thus catalog level photometry may be suitable for many applications that do not require better than $\sim 0.1^m$ accuracy.

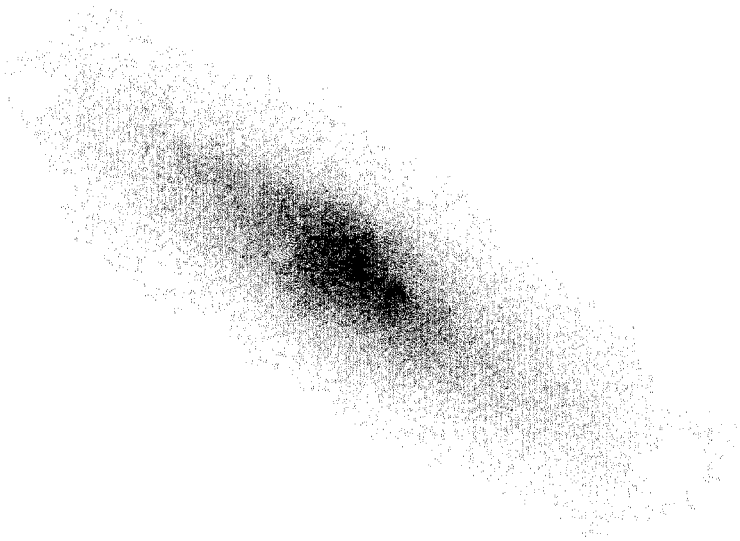

Figure A.1 r-band atlas image for HIPEQ0120-00. The deblender has removed stars but has left the galaxy intact.

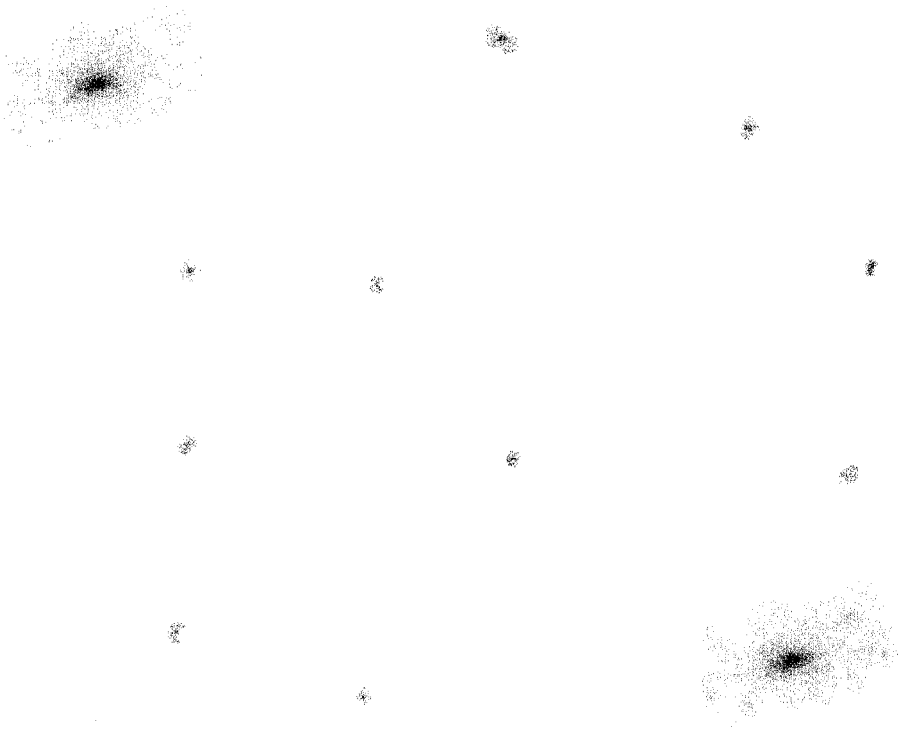

Figure A.2 r-band atlas images for HIPEQ0947+00b. The deblender has divided this galaxy into 11 children. Although the majority of the flux is in the "brightest child", the loss from the other children is 14% of the total flux of the galaxy. The combined image is in the lower right-hand corner of the figure.

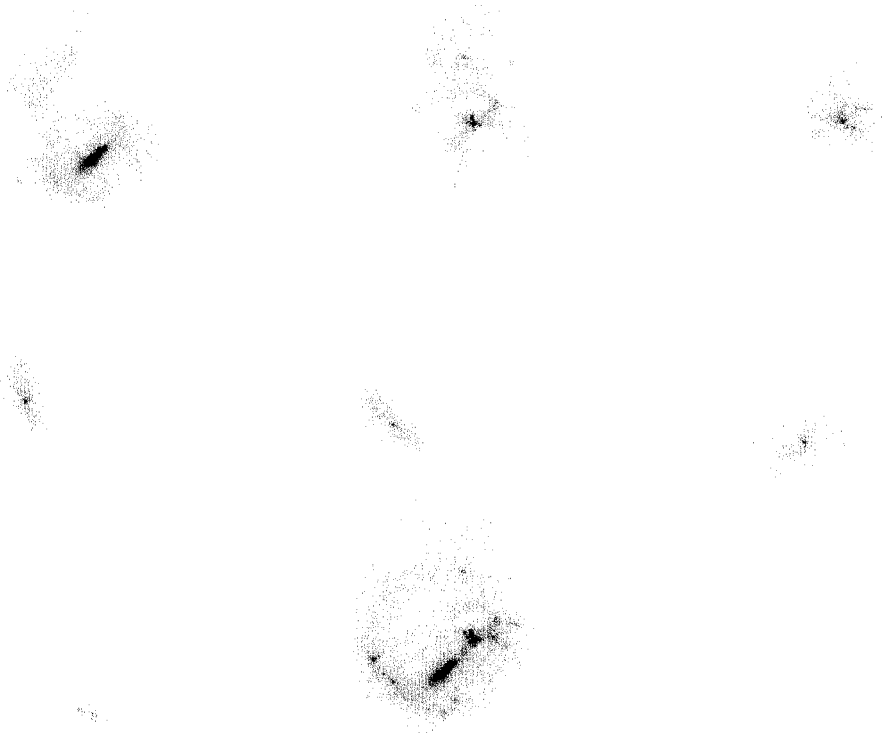

Figure A.3 r-band atlas images for HIPEQ1124+03. The deblender has divided this galaxy into 7 children. The "brightest child" contains only 50% of the total galaxy flux. The irregular morphology of this system is responsible for the large degree of shredding. The combined image is in the lower middle panel of the figure.

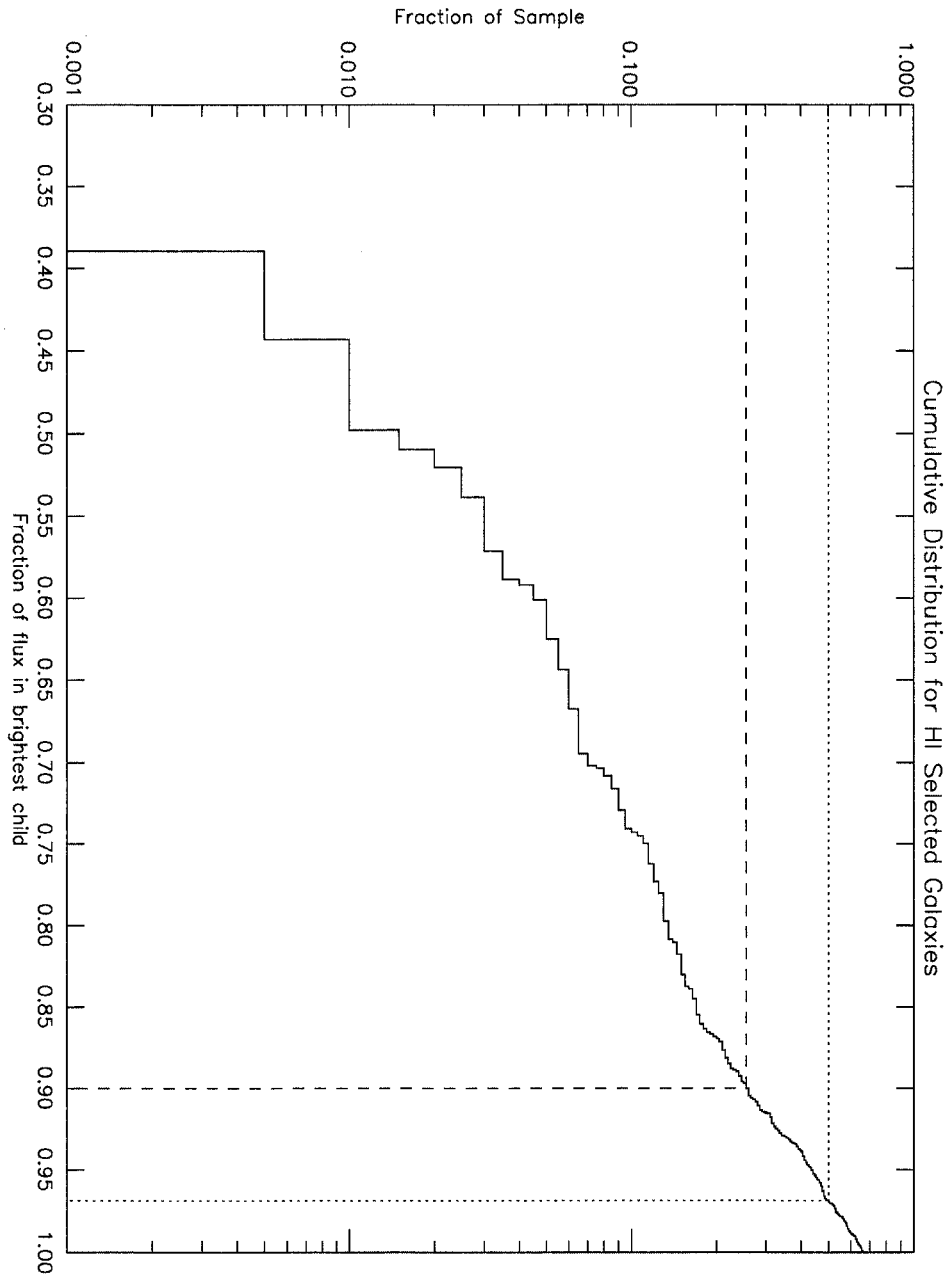

Figure A.4 Cumulative distribution of the fraction of flux in the brightest child of deblended galaxies. The dashed line indicates the level at which galaxies have at least 90% of their flux contained in the brightest child. This accounts for more than 75% of the total sample. The dotted line shows the median value of the sample. Half of the objects have brightest children with more than 96% of the total flux.

This apparent robustness hides a potentially much larger problem in determining the colors of galaxies. If the children from an individual galaxy have drastically different colors, then using solely the brightest child will lead to an erroneous color determination. To test this, the color difference between the reconstructed HIPASS/SDSS galaxies and their brightest children is examined. Figure A.5 shows the $r-i$ (top left), $g-r$ (top right), $u-r$ (bottom left) and $r-z$ (bottom right) color difference (total-brightest child) as a function of the fraction of total flux in the brightest child. Most of the color differences do not exceed 0.2^m. However, there are a few brightest children that have drastically different colors than their parent galaxy. These differences are due to HII regions as well as color gradients in the galaxies themselves (spiral arms are often deblended and have different colors than bulges). Although catalog level photometry can be used for some limited science, without proper treatment of deblending, the colors of most large galaxies can only be measured to within $\sim 0.1-0.2^m$.

Currently deblending *cannot* be corrected at the catalog level. If photometric uncertainties on the order of 10% or better are desired, then including the flux from a galaxy's deblended children is necessary. In this thesis, we have opted to rebuild the galaxies by identifying the appropriate children and combining them (see Chapter 3). Another option is to go back to the original SDSS calibrated fields and extract the galaxy photometry directly. For a small number of galaxies, this is likely to be the most efficient method. However, the excellent foreground star extraction and source identification that Photo performs are not availible in this alternative. In either case, a tedious amount of manual input is required to prepare the images for photometry.

A.3 Inclination

A.3.1 Petrosian Quantities

Because galaxies have different radial surface brightness profiles and have poorly defined edges, correctly determining fluxes for a large sample of galaxies is non trivial. Biases occur when measuring total galaxy flux with apertures based on isophotes or fractions of the central surface brightness. Petrosian (1976) defined a circular aperture radius based on

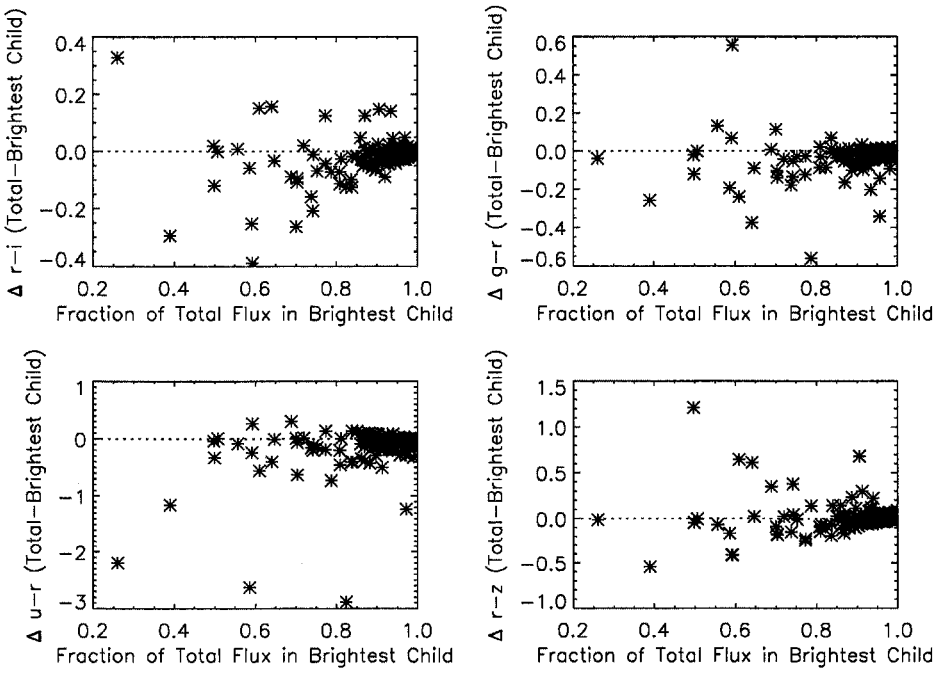

Figure A.5 $r-i$ (top left), $g-r$ (top right), $u-r$ (bottom left) and $r-z$ (bottom right) color difference (total-brightest child) as a function of the fraction of total flux in the brightest child. Although most differences are smaller than $\sim 0.2^m$, there are a few significant outliers that have drastically difference colors. Without proper treatment of deblending, the colors of most large galaxies can only be measured to within $\sim 0.1 - 0.2^m$.

the shape of the azimuthally averaged light profile of the galaxy. The Petrosian magnitudes recover most of the galaxy flux and are robust against most changes in the surface brightness profile. The Petrosian system has been adopted (and slightly modified) by SDSS (Strauss et al. 2002) and the full details of this method will be discussed in Chapter 4. In addition to measuring the Petrosian magnitudes, the SDSS software measures the radii containing 50% and 90% of the Petrosian flux. I will refer to these quantities as R50 and R90 respectively.

As in the original system (Petrosian 1976), Petrosian photometry in SDSS is measured with circular apertures. This is computationally much faster as it does not rely on *a priori* knowledge of the galaxy shape. However, some of the Petrosian quantities derived are significantly affected by the inclination of the galaxy. The difference between the circular and elliptical Petrosian quantities is best seen in the R50 and R90 (50% and 90%) radii. Figure A.6 graphically demonstrates this by overplotting both the circular (green and black) and the elliptical (red and blue) R50 and R90 radii. It is easy to see in this example that the the elliptical quantities are larger than the circular. This makes sense because the circular aperture will encounter more flux along the minor axis and reach the 50% and 90% values before the elliptical aperture does.

The impact of using circular apertures is of greatest concern at large angular sizes but, as we show, is not in any way limited to them. Petrosian quantities for galaxies of almost *all* sizes are affected by the inclination until galaxies become smaller than a few times the seeing. Strauss et al. (2002) briefly examine the effect that inclination has on Petrosian flux but their analysis is limited. Other studies have mentioned the possibility that inclination effects might play a role in SDSS catalog values (Blanton et al. 2003a) but offer no solutions or thorough examination of the problem. In this section we outline the impact of inclination on photometric quantities when using circular apertures to derive Petrosian quantities. Using a simulated set of data, we derive mean corrections that can be directly applied to the catalog data. We show that these corrections are sound by applying them to my catalog of galaxies as well as another simulated data set that was run through `PHOTO`.

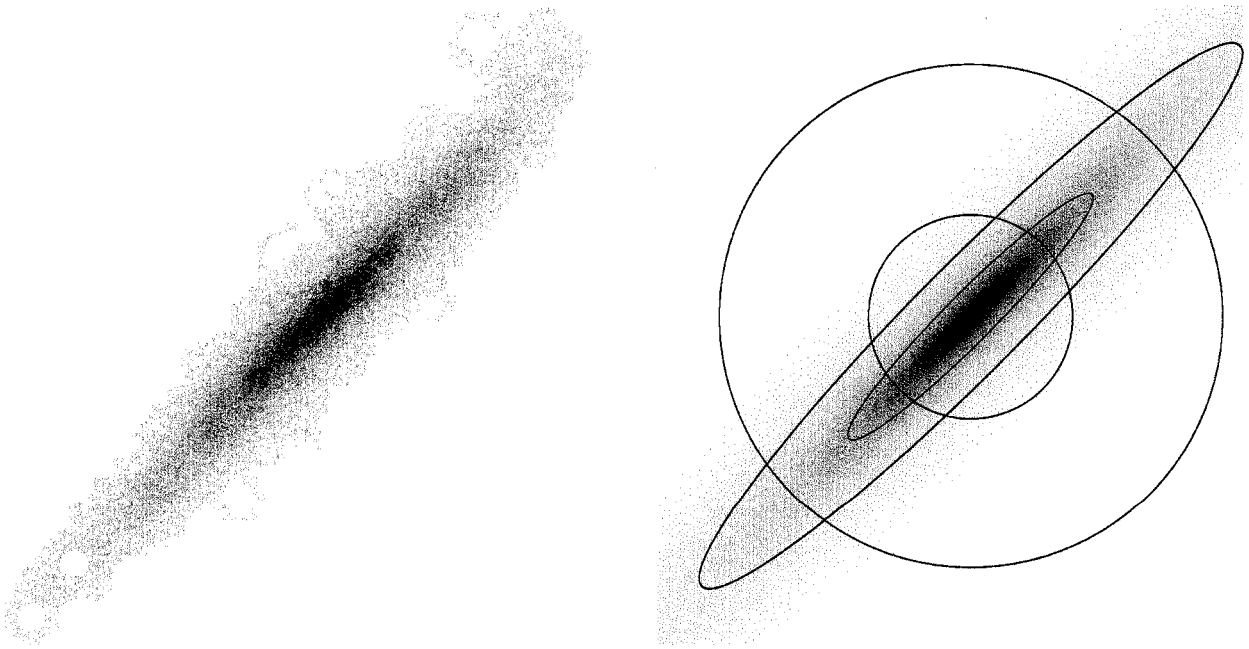

Figure A.6 r-band combined atlas image for HIPEQ0222-00 (left) and exponential disk model of HIPEQ0222-00 with the circular R50 and R90 radii plotted in green and black respectively and the elliptical R50 and R90 radii plotted in red and blue respectively. Note that the elliptical radii extend further than their circular counterparts.

A.3.2 Deriving Inclination Corrections

To investigate how the the circular and elliptical measures change as a function of inclination, we have constructed two sets of model galaxies and measured their circular and elliptical Petrosian quantities. One set of models consists of 3600 exponential disk galaxies with varying scale lengths randomly chosen between 2 and 20 pixels. The other set consists of 3600 galaxies with de Vaucouleurs profiles that have effective radii randomly chosen between 10 and 62 pixels. All of the galaxies were given position angles of $\pi/4$ and were centered in 300×300 pixel arrays. The axis ratios (semi-minor axis over semi-major axis; a proxy for inclination) were also chosen at random between values of 0.1 and 1. Because these models were used for a comparison with SDSS data, we apply a pixel scale of $0.396''$/pixel and convolve each model galaxy with a two-dimensional Gaussian to reproduce the effect of the typical $1.4''$ seeing.

The resulting model galaxies were then run through a photometric pipeline that we will describe in detail in Chapter 3. Sérsic model fits were performed to measure the axis ratio, which is altered by the seeing. Then both elliptical and circular Petrosian quantities were extracted for every galaxy using a method similar to the SDSS pipeline (see Chapter 3). The resulting elliptical and circular sizes and fluxes were then compared to each other to quantify the inclination effect. All axial ratios used to make the following figures are the post-seeing measured axial ratios and not the original input model ratios. This distinction will allow realistic corrections to be applied to the Photo outputs.

Figure A.7 shows the ratio of the R50 values computed for elliptical and circular apertures in my photometric pipeline. As expected, the elliptical aperture yields a larger value as the inclination of the galaxy increases. The colors represent different ranges of scale lengths. Although the scatter increases with smaller scale lengths due to the effects of seeing, the mean relation remains the same. It is also clear that this effect is not solely a large galaxy issue. Galaxies with scale lengths less than $10''$ are significantly affected. The green line is a second-order fit to the mean relation and is given by:

$$\frac{R_{50}, elliptical}{R_{50}, circular} = 1.95 - 1.43(b/a)_{measured} + 0.48(b/a)^2_{measured} \tag{A.1}$$

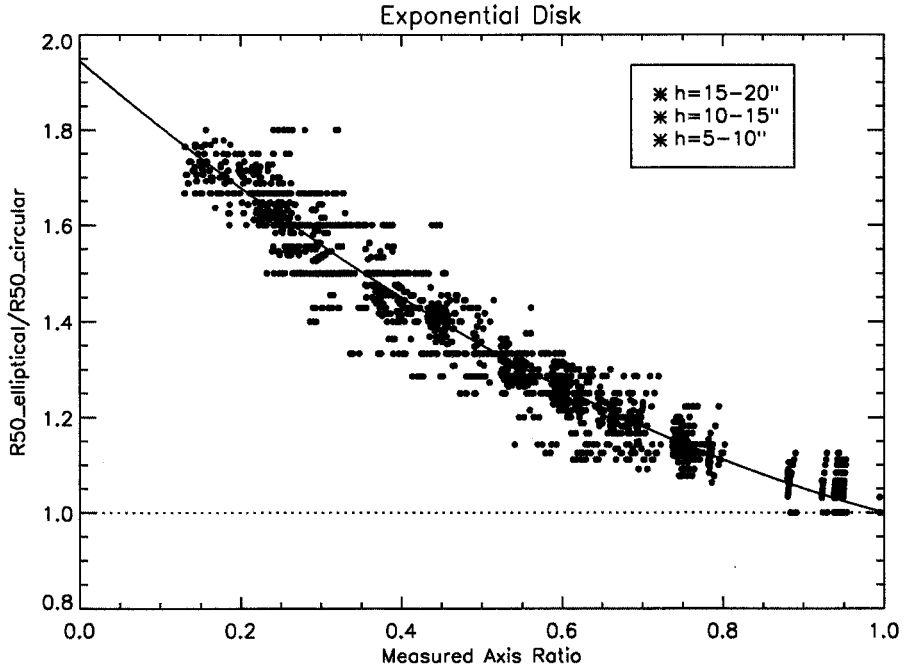

Figure A.7 Comparison of our photometric pipeline's elliptical and circular measured R50 values as a function of axis ratio for the exponential disk model galaxies. The blue, red and black represent disks with different ranges of scale lengths (15-20″, 10-15″ and 5-10″ respectively). Although the scatter increases with smaller scale lengths, the mean relation remains the same. The green line is a second-order fit to the relation, is given in Equation A.1.

where b/a is the axis ratio and $\frac{R_{50},elliptical}{R_{50},circular}$ is a multiplicative correction than can be applied to exponential galaxies analyzed with circular Petrosian quantities in the SDSS photo output.

The de Vaucouleurs models yield a similar result, shown in Figure A.8. The colors represent galaxies with different ranges of effective radii. At small axis ratios, the scatter in this relation is very large. This is because the de Vaucouleurs models are greatly affected by seeing at small axis ratios, due to their highly concentrated profiles. Because it is rare to find highly inclined galaxies that are well fit by de Vaucouleurs profiles, we limit the fit to the relation for axis ratios ≥ 0.3. This fit is shown in green and is given by:

$$\frac{R_{50}deV, elliptical}{R_{50}deV, circular} = 2.17 - 1.99(b/a)_{observed} + 0.82(b/a)^2_{observed}. \qquad (A.2)$$

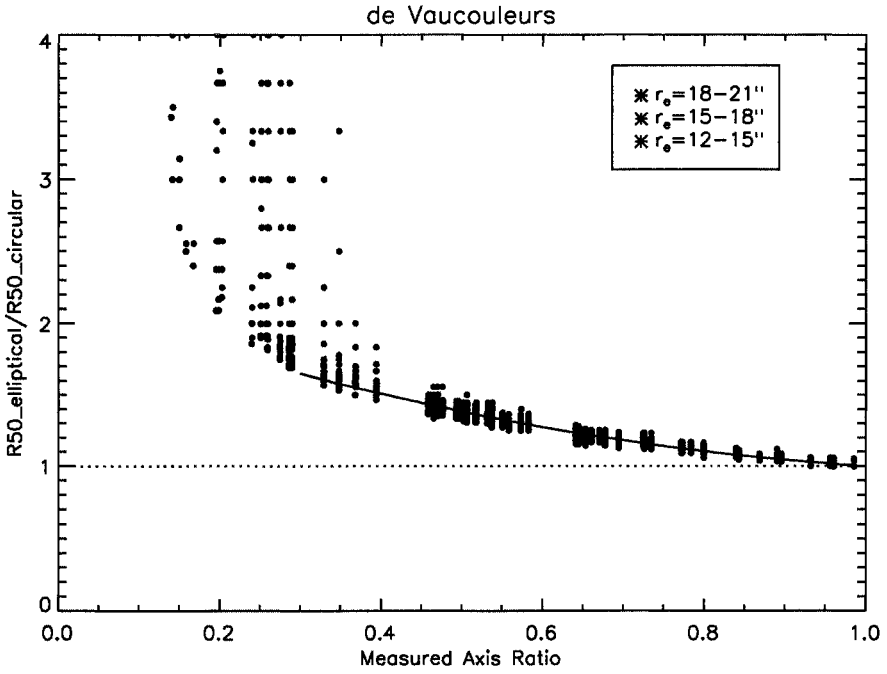

Figure A.8 Comparison of our photometric pipeline's elliptical and circular measured R50 values as a function of axis ratio for the de Vaucouleurs model galaxies. The blue, red and black represent galaxies with different ranges of effective radii (18-21″, 15-18″ and 12-15″ respectively). Although the scatter increases with smaller scale lengths, the mean relation remains the same until very high inclinations, where seeing significantly effects the profile shape for the small galaxies. The green line is a second-order fit to the relation for axis ratios greater than 0.3. The functional form is given in Equation A.2.

Figures A.9 and A.10 examine the impact of using circular apertures for the larger R90. Both Figures continue to demonstrate the problem with using circular apertures without correcting for inclination. The dispersive effects of seeing at small axis ratios are more amplified in the R90 cases. Again we have chosen to fit the de Vaucouleurs models for axis ratios greater than 0.3. The green lines in both Figures indicate the best second-order fit to the relations and are given by the Equations:

$$\frac{R_{90}, elliptical}{R_{90}, circular} = 1.45 - 0.24(b/a)_{observed} - 0.21(b/a)^2_{observed} \quad \text{(A.3)}$$

and

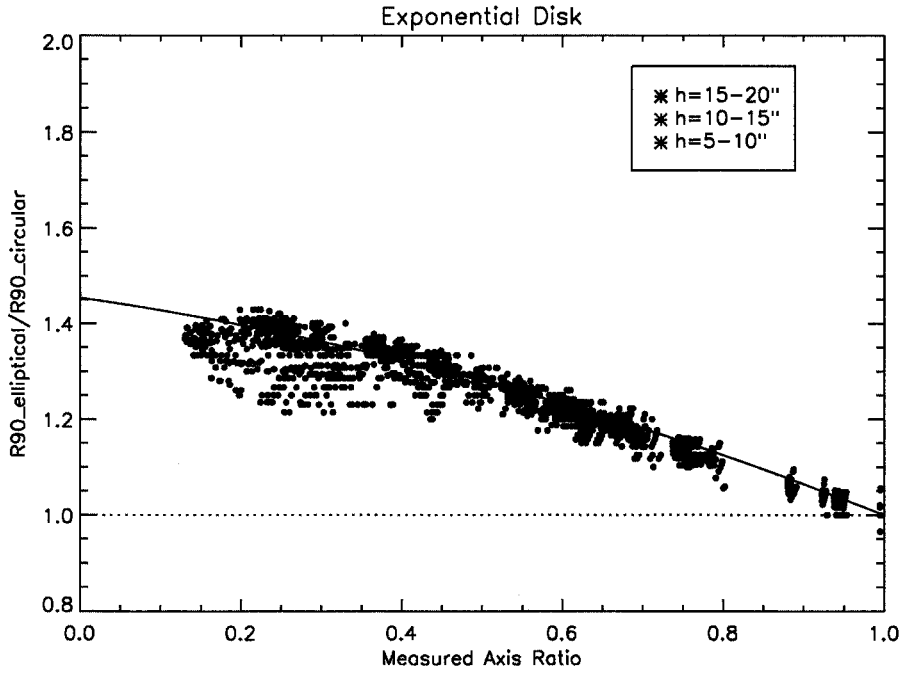

Figure A.9 Comparison of our photometric pipeline's elliptical and circular measured R90 values as a function of axis ratio for the exponential disk model galaxies. The blue, red and black represent disks with different ranges of scale lengths (15-20″, 10-15″ and 5-10″ respectively). Although the scatter increases with smaller scale lengths, the mean relation remains the same until small axis ratios, where seeing significantly affects the profile shape for the small galaxies. The green line is a second-order fit to the relation and is given in Equation A.3.

$$\frac{R_{90}deV, elliptical}{R_{90}deV, circular} = 2.13 - 1.89(b/a)_{observed} + 0.76(b/a)^2_{observed}. \quad \text{(A.4)}$$

Figures A.11 and A.12 show the difference in Petrosian flux between using circular and elliptical apertures, for the exponential disk and de Vaucouleurs models respectively. For each method, we plot the fraction of enclosed flux compared to the true flux for each galaxy. Because the circular Petrosian radius is systematically smaller than the proper elliptical radius at smaller axis ratios, the flux measured within the two Petrosian radii will be systematically different. For a face-on exponential disk galaxy, the Petrosian flux is very close to the total flux, and misses only 0.7% . However, for a face-on de Vaucoleurs profile galaxy, the Petrosian flux is only 81.6% of the total galaxy flux, due to the slow fall-off of

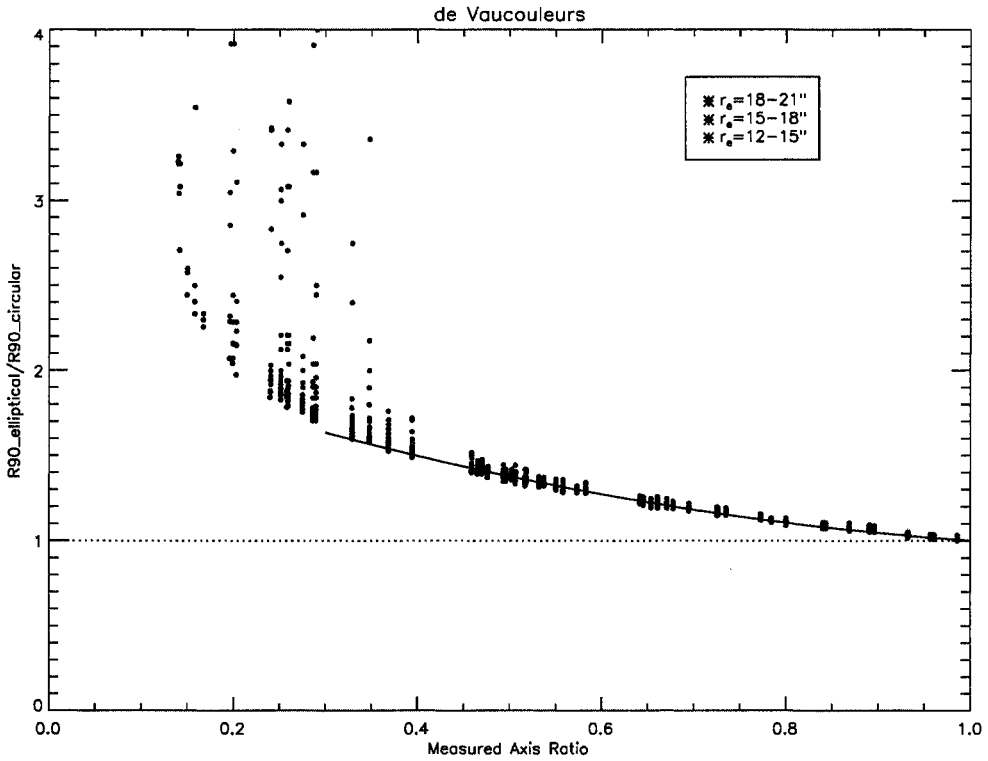

Figure A.10 Comparison of our photometric pipeline's elliptical and circular measured R90 values as a function of axis ratio for the de Vaucouleurs model galaxies. The blue, red and black represent galaxies with different ranges of effective radii (18-21″, 15-18″ and 12-15″ respectively). Although the scatter increases with smaller scale lengths, the mean relation remains the same until very high inclinations, where seeing significantly effects the profile shape for the small galaxies. The green line is a second-order fit to the relation for axis ratios greater than 0.3. The functional form is given in Equation A.4.

the de Vaucouleurs profile at large radii. Figures A.11 and A.12 show the ratio of Petrosian flux to the total flux for exponential disk galaxies (Figure A.11) and de Vaucouleurs profiles (Figure A.12) as a function of axis ratio assuming elliptical apertures (top) and circular apertures (bottom). The colors represent galaxies with different ranges of scale lengths as in Figures A.7-A.10. The dashed line in both panels is the expected analytical value for the Petrosian flux ratio. The flux derived from the elliptical aperture exactly traces this value, whereas the flux enclosed in the circular aperture falls short at small axis ratios. The flux in the elliptical apertures have a larger fraction of the flux than predicted by the analytical models. This small discrepancy is because these models have been convolved with seeing and the Petrosian radius (and therefore the photometric aperture) will be slightly larger, yielding more flux.

Although using circular apertures does affect the total flux, the magnitude of the effect is not significant. The Petrosian radii are sufficiently extended that large fractional changes in their extent make little change in the enclosed flux. For completeness, however, we include a fit giving the required correction to the Petrosian flux (as measured by SDSS) as a function of measured axial ratio. The green line in the bottom panels is a fit to the circular ratio. For the exponential disk model (Figure A.11) this fit is identical to the same relation shown in Strauss et al. (2002). The solid black line in Figure A.12 is the de Vaucouleurs relation from Strauss et al. (2002). Because the steep inner profiles of the de Vaucouleurs models are greatly affected by seeing, the lack of seeing in the Strauss et al. (2002) models accounts for the discrepancy between the green and black lines in Figure A.12. For the exponential disk model, the functional form is given by:

$$\frac{flux, total}{flux, circular} = 1/(0.963 + 0.68(b/a)_{measured} - 0.38(b/a)^2_{measured}) \qquad (A.5)$$

where $\frac{flux,total}{flux,circular}$ is a correction that will convert the Photo output back to the total flux. To only correct for the inclination effect $\frac{flux,total}{flux,circular}$ needs to be multiplied by the exponential disk Petrosian ratio analytical value of 0.993. For the de Vaucouleurs profile, the flux can be corrected for inclination using:

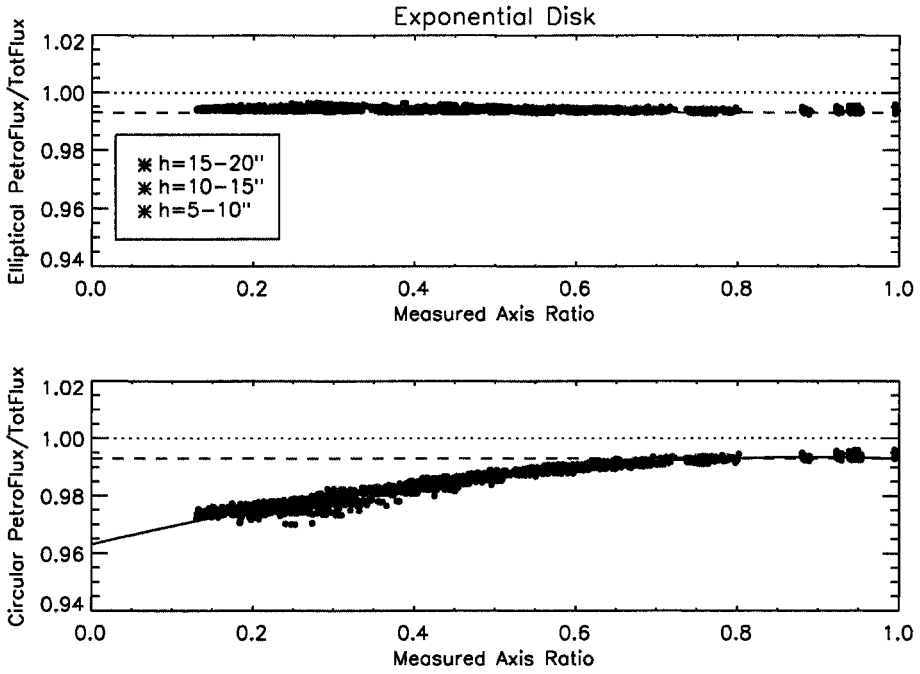

Figure A.11 Ratio of elliptical Petrosian flux to the total flux in exponential disk galaxies as a function of axis ratio (top) and the ratio of circular Petrosian flux to the total flux in exponential disk galaxies (bottom). The colors represent galaxies with different ranges of scale lengths. The dashed line in both panels is the analytical value for the Petrosian flux ratio. The elliptical measures exactly trace this value whereas the circular measures fall short at small axis ratios. Although there is some lost flux in the circular case, it is not a significant amount. The green line in the bottom panel is a fit to the circular ratio and is given in Equation A.5 and mirrors the same relation shown in Strauss et al. (2002).

$$\frac{flux_{deV}, total}{flux_{deV}, circular} = 1/(0.820 + 0.056(b/a)_{measured} - 0.045(b/a)^2_{measured}) \quad \text{(A.6)}$$

where $flux\_deV_{correction}$ is a correction that will convert the Photo output back to the total flux. In order to correct for the inclination effect only, $flux\_deV_{correction}$ needs to be multiplied by the de Vaucouleurs Petrosian ratio analytical value of 0.816.

A.3.3 Surface Brightness

In many SDSS papers, the Petrosian radii and fluxes are used to determine other physical quantities. These too will be affected by the inclination effects. One of the most com-

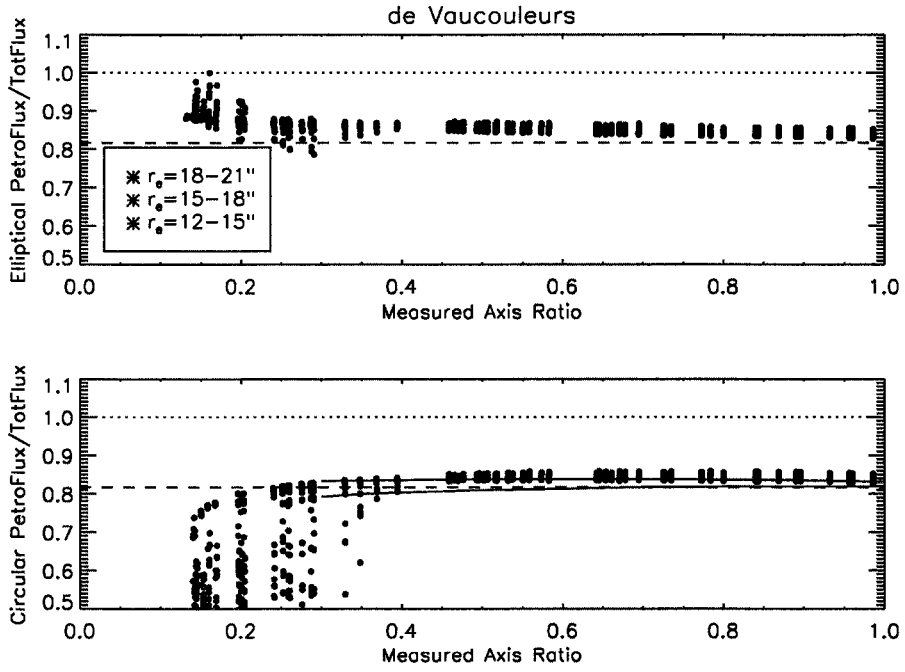

Figure A.12 Ratio of elliptical Petrosian flux to the total flux in de Vaucouleurs model galaxies as a function of axis ratio (top) and the ratio of circular Petrosian flux to the total flux in de Vaucouleurs model galaxies (bottom). The colors represent galaxies with different ranges of scale lengths. The dashed line in both panels is the analytical value for the Petrosian flux ratio. The elliptical measures maintain a constant ratio value but have a larger fraction of the flux than predicted by the analytical models. This is because these models have been convolved with seeing and the Petrosian radius (and therefore the photometric aperture) will be slightly larger, yielding more flux. Although there is some lost flux in the circular case, it is not a significant amount. The green line in the bottom panel is a fit to the circular ratio and is given in Equation A.6. The black solid line is the relation from Strauss et al. (2002). Again the elevated flux levels are due to seeing effects.

monly used is the Petrosian surface brightness, defined as the average surface brightness within the R50 (50%) radius. Figure A.13 shows the ratio of Petrosian surface brightnesses calculated within elliptical and circular apertures for the exponential disk model galaxies. For nearly face-on galaxies with large axis ratios, the differences between the circular and elliptical apertures are minor. However, at smaller values of the axis ratio, the differences become significant. Deviations of 20% ($\sim$0.2 mag/$\Box''$) are already apparent at $b/a \sim 0.4$, corresponding to inclinations of $\sim 66°$. Deviations of >50% ($\sim$0.7 mag/$\Box''$) are present at $b/a \leq 0.3$, or inclinations $> 73°$. Since spectral target selection in SDSS uses the Petrosian surface brightness (Strauss et al. 2002), it is likely that this effect creates a substantial bias against inclined LSB galaxies in the spectroscopic sample. Correcting for inclination in the flux and R50 values (Equations A.1 & A.5) before calculating the Petrosian surface brightness will remedy the discrepancies bewtween the elliptical and circular aperture measures.

The surface brightness ratio for de Vaucouleurs profile galaxies (shown in Figure A.14) does not show the same dramatic increase at small values of axis ratio. Although there is large scatter at low axis ratio values, this is solely due to the seeing and not an intrinsic effect of the inclination problem. For $b/a > 0.3$, the de Vaucouleurs surface brightness ratio is very similar to the exponential disk ratio. Severe changes in both the flux and R50 ratios for the de Vaucouleurs models (Figures A.8 & A.12) cause the large deviations in the surface brightness ratio for $b/a < 0.3$. However, since there are not many de Vaucouleurs profile galaxies with $b/a < 0.3$, these deviations should not affect any science results.

A.3.4 Concentration Index

Many SDSS studies have utilized the R90/R50 ratio as a morphological "concentration index" (e.g. Strateva et al. 2001; Kauffmann et al. 2003). Because the values of R50 and R90 change with inclination, the concentration index may be considerably discrepant at small axis rations. In severe cases, this shift may lead a highly inclined galaxy to be misclassified. Figures A.15 and A.16 demonstrate the effect that inclination has on the concentration index by comparing the R90/R50 ratio for the elliptical aperture to the circular case used

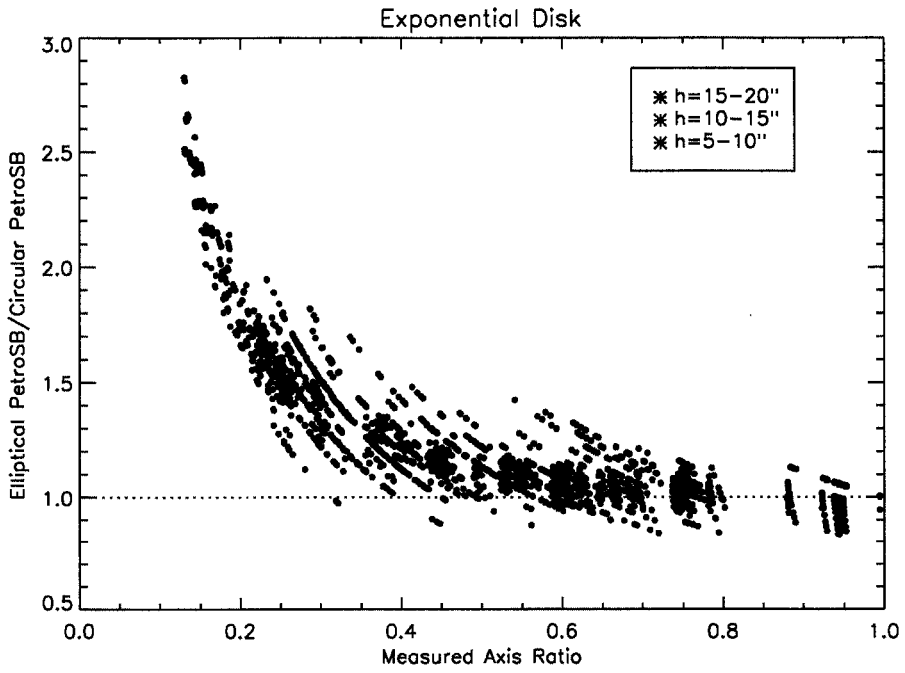

Figure A.13 Ratio of elliptical to circular Petrosian surface brightness for the exponential disk models. At low inclinations, the Petrosian surface brightness does not seem to differ between the circular and elliptical cases. However, at high inclinations the difference becomes significant. This difference may have an effect on the spectral targeting described in Strauss et al. (2002)

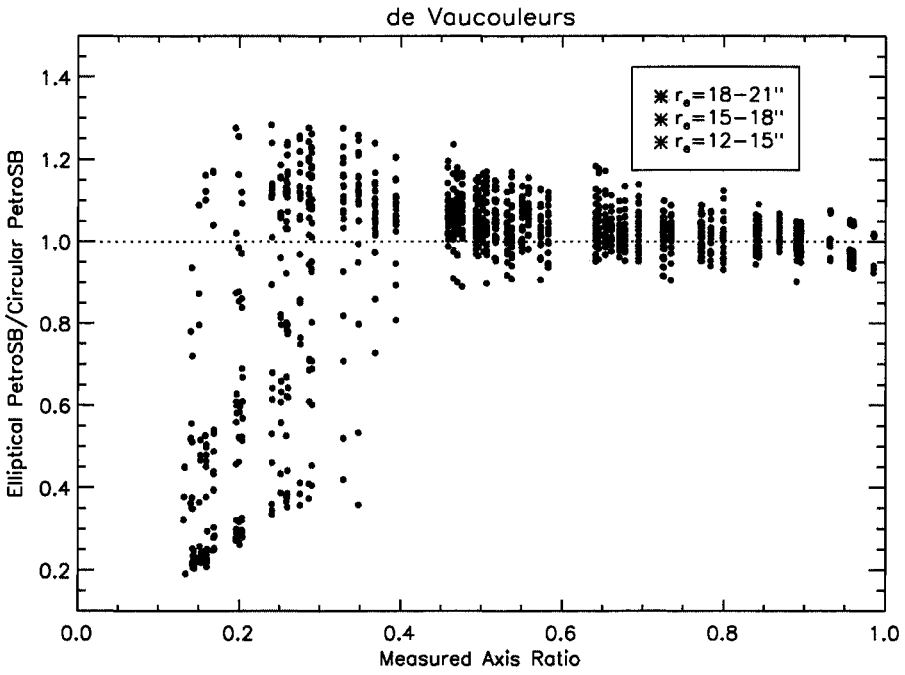

Figure A.14 Ratio of elliptical to circular Petrosian surface brightness for the de Vaucouleurs profile model galaxies as a function of axis ratio. For axis ratios larger than 0.4 (where seeing effects are minimal) there is no strong deviation from unity.

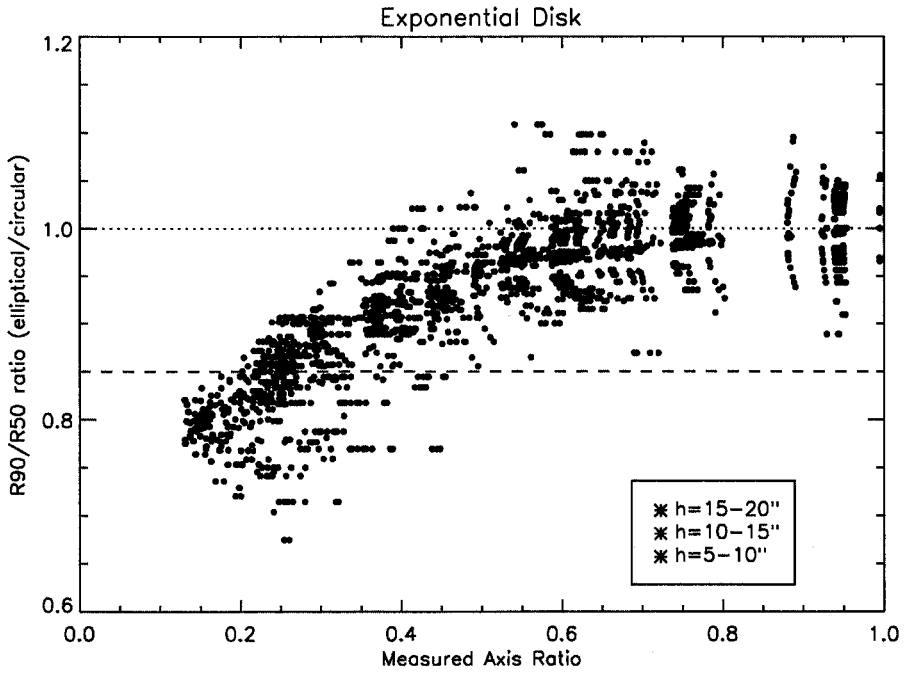

Figure A.15 The ratio of R90/R50 (concentration index) for the elliptical and circular apertures in the exponential disk case versus axis ratio. The different colors indicate different ranges of scale lengths. The dashed line is the empirically derived boundary between early and late type galaxies. At small values of the axis ratio, the circular concentration index gets large enough to cross the dashed boundary. These inclined galaxies would be misclassified using SDSS catalog data.

by SDSS. An exponential disk model has a concentration index of 2.3, and the effect of the circular aperture is to increase the value of the concentration index for galaxies with higher inclinations. The dashed line in Figure A.15 represents the boundary at which an exponential disk galaxy would be classified as an early-type galaxy with a concentration index > 2.6 (Strateva et al. 2001). For the exponential disk model, the effect is quite important. Highly inclined late-type galaxies will have artificially high ratios of R90/R50, and be misclassified as early-type galaxies. Even at lower inclinations, this effect certainly plays a role in increasing the scatter in the concentration index distribution. The concentration index for the de Vaucouleurs models does not seem to be affected by inclination; early type galaxies will be safely classified as early type galaxies using the concentration index.

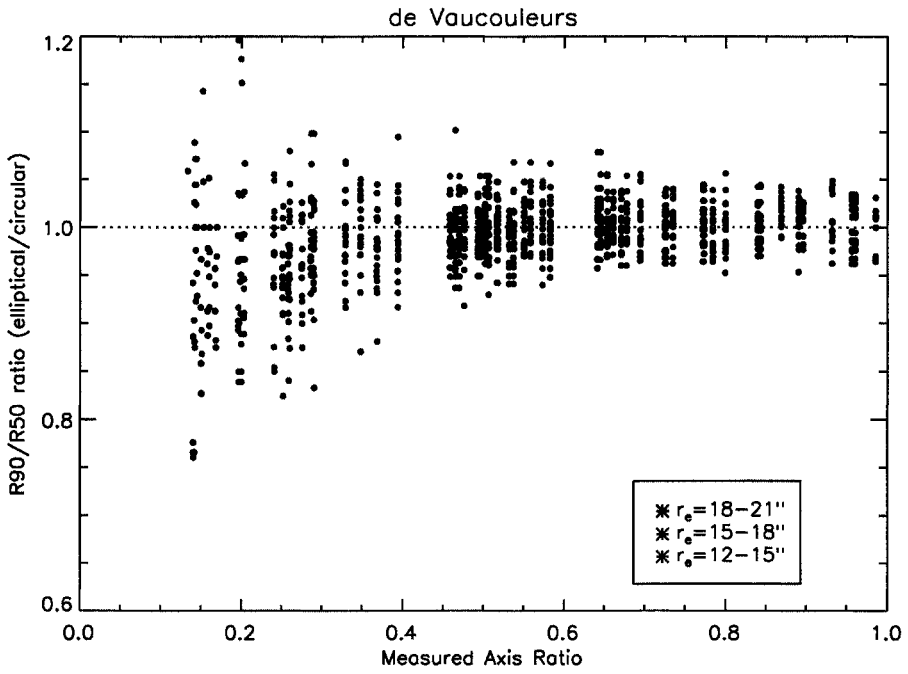

Figure A.16 The ratio of R90/R50 (concentration index) for the elliptical and circular apertures in the de Vaucouleurs model case as a function of axis ratio. The different colors indicate different ranges of effective radii. No significant deviation is seen as a function of axis ratio.

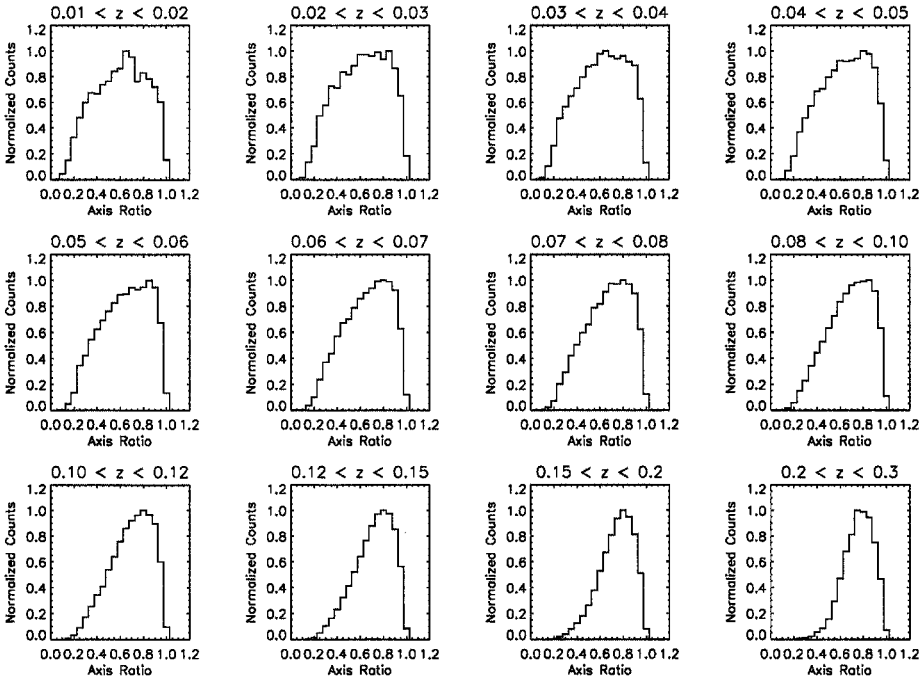

Figure A.17 Axis ratio distributions at different volume cuts for the DR4 main galaxy sample. The number of galaxies with measured small axis ratios falls off at larger distance due to seeing effects. However, a significant number of highly inclined galaxies remains for galaxies with $z < 0.1$.

A.3.5 Inclination Distribution of SDSS galaxies

We have shown that using circular apertures to derive Petrosian quantities for highly inclined galaxies can lead to large deviations from those derived using elliptical apertures. But how much does inclination affect SDSS derived quantities? As the angular size of galaxies gets smaller, seeing circularizes the galaxy axis ratios and the inclination errors should become very small. Figure A.17 shows the distribution of axis ratios for the DR4 main galaxy sample (see Chapter 2). Each panel plots the distribution at a different redshift range. As expected, the more distant galaxies have fewer measurable highly inclined systems due to the effects of seeing. In the nearby universe, the inclination of a galaxy certainly affects the circularly measured Petrosian quantities. However, even in the most distant redshift bins, there are still a significant number of inclined systems.

Because of the magnitude limit ($r < 17.77$), the main galaxy sample does not extend

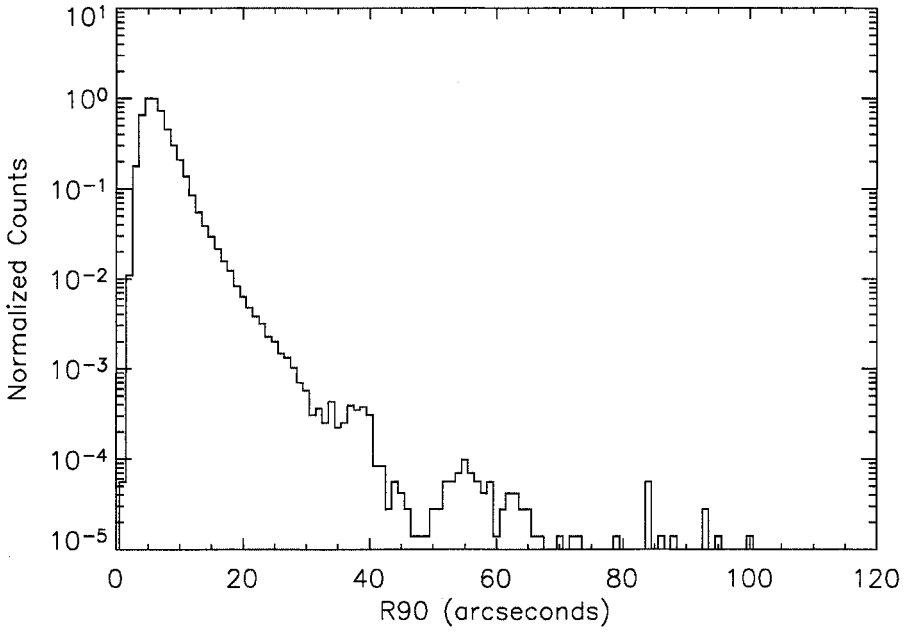

Figure A.18 The R90 distribution for the DR4 main galaxy sample. There are a significant number of galaxies with R90 $> 11''$, making the Petrosian quantities derived, unreliable.

much beyond $z > 0.3$. As evidenced by Figure A.17, main galaxy studies that include Petrosian quantities must take inclination into account. Some of the scatter in the Petrosian quantities used in previous studies (e.g. Strateva et al. 2001; Shen et al. 2003; Kauffmann et al. 2003), can be attributed to differences between the more physical elliptical aperture photometry and the circular aperture photometry used by SDSS.

For our model galaxies, the inclination effects persist even for galaxies with scale lengths as small as a few arcseconds. For an exponential disk galaxy, a scale length of a $3''$ translates to an R90 radius of $11''$. Figure A.18 show the R90 distribution for the DR4 main galaxy sample. There are a significant number of galaxies with R90 $> 11''$. The Petrosian quantities derived for these galaxies will be affected by SDSS's use of a circular aperture. This may be the a source of some of the scatter in previous SDSS results.

A.3.6 Applying Inclination Corrections to the HI Selected Data

In the previous sections we have derived several empirical relations for correcting the SDSS catalog output Petrosian quantities properly with elliptical apertures. These relations were derived using idealized model galaxies. We now test their performance when applied to real data. The HIPASS/SDSS sample is an obvious data set on which to test the ability to correct for inclination. As part of our photometric pipeline (described in Chapter 3), we measure photometry with both the circular and elliptical apertures. Therefore, we can reproduce many of the Figures shown above and see how well the correction equations describe the differences between using the circular and elliptical apertures on realistic galaxies. The r-band HIPASS/SDSS sample data are used for these comparisons.

Figure A.19 shows the ratio of R50 calculated with elliptical vs. circular apertures for the HIPASS/SDSS sample of galaxies. The blue line is the correction for the exponential disk galaxies and the red line is the de Vaucouleurs correction (Equations A.1 & A.2). The two model corrections trace the range of measured ratio values to within a few percent. We have not explored the morphological and/or color differences between the galaxies that are better fit by the exponential disk correction and the systems that are closer to the de Vaucouleurs relations and we leave this for a later study.

Figure A.20 shows the ratio between R90 calculated in elliptical and circular apertures for the HIPASS/SDSS sample. As before, the blue line is the correction derived for the exponential disk galaxies and the red line is the de Vaucouleurs correction (Equations A.3. & A.4). The range of differences is much larger at small axis ratios, but is bordered by the expected model corrections for the two profile shapes.

The ratio of the Petrosian flux (elliptical/circular) as well as the derived corrections are shown in Figure A.21. The corrections do not well trace the small differences between the elliptical and circular apertures. This demonstrates that the dominant difference between circular and elliptical apertures in the HIPASS/SDSS sample is small (only a few percent) and is not due to inclination. It also suggests that even with slight changes due to inclination, correcting flux for inclination is not necessary. However, because the Petrosian flux does not report the entire flux of a galaxy, a correction still needs to be applied if the total flux

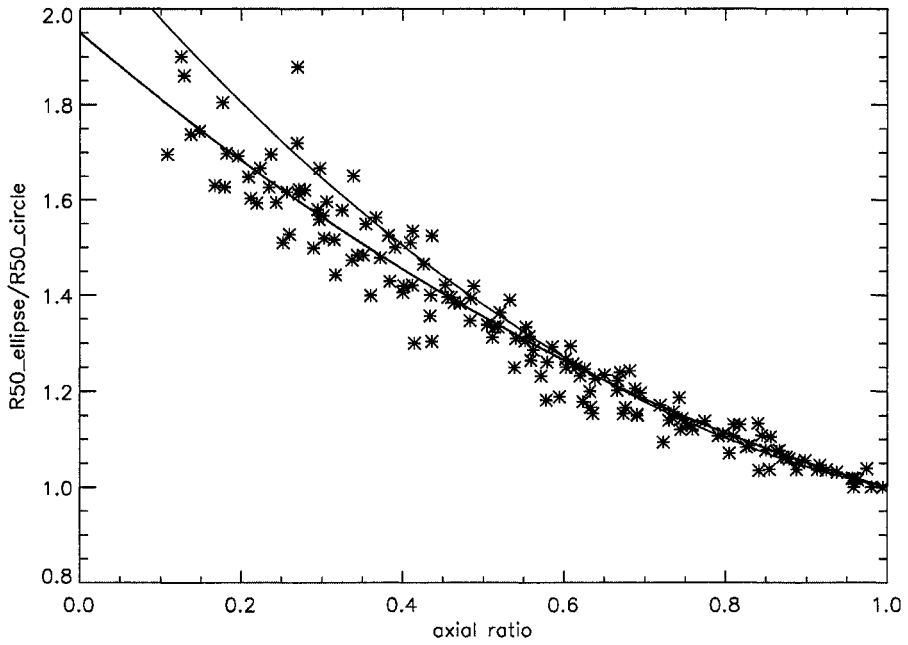

Figure A.19 The elliptical to circular R50 ratio for the HI selected sample of galaxies as a function of axis ratio. The blue line is the correction for the exponential disk galaxies and the red line is the de Vaucouleurs correction. The corrections appear to fit the data reasonably well. The spread in the data also seems to follow the divergence of the two model corrections.

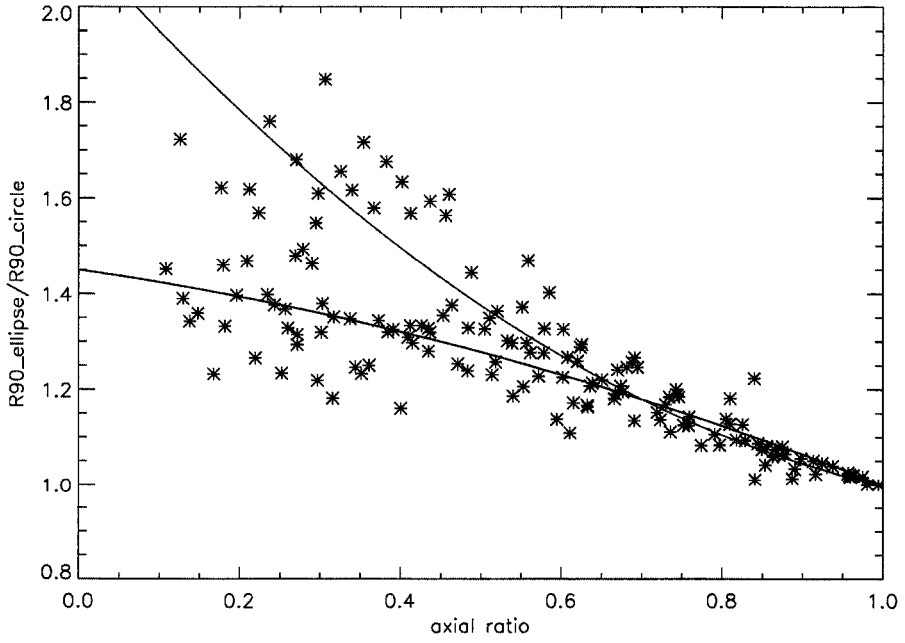

Figure A.20 The elliptical to circular R90 ratio for the HI selected sample of galaxies as a function of axis ratio. The blue line is the correction for the exponential disk galaxies and the red line is the de Vaucouleurs correction. The two different model corrections seem to cover the span of the data.

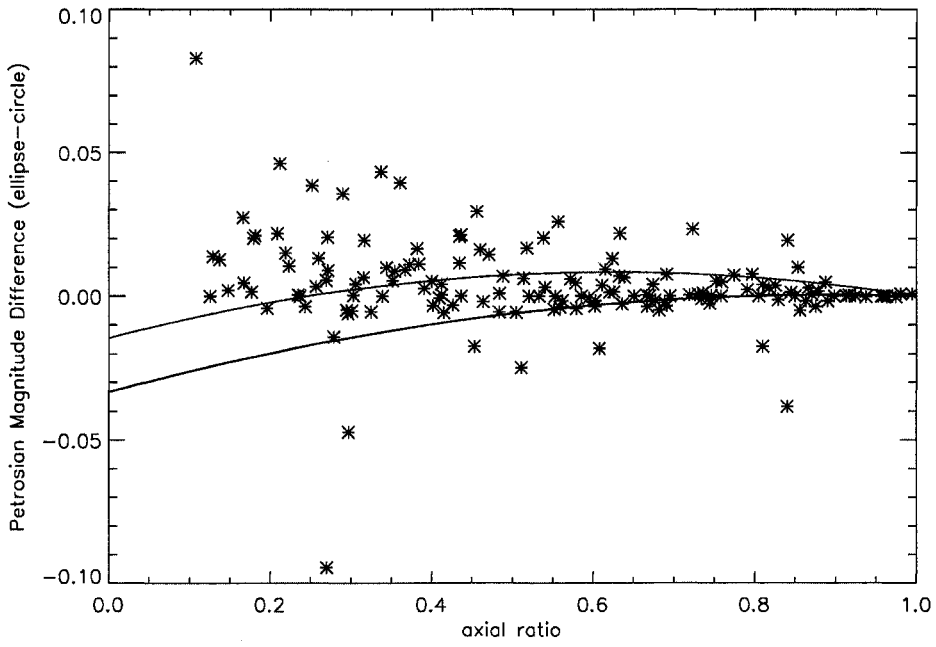

Figure A.21 Ratio of the Petrosian Flux for the elliptical and circular apertures as a function of axis ratio. Exponential disk and de Vaucouleurs model corrections are overplotted in blue and red respectively. The deviation from zero is not well fit by either correction. This suggests that other uncertainties dominate the elliptical/circular relation and that correcting for inclination is not important for real data.

is desired.

Figure A.22 shows the Petrosian surface brightness difference between the elliptical and circular aperture methods. I have converted the surface brightness to magnitude units to demonstrate the amplitude of the inclination effect. In the most extreme case, the surface brightness differs by over a magnitude! The exponential disk correction fits the data very well and the de Vaucouleurs correction helps to explain some of the outliers.

The ratio of concentration index is the relation that is least well described by the correction equations. Figure A.23 show this ratio of concentration index for the elliptical and circular cases. Although the two model corrections do fit the spread for much of the data, there are still quite a few galaxies that are not well corrected by either model. However, because it involves the noisier measurement of R90, and requires larger corrections, the

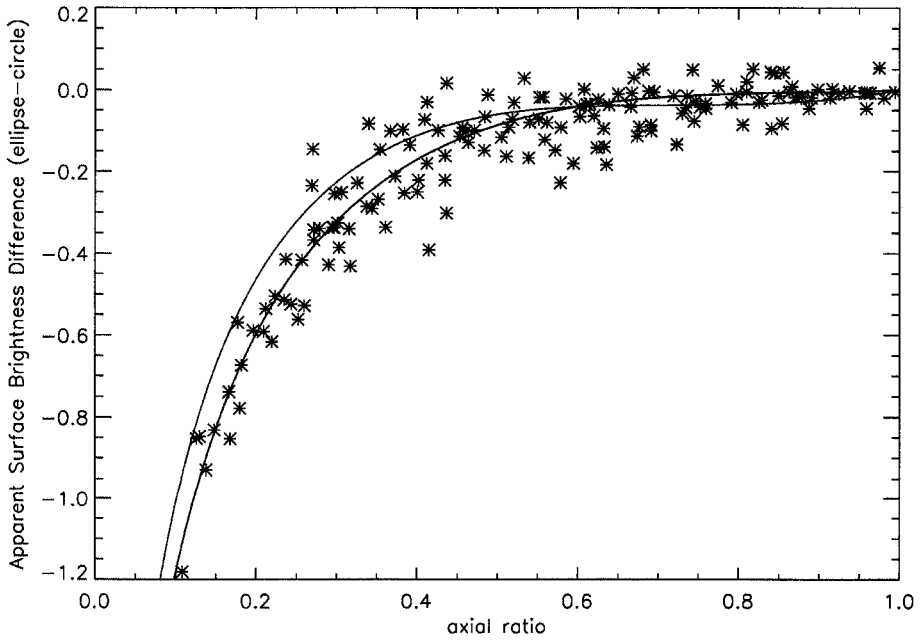

Figure A.22 Petrosian surface brightness as a function of axial ratio. Exponential disk and de Vaucouleurs model corrections are overplotted in blue and red respectively. The exponential disk correction fits the data very well and the de Vaucouleurs correction helps to explain some of the outliers.

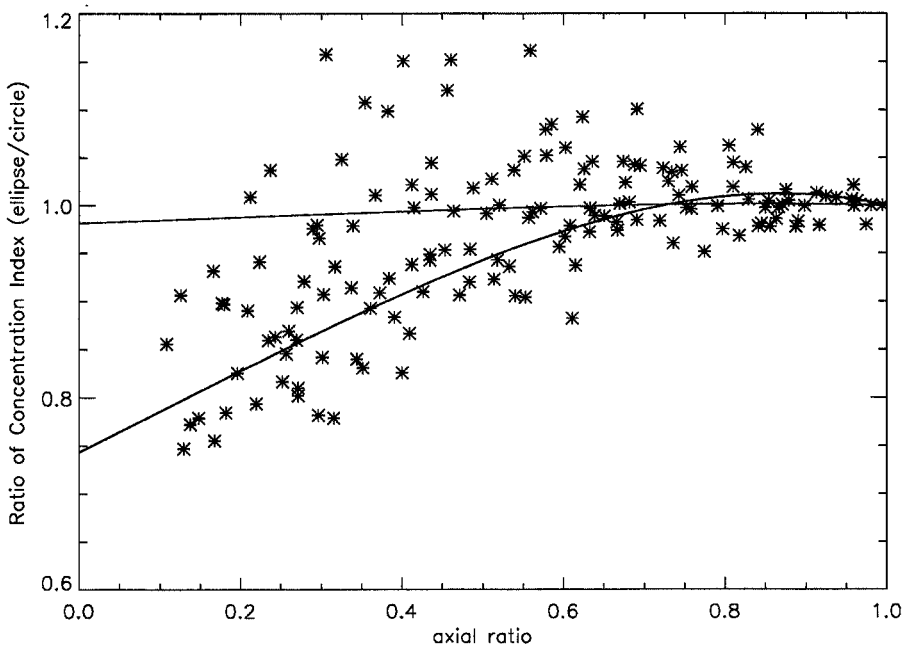

Figure A.23 Ratio of concentration index for the elliptical and circular aperture cases versus axial ratio. Exponential disk and de Vaucouleurs model corrections are overplotted in blue and red respectively. There is tremendous scatter in this plot at most axis ratio values. Although the two model corrections do fit the spread of most of the data, there are still quite a few galaxies that are not well corrected by either model.

scatter around the relation is not unexpected, particularly for the lower surface brightness systems, which are prevalent in the HIPASS/SDSS sample. Further investigation may yield a better way to correct the concentration index for inclination.

A.3.7 Can Photo Outputs be Corrected for Inclination?

The derived corrections for inclination can explain the differences from circular apertures that we measure using elliptical apertures with our photometric pipeline on the HIPASS/SDSS sample. However, the question remains, can these corrections be applied to the `PHOTO` outputs in the SDSS catalogs? This is a challenging question to answer because `PHOTO` does not return elliptical aperture photometry. In order to properly answer this question, we use a similar set of model galaxies to those used to derive the corrections

and run them through the actual SDSS photometric pipeline. We created a sample of 90 exponential disk galaxies and 90 de Vaucouleurs profile galaxies of various axis ratios (from 0.1 to 1) and scale sizes. We convolved each galaxy with a Gaussian to simulate 1.5″ seeing and added Poisson, sky, dark, and read noise. Each galaxy was then added to a real SDSS `field` in `Run` 1453 and `CamCol` 3 (`fields` 30-74). The `fields` were run through `PHOTO` and all of the standard output files were produced. We visually inspected all of the nearby `atlas images` at each galaxy position and selected the `brightest child` or the `parent` (if there was no foreground contamination). A few of the galaxies were not properly deblended but the impact of the deblending was not large due to the smooth nature of the input galaxies. However, this test did demonstrate that `PHOTO` will deblend galaxies even if they have smooth light distributions. Despite our earlier warnings, we dis not correct for deblending and simply acknowledge that some of the scatter in our results is due to missing flux from bad deblends.

To calculate elliptical apertures for each of these galaxies, we ran our photometric pipeline on the selected `atlas` images. To convince the reader that this is an acceptable way to examine the problem, we have provided comparisons of the circular photometry from our pipeline and from `PHOTO`. Figures A.24-A.27 demonstrate our ability to reproduce the `PHOTO` circular quantities with our pipeline. For the most part we can reproduce the `PHOTO` Petrosian sizes to within a few percent. All axis ratios used in these and all remaining plots are from the `PHOTO` outputs. We use the iso_B/iso_A parameters for each atlas image as the measured axis ratio. The R90 for the de Vaucouleurs galaxies (Figure A.27) has the largest offset, but is still only a few percent and is most likely due to my courser integration method (see Chapter 3). Figures A.24-A.27 demonstrate that we can adequately reproduce `PHOTO` measurements and that our elliptical aperture photometry can therefore provide a reasonable comparison to the `PHOTO` circular photometric outputs.

Using the elliptically derived quantities from our photometric pipeline and the circular outputs from `PHOTO`, we test the ability to make inclination corrections on `PHOTO` outputs. Figures A.28-A.31 show the R50 and R90 ratios for both the exponential disk and de Vaucouleurs model galaxies as a function of measure axis ratio. The derived corrections are overplotted on each plot. The corrections clearly fit the deviations from unity in all 4 cases.

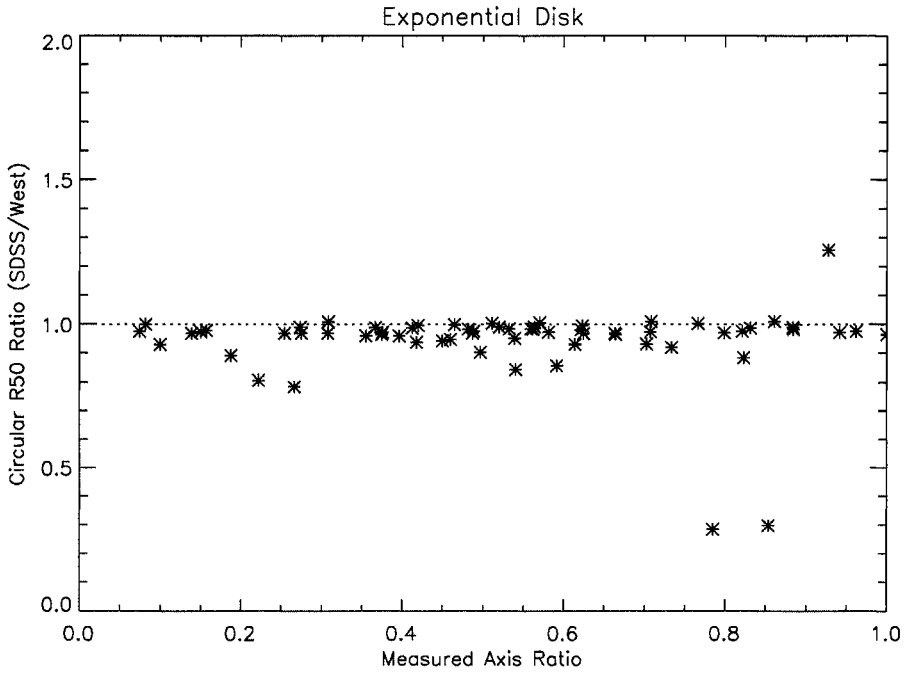

Figure A.24 Ratio of the SDSS circular aperture outputs to our circular outputs for R50 as a function of axis ratio for the exponential disk models.

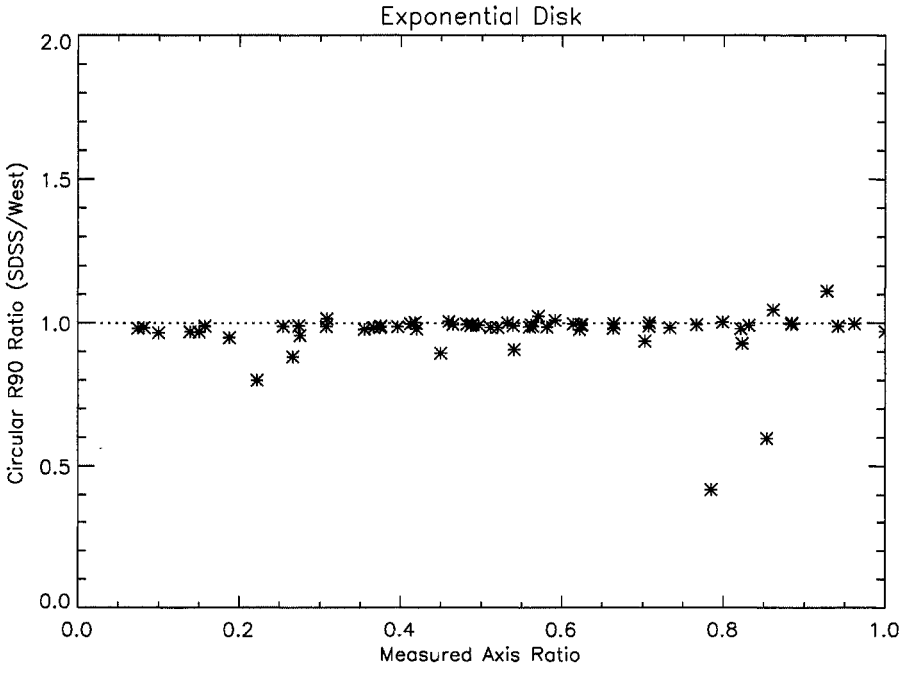

Figure A.25 Ratio of the SDSS circular aperture outputs to our circular outputs for R90 as a function of axis ratio for the exponential disk models.

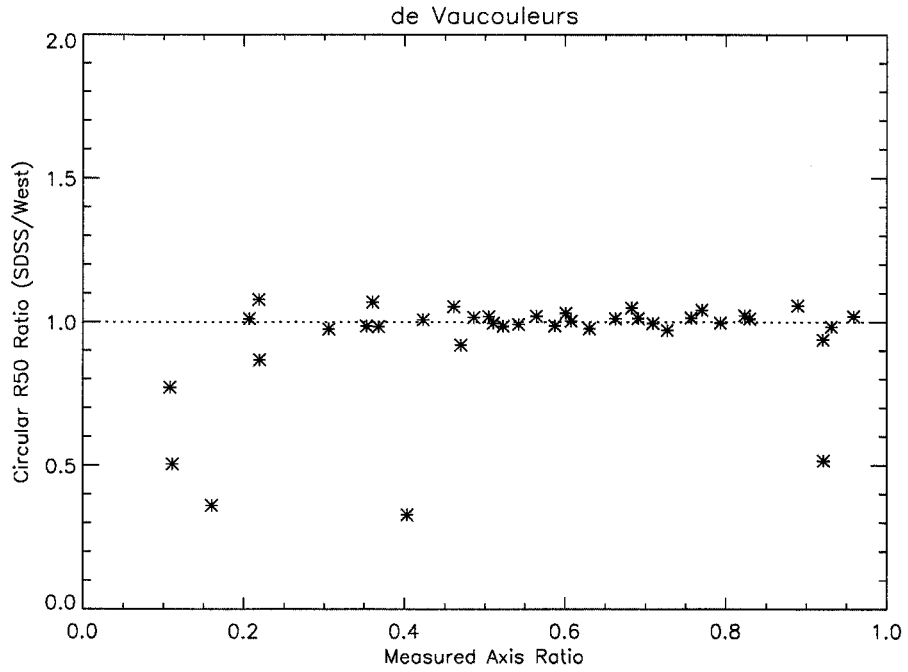

Figure A.26 Ratio of the SDSS circular aperture outputs to our circular outputs for R50 as a function of axis ratio for the de Vaucouleurs models.

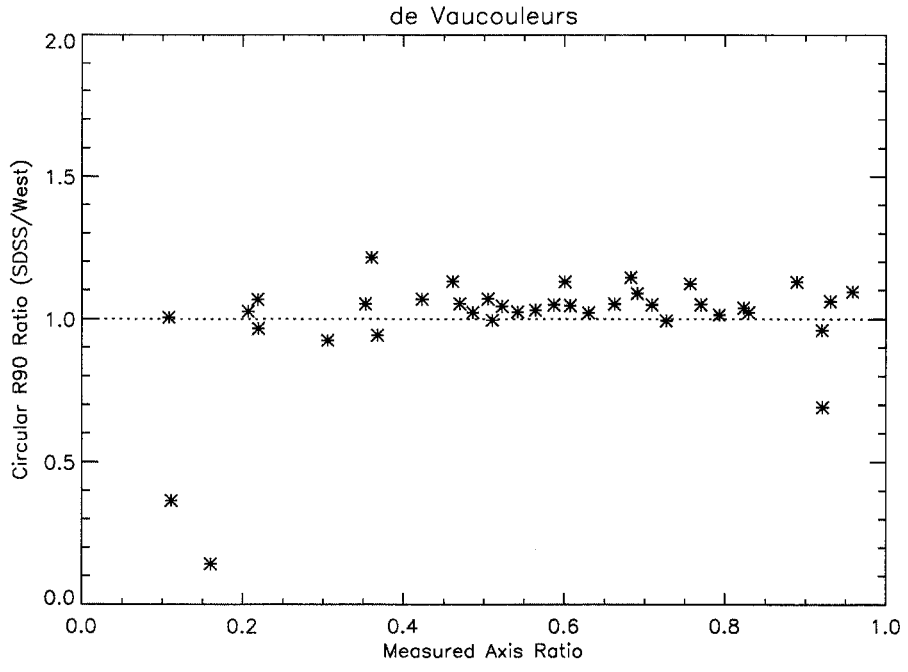

Figure A.27 Ratio of the SDSS circular aperture outputs to our circular outputs for R90 as a function of axis ratio for the de Vaucouleurs models.

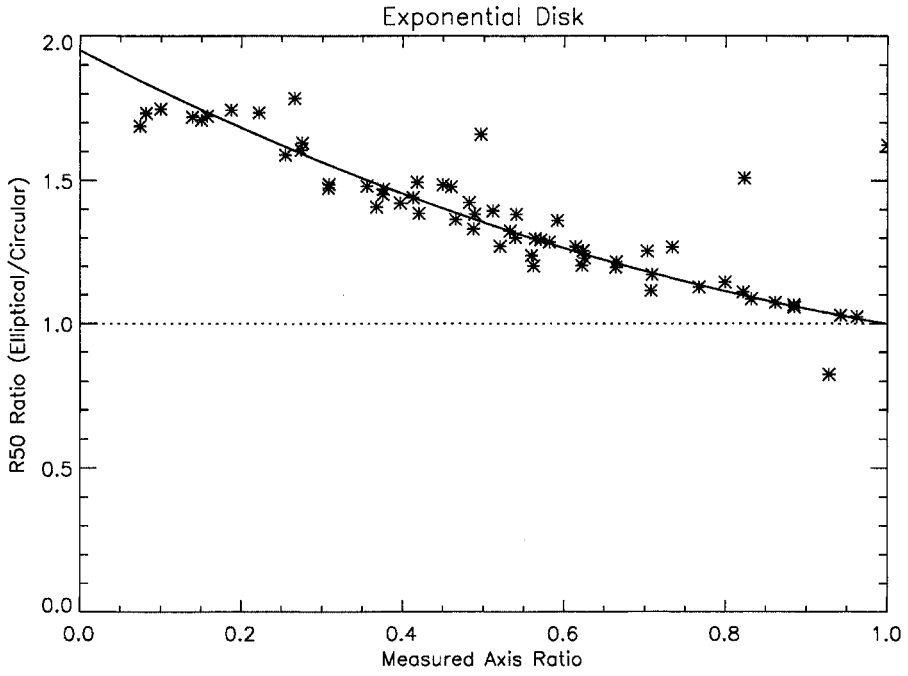

Figure A.28 Elliptical R50 from our photometric pipeline compared to the PHOTO R50 value as a function of axis ratio for the exponential disk galaxies. The blue line is the derived inclination correction. This correction is a good fit to the data and can be used to correct PHOTO outputs in future SDSS work.

We conclude that it is indeed possible to apply our derived inclination corrections directly to PHOTO outputs. The scatter is on the order of a few percent and at small values of axis ratio, is a tiny fraction of the total inclination error.

The question remains of how to properly assign a galaxy to either the exponential or the de Vaucouleurs case. PHOTO performs fits of both profiles to each galaxy and computes the quality of each. This is recorded in the deV_lnL and exp_lnL variables respectively. For the model galaxies that were reduced by Photo in this section, the correct model was always identified. However, these were galaxies that had perfect exponential or de Vaucouleurs profiles. It is unclear if the deV_lnL and exp_lnL parameters measured by SDSS for more realistic galaxies are the best way to differentiate between which correction to use. There is strong evidence for exponential and de Vaucouleurs profiles separating in color space (Strateva et al. 2001; Blanton et al. 2003a; Kannappan 2004; Baldry et al. 2004), which

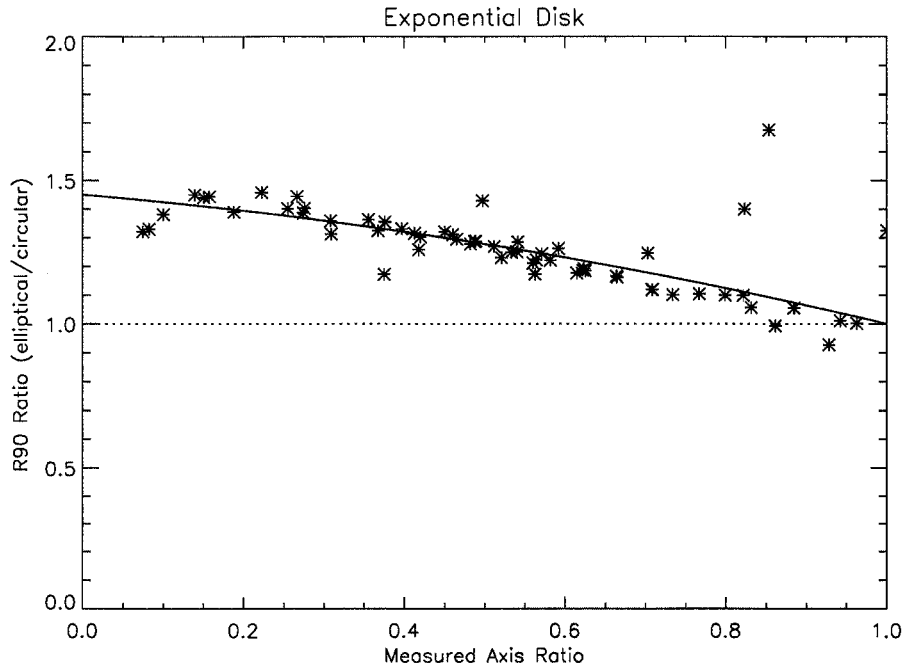

Figure A.29 Elliptical R90 from our photometric pipeline compared to the PHOTO R90 value as a function of axis ratio for the exponential disk galaxies. The blue line is the derived inclination correction. This correction is a good fit to the data and can be used to correct PHOTO outputs in future SDSS work.

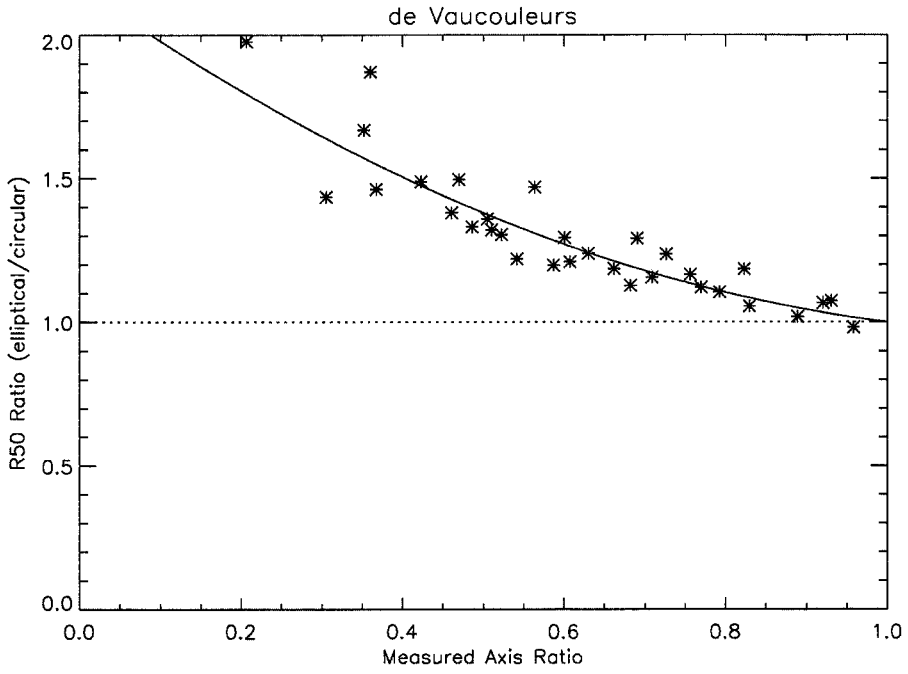

Figure A.30 Elliptical R50 from our photometric pipeline compared to the PHOTO R50 value as a function of axis ratio for the de Vaucouleurs model galaxies. The red line is the derived inclination correction. This correction is a good fit to the data and can be used to correct PHOTO outputs in future SDSS work.

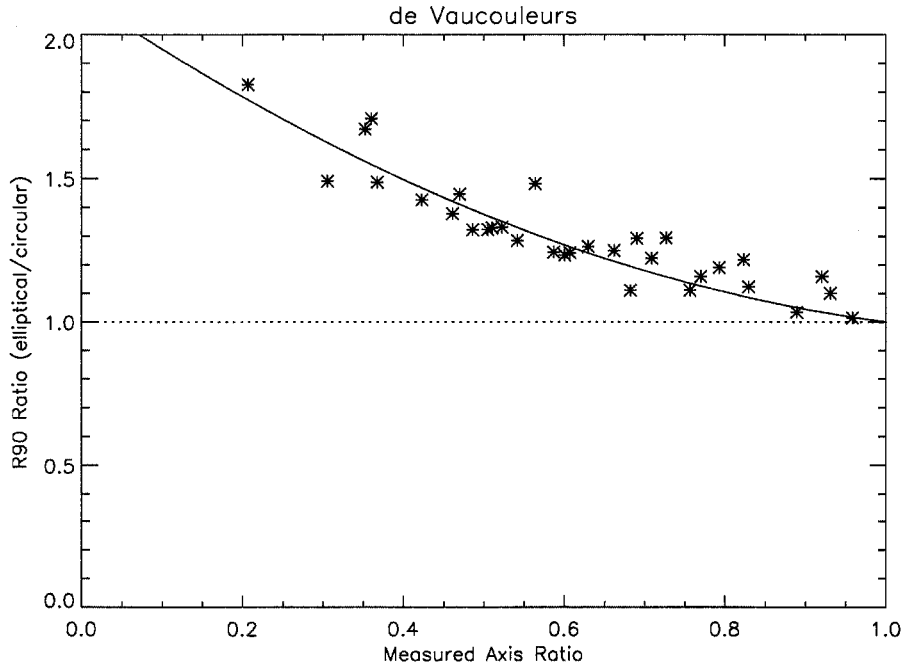

Figure A.31 Elliptical R90 from our photometric pipeline compared to the PHOTO R90 value as a function of axis ratio for the de Vaucouleurs model galaxies. The red line is the derived inclination correction. This correction is a good fit to the data and can be used to correct PHOTO outputs in future SDSS work.

may be utilized in determining which correction to apply. Future work will investigate how the elliptical/circular ratios vary with galaxy properties and will determine the optimal method for selecting which correction equation to use.

A.4 Sky Subtraction

Whereas inclination does not seem to have a large effect on the flux measurements of photo, the error from sky subtraction of angularly large galaxies can be enormous. The error arises from the sky subtraction method itself. To compute the sky, `PHOTO` moves a 256×256 pixel mask across an SDSS `field` and computes the sky value after performing a sigma clipping algorithm. This value is stored at 128 pixel intervals. When the sky is subtracted from the field, this binned sky is remade by interpolating between the 128 pixel intervals. The problem is that when an object (e.g. galaxy, saturated star, comet) takes up an appreciable fraction of the 256×256 ($1.7' \times 1.7'$) sky mask, then some of that object's flux is included in the sky determination. This effect erroneously reduces the object's flux because the sky is over-subtracted.

Figures A.32 and A.33 demonstrate the problem for two large galaxies from the HIPASS/SDSS sample (HIPEQ1232+00a & HIPEQ1232+00b). The top panel of both Figures shows a `field` with only the sample galaxy's `atlas images` included (see Chapter 3). The bottom panels show the reconstructed sky frame for the respective SDSS `field`. The problem is quite obvious; an accurate sky subtraction should yield a smooth surface, and yet the sky field clearly includes galaxy flux. The removal of galaxy flux and its inclusion in the background sky subtraction has dramatic repercussions for the derived fluxes of large galaxies in SDSS.

To investigate the magnitude of the sky subtraction problem, we recalculated a proper sky frame by masking out all of the objects on the `field` and fitting a plane to the sky (see Chapter 3 for details). We then ran our photometric software on the `atlas images` with two different versions of sky subtraction applied: 1) the standard SDSS sky subtraction applied to the `PHOTO` outputs; and 2) our version of sky subtraction (see Chapter 3). The difference is profound. Naively plotting the r-band flux difference as a function of area enclosed by

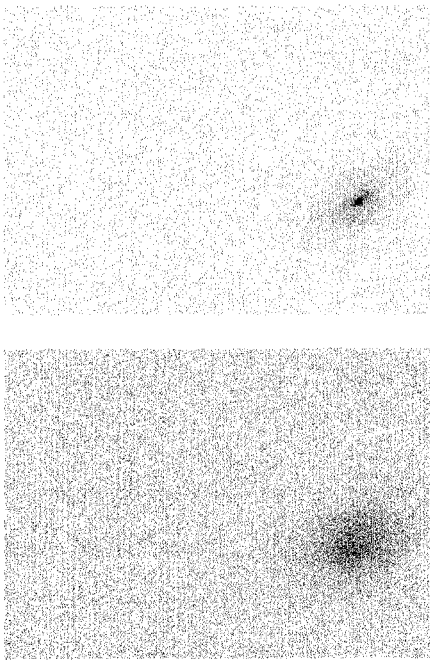

Figure A.32 (Top) Reconstructed `field` for HIPEQ1232+00a with only the relevant `atlas images` included in the `field`. (Bottom) Rebuilt `PHOTO` sky for galaxy HIPEQ1232+00a. This `field` is what `PHOTO` subtracted from the corrected frame before photometry was performed. Flux from the galaxy is clearly seen on this image and is strong evidence for a sky subtraction error.

Figure A.33 (Top) Reconstructed `field` for HIPEQ1232+00b with only the relevant `atlas images` included in the `field`. (Bottom) Rebuilt `PHOTO` sky for galaxy HIPEQ1232+00b. This `field` is what `PHOTO` subtracted from the corrected frame before photometry was performed. A substantial amount of flux from the galaxy is clearly seen on the image.

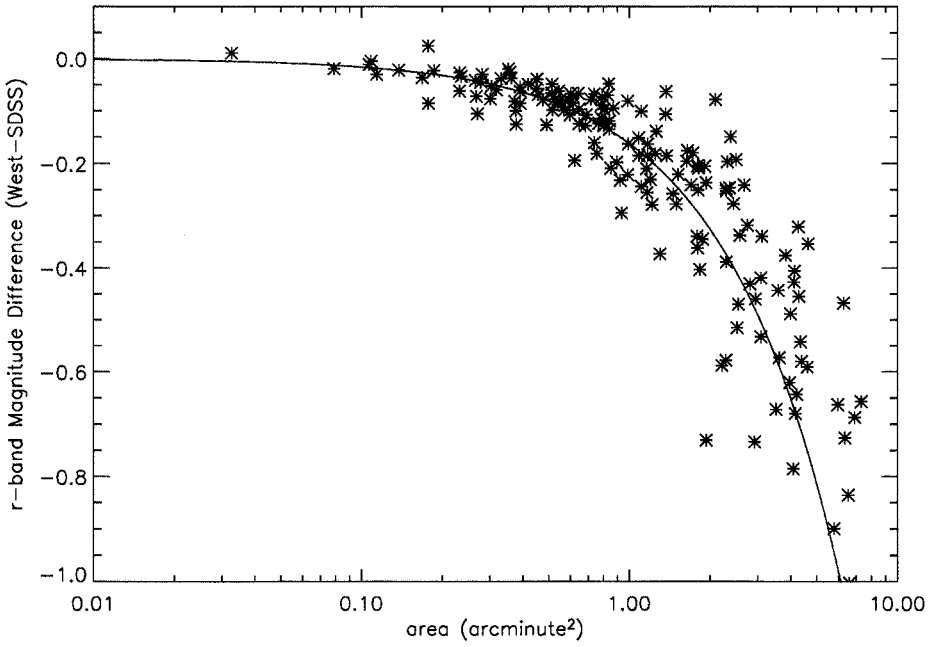

Figure A.34 Difference between the r-band magnitude derived using our sky subtraction pipeline and that of the SDSS as a function of R90 area for the HI selected sample. For areas larger than $\sim 0.5\Box'$, the loss from bad sky subtraction is substantial.

the R90 ellipse indicates the scope of this error (Figure A.34). While the effect is negligible for small galaxies ($< 0.5\ \Box'$), galaxies with angular areas of $\sim 1\Box'$ have magnitude errors greater than 0.2 magnitudes. The sky subtraction is therefore only important in galaxies with areas larger than a few tenths of a square arcminute, unlike the inclination error that affects small galaxies as well as large.

The scatter in the relation shown in Figure A.34 implies that other parameters beyond angular size affect the flux lost to sky subtraction errors. Instead of looking at the magnitude difference (which is a fractional lost flux), we examined the actual flux lost as a function of both area and surface brightness, and discovered that the dependence on area is tied to the mask size. As galaxies get larger, they fill the sky mask resulting in more of their flux being subtracted. But the amount of flux depends on the surface brightness of the source. A higher surface brightness object with the same area as a low surface brightness object will have more flux taken from it.

Fitting a plane to the logarithms of flux lost, surface brightness and R90 area yield a high quality fit from which the flux lost to sky subtraction can be calculated from observed parameters. To make this correction easier to apply for SDSS users, we have modified the fit parameters to be log(r-band magnitude), log(area) and log(flux lost). Since surface brightness depends on the magnitude and the area, this is a sound substitution and will facilitate accurate catalog corrections. Figure A.35 shows the best fit plane to these three parameters using the galaxies from the HIPASS/SDSS sample. The best fit is given by:

$$\log(flux\_lost) = 9.37 - 8.00 \cdot \log(m_r) + 1.06 \cdot \log(\pi(b/a)\mathrm{R90}^2) \qquad \text{(A.7)}$$

where m_r can be substituted with any of the other 4 band magnitudes as long as the appropriate R90 value is also substituted. The scatter in the $\log(flux\_lost)$ relation is 0.13. The lost flux can be converted back into magnitudes by applying the SDSS photometric equations (given in Chapter 3). The photometric offsets, airmass and the extinction coefficient for each galaxy are also needed. Fortunately, all of these parameters can be obtained from the SDSS database, making sky subtraction corrections feasible at the catalog level.

Again it is important to test if this relation can be applied to the PHOTO outputs. To do this we used the same galaxies that were run through PHOTO for the inclination study and examined the effectiveness at correcting for the lost flux. The method for determining the lost flux was as follows. We ran the sky subtraction code on each galaxy `field` and rebuilt the PHOTO subtracted sky. We subtracted the two "sky" fields and produced a residual sky image. Figure A.36 shows one of the residuals fields. This field would look smooth if sky subtraction errors were negligible. Flux from the model galaxy is clearly seen in the residual image. Then at each galaxy position (as defined by PHOTO), we used the PHOTO derived Petrosian radius to calculate the flux in the residual sky image. This method ensures that we use the *exact* aperture used by PHOTO and therefore can accurately assess the amount of flux lost due to sky subtraction errors.

The final test was accomplished by applying Equation A.7 to the PHOTO outputs and seeing if the same plane is fit to the data. Figure A.37 shows the resulting fit. Most of the galaxies fall on the same plane as those in my HI selected sample. Some of the larger

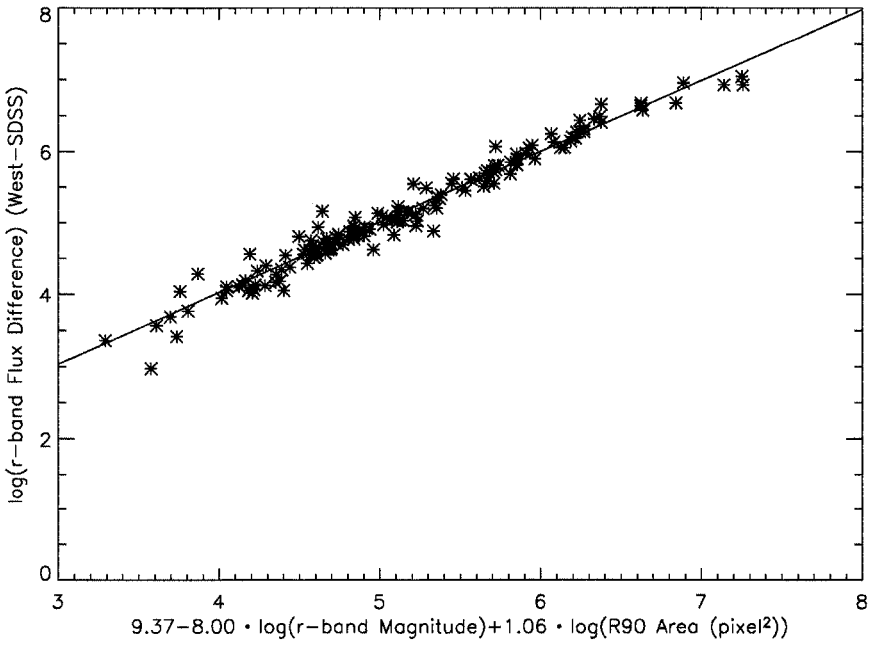

Figure A.35 Projection of the best fit plane to $\log(m_r)$, log(R90 area) and log(r-band flux lost) for the HI selected galaxies. The scatter is less than a half of an order of magnitude. The same relation applies to each of the 4 other band passes. The red line indicates the 2-dimensional fit to this projection.

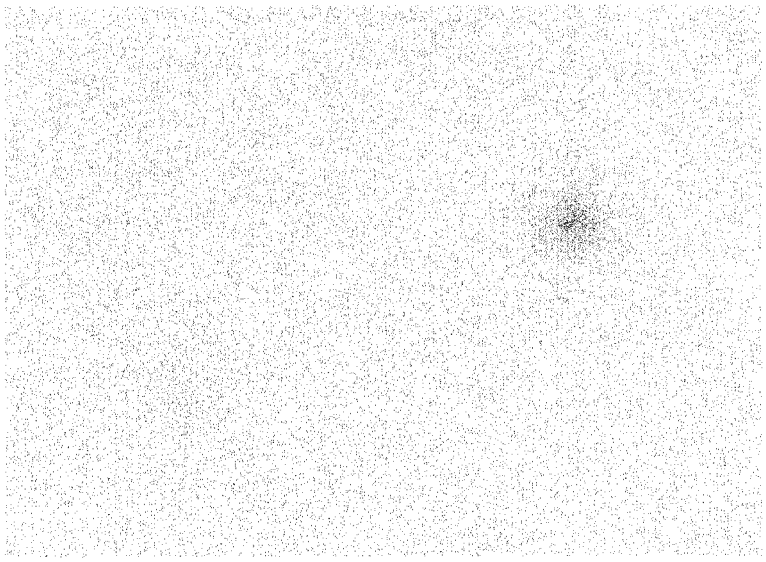

Figure A.36 Residual sky image for one of the model galaxies run through PHOTO. Flux from the galaxy is clearly seen on this image and it strong evidence for a sky subtraction error. This flux was integrated using the PHOTO derived Petrosian radius and used as a measure of the lost flux.

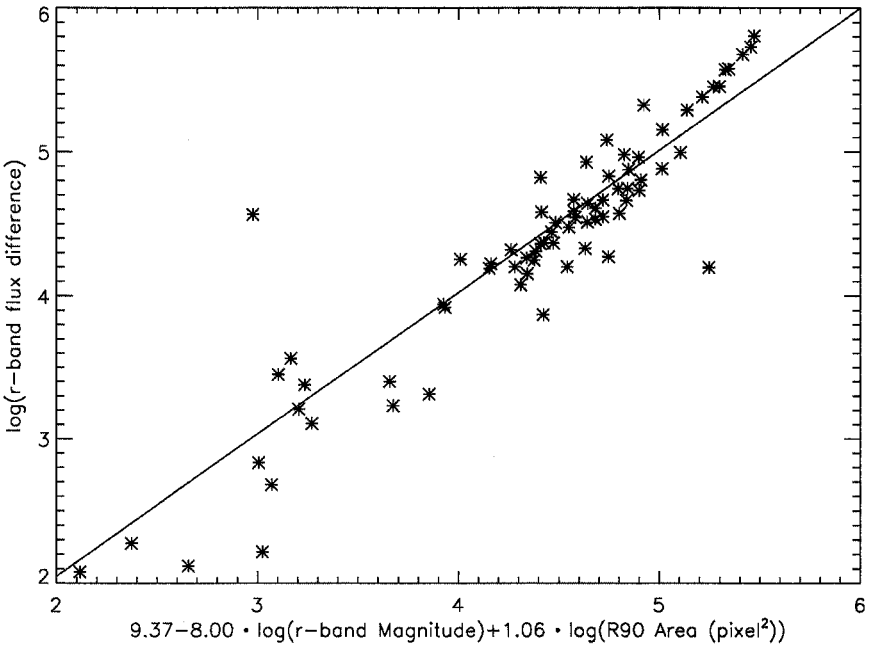

Figure A.37 Two-dimensional projection of the $\log(m_r)$, log(R90 area) and $\log(r$-band flux loss) for the model galaxies on the same 3D coordinate system defined by Equation A.7. The red line is the best fit line to the HI selected sample and demonstrates the quality of the derived sky subtraction correction for this set of model galaxies. Much of the deviation from the plane can be explained by deblending errors that were not taken into account in this study.

galaxies appear to have more flux missing than Equation A.7 predicts. This is likely due to the deblending of these large galaxies. In fact, much of the scatter is most likely caused by bad deblending that will lead to incorrect measurements of the area and magnitude values. However, although the scatter is larger than in Figure A.35, the mean relation provides an excellent first-order correction for sky subtraction and can be directly applied to the SDSS catalog data.

A.4.1 Size Distribution of SDSS Galaxies

Although the magnitude of the sky subtraction errors can be quite large, this problem does not have much of an impact on most SDSS science. The main galaxy samples used in most studies do not have many large galaxies because they intentionally avoid nearby galaxies,

which have large angular extent. Figure A.18 shows the R90 angular size distribution for the DR4 main galaxy sample. Most of the galaxies have R90 smaller than $20''$. More importantly, only a few galaxies with R90 extents larger than $1'$ exist in the main galaxy sample, making the need for sky subtraction corrections virtually unnecessary. Therefore, unlike the errors due to inclination effects, the sky subtraction errors are *only* important for galaxies in the very nearby universe including most galaxies in the HIPASS/SDSS sample.

A.5 Summary

Working with large galaxies in the SDSS can be quite challenging. Deblending, inclination and sky subtraction all introduce significant errors to a catalog level analysis of galaxy properties. In this appendix we have not only demonstrated the existence of these three problems but quantitatively explored the amplitude and behavior of each. We have presented a series of solutions for correcting the problems at the SDSS catalog level and shown that these solutions correctly rectify the problems. More work is required to accurately correct for deblending in an automated way and the issue of what model to use for the inclination correction is still unresolved. This study will make large galaxy science with SDSS attainable to the greater community and will increase our ability to understand the nearby universe.

Appendix B

VISUAL DATA

This appendix contains the visual imagery that make up the HIPASS/SDSS HI selected sample. Some of the excitement of studying galaxies comes from looking beyond the numeric quantities and enjoying the pretty pictures. Much can be learned from visually inspecting the optical and radio data products. We provide this appendix to display the data that are included in this thesis. For each galaxy in the sample, we include a gri color composite image, an image in each of the five SDSS bands (u, g, r, i, z), the Sérsic and bulge-disk models (see Chapter 3 for more details) and the HI spectrum.

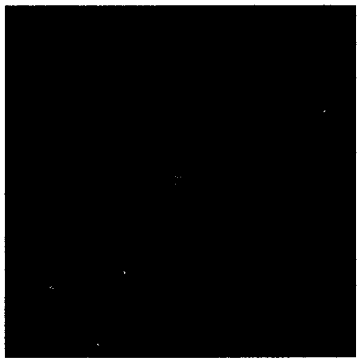

HIPEQ0014−00

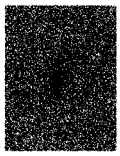
u

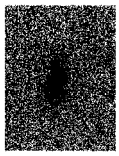
g

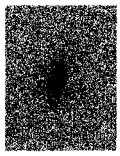
r

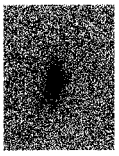
i


z

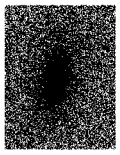
Sersic Fit

HI Spectrum

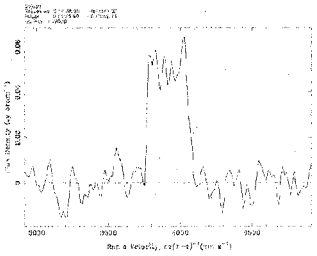

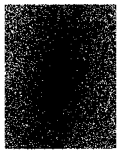
Bulge−Disk Fit

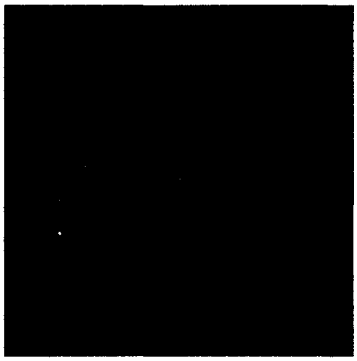

HIPEQ0027−01a

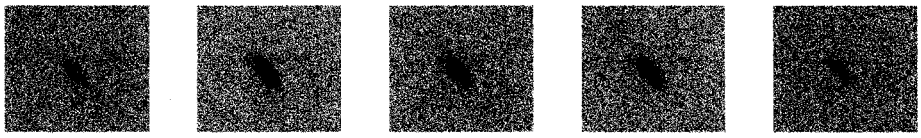

u g r i z

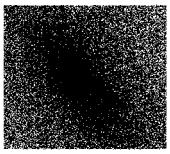

Sersic Fit

HI Spectrum

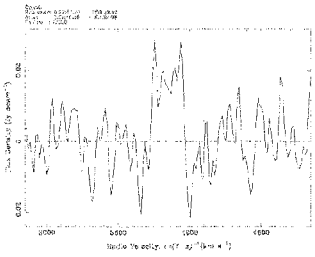

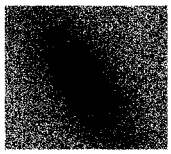

Bulge−Disk Fit

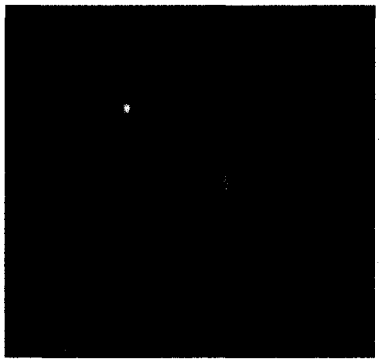

HIPEQ0033−01

u g r i z

Sersic Fit

HI Spectrum

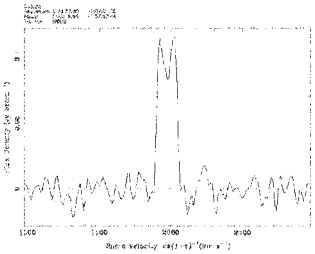

Bulge−Disk Fit

HIPEQ0043−00

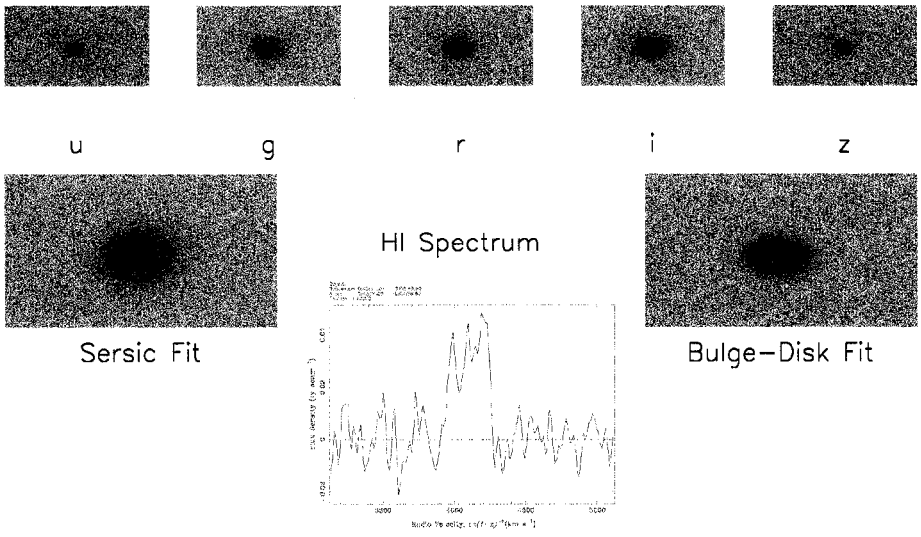

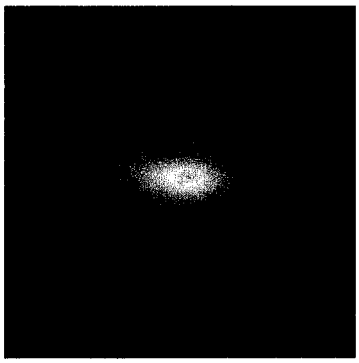

HIPEQ0051−00

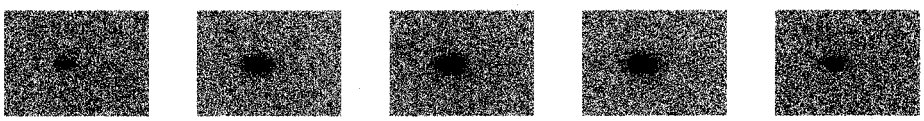

u g r i z

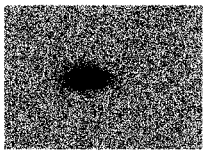

Sersic Fit

HI Spectrum

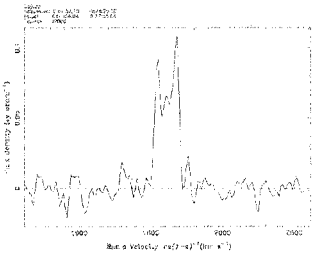

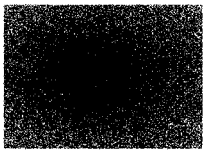

Bulge−Disk Fit

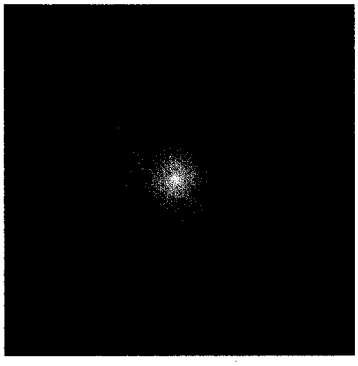

HIPEQ0058+00

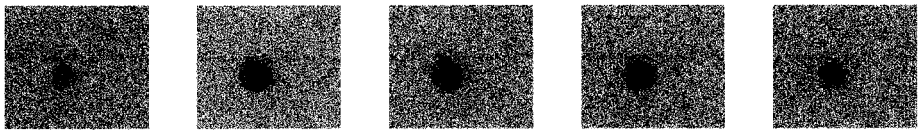

u g r i z

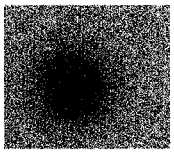

Sersic Fit

HI Spectrum

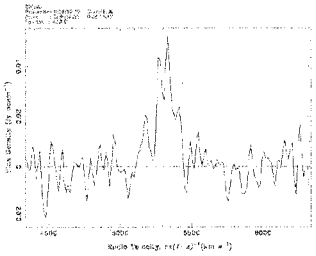

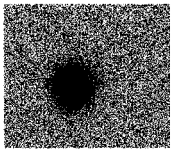

Bulge−Disk Fit

HIPEQ0107+01

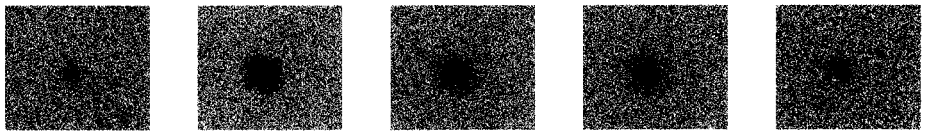

u g r i z

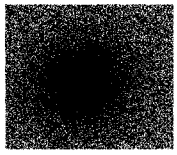

Sersic Fit

HI Spectrum

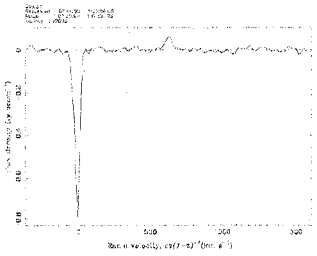

Bulge–Disk Fit

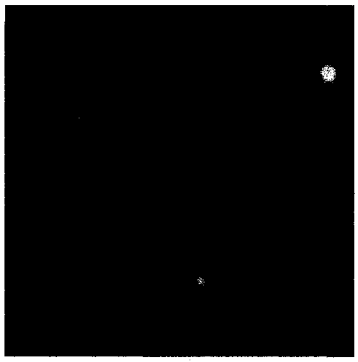

HIPEQ0119+00

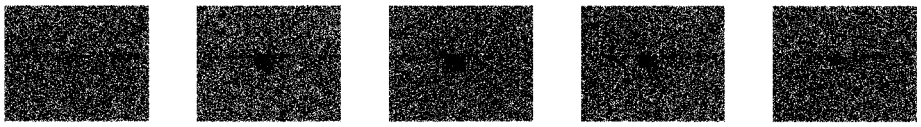

u g r i z

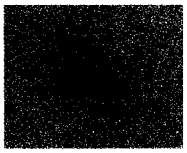

Sersic Fit

HI Spectrum

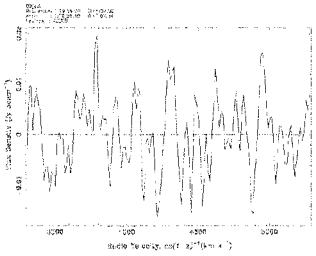

Bulge−Disk Fit

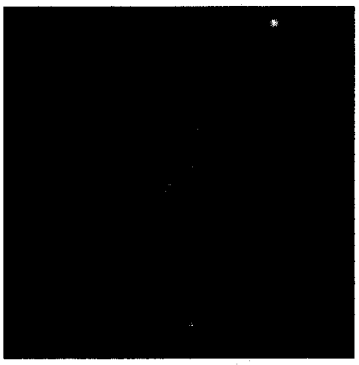

HIPEQ0120−00

u

g

r

i

z

Sersic Fit

HI Spectrum

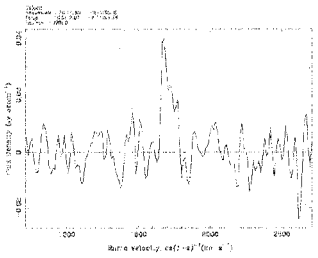

Bulge−Disk Fit

HIPEQ0122+00

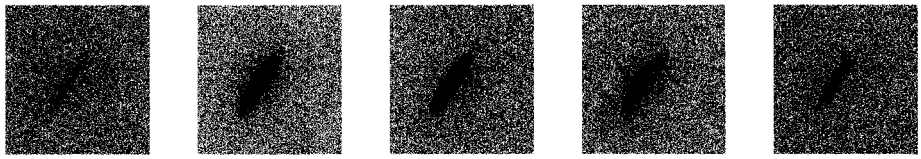

Sersic Fit

HI Spectrum

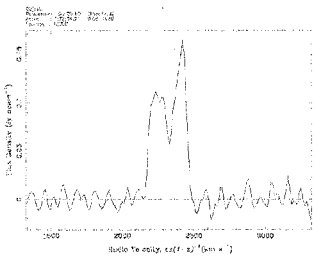

Bulge−Disk Fit

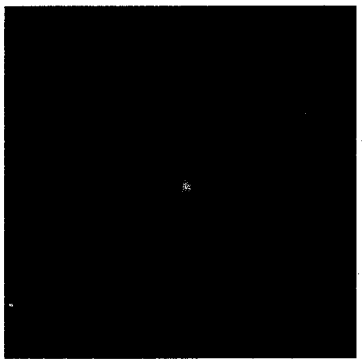

HIPEQ0123−00

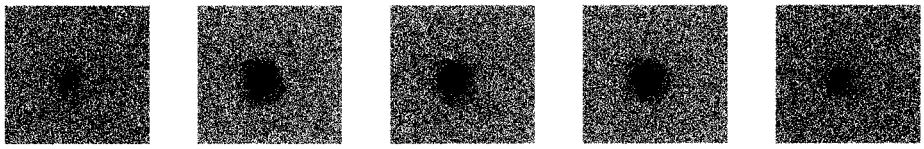

u g r i z

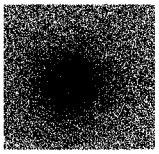

Sersic Fit

HI Spectrum

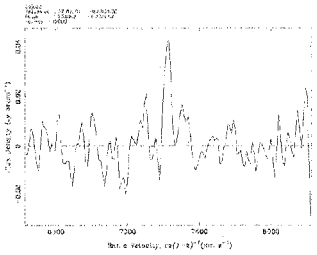

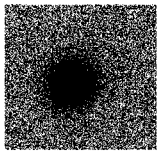

Bulge−Disk Fit

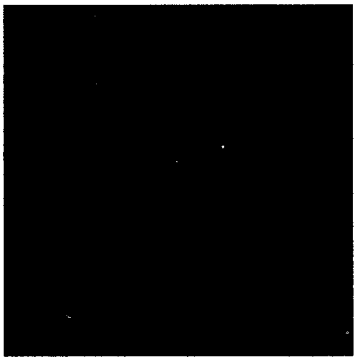

HIPEQ0126+00a

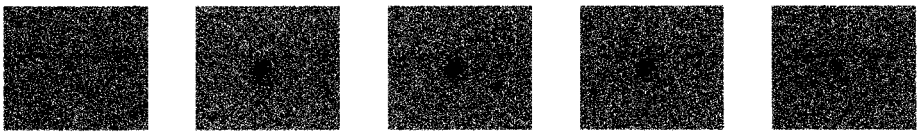

u g r i z

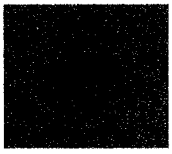

Sersic Fit

HI Spectrum

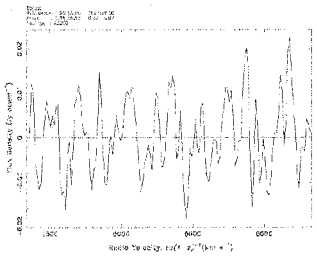

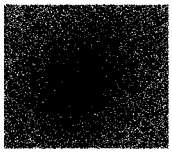

Bulge–Disk Fit

HIPEQ0126−00b

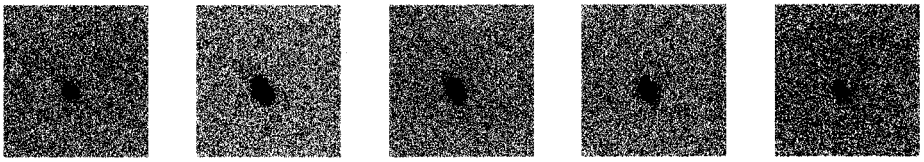

u g r i z

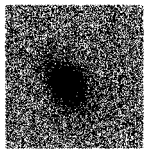

Sersic Fit

HI Spectrum

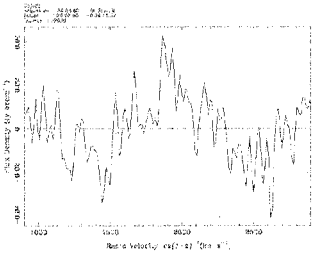

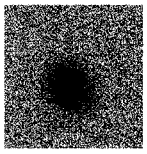

Bulge−Disk Fit

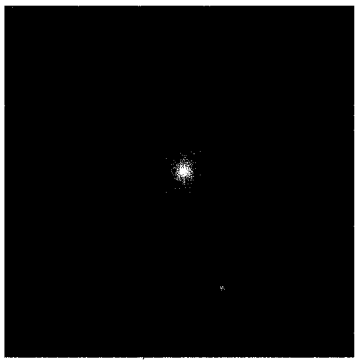

HIPEQ0154−00

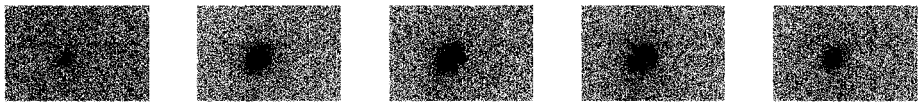

u g r i z

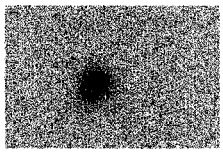

Sersic Fit

HI Spectrum

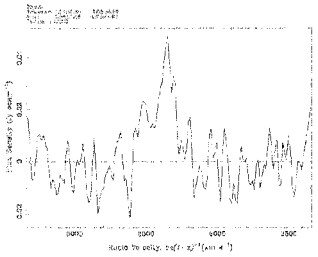

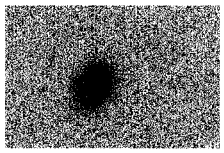

Bulge−Disk Fit

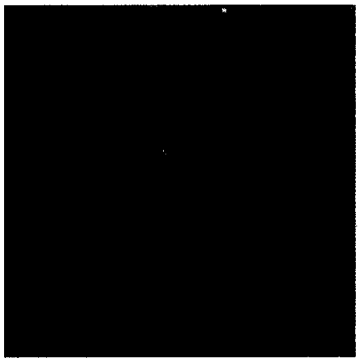

HIPEQ0222−00

u

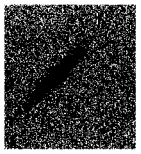

g

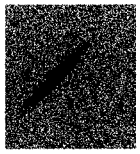

r

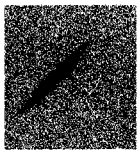

i

z

Sersic Fit

HI Spectrum

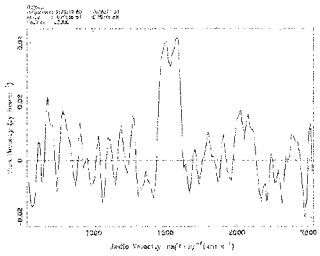

Bulge−Disk Fit

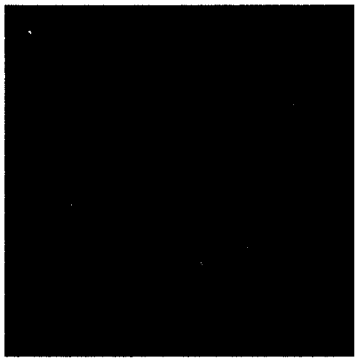

HIPEQ0228−01

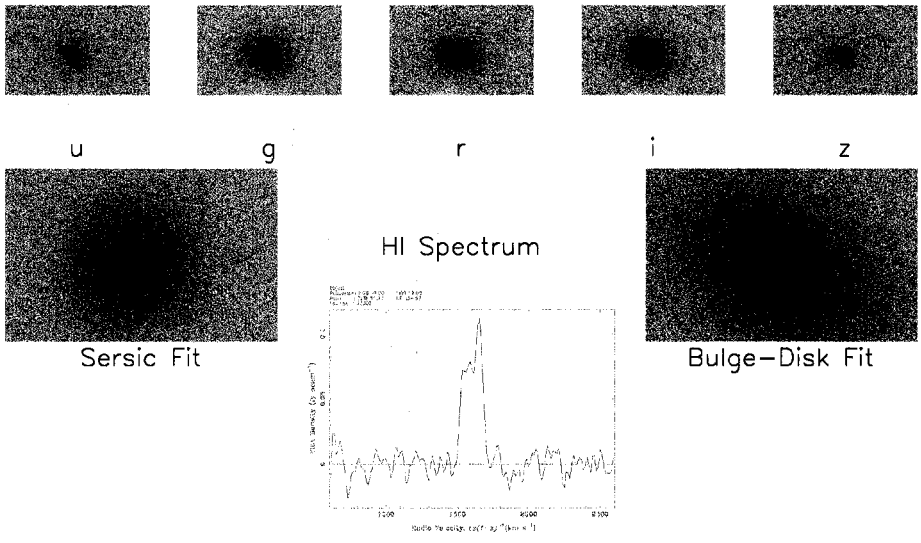

HIPEQ0230+00

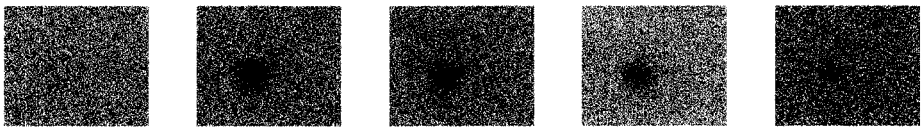

u g r i z

Sersic Fit

HI Spectrum

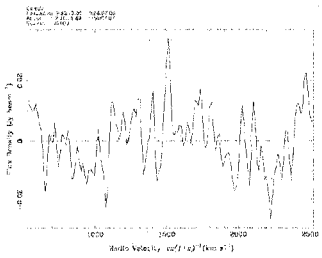

Bulge–Disk Fit

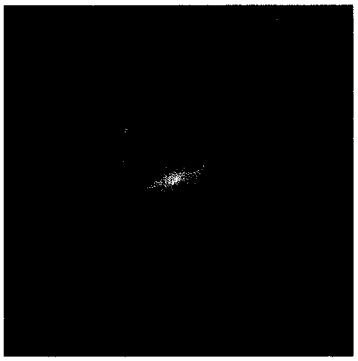

HIPEQ0230−01

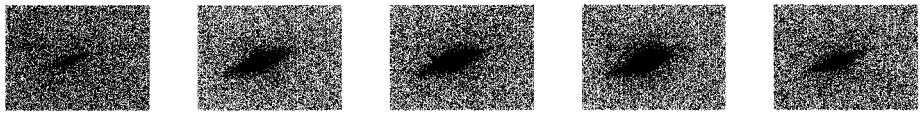

u g r i z

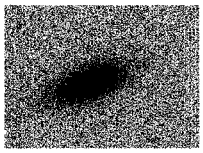

Sersic Fit

HI Spectrum

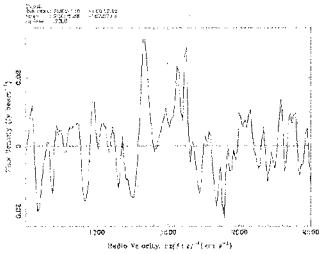

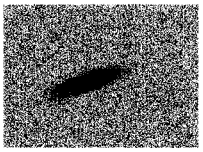

Bulge−Disk Fit

HIPEQ0231+00

u g r i z

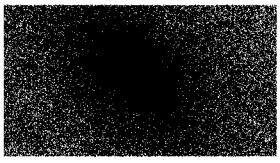

Sersic Fit

HI Spectrum

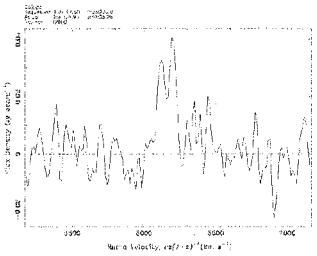

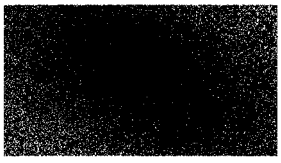

Bulge−Disk Fit

HIPEQ0236+00

u g r i z

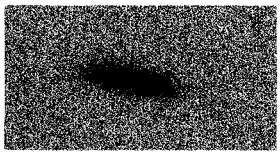

Sersic Fit

HI Spectrum

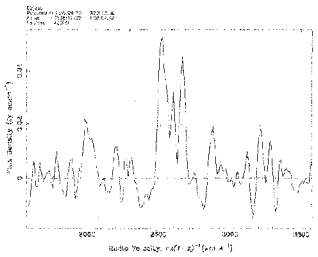

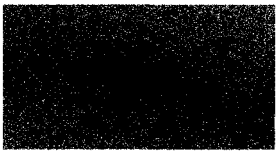

Bulge−Disk Fit

HIPEQ0238+00

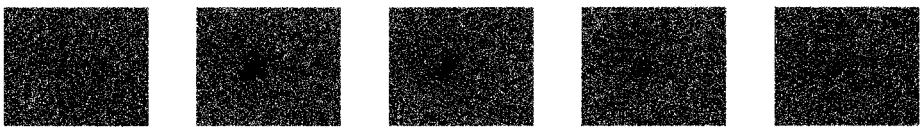

u g r i z

Sersic Fit

HI Spectrum

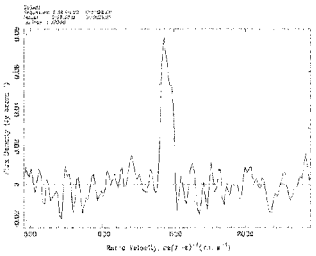

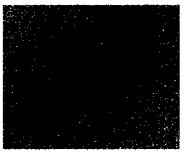

Bulge–Disk Fit

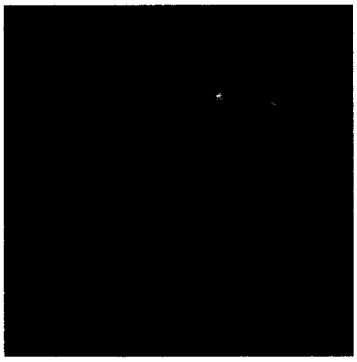

HIPEQ0240+01

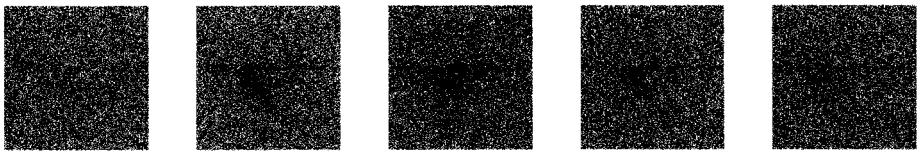

u g r i z

Sersic Fit

HI Spectrum

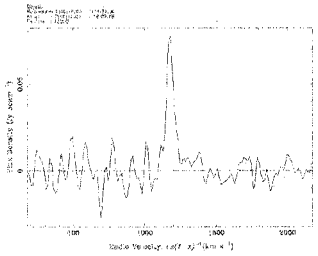

Bulge–Disk Fit

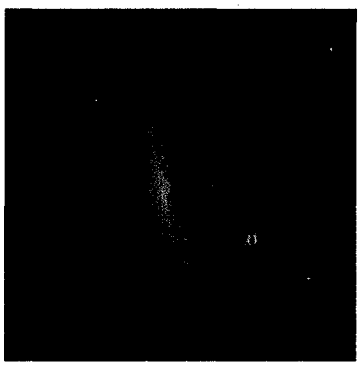

HIPEQ0241+00

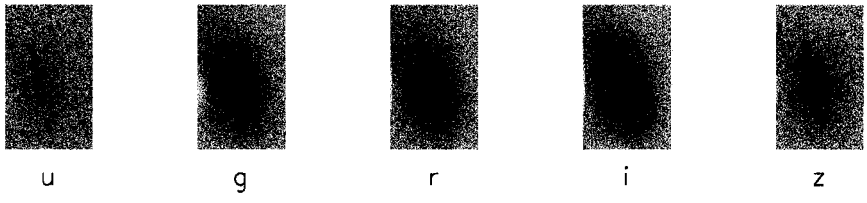

u g r i z

Sersic Fit

HI Spectrum

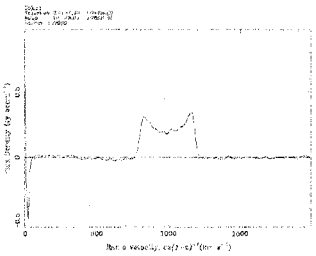

Bulge−Disk Fit

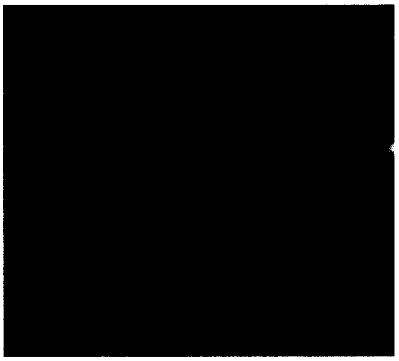

HIPEQ0244+00

u g r i z

Sersic Fit

HI Spectrum

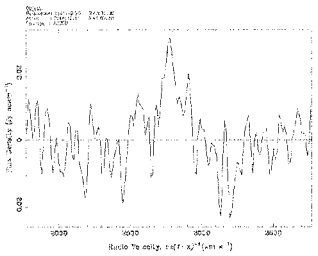

Bulge–Disk Fit

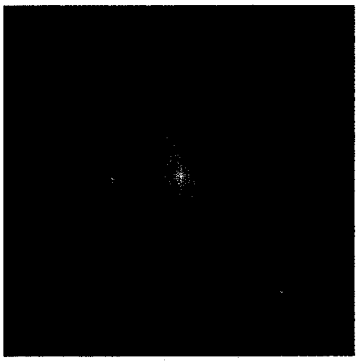

HIPEQ0246−00a

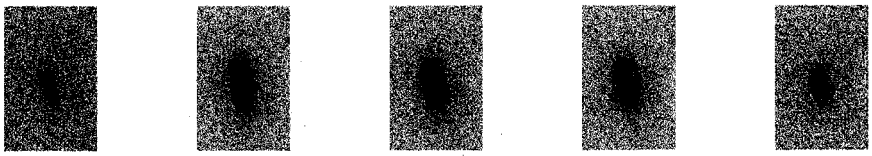

u g r i z

Sersic Fit

HI Spectrum

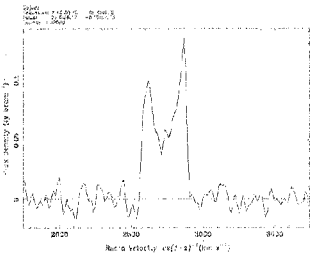

Bulge−Disk Fit

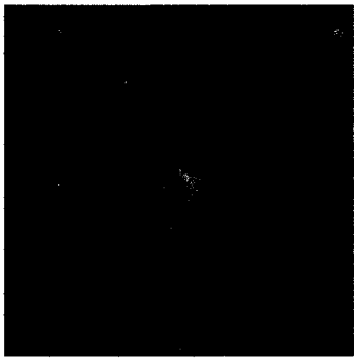

HIPEQ0246−00b

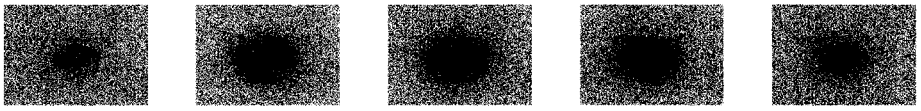

u g r i z

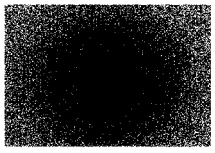

Sersic Fit

HI Spectrum

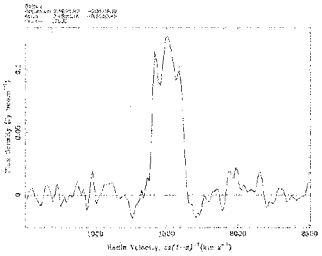

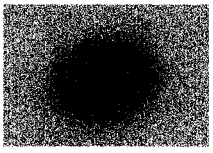

Bulge−Disk Fit

HIPEQ0249−00a

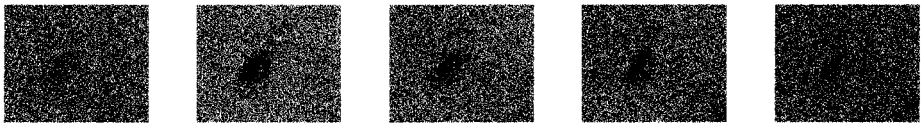

u g r i z

Sersic Fit

HI Spectrum

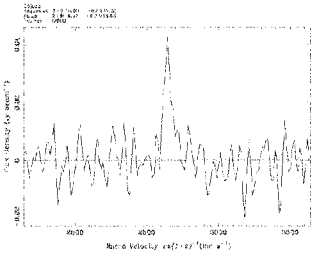

Bulge−Disk Fit

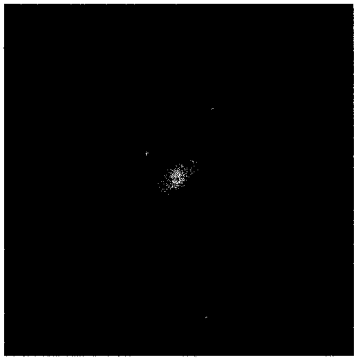

HIPEQ0249−00b

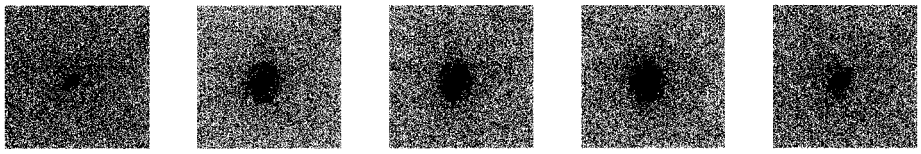

u g r i z

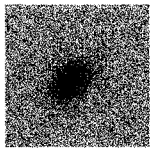

Sersic Fit

HI Spectrum

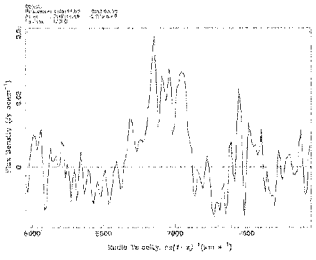

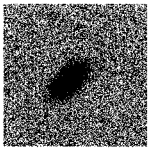

Bulge−Disk Fit

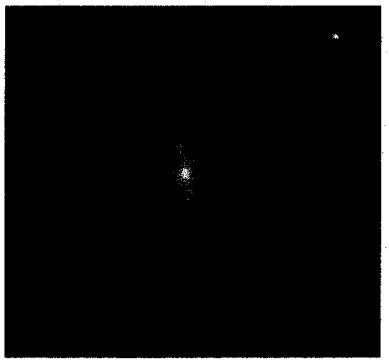

HIPEQ0249−00

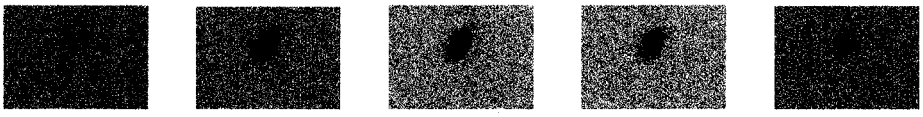

u g r i z

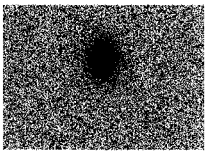

Sersic Fit

HI Spectrum

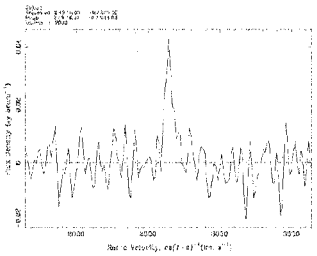

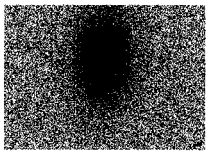

Bulge−Disk Fit

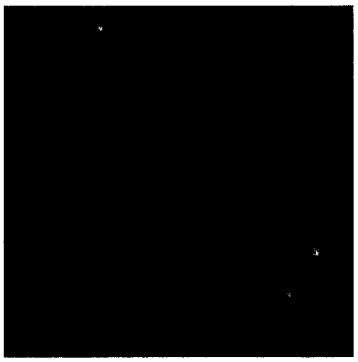

HIPEQ0251−01

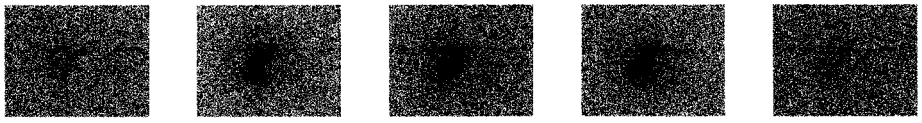

u g r i z

Sersic Fit

HI Spectrum

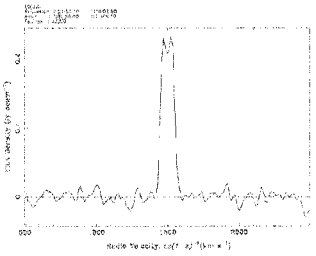

Bulge−Disk Fit

HIPEQ0300+00

u g r i z

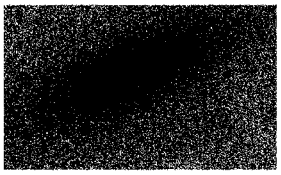

Sersic Fit

HI Spectrum

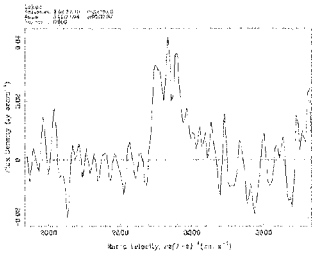

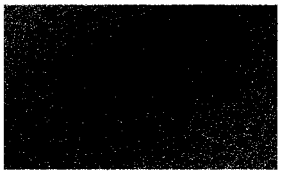

Bulge−Disk Fit

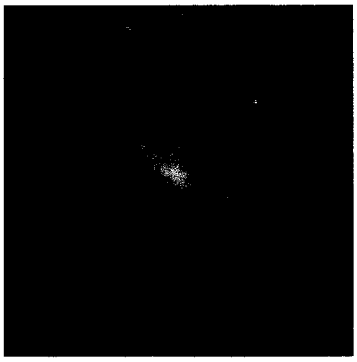

HIPEQ0301−00

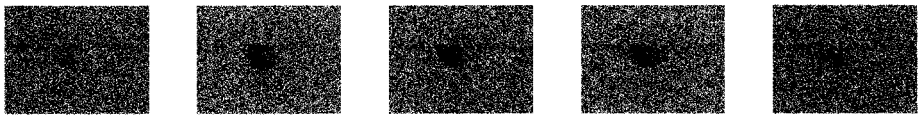

u g r i z

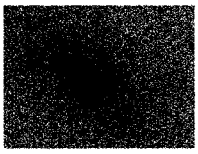

Sersic Fit

HI Spectrum

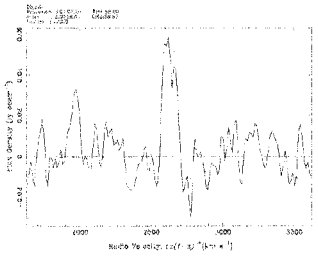

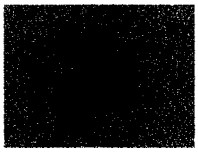

Bulge−Disk Fit

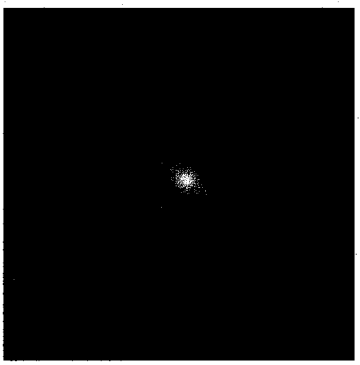

HIPEQ0306−00

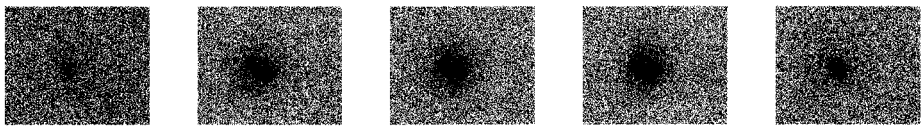

u g r i z

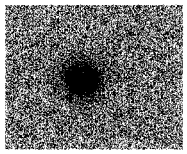

Sersic Fit

HI Spectrum

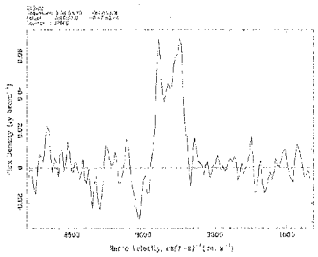

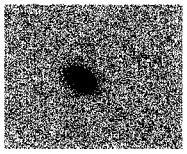

Bulge−Disk Fit

HIPEQ0316−00

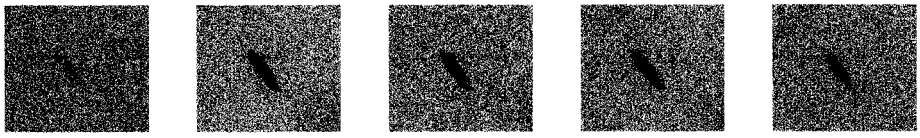

u g r i z

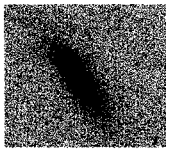

Sersic Fit

HI Spectrum

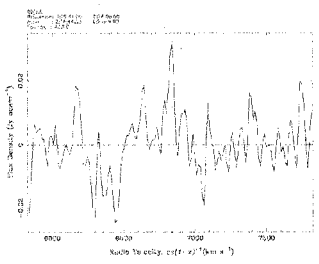

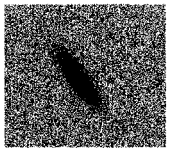

Bulge−Disk Fit

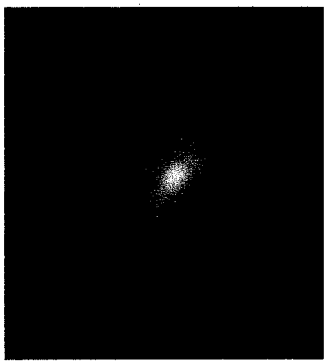

HIPEQ0320−06


u


g


r

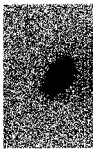
i


z


Sersic Fit

HI Spectrum

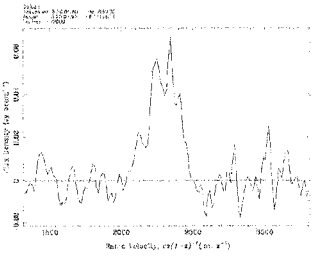


Bulge−Disk Fit

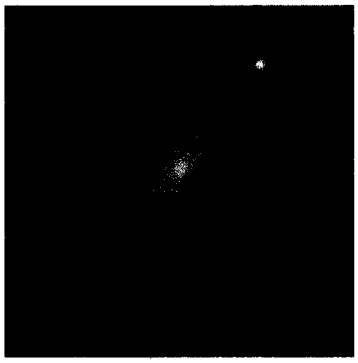

HIPEQ0351−00

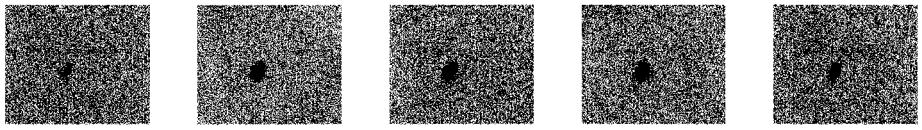

u g r i z

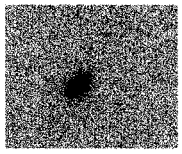

Sersic Fit

HI Spectrum

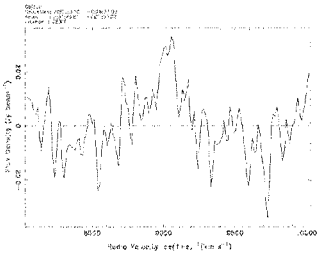

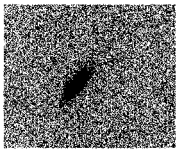

Bulge−Disk Fit

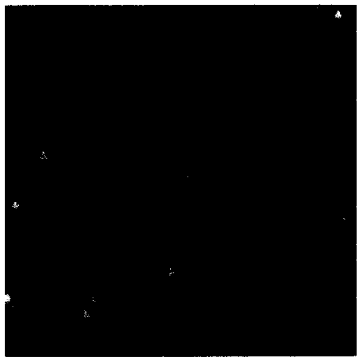

HIPEQ0809+00

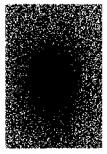

Sersic Fit

HI Spectrum

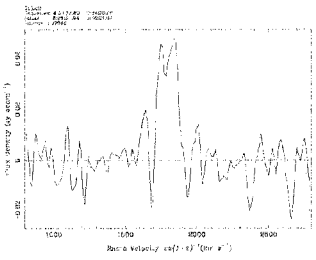

Bulge−Disk Fit

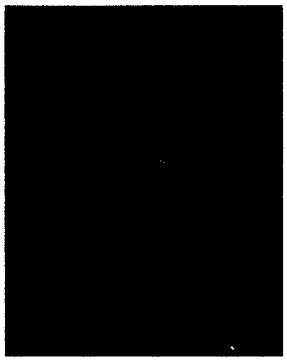

HIPEQ0821−00

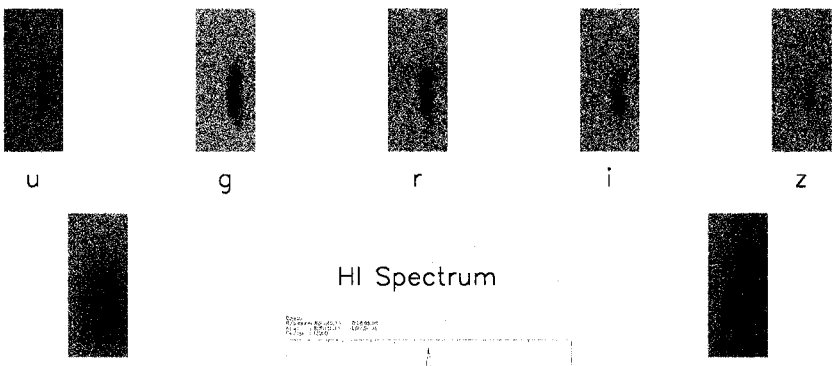

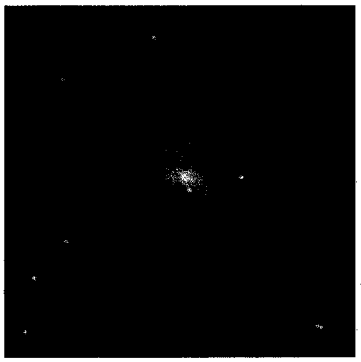

HIPEQ0821+03b

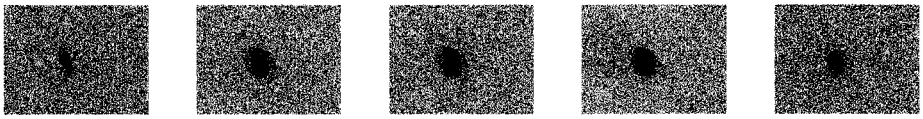

u g r i z

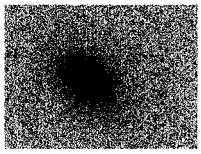

Sersic Fit

HI Spectrum

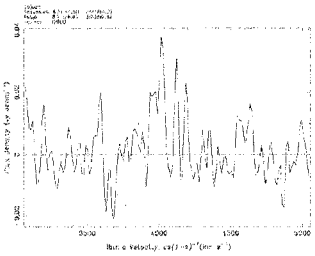

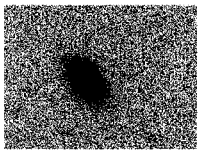

Bulge−Disk Fit

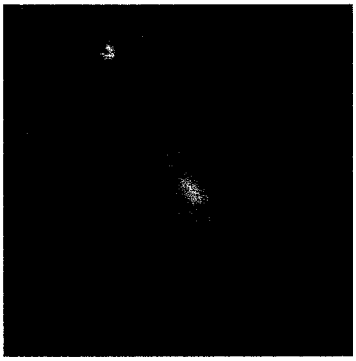

HIPEQ0822−00

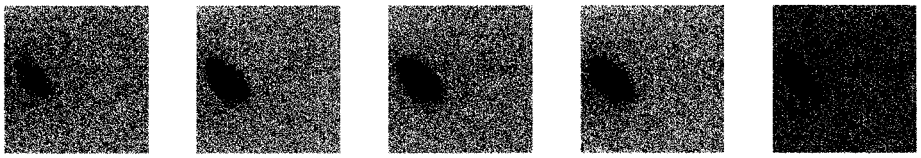

u g r i z

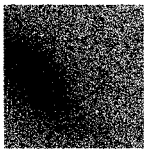

Sersic Fit

HI Spectrum

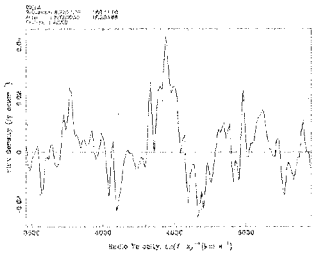

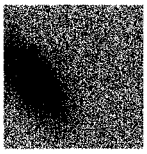

Bulge−Disk Fit

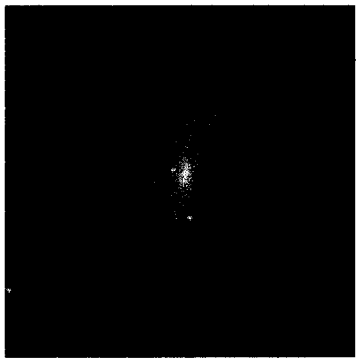

HIPEQ0825−00

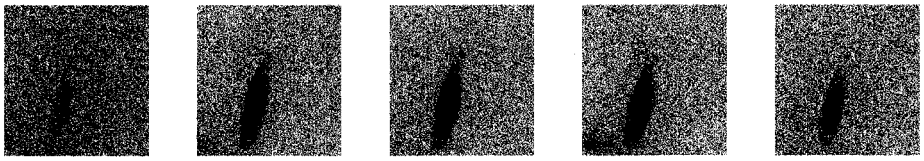

u g r i z

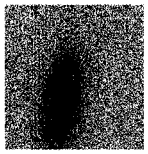

Sersic Fit

HI Spectrum

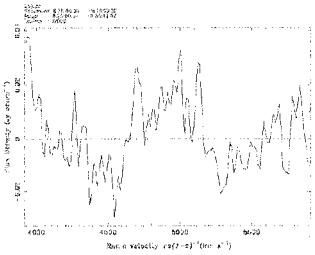

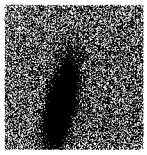

Bulge−Disk Fit

HIPEQ0855+02

u g r i z

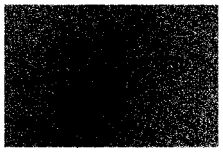

Sersic Fit

HI Spectrum

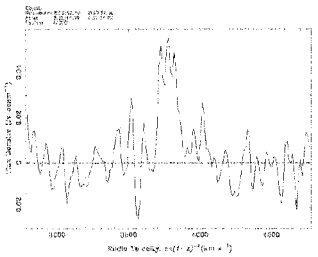

Bulge–Disk Fit

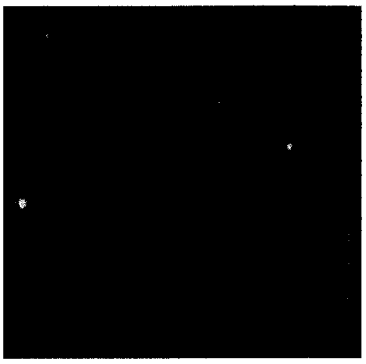

HIPEQ0856+00

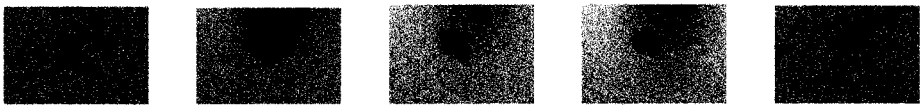

u g r i z

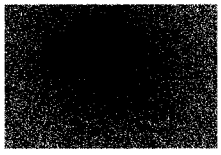

Sersic Fit

HI Spectrum

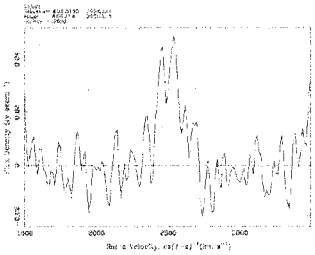

Bulge–Disk Fit

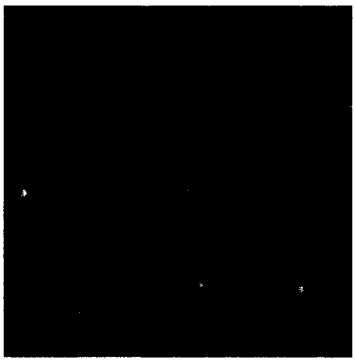

HIPEQ0923−00

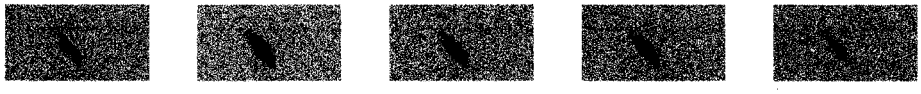

u g r i z

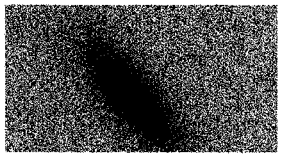

Sersic Fit

HI Spectrum

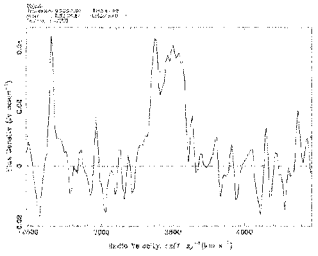

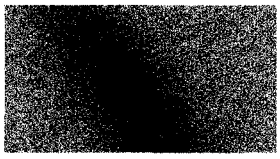

Bulge−Disk Fit

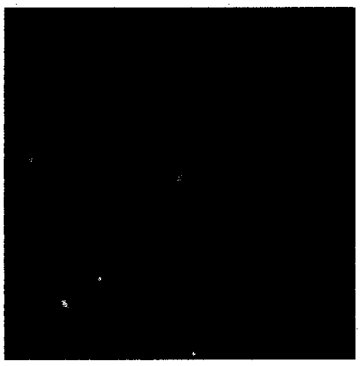

HIPEQ0930+04

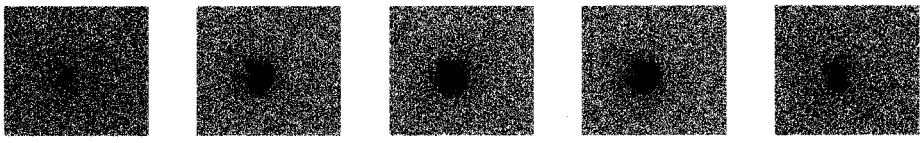

u g r i z

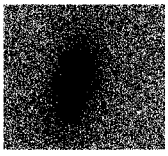

Sersic Fit

HI Spectrum

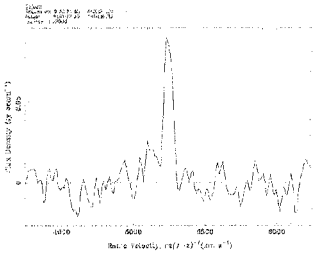

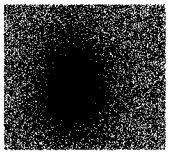

Bulge–Disk Fit

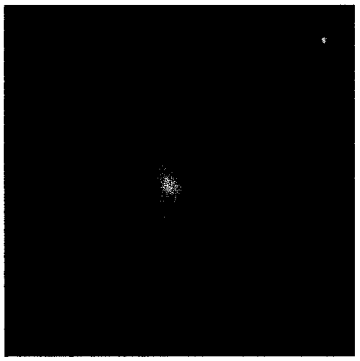

HIPEQ0936+01

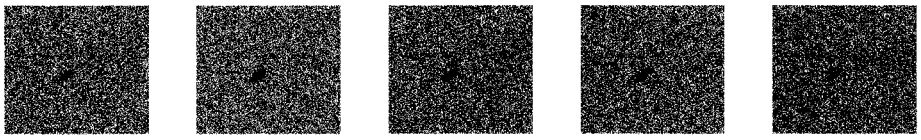

u g r i z

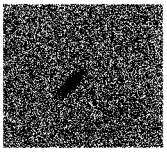

Sersic Fit

HI Spectrum

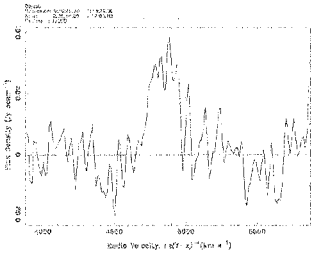

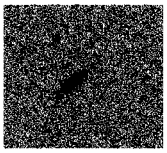

Bulge−Disk Fit

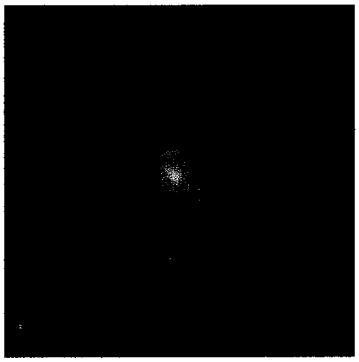

HIPEQ0942+00

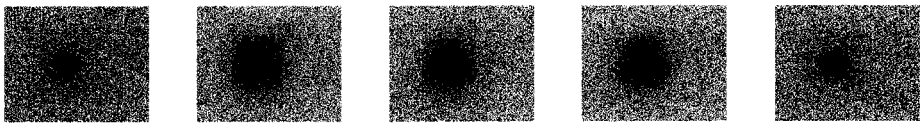

u g r i z

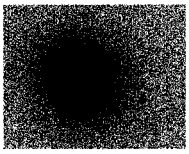

Sersic Fit

HI Spectrum

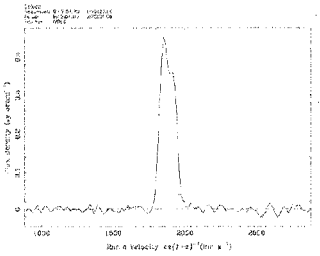

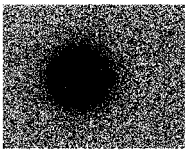

Bulge–Disk Fit

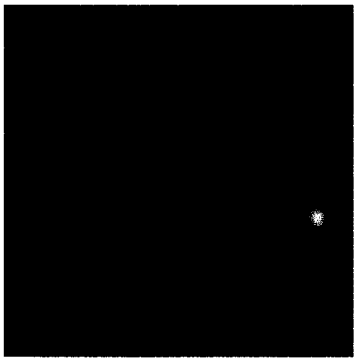

HIPEQ0944−00b

u g r i z

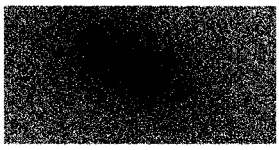

Sersic Fit

HI Spectrum

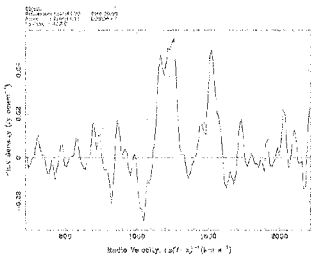

Bulge−Disk Fit

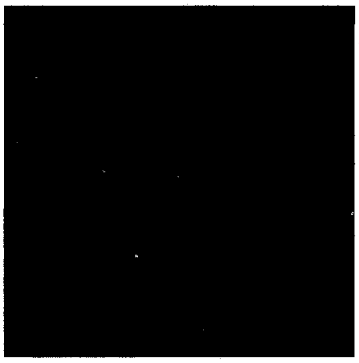

HIPEQ0945+01

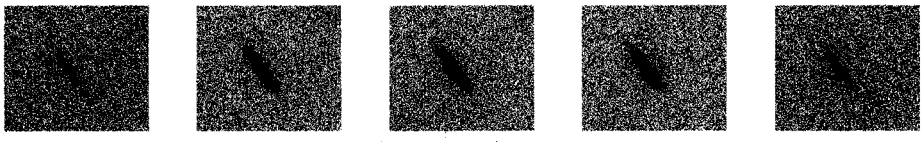

u g r i z

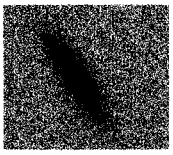

Sersic Fit

HI Spectrum

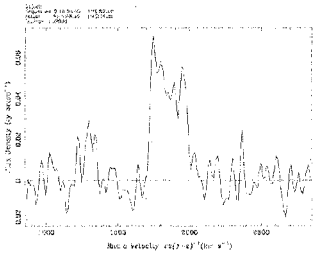

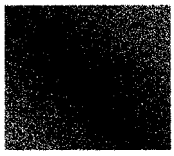

Bulge–Disk Fit

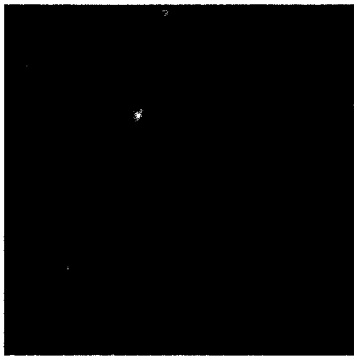

HIPEQ0946+02

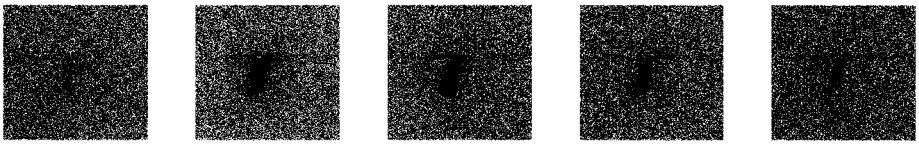

u g r i z

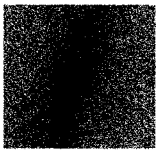

Sersic Fit

HI Spectrum

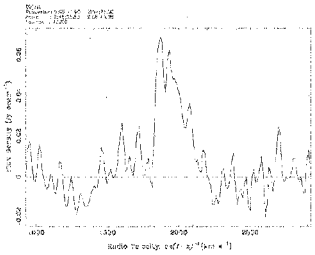

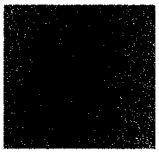

Bulge−Disk Fit

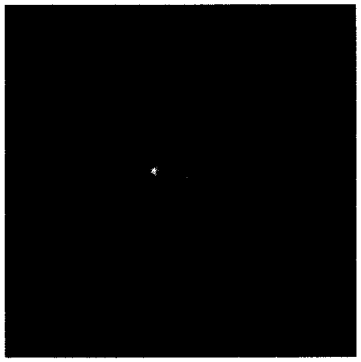

HIPEQ0947+00a

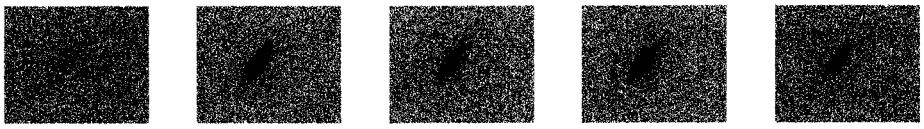

u g r i z

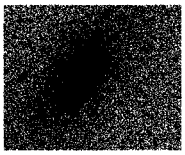

Sersic Fit

HI Spectrum

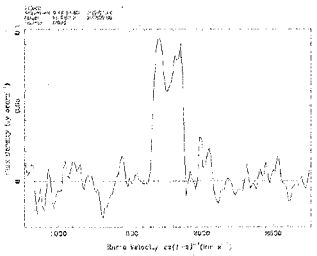

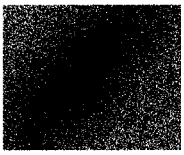

Bulge–Disk Fit

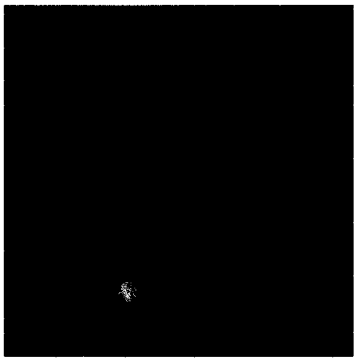

HIPEQ0947+00b

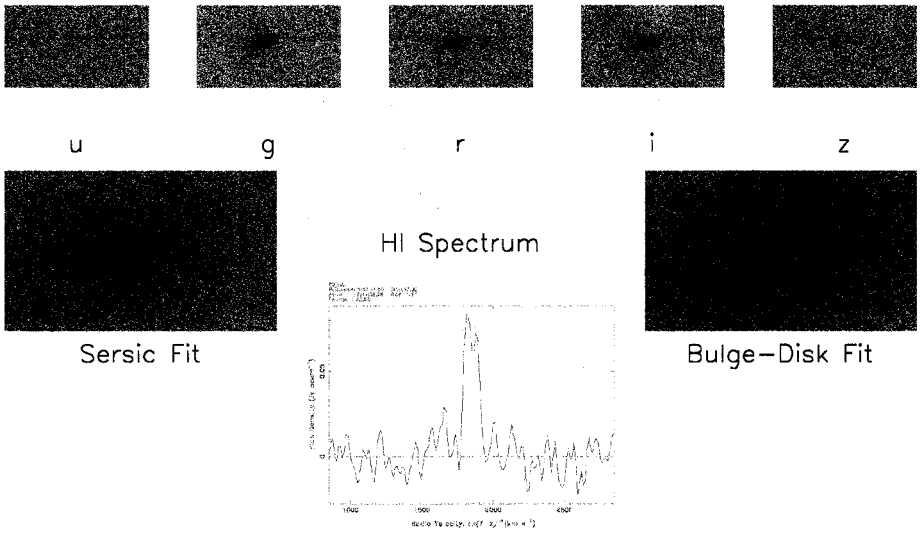

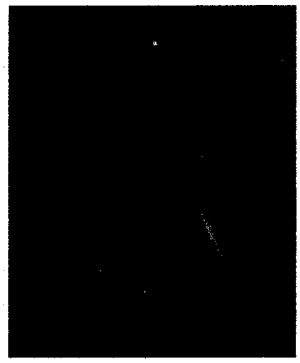

HIPEQ0953+01


u


g


r


i


z


Sersic Fit

HI Spectrum

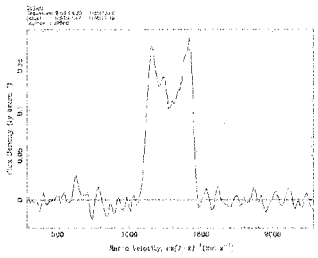


Bulge−Disk Fit

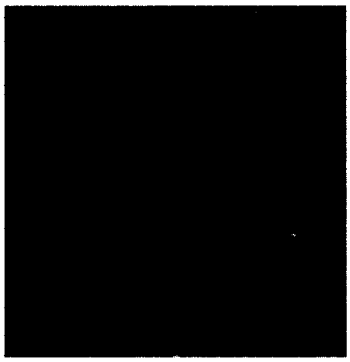

HIPEQ0954+01a

u g r i z

Sersic Fit

HI Spectrum

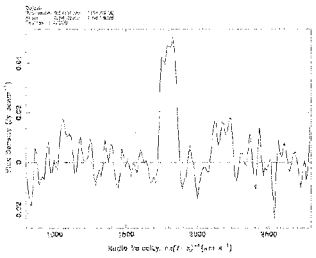

Bulge−Disk Fit

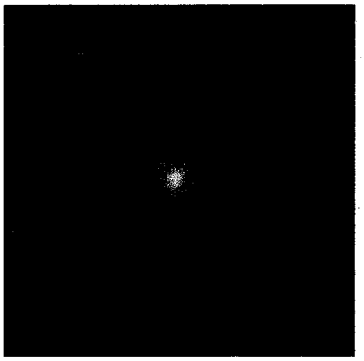

HIPEQ0954+02a

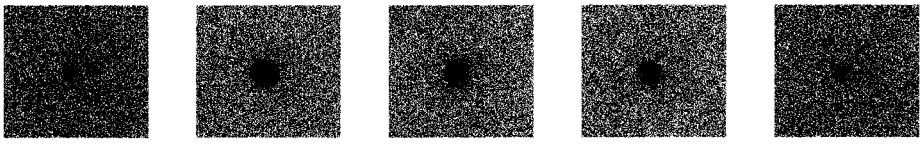

u g r i z

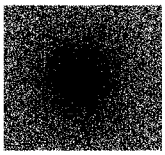

Sersic Fit

HI Spectrum

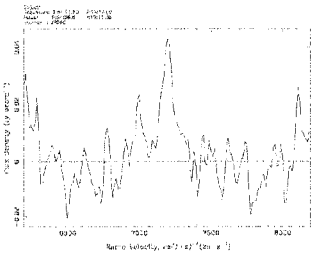

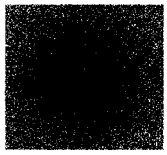

Bulge−Disk Fit

HIPEQ0955+04a

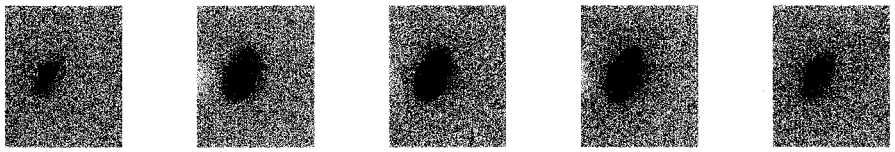

u g r i z

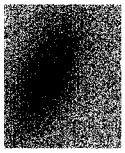

Sersic Fit

HI Spectrum

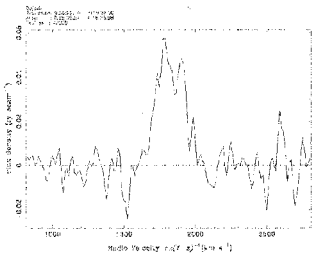

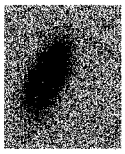

Bulge−Disk Fit

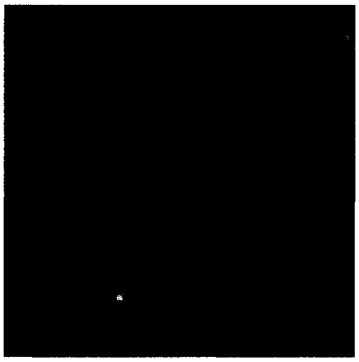

HIPEQ0958+01

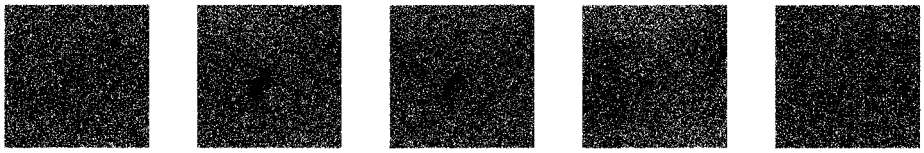

u g r i z

Sersic Fit

HI Spectrum

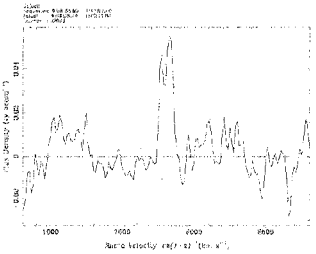

Bulge–Disk Fit

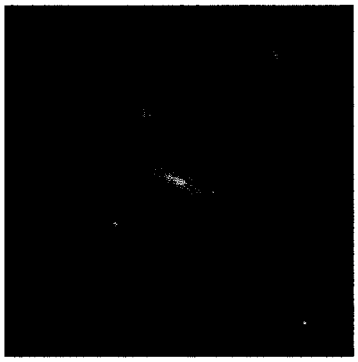

HIPEQ1000+03

u g r i z

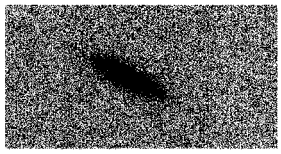

Sersic Fit

HI Spectrum

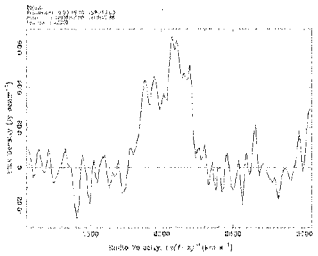

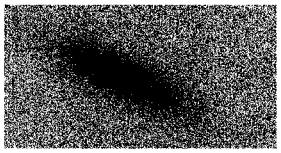

Bulge−Disk Fit

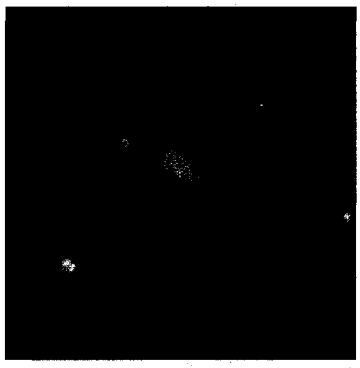

HIPEQ1010+05

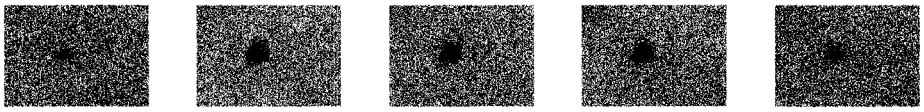

u g r i z

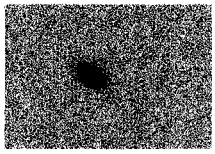

Sersic Fit

HI Spectrum

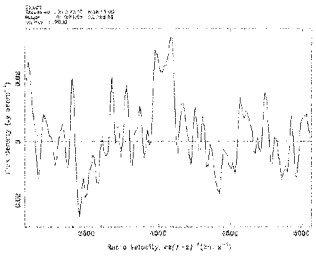

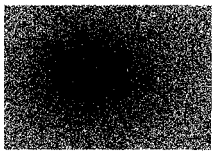

Bulge−Disk Fit

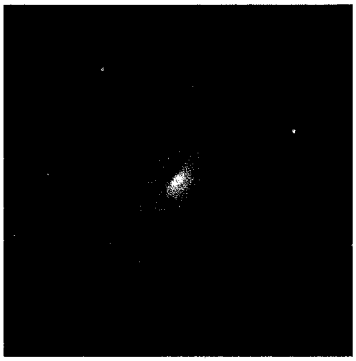

HIPEQ1014+03

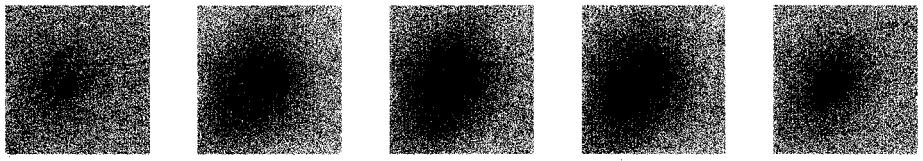

u g r i z

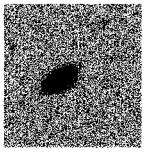

Sersic Fit

HI Spectrum

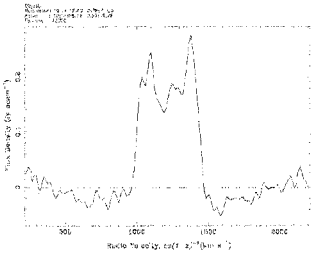

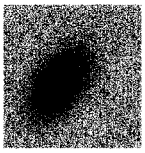

Bulge−Disk Fit

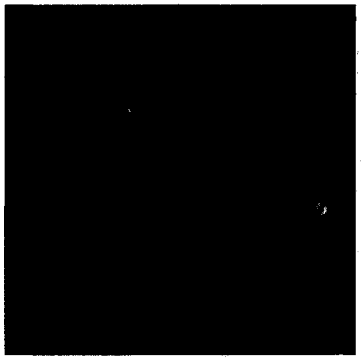

HIPEQ1015+02

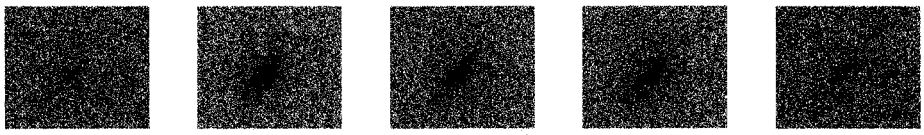

u g r i z

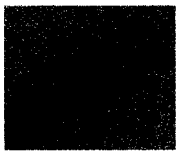

Sersic Fit

HI Spectrum

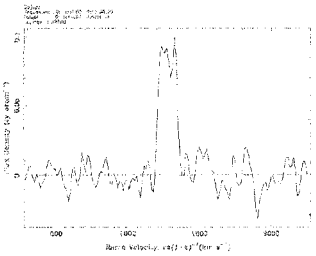

Bulge–Disk Fit

HIPEQ1026+03

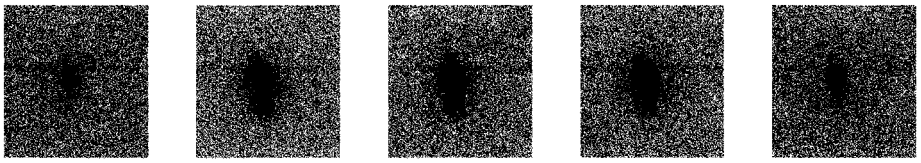

u g r i z

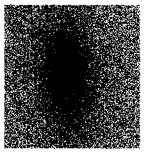

Sersic Fit

HI Spectrum

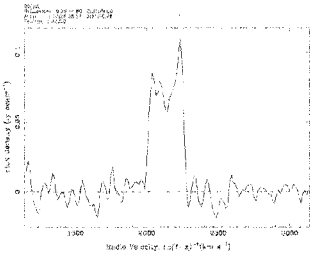

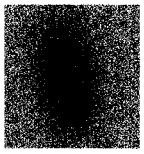

Bulge−Disk Fit

HIPEQ1028+03

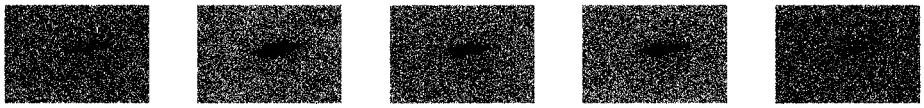

u g r i z

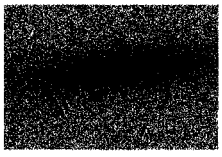

Sersic Fit

HI Spectrum

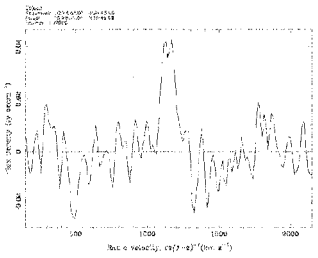

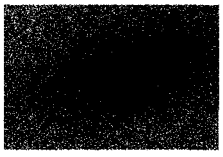

Bulge–Disk Fit

HIPEQ1031+04

u g r i z

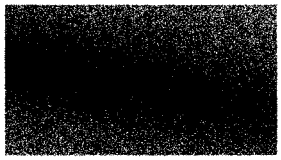

Sersic Fit

HI Spectrum

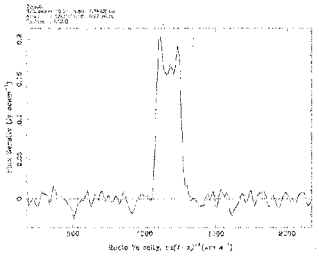

Bulge–Disk Fit

HIPEQ1039+01

u g r i z

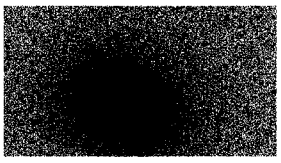

Sersic Fit

HI Spectrum

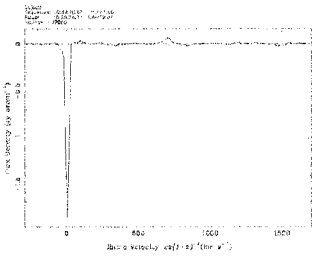

Bulge–Disk Fit

HIPEQ1041+00

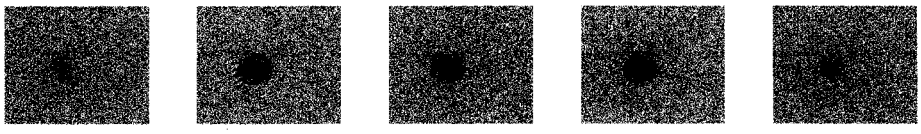

u g r i z

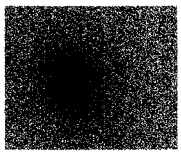

Sersic Fit

HI Spectrum

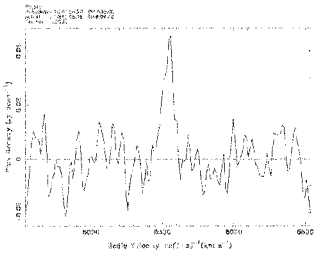

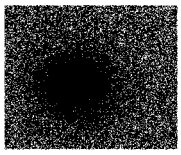

Bulge−Disk Fit

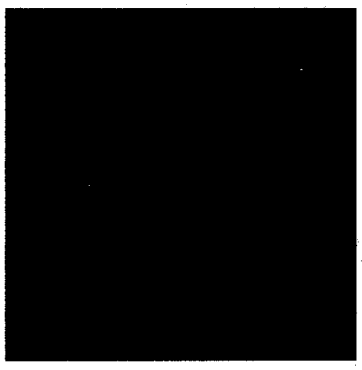

HIPEQ1046+01

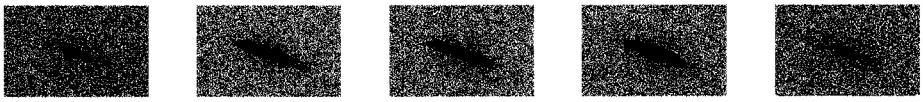

u g r i z

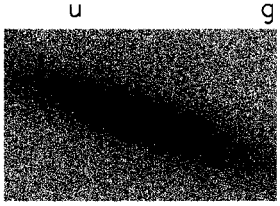

Sersic Fit

HI Spectrum

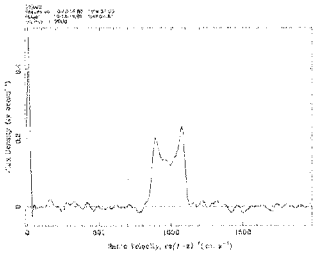

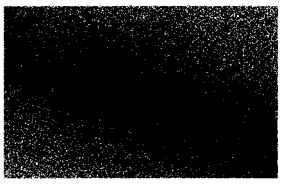

Bulge–Disk Fit

HIPEQ1050+01

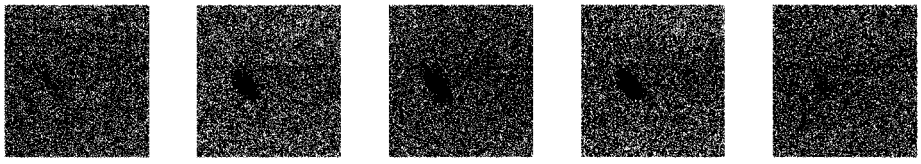

u g r i z

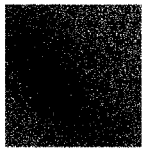

Sersic Fit

HI Spectrum

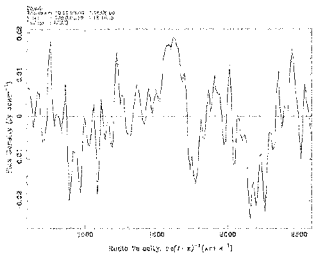

Bulge−Disk Fit

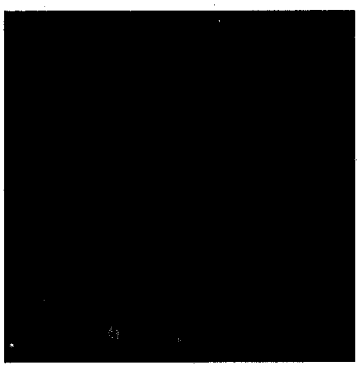

HIPEQ1051+04a

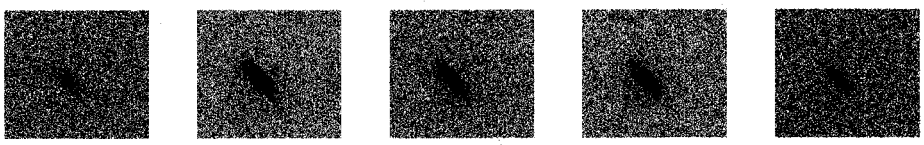

u g r i z

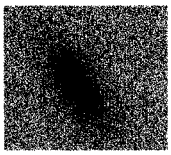

Sersic Fit

HI Spectrum

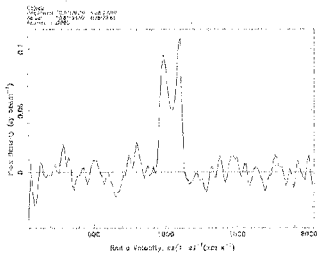

Bulge–Disk Fit

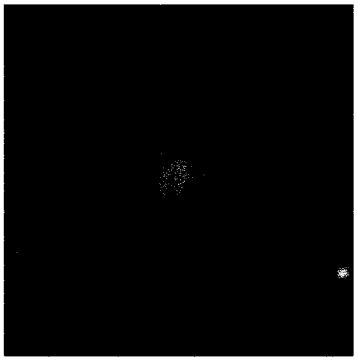

HIPEQ1052+00

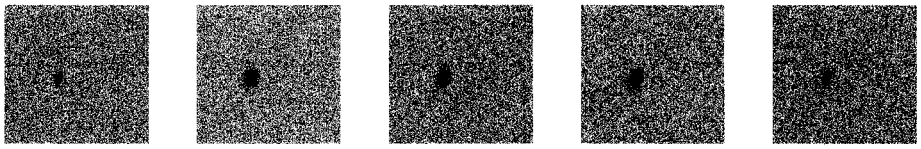

u g r i z

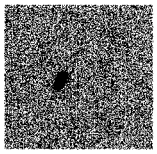

Sersic Fit

HI Spectrum

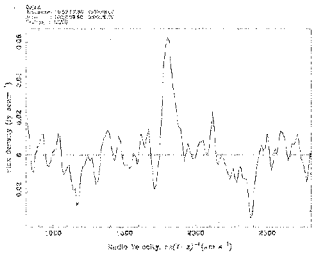

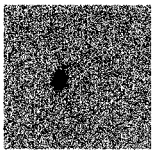

Bulge−Disk Fit

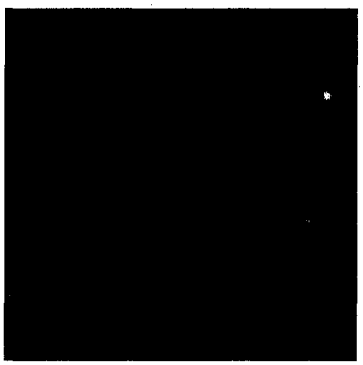

HIPEQ1053+02

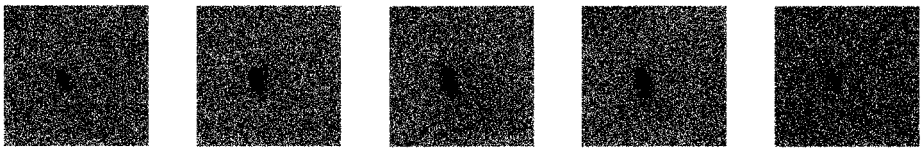

u g r i z

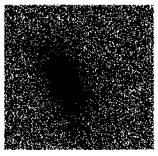

Sersic Fit

HI Spectrum

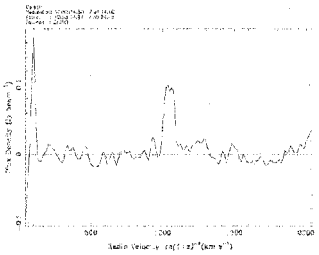

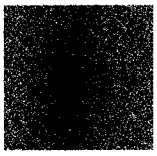

Bulge–Disk Fit

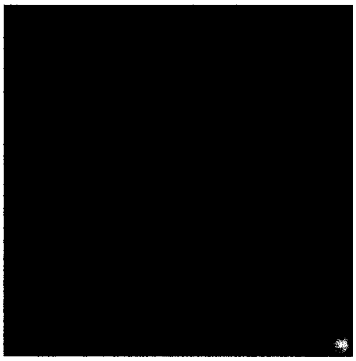

HIPEQ1055+02

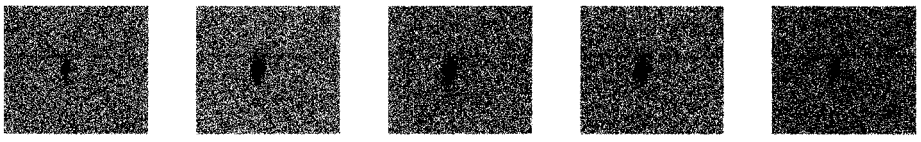

u g r i z

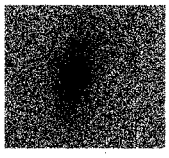

Sersic Fit

HI Spectrum

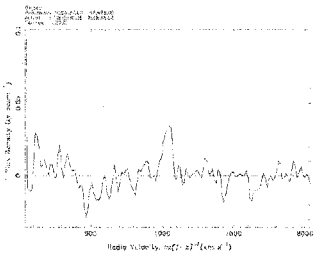

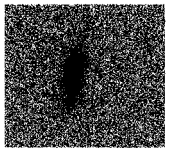

Bulge–Disk Fit

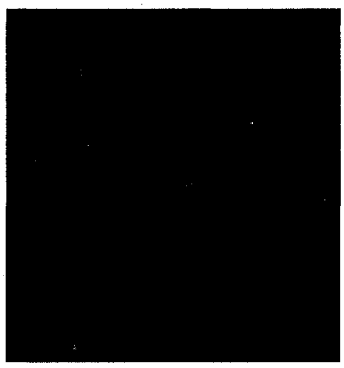

HIPEQ1101+03

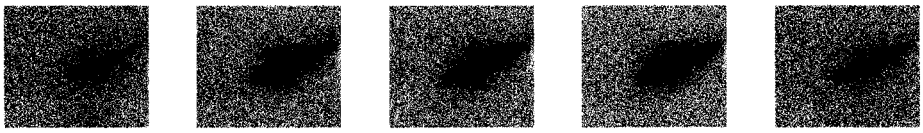

u g r i z

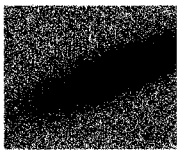

Sersic Fit

HI Spectrum

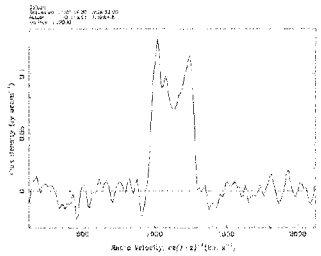

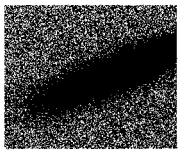

Bulge−Disk Fit

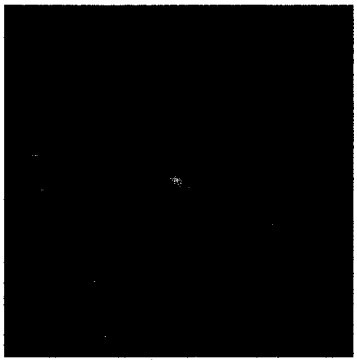

HIPEQ1109−00

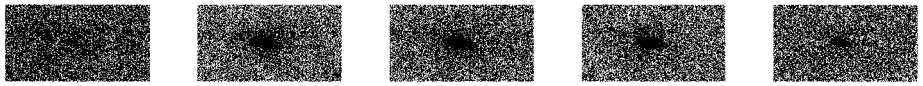

u g r i z

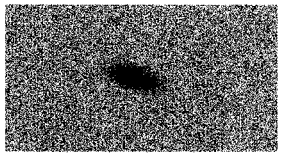

Sersic Fit

HI Spectrum

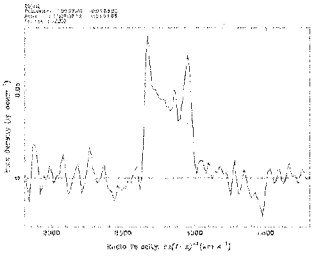

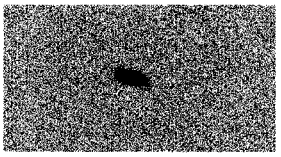

Bulge−Disk Fit

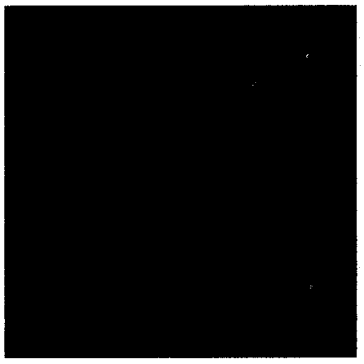

HIPEQ1110+01

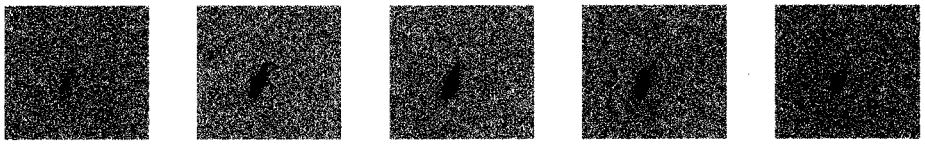

u g r i z

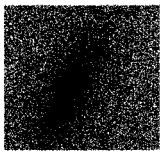

Sersic Fit

HI Spectrum

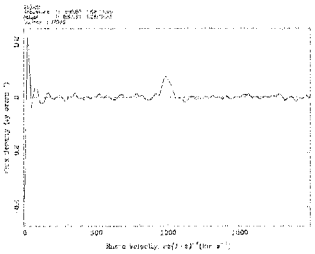

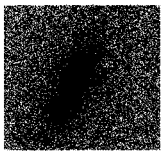

Bulge–Disk Fit

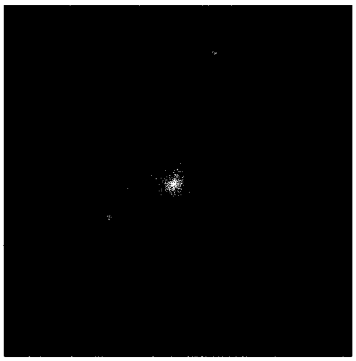

HIPEQ1113+05

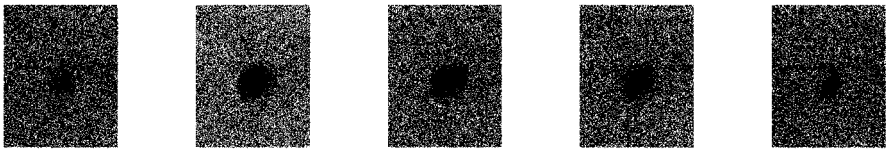

u g r i z

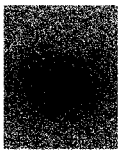

Sersic Fit

HI Spectrum

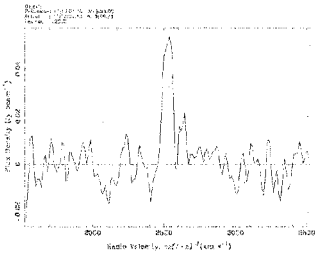

Bulge−Disk Fit

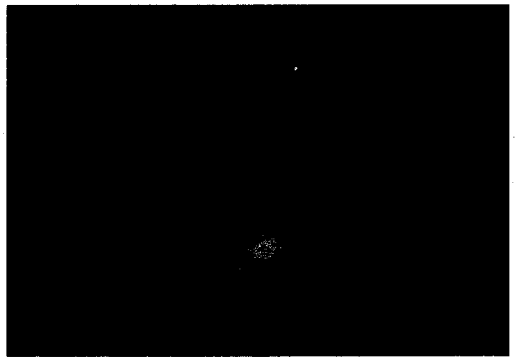

HIPEQ1117+04a

u g r i z

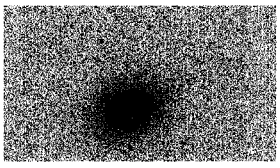

Sersic Fit

HI Spectrum

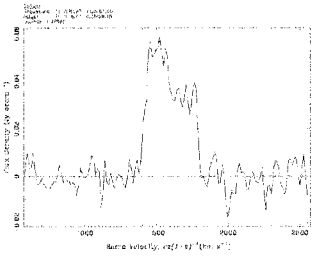

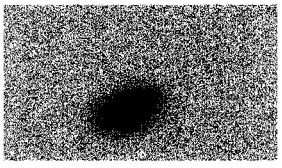

Bulge–Disk Fit

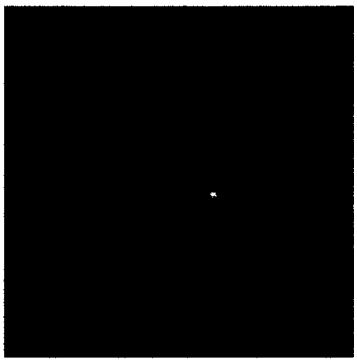

HIPEQ1119+02

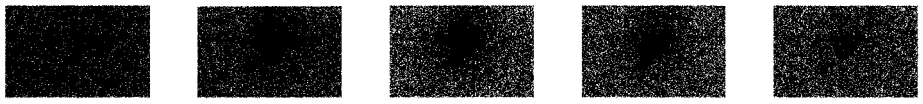

u g r i z

Sersic Fit

HI Spectrum

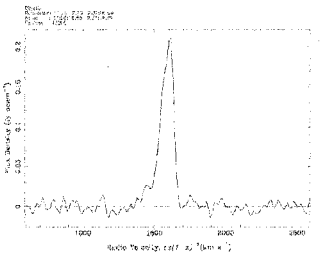

Bulge–Disk Fit

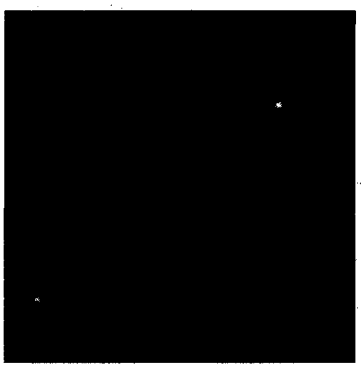

HIPEQ1124+03

u g r i z

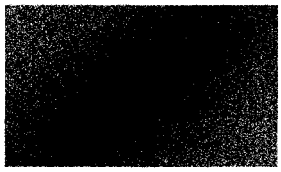

Sersic Fit

HI Spectrum

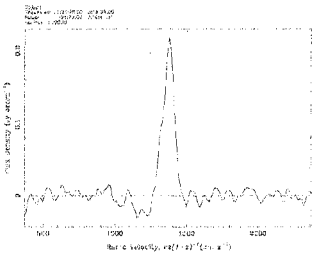

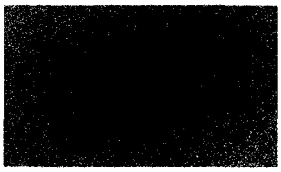

Bulge−Disk Fit

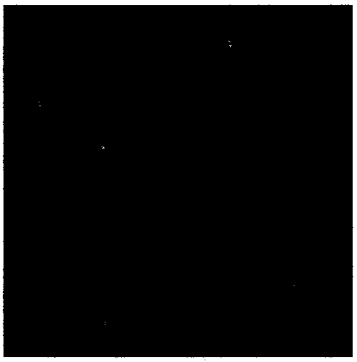

HIPEQ1127−01

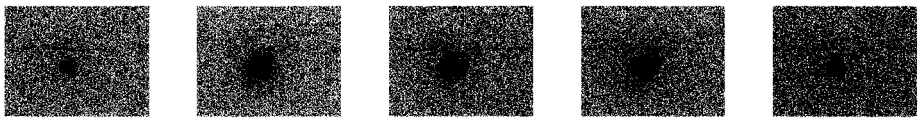

u g r i z

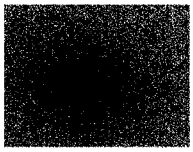

Sersic Fit

HI Spectrum

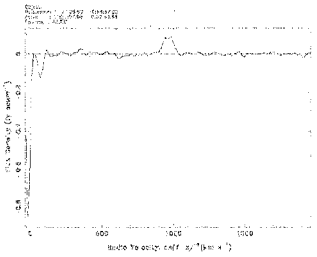

Bulge−Disk Fit

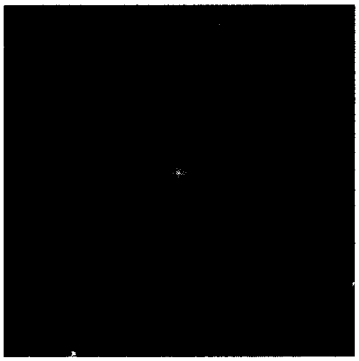

HIPEQ1131−02

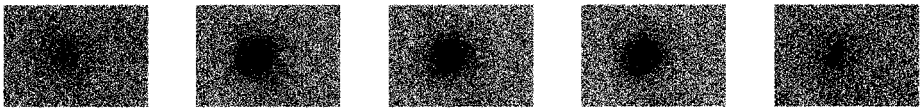

u g r i z

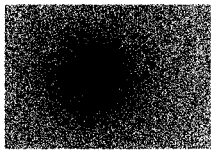

Sersic Fit

HI Spectrum

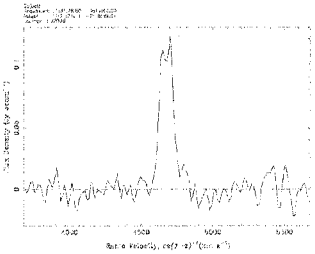

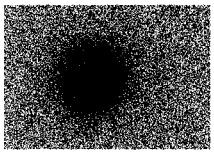

Bulge−Disk Fit

HIPEQ1133−03

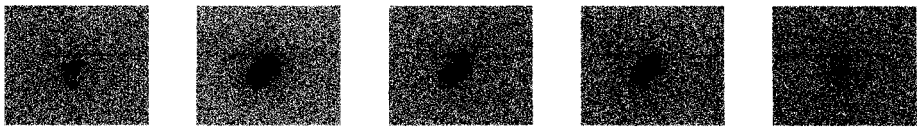

u g r i z

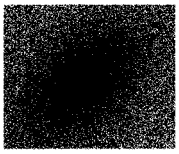

Sersic Fit

HI Spectrum

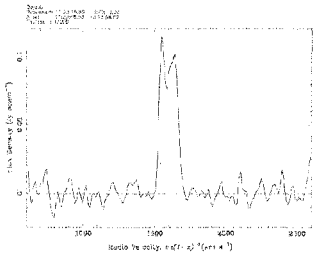

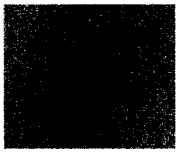

Bulge−Disk Fit

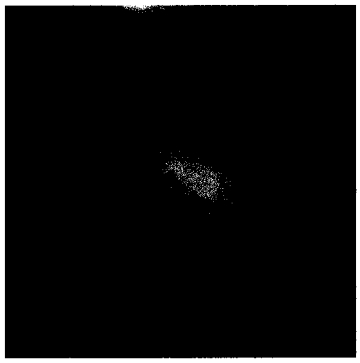

HIPEQ1136+00

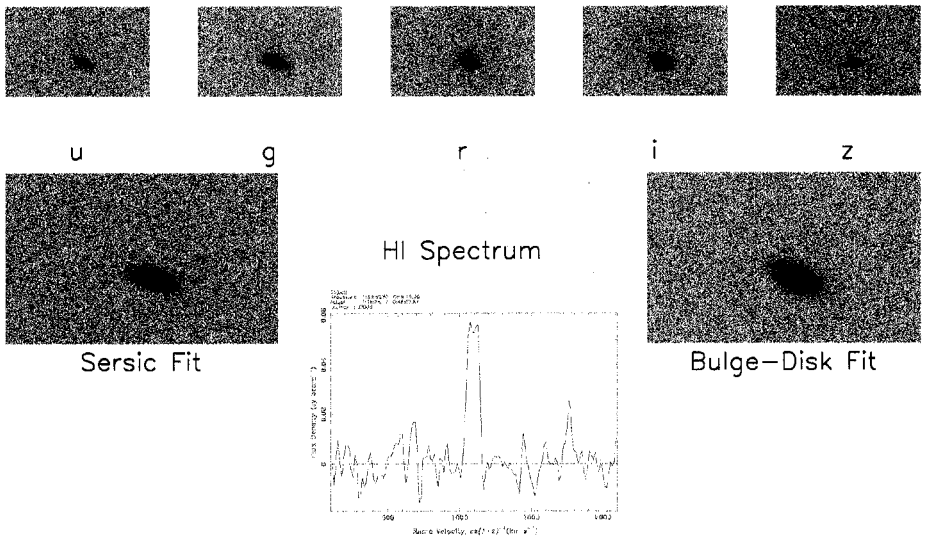

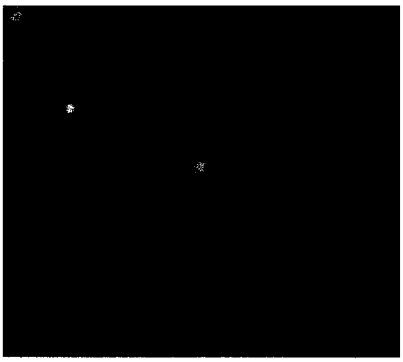

HIPEQ1138+03

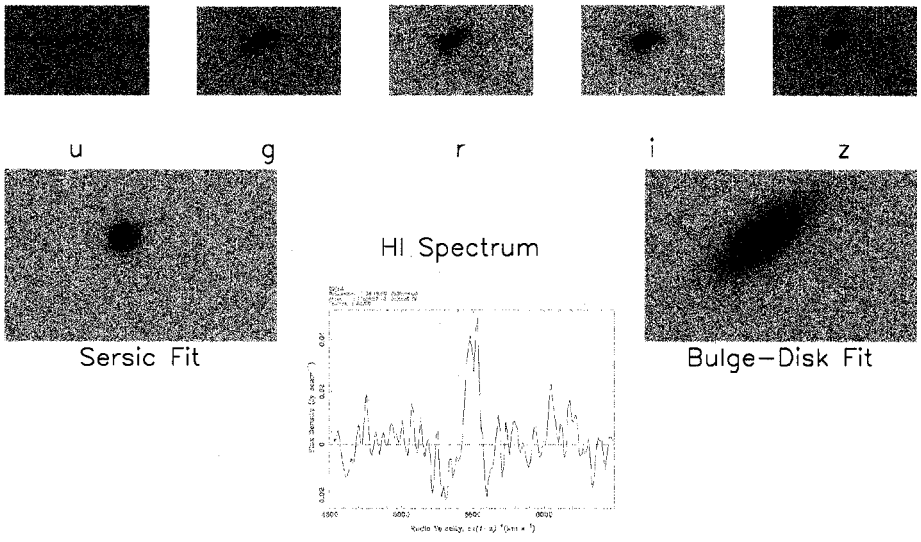

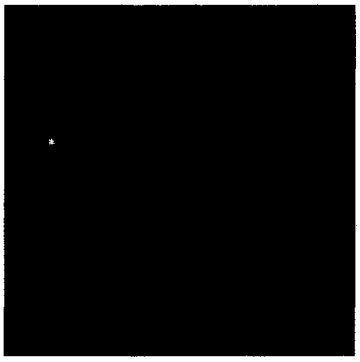

HIPEQ1143−01

u g r i z

Sersic Fit

HI Spectrum

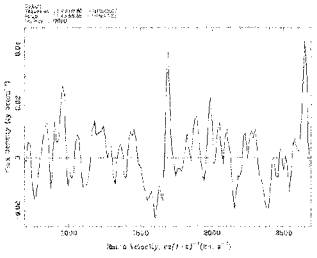

Bulge−Disk Fit

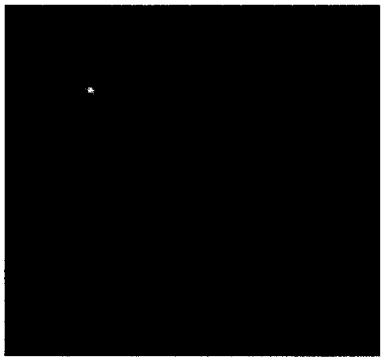

HIPEQ1145+02

u g r i z

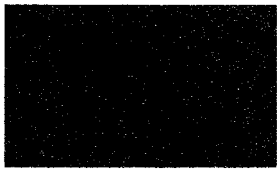

Sersic Fit

HI Spectrum

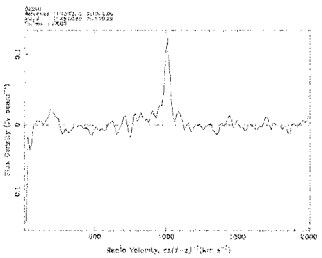

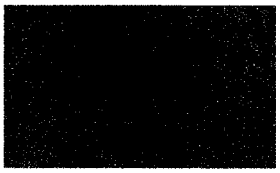

Bulge−Disk Fit

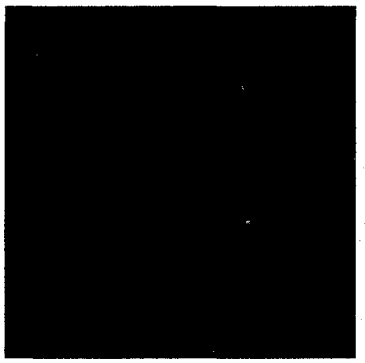

HIPEQ1148−02

u g r i z

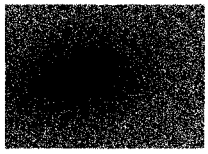

Sersic Fit

HI Spectrum

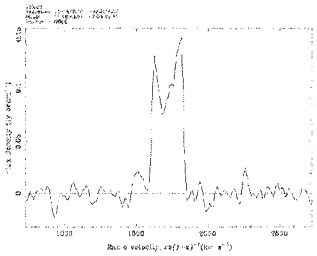

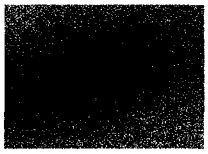

Bulge−Disk Fit

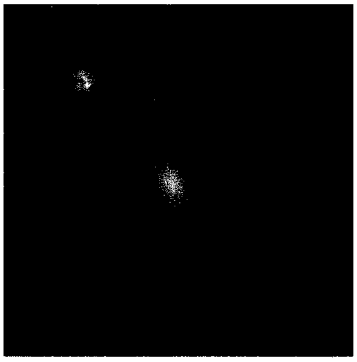

HIPEQ1151−02

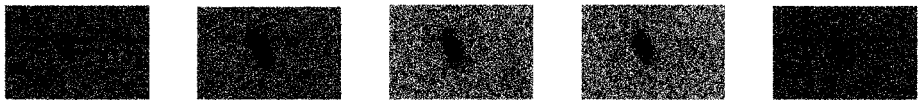

u g r i z

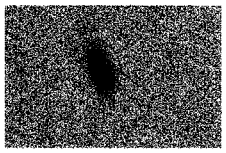

Sersic Fit

HI Spectrum

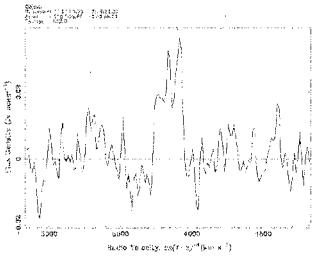

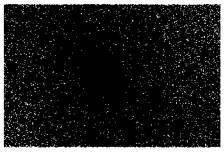

Bulge−Disk Fit

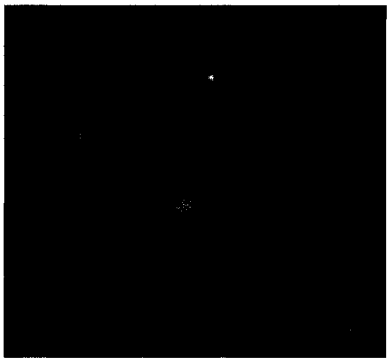

HIPEQ1152+01

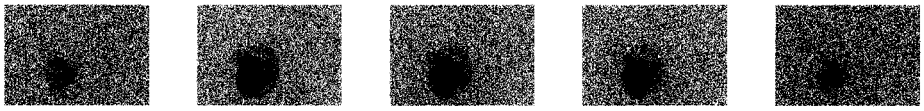

u g r i z

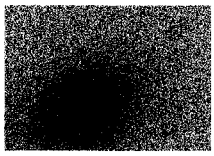

Sersic Fit

HI Spectrum

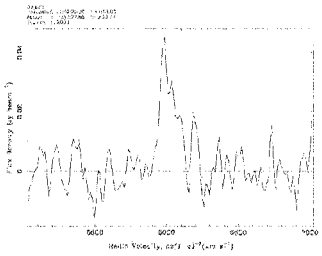

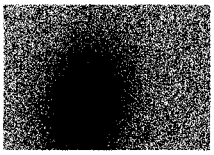

Bulge–Disk Fit

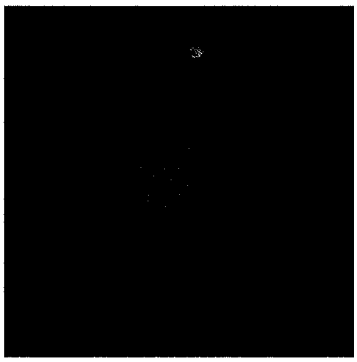

HIPEQ1152−02

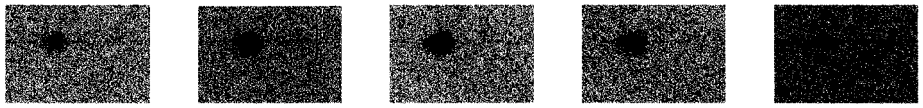

u g r i z

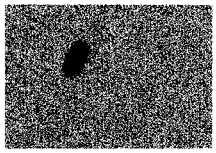

Sersic Fit

HI Spectrum

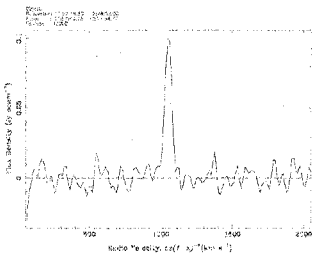

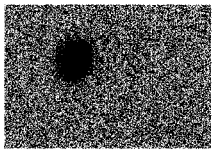

Bulge−Disk Fit

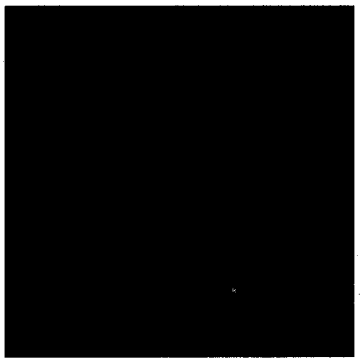

HIPEQ1152−03b

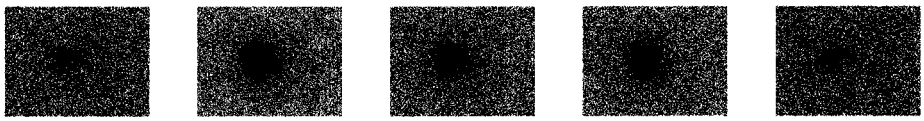

u g r i z

Sersic Fit

HI Spectrum

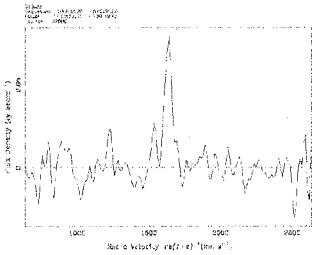

Bulge−Disk Fit

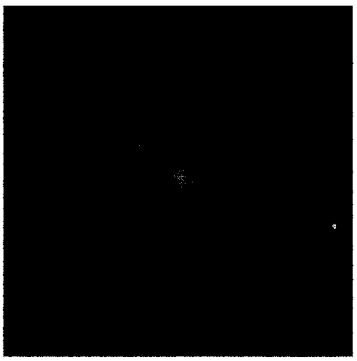

HIPEQ1155+01

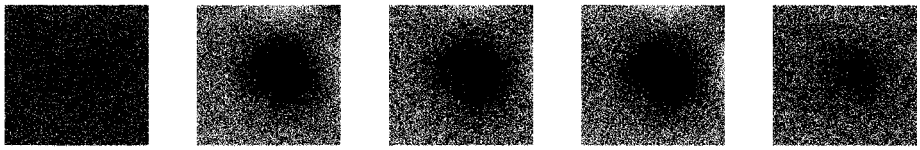

u g r i z

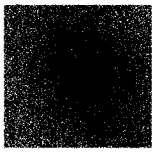

Sersic Fit

HI Spectrum

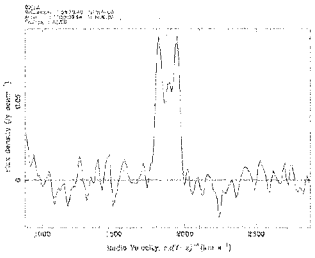

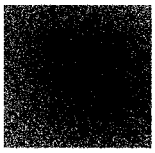

Bulge−Disk Fit

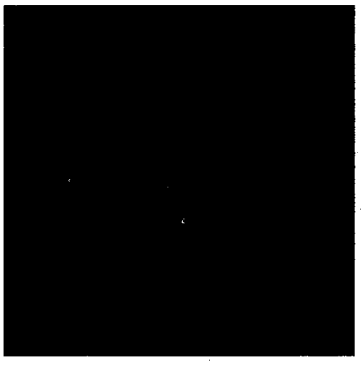

HIPEQ1200−00

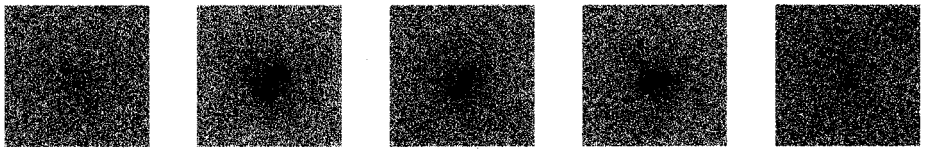

u g r i z

Sersic Fit

HI Spectrum

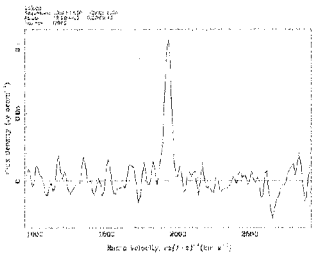

Bulge−Disk Fit

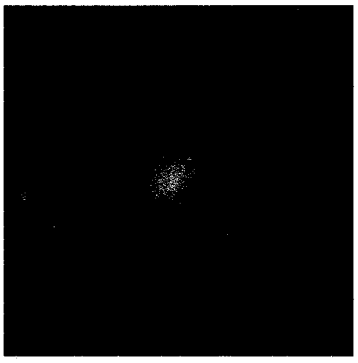

HIPEQ1200−01

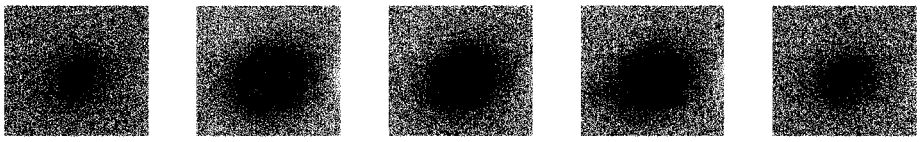

u g r i z

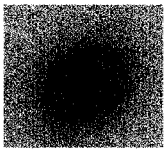

Sersic Fit

HI Spectrum

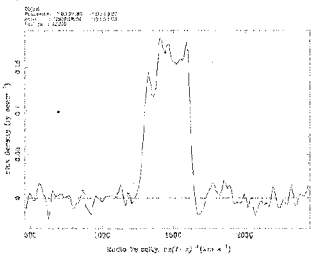

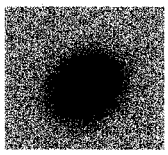

Bulge−Disk Fit

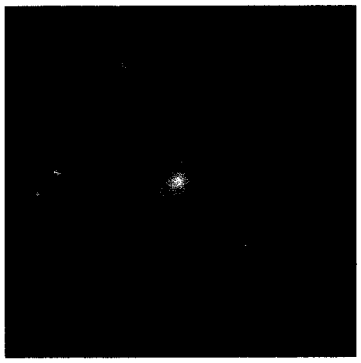

HIPEQ1202+01

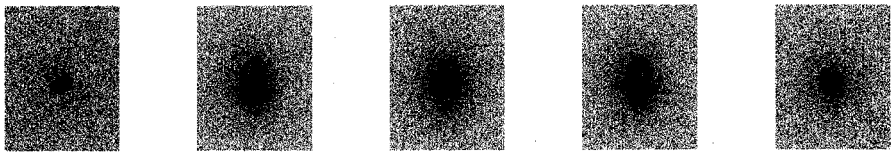

u g r i z

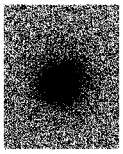

Sersic Fit

HI Spectrum

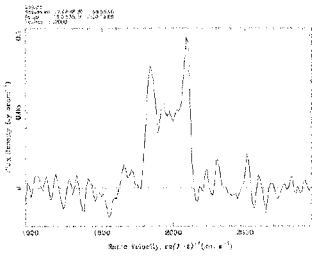

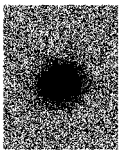

Bulge−Disk Fit

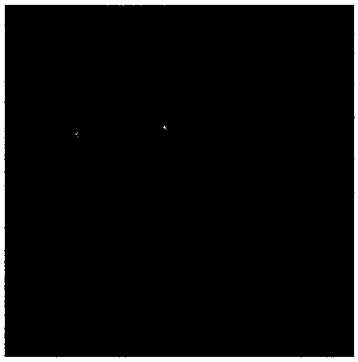

HIPEQ1204−01

u g r i z

Sersic Fit

HI Spectrum

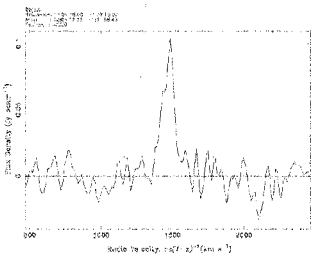

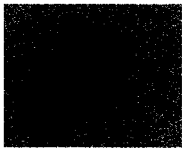

Bulge−Disk Fit

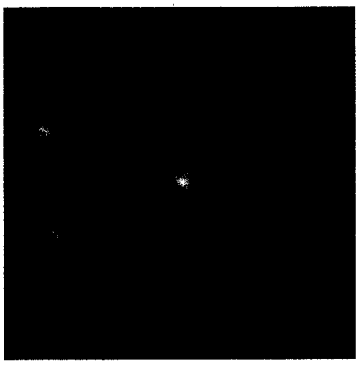

HIPEQ1204−02

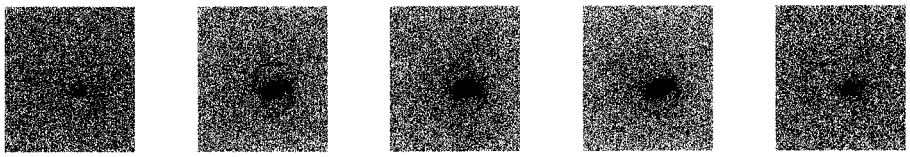

u g r i z

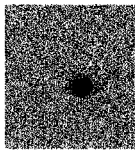

Sersic Fit

HI Spectrum

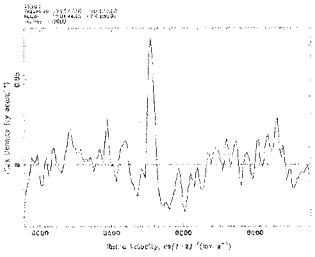

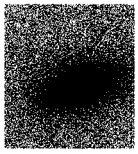

Bulge−Disk Fit

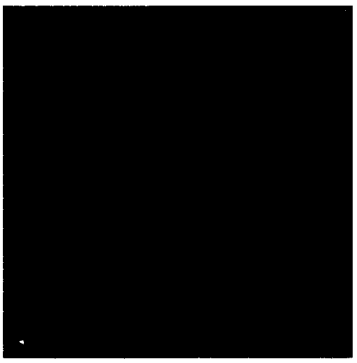

HIPEQ1210+02

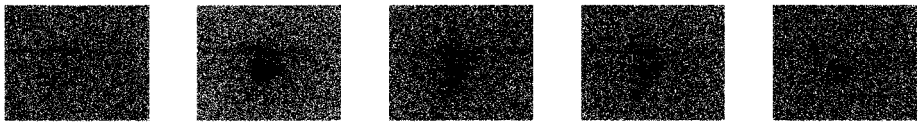

u g r i z

Sersic Fit

HI Spectrum

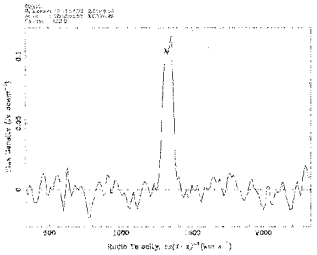

Bulge–Disk Fit

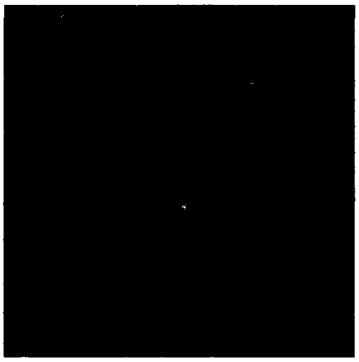

HIPEQ1215+04a

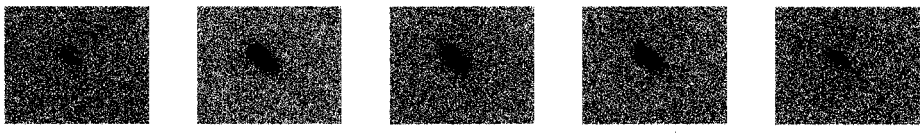

u g r i z

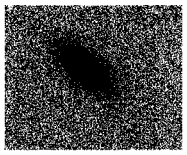

Sersic Fit

HI Spectrum

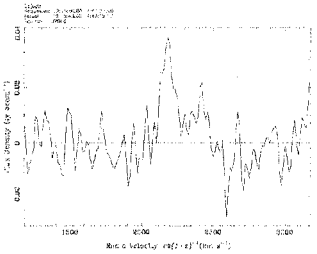

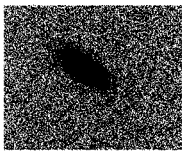

Bulge−Disk Fit

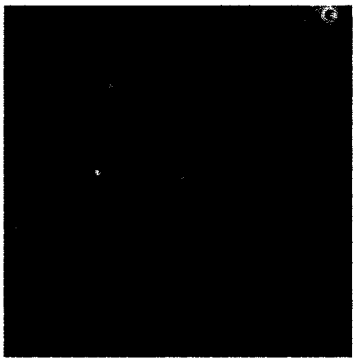

HIPEQ1216−03

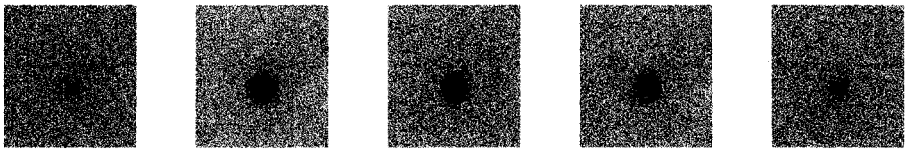

u g r i z

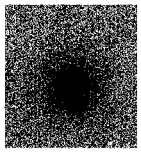

Sersic Fit

HI Spectrum

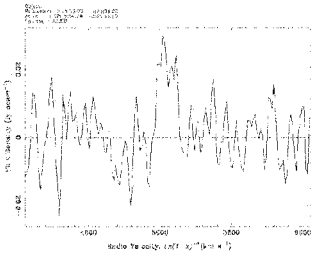

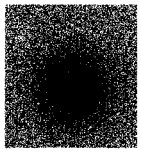

Bulge−Disk Fit

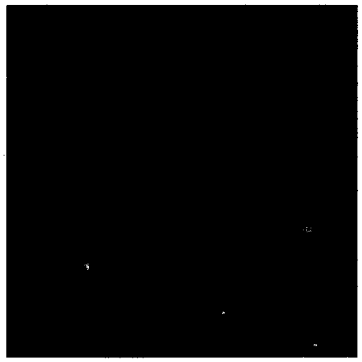

HIPEQ1218+00

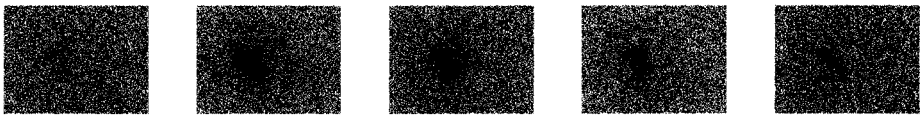

u g r i z

Sersic Fit

HI Spectrum

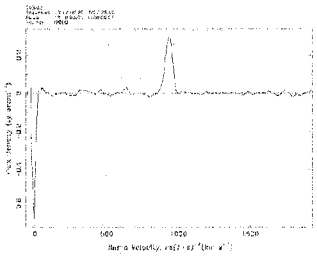

Bulge−Disk Fit

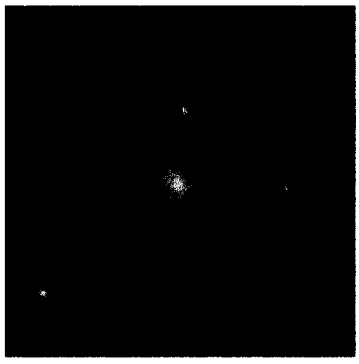

HIPEQ1218−01

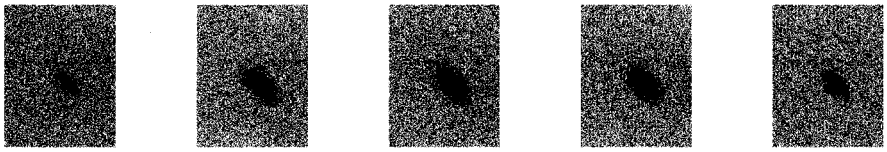

u g r i z

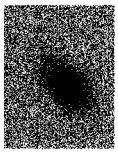

Sersic Fit

HI Spectrum

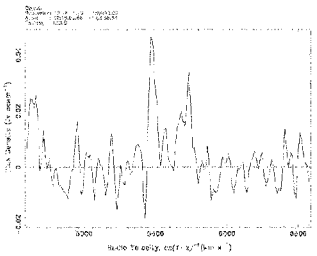

Bulge−Disk Fit

HIPEQ1219+03

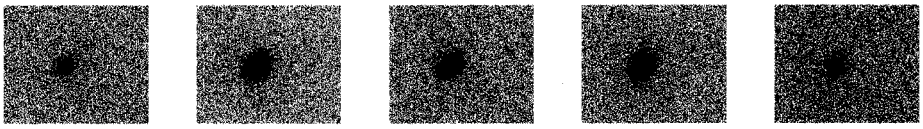

u g r i z

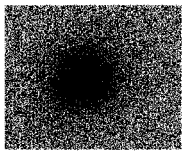

Sersic Fit

HI Spectrum

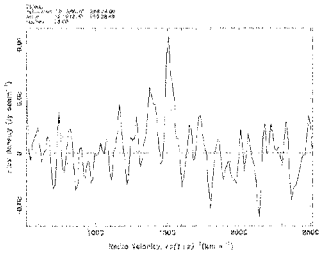

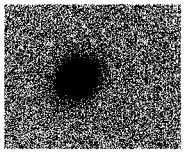

Bulge–Disk Fit

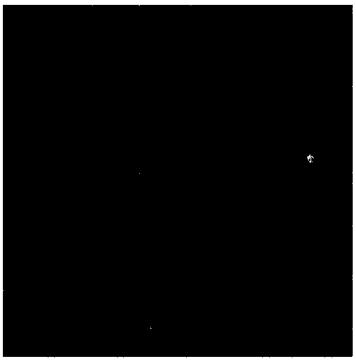

HIPEQ1220+00

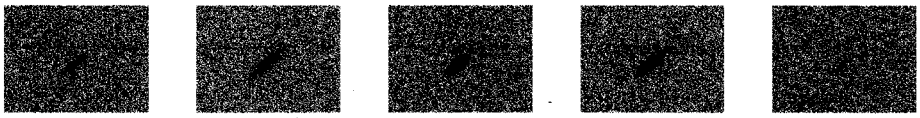

u g r i z

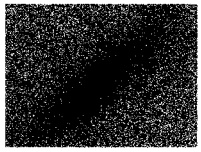

Sersic Fit

HI Spectrum

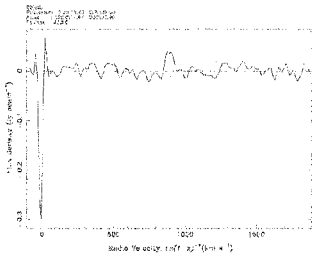

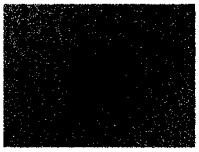

Bulge–Disk Fit

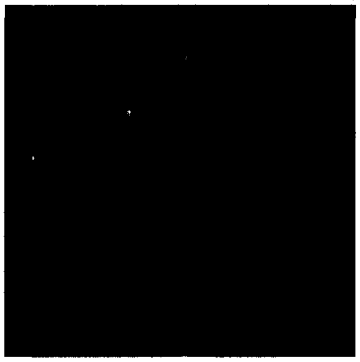

HIPEQ1220+01

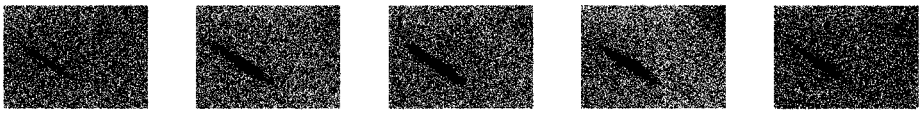

u g r i z

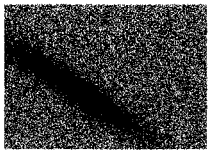

Sersic Fit

HI Spectrum

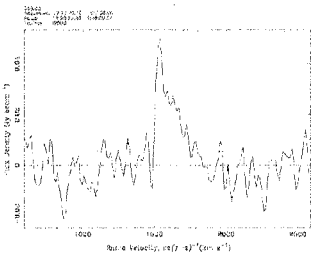

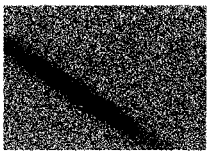

Bulge−Disk Fit

HIPEQ1221+03

u g r i z

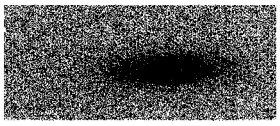

Sersic Fit

HI Spectrum

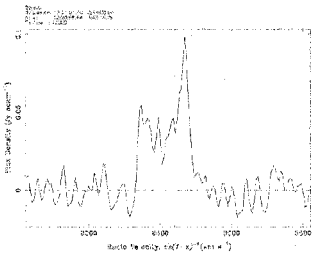

Bulge−Disk Fit

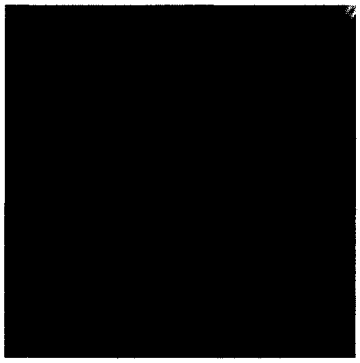

HIPEQ1223+00

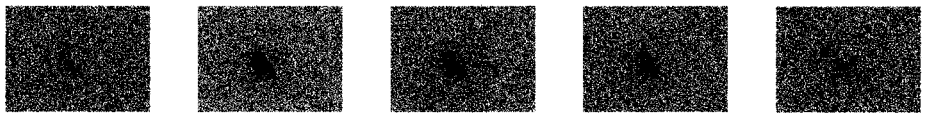

u g r i z

Sersic Fit

HI Spectrum

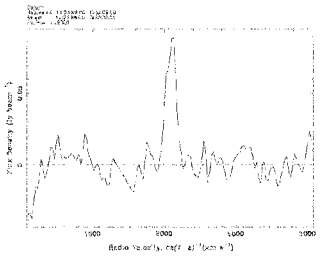

Bulge–Disk Fit

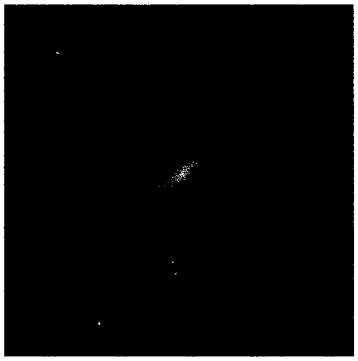

HIPEQ1223−03b

u g r i z

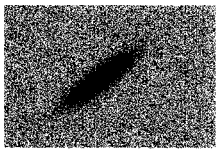

Sersic Fit

HI Spectrum

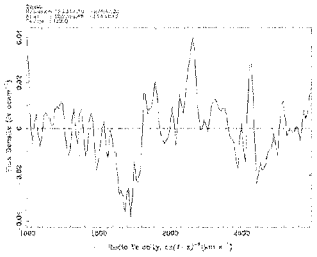

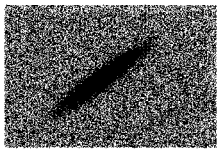

Bulge−Disk Fit

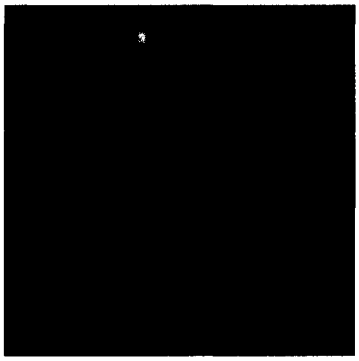

HIPEQ1224+00

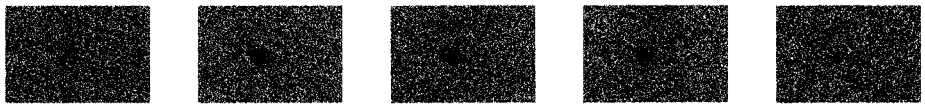

u g r i z

Sersic Fit

HI Spectrum

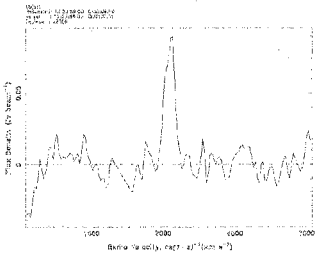

Bulge–Disk Fit

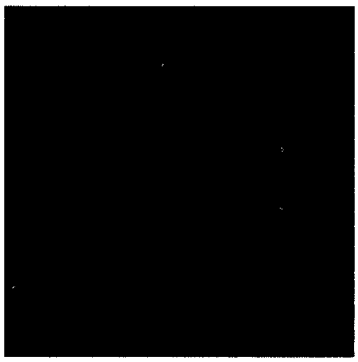

HIPEQ1224+03b

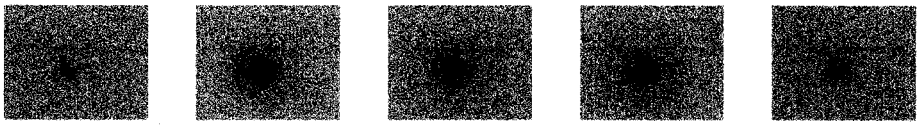

u g r i z

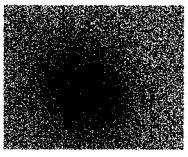

Sersic Fit

HI Spectrum

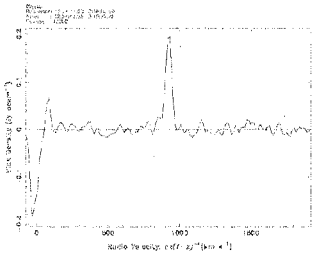

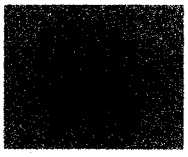

Bulge–Disk Fit

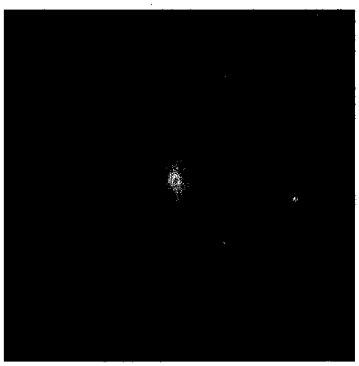

HIPEQ1225+00

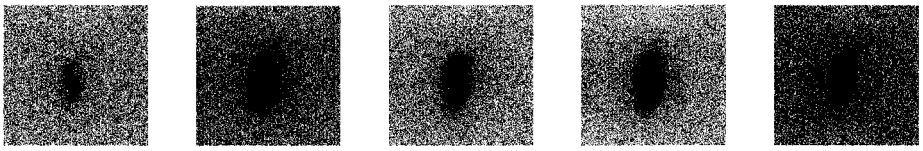

u g r i z

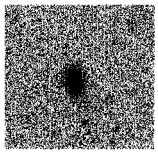

Sersic Fit

HI Spectrum

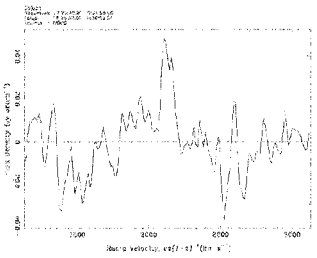

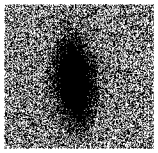

Bulge−Disk Fit

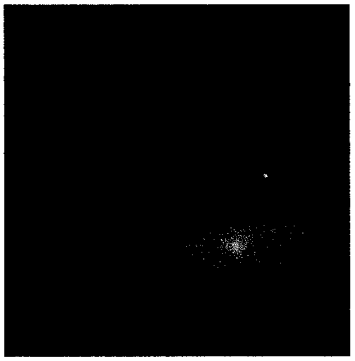

HIPEQ1226+02

u g r i z

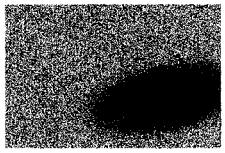

Sersic Fit

HI Spectrum

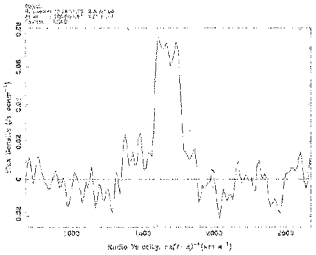

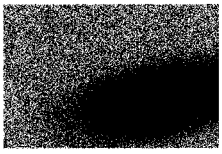

Bulge–Disk Fit

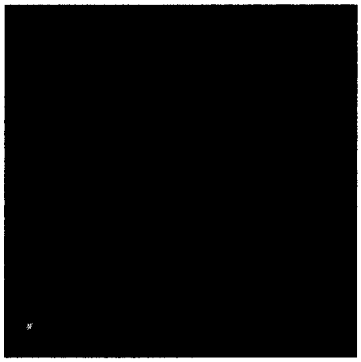

HIPEQ1227+01

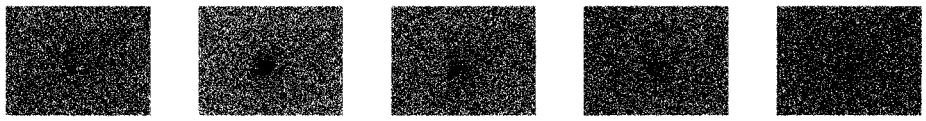

u g r i z

Sersic Fit

HI Spectrum

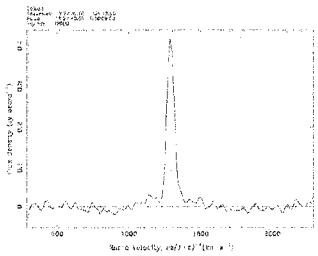

Bulge−Disk Fit

HIPEQ1228+02

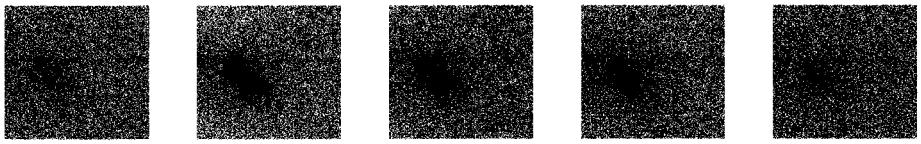

u g r i z

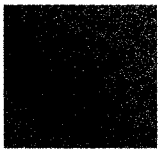

Sersic Fit

HI Spectrum

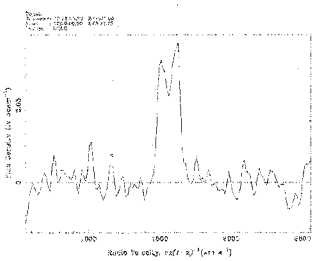

Bulge–Disk Fit

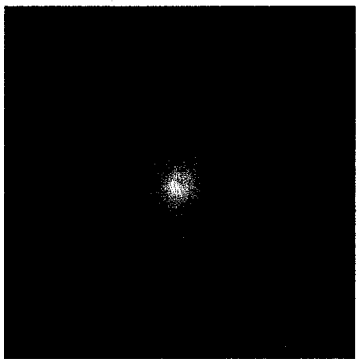

HIPEQ1228+03

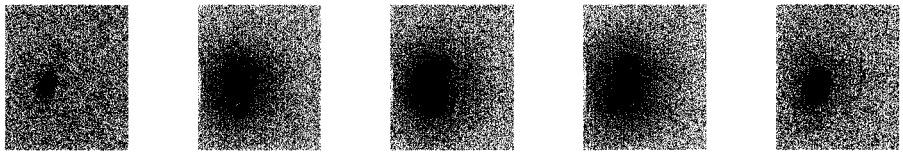

u g r i z

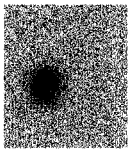

Sersic Fit

HI Spectrum

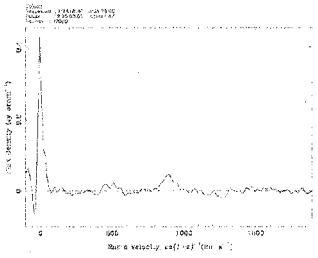

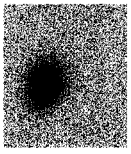

Bulge−Disk Fit

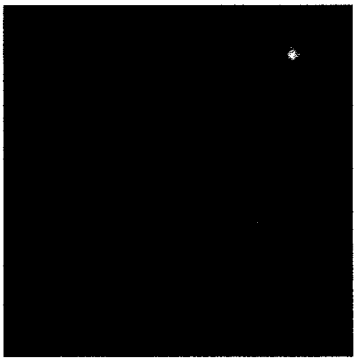

HIPEQ1229+00

u

g

r

i

z

Sersic Fit

HI Spectrum

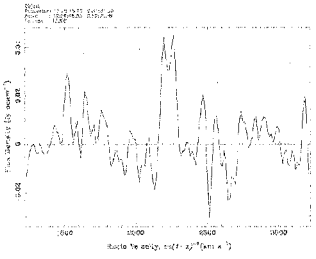

Bulge–Disk Fit

HIPEQ1230+02

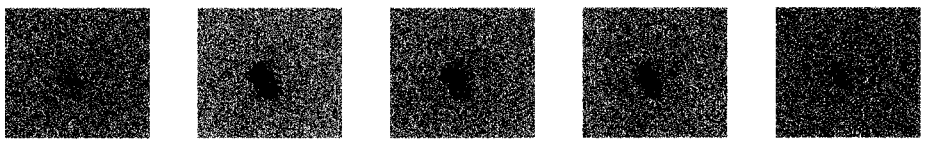

u g r i z

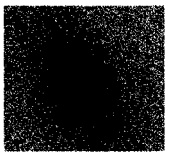

Sersic Fit

HI Spectrum

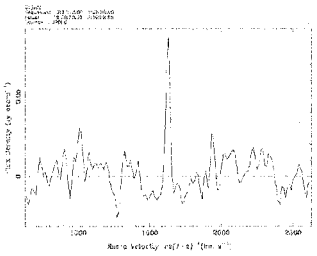

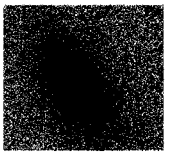

Bulge−Disk Fit

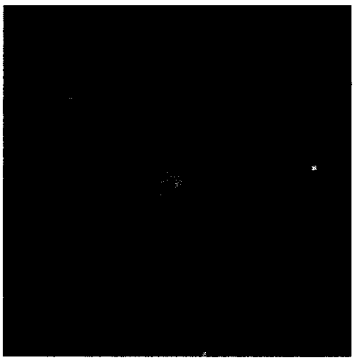

HIPEQ1230+03

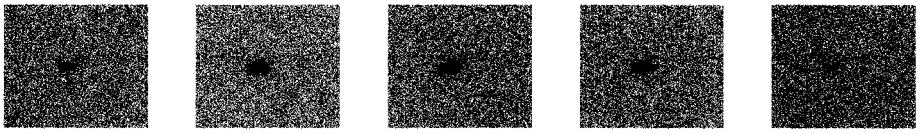

u g r i z

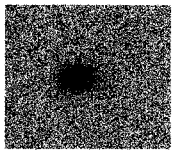

Sersic Fit

HI Spectrum

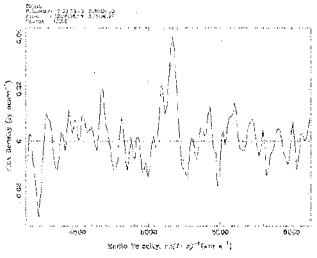

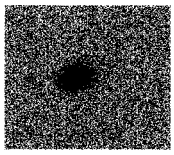

Bulge−Disk Fit

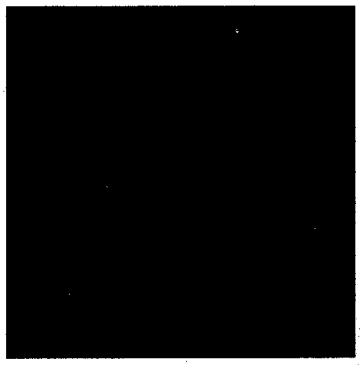

HIPEQ1232+00a

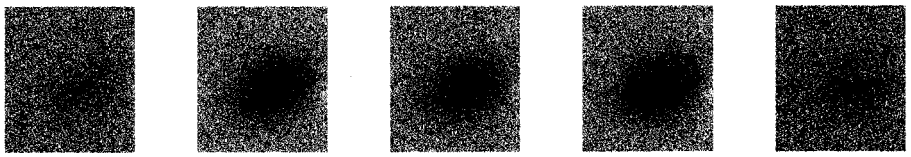

u g r i z

Sersic Fit

HI Spectrum

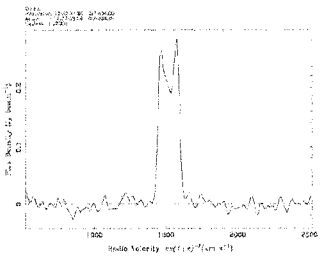

Bulge–Disk Fit

HIPEQ1232+00b

u g r i z

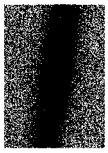

Sersic Fit

HI Spectrum

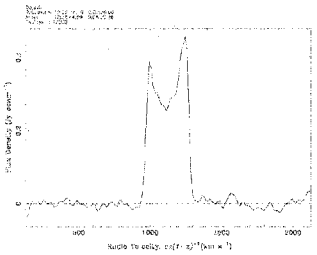

Bulge−Disk Fit

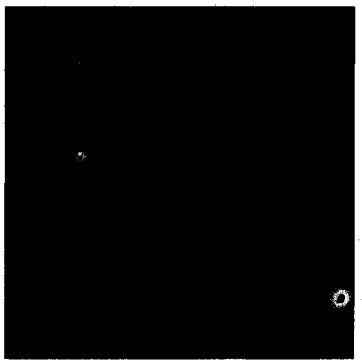

HIPEQ1233−02

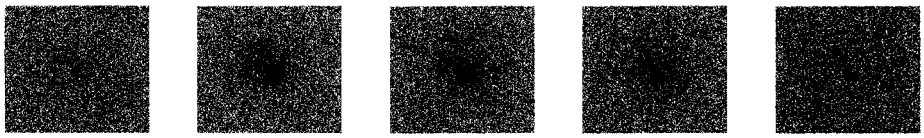

u g r i z

Sersic Fit

HI Spectrum

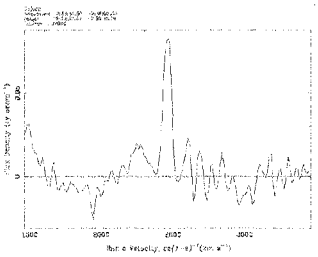

Bulge−Disk Fit

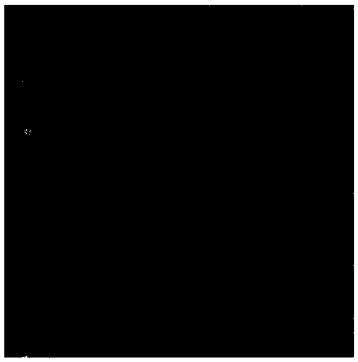

HIPEQ1236+03

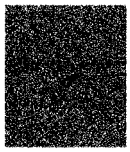
u


g

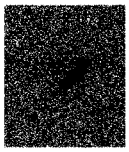
r


i

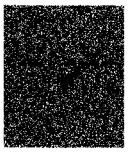
z


Sersic Fit

HI Spectrum

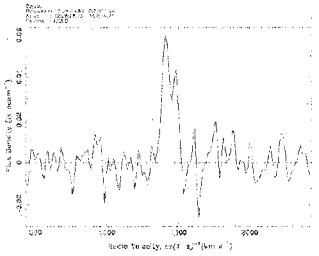


Bulge−Disk Fit

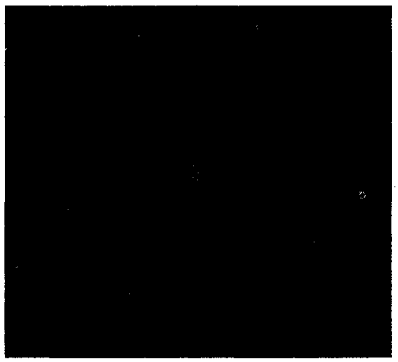

HIPEQ1239−00

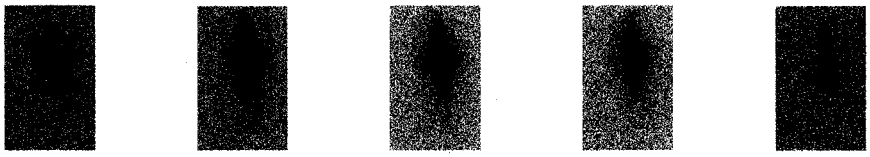

u g r i z

Sersic Fit

HI Spectrum

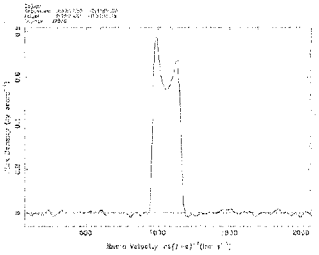

Bulge−Disk Fit

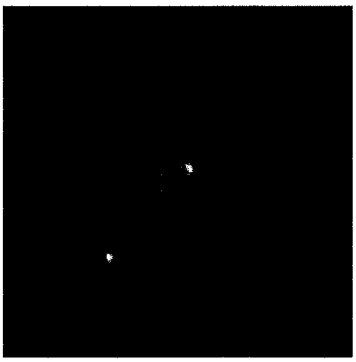

HIPEQ1241+01

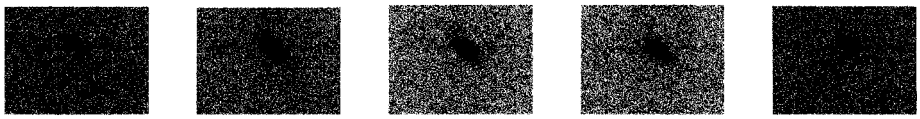

u g r i z

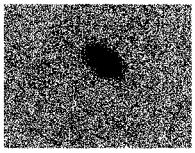

Sersic Fit

HI Spectrum

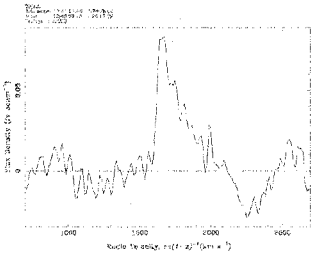

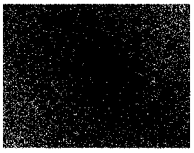

Bulge–Disk Fit

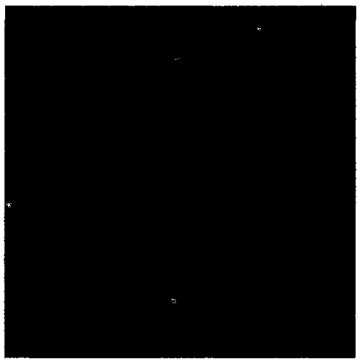

HIPEQ1241−02

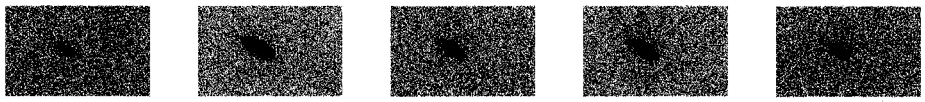

u g r i z

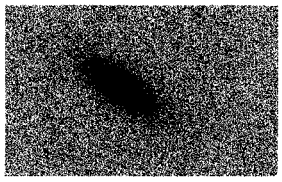

Sersic Fit

HI Spectrum

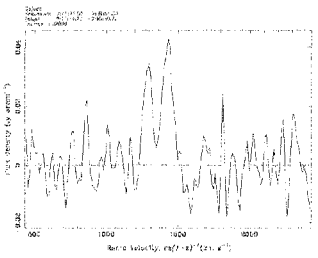

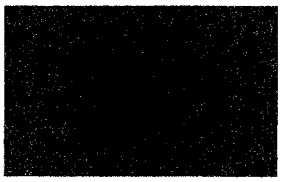

Bulge−Disk Fit

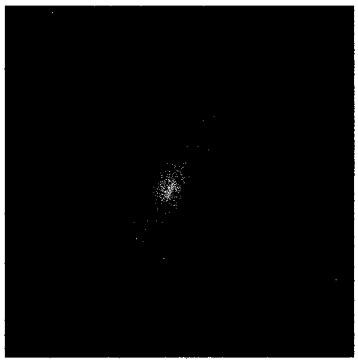

HIPEQ1242−00

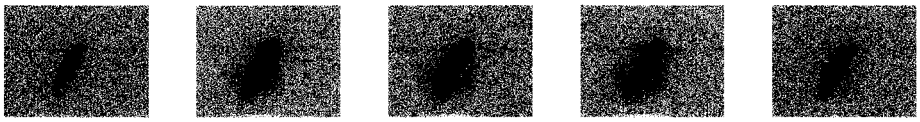

u g r i z

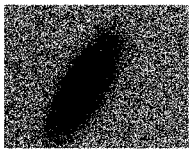

Sersic Fit

HI Spectrum

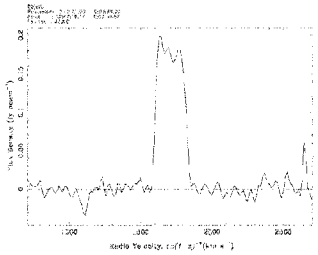

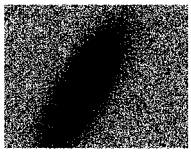

Bulge−Disk Fit

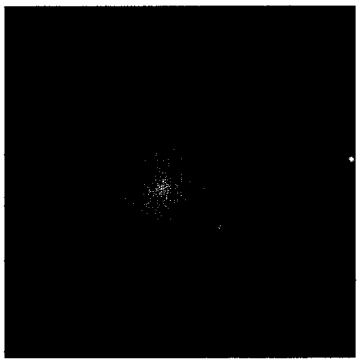

HIPEQ1242−01a

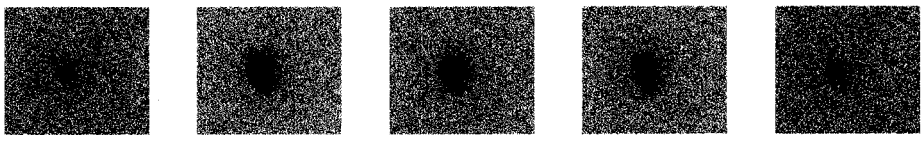

u g r i z

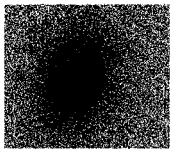

Sersic Fit

HI Spectrum

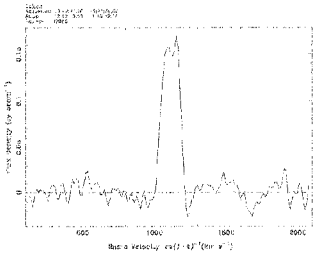

Bulge−Disk Fit

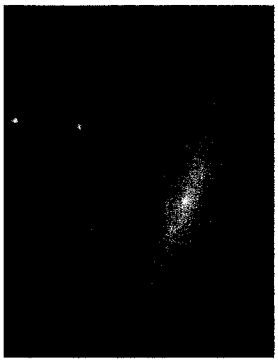

HIPEQ1242−01b

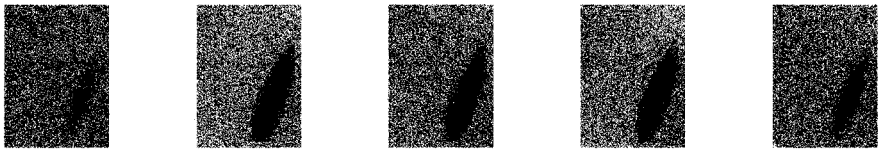

u g r i z

Sersic Fit

HI Spectrum

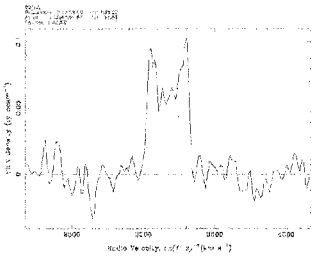

Bulge−Disk Fit

HIPEQ1242+03b

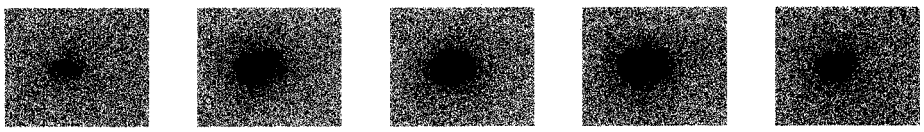

u g r i z

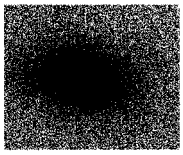

Sersic Fit

HI Spectrum

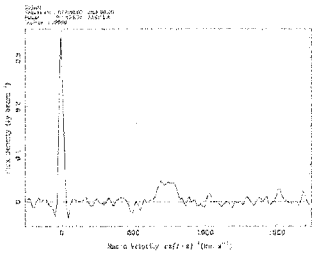

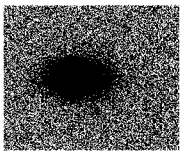

Bulge–Disk Fit

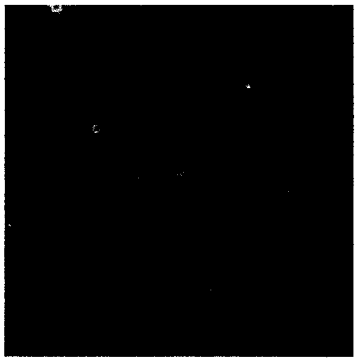

HIPEQ1243−00

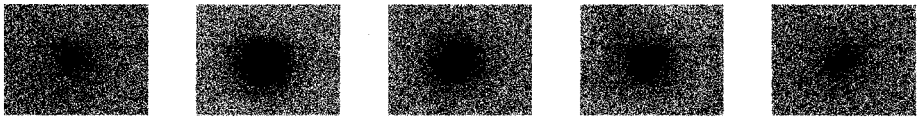

u g r i z

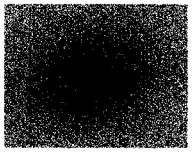

Sersic Fit

HI Spectrum

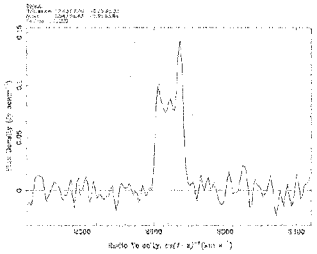

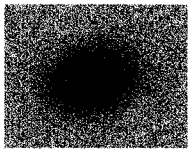

Bulge−Disk Fit

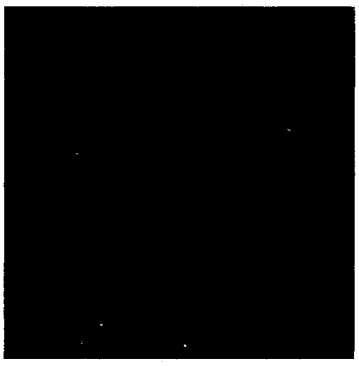

HIPEQ1244+00

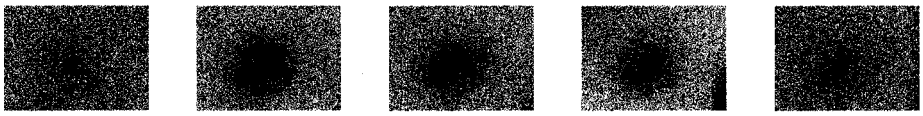

u g r i z

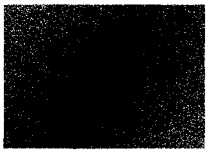

Sersic Fit

HI Spectrum

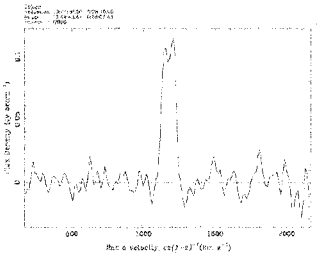

Bulge–Disk Fit

HIPEQ1244−02

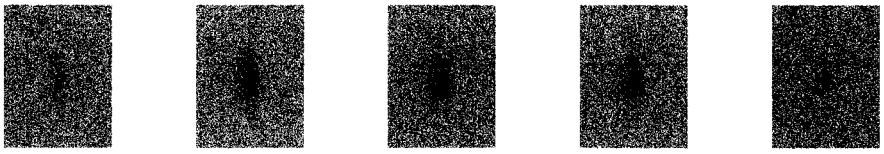

u g r i z

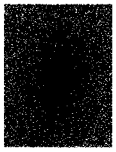

Sersic Fit

HI Spectrum

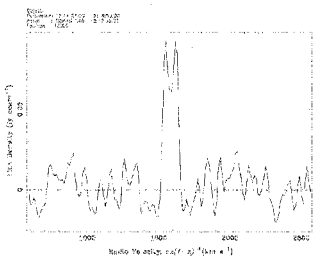

Bulge−Disk Fit

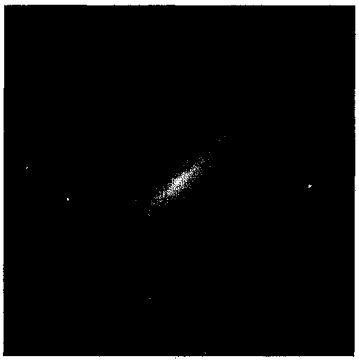

HIPEQ1245−00

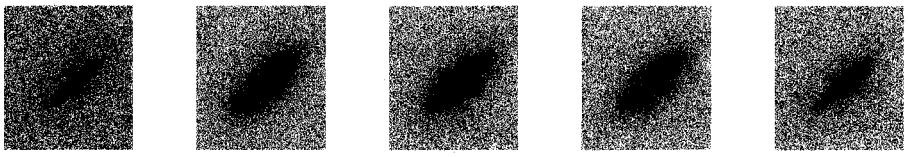

u g r i z

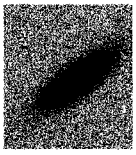

Sersic Fit

HI Spectrum

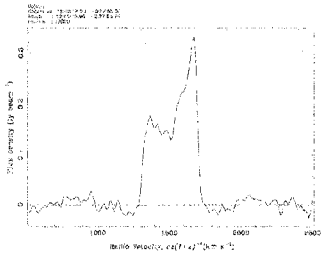

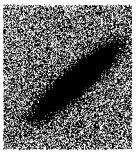

Bulge−Disk Fit

HIPEQ1249+03

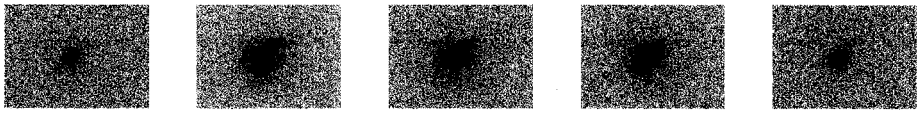

u g r i z

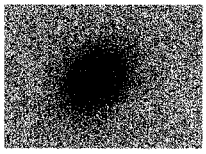

Sersic Fit

HI Spectrum

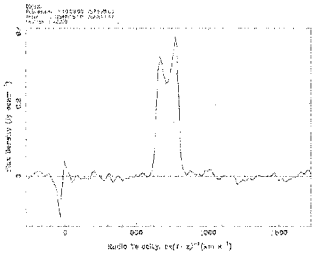

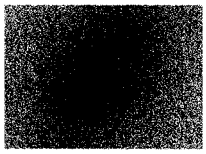

Bulge–Disk Fit

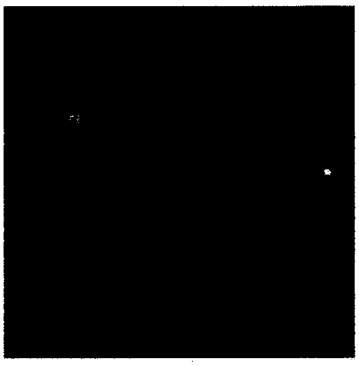

HIPEQ1249+04

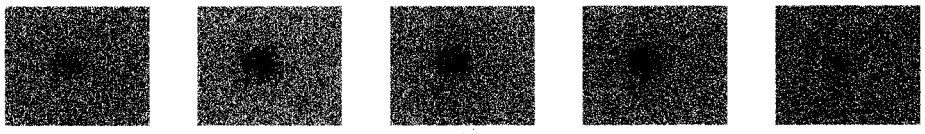

u g r i z

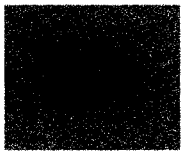

Sersic Fit

HI Spectrum

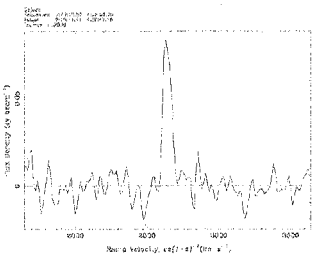

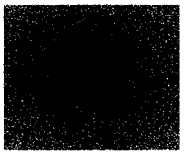

Bulge–Disk Fit

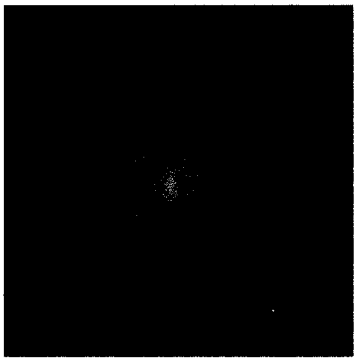

HIPEQ1250+05

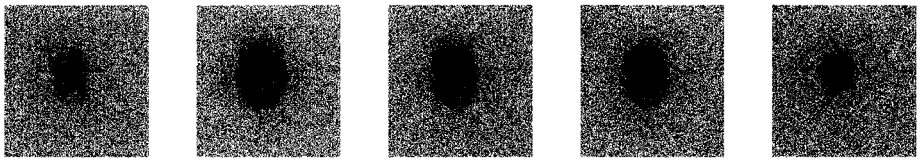

u g r i z

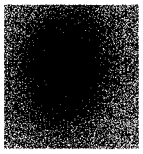

Sersic Fit

HI Spectrum

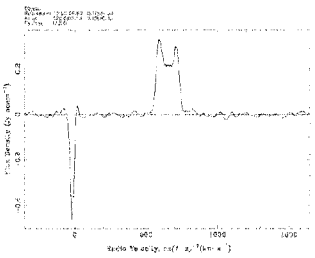

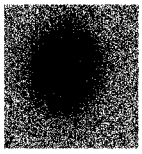

Bulge−Disk Fit

HIPEQ1253+01

u g r i z

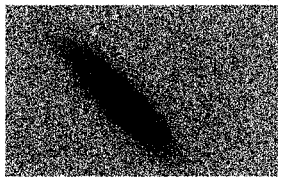

Sersic Fit

HI Spectrum

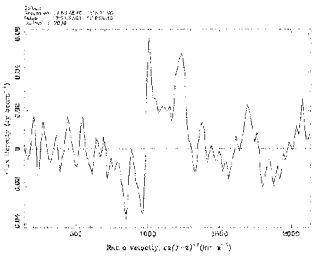

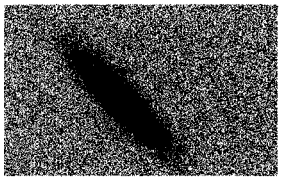

Bulge−Disk Fit

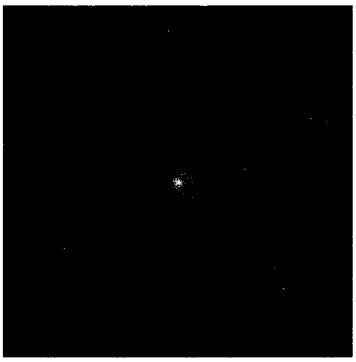

HIPEQ1253+02

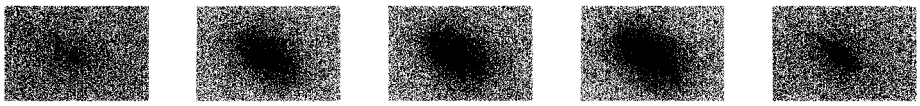

u g r i z

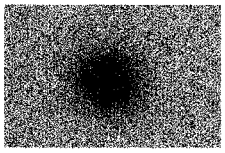

Sersic Fit

HI Spectrum

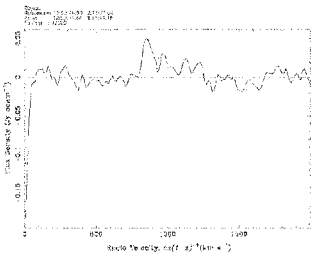

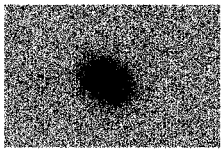

Bulge−Disk Fit

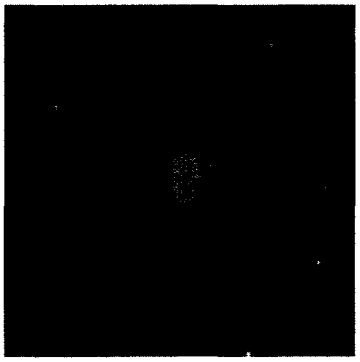

HIPEQ1253+04

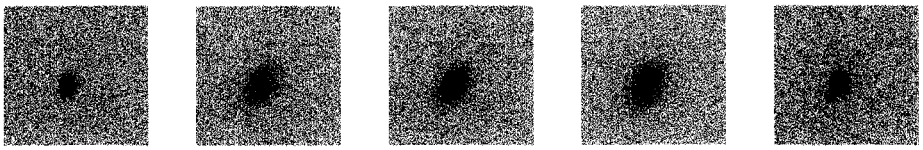

u g r i z

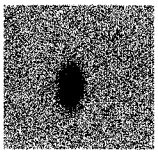

Sersic Fit

HI Spectrum

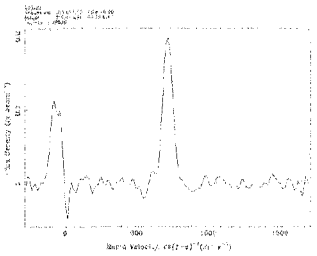

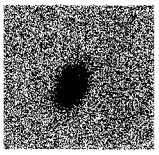

Bulge–Disk Fit

HIPEQ1255−00

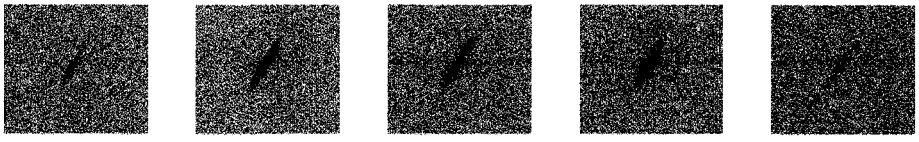

u g r i z

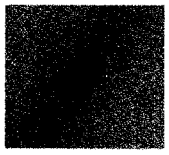

Sersic Fit

HI Spectrum

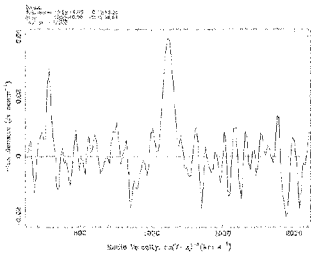

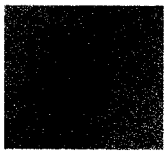

Bulge−Disk Fit

HIPEQ1255+00

u g r i z

Sersic Fit

HI Spectrum

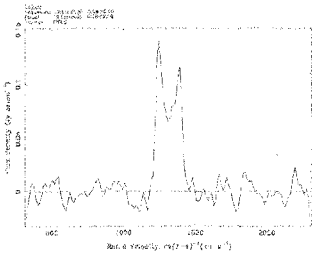

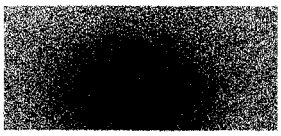

Bulge–Disk Fit

HIPEQ1255+02

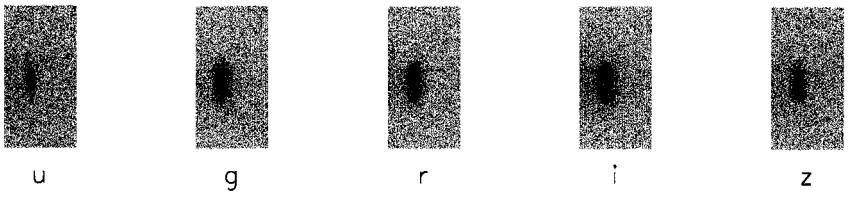

Sersic Fit

HI Spectrum

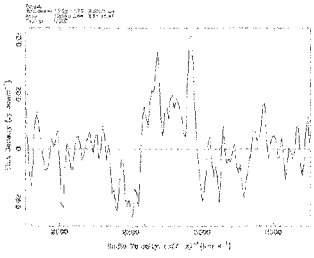

Bulge–Disk Fit

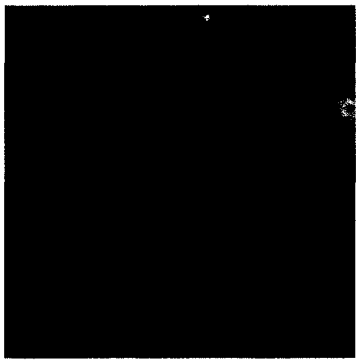

HIPEQ1256+03

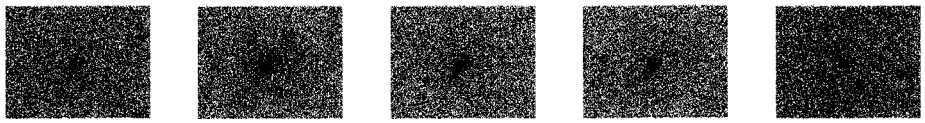

u g r i z

Sersic Fit

HI Spectrum

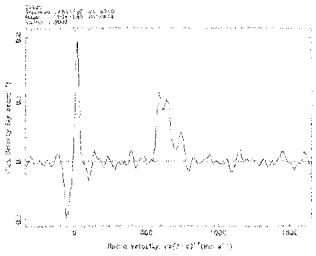

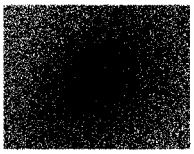

Bulge–Disk Fit

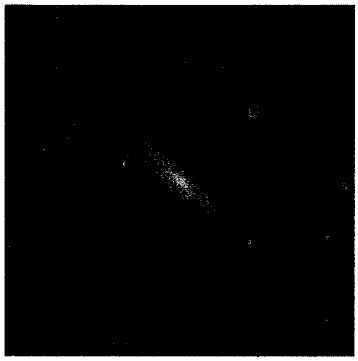

HIPEQ1257−01

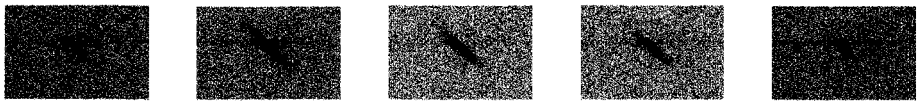

u g r i z

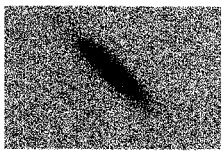

Sersic Fit

HI Spectrum

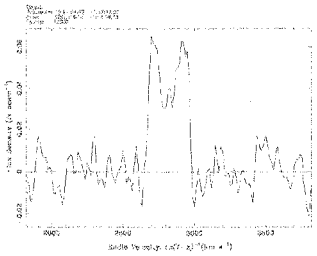

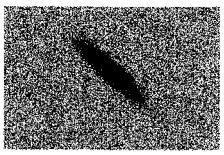

Bulge−Disk Fit

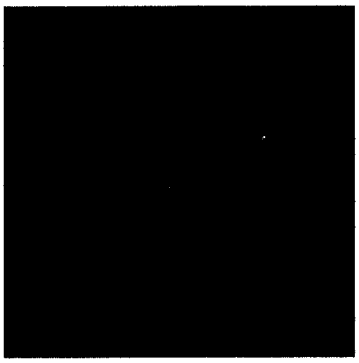

HIPEQ1257+02

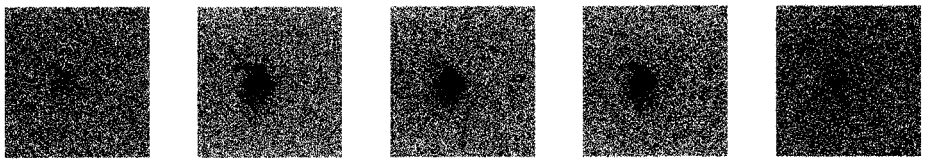

u g r i z

Sersic Fit

HI Spectrum

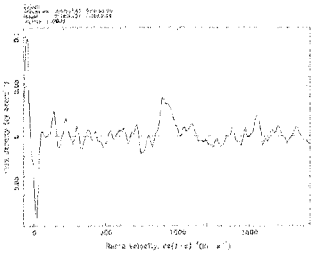

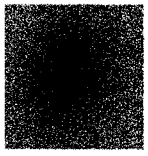

Bulge–Disk Fit

HIPEQ1258+02

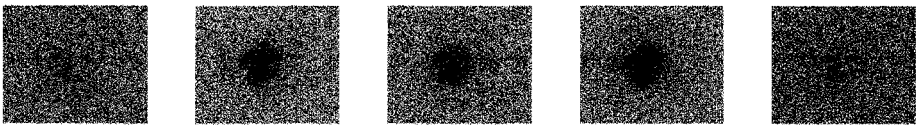

u g r i z

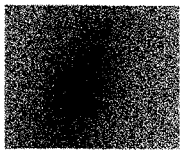

Sersic Fit

HI Spectrum

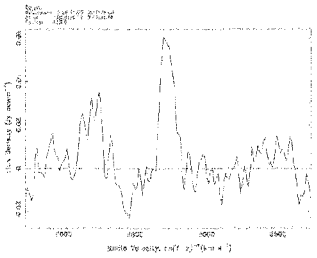

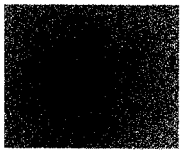

Bulge–Disk Fit

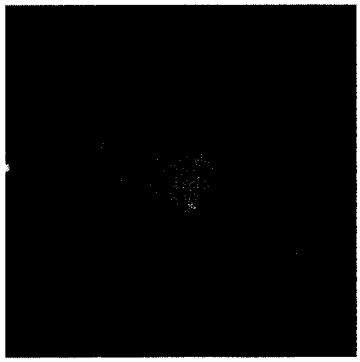

HIPEQ1300+02a

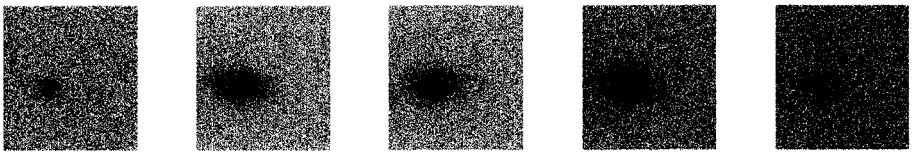

u g r i z

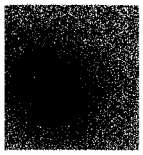

Sersic Fit

HI Spectrum

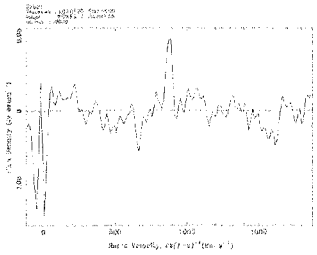

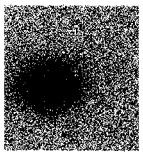

Bulge–Disk Fit

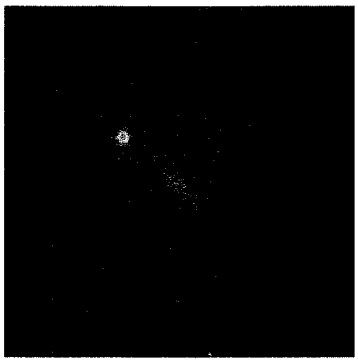

HIPEQ1300+02b

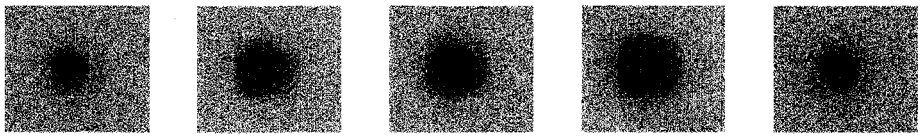

u g r i z

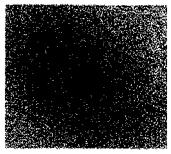

Sersic Fit

HI Spectrum

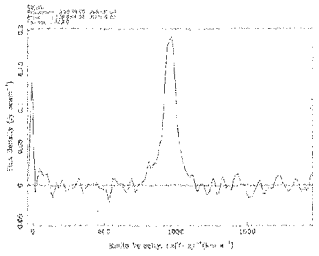

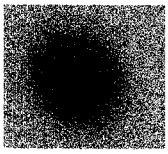

Bulge–Disk Fit

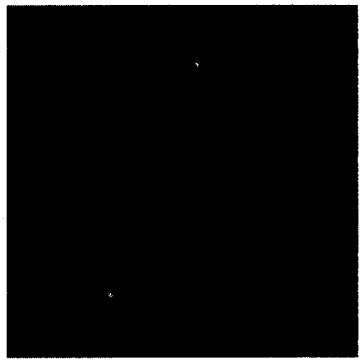

HIPEQ1303+03

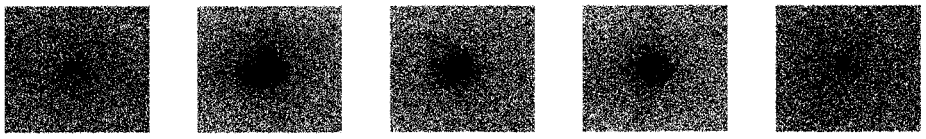

u g r i z

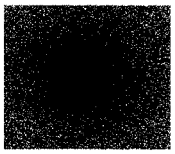

Sersic Fit

HI Spectrum

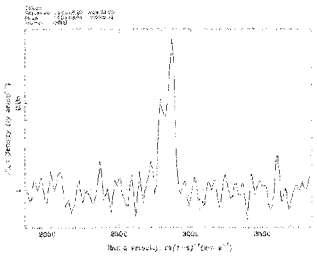

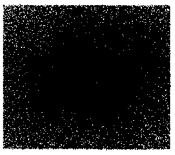

Bulge–Disk Fit

HIPEQ1304−02

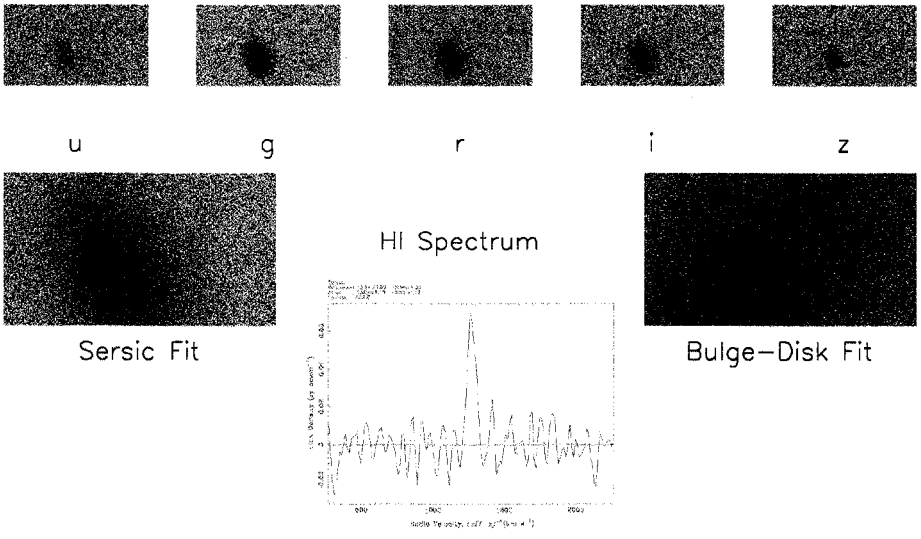

HIPEQ1304−03

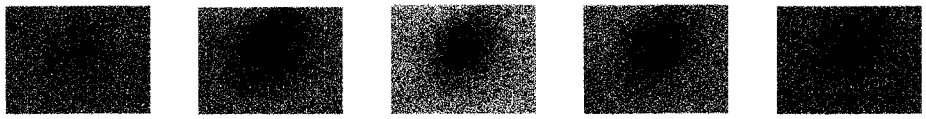

u g r i z

Sersic Fit

HI Spectrum

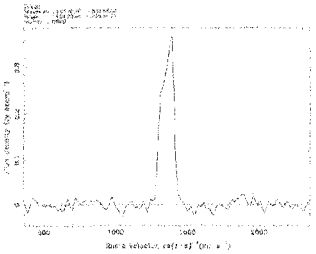

Bulge−Disk Fit

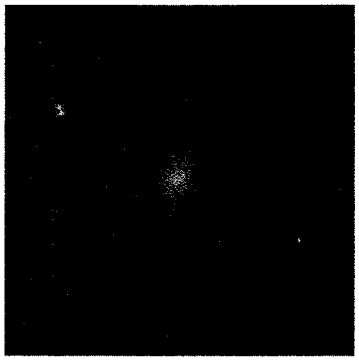

HIPEQ1307−00

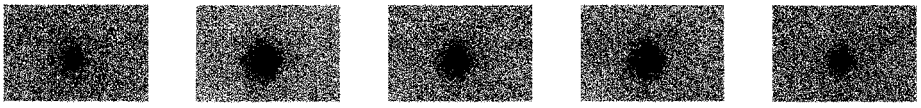

u g r i z

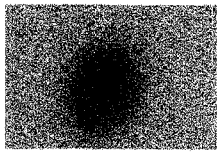

Sersic Fit

HI Spectrum

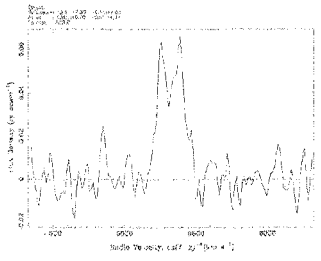

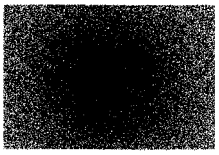

Bulge−Disk Fit

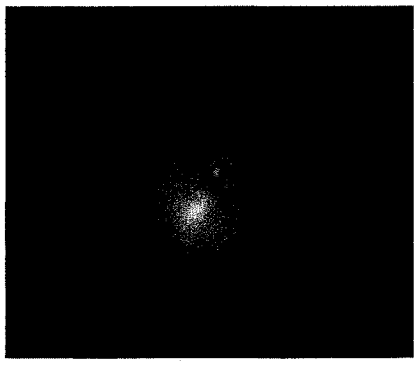

HIPEQ1308−02

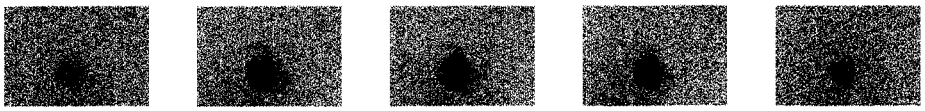

u g r i z

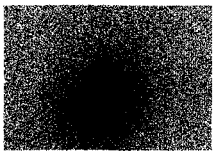

Sersic Fit

HI Spectrum

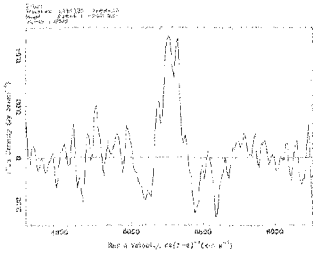

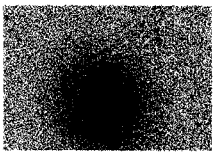

Bulge−Disk Fit

HIPEQ1311+03a

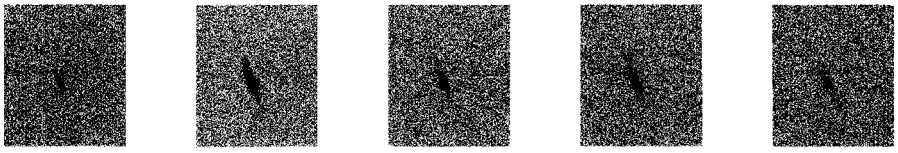

u g r i z

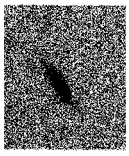

Sersic Fit

HI Spectrum

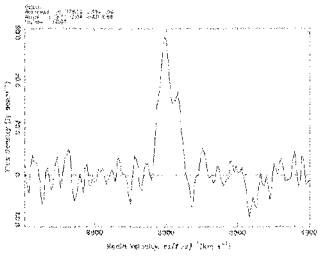

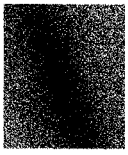

Bulge–Disk Fit

HIPEQ1312+03

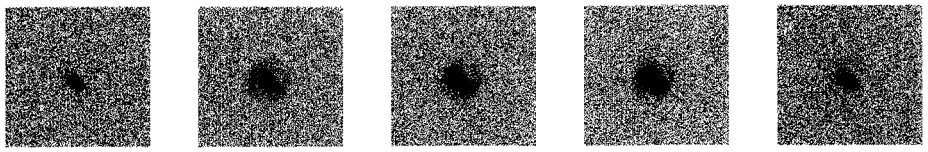

u g r i z

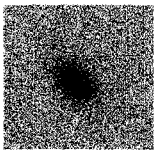

Sersic Fit

HI Spectrum

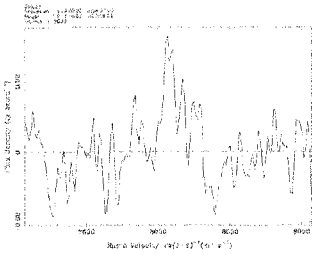

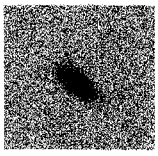

Bulge−Disk Fit

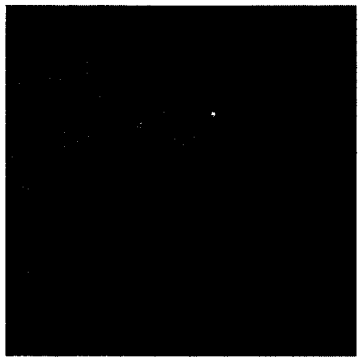

HIPEQ1312+05

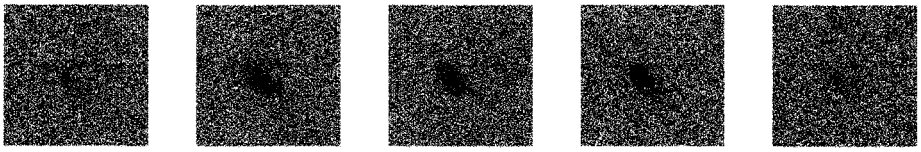

u g r i z

Sersic Fit

HI Spectrum

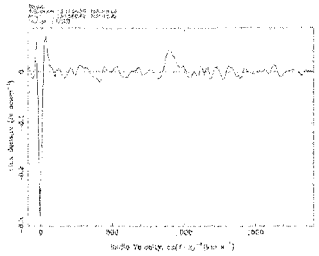

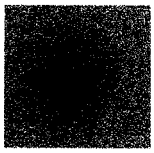

Bulge–Disk Fit

HIPEQ1313+06

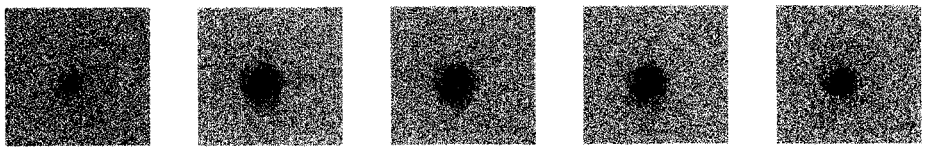

u g r i z

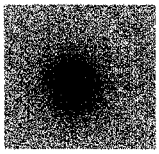

Sersic Fit

HI Spectrum

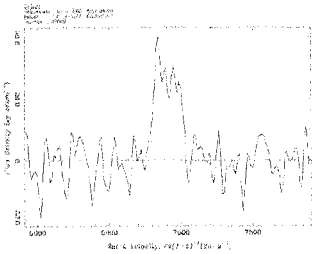

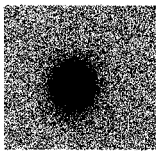

Bulge−Disk Fit

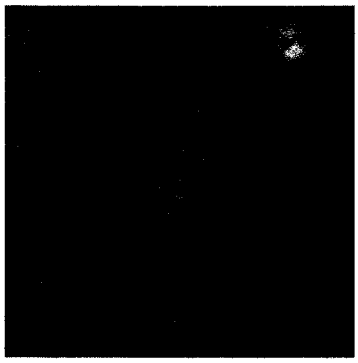

HIPEQ1317−00

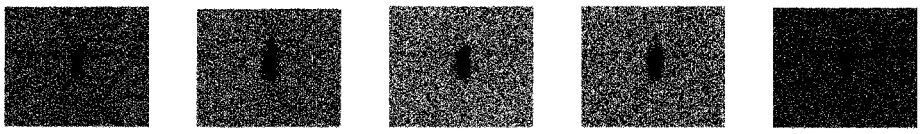

u g r i z

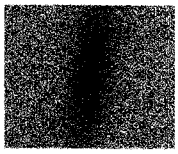

Sersic Fit

HI Spectrum

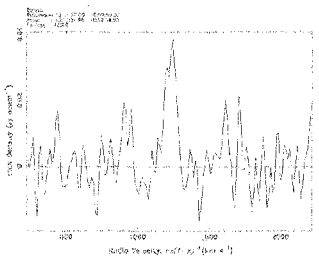

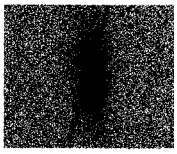

Bulge−Disk Fit

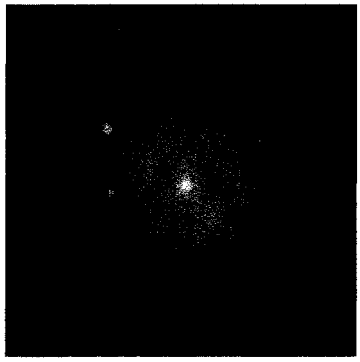

HIPEQ1318−01

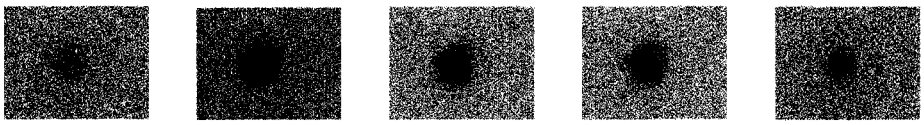

u g r i z

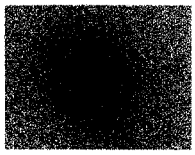

Sersic Fit

HI Spectrum

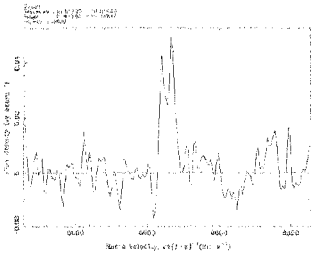

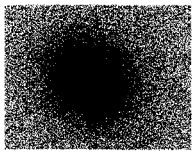

Bulge−Disk Fit

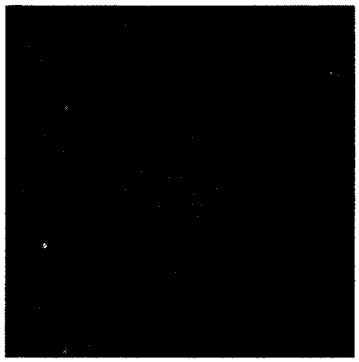

HIPEQ1320+05

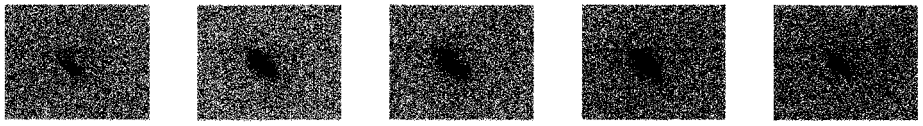

u g r i z

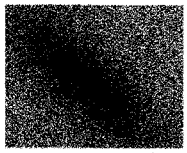

Sersic Fit

HI Spectrum

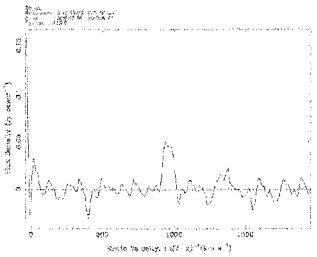

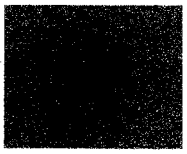

Bulge–Disk Fit

HIPEQ1327+02

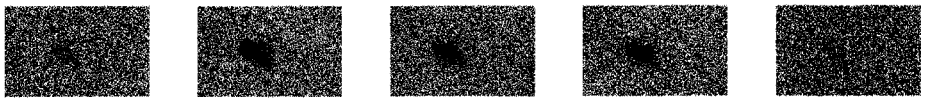

u g r i z

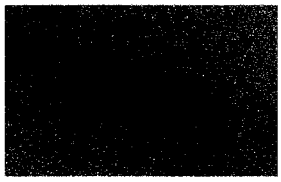

Sersic Fit

HI Spectrum

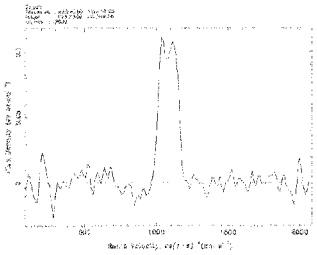

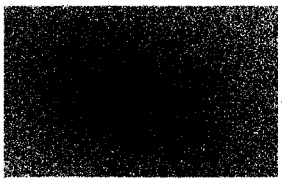

Bulge−Disk Fit

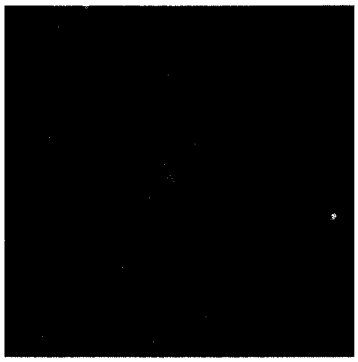

HIPEQ1329−00

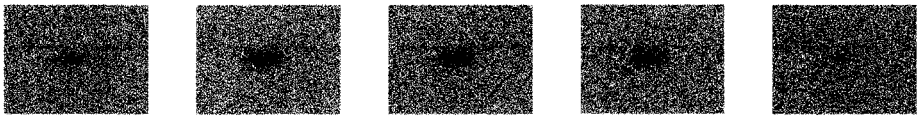

u g r i z

Sersic Fit

HI Spectrum

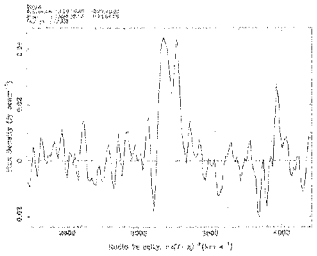

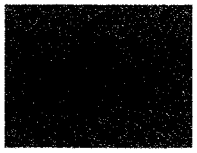

Bulge−Disk Fit

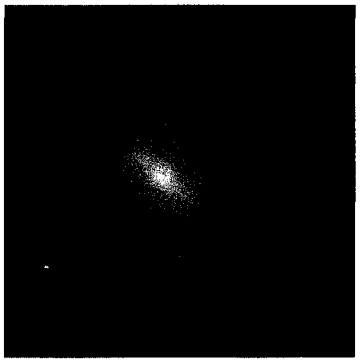

HIPEQ1332+01

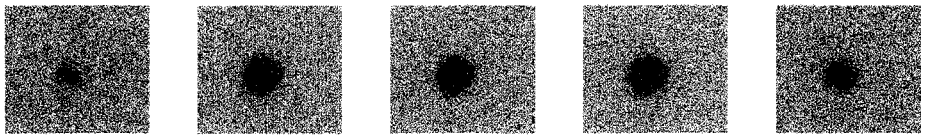

u g r i z

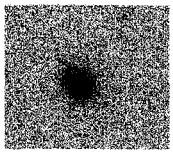

Sersic Fit

HI Spectrum

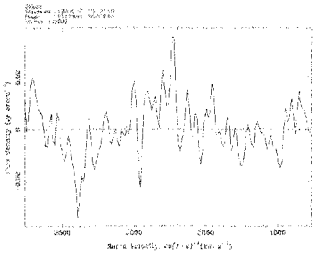

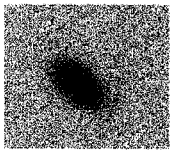

Bulge–Disk Fit

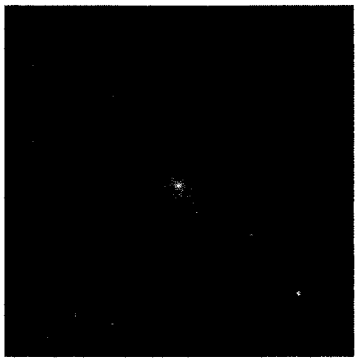

HIPEQ1335+01

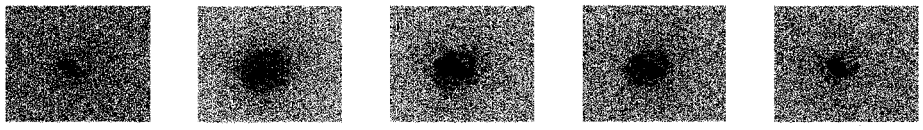

u g r i z

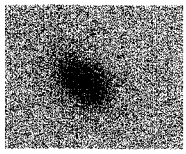

Sersic Fit

HI Spectrum

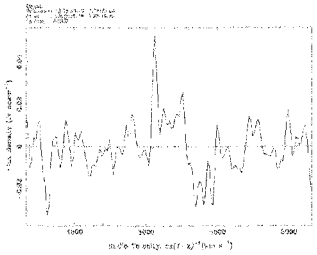

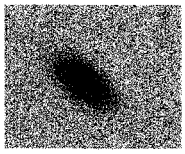

Bulge–Disk Fit

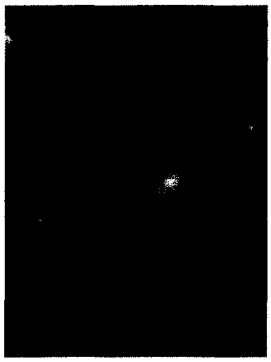

HIPEQ1341+05

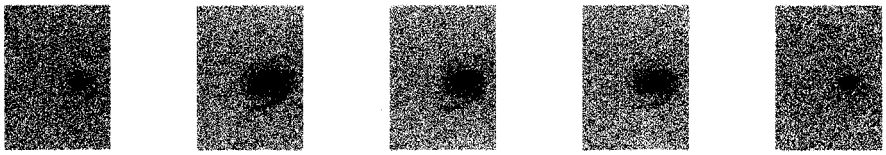

u g r i z

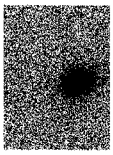

Sersic Fit

HI Spectrum

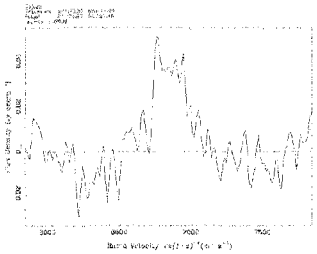

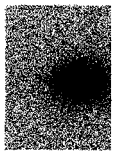

Bulge−Disk Fit

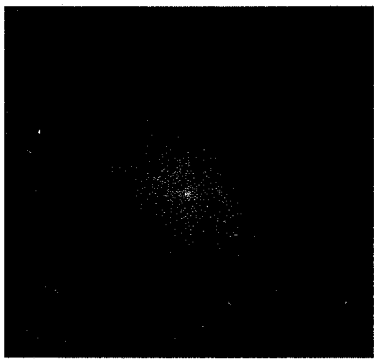

HIPEQ1348+03

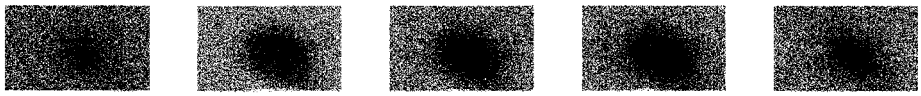

u g r i z

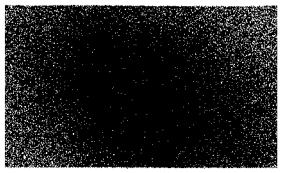

Sersic Fit

HI Spectrum

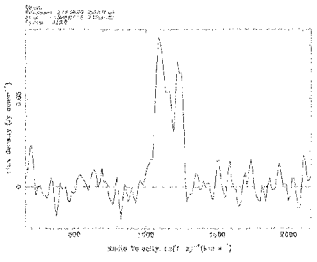

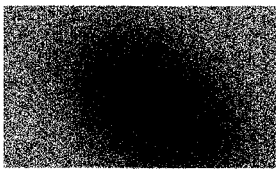

Bulge−Disk Fit

HIPEQ1352−01

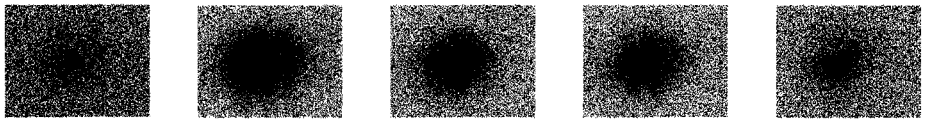

u g r i z

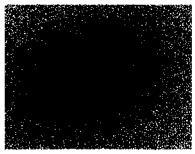

Sersic Fit

HI Spectrum

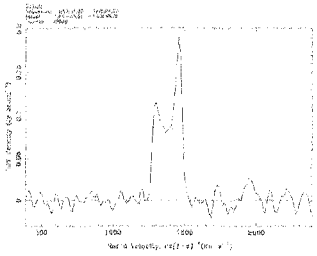

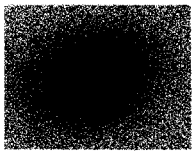

Bulge−Disk Fit

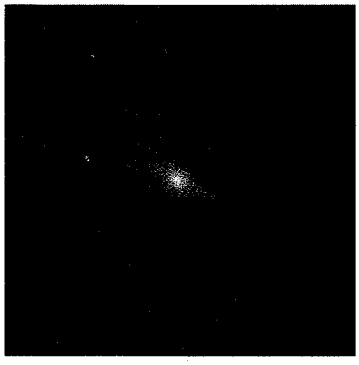

HIPEQ1352+02a

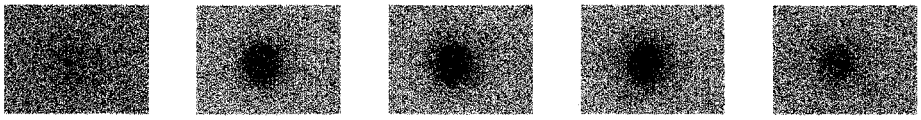

u g r i z

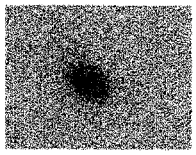

Sersic Fit

HI Spectrum

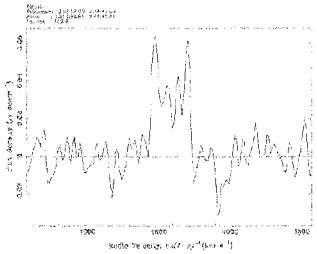

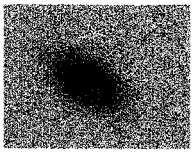

Bulge–Disk Fit

HIPEQ1400+02

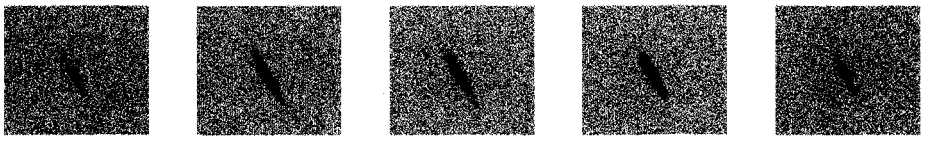

u g r i z

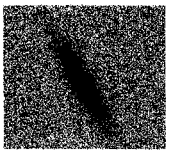

Sersic Fit

HI Spectrum

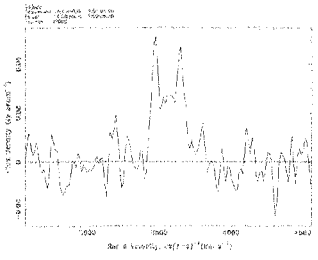

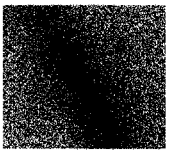

Bulge–Disk Fit

HIPEQ1411−01

u g r i z

Sersic Fit

HI Spectrum

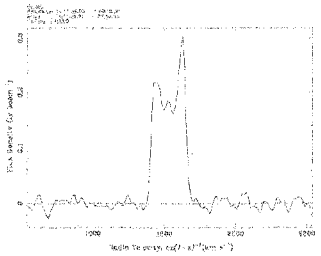

Bulge−Disk Fit

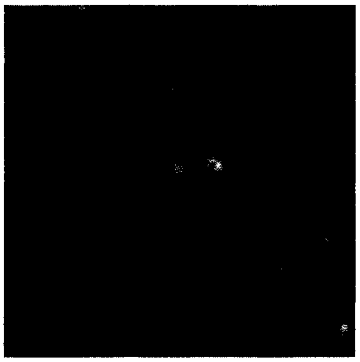

HIPEQ1415+04

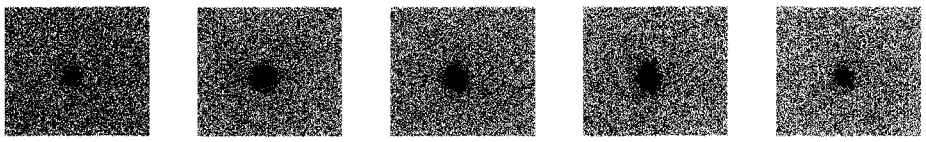

u g r i z

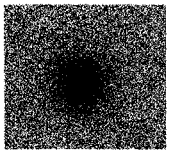

Sersic Fit

HI Spectrum

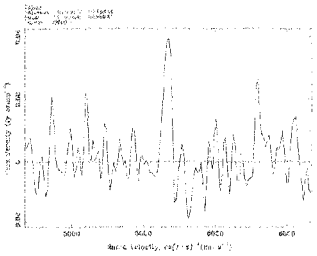

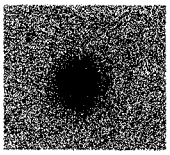

Bulge−Disk Fit

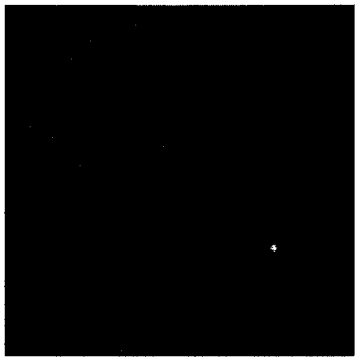

HIPEQ1416+03

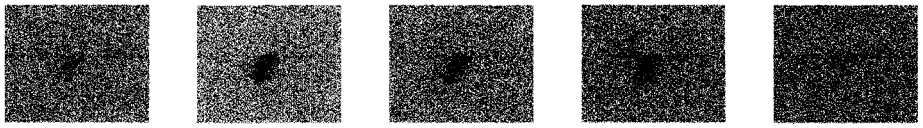

u g r i z

Sersic Fit

HI Spectrum

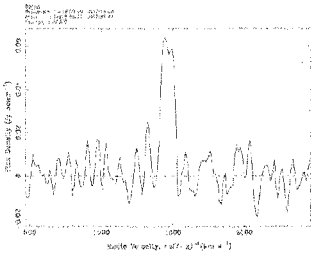

Bulge–Disk Fit

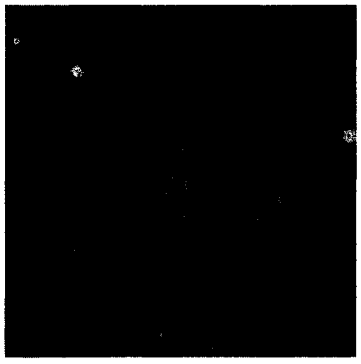

HIPEQ1422−00

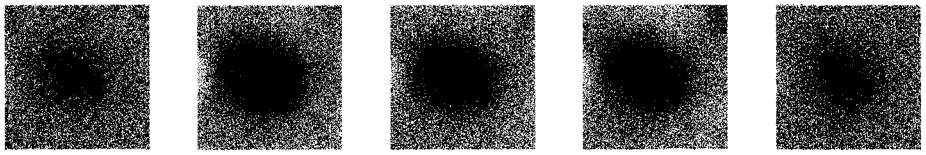

u g r i z

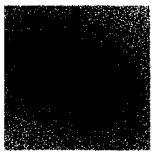

Sersic Fit

HI Spectrum

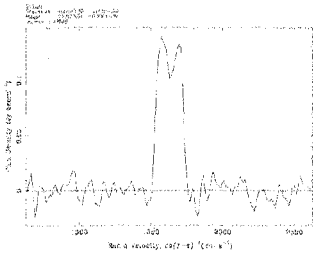

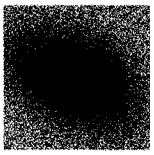

Bulge−Disk Fit

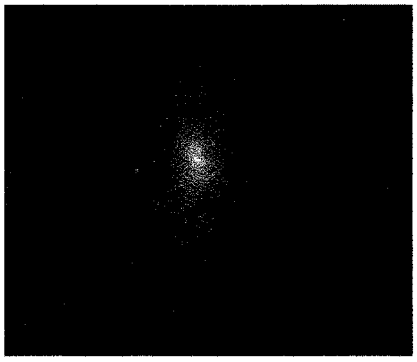

HIPEQ1429−00

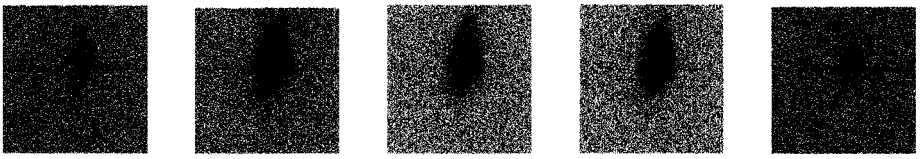

u g r i z

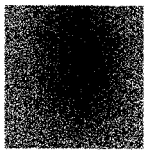

Sersic Fit

HI Spectrum

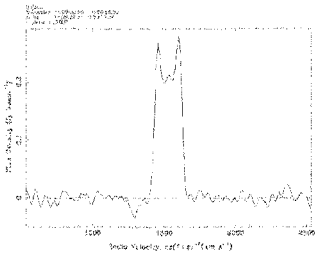

Bulge−Disk Fit

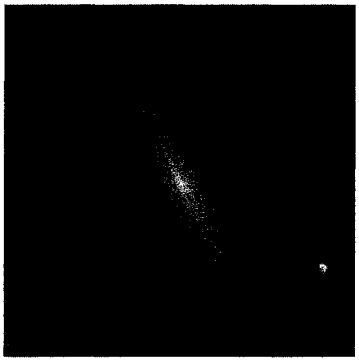

HIPEQ1432+00

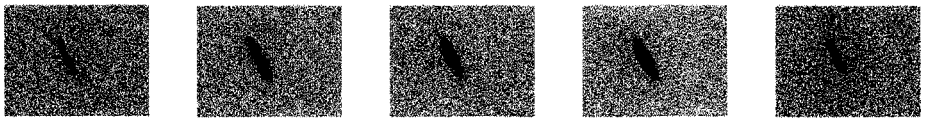

u g r i z

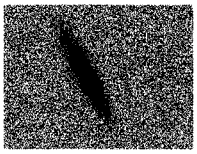

Sersic Fit

HI Spectrum

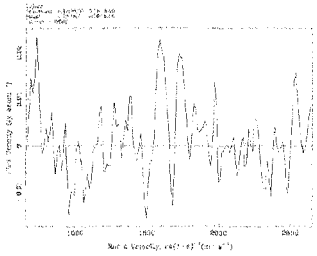

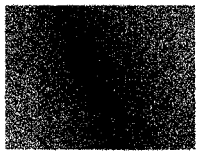

Bulge−Disk Fit

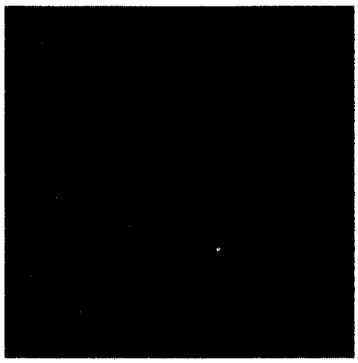

HIPEQ1433+01

u g r i z

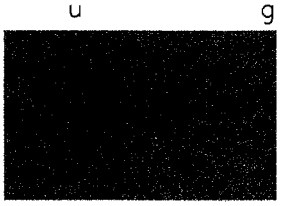

Sersic Fit

HI Spectrum

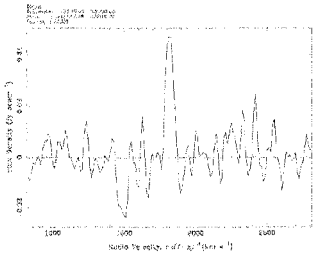

Bulge–Disk Fit

HIPEQ1433+02

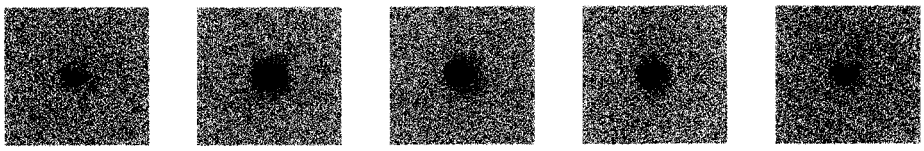

u g r i z

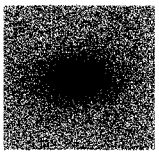

Sersic Fit

HI Spectrum

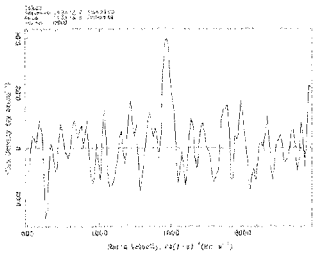

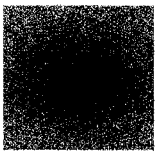

Bulge−Disk Fit

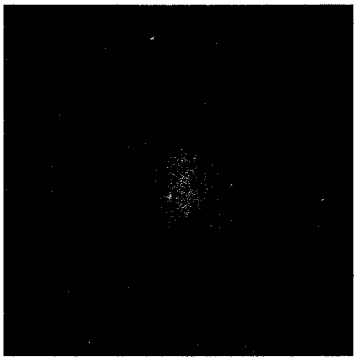

HIPEQ1437−00

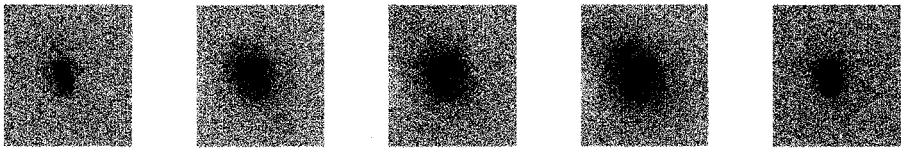

u g r i z

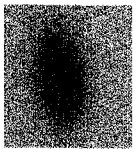

Sersic Fit

HI Spectrum

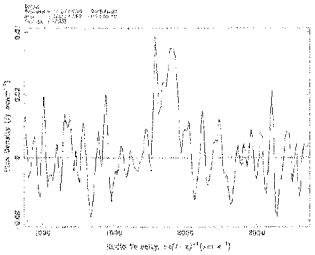

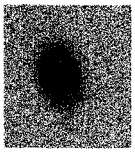

Bulge−Disk Fit

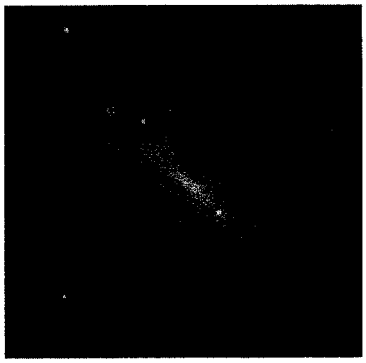

HIPEQ1437+02

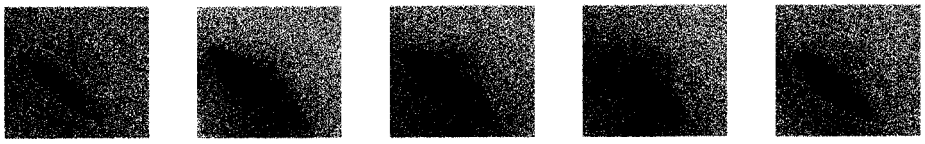

u g r i z

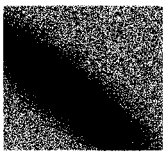

Sersic Fit

HI Spectrum

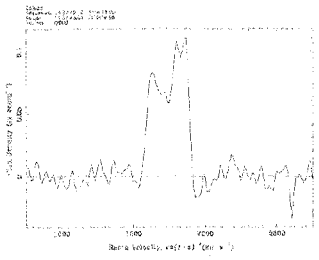

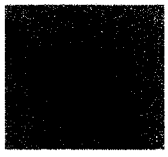

Bulge–Disk Fit

HIPEQ1439−00

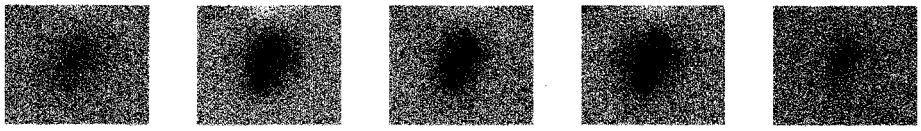

u g r i z

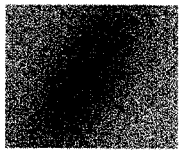

Sersic Fit

HI Spectrum

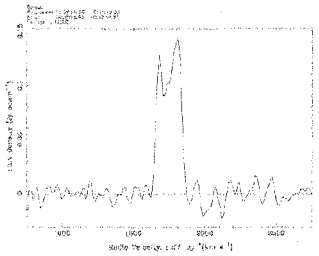

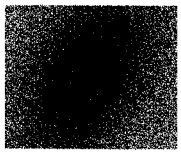

Bulge−Disk Fit

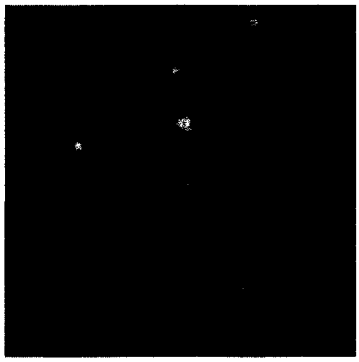

HIPEQ1439+02

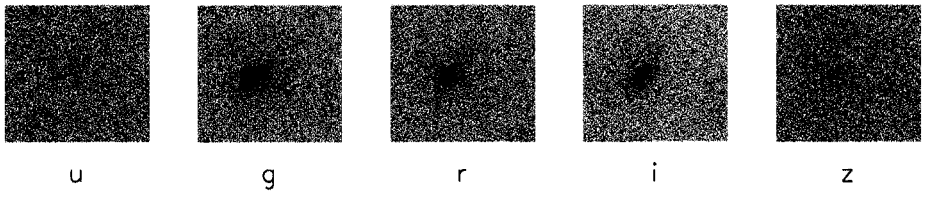

Sersic Fit

HI Spectrum

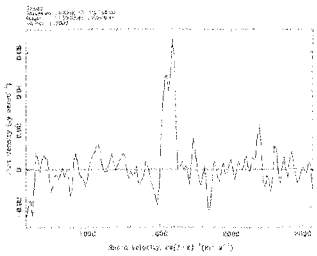

Bulge–Disk Fit

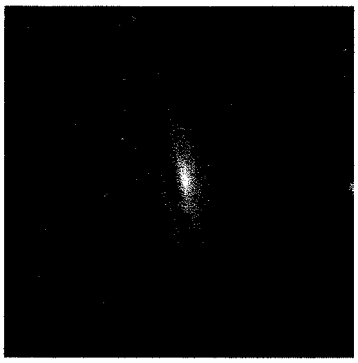

HIPEQ1440−00

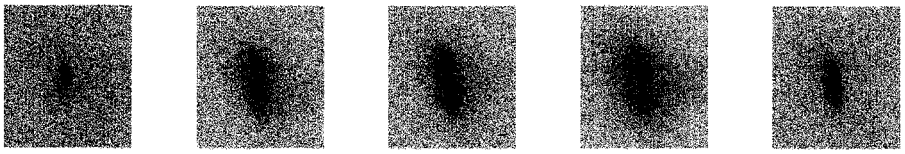

u g r i z

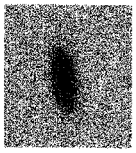

Sersic Fit

HI Spectrum

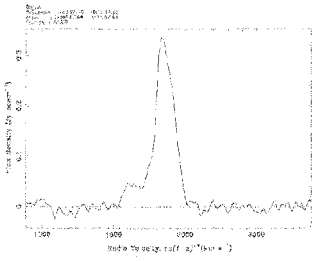

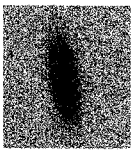

Bulge−Disk Fit

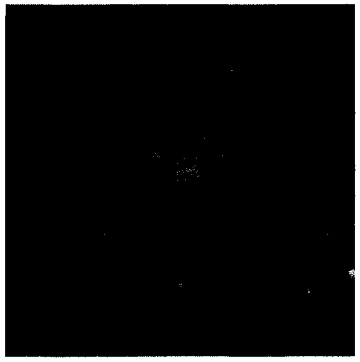

HIPEQ1440+02

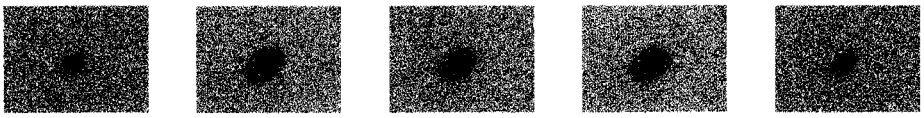

u g r i z

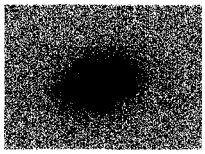

Sersic Fit

HI Spectrum

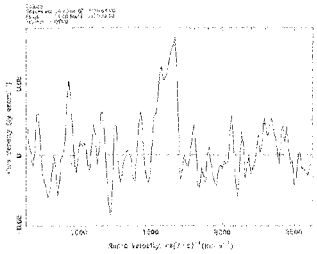

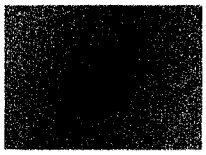

Bulge–Disk Fit

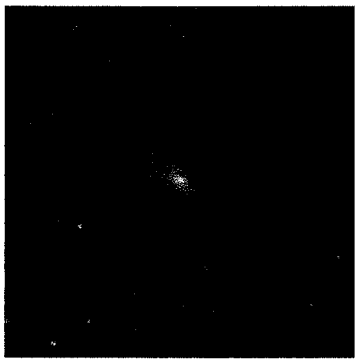

HIPEQ1444+01a

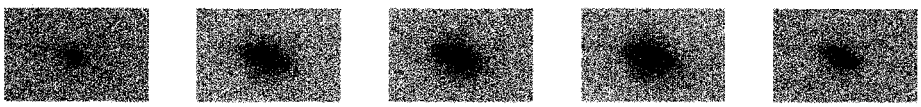

u g r i z

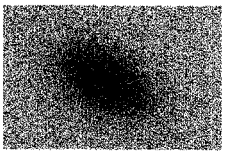

Sersic Fit

HI Spectrum

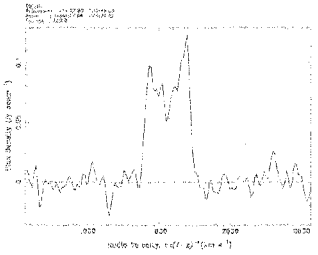

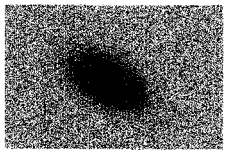

Bulge–Disk Fit

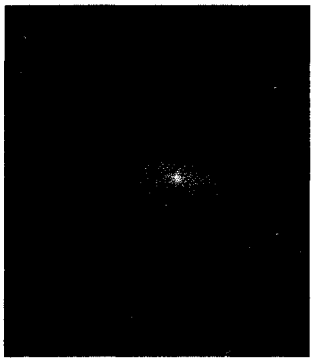

HIPEQ1500+01

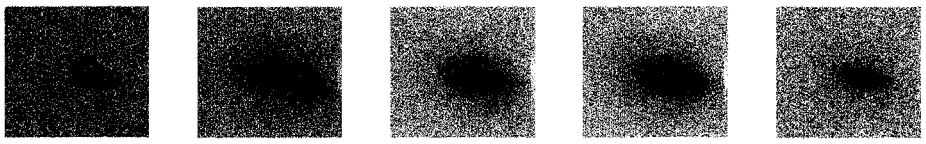

u g r i z

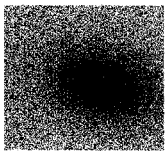

Sersic Fit

HI Spectrum

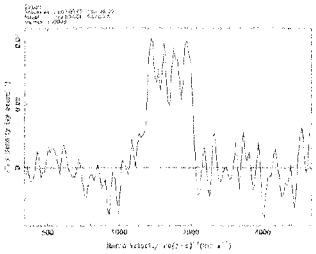

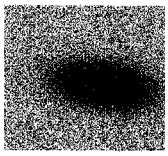

Bulge−Disk Fit

HIPEQ1504−00

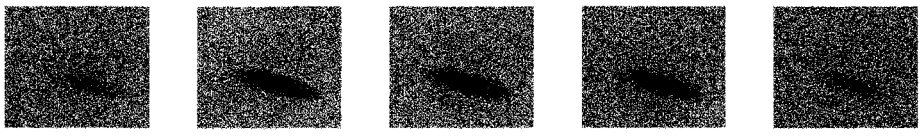

u g r i z

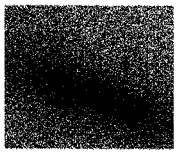

Sersic Fit

HI Spectrum

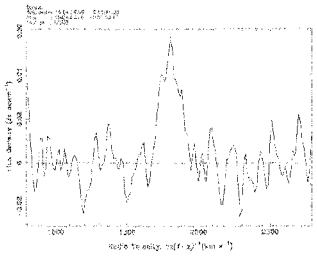

Bulge−Disk Fit

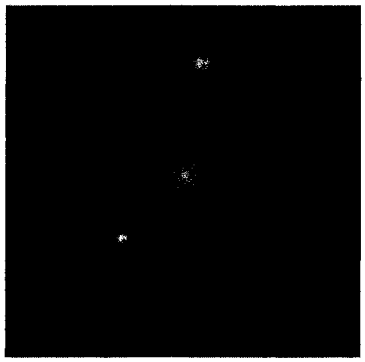

HIPEQ1504+02

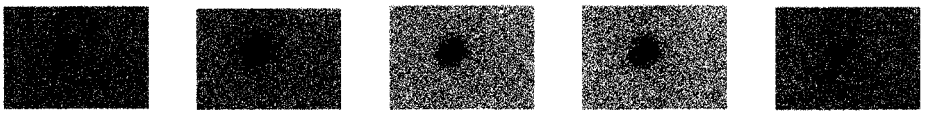

u g r i z

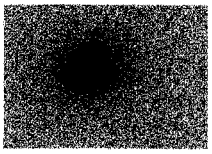

Sersic Fit

HI Spectrum

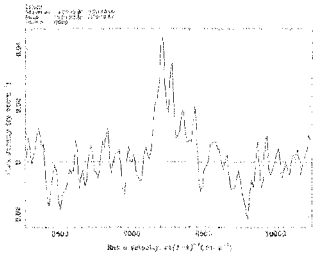

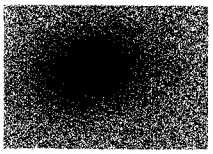

Bulge–Disk Fit

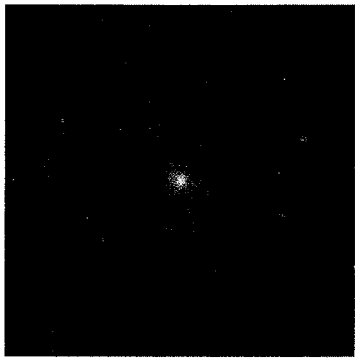

HIPEQ1507+01

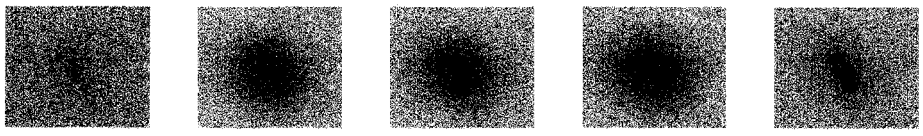

u g r i z

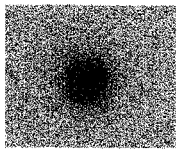

Sersic Fit

HI Spectrum

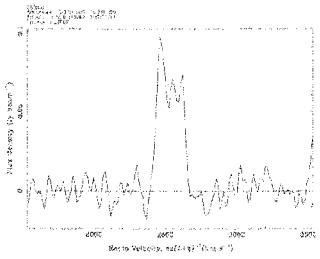

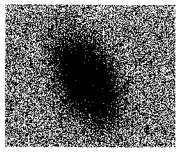

Bulge−Disk Fit

HIPEQ1542+00

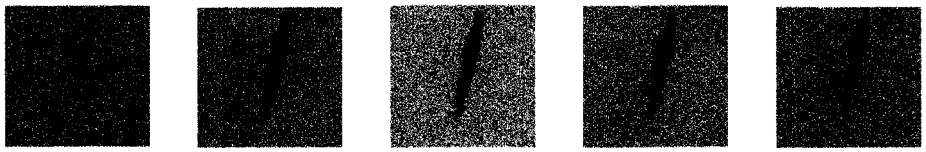

u g r i z

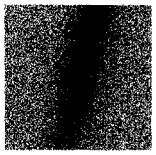

Sersic Fit

HI Spectrum

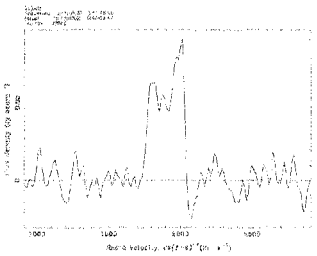

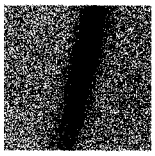

Bulge−Disk Fit

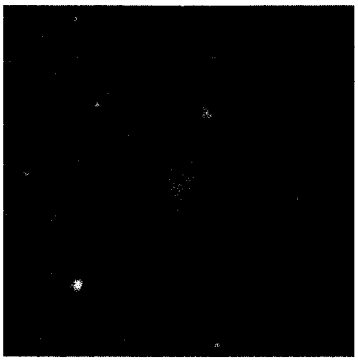

HIPEQ1544+02

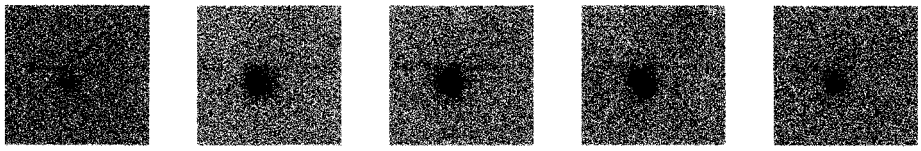

u g r i z

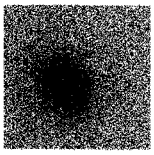

Sersic Fit

HI Spectrum

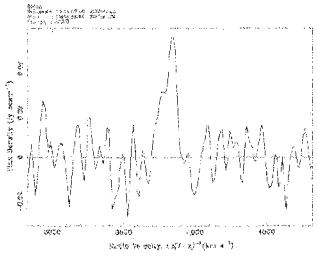

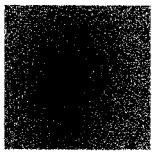

Bulge–Disk Fit

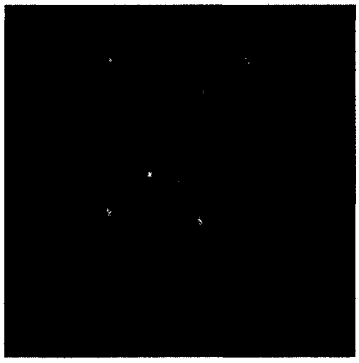

HIPEQ1545+00

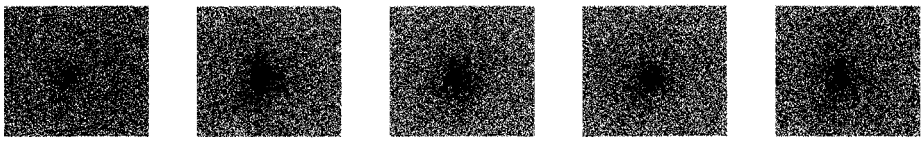

u g r i z

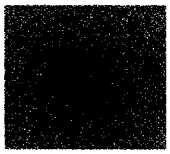

Sersic Fit

HI Spectrum

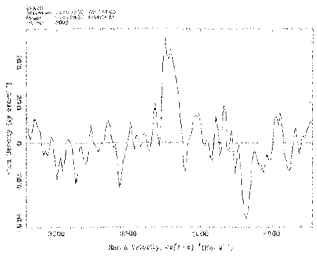

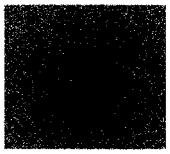

Bulge–Disk Fit

HIPEQ1601+01a

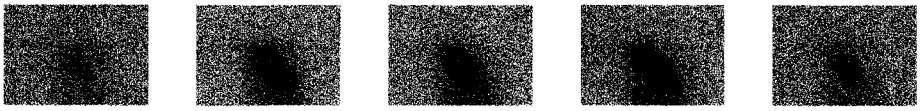

u g r i z

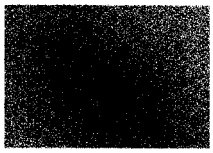

Sersic Fit

HI Spectrum

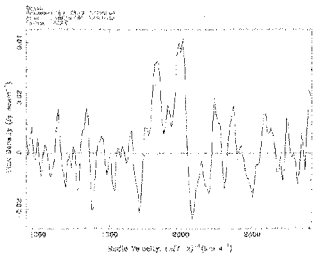

Bulge–Disk Fit

HIPEQ1609−00

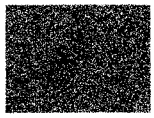
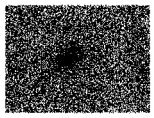
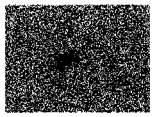
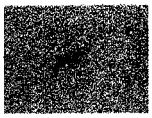
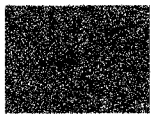

u g r i z

Sersic Fit

HI Spectrum

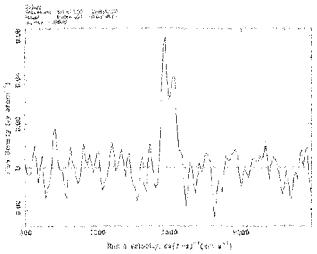

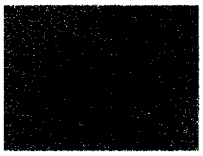

Bulge−Disk Fit

HIPEQ1613−00

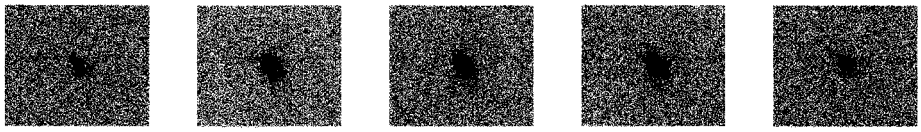

u g r i z

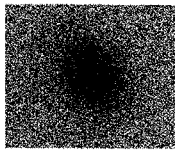

Sersic Fit

HI Spectrum

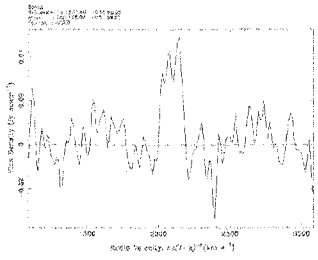

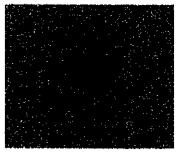

Bulge−Disk Fit

HIPEQ1614−00

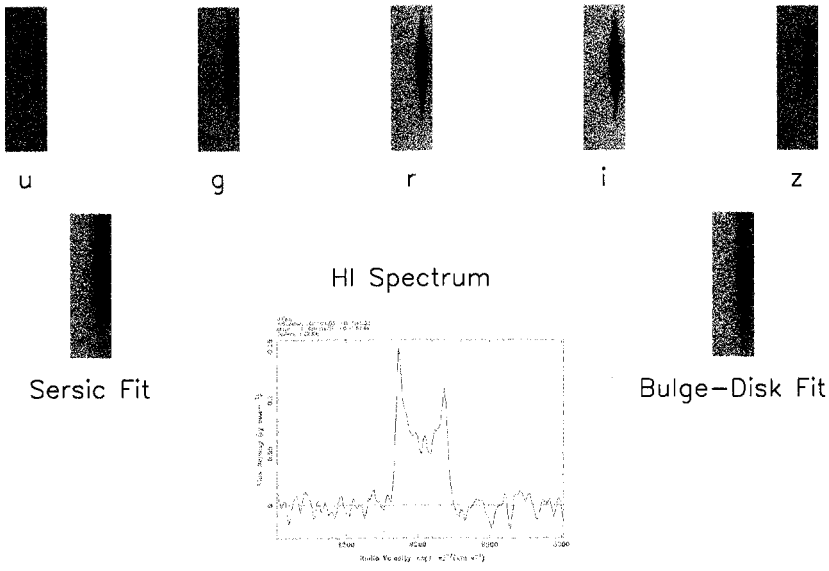

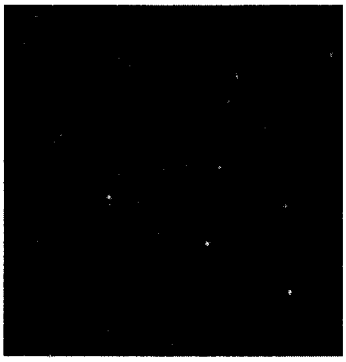

HIPEQ1614+00

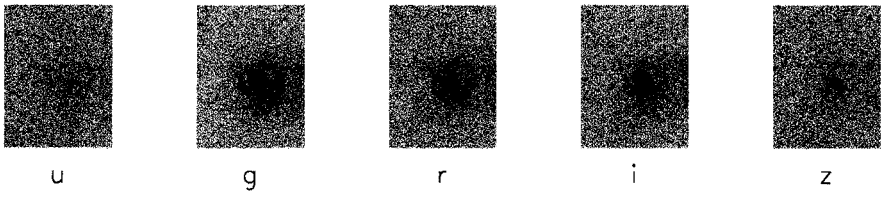

u g r i z

Sersic Fit

HI Spectrum

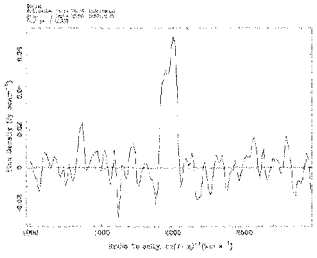

Bulge−Disk Fit

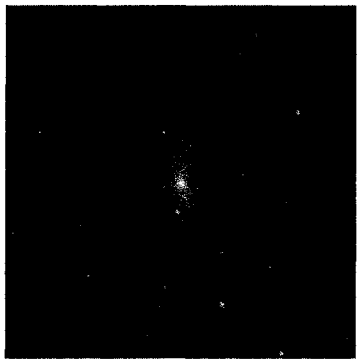

HIPEQ2036−04

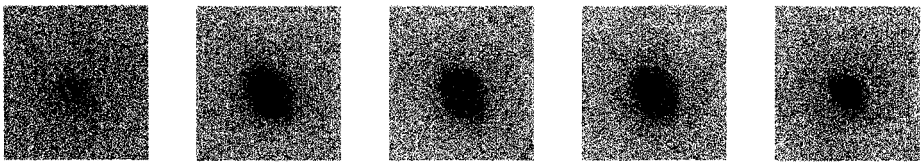

u g r i z

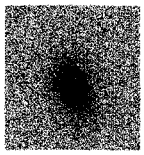

Sersic Fit

HI Spectrum

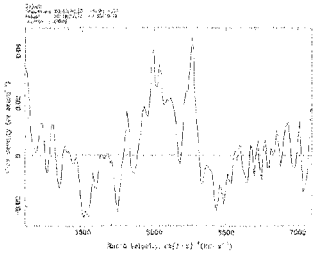

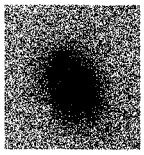

Bulge−Disk Fit

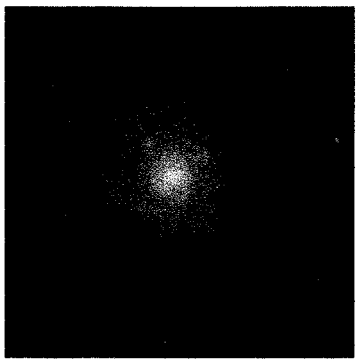

HIPEQ2314+00

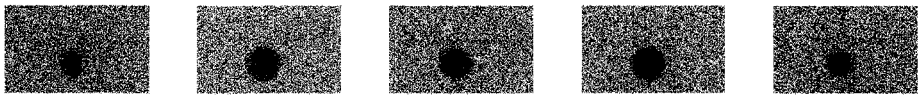

u g r i z

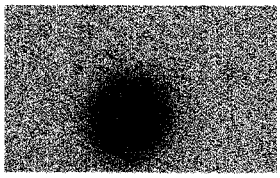

Sersic Fit

HI Spectrum

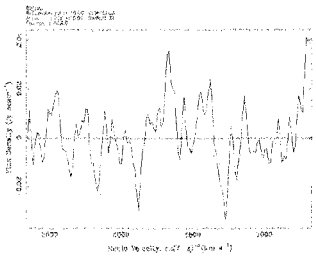

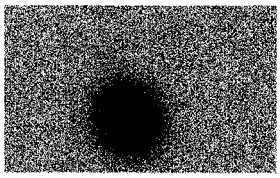

Bulge–Disk Fit

HIPEQ2324−00

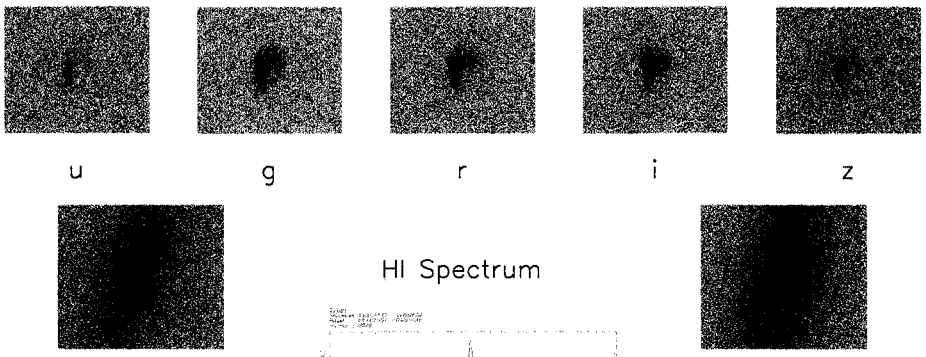

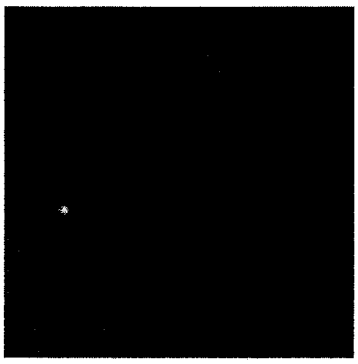

HIPEQ2335+01

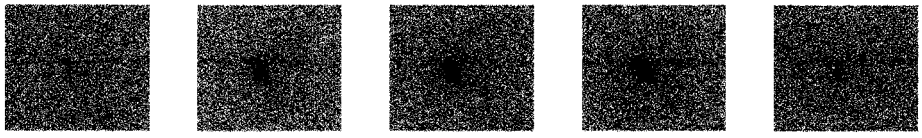

u g r i z

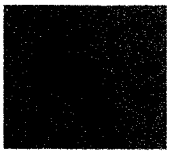

Sersic Fit

HI Spectrum

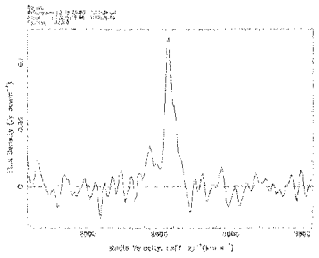

Bulge–Disk Fit

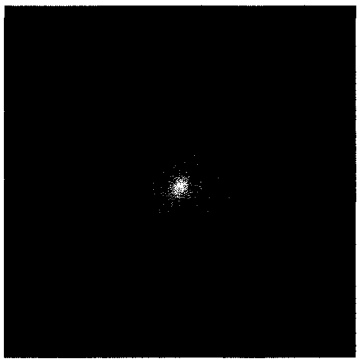

HIPEQ2336+00

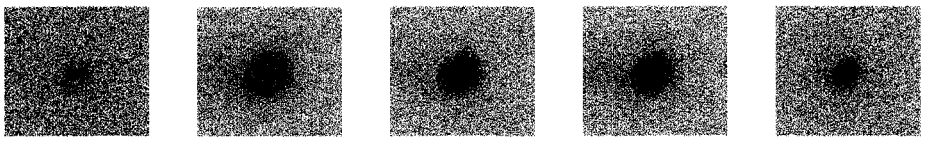

u g r i z

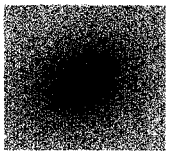

Sersic Fit

HI Spectrum

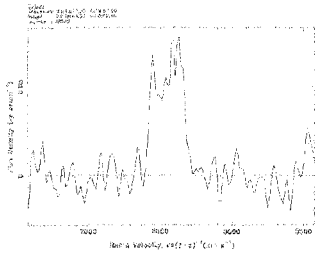

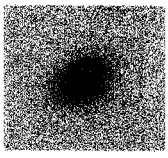

Bulge–Disk Fit

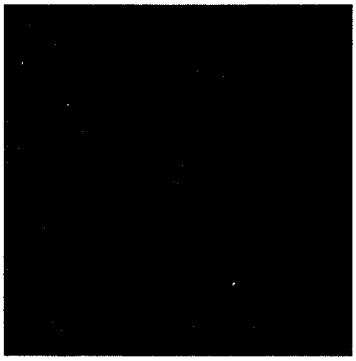

HIPEQ2337+00

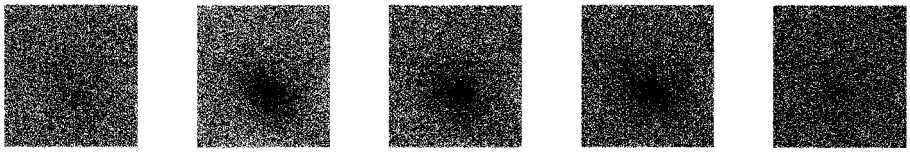

u g r i z

Sersic Fit

HI Spectrum

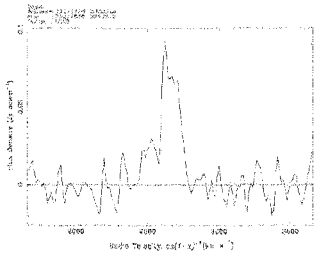

Bulge–Disk Fit

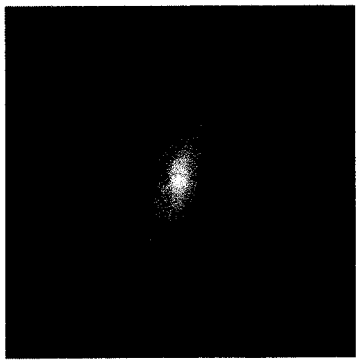

HIPEQ2340+01

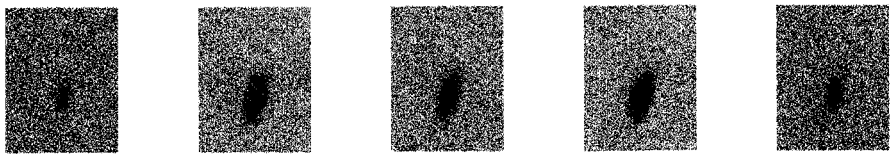

u g r i z

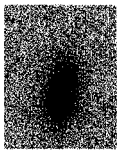

Sersic Fit

HI Spectrum

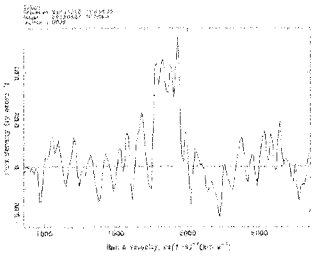

Bulge−Disk Fit

VITA

Andrew West was born on February 26, 1977 and grew up in Northern California. He attended Mountain Meadow Waldorf School through 8th grade, where he was first exposed to astronomy. His grandmother bought him a 4-inch telescope when he was 10 years old, a gift that amplified his interest in astronomy. After graduating from Ukiah High School in 1995, Andrew attended Haverford College in PA, where he studied Astronomy and Physics. He returned to the west coast in 1999 for graduate school at the University of Washington in Seattle, where he has studied under both Julianne Dalcanton and Suzanne Hawley. Andrew defended his Ph.D. in May 2005 and will be starting a postdoc at U.C. Berkeley in the fall of 2005. Andrew has maintained his interest in music and has continued to play the trombone throughout his undergraduate and graduate career in various ensembles. He ran varsity track in college and took up ultimate frisbee upon entering graduate school.